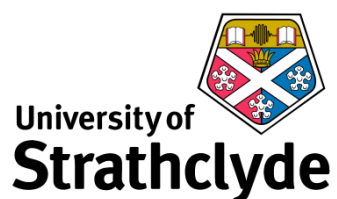


The Design and Synthesis of Targeted BET Inhibitors

Craig Michael Robertson



Epinova Discovery Performance Unit, GlaxoSmithKline

Department of Pure & Applied Chemistry, University of Strathclyde

Supervised by Dr Jack Brown and Professor William Kerr

Abstract

The field of epigenetics is an exciting new area for drug discovery. In particular, modulating proteins at the level of gene expression has already been verified as a valuable tool in treating disease. Within this area, bromodomain containing proteins recognise the epigenetic code on histone proteins, modulating gene expression. The bromodomains contained within the BET family have been implicated in multiple disease indications, including cancer, inflammation and viral infections. Furthermore, the BET family of bromodomains have been widely disclosed as amenable to inhibition by small molecules.

However, of the four bromodomain containing proteins within the BET family, three (Brd2, Brd3 and Brd4) are expressed ubiquitously. Therefore inhibition of BET bromodomain function has the potential to affect all cell types, not just those associated with disease.

In this regard, a targeted drug delivery system could minimise the broader systemic effects of BET inhibition and potentially improve the therapeutic index associated with this pharmacology. To this end, this thesis will focus on the use of an esterase sensitive motif (ESM) pro-drug targeting strategy. The ESM, developed by Chroma Therapeutics, consists of an amino acid ester which is selectively hydrolysed by the tissue-specific esterase human carboxyesterase 1 (hCE-1), mainly localised in the immune cells, monocytes and macrophages. However, the incorporation of this targeting motif contributes around 200 molecular weight to a small molecule inhibitor. Therefore, a small, ligand efficient BET bromodomain inhibitor was identified to initiate the work described within this thesis.

The first section of results within this thesis describes attempts made to further improve the ligand efficient fragment. While modifying the electronics of a phenyl ring contained within this fragment did not give an improved profile, replacement of this ring with a pyridyl group showed promise for the future physicochemical properties of this series.

Subsequently, the ESM was successfully incorporated onto this template, with the hydrolysis of the ESM, within target cells, being demonstrated. However, the resulting acid, produced in large quantities within the target cell, was less potent in biochemical assays of BET inhibition than the parent ester. Additional investigation

of the linker between the aryl and amino acid ester demonstrated, for the first time, the importance of linker length in the observed potency of the acid and in modulating hydrolysis rate of the ester at the site of action.

In the second results section, the aim was to introduce selectivity over the wider bromodomains. To achieve this, while maintaining desirable physicochemical properties, the aim was to utilise saturated groups to interact with the WPF shelf region of the BET bromodomains. Optimisation was conducted through a number of iterations, making use of modern medicinal chemistry techniques including: structure-based design, small molecule X-ray data and computational modelling.

Overall, work towards this thesis has taken a fragment molecule and optimised it towards a well-rounded lead molecule with excellent potency and physicochemical properties. The lead molecule has provided a platform to progress this series into lead optimisation within our laboratory with the aim of discovering a clinical candidate molecule to be evaluated in the treatment of rheumatoid arthritis.

The human biological samples used within this thesis were sourced ethically and their research use was in accord with the terms of the informed consents.

All animal studies discussed within this thesis were ethically reviewed and carried out in accordance with Animals (Scientific Procedures) Act 1986 and the GSK Policy on the Care, Welfare and Treatment of Animals.

Abbreviations

AcK	Acetyl-lysine
ADC	Antibody Drug Conjugate
ADME	Absorption, Distribution, Metabolism and Excretion
ADMET	Absorption, Distribution, Metabolism, Excretion and Toxicity
AIDS	Acquired Immune Deficiency Syndrome
AMP	Artificial Membrane Permeability
AMU	Atomic Mass Units
ApoA1	Apolipoprotein A1
AUC	Area Under the Curve
BBB	Blood-brain-barrier
BCP	Bromodomain Containing Protein
BET	Bromodomain and Extra C-Terminal
bp	Base Pairs
BSci	Biological Sciences
cAMP	Cyclic Adenosine Monophosphate
cChromLogD	Calculated ChromLogD
Cdk9	Cyclin-dependent Kinase 9
CDS	Chemical Drug-delivery System
CF	Cystic Fibrosis
ChromLogD	Chromatographic LogD
CLND	Chemiluminescent Nitrogen Detection
C _{max}	Maximum Concentration
CNS	Central Nervous System
CREB	cAMP-response Element Binding Protein
CREBBP	CREB Binding Protein
CTCL	Cutaneous T-cell Lymphoma
CTD	C-Terminal Domain
CV	Column Volume
DCM	Dichloromethane
DEA	Diethanolamine
DIAD	Diisopropyl Azodicarboxylate
DIBAl-H	Diisobutylaluminium Hydride
DIPEA	Diisopropylethylamine
DMAP	4-(<i>N,N</i> -Dimethylamino)pyridine
DMF	<i>N,N</i> -Dimethylformamide
DMPK	Drug Metabolism and Pharmacokinetics
DMSO	Dimethylsulfoxide
DNA	Deoxyribonucleic Acid
DOC	Sodium Deoxycholate
DPU	Discovery Performance Unit
ED ₅₀	Dose which delivers the desired effect within 50% of the population
EDC	<i>N</i> -(3-Dimethylaminopropyl)- <i>N'</i> -ethylcarbodiimide
EPR	Enhanced Permeability and Retention

ESI	Electrospray Ionisation
ESM	Esterase Sensitive Motif
ET	Extra-terminal
eXP	Enhanced Cross-screening Panel
FaSSIF	Fasted State Simulated Intestinal Fluid
FDA	Food and Drug Administration
FP	Fluorescence Polarisation
FRET	Fluorescence Resonance Energy Transfer
GSK	GlaxoSmithKline
h	Hour
HAC	Heavy Atom Count
HAMA	Human Anti-mouse Antibodies
HAT	Histone Acetyltransferase
hCE	Human Carboxylesterase
hCE-1	Human Carboxylesterase 1
HDAC	Histone Deacetylase
HDL	High-density Lipoprotein
HLM	Human Liver Microsomes
HOBt	Hydroxybenzotriazole
HPLC	High Performance Liquid Chromatography
HRMS	High Resolution Mass Spectroscopy
HSA	Human Serum Albumin
HTS	High-throughput Screening
hWB	Human Whole Blood
IBX	2-Iodoxybenzoic Acid
IC ₅₀	Concentration required for 50% Inhibition
Ig	Immunoglobulin
IR	Infrared
IVC	<i>In Vitro</i> Clearance
LCMS	Liquid Chromatography Mass Spectroscopy
LDL	Low-density Lipoprotein
LE	Ligand Efficiency
LogD	Log of the Distribution Coefficient
LogP	Log of the Partition Coefficient
LPS	Lipopolysaccharide
mAb	Monoclonal Antibodies
MCP-1	Monocyte Chemoattractant Protein-1
mCPBA	<i>meta</i> -Chloroperoxybenzoic Acid
MIDA	<i>N</i> -Methyliminodiacetic Acid
min	Minute
MM	Multiple Myeloma
MR	Molar Refractivity
mRNA	Messenger RNA
MWt	Molecular Weight
NBS	<i>N</i> -Bromosuccinimide
NMC	NUT Midline Carcinoma

GSK Confidential Information – Do not copy

NMR	Nuclear Magnetic Resonance
NUT	Nuclear Protein in Testis
PBMC	Peripheral Blood Mononuclear Cell
pdb	Protein Data Bank
PFI	Property Forecast Index
pIC ₅₀	- Log[IC ₅₀]
PLE	Pig Liver Esterase
PPL	Porcine Pancreatic Lipase
PTCL	Peripheral T-cell Lymphoma
P-TEFb	Positive Transcription Elongation Factor b
PTM	Post-translational Modification
qPCR	Quantitative Polymerase Chain Reaction
RA	Rheumatoid Arthritis
Rf	Retention Factor
RNA	Ribonucleic Acid
RNAi	RNA Interference
RT	Room Temperature
rt	Retention Time
SA	Specific Activity
SGC	Structural Genomics Consortium
siRNA	Short Interfering RNA
STAB-H	Sodium Triacetoxyborohydride
t _{1/2}	Half Life
TBAF	Tetra- <i>n</i> -butylammonium Fluoride
TD ₅₀	Dose which causes toxicity within 50% of the population
TFA	Trifluoroacetic Acid
THF	Tetrahydrofuran
THP	Tetrahydropyran
TI	Therapeutic Index
TLC	Thin Layer Chromatography
TMS	Tetramethylsilane
TNF α	Tumour Necrosis Factor α
TPP	Target Product Profile
TPSA	Total Polar Surface Area
UPLC	Ultra Performance Liquid Chromatography
UV	Ultraviolet
WPF	Tryptophan, Proline, Phenylalanine
SAR	Structure-activity Relationship

Contents

Abstract	i
Abbreviations	iii
Contents	vi
Acknowledgements.....	ix
1 Introduction.....	1
1.1 Genetics and DNA.....	1
1.2 Epigenetics.....	4
1.2.1 DNA Methylation.....	5
1.2.2 Histone Modification	6
1.2.3 Acetylated Lysine	10
1.2.4 Bromodomains	15
1.3 Early BET Bromodomain Inhibitors.....	19
1.3.1 Azepine- and Diazepine-centred BET Inhibitors.....	23
1.3.2 Isoxazole-containing BET Inhibitors.....	24
1.3.3 Novel Acetyl-lysine Mimetics	26
1.4 BET Inhibitors in the Clinic.....	29
1.4.1 Potential Risks of Clinical BET Inhibitors	31
1.5 Targeted Drug Delivery.....	32
1.5.1 Therapeutic Index.....	32
1.5.2 Nano-particles and Liposomes	33
1.5.3 Comparing Prodrugs and Antibody-Drug Conjugates	36
1.5.4 Prodrugs.....	37
1.5.5 Antibody Drug Conjugates.....	39
1.6 Targeted Prodrugs.....	47
1.6.1 Targeting Drugs to the Central Nervous System (CNS).....	47
1.6.2 Targeting Drugs to Specific Cells.....	50
1.7 Targeting Molecules to the Macrophage.....	52

1.7.1	Human Carboxyl Esterases (hCE)	52
1.7.2	Esterase Sensitive Motif (ESM)	54
1.8	Project Aim and Objectives	60
1.9	Compound Profiling	60
1.9.1	Screening Cascade	60
1.9.2	Target Product Profile	63
2	Fragment Optimisation and Targeting	67
2.1	Proposed Work	67
2.2	Fragment Identification	68
2.2.1	Initial Aims	70
2.3	Fragment Optimisation	71
2.3.1	Investigating the ZA Channel	72
2.3.2	Investigations into Phenyl Ring Replacements to Reduce LogD	78
2.3.3	Reducing Lipophilicity via the Acetyl Lysine Mimetic	83
2.4	ESM Incorporation	87
2.4.1	Phenyl Pyridone Fragment	87
2.4.2	Synthesis of Pyridyl Core Replacements	96
2.4.3	Properties of Initial ESM-functionalised BET Inhibitor 2.58e	108
2.5	Investigating Acid Potency	114
2.6	Alternative Methods to Reduce Lipophilicity	135
2.7	Summary	140
3	BET Pharmacophore Optimisation	143
3.1	Non-BET Bromodomains	143
3.1.1	Inhibitors of the non-BET Bromodomains	144
3.2	Introducing Selectivity for BET over the non-BET Bromodomains	148
3.2.1	Investigating Selectivity by Targeting the WPF Shelf	152
3.3	Interrogating the WPF Shelf Group	195
3.3.1	Branching	195

3.3.2	Demethylation	205
3.4	Summary	222
4	Conclusions and Further Work.....	227
5	Experimental.....	234
5.1	General Experimental Details	234
5.2	Experimental	238
6	References	385
7	Appendix 1	401
7.1	Macrophage Retention Assay Calculations.....	401
7.1.1	Acid 2.95e	401
7.1.2	Ester 2.58e	401
8	Appendix 2	402
8.1	BROMOscan™ Bromodomain Phylogenetic Tree	402
9	Appendix 3	403
9.1	Assay Protocols.....	403

Acknowledgements

The preparation of this thesis would not have been possible without the support I have had throughout my PhD studies. First and foremost, I would like to extend my biggest thanks to my supervisors Dr Jack Brown and Professor William Kerr.

As my industrial supervisor, I am grateful for Jack's close supervision and guidance. I appreciate all the time given for proof-reading as well as support when presenting my work.

I also extend my gratitude to Billy, as my academic supervisor, for the advice and discussions throughout my PhD. Additionally, I am thankful for his meticulous proofing of my key reports and final thesis.

As fellow members of "Cohort 1", I would like to thank Rob, Natalie, Ben, Aymeric, Jonathan, Sam and Laura. This shared help and advice aided our progression through this new PhD programme.

I must also thank the labs I worked within during my studies. Firstly, 2T113 in Epinova, who were all very welcoming and happy to share their wisdom. In addition, I would like to thank the Kerr group for the good times had during my three month secondment. It was an excellent experience, working with iridium catalysts, very different, but with a similar strategy.

A special mention is also owed to Sean Lynn and Richard Upton (NMR support), Bill Leavens (HRMS) and Ian Lynch (IR) for their advice and support in data collection.

Many thanks go to my wife, Naomi. Her incredible, continuous support, despite not knowing what I was working on, made the difficult times easier. I would also like to acknowledge the help Naomi gave me in the art of Chemdraw to aid some of my home-made figures. My thanks also extend to my parents, for their continued support and understanding when times got busy, especially during the preparation of this thesis.

Finally, I would also like to thank our team mascot, the Bromo-gnome for his watchful eye over my reactions and good luck he brought to my endeavours.

1 Introduction

1.1 Genetics and DNA

The information an organism requires to function, grow and replicate is encoded in its DNA.¹ Hence, each cell contains its own copy of this vital information. However, on occasions, changes in the genetic code can cause genetic disorders. Some, such as cystic fibrosis (CF), involve small deletions from the DNA code, causing the formation of dysfunctional proteins. Once the genetic cause is understood, the Mendelian^{2,3} heredity of the mutated code can be followed through generations (Figure 1.1), aiding the diagnosis of genetic diseases.

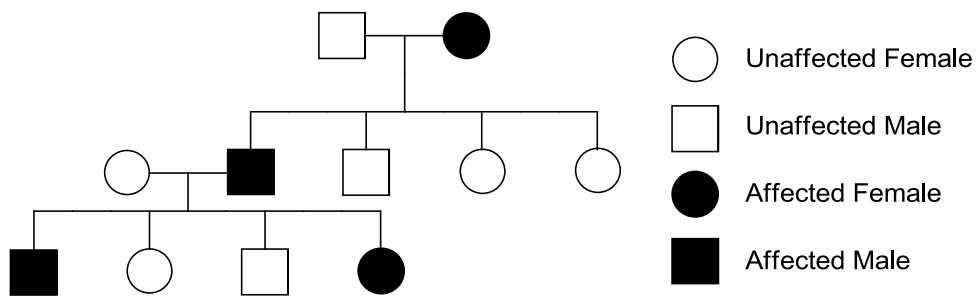


Figure 1.1: Pedigree diagram following genetic traits, such as disease

Mutations which cause disease arise from changes of the DNA code. The DNA is coded by the sequential arrangement of four nucleotides, adenine (A), cytosine (C), guanine (G) and thymine (T) (Figure 1.2). These four DNA bases form hydrogen bonded pairs and arrange into two strands of DNA, structured as a double-helix.⁴ The human genome project, completed in 2003, measured the entire human DNA sequence and found it to contain almost 3 billion base pairs (bp).⁵

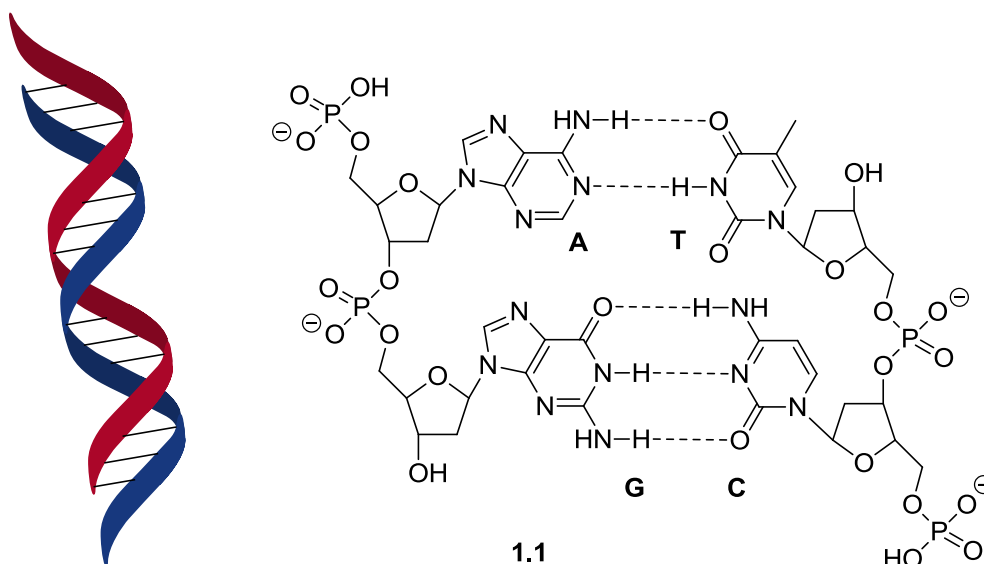


Figure 1.2: DNA base pairing

Cells of the human body each contain a complete copy of these near 3 billion bp, measuring 1.6 m of DNA in total. Separated into smaller lengths called chromosomes, the large quantity of DNA must fit within the nucleus, measuring only 5 μm in diameter.⁶ Indeed, the DNA must be efficiently packaged and is achieved via a number of structures (Figure 1.3). Firstly, the DNA is wrapped around a bundle of histone proteins to form a nucleosome before further condensing to form a chromatin fibre. The chromatin is then able to further loop and fold to form tightly coiled chromatid, half of the chromosome required to pass the information to the daughter cells during cell division.

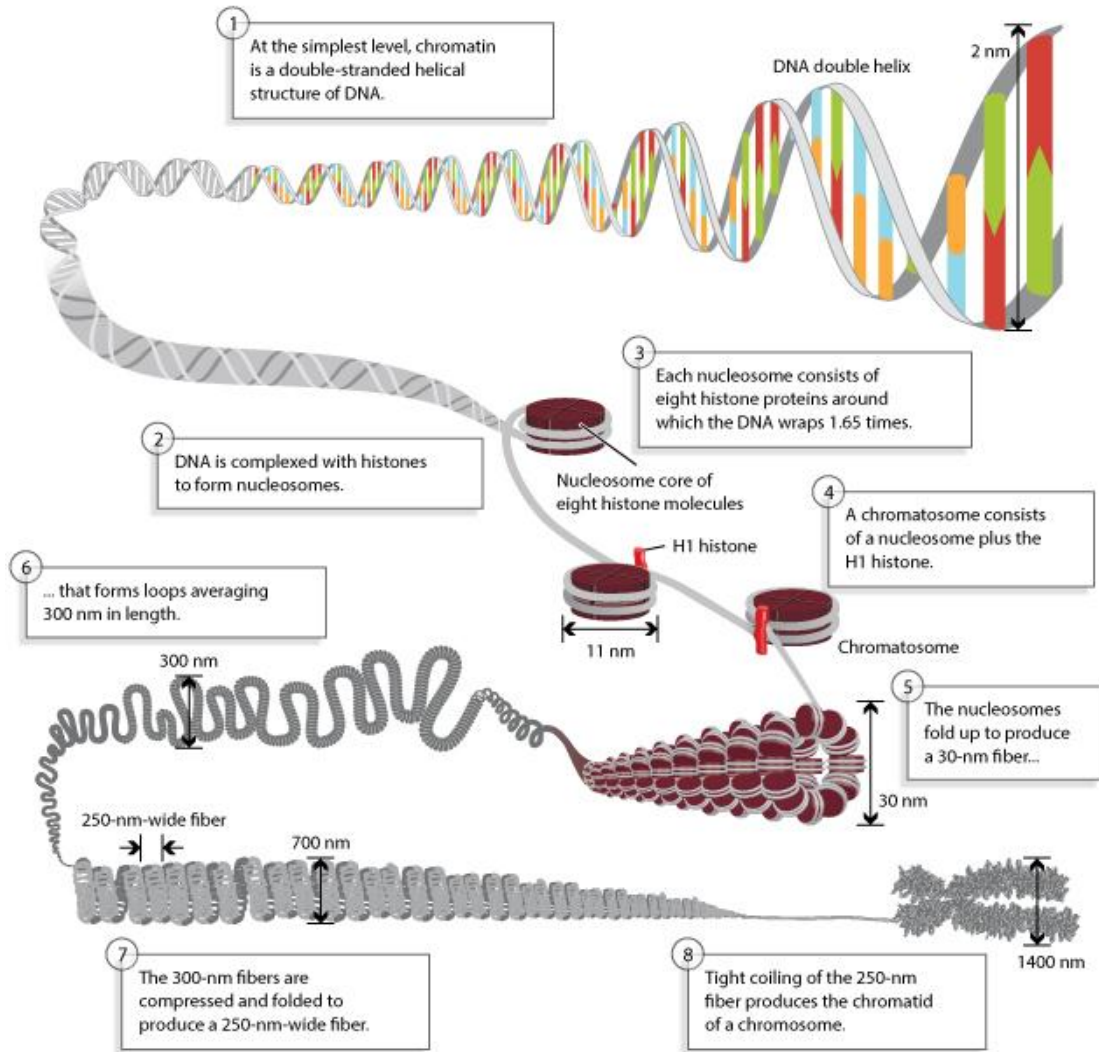
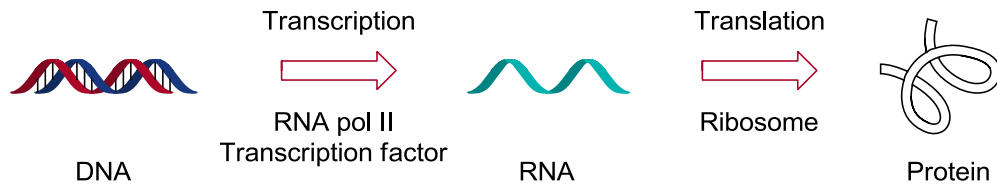


Figure 1.3: DNA packaging⁷

Contained within the DNA are genes, which are, in essence, the instructions required to make specific proteins. In order to synthesise proteins, the DNA must firstly be transcribed into messenger RNA (mRNA), a single-stranded ribonucleic acid (Scheme 1.1). RNA polymerase II plays a pivotal role in transcription as this is the enzyme which builds the mRNA sequence. It first binds to a gene promoter region recognition site before initiating transcription. In addition, other proteins called transcription factors are able to bind to promoter regions within the DNA sequence and enhance the activity of RNA polymerase II. The mRNA code must then be translated to produce the desired protein. This is mediated by large proteins called ribosomes, which read the mRNA code, introduce the required individual amino acid and build the protein sequence, residue by residue.



Scheme 1.1: Flow of information from DNA to proteins

Every cell, barring red blood cells, contains a complete copy of the organism's DNA and, therefore, has the potential to synthesise every protein coded in the DNA. However, not all of the genes present in DNA are expressed (transcribed and translated into proteins) at the same time. Indeed, control over gene expression allows for the production of differentiated cell types from the pluripotent stem cell (Figure 1.4).⁸ Researchers questioned the control mechanisms which restrict the expression of genes to specific cell types and at certain times. Also, how does one account for the variety of cell types and cell functions given their common progenitor cell and ultimately, genetic code? The answers to these questions may lie in the emerging field of epigenetics.

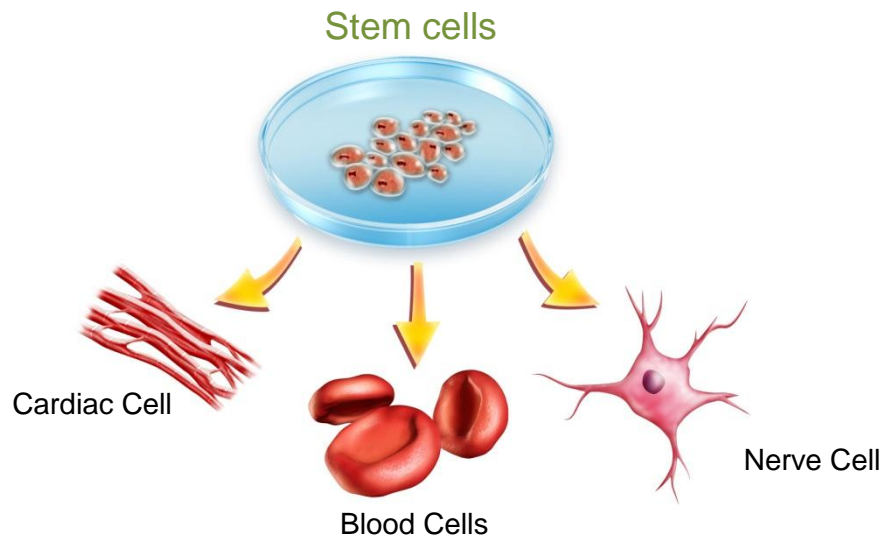


Figure 1.4: Differentiation of stem cells⁹

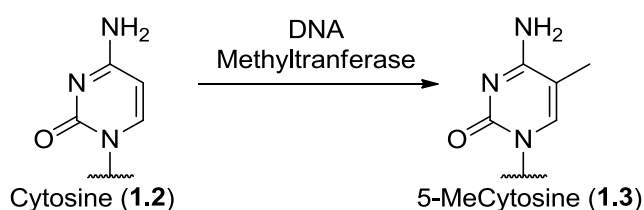
1.2 Epigenetics

The term “epigenetics” comes from the greek prefix ‘epi’ meaning ‘above’, thus literally means “above genetics”. It can be summarised as heritable changes in phenotype, the observable characteristics of an organism, which occur without changing the underlying DNA sequence.¹⁰ Epigenetics allows organisms to quickly adapt to changes in their environment without requiring genetic mutation.¹¹

It is now understood that gene expression is controlled by changing the affinity of transcription factors, proteins which enhance transcription, and RNA polymerase II, the enzyme responsible for forming mRNA, for DNA.¹² This change in affinity can be brought about through two main mechanisms: DNA base modification or changes to how tightly packed the DNA is within the nucleosome. Based on this, in terms of molecular biology, these mechanisms will be discussed in turn.

1.2.1 DNA Methylation

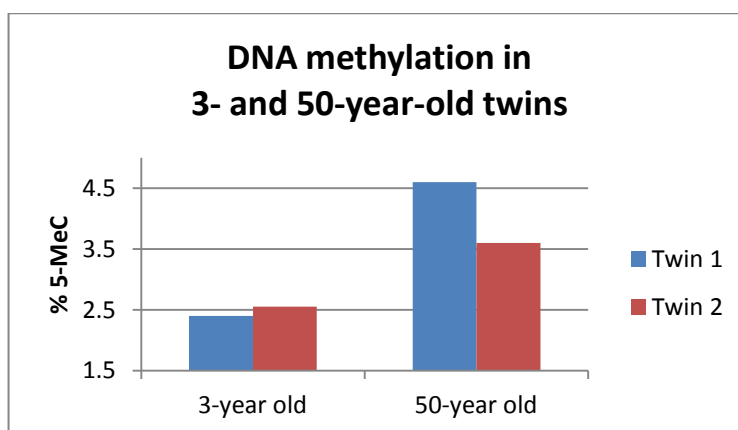
Firstly, the DNA can be chemically altered through methylation of the DNA base cytosine (1.2) (Scheme 1.2). This methylation occurs at areas rich in cytosine-guanine dinucleotides termed CpG islands, found within gene promoter regions.¹³ The effect of DNA methylation is to silence genes; in other words, cytosine methylation prevents transcription in a permanent fashion.¹⁴



Scheme 1.2: Methylation of Cytosine by DNA Methyltransferase (DMT)

To explain this silencing affect, two hypotheses have been proposed. First, transcription factors are thought to have reduced affinity for methylated DNA. Alternatively, blocking proteins recognise and bind to the modified DNA, preventing transcription.¹⁴

Changes in an organism's environment can affect this epigenetic marker, which can be perfectly exemplified in monozygotic twins. Importantly, identical twins have exactly the same DNA sequence, thus ensuring any differences in observed phenotype are caused by changes in the epigenetic state. As can be seen in Graph 1.1, three year old twins show identical levels of 3-methylcytosine. Similar environmental factors during early childhood maintain similar epigenetic profiles. The same twins, aged 50, demonstrate a very different epigenetic profile, with significant differences in DNA methylation levels, diverging with differing lifestyles. Therefore, the epigenetic state of any given individual is highly promiscuous and prone to change.



Graph 1.1: Epigenetic divergence during aging¹⁵

Aberrant DNA methylation, and the resultant gene silencing, has been directly linked to disease. A poignant example is the hypermethylation of DNA, specifically, of the promoter region of tumour suppressor gene *p16*, which has been observed in cancers of the lung and throat of regular smokers.^{16,17} Hypermethylation at this promoter region results in silencing of the tumour suppressing protein. The upregulation of DNA methyltransferases and the resulting hypermethylation is currently thought to be a protective mechanism against DNA damage, maintaining the structural integrity¹⁸ of the DNA by preventing transposition of lengths of DNA between chromosomes which can be highly mutagenic.¹⁹ Conversely, it is hypothesised that hypermethylation of the *p16* tumour suppressor promoter region is the cause of these cancers. As a result, the body's hypermethylation protective mechanism can also have other deleterious effects. Additionally, this hypermethylation is also observed in normal tissue, preceding cancer. Therefore, hypermethylation may be an important early-detection method for oral and lung cancers. In addition, DNA methylation may be implicated in a number of other diseases such as Alzheimer's,²⁰ atherosclerosis,²¹ chronic inflammatory diseases,²² diabetes,²³ lupus²⁴ and osteoarthritis.²⁵

1.2.2 Histone Modification

The second mechanism involved in altering the transcription of the genetic code is modulation of nucleosome-mediated accessibility of the DNA to transcription factors and RNA polymerase II. To understand how the DNA associates with the histone proteins within the nucleosome, additional detail is required around the structural aspects of the nucleosome. As previously mentioned, the nucleosome consists of

the DNA wrapped around a bundle of histone proteins and, more specifically, an octet, two each of proteins H2A, H2B, H3 and H4.

An X-ray crystal structure of the nucleosome is shown in Figure 1.5, showing the DNA double helix wrapped around the eight helical histone proteins. An important observation from this crystal structure is the presence of randomly coiled amino acid “tails” protruding from the nucleosome.

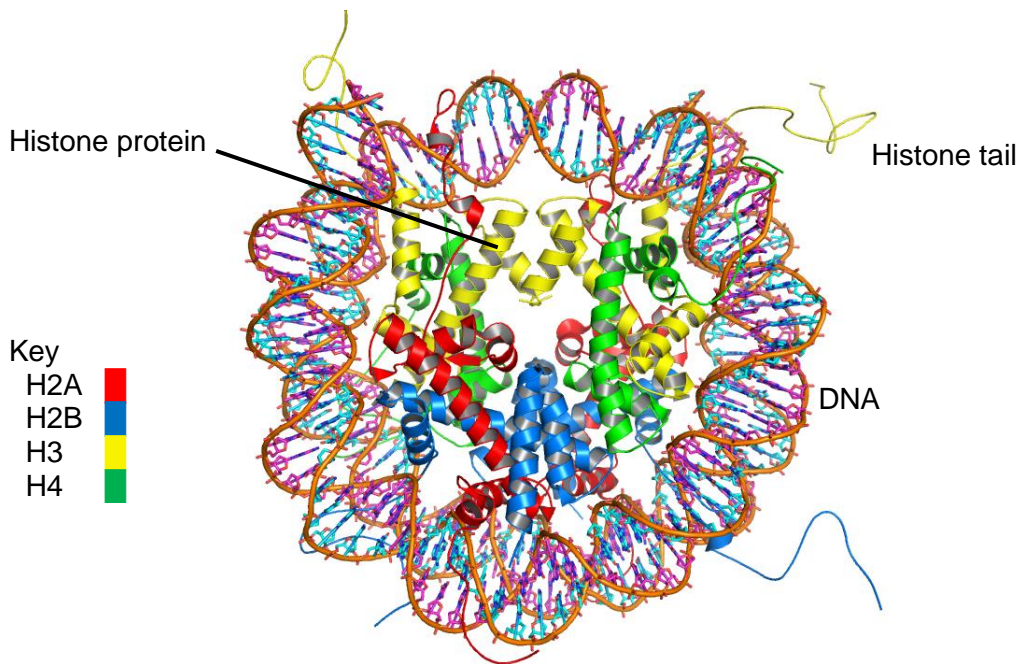


Figure 1.5: X-ray crystal structure of DNA wrapped around the octamer of histone proteins (Protein Data Bank: pdb 1KX5)²⁶

To further highlight the importance of the histone tails, the nucleosome can be shown diagrammatically in Figure 1.6. Viewing the histone proteins as spheres, the DNA encloses the proteins apart from the histone tails. These histone tails are susceptible to post-translational modifications (PTM), which are chemical changes to the constituent amino acids after protein biosynthesis.

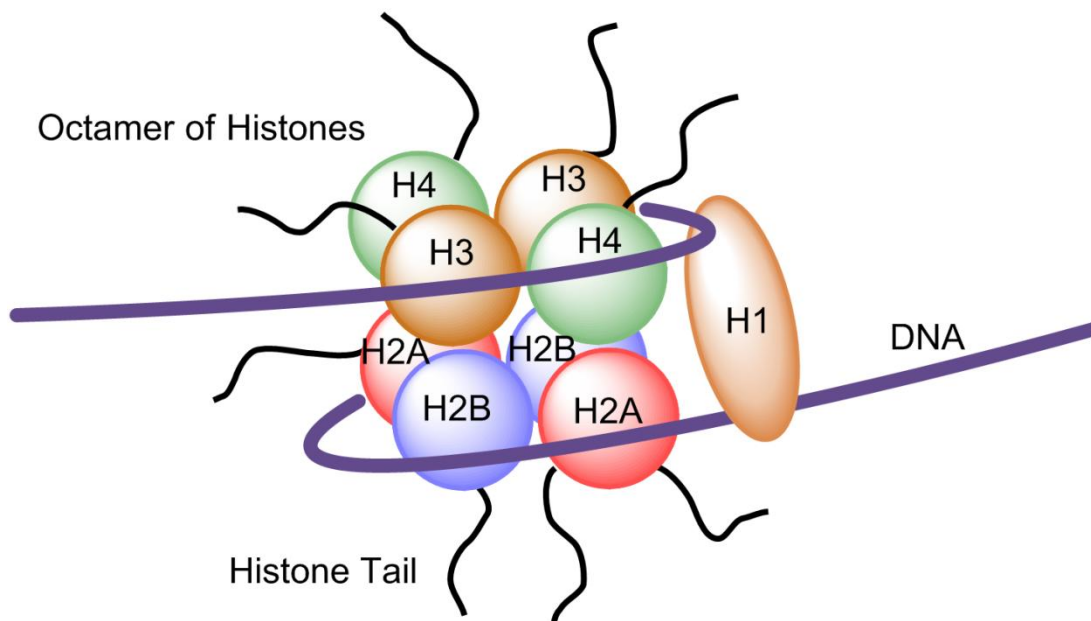


Figure 1.6: DNA wrapped around histone proteins forming a nucleosome

PTM of histone tail amino acids was first observed by Phillips in 1961 when acetate was found after acid hydrolysis of histone proteins, suggesting acetyl groups were present on histone amino acids.²⁷ Further investigations, at the Rockefeller Institute, using ¹⁴C labelled acetate and methionine showed incorporation of acetyl and methyl groups, respectively, onto the histones.²⁸ In 1964, Allfrey *et al.* correctly postulated that these groups modified the ability of the associated DNA to be transcribed into RNA.²⁸ In addition to methylation and acetylation, histone tail PTMs also include phosphorylation,²⁹ ubiquitination³⁰ and sumoylation,³¹ amongst others (Figure 1.7).^{32,33} The importance of these histone modifications has resulted in the Brno nomenclature having been developed.³⁴ For example, acetylation of lysine 9 of histone 3 can be written as H3K9ac.

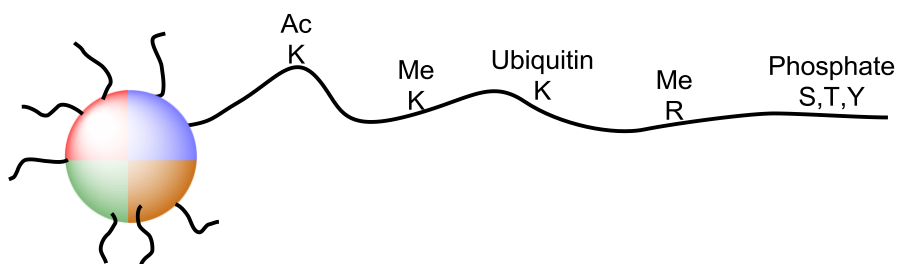


Figure 1.7: Schematic of histone tail modifications

Compared to the DNA methylation discussed previously, histone tail PTMs are more dynamic.³⁵ This is due to the large variety of enzymes tasked with the addition and

removal of the various histone marks. However, due to the expansive nature of PTM regulation, the area of focus, in the context of this thesis, will be the acetylation of lysine residues.

Lysine, at physiological pH is protonated at the ϵ -amine, while DNA contains a negatively charged phosphate backbone. This results in a charge interaction between the DNA and the histone causing the DNA to be tightly bound in a structure termed heterochromatin (Figure 1.8). However, introduction of an acetyl group neutralises the positive charge and removes the charge interaction, leading to a more loosely packaged structure called euchromatin (Figure 1.8).

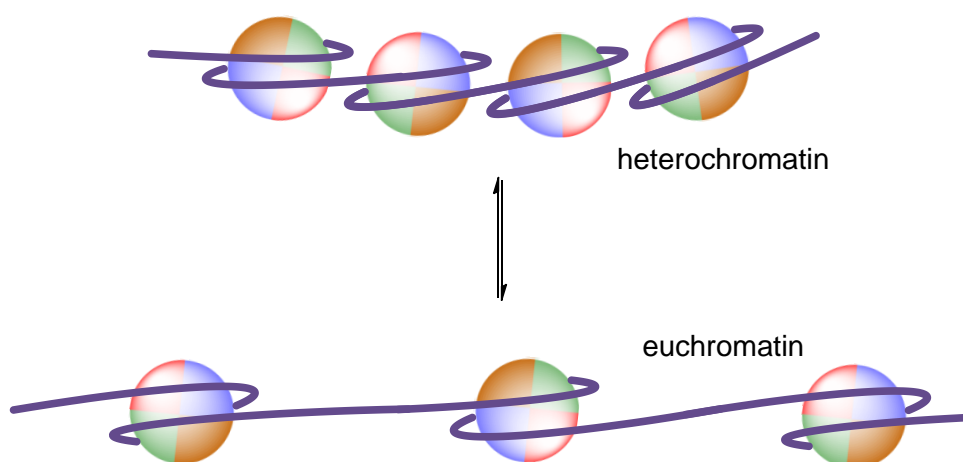


Figure 1.8: Comparison of heterochromatin (closed) and euchromatin (open)

Due to the looser packing, the more open structure of euchromatin is more accessible for transcription factors and RNA polymerase II. Therefore, the DNA is more readily transcribed.³⁶ Conversely, the less accessible heterochromatin prevents transcription.

However, given the number and variety of PTMs that can have different effects on transcription the euchromatin/heterochromatin model is now considered an oversimplification.³⁷ Additionally, the flexibility within these modifications enables different combinations of histone marks to be added creating a “histone code” to affect transcription.³⁸

To illustrate the influence of the histone code, the metamorphosis of a monarch caterpillar to the monarch butterfly will be exemplified. As the caterpillar and butterfly are the same organism, at different stages of its life cycle, the DNA sequence is identical (Figure 1.9). The complete change in appearance must be due to

epigenetics, that is, how the genes are expressed. Using a lepidopteran model, Mukherjee *et al.* were able to show that affecting the acetylation state of the histone proteins, and subsequent gene expression, could promote or delay the onset of pupation within the moth species *Galleria mellonella*.³⁹ As such, the balance of histone acetylation is important to survival with acetylation levels also having been found to affect wound healing and immunity.³⁹

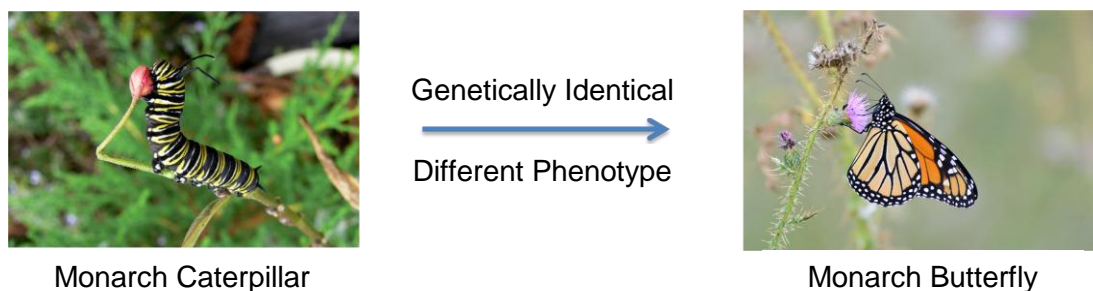


Figure 1.9: Phenotypic changes after metamorphosis of a caterpillar to a butterfly⁴⁰

Consequently, dysregulation of the epigenetic code could lead to aberration in gene expression, affecting development, growth and disease. As observed within the insect model, modulators of epigenetic mechanisms can affect disease at the transcriptional level without altering the DNA sequence. Modulating the epigenetic code could, therefore, be a powerful and dynamic method of treating disease. To understand the effects of altering the acetylation state of histone protein tails, the regulation of this epigenetic marker must be considered.

1.2.3 Acetylated Lysine

In terms of research and drug discovery, modulation of the acetyl lysine mark has been the most successful to date. To understand why, we must look at how this marker is maintained: added, removed and read (Figure 1.10).

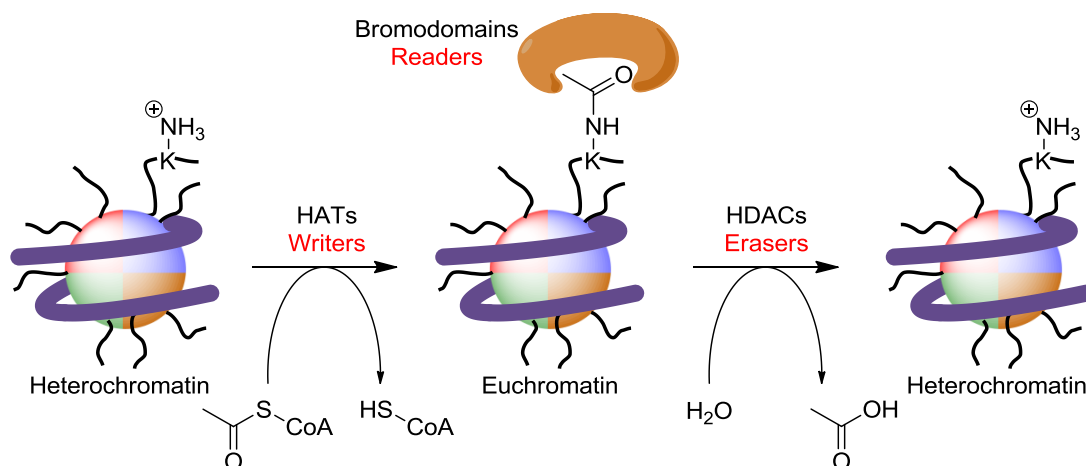


Figure 1.10: Writing, reading and erasing lysine acetyl marks

Firstly, histone acetyltransferase (HAT) enzymes write the code by adding the acetyl marks to the lysine residues. As HATs are a family of enzymes, a number of efforts have been made to inhibit their function. In this regard, the first known HAT inhibitor Lys-CoA (**1.4**) was described by Lau in 2000, an unnatural analogue of the acyl donor acetyl-CoA, which demonstrated sub-micromolar inhibition of the p300 HAT (Figure 1.11).⁴¹ To this date, however, targeting the HAT enzymes has not produced a marketed drug or clinical compound,⁴² due to lack of potency, metabolic instability and the multiple effects of HAT inhibitors *in vivo*.^{42,43} Despite these challenges, work is ongoing in the field to discover a clinical use for inhibitors of the HAT enzymes.

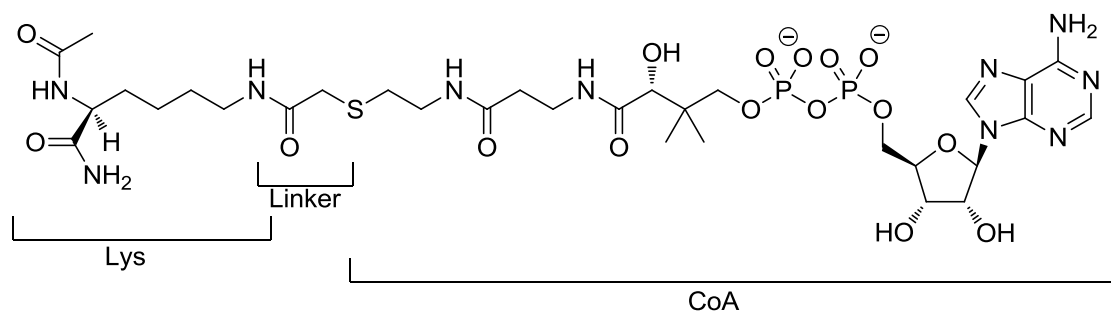
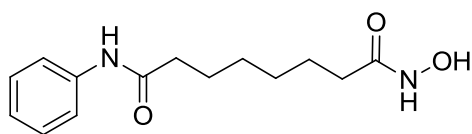
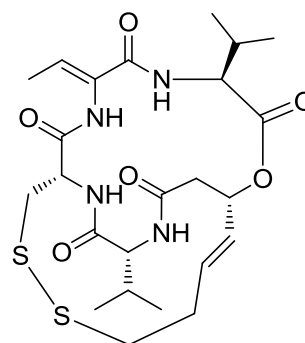


Figure 1.11: First HAT inhibitor, Lys-CoA (1.4)

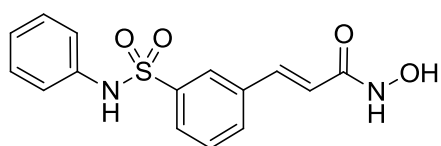
Conversely, histone deacetylase (HDAC) enzymes remove the acetyl mark unmasking the primary amine. The inhibition of the HDAC mechanism has been the most successful clinical strategy pursued to date. Four HDAC inhibitors have been FDA approved: vorinostat, romidepsin, belinostat and panobinostat (Figure 1.12).⁴⁴



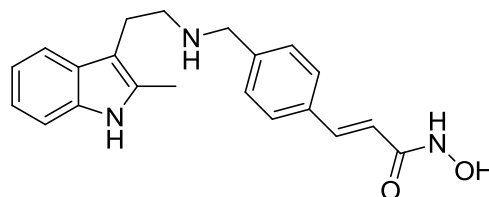
Vorinostat (1.5)



Romidepsin (1.6)



Belinostat (1.7)



Panobinostat (1.8)

Figure 1.12: Four FDA approved HDAC inhibitors

All four drugs inhibit the enzyme by binding to a zinc ion within the active site of the HDAC. This competitive inhibition can be exemplified using vorinostat. The hydroxamate of vorinostat is able to form a bidentate interaction with the zinc ion (Figure 1.13). Similar to the native substrate, acetylated lysine, the long carbon chain extends out of the active site. Finally, the aryl amide forms the capping group, making interactions with the lipophilic surface of the protein.

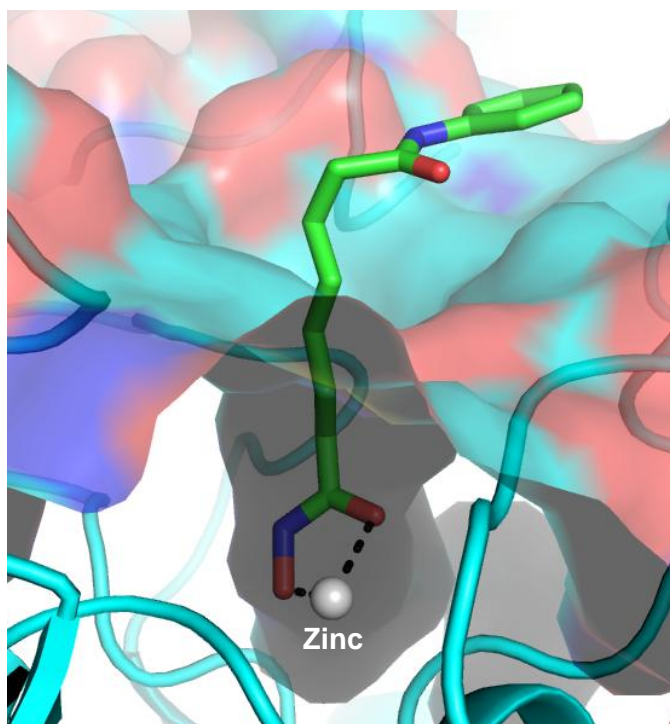
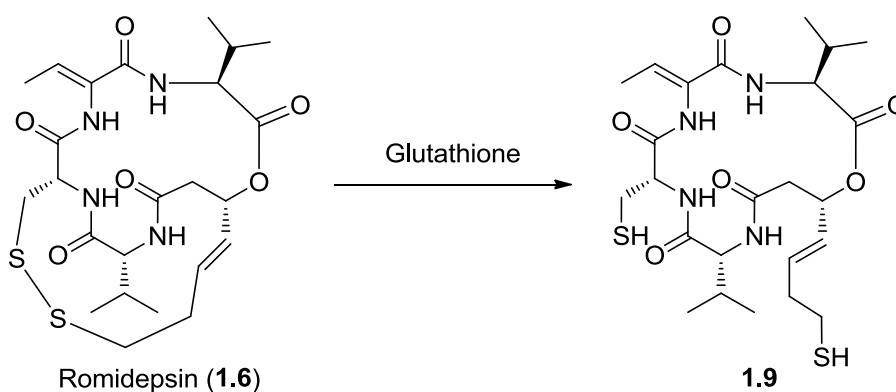


Figure 1.13: X-ray crystal structure of vorinostat (**1.5**) bound to the active site of HDAC2 (Protein Data Bank: pdb 4LXZ)⁴⁵

In 2006, vorinostat (**1.5**) became the first FDA-approved HDAC inhibitor, and is used for the treatment of cutaneous T-cell lymphoma (CTCL), a group of rare cancers, caused by proliferating T cells localised in the skin.⁴⁶ HDAC inhibition using vorinostat prevents the deacetylation of histone tails and leads to hyperacetylation, resulting in modulation of cell cycle proteins, as well as inflammatory proteins. The effect is to inhibit cancer cell proliferation and induce apoptosis.⁴⁷

For the same indication, CTCL, the FDA approved the structurally differentiated HDAC inhibitor romidepsin (**1.6**) in 2009.⁴⁸ A cyclic peptide, romidepsin is the only approved HDAC inhibitor lacking the hydroxamic acid group, to date. Originally discovered as a natural product from the bacteria *Chromobacterium violaceum*,⁴⁹ romidepsin was found to be a pro-drug activated by reduction of the disulfide bond (Scheme 1.3).⁵⁰ The resulting thiol binds to the HDAC's zinc atom, inhibiting the enzyme activity.



Scheme 1.3: Glutathione-mediated reduction of romidepsin to form the active species 1.9

Accelerated approval was granted for belinostat (**1.7**) in 2014 for the treatment of peripheral T-cell lymphoma (PTCL),^{51,52} a fast-growing group of cancers distinct from CTCL.⁵³ While romidepsin is one of two drugs previously having gained accelerated approval for the same indication, the unmet medical need permits the FDA to approve three separate drugs under the accelerated scheme.⁵¹

More recently, in February 2015, the FDA approved the use of panobinostat (**1.8**) for multiple myeloma (MM),⁵⁴ a cancer of blood plasma cells. Again, approval was achieved on the accelerated approval programme as a combined therapy with two current MM drugs, bortezomib and dexamethazone.⁵⁴

The accelerated approval for the latter two drugs is based on the promising results within their phase II trials. Phase III trials are on-going while data is also collected from patients on the approved drugs.⁵⁵

From these four compounds, the clinical application of HDAC inhibitors can be seen. However, all four are pan-HDAC inhibitors, having similar potency at more than one of the 4 distinct HDAC enzyme classes. The next wave of HDAC inhibitors, which are selective for a single class, are now progressing into the clinic.⁵⁶ It is partly because of these successes that the area of epigenetic modulation by small molecules holds such promise for intervention in human disease.

1.2.4 Bromodomains

With the excellent progress observed in the field of HDAC inhibition, interfering with the removal of the acetyl lysine mark, the high therapeutic potential for disrupting the reading of the acetyl lysine code is an important foundation for this thesis. Proteins containing bromodomains are involved in the recognition of acetylated lysine residues on histone tails, through a formal protein-protein interaction. Bromodomains are named from the prior discovery of the related *brahma* gene in *Drosophila*.⁵⁷

To date, 61 human bromodomains have been identified within 46 distinct proteins.⁵⁸ Bromodomains consist of a sequence of around 110 amino acids. The homology in this full sequence, not limited to the binding site, is used to group the bromodomains into a phylogenetic tree (Figure 1.14).⁵⁸

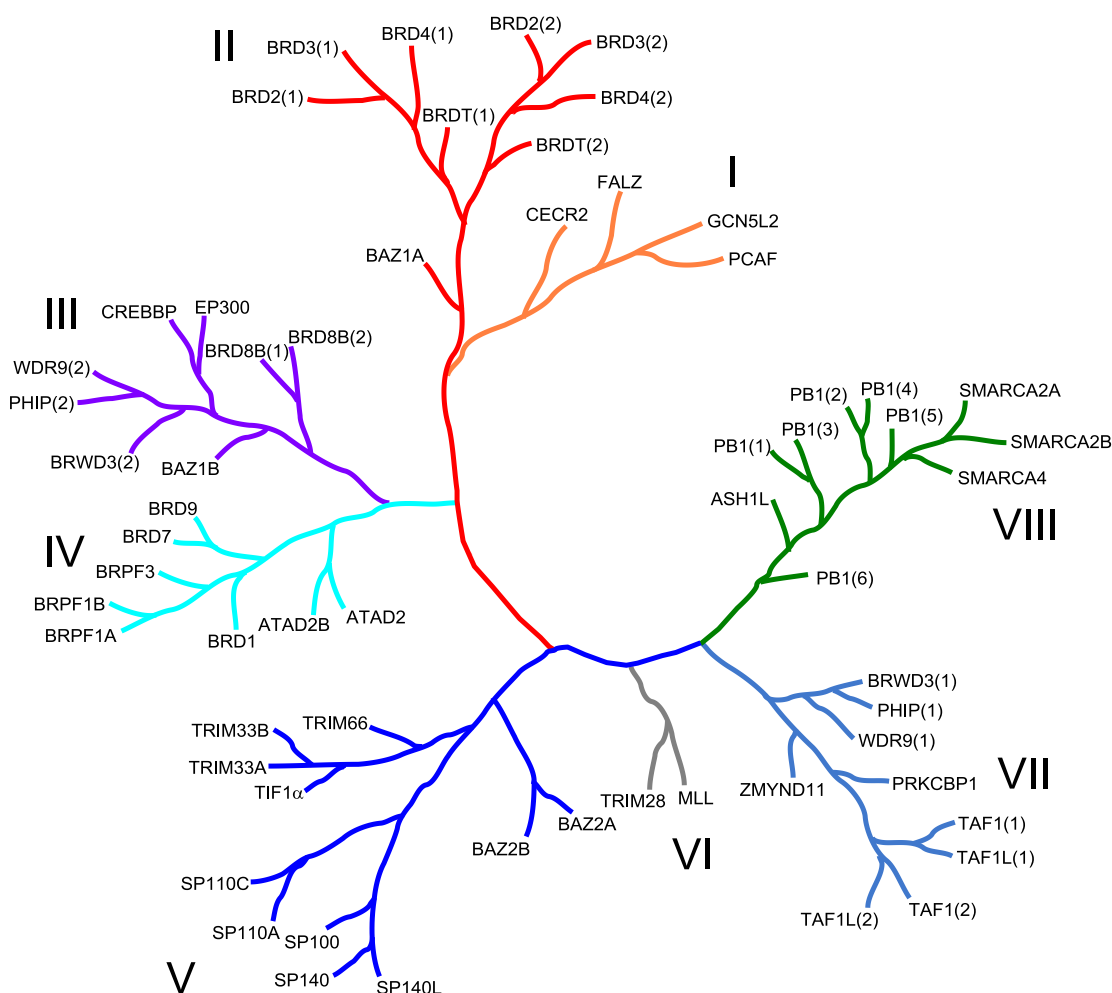


Figure 1.14: Bromodomain Phylogenetic Tree

Within this tree, the bromodomains can be grouped into eight families, of which the focus of this thesis will be group II, the Bromodomain and Extra C-Terminal (BET) family. This family contains four proteins: Brd2, 3, 4 and T. The Brd2, 3 and 4 proteins are ubiquitously expressed, whereas BrdT is localised within the testes and ovaries.^{59,60,61} Each of these BET proteins contains two bromodomains, BD1 and BD2, as well as an extra-terminal (ET) domain (Figure 1.15). While the bromodomain's ability to regulate transcription has been known for over 20 years, the role of the extra-terminal domain has remained elusive.⁵⁷ However, in 2011, scientists at the Harvard Medical School published the potential transcriptional regulatory effects of this ET domain.⁶²

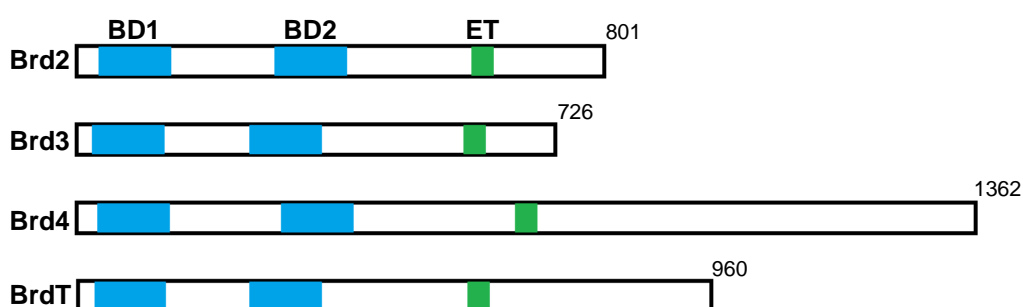


Figure 1.15: The four BET proteins: Brd2, 3, 4 and T

The BD1 bromodomains are found near the *N*-terminus of the protein, whereas the BD2 bromodomains are situated towards the centre of the proteins before the extra-terminal domain, located nearer the *C*-terminus. Homology among the four BD1 bromodomains is very similar, likewise within the BD2 bromodomains. Although very similar, larger differences exist between BD1 and BD2.

To understand how these bromodomains bind acetylated lysine, the structure of Brd4 BD1 will be exemplified. Brd4 BD1 is a typical bromodomain, consisting of a left-handed bundle of four α -helices: α A, α B, α C and α Z. The helices are linked by two loops, the ZA and BC loops, which help to define the binding pocket (Figure 1.16).

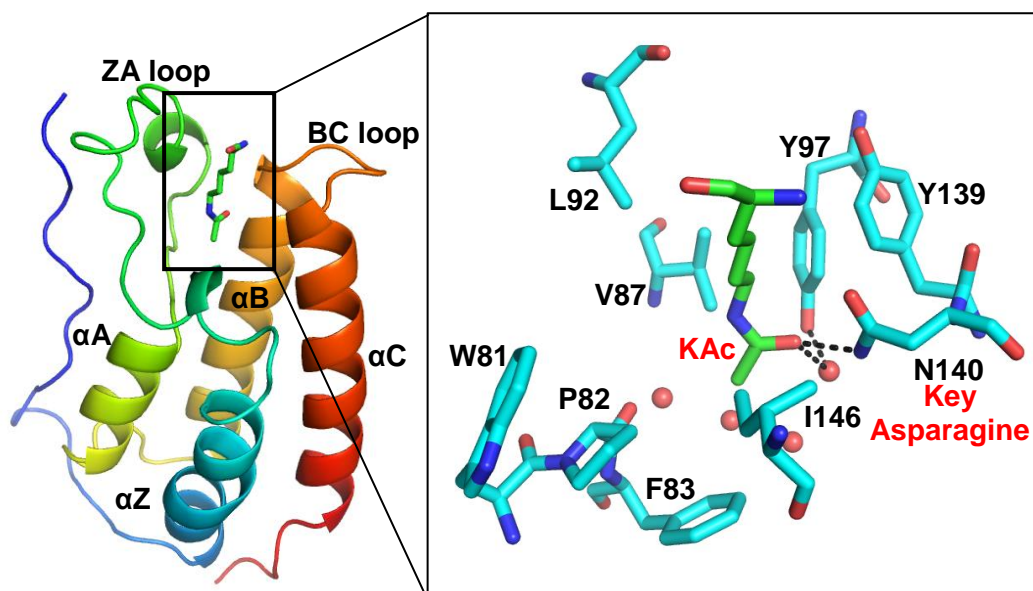


Figure 1.16: X-ray crystal structure of acetylated lysine within Brd4 BD1

Focusing on the acetyl-lysine binding pocket, hydrogen bonding forms the key interactions when binding to an acetylated lysine residue. Firstly, the acetyl carbonyl oxygen forms a direct hydrogen bond to asparagine 140 (N140). This residue is conserved across most bromodomains. In addition to this, a through-water interaction is formed to tyrosine 97 (Y97), which is conserved amongst all but three of the known human bromodomains.⁶³

These simple molecular interactions between the acetyl group and the bromodomain, allow epigenetic information contained within these chemical moieties to be manifested as differences in gene transcription. A well-studied example are the bromodomains within Brd4 of the previously mentioned BET family. Firstly, one of the bromodomains within the Brd4 protein reads the acetyl marker present on the histone tail. The binding of Brd4 to the acetylated histone tail promotes the recruitment of the larger protein complex, positive transcription elongation factor b (P-TEFb), depicted in Figure 1.17. P-TEFb consists of a dimer of cyclin-dependent kinase 9 (Cdk9), in addition to one of three isoforms of cyclin regulatory cofactor: T1, T2 or K.⁶⁴ The kinase, Cdk9, associated with Brd4 is brought into proximity with the C-terminal domain (CTD) of RNA polymerase II, the protein involved in transcribing DNA into mRNA. Phosphorylation of serine 2 of the CTD by Cdk9 activates RNA polymerase II, promoting gene transcription.⁶⁵ It has also been demonstrated that Brd2 and Brd3 are involved in promoting transcription, although the mechanism is not yet understood.⁶⁶

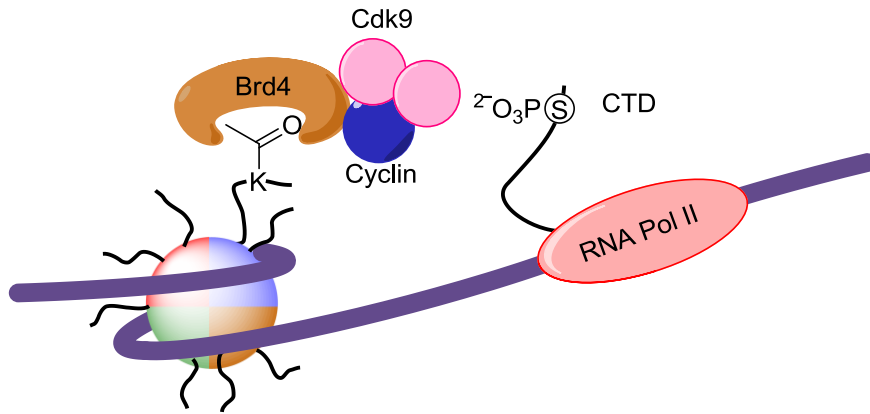


Figure 1.17: P-TEFb Brd4 mechanism⁶⁵

If the initial binding event between the acetylated histone tail and the bromodomain is disrupted, the P-TEFb complex cannot be recruited (Figure 1.18). This would prevent the phosphorylation of RNA polymerase II, hence halting transcription. As the BET family of proteins, such as Brd4, are associated with the transcription of a range of disease relevant genes,⁶⁴ the rationale for attempting to drug them is strong.⁶⁷ Also, considering the well defined acetyl-lysine binding pocket within each bromodomain, this interaction has recently been shown to be amenable to inhibition by small molecules.⁵⁸

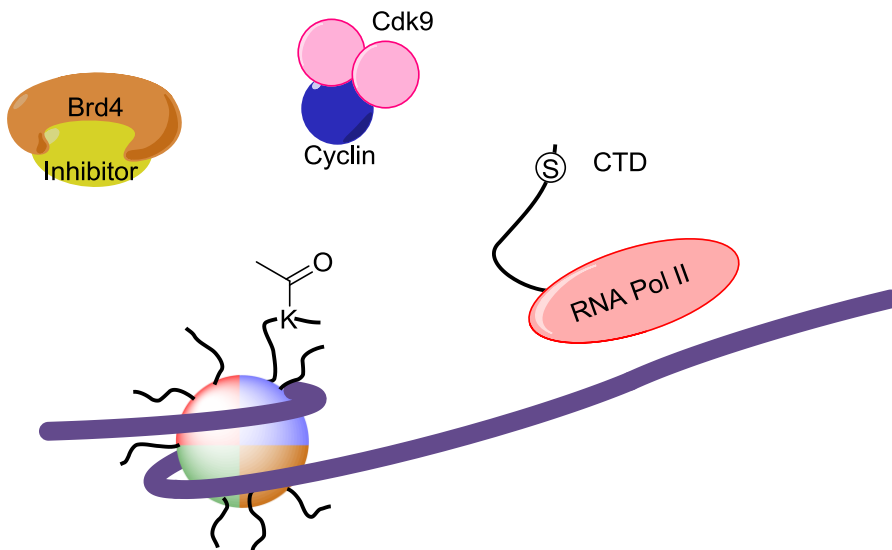


Figure 1.18: Disruption of the bromodomain-acetyl-lysine binding prevents transcription

1.3 Early BET Bromodomain Inhibitors

Disrupting the code-reading BET family of bromodomains with a small molecule inhibitor was first disclosed in the patent literature by Mitsubishi-Tanabe Pharma. Their first patent⁶⁸ detailed structures containing a diazapine core, which were not initially known to be BET bromodomain inhibitors, however, subsequent patents described these molecules as such.⁶⁹ Scientists at the Structural Genomics Consortium (SGC) in Oxford, in collaboration with the Harvard Medical School, used the general structure to begin their own optimisation. From these studies, (+)-JQ-1 (**1.10**) (Figure 1.19) was discovered as a potent and selective inhibitor of the BET family of bromodomains.⁷⁰

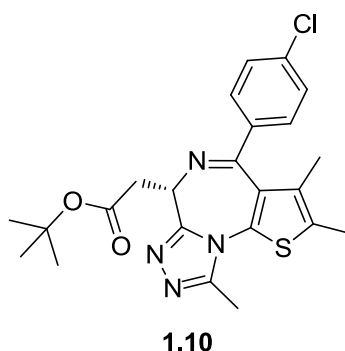


Figure 1.19: (+)-JQ-1

Initial studies with this molecule utilised a nuclear protein in testis (NUT) midline carcinoma (NMC) cell line. This was due to the known intrinsic importance of two of the BET proteins, Brd3 and Brd4, within the mechanism of NMC. Mainly affecting children, NMC is a rare and lethal cancer with an average survival time of just 6.7 months following diagnosis.⁷¹ Unexpectedly, this cancer does not affect a particular cell type, with the disease differing from patient to patient. NMC is caused by the translocation of the *NUT* gene to *Brd4*, or less commonly, *Brd3*.⁷² Expression of this faulty gene results in the formation of a fusion protein, consisting of both of these, normally separate, proteins (Figure 1.20). Association of this fusion, cancer inducing, oncoprotein to chromatin maintains cells within an undifferentiated and proliferative state.⁷³

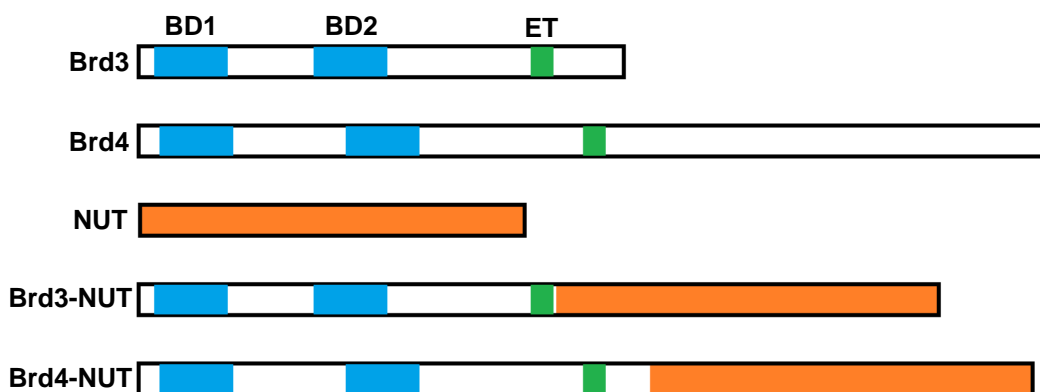


Figure 1.20: Formation of Brd3-NUT and Brd4-NUT fusion proteins

Previous studies using NMC cancer cells have shown the use of short interfering RNA (siRNA), to block the fusion protein synthesis, causes cell cycle arrest, preventing cell division and cancer growth.⁷³ In a similar fashion, returning to (+)-JQ-1, *in vitro* and *in vivo* studies were carried out using NMC cell lines.⁷⁰ *In vitro*, (+)-JQ-1 was able to stimulate observable differentiation, away from the cancerous phenotype, in under 24 hours. Further, Filippakopoulos *et al.* were able to undertake a mouse xenograft experiment using patient-derived NMC cancer tissue, observing tumour shrinkage in mice treated with (+)-JQ-1, while using vehicle (delivery solvent) alone showed tumour growth. It is thought that (+)-JQ-1 is able to bind to the bromodomain of the fusion protein. This prevents the oncoprotein from binding to chromatin returning the cells to a normal state.⁷⁰

Interestingly, these studies were published within the same edition of *Nature* as a structurally related inhibitor I-BET762 (1.11) (Figure 1.21), which was discovered by scientists at GSK, in parallel to (+)-JQ-1.⁷⁴

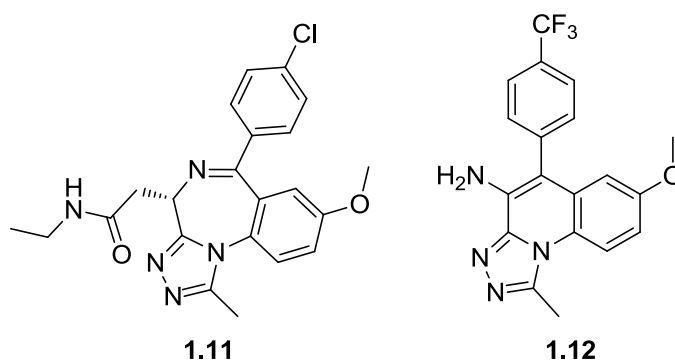


Figure 1.21: I-BET762 (1.11) and the previously discovered inhibitor, 1.12

Prior to the discovery of I-BET762, 5-aryltriazoloquinoline **1.12** (Figure 1.21) was identified through a phenotypic screen geared towards measuring the upregulation of Apolipoprotein A1 (ApoA1).⁷⁵ Importantly, ApoA1 is known to increase the amount of high-density lipoprotein (HDL) *in vivo*. Atherosclerosis is caused by low levels of HDL and high levels of low-density lipoprotein (LDL). As a result, the upregulation of ApoA1 and subsequent increased HDL levels, can aid the reduction of LDL. Overall, increasing ApoA1 levels is thought to be a potential treatment for atherosclerosis. Unfortunately, compound **1.12** showed poor bioavailability so could not be further progressed.⁷⁶

During the subsequent discovery of I-BET762, using the ApoA1 phenotypic assay, the molecular target for these compounds' effects continued to be unknown within GSK and the literature at the time. Therefore, experiments were carried out to elucidate the mechanism of their action. A chemoproteomics study was conducted using compound **1.13**, a tethered analogue of I-BET762 (Figure 1.22). Hepatocyte cell lysate, containing all the cellular proteins, was added to compound **1.13** and the resulting unbound proteins were washed away. The remaining bound proteins were characterised and found to be bromodomain containing proteins Brd2, Brd3 and Brd4, from the BET family. Thus, the upregulation of ApoA1 was thought to be caused by BET bromodomain inhibition. Upon further profiling, I-BET762 was deemed unsuitable as a drug for cardiovascular disease. However, given the rationale for using BET inhibitors in NMC, I-BET762 may offer some clinical benefit to those suffering from this latter disease.⁷⁷

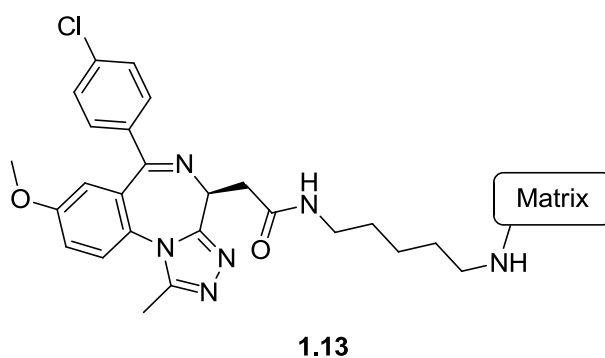


Figure 1.22: Matrix supported analogue **1.13** used in chemoproteomics study

In addition, the advantage to having access to a known potent and selective BET inhibitor, such as I-BET762 (1.11), was that the ability of these compounds to combat inflammation could be evaluated preclinically. Using isolated macrophages, I-BET762 was shown to downregulate the production of many of the signalling proteins, such as cytokines and interleukins, produced by the immune system in response to foreign molecules derived from bacteria upon infection.⁷⁴ Further, an exciting result was seen in an animal sepsis model where mice were administered with a terminal dose of lipopolysaccharide (LPS), part of the bacterial cell wall. The experiments showed that I-BET762 could be administered *in vivo* to give not only a preventative but also a therapeutic effect, after the mice showed extreme symptoms from cytokine storm, through over activation of the immune system (Figure 1.23).⁷⁴ Within two days of LPS administration, in the absence of I-BET762, the mice died as expected. Remarkably, mice treated with the BET inhibitor pre- or post-administration of LPS show 100% survival out to four days. This further demonstrated the therapeutic potential of BET inhibition in life threatening immune disease modification.

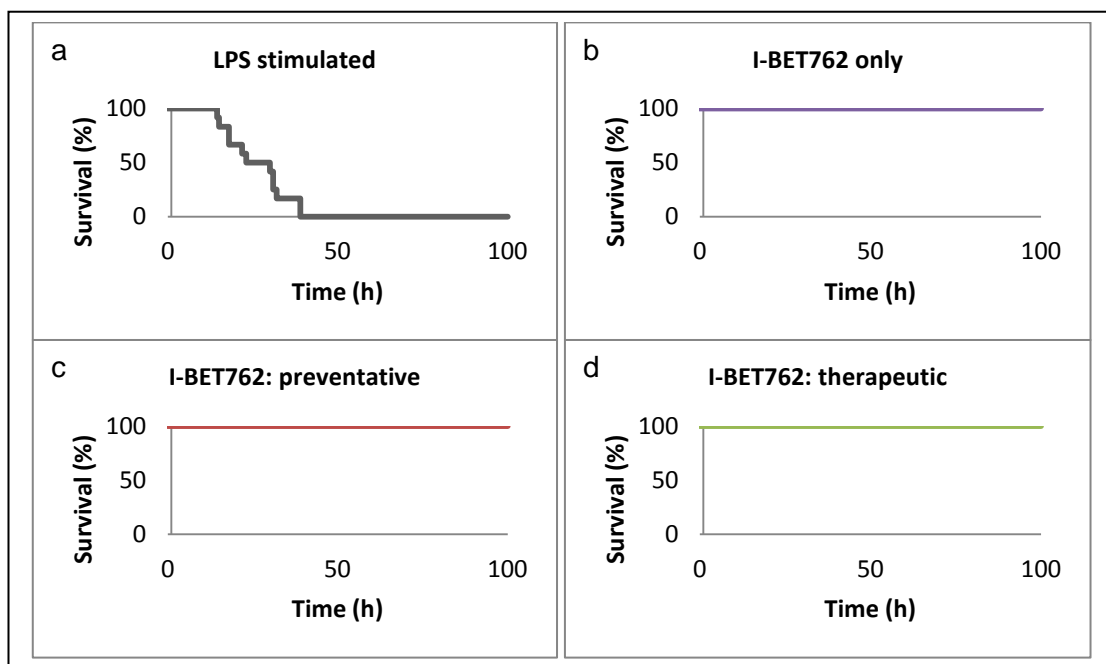
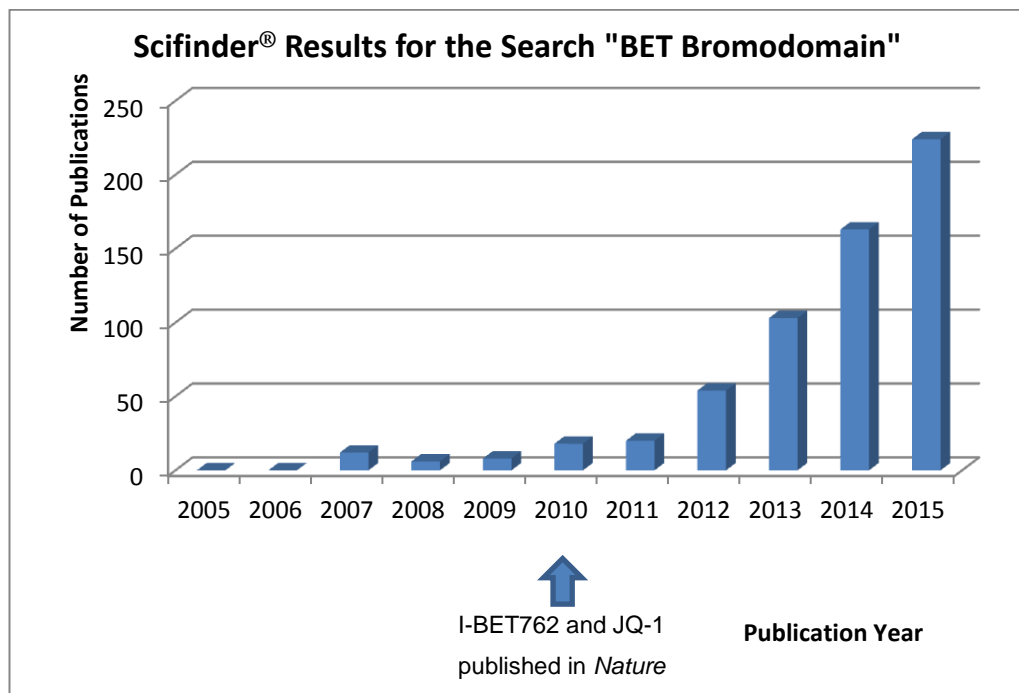


Figure 1.23: Survival rates after induced disease by LPS and treatment with I-BET762.⁷⁴ LPS-treated C57BL/6 mice (5 mg per kg, IP, n=12 per group) that were injected IV (a) solvent control, (b) without LPS administered with 30 mg per kg of I-BET762, 30 mg per kg of I-BET762 (c) 1 h before or (d) 1.5 h after LPS administration.

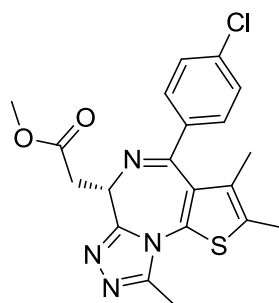
Since these seminal papers on the inhibitors I-BET762 and (+)-JQ-1, published in the same 2010 edition of *Nature*, research interest within the field of bromodomains has grown exponentially (Graph 1.2).



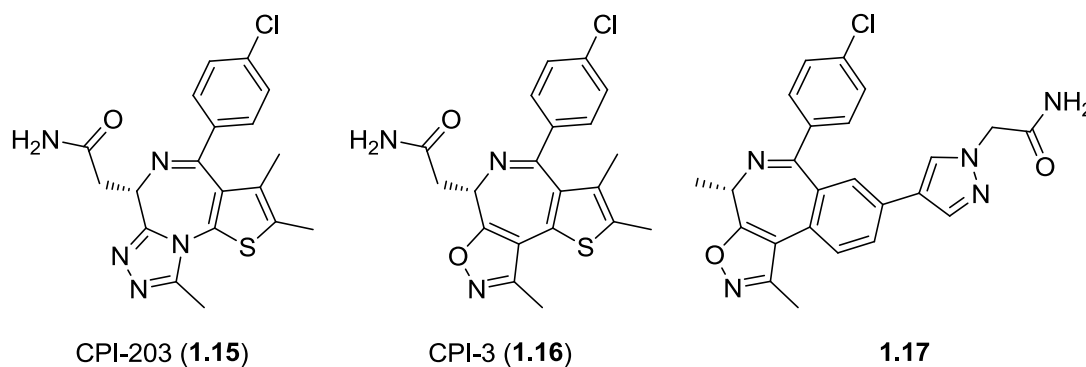
Graph 1.2: Scifinder® results for the search "BET bromodomain" each year since 2005

1.3.1 Azepine- and Diazepine-centred BET Inhibitors

In addition to these first two successful inhibitors, (+)-JQ-1 and I-BET762, other research groups have had success discovering molecules centred around a diazapine or azepine core. MS417 (**1.14**), the methyl ester derivative of (+)-JQ1, was developed by scientists at the Mount Sinai School of Medicine (Figure 1.24). Their inhibitor demonstrated 30 nM potency at Brd4 BD1, with excellent 1000-fold selectivity against CREBBP, a bromodomain out with but containing a closely related binding site to the BET family. *In vitro* studies in kidney cells showed the ability of MS417 to inhibit the production of pro-inflammatory cytokines.⁷⁸

MS417 (**1.14**)**Figure 1.24: MS417**

Researchers at Constellation Pharmaceuticals have published a number of iterations around the diazepine- and azepine-centred BET inhibitors (Figure 1.25). Although the development of CPI-203 (**1.15**) has not been disclosed, combining this inhibitor with marketed drugs, was shown to have enhanced anti-tumour effects.⁷⁹⁻⁸¹

**Figure 1.25: Developmental iterations by Constellation Pharmaceuticals**

The structurally orthogonal isoxazole acetyl-lysine mimetic was discovered from a fragment hit, by the same group and was developed into CPI-3 (**1.16**), a 26 nM inhibitor of Brd4 BD1.⁸² This compound has good pharmacokinetics and a half life of 1.4 hours in rat, but only 31% oral bioavailability.⁸² However, Hewitt *et al.* wanted to improve the PK profile and, recently, they published further optimisations. From CPI-3 they developed compound **1.17**, with reduced *in vitro* clearance which translated into a longer half life of 3 hours and an excellent oral bioavailability of 92% in rat.⁸³

1.3.2 Isoxazole-containing BET Inhibitors

The intense research in this field has produced additional functional groups that mimic the acetylated lysine motif. A key example, with much use within the literature, is the isoxazole. The Conway group have developed OXFBD02 (**1.18**) and OXFBD03 (**1.19**), shown in Figure 1.26.^{84,85} These two compounds are structurally

very similar, differing in an acetyl group. While these compounds have sub-micromolar activity, the selectivity profile for the lead compound, **1.19**, over the non-BET bromodomains is poor, with a bias of 7-fold over the structurally-related bromodomain CREBBP.

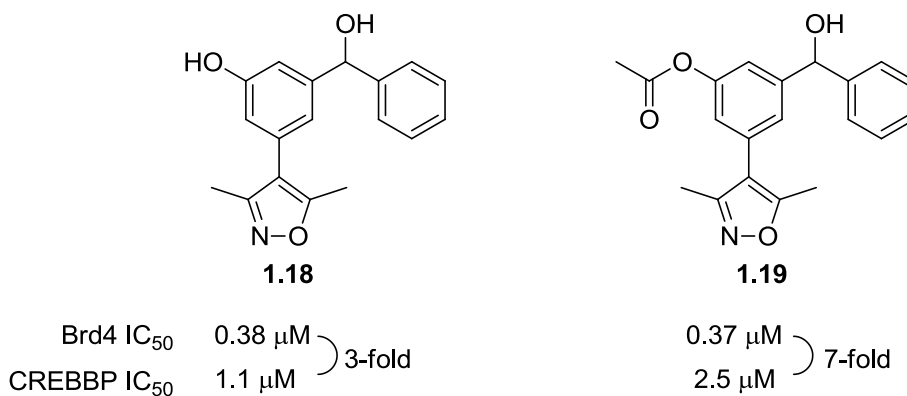


Figure 1.26: Lead compounds developed by the Conway group

GSK have also had success with the dimethylisoxazole group. One strategy they employed was a fragment-based approach. Their efforts also yielded a sub-micromolar BET bromodomain inhibitor **1.20**.⁸⁶ However, the lead compound showed poor solubility and subsequent attempts to improve solubility proved detrimental to the biochemical potency (**1.21**, Figure 1.27).⁸⁶

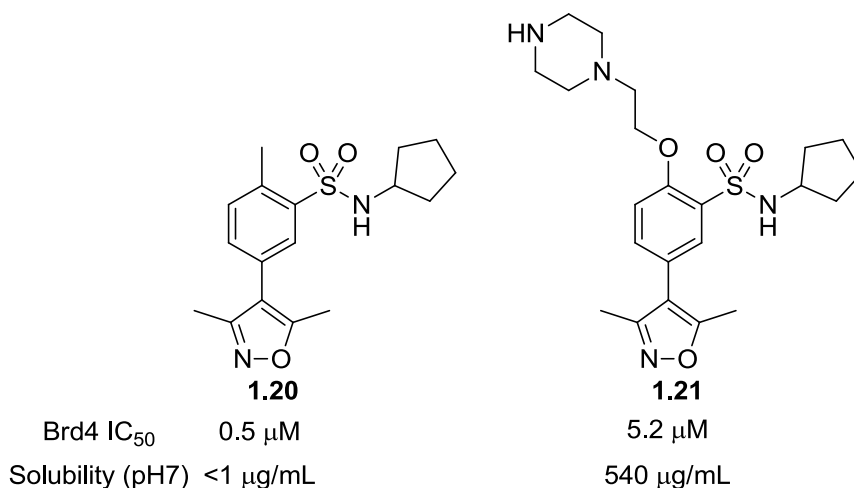


Figure 1.27: GSK's isoxazole-based fragment-derived inhibitors

Continuing with the dimethylisoxazole motif, GSK also discovered I-BET151 (**1.22**) (Figure 1.28). With a biochemical pIC₅₀ of 6.1 at Brd4, this compound demonstrated good levels of IL-6 cytokine inhibition within a human peripheral blood mononuclear cell (PBMC) cellular assay, with a pIC₅₀ of 6.7.⁸⁷ Additionally, thermal shift assays

demonstrated no interactions with and, therefore, very high selectivity over, the non-BET bromodomains.

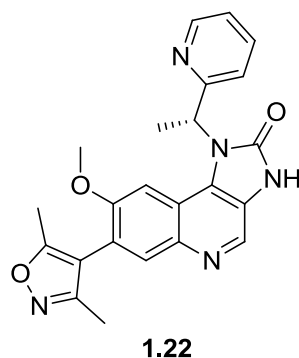


Figure 1.28: Structure of I-BET151

Recently, Ran and co-workers described their structurally differentiated, I-BET151 inspired BET inhibitor.⁸⁸ Finding the dimethylisoxazole moiety to be optimal, they focused on the novel [6,5,6] tricyclic γ -carboline core. Substitution in the 4-position gave them improved potency, leading to compound **1.23** as their lead molecule (Figure 1.29).⁸⁸ While 2-fold less potent at Brd4 BD1, their inhibitor is 6-fold more potent at Brd4 BD2 than I-BET151 within their assays. It was also demonstrated that the biochemical potency translated into excellent cellular activity within two cancer cell lines.

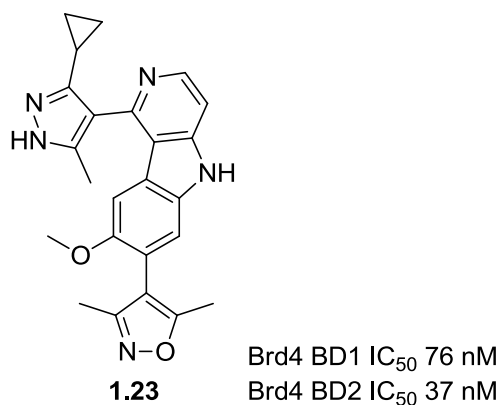


Figure 1.29: Lead compound 1.23 developed by Ran and co-workers

1.3.3 Novel Acetyl-lysine Mimetics

In addition to the triazole and isoxazole acetyl-lysine mimetics, the large amount of interest in this field has seen the publication of additional, novel functional groups to mimic acetylated lysine.

For the purpose of discovering novel acetyl-lysine mimetics, the Conway group tested compound **1.24** (Figure 1.30), which was found to deliver a promising level of potency (3 μM at Brd2 BD1).⁸⁵ Computational modelling studies suggested two possible binding modes, through the dimethylisoxazole or using the quinazolinone functionality. Subsequently, X-ray crystallography, in Brd4 BD1, confirmed the dimethylisoxazole as the AcK mimetic.⁸⁵ However, Chung and co-workers at GSK showed, through crystallography, that the quinazolinone **1.25** can act as a weak binding, ligand efficient bromodomain inhibitor.⁸⁹ Scientists at Pfizer further investigated this fragment to introduce an arylsulfonamide. The most optimal compound, PFI-1 (**1.26**), was selected as a chemical probe (Figure 1.30). This compound balanced potency (pIC_{50} 6.7) with lipophilicity (cLogP 1.3). Although the wider bromodomain selectivity profile was not elucidated, the selectivity over CREBBP, a bromodomain fragment **1.25** showed activity at, was optimised to over 100-fold.⁹⁰ Moving into *in vivo* experiments with this probe the bioavailability was lower than expected, hypothesised to be due to low gut solubility.⁹⁰

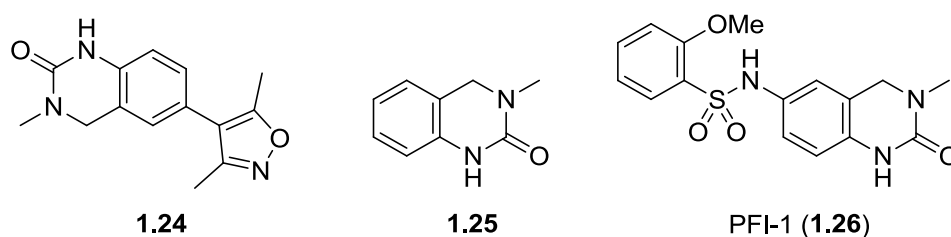


Figure 1.30: Quinazolinone BET inhibitors

Scientists from the Chinese Academy of Science also used a fragment-based approach to discover 2-thiazolidinones as an efficient mimic of acetylated lysine. From the initial fragment hit, **1.27**, Zhao *et al.* optimised the substitution around the pendant phenyl ring towards their lead molecule **1.28** (Figure 1.31).⁹¹ While they were able to synthesise sub-micromolar inhibitors, their cellular activity was low, which they hypothesised was due to poor permeability.

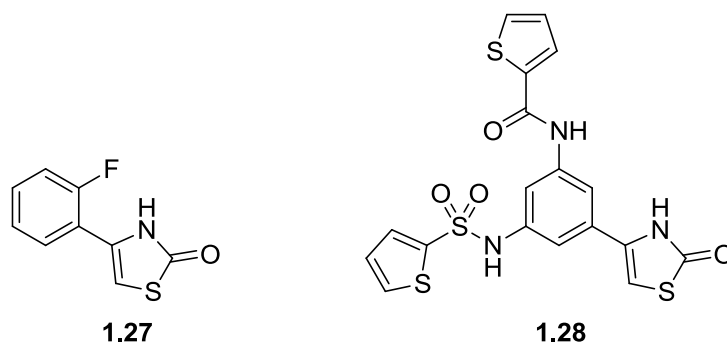


Figure 1.31: 2-Thiazolidinones based inhibitors

The laboratory of Zhou and co-workers disclosed the diazobenzene series of bromodomain inhibitors. This template was derived from the CREBBP bromodomain inhibitor **1.29**.⁹² The *ortho*-methyl phenol mimics the acetylated lysine. This was found to be optimal for binding to both CREBBP and the BET bromodomains. During their optimisation, it was found that substitution in the *para*-position of the second aryl ring gave additional BET potency. This led to MS436 (**1.30**), a <85 nM inhibitor of Brd4 BD1, limited by the affinity of the ligand used in their assay (Figure 1.32).⁹³ Considering the starting point was a CREBBP ligand, MS436 showed selectivity of at least 25-fold for Brd4 BD1 over CREBBP. While this compound was shown to have cellular activity, the developability profile, such as the DMPK properties, of this compound was not demonstrated.

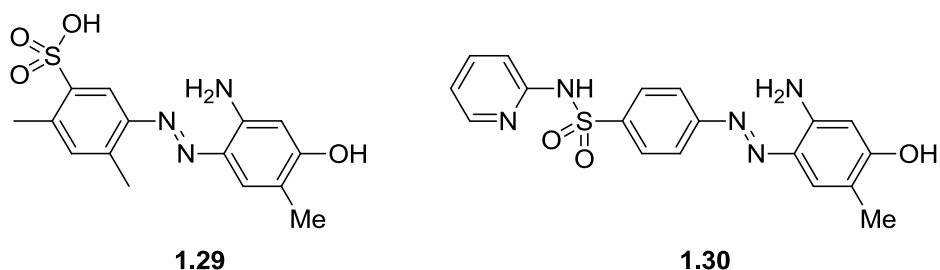


Figure 1.32: Diazobenzene BET inhibitors

In addition to the dimethylisoxazole-containing inhibitor I-BET151, scientists at GSK discovered the tetrahydroquinoline template (**1.31**) from a high-throughput screening (HTS) campaign.⁹⁴ The hit was developed into the lead molecule I-BET726 (**1.32**) (Figure 1.33) with a binding affinity of 100 nM or less at the BET bromodomains. Additionally, I-BET726 was also at least 100-fold selective over the non-BET bromodomains. Furthermore, the pharmacokinetic profile of I-BET726 was suitable for the progression into a murine septic shock model, similar to that carried out with I-BET762, previously. In this study only a quarter of the untreated mice survived to

five days, whereas, when treated therapeutically with I-BET726, only 44% of the mice died, demonstrating increased survival of the treated group.⁹⁴

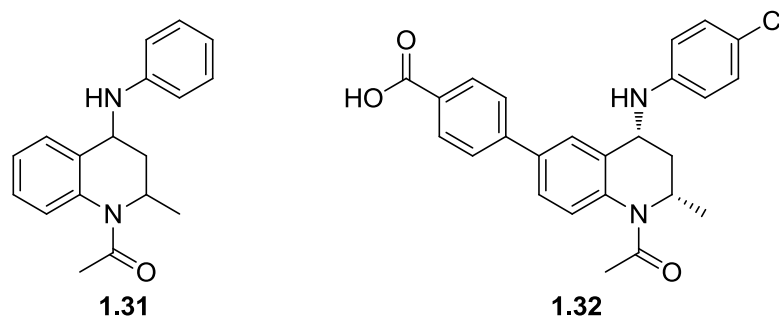
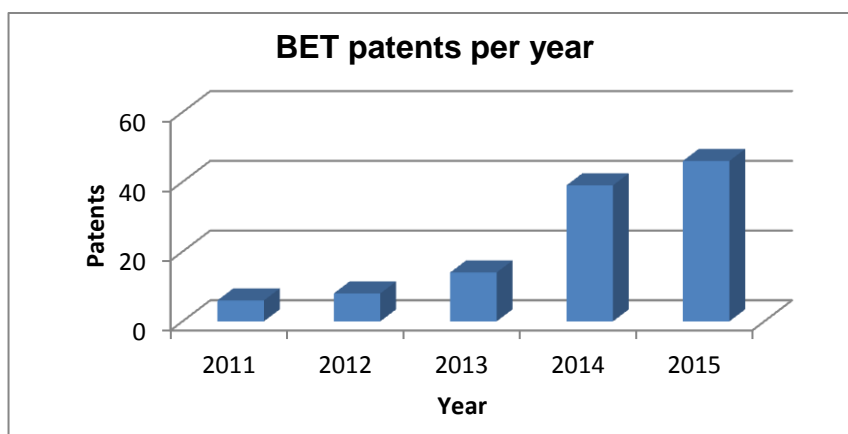


Figure 1.33: Development of I-BET726 (1.32)

In addition to the increasing wealth of knowledge from the article literature, the patent literature in this area has grown exponentially within the past five years (Graph 1.3). Through this, an array of chemotypes to mimic acetyl-lysine have been disclosed.⁹⁵



Graph 1.3: BET patents per year

1.4 BET Inhibitors in the Clinic

Despite I-BET762's unsuitability for atherosclerosis, it was investigated for an alternative indication, NMC. I-BET762 has progressed into phase I/II clinical trials recruiting volunteers for NMC and additional cancer types.⁷⁷

An important contribution to the field of BET inhibitors has been achieved by scientists at Resverlogix. RVX-208 (**1.34**) (Figure 1.34), a derivative of the plant polyphenol resveratrol (3,4',5-trihydroxy-*trans*-stilbene) (**1.33**),⁹⁶ proved to be an efficient upregulator of ApoA1 in phenotypic assays.⁹⁷ RVX-208 is in clinical trials for the treatment of atherosclerosis. Having successfully completed a phase II trial in

2010,⁹⁸ phase IIb trials have been initiated for the same indication.⁹⁹ Additionally, RVX-208 has recently completed phase II trials for type 2 diabetes, although results are yet to be published.¹⁰⁰ Having developed this promising drug through phenotypic screening, its mechanism of action initially remained elusive. However, on the publication of GSK's *Nature* paper in 2010,⁷⁴ describing the upregulation of ApoA1 by I-BET762, it was hypothesised that RVX-208 was having its effect through the same mechanism. Subsequently, both Resverlogix⁹⁶ and the SGC⁹⁷ investigated the potential that RVX-208 also functions through the inhibition of the BET family of bromodomains. Indeed, RVX-208 was shown to be a potent and selective inhibitor of the BET family of bromodomains. Both investigations additionally describe the preferred binding for the BD2 domain of Brd2, Brd3 and Brd4.^{96,97}

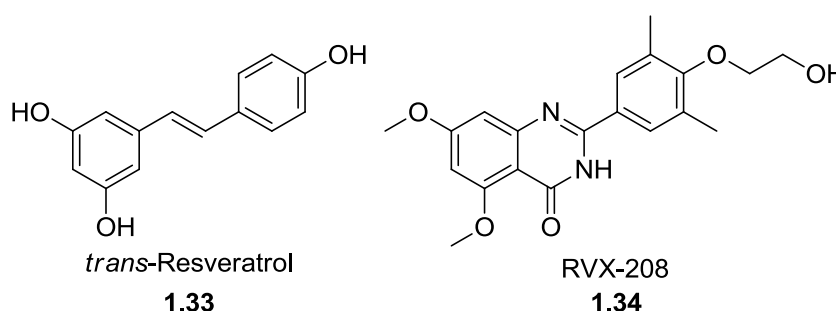


Figure 1.34: Structure of Resveratrol (1.33) and RVX-208 (1.34)

Resverlogix also completed a side-by-side cellular comparison with (+)-JQ1. As expected, both molecules upregulate Apo-A1 transcription. Similarly, both molecules suppressed the transcription of the *IL-6* (interleukin-6) gene without affecting tumour necrosis factor α (TNF α) mRNA production, further supporting this mechanism of action.⁹⁶ Hence, Resverlogix has since progressed RVX-208 into the clinic for atherosclerosis.¹⁰¹

A number of other pharmaceutical companies have developed BET inhibitors. Four further compounds have progressed into the clinic. OncoEthix disclosed a thienodiazopine-based BET inhibitor OTX015 **1.35**⁹⁵ (Figure 1.35), which is currently in a clinical trial for acute leukaemia and other haematological malignancies.¹⁰² CPI-0610 **1.36**¹⁰³ (Figure 1.35), discovered by Constellation Pharmaceuticals, will be investigated for the treatment of patients with progressive lymphoma.¹⁰⁴ Additionally, scientists at Tensha Therapeutics developed their compound, TEN-010, which is being investigated as a treatment for NMC.¹⁰⁵ Recently, Bayer have progressed into a first time in man study with BAY1238097.¹⁰⁶ Unfortunately, Tensha Therapeutics

and Bayer have not released the exact structure of their clinical compounds preferring not to specify from their patents.⁸⁸

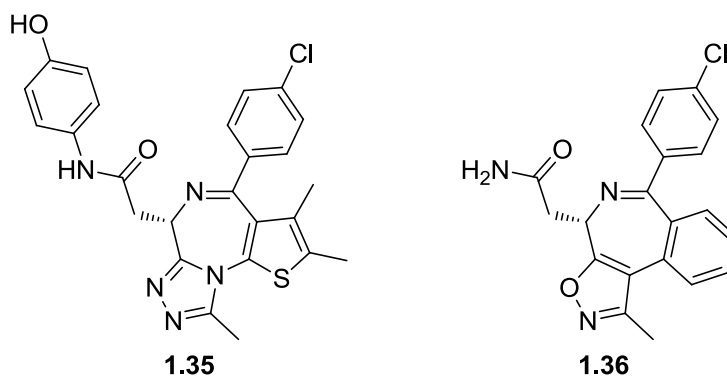


Figure 1.35: Clinical BET inhibitors from OncoEthix and Constellation Pharmaceuticals

In addition, Incyte Corporation and Gilead Sciences recently started recruiting participants for the phase I trials of their compounds INCB054329¹⁰⁷ and GS-5829,¹⁰⁸ respectively. As these eight compounds are progressed through clinical trials, the overall profile of these BET inhibitors, in human, will be elucidated.

1.4.1 Potential Risks of Clinical BET Inhibitors

As no bromodomain inhibitors have reached the market, the clinical biology associated with these compounds is not fully understood. There have been numerous papers describing the benefits of inhibiting the BET family of bromodomains: inflammation, cancer, anti-viral and contraceptive. However, due to this wide variety of mechanisms controlled by the BET family of bromodomains and the ubiquitous expression of Brd2, 3 and 4, the issue of on-target toxicity has to be considered.

Studies in mice have been used to attempt to understand the potential risks of removing the function of the BET bromodomains. Unfortunately, Houzelstein *et al.* showed that mice with two copies of a genetically inactivated *Brd4* gene were unviable, and die at an early embryonic stage.¹⁰⁹ Additionally, heterozygotes with only one functioning copy of the *Brd4* gene demonstrated growth defects affecting the skin, liver, testis, eyes and brain of the young mice.¹⁰⁹ The reduced quantity of Brd4 is thought to cause these growth defects, partially by the slower proliferation of these cells.

In light of these results, Bolden *et al.* used RNA interference (RNAi) in mice to reversibly switch Brd4 expression off.¹¹⁰ *In vitro*, the RNAi gave a similar gene

expression profile as the BET inhibitor, JQ-1. Therefore, this model was progressed into *in vivo* experiments. The most efficient RNAi occurred in the skin and intestine. Firstly, the skin showed structural deformities leading to hair loss. Also, contrary to Bolden's hypothesis, the epidermal cells increased in proliferation. The intestine, on the other hand, remained intact despite loss of intestinal stem cells. While these results are an induced model using RNA interference, it gives an insight into potential toxicities that may be incurred through long-term BET inhibition.

Overall, as with many drug targets, inhibiting the BET bromodomains has potential risks. Considering the ubiquitous expression of these proteins, pharmacology across all tissues may be observed. This may be beneficial or lead to toxicities, such as those observed by inhibiting BET protein expression. Therefore, combining a potent small-molecule BET inhibitor with a more specific cell targeting approach may lead to molecules with an improved safety profile.

1.5 Targeted Drug Delivery

Delivering a drug molecule, intact, to its site of pharmacological action is a challenging aspect of drug discovery and development. Absorption, Distribution, Metabolism and Excretion (ADME) must all be balanced to achieve the desired effect at the biological target. However, the majority of marketed drugs not only reach their intended site of action, but are also delivered to other systemic organs and tissues. Due to the presence of drug at undesired sites, the potential for toxicity is much larger.

A targeted approach to drug delivery was envisaged by Paul Ehrlich in the early 20th century: the "Magic Bullet" approach.¹¹¹ This hypothetical drug entity was envisaged to have two main properties. Firstly, it must be able to selectively recognise and bind to the desired target only. Secondly, the magic bullet should provide a therapeutic effect at the bound target.

1.5.1 Therapeutic Index

Overall, Ehrlich's vision was towards a drug with excellent therapeutic properties without the potential toxic side effects. This would be the ideal profile, however, due to the dosing of a foreign molecule into the body, the drug is likely to have toxic effects at a certain concentration. The therapeutic index (TI) is used to quantify the difference between the desired effects and the toxic effects. This can be visualised

in Equation 1.1 with the TI being the ratio between the concentration of drug that produces adverse effects within half of the population (TD_{50}) to the concentration that gives a efficacy in 50% of the population (ED_{50}).^{112,113} These values can be demonstrated with a desired profile shown in Figure 1.36. Low doses would lead to the desired effect, while much larger doses are needed before adverse effects are observed. As such, the drug discovery strategy requires the TI to be as large as possible.

$$TI = \frac{TD_{50}}{ED_{50}}$$

Equation 1.1: Therapeutic Index

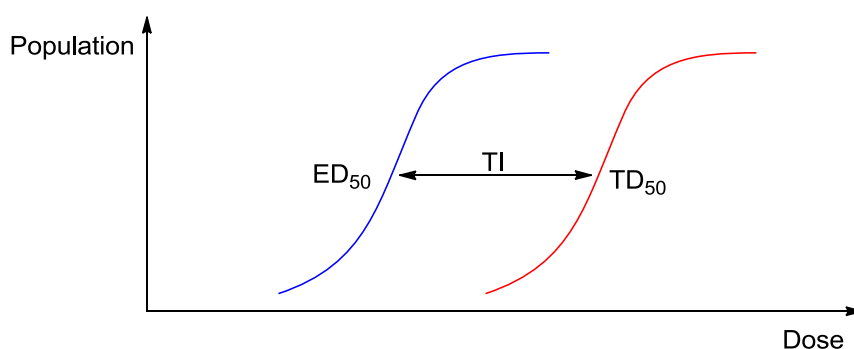


Figure 1.36: Graphical representation of TI

Since Ehrlich's vision, a number of methods have been more recently investigated to realise this hypothetical targeted entity, including: nano-particles,¹¹⁴ liposomes,¹¹⁵ monoclonal antibodies¹¹⁶ and prodrugs.¹¹⁷ This overview will highlight these methods, with a more in-depth discussion of the advantages and disadvantages of using monoclonal antibodies (mAb), their drug conjugates and prodrugs as targeting methods.

1.5.2 Nano-particles and Liposomes

Both nano-particles and liposomes can be used to deliver drug molecules to the site of action. The term nano-particle is broad, relating to a number of species including biologically derived molecules (such as lipids or carbohydrates) or more biologically inert, carbon, silica or metal supports.¹¹⁴ Drug molecules can subsequently be attached to these supports facilitating delivery to the site of action.

Nano-particle supported drug molecules are commonly used to deliver molecules to tumours. This targeting strategy exploits the often abnormal blood vessels that serve cancer cells due to angiogenesis.¹¹⁸ The abnormal vasculature is termed as "leaky",

relating to the larger than normal entities that are able to permeate the vessel walls.¹¹⁹ The larger size of the nano-particle can exploit the different sizes of vessel openings in normal versus cancerous growths. Nano-particles can then release the drug pay-load within the tumour, giving a local high concentration relative to other compartments. Overall, the use of nano-particles is a passive drug targeting method, relying on an enhanced permeability and retention (EPR) effect. An excellent example of this effect in action is the nano-particle DOC-Heparin. Unconjugated heparin, a 5000 Da sulfated carbohydrate has anticoagulant and anti-angiogenesis effects. However, heparin alone was unsuitable for antitumour therapies due to its high systemic anticoagulant effects at the required dose. Conjugating this macromolecule with the steroid sodium deoxycholate (DOC) **1.37** was hypothesised to form the basis of a more targeted approach. DOC-heparin **1.38** (Figure 1.37) demonstrated an improved therapeutic index compared with the parent heparin by reducing the systemic anticoagulant effects.^{120,121} It is claimed these 185 nm DOC-heparin particles are still active via the EPR effect, with the steroidal moiety improving the targeting once through the leaky vessel membrane.

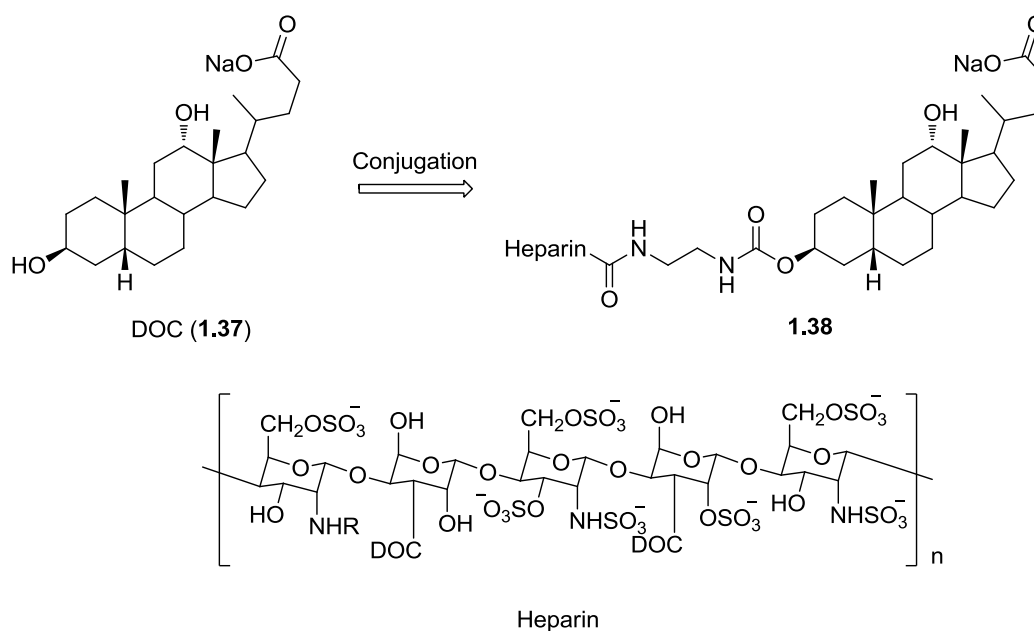


Figure 1.37: DOC (sodium deoxycholate)-Heparin **1.38**

One often used subset of nano-particles are liposomes. Liposomes differ from solid nanoparticles by encompassing the drug molecule within a membrane. A successful example of the use of liposomes is Doxil (**1.40**).¹²² Doxorubicin (**1.39**) is a cytotoxic anticancer drug, which acts by intercalating DNA and binding to DNA-associated

enzymes.¹²³ To reduce systemic cytotoxicity, doxorubicin, the drug payload, is encapsulated within a PEGylated liposome (Figure 1.38), consisting of hydrogenated phosphatidylcholine, cholesterol and distearoyl-phosphatidylethanolamine.¹²⁴ The PEGylation is required in this strategy to protect the liposome from phagocytosis, which would otherwise destroy the delivery vehicle.¹²⁵ Doxil has been observed to have improved properties, showing retention and up to six times more anticancer activity, while reducing toxicity, relative to doxorubicin.^{126,125} Doxil was approved for a number of cancer types between 1995 and 2007.¹¹⁵ A limitation to this technology lies in the fact that liposomes have been observed to be unstable within the gastrointestinal tract due to the action of bile salts as surfactants.¹²⁷ Therefore, unless they are elaborately functionalised, to reduce this risk, they must be administered intravenously. An additional challenge to this delivery method is the loading of the drug, at the desired concentration, within the pre-formed liposome due to the small volumes encapsulated within these small structures.¹²⁸ Currently, the loading method must be tailored to the specific drug molecule, with particular difficulties arising if the drug is extremely hydrophilic or lipophilic. Hydrophilic drugs are less able to cross the liposome membrane once at the site of action. Conversely, hydrophobic drugs associate with the membrane and are less readily retained by the structure.¹²⁹

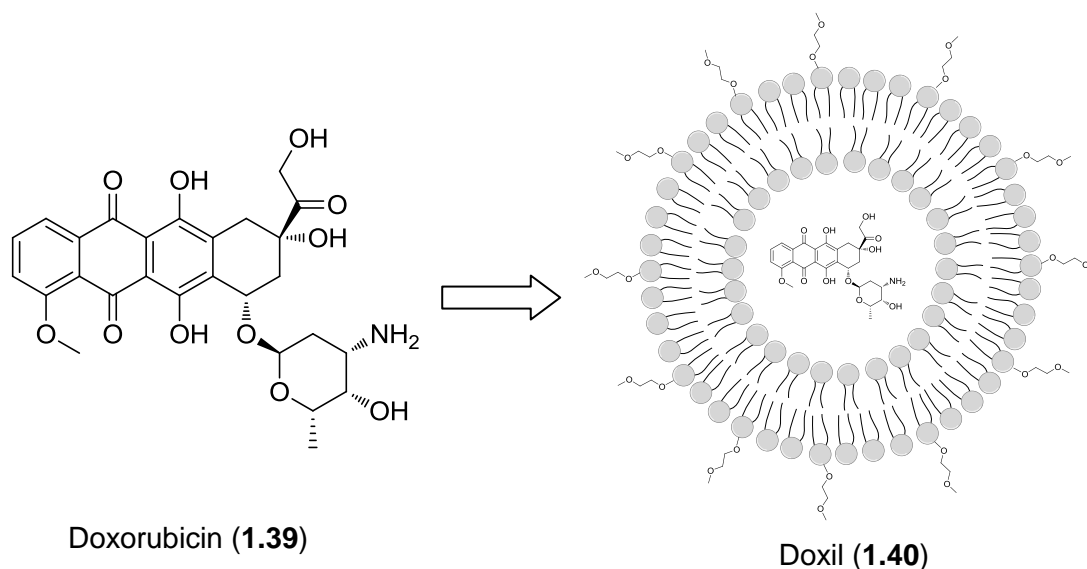


Figure 1.38: Liposome based drug Doxil

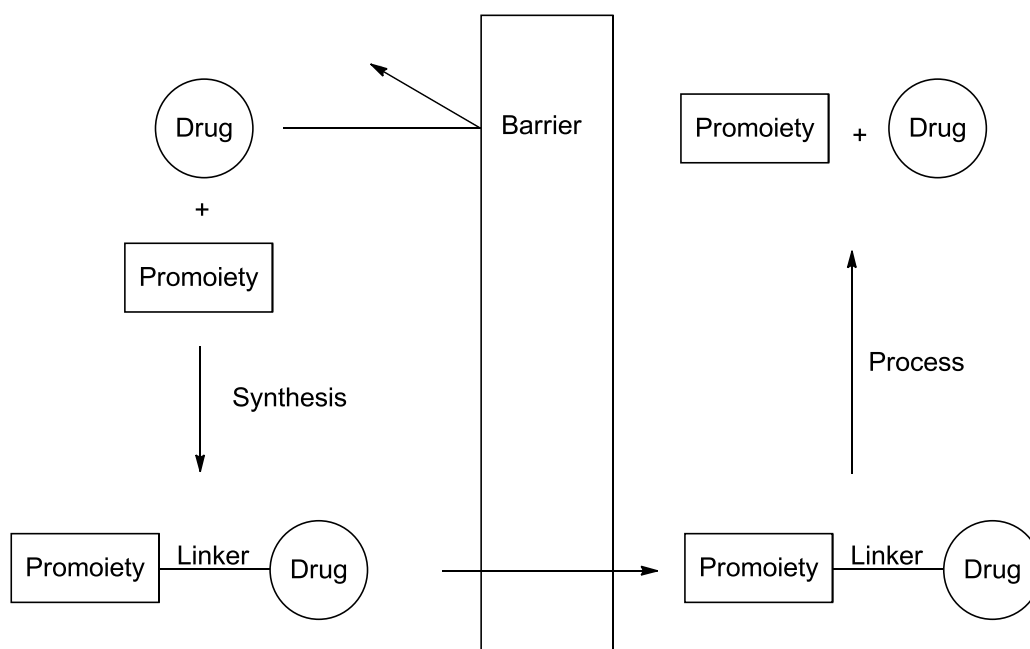
Liposomes have been the most widely used nano-particle delivery system for drug molecules, predominantly using EPR to target cancer.¹³⁰ While this has been a very

useful passive targeting approach, an active form may be more effective at reaching the target.

1.5.3 Comparing Prodrugs and Antibody-Drug Conjugates

Two additional targeting strategies, which are relevant to this current programme of work, are prodrugs and the related antibody drug conjugate (ADC) approach. The term prodrug was introduced by Adrian Albert in 1958 to describe a molecule which has to be converted into the active drug before it has its biological effect.¹³¹

Prodrugs typically consist of the drug molecule linked to a promoiety. An enzymatic or chemical transformation leads to release of the promoiety and the formation of the active drug (Scheme 1.4).¹³² This approach is considered when a barrier, such as bioavailability, solubility or toxicity, is encountered.

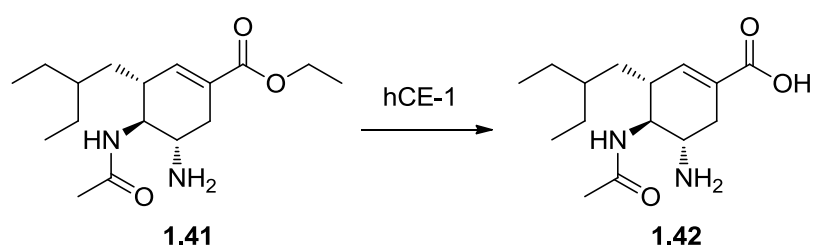


Scheme 1.4: Typical prodrug strategy¹³³

In a somewhat related concept, antibody-drug conjugates are the combination of the highly specific binding of an antibody for a single antigen with a very potent drug molecule. Therefore, both typical small-molecule prodrugs and antibody-drug conjugates can be viewed as having the drug attached to a promoiety, despite the macromolecular size relating to the latter class.

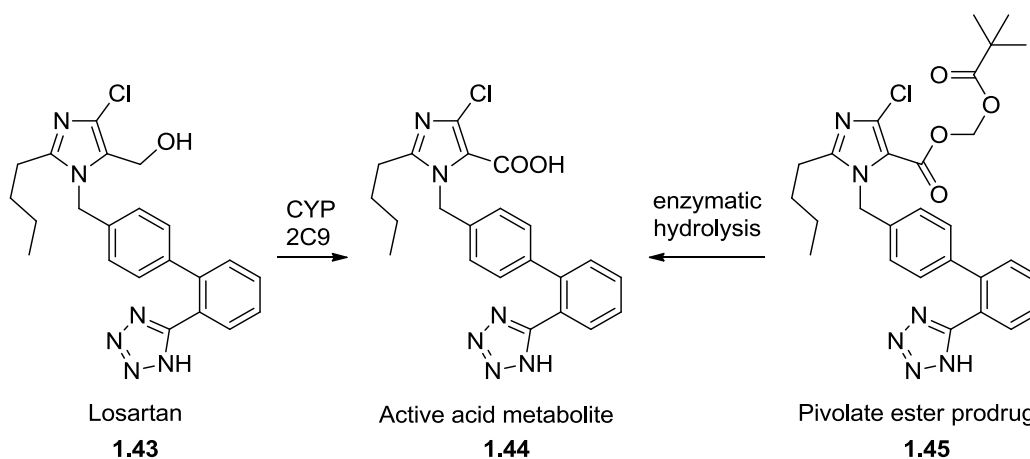
1.5.4 Prodrugs

The most commonly used prodrug strategy is to improve the gut absorption of an orally dosed drug.¹³⁴ To improve the permeability of polar drugs, a masking prodrug strategy may be beneficial, thereby increasing the lipophilicity relative to the parent. Ester prodrugs are chemically easily introduced. In order to facilitate their hydrolysis to the bioactive parent, there are a number of esterases within the blood, liver, gut and other organs and tissues. An excellent example of an ester prodrug strategy is the anti-influenza drug Oseltamivir (**1.41**), hydrolysed in the liver by human carboxylesterase 1 (hCE-1) (Scheme 1.5). Within rat, the bioavailability of the active acid **1.42** was poor at 5%. Pleasingly, the addition of the ester increased bioavailability, in humans, to 80%.¹³⁵



Scheme 1.5: Hydrolysis of Oseltamivir (1.41) by carboxylesterase (hCE-1)

However, some prodrugs do not contain a clear promoiety. Losartan **1.43**, an angiotensin II type 1 receptor agonist, is an example of this (Scheme 1.6).¹³⁶ Losartan contains a primary alcohol which is oxidised to the carboxylic acid **1.44** by the specific cytochrome P450 enzyme, CYP2C9. The more potent acid metabolite is only formed in 14%, but it has a longer duration of action than the parent Losartan. However, because of inter-patient variability, the use of CYP2C9 activation was not well tolerated in all patient populations. Further work identified the more typical ester prodrug **1.45**, which is hydrolysed *in vivo* to produce the desired acid.¹³⁶ Overall, these two different prodrug strategies achieve the same function of masking polarity and, consequently, improving the absorption of the active acid species **1.44**.



Scheme 1.6: Losartan and pivate prodrugs

Conversely, absorption of drug molecules may be enhanced by improving solubility, for example, through the addition of a phosphate ester.¹³⁷ An example of introducing a phosphate group to aid solubility is estramustine phosphate (Estracyt) (**1.47**) (Figure 1.39).¹³⁸ This prodrug had a much improved solubility compared to the non-ionisable parent estramustine (Emcyt) (**1.46**). No studies have been published on the oral bioavailability of the parent.¹³⁹

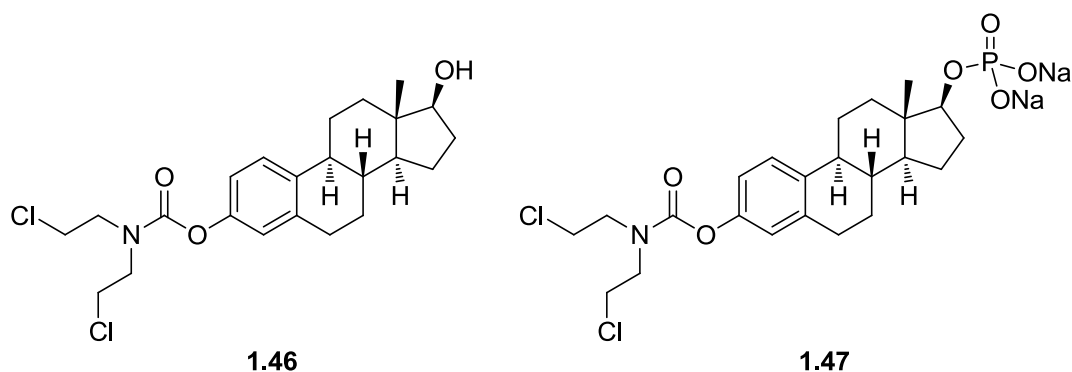


Figure 1.39: Parent drug estramustine (1.46) and phosphate prodrug 1.47

The polarity of the phosphate group aids aqueous solubility. In turn, alkaline phosphatases, located in the gut wall, are able to remove the phosphate group allowing membrane absorption.¹³⁴ However, this solubilising strategy has a number of drawbacks. The calcium counter-ion salts can be very stable, which can reduce uptake. Hence, dairy products, containing calcium, cannot be taken with these prodrugs. Also, the removal of the solubilising group can cause the parent molecule to precipitate at the membrane juncture.¹³⁹ All three of these prodrug examples

demonstrate the importance of adsorption of reaching the site of action and eliciting the desired biological effect.

1.5.5 Antibody Drug Conjugates

1.5.5.1 Monoclonal Antibodies

Antibodies, interchangeably named immunoglobulins (Ig), are a key component of the adaptive immune system. These Y-shaped proteins consist of four disulfide bond-linked proteins (Figure 1.40). The four proteins consist of two identical heavy chains and two identical light chains. Each heavy chain consists of one variable domain (V_H) and three constant domains (C_H). Similarly, each light chain contains one variable domain (V_L) and one constant (C_L). In addition to the two disulfide bonds which hold the heavy and light chains together, two disulfide bonds stabilise the dimerisation of the two heavy chains.¹⁴⁰

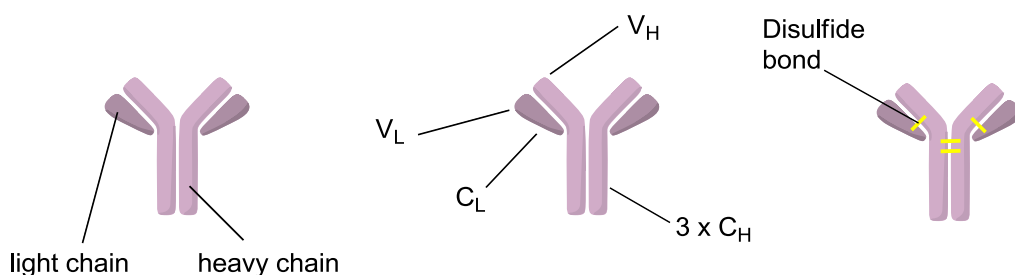


Figure 1.40: Structure of IgG including inter-subunit disulfide bonds

Within the human body, antibodies are produced by B lymphocytes when the cell's surface antibodies detect a foreign antigen.¹⁴¹ The variable region imparts the uniqueness of antibodies produced by different B lymphocytes. On detecting an antigen, the cell replicates and becomes a plasma cell. These mature cells make multiple copies and secrete the specific antibody (Figure 1.41). The antibodies can then bind to the antigens neutralising the threat and marking them for degradation.

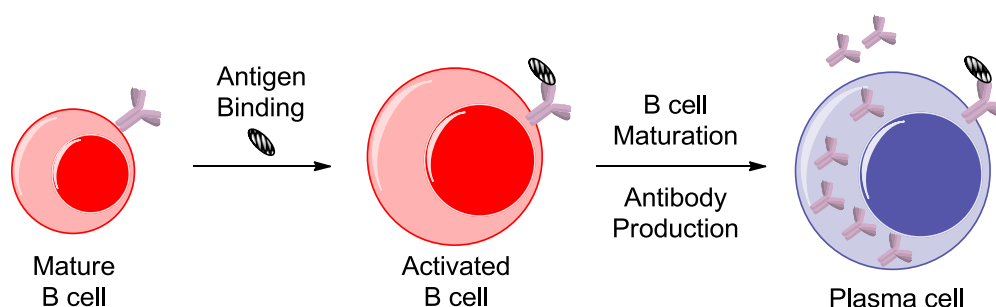


Figure 1.41: B cell activation and maturation

Initial methods used to make antibodies within the laboratory involved purification of a single antigen and immunisation of mice with the antigen.¹⁴² However, this method provided the desired antibodies in poor yield, often including undesired antibodies. A huge step forward was the ability to form monoclonal antibodies (mAb), in other words, a single purified antibody selective for a single antigen. This was achieved by Kohler and Milstein in 1975.¹⁴³ Isolated mouse derived B lymphocytes were immortalised and treated with a specific purified antigen. This method introduced the possibility of producing and ultimately using monoclonal antibodies therapeutically. It is the extremely high selectivity of an antibody for its antigen which makes these species a possible tool for targeted therapy.

The production of antibodies from mouse-derived cells produced murine antibodies. Clinical trials using these murine antibodies, such as the first example using AB 89 to treat a lymphoma patient, showed promising therapeutic effects.¹⁴⁴ However, this trial and others, also using murine antibodies, observed high systemic clearance of the circulating antibody.^{144,142} This was later discovered to be caused by the production of human anti-mouse antibodies (HAMA).¹⁴⁵ The majority of this clearance is by binding of these HAMA to the constant regions of the murine antibody heavy chains. This interaction is common, with 10-40% of patients reacting in this way.¹⁴⁵ This was a large hurdle to the further development of antibody therapy.

The parallel advancement of DNA technology aided the production of human-like antibodies. Due to HAMA binding to the constant regions, the first step was to use this DNA technology to replace the murine antibody protein sequences with sequences naturally found in human antibodies.¹⁴⁶ Despite this, these “chimeric” antibodies still contained a large sequence of murine protein. Further advancements

allowed the formation of “humanised” antibodies, containing human protein sequences for all but the antigen binding sites.¹⁴⁷

The final step was aided by phage display¹⁴⁸ and transgenic mouse technologies,¹⁴⁹ where fully human antibodies were then possible. The half-life of these human antibodies was significantly longer than the mouse antibodies, extending from days to weeks.¹⁴² However, immunogenicity is not eradicated with the use of fully human antibody therapies. A proportion of the patient population may still have an immune response against the therapy, which is not only a problem observed with antibodies, but other recombinant proteins.¹⁵⁰ Overall, monoclonal antibody therapies have been found to be useful for both cancer and rheumatoid arthritis. Humira (Adalimumab) has found much success in the latter field.¹⁵¹ This agent acts by binding TNF α , a pro-inflammatory cytokine, reducing its signalling ability. However, this strategy does not prevent the TNF α being produced. Unfortunately, antibody therapies cannot be taken orally, as these complex proteins are digested in the stomach. Therefore, therapies such as Humira are administered by injection.

Having stated all of the above, combining the specific binding ability of an antibody with the effects of a small molecule inhibitor could give a very selective targeted therapy.

1.5.5.2 Combining Antibodies with Small Molecule Drugs

A number of current cancer therapies are small molecules. Many affect rapidly dividing cells, with examples of such molecular agents being nitrogen mustards **1.48** and cis-platin **1.49** (Figure 1.42). These act by cross-linking DNA, with resulting cytotoxic effects on all rapidly dividing cells. This includes non-cancerous cells as well as those related to the tumour.

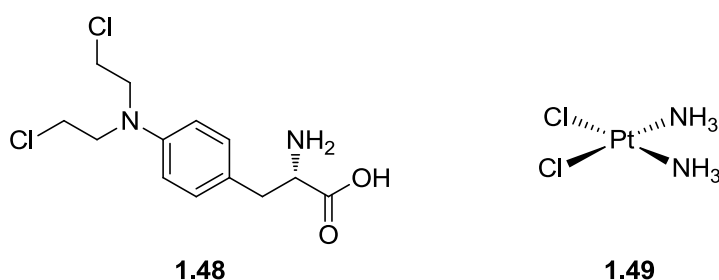


Figure 1.42: Examples of chemotherapeutic agents which target rapidly dividing cells

It was thought that combining cytotoxic small molecules, such as those detailed above, with the highly selective binding of antibodies would give reduced systemic

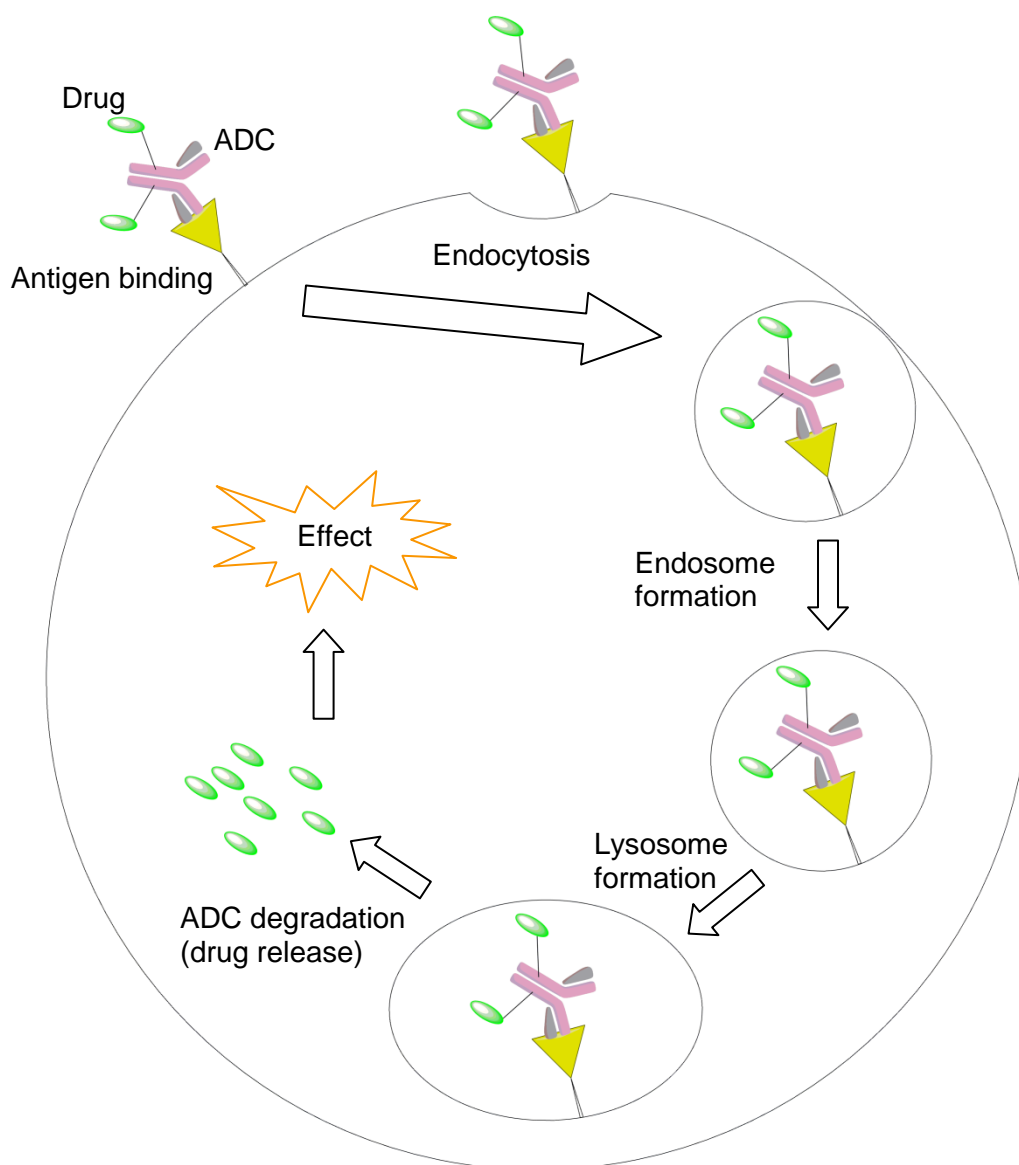


Figure 1.44: Therapeutic mechanism of an ADC

In addition to the linker, the stoichiometry of conjugated drugs is thought to be important in maintaining antibody binding. *In vitro* experiments show improved efficacy when using higher drug loading. Conversely, lower drug loadings lead to similar *in vivo* activity with an improved therapeutic index.¹⁵⁴

There are a number of common methods for drug conjugate attachment. As previously described, antibodies contain four interchain disulfide bonds. Reduction of these four disulfide bonds yields eight sites for alkylation. Alternatively, conjugation can be achieved through acylation of lysine residues, although there can be up to 100 lysines in a single antibody. In both these methods, the number of different conjugation sites can lead to a large variation in the conjugation

stoichiometry. To mitigate this, genetically engineered antibodies can be used, although the location of conjugation remains difficult to control. For example, introduction of additional cysteine residues can be used to form drug conjugates with defined stoichiometry without disrupting interchain disulfide bonds.¹⁵⁵ An alternative strategy involves the replacement of cysteine residues involved in interstrand disulfide bonding to serines. On reducing the remaining antibody disulfide bonds in these modified antibodies, the sites available for conjugation are minimised, leading to improved homogeneity of the resulting ADC.¹⁵⁶ Pleasingly, antibodies lacking the inter-chain disulfide bonding ability were shown to maintain their binding affinity.

An alternative strategy is the introduction of non-natural amino acids, such as *para*-acetylphenylalanine (*p*-AcPhe).¹⁵⁷ This introduces a handle to add the drug conjugate as an oxime or hydrazone. Overall, conjugation is still one of the most challenging aspects within this area of drug design and delivery, with the effects of the number and positioning of conjugated drugs not yet fully understood.

In relation to the successes of this overall approach, the first US Food and Drug Administration (FDA) approval of an antibody-drug conjugate was Mylotarg[®] (Gemtuzumab ozogamicin) (**1.50**) in 2000 for the treatment of acute myeloid leukaemia (Figure 1.45).¹⁵⁸ This approval was granted as part of the FDA accelerated approval programme, prior to the compound progressing through Phase III trials.¹⁵⁹ Gemtuzumab, a humanised antibody targeting CD33, was linked to two or three molecules of calicheamicin γ 1. CD33, importantly in this treatment for myeloid leukaemia, is a transmembrane receptor expressed specifically on myeloid cells.¹⁶⁰ The ADC binds CD33 selectively, is internalised by phagocytosis and degraded to selectively release the cytotoxic agent within myeloid cells.

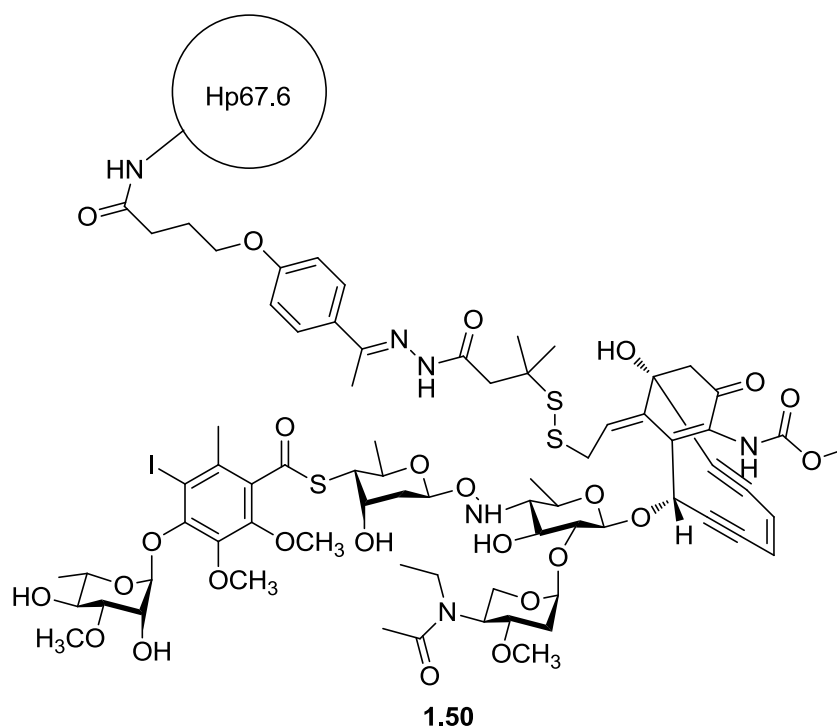
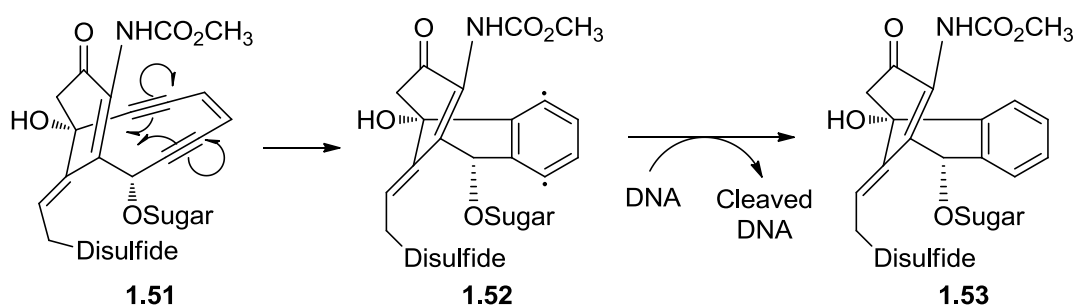


Figure 1.45: Mylotarg (1.50) including antibody Hp67.6 and Calicheamicin γ 1

The cytotoxic agent, Calicheamicin γ 1, is an enediyne antibiotic natural product. It acts by binding DNA and performing a subsequent Bergman-type radical cyclisation¹⁶¹ of the enediyne moiety (Scheme 1.7). A benzyne diradical **1.52** is formed which abstracts protons from DNA inducing a double strand break.¹⁶² This particular antitumor agent, unconjugated, is active at sub-picomolar concentrations.¹⁶³

The linker, used to conjugate the warhead to the antibody was based on a hydrazone. Investigations around this linker found that the geminal dimethyl group improved the anti-tumour properties.¹⁶³ This is likely to be due to improved disulfide stability to reduction by glutathione, allowing more ADC to be internalised prior to cleavage.¹⁶⁴

Scheme 1.7: Bergman-type radical cyclisation of calicheamicin γ 1

Mylotarg, however, was later voluntarily withdrawn by Pfizer.¹⁶⁵ Unfortunately, the ADC was not well tolerated in the Phase III trial compared to standard chemotherapy. It was discovered that the acid-labile linker was unstable within the circulation,¹⁶⁶ and the resulting free drug molecule, with its extremely potent anti-tumour activity, led to off-target effects and a reduced TI.¹⁶⁷

While Mylotarg was unsuccessful in the clinic, there have been a number of recent successes within the field of antibody drug conjugates. Two examples of FDA-approved anti-cancer ADCs are trastuzumab emtansine (Kadcyla) and brentuximab vedotin (Adcetris). Both utilise a thiol-maleimide linker **1.54** (Figure 1.46), which is more stable than the hydrazone present in Mylotarg.¹⁶⁸

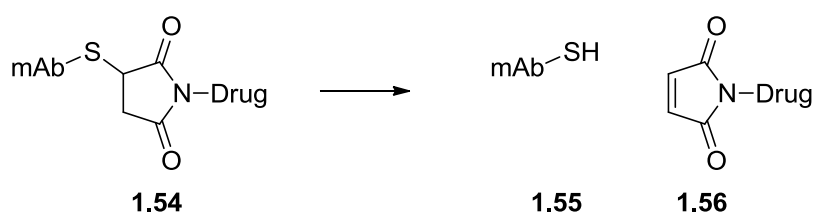


Figure 1.46: Thiol-maleimide linker

While the highly selective delivery of ADCs is attractive, the risks are also large. Synthesis of the conjugate is still imprecise due to the variability of drug loading. It has also been seen with the use of mAb that immune responses against the therapy can retard their effectiveness. The linker of the ADC must also be suitably resistant to cleavage before reaching the desired target.

An additional drawback of antibodies or ADCs as therapeutic agents is the inability to dose orally. These proteins would be quickly degraded in the stomach before they reach the intestine. Instead, they are often injected, either intravenously or subcutaneously.

1.6 Targeted Prodrugs

Whilst ADCs represent the combination of small molecules with a macromolecule, a solely small molecule approach to targeted drug delivery is the use of prodrugs. As mentioned previously, prodrugs are often a secondary strategy within medicinal chemistry.¹⁶⁹ Specifically, problems encountered with the absorption, distribution, metabolism, excretion or toxicity (ADMET) of a compound can potentially be solved with the correct choice of prodrug. While the adjustments to the chemistry of the active drug were sufficient for the highlighted therapeutic molecules, this overview is concerned with the targeted aspect of the prodrug approach. Looking back at the ADMET properties, the targeted approach is most concerned with altering the distribution and toxicity of the compound. Distribution can be minimised with a targeted approach, where the drug would be delivered to the target cells, with minimal quantities affecting other tissues. Reducing the distribution may limit toxicity, whether it is off-target systemic toxicity or on-target at a different site.

Targeted prodrug approaches can deliver active molecules selectively to organs or potentially to specific cell types. Examples of targeting using specific enzymes or environmental conditions to activate the prodrug, will be discussed in the following pages.

1.6.1 Targeting Drugs to the Central Nervous System (CNS)

The blood-brain-barrier (BBB) is an efficient blockade the body uses to protect the central nervous system (CNS).¹⁷⁰ Delivering molecules to the brain represents a significant challenge for medicinal chemists. Lipinski's rule of five, associated with compounds with good solubility and oral bioavailability, is inadequate for predicting BBB permeability.^{171,172} To achieve BBB permeability, a stricter set of guidelines were established.¹⁷² The recommended limits for calculated lipophilicity (cLogP) and total polar surface area (TPSA) were ≤ 3 and $\leq 90 \text{ \AA}^2$, respectively, based on candidate and marketed CNS drugs.¹⁷³

Using a targeted approach may relax these molecular guidelines. An initial example is L-3,4-dihydroxyphenylalanine (L-DOPA) (**1.57**). This drug, a precursor of dopamine (**1.58**) (Figure 1.47), uses the neutral amino acid transporter within the BBB to cross the membrane.¹⁷⁴ Dopamine, on the other hand, cannot cross the BBB into the brain.

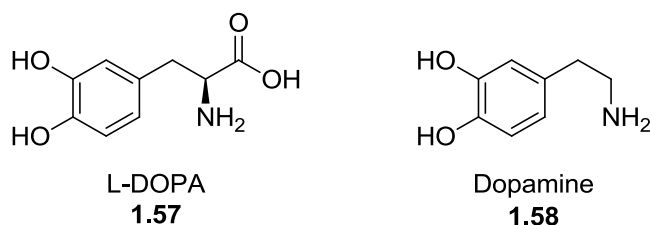
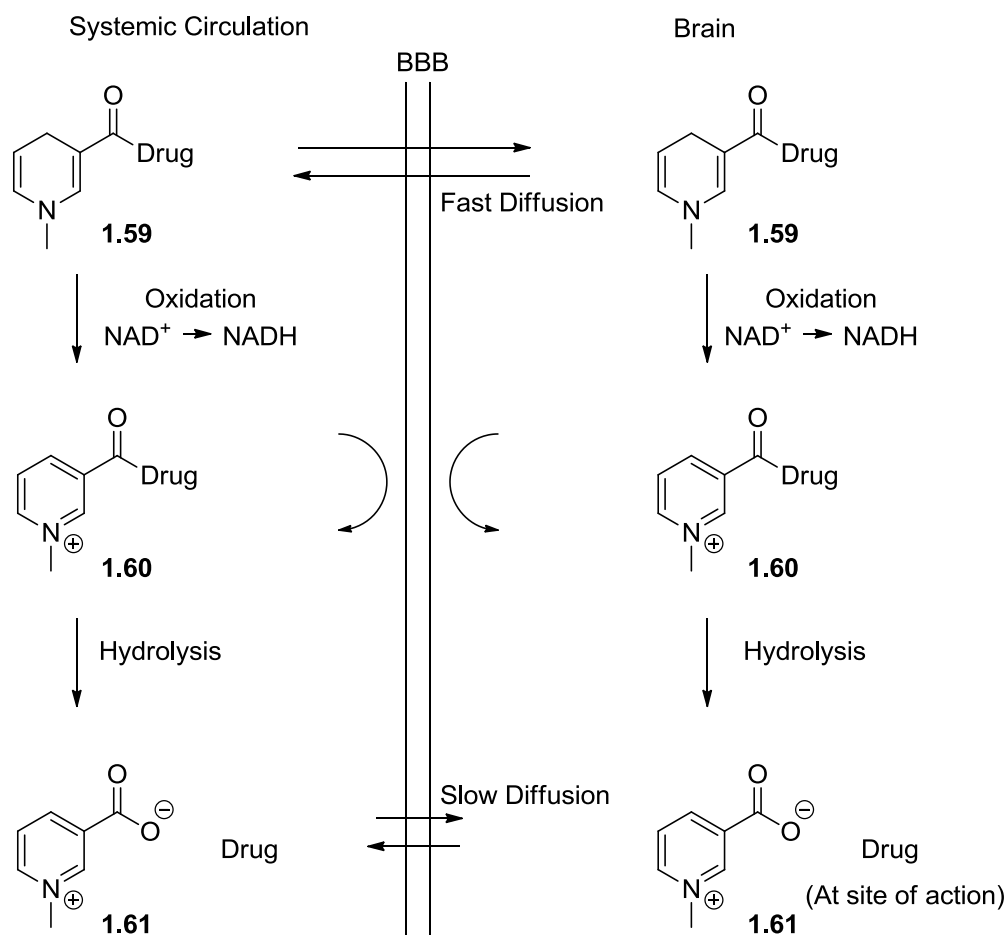


Figure 1.47: Structures of dopamine (1.58) and its prodrug L-DOPA (1.57)

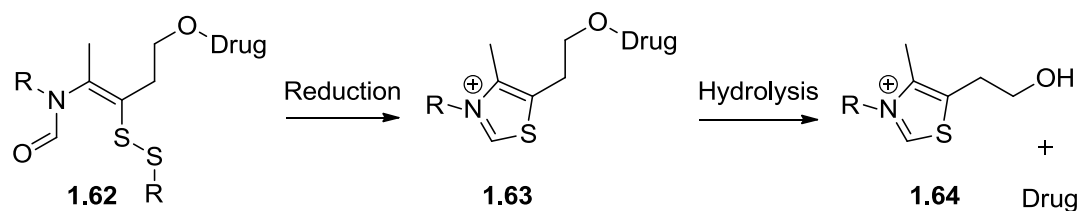
Additional methods have been described to selectively deliver L-DOPA and other drug molecules to the brain in a chemical drug-delivery system (CDS). This involves the formation of a charged intermediate to trap the prodrug within the brain, of which two examples are illustrated below.

In 1981 Bodor *et al.* described the use of a dihydropyridine conjugate **1.59** to cross the BBB.¹⁷⁵ Oxidation, analogous to NAD^+/NADH , which occurs within the CNS, traps the resulting pyridinium species within the brain (Scheme 1.8). Unfortunately, oxidation of the prodrug in the systemic circulation leads to drug clearance. However, within the CNS, release of the drug from this oxidised conjugate **1.60**, by hydrolysis, delivers the drug to the brain. This strategy has been used to investigate delivery of a number of drugs across the BBB, for example AIDS therapy zidovudine,¹⁷⁶ antibiotics,¹⁷⁷ hormones¹⁷⁸ and chemotherapeutic agents,¹⁷⁹ as well as imaging agents.¹⁸⁰

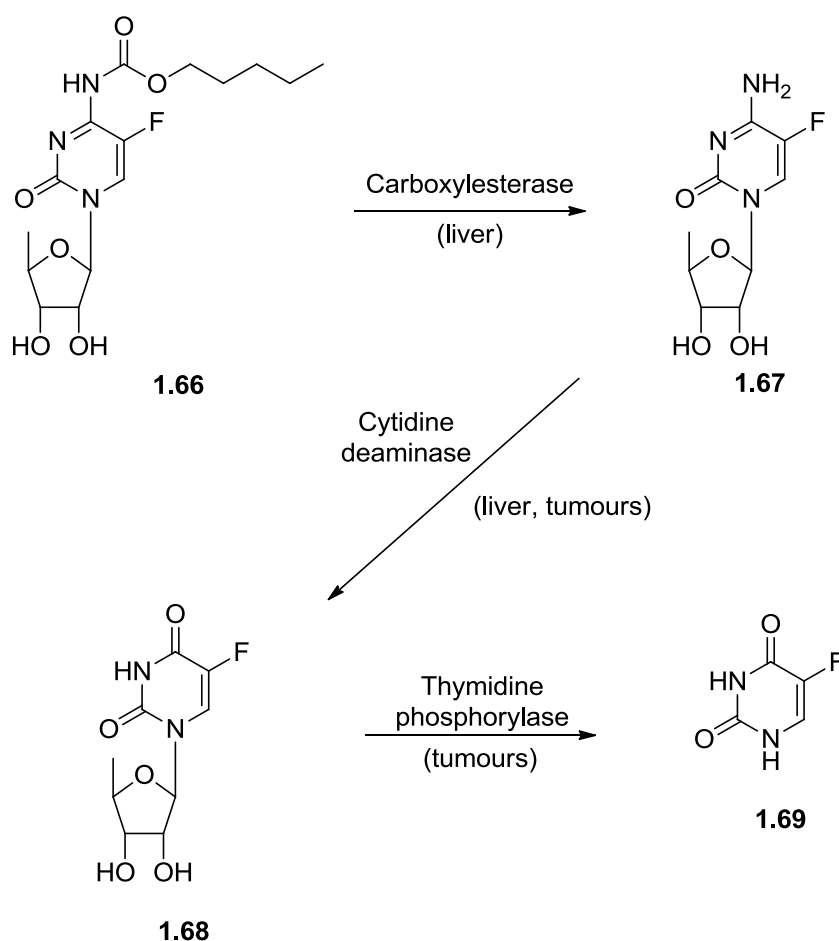


Scheme 1.8: Dihydropyridine/pyridinium chemical drug delivery system (CDS)

An alternative to dihydropyridines is the use of *cis*-2-formylaminoethenylthio derivatives **1.62**.¹⁸¹ The prodrug is reduced *in vivo* to form the quaternary thiazolium **1.63** which is retained in the brain, again, due to its charged nature (Scheme 1.9). Hydrolysis completes the drug delivery. Similar to the dihydropyridine strategy, the activation is not restricted to the CNS. Reduction, mediated by glutathione, was observed within red blood cells.¹⁸¹



Scheme 1.9: *cis*-2-Formylaminoethenylthio drug carrier



Scheme 1.10: Metabolism of Capecitabine (1.66) to 5-FU 1.69

A number of these prodrug targeting strategies use specific enzymes to convert the prodrug into the active drug. In order to use an enzymatic activation method, it is required for the targeted enzyme to have a differentiated tissue expression profile. Furthermore, a challenge associated with this approach is the knowledge required to guide the prodrug design.

Additionally, enzyme expression between patients can be variable. This could lead to different drug efficacies, which can complicate later stage patient treatment. Developing the drug, prior to human studies, can also prove challenging if the enzyme is specific to humans, complicating the required safety and efficacy studies.

Overall, there are a number of strategies available to the medicinal chemist in order to improve the therapeutic index of a drug molecule. Selective targeting of drugs to the site of action, similar to Erlich's vision, has become increasingly possible with these techniques.

As discussed in the first section, inhibiting the BET family of bromodomains has numerous effects within different cell types and disease states. Using a targeted approach could potentially improve the therapeutic window between the desired and undesired effects. One set of immune cells that are positively affected by BET inhibition are those of the myeloid lineage, such as monocytes and macrophages.

1.7 Targeting Molecules to the Macrophage

The macrophage, literally meaning “big eater”, engulfs and degrades foreign molecules and pathogens within tissues. These cells play a pivotal role in the innate immune response. Their second role is to activate the secondary adaptive immune response, both by excreting the degradation products of phagocytosis and through the production of immuno-modulatory signalling molecules. However, the macrophage can be over activated in chronic immuno-inflammatory diseases. These cells are the major cause of joint inflammation and destruction in rheumatoid arthritis (RA) and they can also contribute to tumour growth.^{186,187} Therefore, combating an undesired inflammatory response by targeting a drug to the macrophage would be a very desirable research outcome.

1.7.1 Human Carboxyl Esterases (hCE)

The human carboxylesterase family of enzymes are responsible for hydrolysis or transesterification of xenobiotics, such as cocaine.¹⁸⁸ However, there are five different enzymes belonging to this class present within the human body, named human carboxylesterase-1, -2, -3, -5 and -6.¹⁸⁹ Each of these enzymes is expressed in different amounts in different cell types. Importantly, the human carboxylesterase 1 (hCE-1) enzyme is expressed in high quantities within human macrophage and monocytes. On the other hand, hCE-2 is expressed mainly within the intestine while hCE-3 and -6 are found in the brain.¹⁹⁰ However, the location of hCE-5 expression has not been elucidated in humans with expression of a structurally-related enzyme observed in rats and cats.¹⁹¹ Overall, this restricted expression of hCE-1 has lent itself to its exploitation as part of pro-drug strategies, such as that used by the Chroma platform.¹⁹²

As previously described in Section 1.5, hCE-1 has also been used as part of a prodrug strategy for the anti-influenza drug, Oseltamivir (Tamiflu) (**1.41**), where the

active compound is the acid (Scheme 1.5, Page 37), which is generated through hydrolysis of the ester by hCE-1 present in liver hepatocytes.¹⁹³

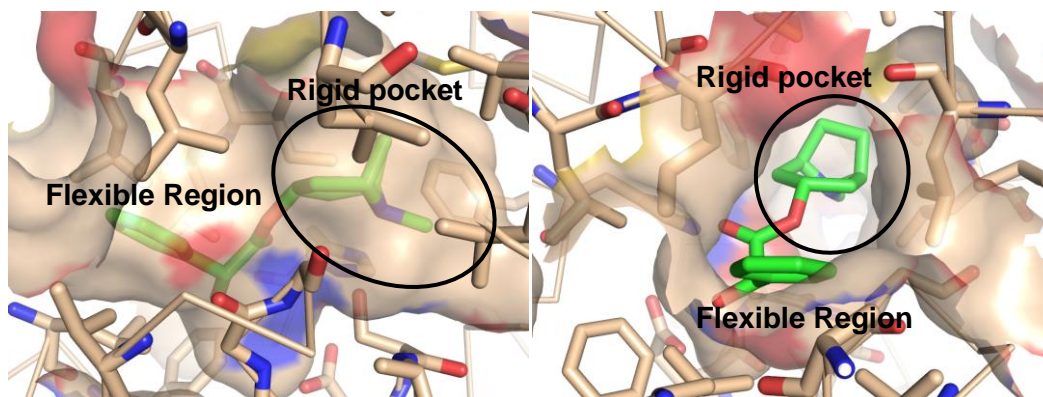


Figure 1.49: X-ray crystal structure of homatropine (1.70) within the hCE-1 active site (Protein Data Bank: pdb 1MX5)¹⁹⁴

To describe the hCE-1 active site, Figure 1.49 shows the exemplar homatropine analogue (1.70) (Figure 1.50) within the active site of hCE-1. A computational Van der Waals surface has been added to show the fit within the pocket. As can be seen, the binding pocket contains two distinct areas, a rigid pocket and a large flexible region.¹⁹⁵ The tropine ester occupies the rigid pocket, while the flexible region can encompass the remainder of larger molecules, such as heroin and cocaine, due to its flexible nature. Figure 1.49 also shows the mandelic acid group in the flexible region. Overall, this allows a wide variety of esters to be hydrolysed by this enzyme, though the rigid pocket aids ester selectivity. To hydrolyse compounds such as homatropine, the protein utilises a catalytic triad of amino acid residues, Ser-221, Glu-353 and His-467, to perform this hydrolysis in a two step process.^{195,196}

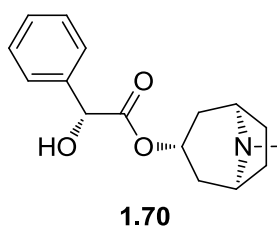


Figure 1.50: Structure of homatropine analogue 1.70

1.7.2 Esterase Sensitive Motif (ESM)

As previously mentioned, Chroma Therapeutics developed a pro-drug strategy, centred on hCE-1, to target specific immune cell types selectively. They discovered that adding an amino acid ester group, which does not interfere with the primary activity of the molecule at its pharmacological target, can exploit the differences in expression of intracellular esterases between cell lines.¹⁹⁷ In relation to this technology, the structure of the amino acid ester group, ESM, can discriminate between the three major carboxylesterases present within human cells, hCE-1, -2 and -3, with hydrolysis only occurring via hCE-1.

The general structure of the ESM (**1.71**) has been well defined by researchers at Chroma Therapeutics, in order to gain the described selectivity (Figure 1.51).¹⁹⁸

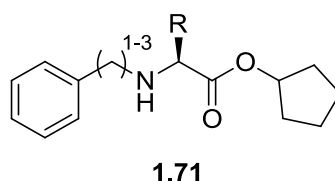


Figure 1.51: General ESM structure

For optimal recognition, the ESM should branch from an aromatic ring, to ensure the molecule extends through the tight mouth of the esterase. The chain to link to the amino acid group can be varied in length from one to three carbons. While working on a monocyte and macrophage targeted kinase inhibitor, researchers discovered that the ESM should be linked to the amino acid through the nitrogen (**1.72**) (*N*-linked) rather than from the amino acid side chain (*C*-linked) (**1.73**) in order to preserve the hCE-1 selectivity (Figure 1.52).¹⁹⁷

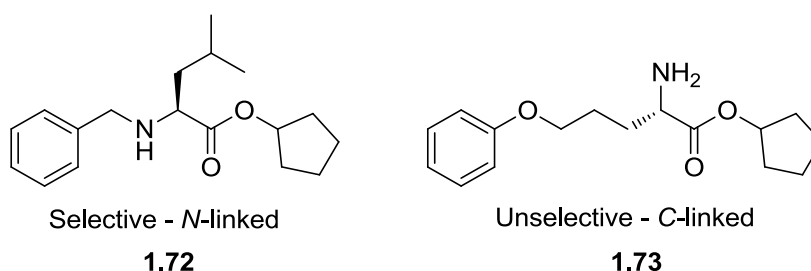


Figure 1.52: Amino acid linkage to gain selectivity

The functionality used as the linker is versatile, the main exception being the amide functional group, which removes selectivity for hCE-1 versus hCE-2. Therefore, from Chroma's patent literature, an alkylamine or sulfonamide are the most effective

groups for retaining esterase selectivity.¹⁹⁹ As exemplified with Tosedostat (**1.74**), containing an amide linker, the ester bond is easily cleaved by the other carboxylesterase enzymes (Figure 1.53).^{192,200}

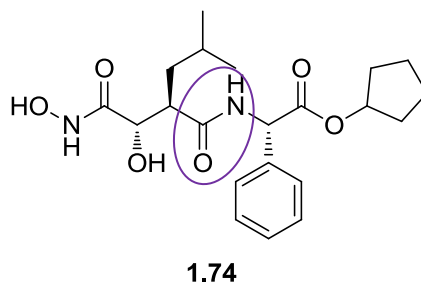


Figure 1.53: Structure of Tosedostat (**1.74**) with highlighted amide linker¹⁹²

The amino acid side chain is also variable, with both natural and un-natural examples being tolerated.¹⁹⁸ Chroma, while investigating the effect of varying the ESM on a known HDAC inhibitor, Vorinostat (**1.5**), compared leucine (**1.76**) and the un-natural amino acid phenyl glycine (**1.75**) (Figure 1.54, Table 1.1). Both had the same (*S*)-stereochemistry at the α -carbon, and both were potent within the enzyme and cellular assays. Importantly, while the ESM-containing molecules were essentially equipotent to vorinostat in the enzyme assay, they were significantly more potent within the cellular assay.¹⁹² This is known as the “ESM effect”. Therefore, the binding pocket can accommodate the amino acid side chain, whether natural or un-natural.

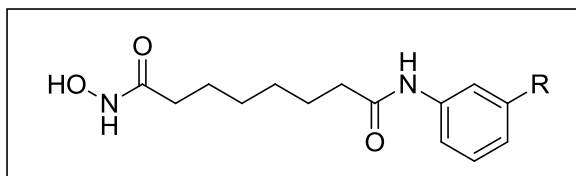


Figure 1.54: Structure of iHDAC Vorinostat with variable R group

(Table 1.1, Table 1.2, Table 1.3)

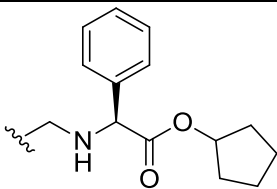
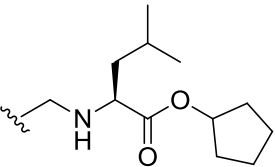
R	H (Vorinostat)		
	1.5	1.75	1.76
Enzyme assay IC ₅₀ (nM)	78	53	75
Cellular assay IC ₅₀ (nM)*	445	24	15

Table 1.1: Comparison of natural and un-natural amino acids as ESM¹⁹²
*Using hCE-1 positive THP-1 cells

The ester functionality, however, is less variable, Chroma having found the cyclopentyl group to be optimal. Smaller esters are not stable enough within the blood, and larger bulky esters, such as *t*-butyl, are not hydrolysed by hCE-1.¹⁹² Chroma again used ESM variants of Vorinostat to investigate the ester group and found that, while the enzyme assay showed the three molecules **1.5**, **1.76** and **1.77** (Table 1.2) to be equipotent, the cyclopentyl ester (**1.76**) was more effectively converted to the acid in hCE-1 positive cells (THP-1). Accordingly, the cyclopentyl ester showed a 30-fold increase in potency compared to Vorinostat (**1.5**) and the non-hydrolysable *t*-butyl ester (**1.77**).¹⁹²

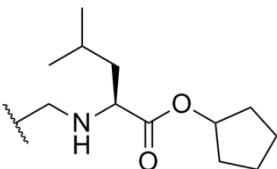
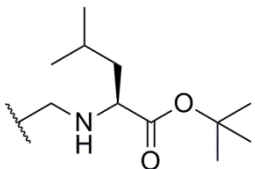
R	H (Vorinostat)		
	1.5	1.76	1.77
Enzyme assay IC ₅₀ (nM)	78	75	73
Cellular assay IC ₅₀ (nM)	445	15	400
hCE-1 positive* Cellular assay IC ₅₀ (nM)	350	630	610
hCE-1 negative**			

Table 1.2: Different cellular potencies of cyclopentyl and *t*-butyl esters¹⁹²
Using *THP-1 cells or **HuT-78 cells

Additionally, in hCE-1 negative HuT-78 cells, the ESM-containing molecules were less potent than Vorinostat. The overall result is that, before hydrolysis, the ester enters the cell by crossing the membrane facilitated by the molecule's lipophilicity. Hydrolysis by hCE-1 specifically converts the cyclopentyl ester to the corresponding acid, which is ionised at physiological pH, less lipophilic and, therefore, less able to permeate out of the cell (Figure 1.55). This results in selective retention of the pharmacologically active acid only within cells expressing hCE-1. Additionally, as both the ester (75 nM) and corresponding acid (290 nM) have HDAC inhibitory effects, the combination of these species, within the target cell types, will elicit the desired response.

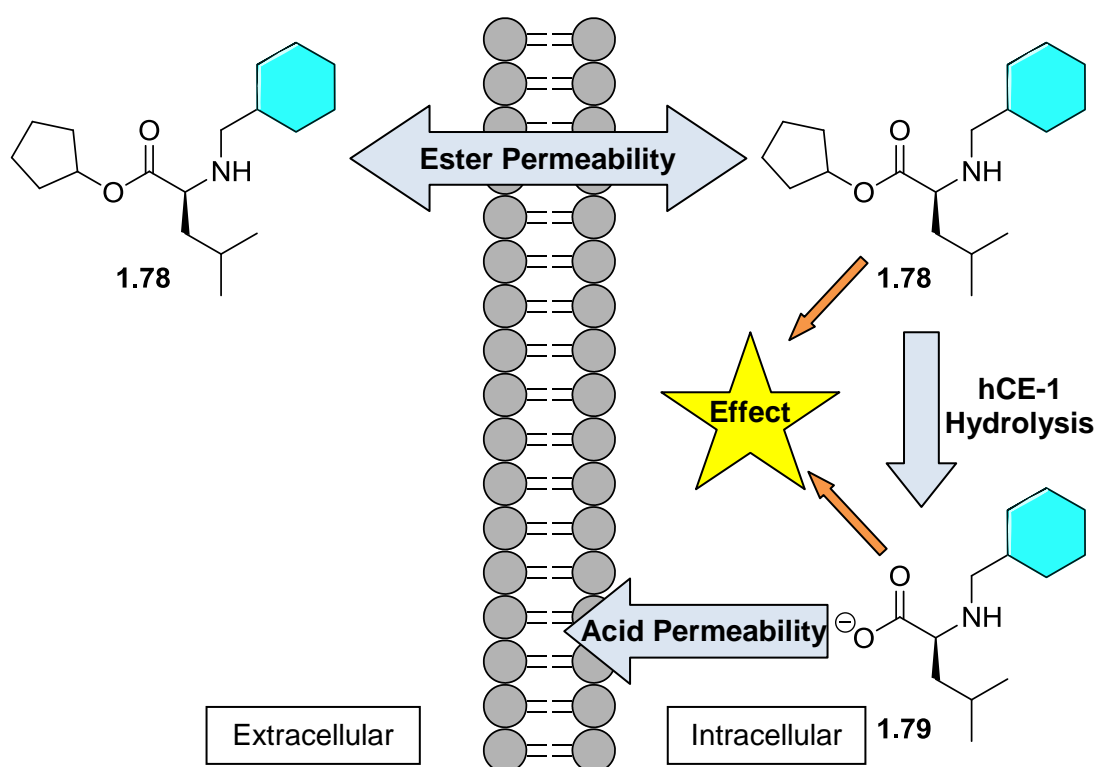


Figure 1.55: Representation of ESM permeability through the lipid membrane.

In relation to the above, Chroma also investigated the generation of the acid within hCE-1 positive and negative cells using different esters of structure **1.76** and **1.77** (Figure 1.54, Table 1.3).¹⁹² This work detailed the production of the acid from hydrolysis of the cyclopentyl ester within the hCE-1 positive cells, while only negligible quantities of the acid were seen in hCE-1 negative cells. The table of data also confirms the *t*-butyl ester was not hydrolysed in either the hCE-1 positive or negative cells.

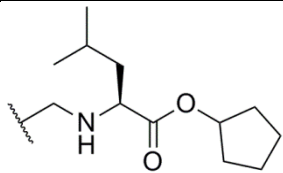
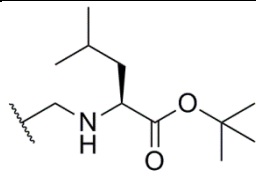
R			
		1.76	1.77
Acid retention by intact cells (ng/10 ⁶ cells)	U-937 (hCE-1 positive)	438 ± 29	1 ± 1
	HuT-78 (hCE-1 negative)	3 ± 1	0

Table 1.3: Acid retention within hCE-1 positive and negative cell lines¹⁹²

There are a number of advantages to developing and utilising this ESM strategy (Figure 1.57). While the acid is being formed within the cell, a local high concentration is formed as the acid is retained, less able to permeate through the membrane. Additionally, due to Le Chatelier's principle, more ester is drawn into the cell to replenish that hydrolysed by hCE-1 (Figure 1.56).

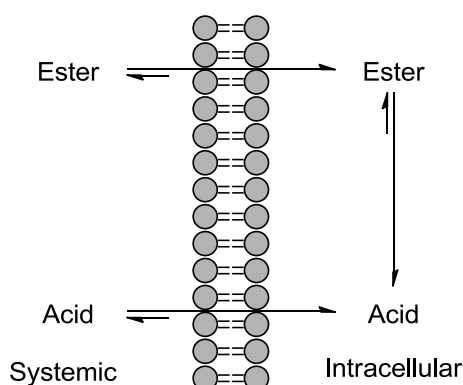


Figure 1.56: Le Chatelier's principle in acid formation and retention

Due to this retention, higher quantities reach the target and, therefore, the drug molecule itself should not require high levels of potency to be active, as retention of the acid metabolite would expect to give an apparent increase in phenotypic potency. As a result, a drug exploiting this should be better tolerated due to fewer side effects, as non-hCE-1 expressing cells should have limited exposure to the drug. The drug should also have a prolonged period of effectiveness as the acid is retained, taking longer to be transported out of the cell. Additionally, hydrolysis within the target cell or during metabolism within the liver should also limit the systemic exposure of the compound. For these reasons, this strategy could be

applicable to BET as dosing a less potent inhibitor without losing activity at the desired target cell would constitute an optimal strategy.

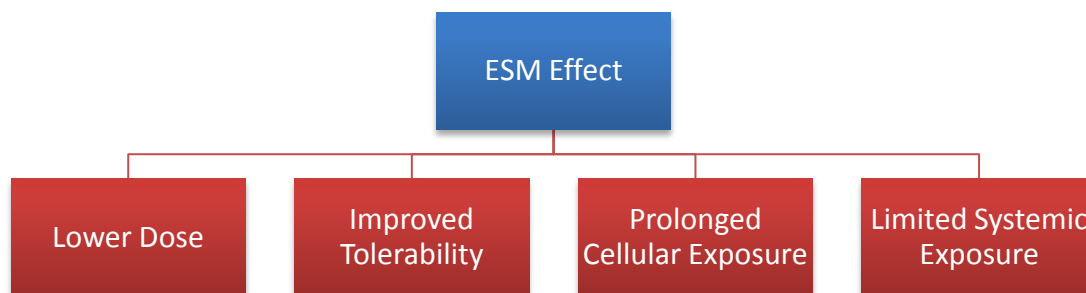


Figure 1.57: Advantages of utilising the ESM strategy

Based on the work described in this section, Chroma Therapeutics found that their ESM iHDAC (**1.80**) (Figure 1.58) compound was more efficacious than the non-targeted iHDAC, with an effective dose of 3 mg/kg/day compared to the 100 mg/kg/day of Vorinostat (**1.5**) in a murine model of arthritis. The ESM iHDAC showed an improved therapeutic index (TI) of 30-fold in comparison to Vorinostat, the parent molecule.¹⁹²

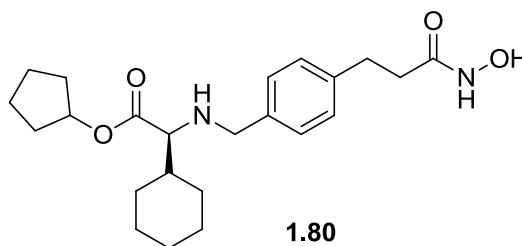


Figure 1.58: ESM iHDAC showing increased TI¹⁹²

The lower dose and larger therapeutic index observed with the ESM-functionalised HDAC inhibitor has made this a potentially promising strategy for other medicinal chemistry programmes. It was hypothesised that this technology would be suitable for combination with a BET inhibitor.

1.8 Project Aim and Objectives

As discussed earlier, BET inhibitors have been implicated in a number of disease areas. The BET inhibitors published, to this date, affect all cells as the BET proteins Brd2, Brd3 and Brd4 are expressed ubiquitously. Additionally, BrdT is also inhibited although this bromodomain is confined within the testis and ovaries. However, broad inhibition of the BET proteins may lead to undesired effects, particularly when dosing in a chronic setting. The aim of this programme of work was to discover a BET inhibitor suitable for chronic immuno-inflammatory diseases, such as rheumatoid arthritis (RA). Chronic drug therapies require an excellent safety profile as they may be prescribed for months or years.

A targeted approach, delivering the BET inhibitor to the target cells central to a disease such as RA is hypothesised to mitigate the potentially challenging pre-clinical safety profile of a non-targeted BET inhibitor. Increasing the effect within target cells while reducing systemic effects would also potentially widen the therapeutic index.

The aim of this PhD programme was therefore to understand the subtleties, in potency, lipophilicity and clearance, regarding the optimisation of a targeted BET inhibitor using the ESM technology. To understand these properties and the wider compound profile, synthesised compounds would be tested within a series of assays. The screening cascade for this project is outlined below.

1.9 Compound Profiling

1.9.1 Screening Cascade

In a medicinal chemistry programme, it is important to collect data on the synthesised compounds to gain perspective on their suitability as potential drug candidates and to differentiate one compound from another. In order to do this, a number of assays are put in place to answer specific questions about the molecule's properties. The tests are ranked in terms of importance at each stage and a screening cascade (Figure 1.59) is then produced. Commonly, compounds are screened through the assays layer by layer. This screening cascade acts as a filter, removing compounds which do not meet the target product profile (TPP). Each layer creates an increasingly selective filter giving a high number of compounds at the first stage of the cascade and fewer at the lower layers.

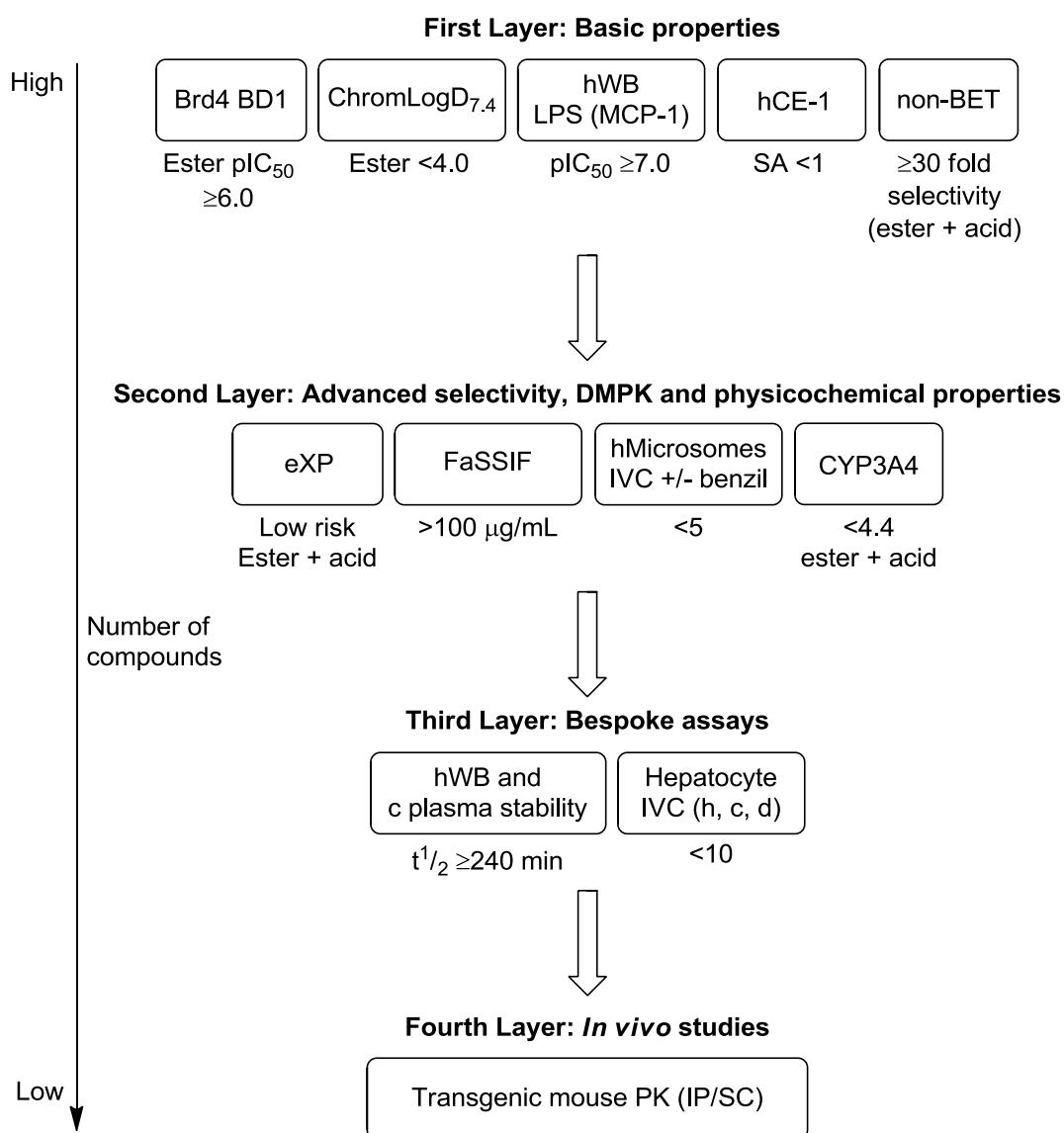


Figure 1.59: Screening cascade

The first layer of the screening cascade for this project involved five key assays. These include the biochemical assay for the target, Brd4 BD1, as well as the non-BET bromodomain assays required for judging selectivity. The cell based, human whole blood potency and the hCE-1 specific activity (SA) combine to give an initial indication as to whether the ESM mechanism is in action. An enhanced potency into the whole blood relative to biochemical potency, due to acid retention, and hydrolysis rate of the ester by hCE-1 are key pieces of data. Finally, the ChromLogD_{7.4} is measured to give an indication to the molecule's physicochemical properties.

The physicochemical properties of compounds are further investigated in the second layer of the screening cascade, looking into the solubility within the pharmacologically relevant fasted state simulated intestinal fluid (FaSSIF) solubility assay. It is at this stage that likely modes of metabolism are investigated to ensure that the compound does not inhibit the cytochrome P450 family of enzymes, the most promiscuous being CYP3A4.²⁰¹ Cytochromes P450 (CYPs) are enzymes that have a central role in the body's defence against foreign molecules. They act through the oxidation of foreign molecules to introduce polarity and attach handles for conjugation of more polar molecules in preparation for excretion. Inhibition of these CYPs can hamper this defence. After confirming this, compound metabolism is measured in an *in vitro* clearance (IVC) assay using isolated human liver microsomes. This assay gives an indication of the likely Phase I metabolism taking place, including oxidation, reduction and ester hydrolysis. Unfortunately, hCE-1, as well as being expressed in cells of the myeloid lineage, is expressed in the liver. In order to separate ester hydrolysis from other modes of metabolism, the carboxylesterase inhibitor, benzil, is used to inhibit esterase activity. This allows measurement of non-esterase-mediated metabolism, thereby allowing optimisation of this property. Finally, within this level, a broader selectivity profile is generated via an enhanced cross-screening panel (eXP) of a diverse set of known biological liabilities.

The third layer of the screening cascade contains more bespoke assays. Following on from the human liver microsome IVC, a more complete picture is formed when whole hepatocytes are used. In this case, Phase I and II metabolism are both accounted for, in which the second phase involves the conjugation of polar molecules, such as glucuronic acid or sulfate.

Having progressed through the human whole blood assay with the desired potency for further profiling, human whole blood stability would not be expected to be a problem. However, it is useful to obtain an absolute value on the stability, with a view to comparing this to pre-clinical species. One of these species, the cynomolgus monkey is important due its close genetic relation to humans with a common ancestor around 25 million years ago.²⁰² Leading on from this, the cynomolgus monkey is a potentially very useful pre-clinical species specifically due to the similarity in the carboxylesterase-1 (CE-1) gene compared to the human form (hCE-1), with 92.9 % homology.²⁰³

The fourth layer is the start of *in vivo* animal experiments. In this case, a transgenic mouse is required in which the hCE-1-like mouse blood esterase has been nullified whilst the human esterase, hCE-1, has been successfully introduced to monocytes and macrophages. This experiment investigates the pharmacokinetics of the molecule after different dosing methods, thereby informing future *in vivo* studies.

1.9.2 Target Product Profile

In order to give some context to the desired target product profile (TPP), a well-profiled compound within our laboratory, benzimidazole **1.81** along with the corresponding acid **1.82**, will be used as a comparison (Figure 1.60). The product profile will be discussed in terms of potencies, physicochemical properties and further developability assays, as well as within the context of the screening cascade.

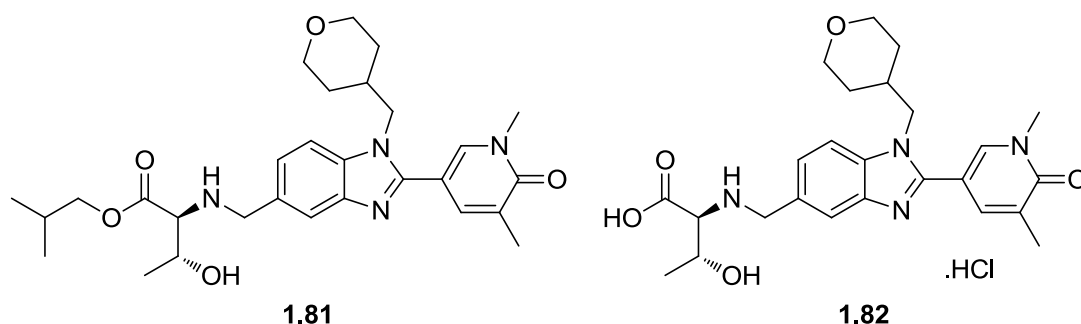


Figure 1.60: Structures of the lead compound and acid from the benzimidazole (BI) series

Beginning with the bromodomain biochemical assays (Table 1.4), compound **1.81**, is potent within the Brd4 BD1 biochemical assay with a pIC_{50} of 7.2, reducing to 6.6 as the acid. The compound was then tested within the human whole blood assay, which showed an excellent potency of 8.4, constituting a 1.2 log unit enhancement, the difference between the hWB potency and the biochemical Brd4 BD1 potency (ΔpIC_{50}). The acid was also tested, and showed a potency of 5.6 due to the carboxylate functionality reducing permeability and therefore potency in the cellular assay. As an enhanced potency was observed in the hWB assay, the specific activity (SA) of human carboxylesterase 1 (hCE-1) was measured for compound **1.81**. An activity of 0.44 was observed, within the confines of the TPP. Too high a specific activity would lead to significant hydrolysis within the liver, too low a SA, on the other hand, prevents enhancement of potency within hCE-1 positive cells. In terms of inhibiting the desired target, compound **1.81** has an excellent profile. To establish its selectivity, it was also tested biochemically against a number of

bromodomains out with the BET family. Pleasingly, the compound was more than 30-fold selective against a number of bromodomains.

	TPP	1.81	1.82
Brd4 BD1 pIC₅₀	-	7.2	6.6
hWB (MCP-1) pIC₅₀	≥ 7.0	8.4	-
ΔpIC₅₀	≥ 1.0	1.2	-
hCE-1 SA (μM/min/μM)	< 1	0.44	-
Non-BET selectivity	≥ 30-fold	> 30-fold	> 30-fold

Table 1.4: Initial biological results for compound 1.81 and its acid 1.82

To understand whether compound **1.81** had suitable physicochemical properties, it was subjected to a series of further tests (Table 1.5). Firstly, the lipophilicity has a large bearing on other physicochemical properties, such as solubility, permeability and protein binding. Compound **1.81** has a good ChromLogD_{7.4} of 3.6, although, due to the presence of three aromatic rings the PFI is a little high, however, it should still have acceptable properties. The solubility of ester **1.81** within the FaSSIF assay was excellent, while the acid also had good solubility as measured by CLND. As desired, within this project, the ester was permeable, while the acid was less so. This mirrors the hWB results observed in Table 1.4, where the acid was weakly active due to the requirement to cross the cell membrane. The desired levels of permeability for the ester may be aided by the low molecular weight, within the desired area.²⁰⁴ The human serum albumin (HSA) binding is low for the ester and higher for the acid. The role of HSA in the body is to transport fatty acids, and is an early measure of plasma protein binding. In this case, compound **1.82** is also a good substrate.²⁰⁵

	TPP	1.81	1.82
ChromLogD_{7.4} / PFI	≤ 6.0	3.6 / 6.6	0.3 / 3.3
Solubility (μg / ml)	> 100	> 950 (FaSSIF)	166 (CLND)
Permeability (nm / s)	> 100	121	< 6.5
MWt	< 550	524	469
HSA (%)	< 90	44	59
HLM IVC (- / + benzil) (mL / min / g)	<5 / <1.5	4.9 / 2.1	- / -

Table 1.5: Physicochemical properties of 1.81 and 1.82

Mirroring the initial biological results, the physicochemical data meets the TPP. Some final tests were required to discover whether this compound was suitable for progression into animal studies. Consequently, a broader safety profile was required. Within our laboratory, an enhanced cross screen panel (eXP) was used. This involves *in vitro* testing of the compound against receptor sites, ion channels, transporters and enzymes. Compound **1.81** was observed to have a good profile against these targets. Subsequently, it was important to ensure the compound was not an inhibitor of the CYP450 enzymes. With a potency of < 4.4 , it was not considered an inhibitor. Having found this, the *in vitro* clearance (IVC) was tested in human liver microsomes (HLM). As stated within the screening cascade discussion, the IVC was tested in the presence and absence of benzil, the hCE inhibitor. In the absence of benzil, the clearance was 4.9 mL/min/g liver, whereas, with benzil, this was reduced to 2.1 mL/min/g liver. Therefore, the underlying contribution from hydrolysis by hCE-1 accounts for more than half of the liver clearance. These values are high, which would predict a highly cleared compound within the liver. Alternative dosing methods to oral administration would bypass first pass metabolism. Methods such as intravenous or subcutaneous can be used, in each case, where the compound is able to achieve systemic circulation without initially passing through the liver.

To discover how stable compound **1.81** would be in the blood of different species, prior to *in vivo* studies, incubation experiments were carried out (Table 1.6). The stability of ester **1.81** was measured in human, dog, minipig, cynomolgus monkey (cyno), rat and mouse blood, with the results presented as the half life. As it can be seen from Table 1.6, compound **1.81** is stable within human and dog blood. The half life in minipig is reduced to two hours. Stability in cyno blood is less than expected, with a half life of only 23 minutes. However, it was expected that the half life in rat and mouse would be low due to the presence of rodent CE-1-like enzymes present in the blood. As shown in Table 1.6, this is indeed the case.

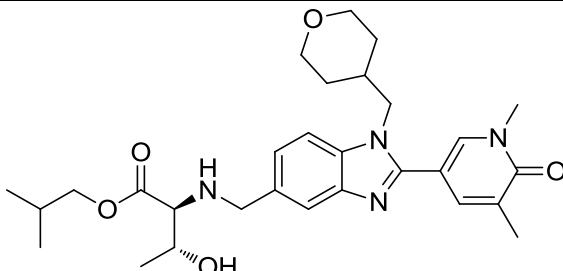
	Species	Whole Blood Half Life (min)
 <p style="text-align: center;">1.81</p>	Human	> 340
	Dog	> 240
	Minipig	120
	Cyno	23
	Rat	5
	Mouse	< 1

Table 1.6: Blood stability of ester 1.81

While compound **1.81** and its acid **1.82** have good properties within the outlined TPP, the half life of ester **1.81** in a number of potential pre-clinical species was disappointing. In order to mitigate the risk within this drug discovery project, the programme of work described herein will investigate a modified chemical template from a fragment-based starting point. Optimisation of this fragment was envisaged to be against the TPP detailed in Table 1.7.

	Ester TPP
Brd4 BD1 pIC₅₀	-
hWB (MCP-1) pIC₅₀	≥ 7.0
ΔpIC₅₀	≥ 1.0
hCE-1 SA (μM/min/μM)	< 1
Non-BET selectivity	≥ 30-fold
ChromLogD_{7.4} / PFI	≤ 4.0 / ≤ 6.0
HLM IVC (- / + benzil) (mL / min / g)	<5 / <1.5
Solubility (μg / ml)	> 100
Permeability (nm / s)	> 100
MWt	< 550
HSA (%)	< 90
Cyno whole blood stability (t_{1/2})	≥ 240 min

Table 1.7: Summarised TPP

2 Fragment Optimisation and Targeting

2.1 Proposed Work

As previously discussed, at the outset of this programme, a fragment-based approach was to be utilised to develop a novel series of ESM-functionalised BET inhibitors. Using fragment-derived start points is a well validated strategy in the discovery of novel, bromodomain inhibitors.²⁰⁶ A number of structurally distinct fragments shown to bind to the BET family of bromodomains, have been described.⁸⁹ On finding a suitable fragment, subsequent growth would enable the properties to be optimised towards the TPP.²⁰⁷

A fragment-based approach offers the ability to start from a molecule with lower activity at the target but with strong binding. The use of ligand efficiency metrics can aid the scientist to determine whether they are introducing a positive binding interaction or are increasing potency through the addition of lipophilicity and non-specific binding. The main value used in this thesis is ligand efficiency (LE), measured in kcal/mole, which correlates the free energy of binding (ΔG) normalised to the number of non-hydrogen atoms or heavy atom count (HAC) (Equation 2).²⁰⁸ This can also be represented in terms of the pIC_{50} .

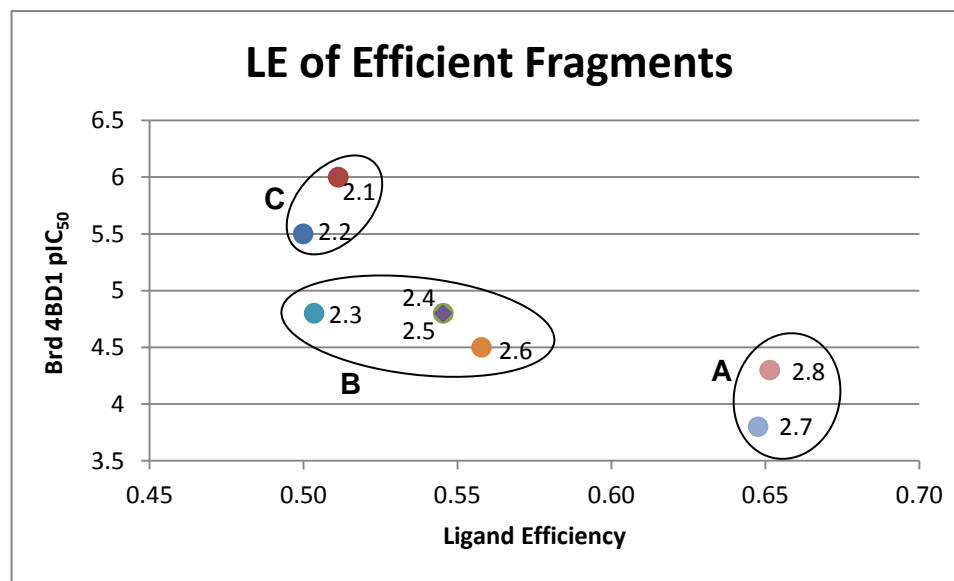
$$LE = \frac{\Delta G}{HAC} \approx 1.37 \times \frac{pIC_{50}}{HAC}$$

Equation 2: Ligand Efficiency

A fragment with a high initial LE is beneficial for further optimisation, where the aim is to at least maintain the LE. Generally, a LE of greater than 0.3 is considered to be efficient throughout the optimisation process towards a drug molecule. This is due to the presumption of, firstly, requiring a 10 nM affinity compound. Secondly, the molecule has a molecular weight of under 500, which is compliant with Lipinski's rules,¹⁷¹ which correlates to an average a HAC of 38. These two properties give a required LE of at least 0.29.²⁰⁹ However, in the work contained within this thesis, LE will be used to guide the early fragment investigations. Later, combining the pharmacophore for hCE-1 with the BET pharmacophore will reduce the overall efficiency and, therefore, LE was deemed to be an inappropriate measure for optimisation of the template.

2.2 Fragment Identification

The initial aim was to identify a suitable fragment. On commencing this work, compounds with measured potency against Brd4 BD1, were analysed. However, this set contained 6691 compounds. For this reason, LE was used to evaluate this large portfolio of potential structures, with a LE of 0.3 being used to triage the initial compound set. Despite removing over 70% of the initial set with this filter, 1808 remained. Therefore, using a more stringent LE cut-off of 0.5 allowed this large number to be cut down to the eight most efficient compounds (Graph 2.1).



Graph 2.1: Plot of ligand efficiency against Brd4 BD1 potency
 2.4: pIC₅₀ ≤4.3; 2.6: pIC₅₀ ≤4.5; 2.8: pIC₅₀ ≤3.8
 (*2.4 and 2.8: pIC₅₀ <4.3 on 1 of 2 test occasions, **2.6: pIC₅₀ <4.3 on 2 of 12 test occasions
 ***2.7: pIC₅₀ <4.3 on 2 of 4 test occasions)

The eight compounds could be separated into three groups based on potency or structural motif. Group A contains the most ligand efficient fragments, with LE values of around 0.65. Group B consists of fused bicyclic systems, while group C has two pyridone compounds.

Firstly, group A contains two compounds, **2.7** and **2.8** (Figure 2.1). Compound **2.7**, a bisfunctionalised pyridazine, was only weakly active at Brd4 BD1, with a pIC₅₀ of 3.8. Compound **2.8** is again very small and ligand efficient. However, it contains a Michael acceptor with the potential for covalent binding.

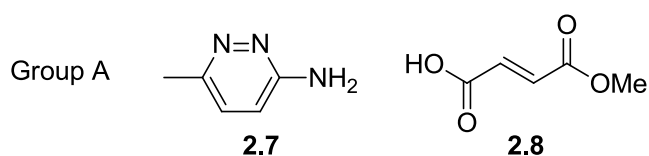


Figure 2.1: Fragment Group A

Group B (Figure 2.2), made up of the fused bicycles, also contain very ligand efficient molecules. However, with a requirement to reduce the aromatic ring count compared to the benzimidazole series, an acetyl lysine mimetic containing two aromatic rings did not constitute a desired start point: **2.4**, **2.5** and **2.6**. On the other hand, compound **2.3**, with a LE of 0.5, was a more acceptable molecule with a pIC_{50} of 4.8.

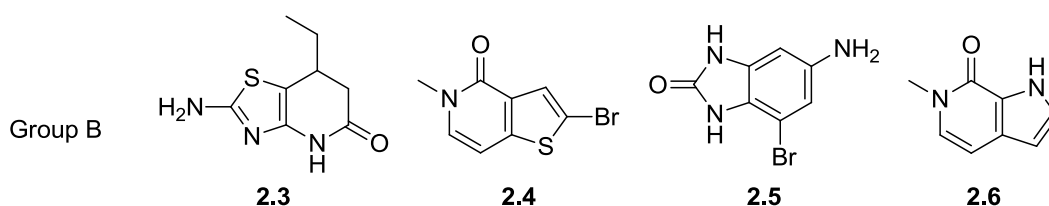


Figure 2.2: Fragment Group B

However, the two molecules of group C (Figure 2.3) also have LE values of approximately 0.5, but are much more potent start points, with pIC_{50} values of 5.5 and 6.0 for compounds **2.2** and **2.1**, respectively. These compounds contain one aromatic ring as the acetyl lysine mimetic plus the additional aryl ring which is open for further functionalisation. It was, therefore, the pyridone fragment which was selected for elaboration and development due to the potential suitability for ESM attachment, as well as its balanced potency and efficiency characteristics. Additionally, an X-ray crystal structure was available for fragment **2.2**,²¹⁰ thus paving the way for structure-based design.

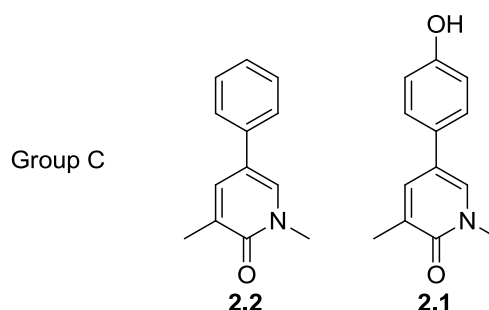


Figure 2.3: Fragment Group C

2.2.1 Initial Aims

Having selected a ligand efficient fragment, the aim was to optimise the fragment to investigate possible improvements in BET biochemical potency through substitution of the core phenyl ring, using LE as a guide. Further efforts were aimed towards the optimisation of the physicochemical properties, especially LogD, by investigating whether nitrogen atoms could be tolerated in the core and pyridone ring systems. These distinct efforts are summarised in Figure 2.4.

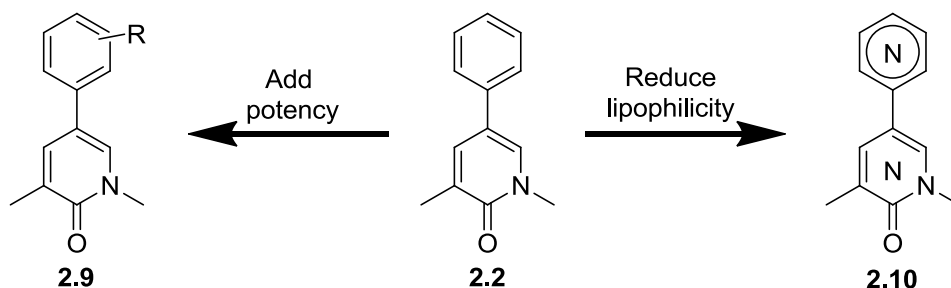


Figure 2.4: Fragment optimisation strategy

Upon identifying the most efficient start point, the ESM would then be incorporated and optimised to mitigate the lipophilic nature of this large group (Figure 2.5). Additionally, this optimisation would be guided by the biological properties of the ESM-functionalised compounds in this template.

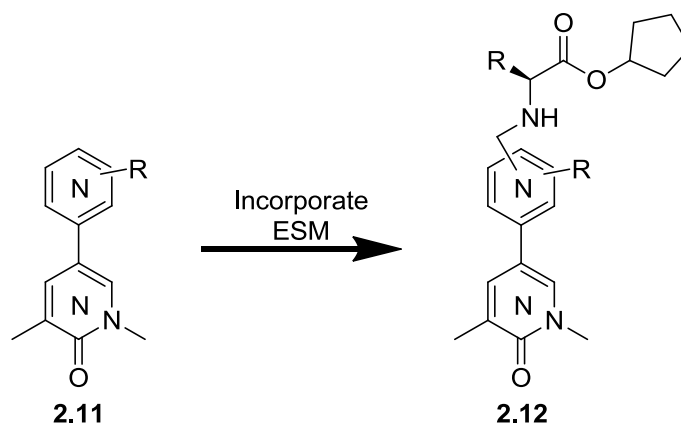


Figure 2.5: ESM incorporation to the optimised scaffold

2.3 Fragment Optimisation

To understand how the fragment could be optimised, an X-ray crystal structure of **2.2** within Brd4 BD1 was analysed. Using this protein crystal structure (Figure 2.6), the dimethylpyridone warhead binds within the acetyl-lysine binding pocket. It does this in a similar fashion to the native acetylated lysine residue, as shown previously, via two key hydrogen bonds: a through-water interaction to tyrosine Y97 and directly to asparagine N140. Additionally, the methyl group is important in binding within the hydrophobic pocket mimicking the acetyl group of the native ligand.

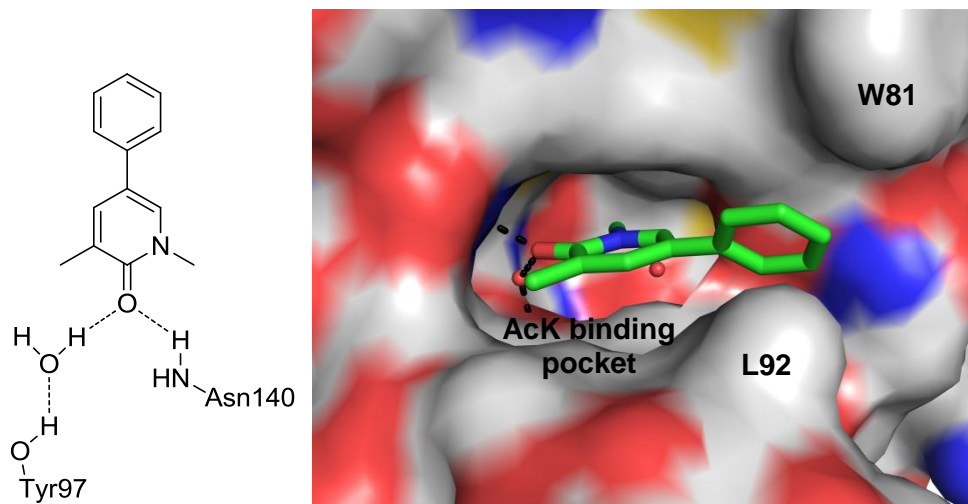


Figure 2.6: X-ray crystal structure of **2.2** in Brd4 BD1 with schematic of key binding interactions

Extending out from the acetyl-lysine binding pocket, the phenyl ring enters the narrow ZA channel region, formed by the amino acid residues; tryptophan 81 (W81) and leucine 92 (L92). From the crystal structure, W81, flanking the ZA channel, was hypothesised to be making an edge-to-face interaction with the phenyl ring, where the δ^+ tryptophan hydrogens interact with the δ^- π -cloud (Figure 2.7).²¹¹

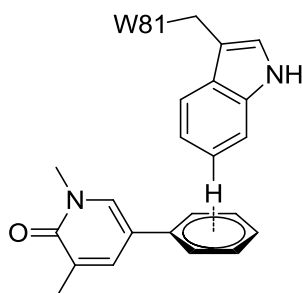
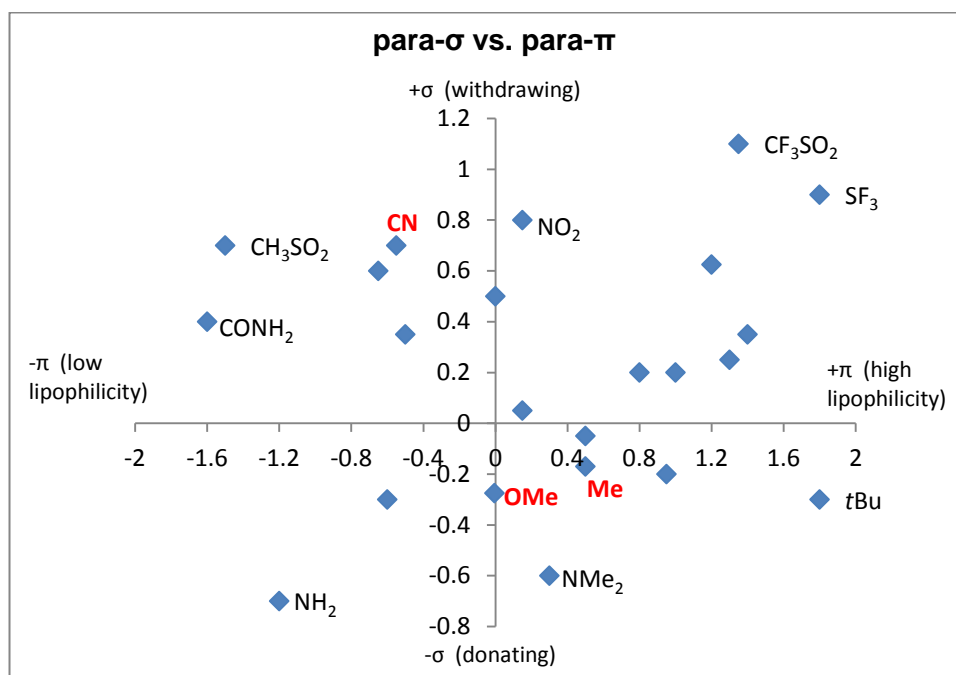


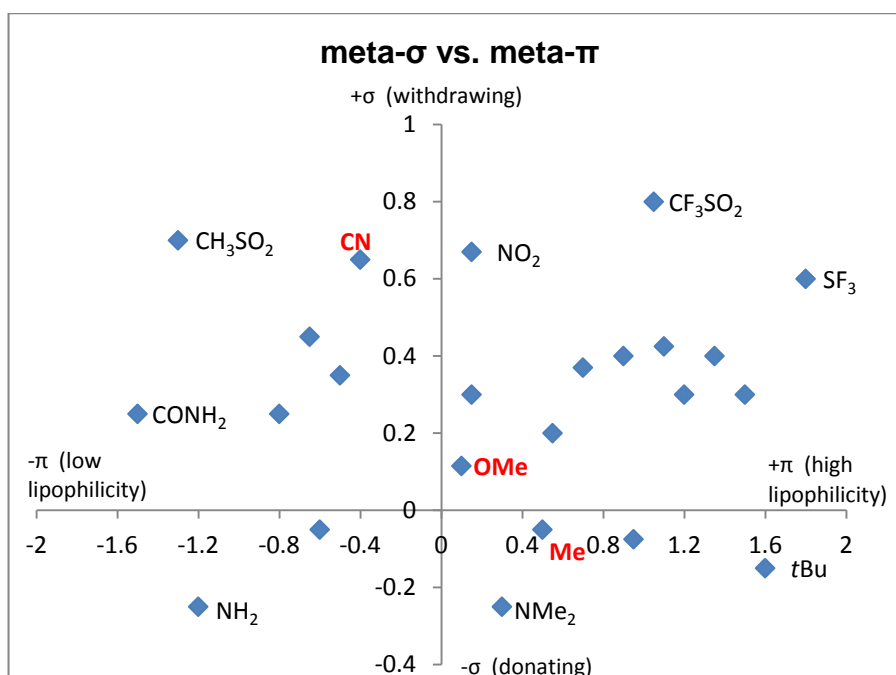
Figure 2.7: Proposed edge to face interaction

2.3.1 Investigating the ZA Channel

To investigate this potential interaction in more detail, an electronics study was undertaken. If a strong edge-to-face interaction is at play, the δ^+ hydrogens of the tryptophan should make a more favourable interaction with a more electron-rich phenyl ring. Taking inspiration from Craig plots, substituents are plotted on these graphs according to the electron-withdrawing/donating properties (σ) versus the lipophilicity (π) of the groups. Two graphs can be used to account for whether the functionality occupies the *para*- or *meta*-positions (Graph 2.2 and Graph 2.3, respectively).



Graph 2.2: *Para* Craig plot with functional groups highlighted²¹²



Graph 2.3: *Meta* Craig plots with functional groups highlighted²¹²

Using these Craig plots as inspiration, and aiming to interrogate the edge-to-face π -interaction hypothesis, three substituent profiles were proposed: electron-withdrawing, -neutral and -donating groups. Also, in order to ensure the effects were due to the differences in electronics, the substituents chosen would be small, to prevent the introduction of adverse steric interactions, and similar in lipophilicity (π) to hydrogen to minimise increases in potency due to lipophilic interactions. To fit these criteria, cyano, methyl and methoxy groups were selected (Table 2.1). The Hammett value for the cyano group shows a good level of electron-withdrawing ability, while the methyl group is near zero. The methoxy group differs between the *meta* and *para* Hammett values due to the different mesomeric and inductive contributions. The hydrophobicity constants (π) are within 0.6 of the baseline unsubstituted value. Additionally, the molar refractivities, the calculation of the size of a substituent, are also very similar.

	CN	Me	OMe	H
σ_m^{213}	0.68	-0.069	0.115	0
σ_p^{214}	0.66	-0.170	-0.268	0
π^{214}	-0.57	0.52	-0.02	0
MR ²¹⁵	7.08	6.34	8.12	1.68

Table 2.1: Properties of proposed functional groups

To fully understand the template, such as the tolerability to substitution, all three isomers, *ortho*-, *meta*- and *para*-compounds, would be synthesised (Figure 2.8).

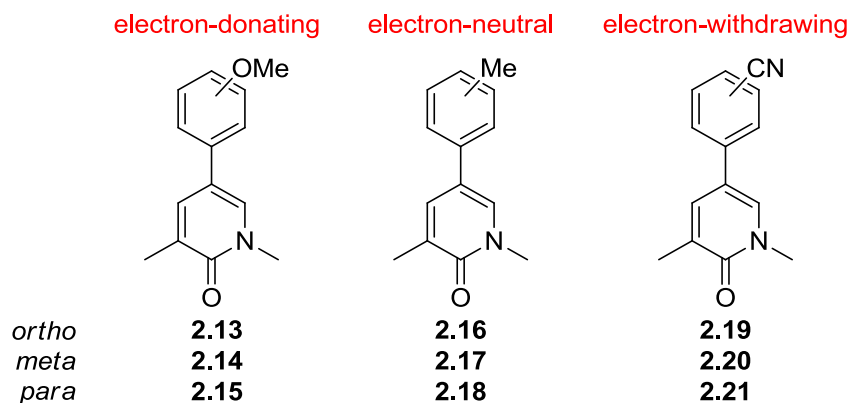
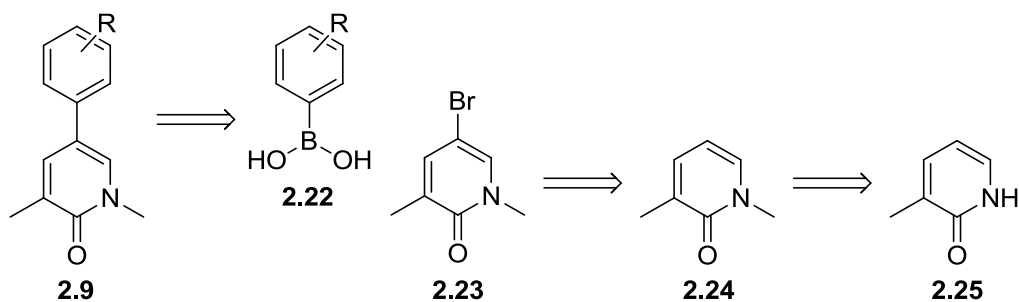


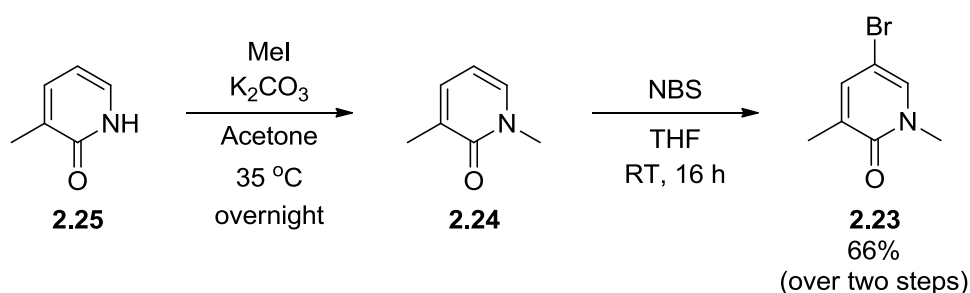
Figure 2.8: Craig plot inspired electronics investigation

A retrosynthetic analysis was applied to these molecules (Scheme 2.1). The aryl-aryl bond could be disconnected to the bromopyridone **2.23** and a boronic acid derivative. Disconnection of the bromine could reach dimethylpyridone **2.24**, which could be made from the commercially available 3-methylpyridone (**2.25**).



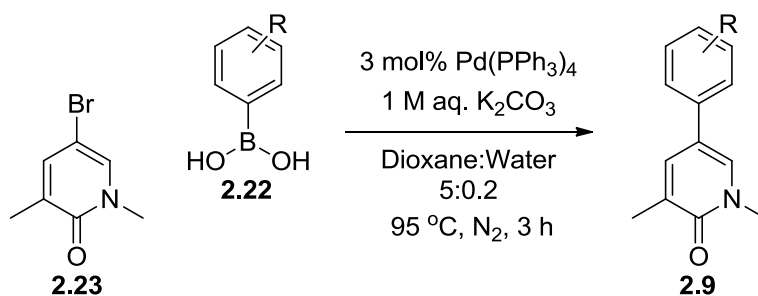
Scheme 2.1: Retrosynthetic analysis of general structure 2.9

In the forward direction, the synthesis of intermediate **2.23** was carried out on multi-gram scale (Scheme 2.2). The first reaction involved methylation of 3-methylpyridone using methyl iodide and potassium carbonate. Filtration yielded the desired intermediate in acceptable purity, before treatment with *N*-bromosuccinimide to selectively introduce the bromine at the 5-position, in good yield, over two steps.



Scheme 2.2: Alkylation and bromination of 2.25

To complete the synthesis of compounds **2.13-2.21**, the corresponding commercially available boronic acids were sourced. The Suzuki-Miyaura cross-coupling reaction was utilised to yield the desired products (Scheme 2.3).^{216,217} Leading on from this, compound yields and biological assay results are presented in Table 2.2, with comparisons made to fragment **2.2** and dimethoxy-substituted example **2.26**, prepared previously within our laboratory.²¹⁸



Scheme 2.3: General Suzuki reaction conditions

Having synthesised methoxy-compounds **2.19-2.21** in good yields, their potencies within the Brd4 BD1 biochemical assay ranged from 5.4 to 5.9, equipotent to the parent fragment **2.2** (5.5), within experimental error (± 0.3). Consequently, including the methoxy groups lowers the ligand efficiency of these compounds.

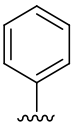
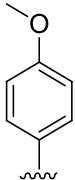
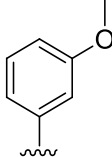
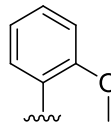
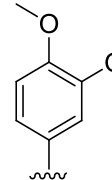
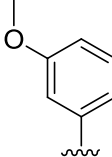
Ar						
Compound number	2.2	2.15	2.14	2.13	2.26	2.27
Yield (%)	-	73	78	67	-	67
Brd4 BD1 pIC ₅₀	5.5	5.8	5.9	5.4	6.2	6.3
LE	0.50	0.47	0.47	0.43	0.44	0.45

Table 2.2: Reaction yields and biological results for methoxy substituted examples

From work carried out previously, the 3,4-dimethoxyphenyl compound (**2.26**) had a good level of potency, improved over fragment **2.2**, but with a lower LE of 0.44.²¹⁸ The *meta*-methoxyphenyl derivative **2.14** was also seen to have good potency (Table 2.2). Considering the reasonable potency of **2.14** and improved potency of compound **2.26** it was therefore interesting to make the 3,5-dimethoxyphenyl compound **2.27**. The result showed almost a half log unit increase beyond the 3-methoxyphenyl, while having essentially the same activity as compound **2.26**. Again, however, the ligand efficiency demonstrated the lack of any new specific interactions, other than those from lipophilic interactions.

Subsequently, the bromodomain assay results for the methyl and nitrile substituted phenyl rings are shown below (Table 2.3, Table 2.4). The methyl variants were synthesised in good yields. However, potencies of compounds **2.16-2.18** are not improved compared to compound **2.2**. Overall, the electron-donating groups, variously substituted around the ring, do not improve the potency of this fragment.

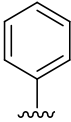
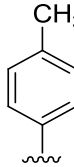
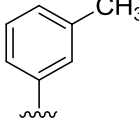
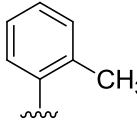
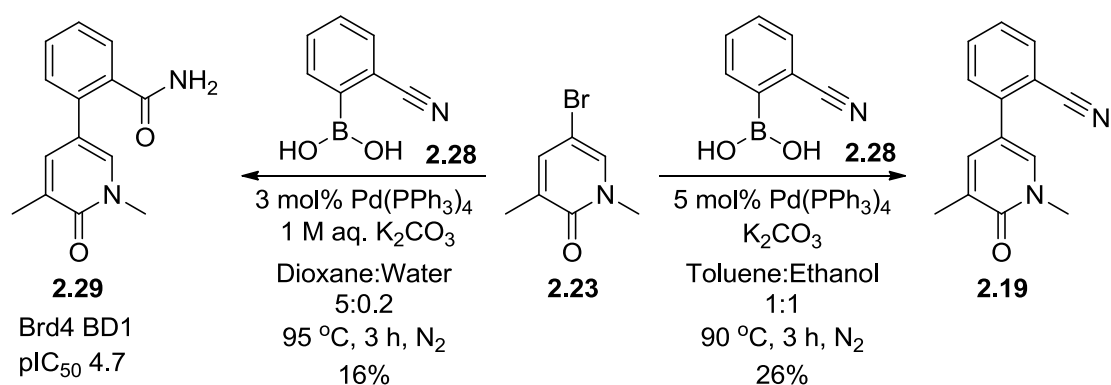
Ar				
Compound number	2.2	2.18	2.17	2.16
Yield (%)	-	73	80	71
Brd4 BD1 pIC ₅₀	5.5	5.4	5.6	5.5
LE	0.5	0.45	0.48	0.46

Table 2.3: Reaction yields and biological results for methyl substituted examples

Lastly, the nitrile-containing examples **2.19-2.21** are shown in Table 2.4. Whilst **2.20** and **2.21** were synthesised in average to good yield, the conditions were found to be incompatible with the *ortho*-example, **2.19** (Scheme 2.4). Instead, an interesting side reaction occurred during the cross coupling with 2-cyanophenylboronic acid (**2.28**). The major product observed was the amide, **2.29**, rather than the desired nitrile compound. A literature search revealed that the cross coupling reaction using 2-cyanophenylboronic acid yields both amide (**2.29**) and nitrile (**2.19**) products (Scheme 2.4).²¹⁹ The palladium may have coordinated to the nitrile, which, under aqueous conditions, facilitated the conversion to the amide. As such, the amide derivative was isolated in low yield and tested for biochemical activity, although, it was found that this larger *ortho*-substituent negatively impacted the potency. To synthesise the desired product the reaction was re-attempted, using non-aqueous conditions with only a small proportion of undesired amide product being observed.



Scheme 2.4: Different cross coupling conditions form two products

Unfortunately, the electron-withdrawing nitrile group was similarly ineffective at improving the potency above that of the original fragment, **2.2** (Table 2.4). Overall, initial studies into the nature of the aromatic ring substitution showed the SAR to be relatively flat with only electron-rich systems offering an increase in biochemical potency with a concurrent reduction in LE. Therefore, it was concluded that an efficient edge-to-face π -interaction is not being achieved in this template. With this result in mind, attention turned to using this aryl ring as a means to modulating the physical properties of the system.

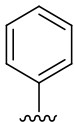
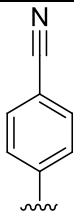
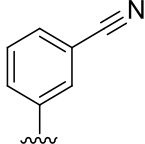
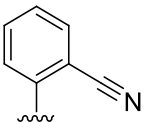
Ar				
Compound number	2.2	2.21	2.20	2.19
Yield (%)	-	40	77	26*
Brd4 BD1 pIC₅₀	5.5	5.5	5.8	5.6
LE	0.5	0.44	0.47	0.44

Table 2.4: Reaction yields and biological results for nitrile substituted examples
*Achieved using non-aqueous cross-coupling conditions (see Scheme 2.4)

2.3.2 Investigations into Phenyl Ring Replacements to Reduce LogD

An effective method of understanding a compound's physical properties is to measure the lipophilicity. The relative quantities of compound partitioned between an organic and aqueous layer can be quoted as the partition coefficient, first described in 1872,^{220,221} although, it was not until 1964²¹⁴ when the partition coefficient (LogP) was standardised as using octanol and water. The LogP measures the intrinsic lipophilicity of the unionised form. However, in drug discovery, the varied pH conditions within the body, such as the fasted stomach (pH 2.7) and intestine (pH 6-8),²²² requires the lipophilicity of the ionised forms to be accounted for. In this procedure, the distribution coefficient (LogD) measures the effective lipophilicity between octanol and a buffered solution at any defined pH. However, distributing between octanol and water is time consuming, therefore, more high through-put methods of measuring LogD, chromatographically (ChromLogD), have been developed using high performance liquid chromatography (HPLC).²²³

Measured ChromLogD values are important in medicinal chemistry optimisation. Minimising ChromLogD has effects on improving solubility, reducing plasma protein binding and minimising intrinsic clearance.²²³ However, the reduced lipophilicity must be balanced with the potential detrimental effects on permeability with hydrophilic molecules.

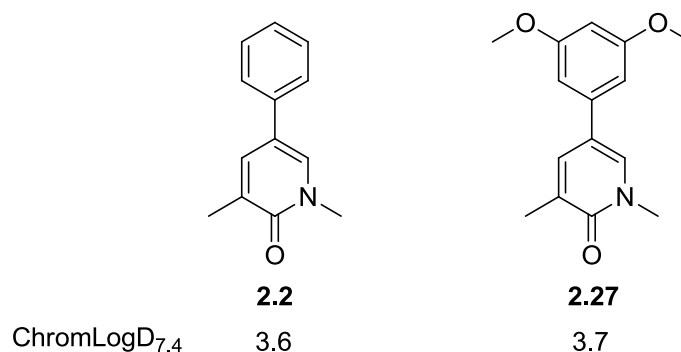


Figure 2.9: Two key compounds from the fragment optimisation and their measured ChromLogD_{7.4}

Overall, fragments, **2.2** and **2.27** have reasonable physical properties (Figure 2.9). However, once the large, lipophilic ESM group is added, it was anticipated that the physical properties of the substituted molecule might require further optimisation. Hence, it was thought that minimising the lipophilicity of the BET active fragment would be advantageous. One common way of modulating physicochemical properties is to replace relatively lipophilic phenyl rings with more polar heterocycles, such as pyridine. However, this must be done without significant loss of binding potency. To understand the potential for introducing nitrogen atoms into the phenyl ring of **2.2**, a range of heterocycles were investigated. The various possible isomers of pyridine were profiled to elucidate where polar functionality can be accommodated and the potential effect on ChromLogD_{7.4}. Integrating an additional nitrogen, in the case of a pyridine, is predicted, using *in silico* modelling, to reduce the cChromLogD_{7.4} from 3.6 to between 1.0 and 2.0 (Figure 2.10), thus potentially paving the way for ESM iBET analogues with improved physicochemical properties to be synthesised.²²⁴

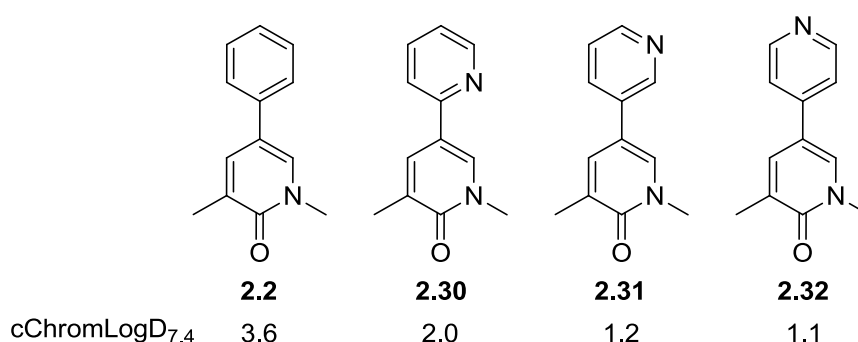
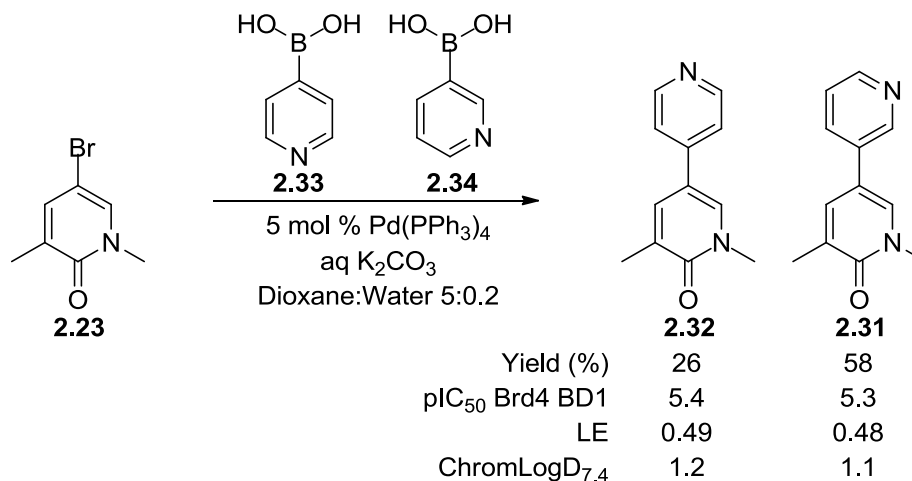


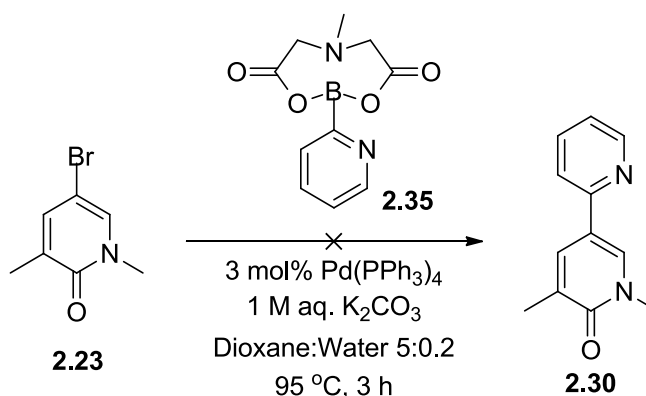
Figure 2.10: Comparison of 2.2 with pyridyl and pyrimidyl compounds

Due to the promising *in silico* modelling, all three pyridine isomers were selected to validate the use of 6-membered nitrogen containing heterocycles to replace the phenyl ring. The different isomers would be synthesised to investigate the optimal position for the nitrogen to be incorporated.



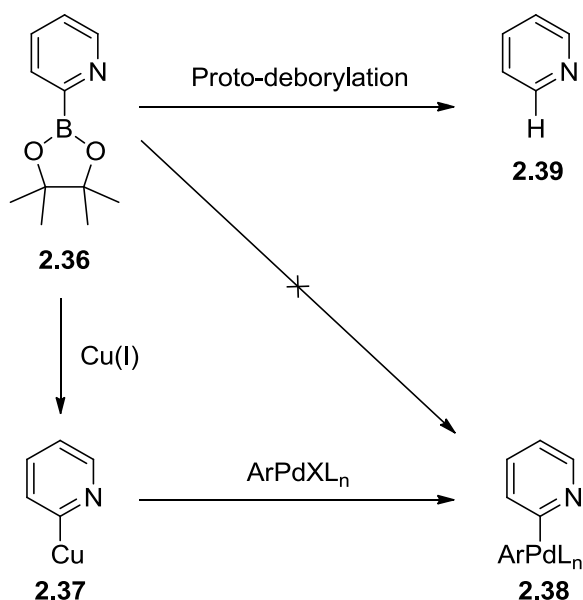
Scheme 2.5: Initial pyridyl Suzuki coupling reactions

Under standard Suzuki conditions, the 3- and 4-pyridyl compounds were isolated in low to moderate yield (Scheme 2.5), providing sufficient material for the compounds to be tested in the Brd4 BD1 biochemical assay. The two pyridine isomers were equipotent, with a similar potency to that of the phenyl analogue **2.2** (pIC₅₀ 5.5), also maintaining the LE compared to the phenyl analogue (LE 0.5). However, when synthesis of the 2-pyridyl **2.30** analogue was attempted under the same conditions, using the stabilised MIDA boronate,²²⁵ no desired product was observed (Scheme 2.6).



Scheme 2.6: Initial attempt of 2-pyridyl Suzuki coupling

Investigation of the relevant background literature revealed various modified conditions to successfully carry out palladium cross-couplings with 2-pyridyl boron species.^{226,227,228} An important modification is the use of copper.²²⁷ This acts to transmetalate into the carbon-boron bond forming **2.37**, stabilising the 2-pyridyl species, before palladium transmetalation **2.38** (Scheme 2.7).



Scheme 2.7: Stabilisation of the pyridyl boron species with copper

From the literature, it was seen that DMF is the solvent of choice for many of these procedures, however, the palladium species, ligand and copper source are variable. Given the perceived instability of 2-pyridyl boronic acids, the corresponding boronic ester **2.36** is widely used in 2-pyridyl Suzuki couplings, along with, more recently, the MIDA boronate **2.35**.²²⁶ It was therefore decided that a range of reaction systems would be investigated with a view to synthesising compound **2.30**. Conditions chosen for this investigation are shown in Table 2.5 and the results summarised in Table 2.6.

Conditions	Boron species	Pd source	Ligand	Cu source	Base	Solvent	Additive
A ²²⁸	Ester	Pd(OAc) ₂	S-phos	Cu(I)Cl	CsCO ₃	DMF	-
B ²²⁶	MIDA	XphosPdcycle	-	Cu(II)OAc	K ₃ PO ₄	DMF	DEA
C ²²⁷	Ester	Pd(OAc) ₂	dppf	Cu(I)Cl	CsCO ₃	DMF	-

Table 2.5: Conditions used to test 2-pyridyl Suzuki coupling on bromopyridinone 2.23

The procedure followed for conditions A resulted in a complete reaction after two hours as judged by LCMS. Therefore, to treat the three reactions equally, the reaction mixtures were analysed by LCMS at this time point. Indeed, reaction C was also seen to have reached completion, despite the literature procedure suggesting a 16 hour reaction time.²²⁷ Reaction A and C were purified by column chromatography yielding reasonable to good quantities of product.

Conversely, the reaction using the MIDA boronate was seen to proceed sluggishly. The reaction was therefore stirred for a total of 24 hours. Despite the extra time allowed for this reaction to reach completion, the reaction had progressed little more than it had after the two hour time point. At this point, the reaction was also worked up, with the aim of isolating both the starting material and product. The crude material was purified by column chromatography using the same gradient as with conditions A and C. Despite this, no product was collected, with only 36% starting material being reisolated. The product is likely to be more UV active than the starting material, so the quantity of product within the mixture was likely to have been small. A peak relating to the proto-debrominated by-product was observed which may constitute a portion of the remaining mass balance.

Conditions	LCMS area (%)	Isolated yield (%)
A	87	72
B	21 (product) 43 (starting material)	- 36 (starting material)
C	92	61

Table 2.6: Observed yields under each set of reaction conditions

The reaction using the MIDA boronate may have been poor due to the slower generation of the active boronic acid *in situ*. This is especially true with the addition of DEA to the reaction, adding an additional step to acid generation.

With a robust experimental procedure in hand, the pyridyl product **2.30** was tested in the biochemical assay and, pleasingly, was found to have a similar potency to the phenyl derivative. Consequently, the LE was also maintained from **2.2** to **2.30**. This is encouraging considering the 1.8 unit difference in measured ChromlogD_{7.4} observed between these compounds (Figure 2.11). Therefore, inclusion of an additional nitrogen at all positions around the ring to lower the lipophilicity is possible within this template.

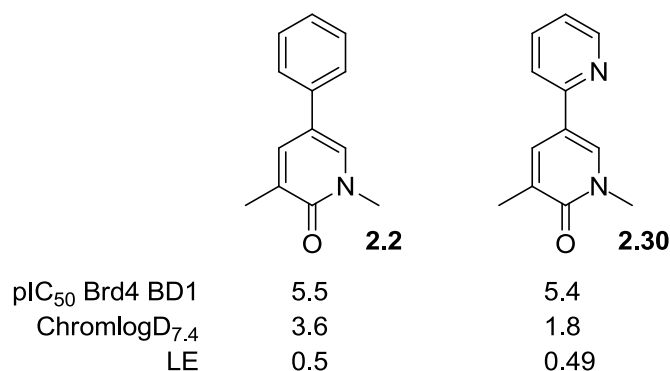
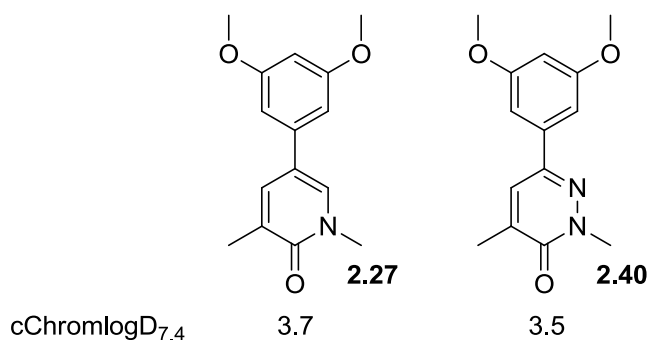


Figure 2.11: Comparison of 2-pyridyl 2.30 back to phenyl 2.2

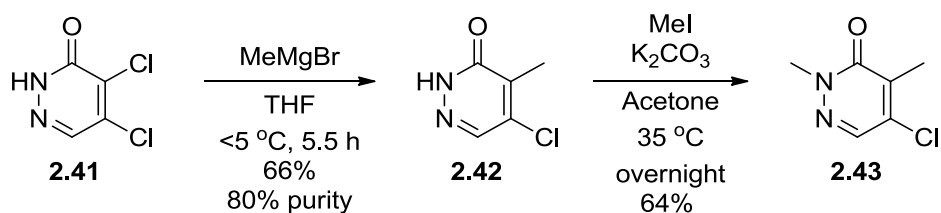
2.3.3 Reducing Lipophilicity via the Acetyl Lysine Mimetic

In a further attempt to understand the potential to reduce the lipophilicity of these molecules, attention turned to the pyridone acetyl lysine mimetic moiety. In a similar fashion as described before, the aim was to substitute one of the ring carbons for a nitrogen (Figure 2.12) envisaging that this would result in a decreased LogD. *In silico* modelling predicted a small decrease in cChromlogD_{7.4} for compound **2.40** compared to previously synthesised **2.27**.

Figure 2.12: Comparison of calculated ChromlogD_{7.4}

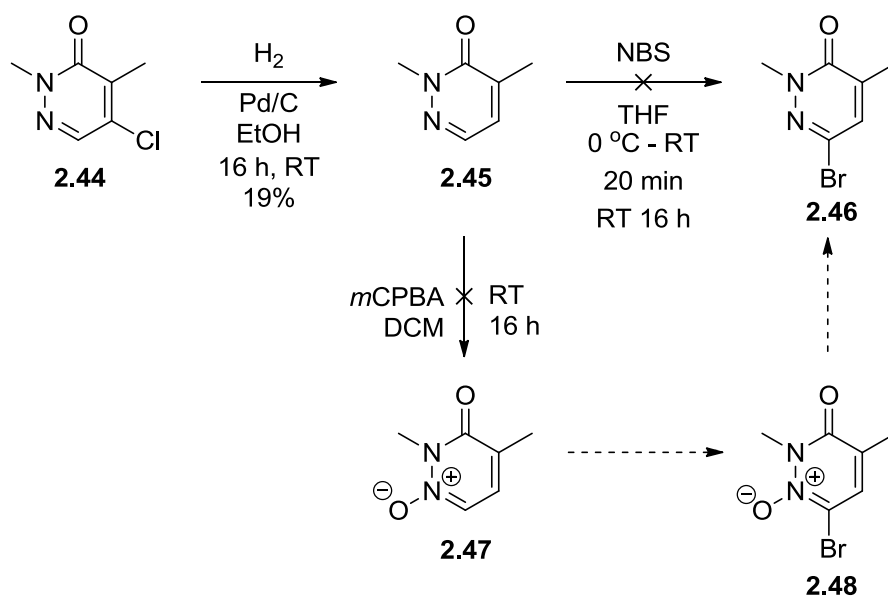
Initially, the synthesis of the key intermediate 6-bromopyridazinone (**2.46**, Scheme 2.9) was investigated. The first two steps of the proposed synthesis of this compound would be similar to those of previous studies within our laboratory (Scheme 2.8).²²⁹ The first step uses methylmagnesium bromide to selectively alkylate the 4-position of **2.41**. The first equivalent deprotonated the pyridazinone **2.41**, observed with an exotherm controlled with a salt/ice bath, with the second completing the desired reaction. The crude product **2.42** from this reaction was used in the subsequent *N*-methylation reaction. The positioning of the methyl group was

confirmed by NMR, with the *N*-methyl carbon appearing around 40 ppm in the ^{13}C spectrum.



Scheme 2.8: Initial two methylation reactions

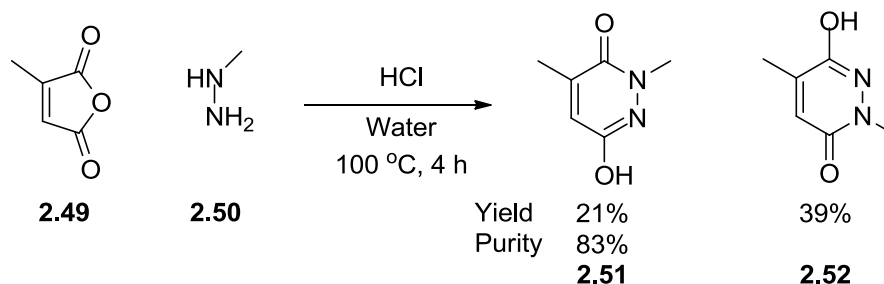
From compound **2.43**, the route diverged from the previous synthesis.²²⁹ The aim was to functionalise in the 6-position rather than the 5-position, the current position of the chlorine. A low yielding hydrogenolysis of the chlorine led to compound **2.45** (Scheme 2.9). This compound was treated with NBS (Scheme 2.9), however, no reaction was observed with this substrate. A literature search revealed the necessity of using the pyridazinone *N*-oxide **2.47** in order to brominate the 6-position, to promote the electrophilic aromatic substitution.²³⁰ However, the common oxidising agent, *m*CPBA, was ineffective in this transformation (Scheme 2.9), with only the starting material observed in the reaction mixture.



Scheme 2.9: Hydrogenolysis and attempted bromination and oxidation

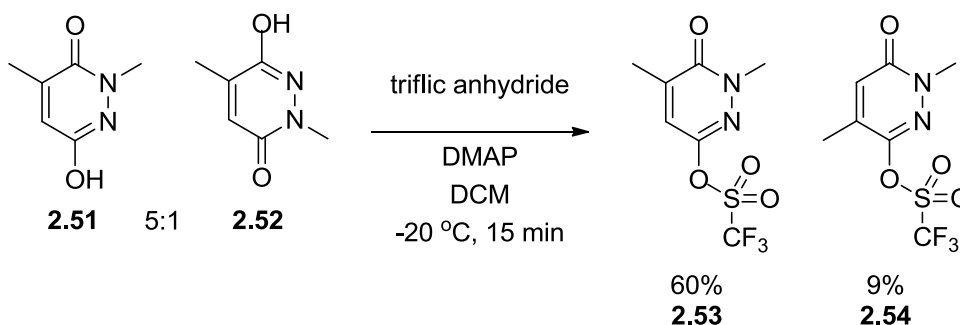
Based on the lack of preparative success detailed above, a new route was required to the desired motif. A procedure was found in the literature which utilised citraconic

anhydride (**2.49**) and methyl hydrazine (**2.50**).²³¹ As expected and previously reported, a mixture of regioisomers was formed from this reaction (Scheme 2.10).



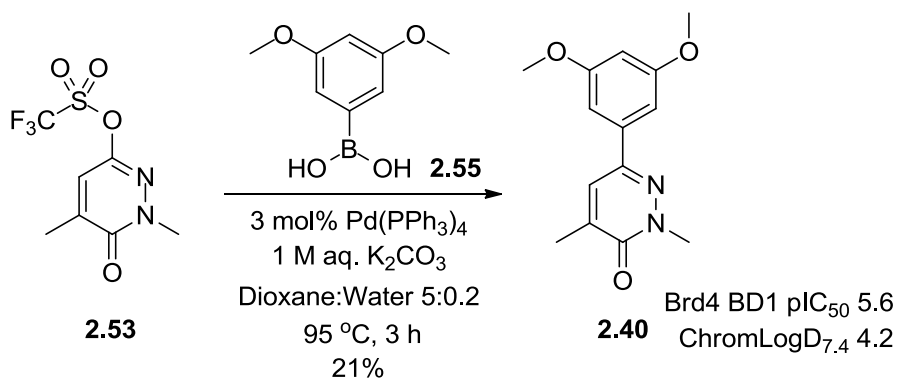
Scheme 2.10: Reaction of citraconic anhydride with methylhydrazine

However, as clearly stated in the procedure, the two products have distinguishable solubilities, with the undesired isomer **2.52** having poorer solubility in water.²³¹ The desired product **2.51** was isolated containing minimal quantities of the undesired isomer. This material was used in the next step, formation of the corresponding trifluoromethanesulfonate (Scheme 2.11).²³² This group is described as a pseudo-halogen because of its usefulness as a leaving group. In this programme, it was to be used within the Suzuki cross-coupling reaction.



Scheme 2.11: Formation of the triflate

On formation of the triflate, which was less polar than the free alcohol, the isomers were successfully separated by column chromatography. The resulting desired triflate **2.53** was reacted with dimethoxyphenyl boronic acid (**2.55**) under Suzuki coupling conditions (Scheme 2.12). This gave the desired compound **2.40** in low yield. The compound, nonetheless, was tested within the bromodomain biochemical assay.



Scheme 2.12: Coupling of the pyridazinone triflate 2.56 with boronic acid 2.58

The potency of **2.40** within the Brd4 BD1 biochemical assay was lower than anticipated at 5.6. Additionally, in comparison with **2.27**, compound **2.40** was 5-fold less potent (Figure 2.13). This may be due to the more electron-deficient nature of the pyridazinone ring having a detrimental effect on the key hydrogen bonding interactions within the acetyl lysine binding pocket.

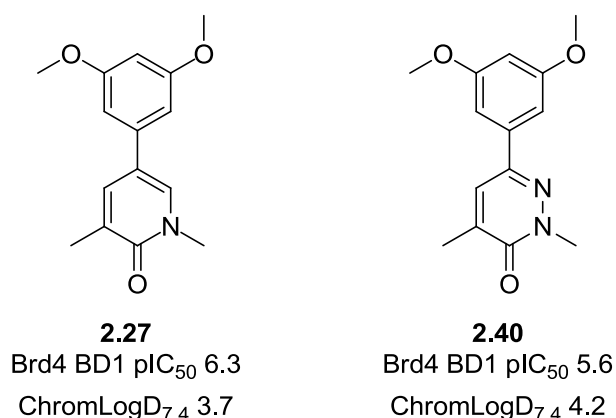


Figure 2.13: Comparison of pyridone 2.27 with pyridazinone 2.40

In addition to this, the pyrazinone derivative **2.57** was synthesised in an alternative series (Figure 2.14) elsewhere within in our laboratory.²³³ Unfortunately, compound **2.57** had a disappointing potency within the Brd4 biochemical assay with a log unit decrease compared to the parent compound **2.56**. Surprisingly, neither of these compounds showed a significant reduction in ChromLogD_{7.4}, and in the case of the pyridazinone, **2.40**, the measured ChromLogD_{7.4} was higher than the parent pyridinone **2.27**. Therefore, without the desired decrease in lipophilicity to balance the decrease in potency, these acetyl lysine mimetic modifications did not have the desired effect and further investigation into this sub-set of the series was abandoned.

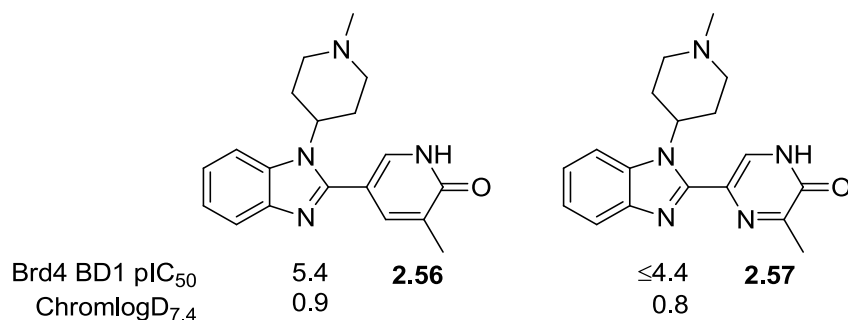


Figure 2.14: Pyrazinone derivative compared to pyridone in a related series²³³
 *2.57: pIC₅₀ <4.3 on 1 of 2 test occasions

The initial aim of this investigation, to explore the scope of introducing additional heteroatoms to reduce the ChromlogD_{7.4} was successful. Chemistry was enabled to synthesise the more challenging 2-pyridyl compounds which, along with the 3- and 4-pyridyl, had similar potency to the initial phenyl fragment **2.2**. With the 1.6 log unit decrease in lipophilicity whilst maintaining biochemical potency, these compounds offer a viable alternative to the simple phenyl ring. The pyridazinone compound **2.40** was also synthesised after successful route optimisation, however, this delivered a less than desirable physicochemical outcome.

Therefore, from these fragment investigations, the phenyl substitution investigated in the first instance was not carried forward. However, the initial fragment and pyridyl examples were deemed suitable for incorporation of the amino acid ester, esterase sensitive motif (ESM).

2.4 ESM Incorporation

2.4.1 Phenyl Pyridone Fragment

Prior to the commencement of this body of work, the leucine-based ESM group was attached to this fragment within our laboratory to investigate the initial validity of the strategy.²³³ The ESM-functionalised dimethylpyridone (**2.58a**) showed no decrease in potency compared to corresponding fragment **2.2**, however, the acid **2.59a** was only weakly active (Figure 2.15). This represented an area for further understanding and optimisation.

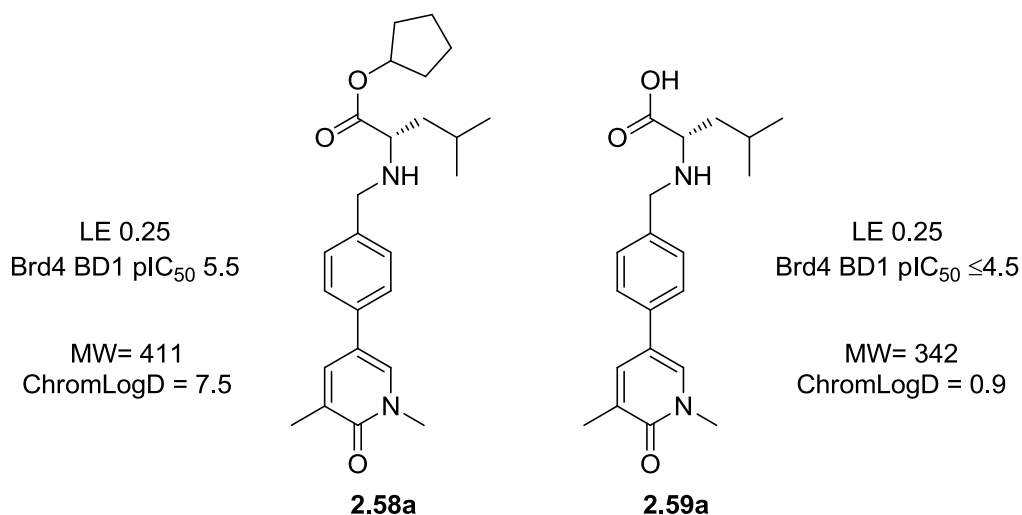


Figure 2.15: Baseline dimethylpyridinone ESM compounds²³³
 *2.59a: pIC₅₀ <4.3 on 2 of 3 test occasions

The ESM, *para* to the pyridone is thought to be directed through the tight ZA channel region which contains a network of water molecules. The direction of the ESM through the ZA channel was observed in a model of proposed compound **2.58e** in Brd4 BD1 (Figure 2.16).

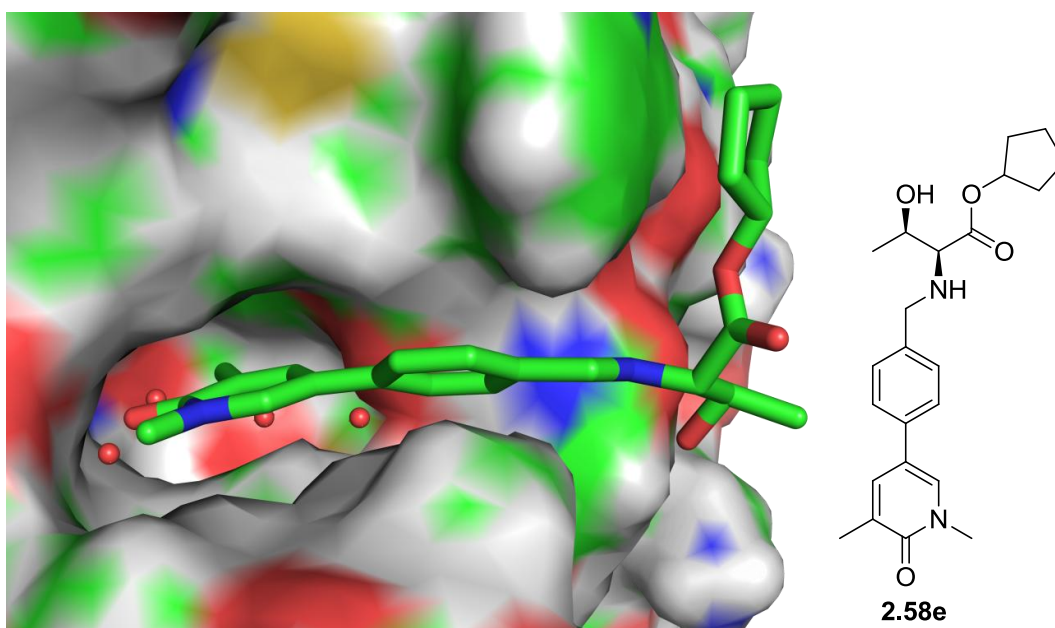


Figure 2.16: Model of ESM-functionalised compound 2.58e in Brd4 BD1

Hence, a number of alternative amino acids were chosen to investigate a potentially more optimal ESM for this template than the commonly used leucine amino acid. To this end, compounds with the general structure **2.60**, shown in Figure 2.17, were identified for synthesis.

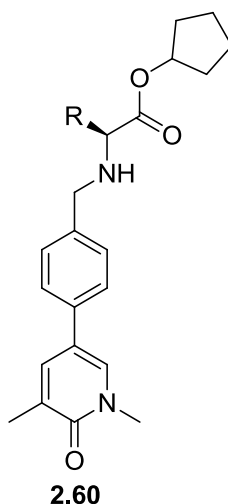


Figure 2.17: General structure 2.60

Firstly, it was hypothesised that reducing the size of the alkyl side chain, from the leucine (**2.61**) previously used, to valine (**2.62**) and alanine (**2.63**) (Figure 2.18) might offer some insight into the steric requirements of this position of the protein.

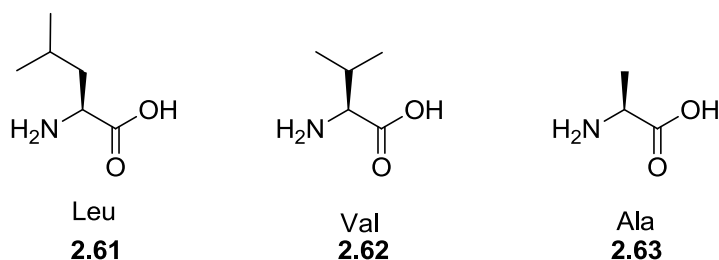


Figure 2.18: Amino acids with alkyl side chains

Also, due to the water network within the ZA channel, more polar side chains were considered. It was proposed that a hydroxyl side chain may be able to contribute to the hydrogen bonding network present in this part of the protein. Additionally, both serine (**2.64**) and threonine (**2.65**) would be used to investigate any potential role of steric bulk in this region of the BET proteins (Figure 2.19).

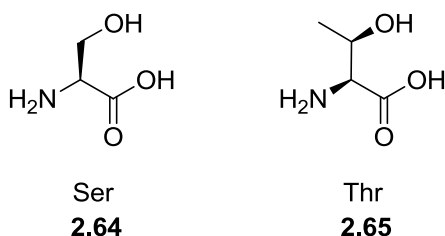
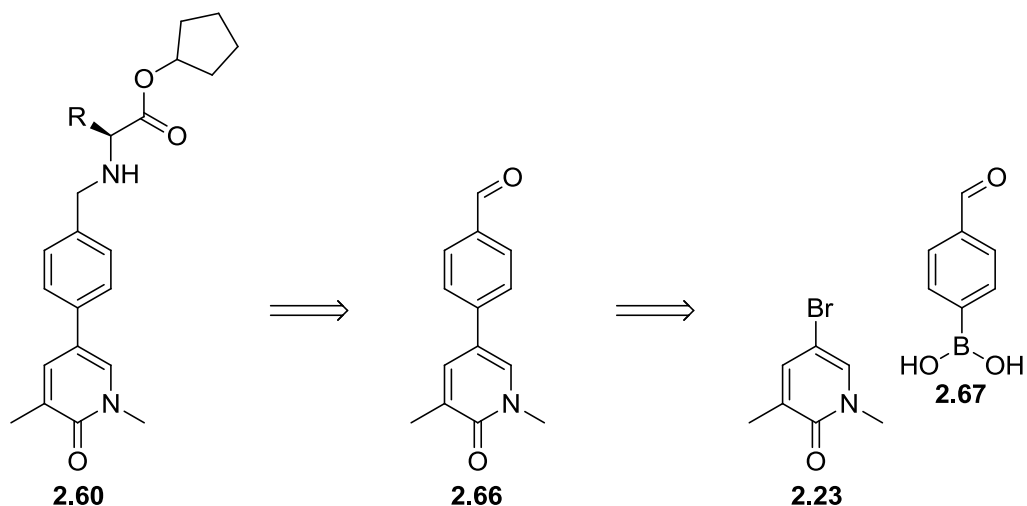
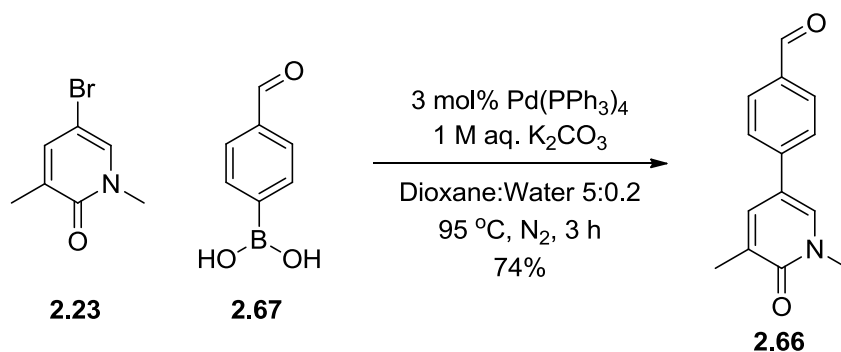


Figure 2.19: Polar, hydroxyl containing amino acids

To synthesise such compounds, a retrosynthesis was proposed (Scheme 2.13). The ESM-functionalised BET inhibitor **2.60** could be disconnected to aldehyde **2.66**, which could be made from the benzaldehyde boronic acid **2.67** and the previously used bromopyridone **2.23**. The four amino acids, valine, alanine, serine and threonine were used initially as their cyclopentyl esters.

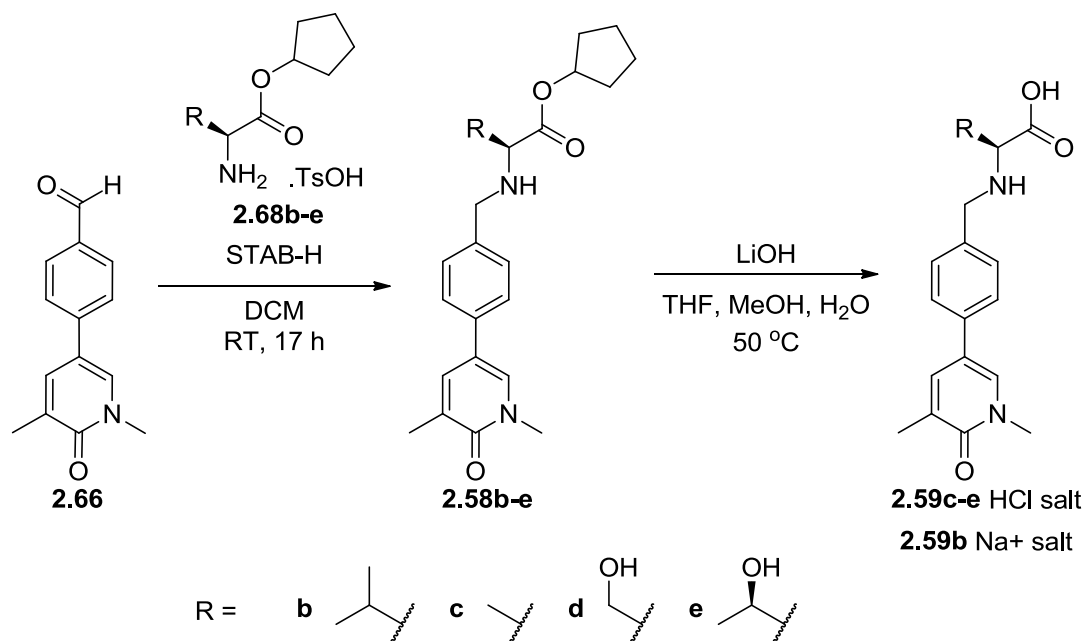
Scheme 2.13: Retrosynthesis of **2.60**

To initiate the synthesis of alternative amino acid ester containing molecules **2.60**, the bromodimethylpyridone intermediate **2.23** was coupled with benzaldehyde boronic acid **2.67** under the previously used Suzuki cross-coupling conditions (Scheme 2.14). This key intermediate **2.66** was isolated in good yield after precipitating from the reaction mixture, on addition of water during work-up.

Scheme 2.14: Synthesis of benzaldehyde intermediate **2.66**

The conditions to couple the amino acid ester toic acid salts to alternative aldehyde derivatives was investigated within our laboratory.²³⁴ It was found that two equivalents of the amino ester gave good yields, while using the toic acid salts of

these substrates prevented any need to add extra acid. These optimised conditions were utilised and yielded the desired products **2.58b-e** in good yields (Scheme 2.15) to complement the previously synthesised **2.58a**.



Scheme 2.15: Reductive aminations using optimised conditions and subsequent ester hydrolysis

The resulting esters were hydrolysed using lithium hydroxide and, after purification and treatment with aqueous hydrochloric acid, the products were isolated as the hydrochloride salts in good to excellent yields (Scheme 2.15). Interestingly, the valine derivative **2.58b** showed a very slow reaction rate, requiring a large excess of base. This observation was typical to similar valine ESM compounds within our laboratory.²³⁵ This may be due to valine having increased restricted rotation of the side chain and, subsequently, more steric hinderance around the carbonyl group.²³⁶ Also, the formation of the hydrochloride salt of the valine derivative proved problematic. As a result, the sodium salt was produced and isolated.

The products from these reductive aminations and the subsequent ester hydrolysis products were tested for inhibitory activity against Brd4. The yields and biological results are shown in Table 2.7. Having isolated the products in moderate to good yield, esters **2.58a-e** are all equipotent with a Brd4 BD1 pIC₅₀ around 5.5. Additionally, the acids are also all equipotent, whilst being consistently around 1 log unit less potent than the parent ester.

Amino acid side chain (R)	Cyclopentyl Ester (2.58)					Acid (2.59)				
	Leu (a)	Val (b)	Ala (c)	Ser (d)	Thr (e)	Leu (a)	Val* (b)	Ala (c)	Ser (d)	Thr (e)
Yield (%)	-	45	73	83	76	-	51	88	67	69
Brd4 BD1	5.5	5.7	5.6	5.5	5.7	≤4.5**	4.8	4.6	4.7	4.6

Table 2.7: Biochemical results of varied ESM compounds (*sodium salt)
****2.59a: pIC₅₀ <4.3 on 2 of 3 test occasions**

The initial results suggest that the ZA channel is capable of accommodating a variety of amino acid side chains, with similar biochemical potencies being achieved across all derivatives. However, there is no evidence of gaining a hydrogen bonding interaction with the addition of the hydroxyl group in serine and threonine, when compared to alanine and valine. Unfortunately, the corresponding acids all have low biochemical potencies at Brd4 BD1 and, consequently, a significant drop-off in potency is observed going from the ester to acid, indicating the acid is not optimally placed in the protein. Despite this, the esters were tested within the human whole blood assay. This measures the inhibition of MCP-1 release by cells of the monocyte lineage, when stimulated with LPS. In this project the results from this assay depend upon hCE-1 hydrolysis rate, cell permeability and overall BET potency.

A typical profile was seen with the lead compound **2.69** within our laboratory at the time of this work (Figure 2.20, Table 2.8).²³⁷ Despite the cyclopentyl compound **2.69** having modest biochemical potency, the human whole blood results show an enhancement in potency. This is particularly striking as compounds typically demonstrate a loss of potency within the human whole blood assay. This is due to whole blood containing a number of biological barriers that a compound must first overcome before reaching the intracellular BET proteins. This is an example of the beneficial effect of including an ESM within this molecule where by the cyclopentyl ester is being hydrolysed to the acid which is in high concentration at the site of action. In comparison, the more stable *t*-butyl ester **2.70** shows a more standard drop-off in whole blood potency because of the inability of the *t*-butyl ester to be converted to the retained acid by hCE-1.

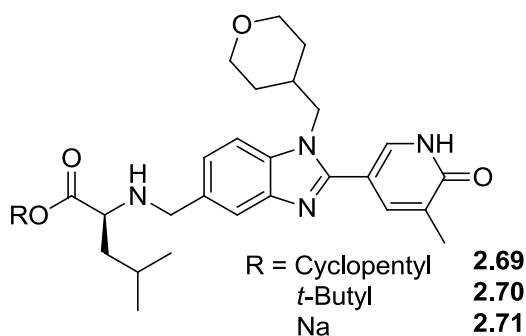


Figure 2.20: Scaffold of lead compound

Ester (R)	Cyclopentyl (2.69)	t-Butyl (2.70)	Na (Acid) (2.71)
Biochemical Brd4 BD1 pIC ₅₀	6.1	6.1	5.8
hWB _{DPU} (MCP-1) pIC ₅₀	7.5	5.8	<5.0
ΔpIC ₅₀	+1.4	-0.3	-
ChromLogD _{7.4}	5.4	5.3	0.6
Solubility	185	≥282	≥189
AMP	380	370	<3

Table 2.8: Biochemical and hWB profile of lead compound 2.69

The whole blood results for esters **2.58a-e** (Figure 2.21) are shown in Table 2.9.

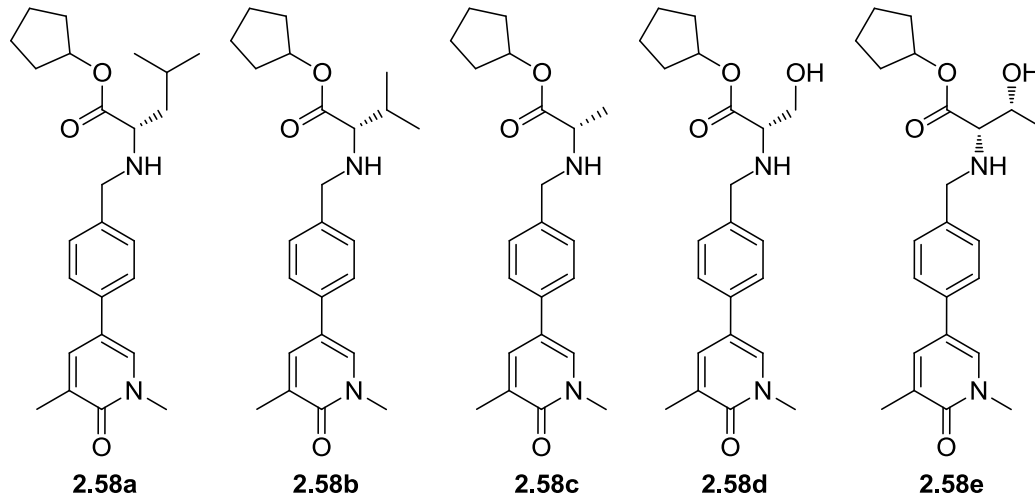


Figure 2.21: Esters submitted for whole blood studies

Compound	2.58a	2.58b	2.58c	2.58d	2.58e	2.2
Biochemical Brd4 BD1 pIC ₅₀	5.5	5.7	5.6	5.5	5.7	5.5
hWB _{DPU} (MCP-1) pIC ₅₀	5.8	5.9	6.2	6.4	6.5	5.2
ΔpIC ₅₀	+0.3	+0.2	+0.6	+0.9	+0.8	-0.3
ChromLogD _{7.4}	7.5	7.1	5.2	3.7	4.4	3.6

Table 2.9: The effect on MCP-1 hWB potency on changing the ESM

From the data in Table 2.9, it can be seen that all these molecules have measurable potencies in whole blood, despite their low BET biochemical potency. Indeed, non-ESM-containing compounds with Brd4 BD1 potencies of less than 6.0 typically have a low or undetectable whole blood potency, such as the non-ESM control compound, **2.2**. This is because plasma protein binding and membrane permeability restrict the quantity of compound available at the intracellular target. Conversely, ESM-containing compounds **2.58a-e** have pleasing whole blood potencies, however, the most promising compounds are those where the ESM is based on the hydroxyl containing amino acids (**2.58d** and **2.58e**). These two compounds have around one log unit increase in potency in this cell assay compared to their biochemical potency, despite both the ester or acid molecules synthesised above having identical BET biochemical potencies. The corresponding hydroxyl containing acids are significantly more polar compared to the compounds without the hydroxyl, hence, there may be less compound able to cross the membrane, back out of the cell, aiding cell retention at the site of action. Despite the acid of these compounds having low biochemical potency, the whole blood potencies are very promising, with a ΔpIC₅₀, the enhancement from biochemical to whole blood potency, nearing that of compound **2.69**. Indeed, comparing compound **2.2** with **2.58e**, the value of the ESM can be seen: for the same level of BET inhibition, a 25-fold increase in efficacy within human whole blood can be achieved (Figure 2.22). By extension, this exciting result suggests that up to 25-fold improvement in TI could be achieved using this approach.

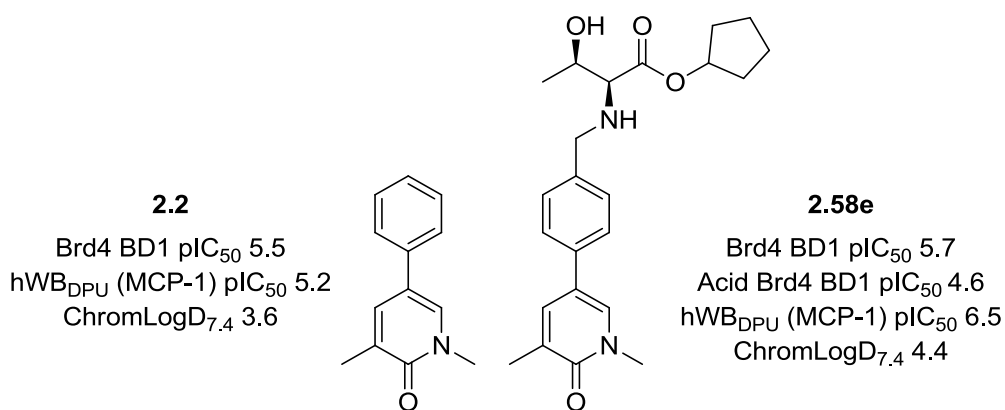


Figure 2.22: ESM-functionalised compound 2.58e and fragment 2.2

Compound **2.58e** (Figure 2.22), containing the threonine amino acid ester, provided a good whole human whole blood potency coupled with an excellent Δ pIC₅₀. However, despite using the more polar hydroxyl-containing side chain, the ChromLogD_{7.4} is higher than desired within the TPP.

To mitigate this observation, the potential of using a pyridyl core aromatic ring was re-examined. A summary of the previous findings are highlighted in Figure 2.23, comparing compounds **2.30**, **2.31**, and **2.32** to fragment **2.2**. The more solvent exposed nitrogen of the 3- and 4-pyridyl isomers (**2.31** and **2.32**, respectively) had the lowest lipophilicities. In addition to this, the 2-pyridyl isomer **2.30** showed a 1.8 log unit decrease in LogD value, relative to fragment **2.2**. Pleasingly, the three pyridyl isomers were equipotent within the Brd4 BD1 biochemical assay compared to the phenyl compound **2.2**.

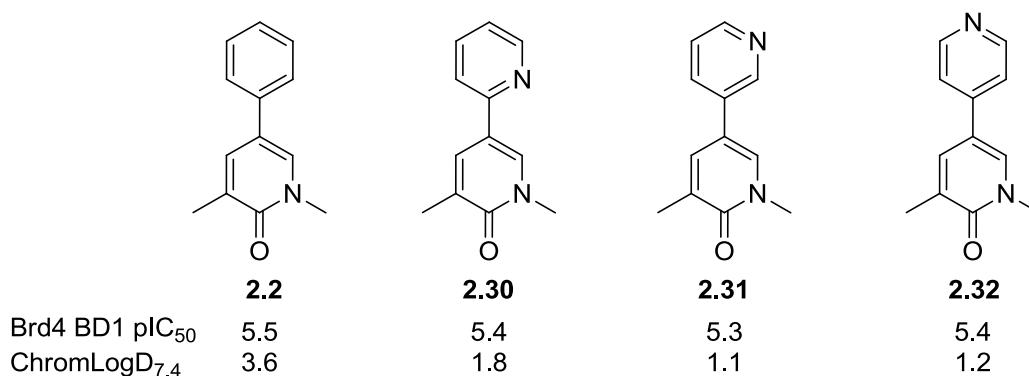


Figure 2.23: Three pyridyl isomers compared to phenyl example 2.2

Comparing these results, all three isomers were beneficial in reducing ChromLogD_{7.4}, relative to **2.2**. With this result and the regiochemistry of ESM attachment in mind, both the 2- and 3-pyridyl isomers (Figure 2.24) were proposed

as cores to be functionalised with the ESM. Computational prediction of lipophilicity (cChromLogD_{7.4}) for threonine ESM-functionalised pyridyl compounds compared favourably with the calculated value for compound **2.58e**, supporting the hypothesis for synthesising these analogues. The 2-pyridyl **2.72e** and 3-pyridyl **2.73e** compounds were predicted to reduce the overall lipophilicity by more than one log unit, with cChromLogD_{7.4} values of 3.3 and 3.0, respectively. Should these predicted values translate into measured ChromLogD_{7.4} values, this would represent a positive evolution relative to **2.58e**, provided associated properties, such as BET biochemical and human whole blood potencies, were at least maintained.

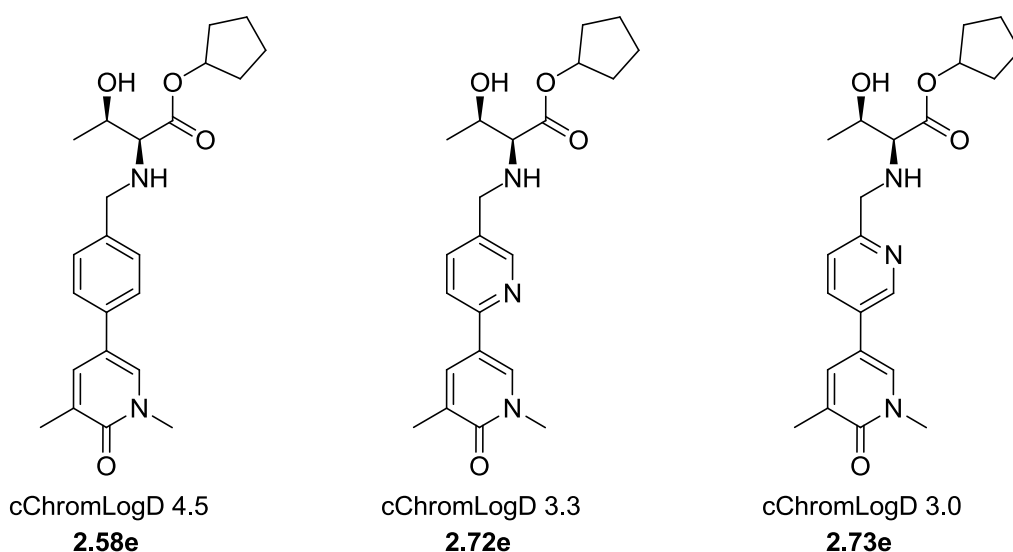
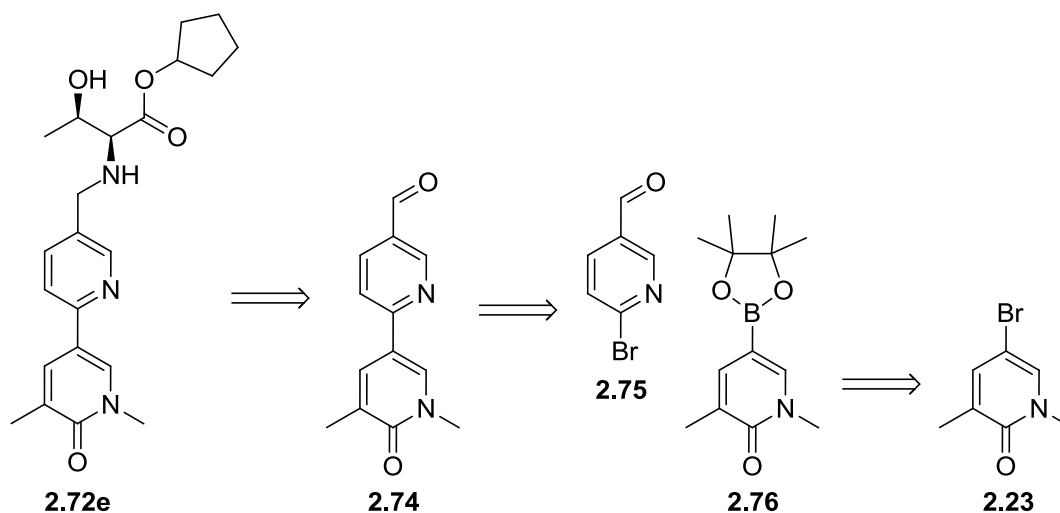


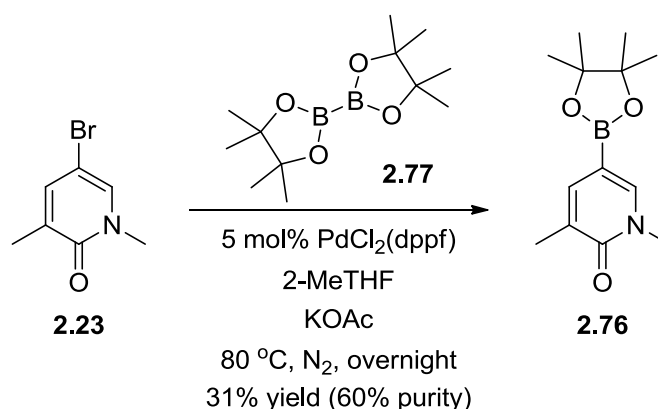
Figure 2.24: ESM functionalised pyridyl compounds

2.4.2 Synthesis of Pyridyl Core Replacements

A retrosynthetic analysis was performed for the 2-pyridyl example **2.72e** (Scheme 2.16). The desired ESM-functionalised compound could be made from aldehyde **2.74** via reductive amination with the appropriate amino acid ester. A Suzuki cross coupling could form the desired bi-aryl bond using pyridone boronic ester **2.76**, which could itself be formed from the available bromo pyridone **2.23**.

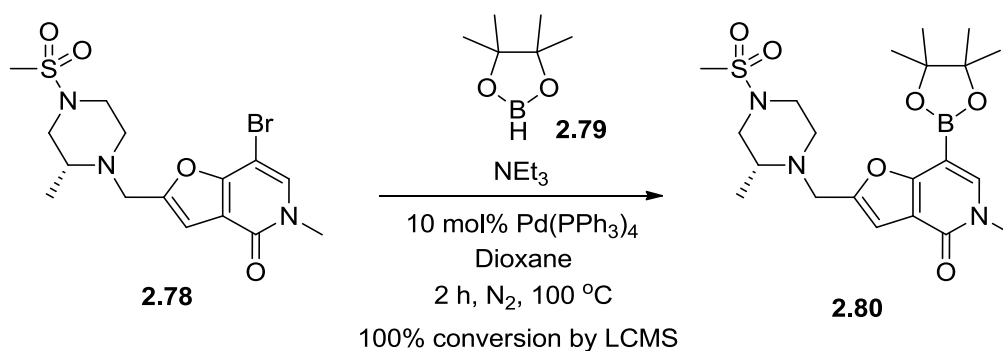
Scheme 2.16: Retrosynthesis of pyridyl compound **2.72e**

However, an issue was foreseen with the initial Miyaura²³⁸ boronation of bromopyridone **2.23**. Similar transformations had previously been carried out in both the literature²³⁹ and within our laboratory,²⁴⁰ however, replicating this method had proven to be low yielding and had provided low purity product (Scheme 2.17). A large portion of protodeboronated by-product was also observed with these conditions.



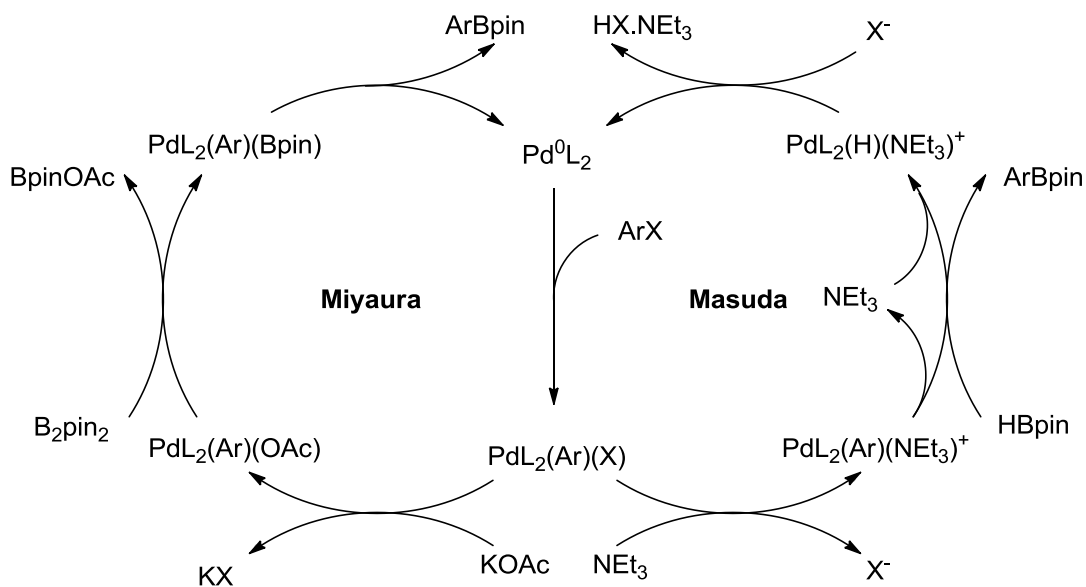
Scheme 2.17: Poor yielding pyridone boronation

Conditions have recently been developed within our laboratory, when synthesising functionalised boronic ester **2.80** (Scheme 2.18),²⁴¹ based on the Masuda boronation.²⁴² The method utilises palladium tetrakis triphenylphosphine alongside six equivalents of both pinacolborane (**2.79**) and triethylamine. Using the newly developed conditions the boron-containing intermediate **2.80** was synthesised within our laboratory with good conversion and used crude in dioxane within the subsequent desired Suzuki reaction.²⁴¹



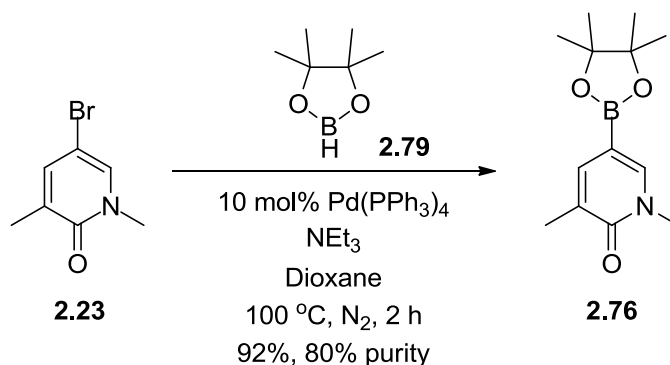
Scheme 2.18: Alternative borylation conditions

These conditions were subsequently used in the synthesis of dimethylpyridone boronic ester **2.76** and proved to be very efficient and much improved over the original procedure. This contrasting palladium activation mechanism, as shown in Scheme 2.19, using triethylamine²⁴³ compared to acetate,²³⁸ may be the basis of the improved reaction profile. During the Miyaura borylation, the acetoxypalladium species undergoes transmetalation with bispinacolatodiboron before reductive elimination forms the desired product. However, using the Masuda procedure, metathesis with pinacolborane is proposed to form the desired product, preventing protodebromination. Reductive elimination reforms the palladium catalyst forming trialkylammonium halide by-product.



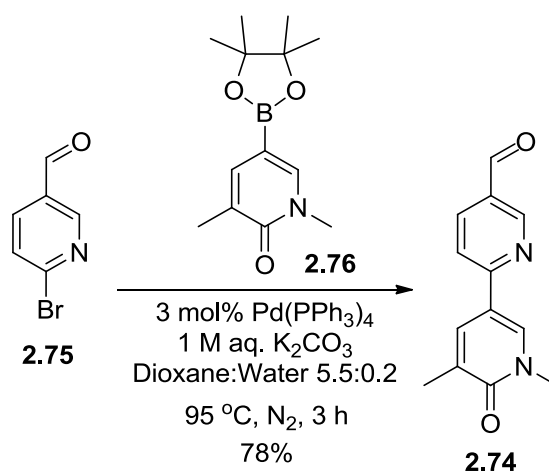
Scheme 2.19: Comparison of Miyaura and Masuda borylation mechanisms

As product **2.76** was previously observed to be stable to chromatography, the compound was purified to good purity, with pinacol being the main residual impurity (Scheme 2.20).



Scheme 2.20: New method for boronic ester formation

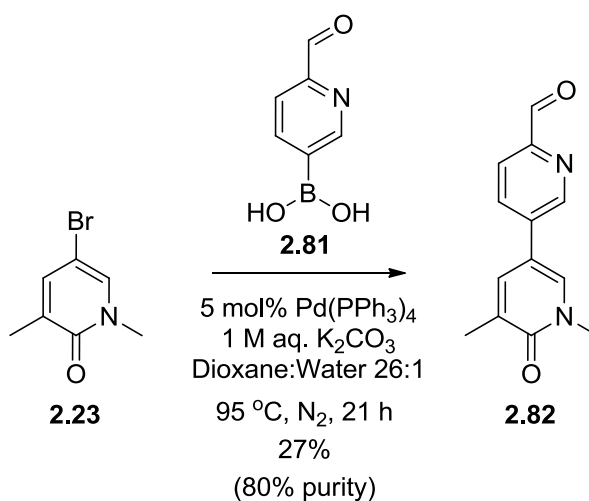
Boronic ester **2.76** was reacted in a Suzuki cross-coupling with commercially available bromo aldehyde **2.75** (Scheme 2.21). The desired pyridyl aldehyde intermediate **2.74** was formed in good yield.



Scheme 2.21: Synthesis of 2-pyridyl aldehyde 2.74

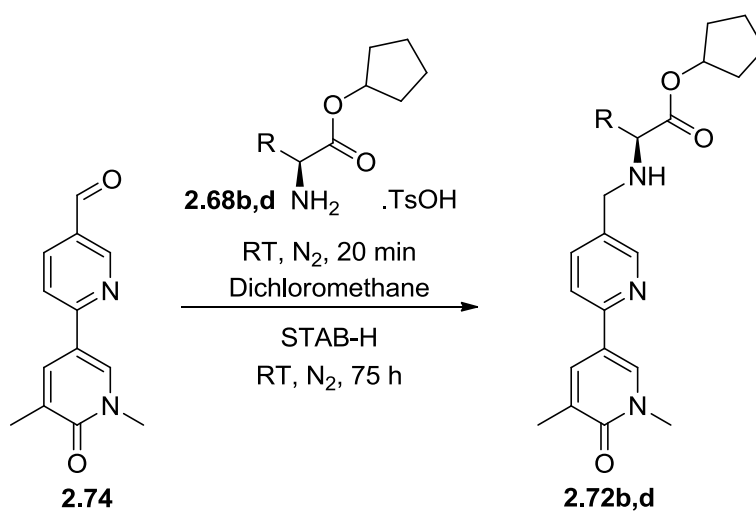
Conversely, the 3-pyridyl aldehyde boronic acid (**2.81**) was commercially available facilitating the cross-coupling with the bromo pyridone **2.23** (Scheme 2.22). The commercial availability of the boronic acid **2.81**, in this case, removed a synthetic step from the reaction sequence. The cross coupling with the 3-pyridyl aldehyde boronic acid **2.81** proved to be poor yielding. Firstly, the reaction proceeded at a much slower rate than other examples using the same conditions. Secondly, a portion of the reduced aldehyde was observed by LCMS. Both observations are

potential evidence of the palladium coordinating between the pyridyl nitrogen and the aldehyde.

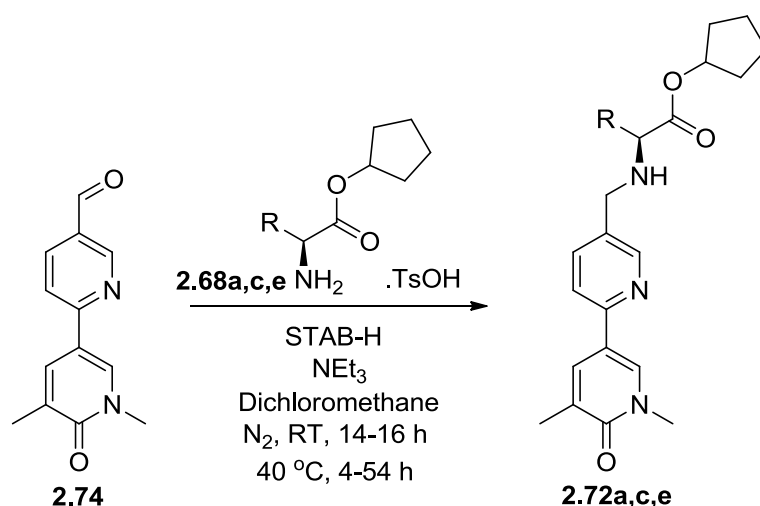


Scheme 2.22: Synthesis of 3-pyridyl aldehyde 2.82

Once the aldehyde intermediates (**2.74** and **2.82**) had been synthesised, the next step was to functionalise both with the ESM. As this template was early in development, five amino acid esters were selected: leucine, valine, alanine, serine and threonine (Scheme 2.23, Scheme 2.24) as before. These particular amino esters were chosen to vary the size of the ESM and to introduce polar hydroxyl groups. Initially, the reductive aminations with aldehyde **2.74** were carried out.



Scheme 2.23: Reductive aminations using 2-pyridyl aldehyde 2.74

Scheme 2.24: Reductive aminations using 2-pyridyl aldehyde **2.74**

The valine **2.72b** and serine **2.72d** derivatives were synthesised using the conditions previously described, within our laboratory, without acid or base additive. However, the leucine, alanine and threonine (**2.72a**, **2.72c** and **2.72e**) derivatives were synthesised with additional triethylamine within the reaction, using general base catalysis, in an attempt to minimise the potential formation of reduced aldehyde by-products.²⁴⁴ From the yields in Table 2.10, the triethylamine does not show enhanced yields for compounds **2.72a**, **2.72c** or **2.72e**.

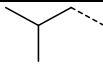
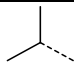
R			Me	OH	OH
	2.72a	2.72b	2.72c	2.72d	2.72e
Yield (%)	58	64	35	37	14
ChromLogD _{7.4}	6.6	6.0	4.2	2.6	3.5
Brd4 BD1 pIC ₅₀	5.3	5.4	5.2	5.1	5.1
hWB _{DPU} (MCP-1) pIC ₅₀	6.6	5.2	5.6	5.6	5.7
ΔpIC ₅₀	1.3	-0.2	0.4	0.5	0.6

Table 2.10: Results for 2-pyridyl esters **2.72a-e**

Pleasingly, esters **2.72c-e** demonstrated lower ChromLogD_{7.4} values relative to lead compound **2.58e** (Figure 2.25). Indeed, the cChromLogD_{7.4} compared favourably with the measured value demonstrating that, in this example, the model of lipophilicity predicts well for synthesised compounds. In terms of Brd4 BD1 potency, compounds **2.72a-e** are equipotent, although lower than the phenyl compound **2.58e** (Figure 2.25). Similarly, the human whole blood potencies are poorer, for

compounds **2.72b-e**, than the pIC_{50} 6.5 of the lead compound **2.58e** (Figure 2.25), which is closer to the target profile. It is noteworthy that compound **2.72a** had a much higher whole blood potency than the other compounds in this series, however, the lipophilicity is very high and moving in the wrong direction for optimisation.

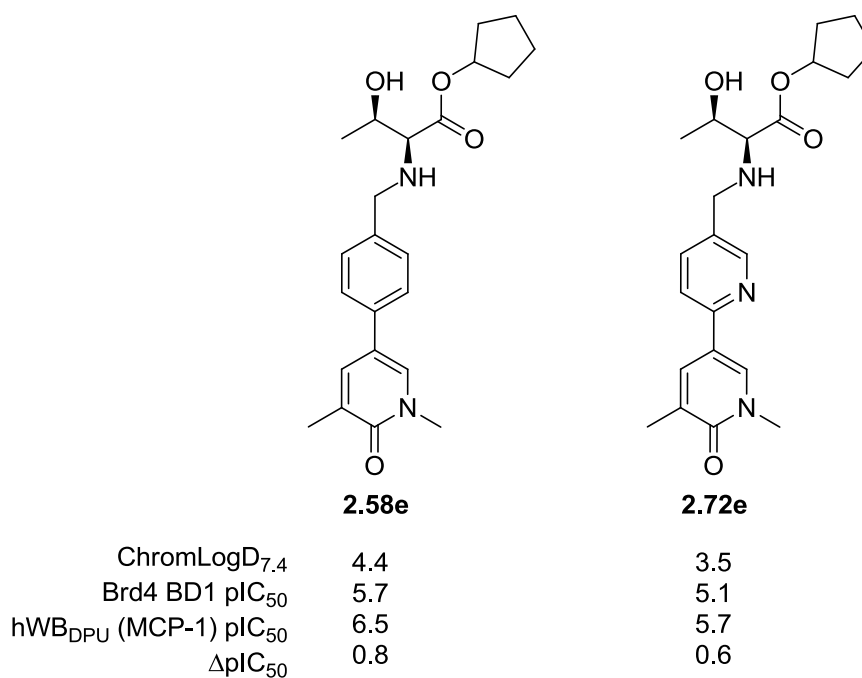
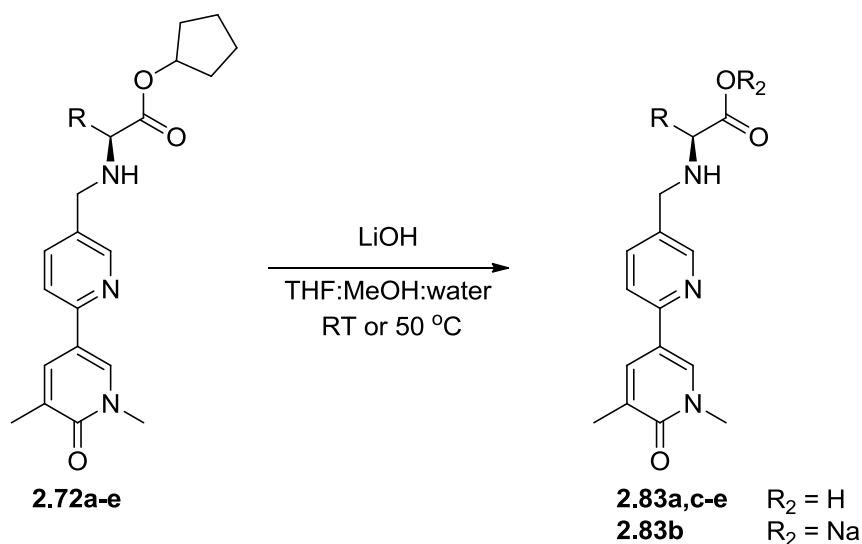


Figure 2.25: Comparison of pyridyl 2.72e with compound 2.58e

To understand the reduced whole blood potencies of these compounds when compared to phenyl derivative **2.58e**, it was hypothesised that the acid potency is key to the whole blood potency, due to its generation within cells. To explore this hypothesis, the corresponding acids **2.83a-e** were synthesised in good yields (Scheme 2.25). Due to the observed insolubility of the leucine and valine derived products in DMSO, different salt forms of these compounds were investigated. Unfortunately, the hydrochloride salts could not be isolated in acceptable purity, as judged by their 1H NMR spectra and these were therefore isolated as the free acid, or the sodium salt, in the case of the valine derivative **2.83b**.



Scheme 2.25: 2-Pyridyl acid generation

The Brd4 BD1 potencies of acids **2.83a-e** proved to be disappointing with a pIC_{50} of 4.5 or lower (Table 2.11). The compounds with alkyl amino acid side chains demonstrate a log unit drop off in potency between the ester and acid, whilst the more polar amino acids are similarly poor.

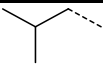
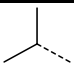
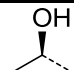
R			Me	OH	
	2.83a	2.83b	2.83c	2.83d	2.83e
Yield	72	71	82	76	72
Salt	-	Sodium	-	-	-
Brd4 BD1 pIC_{50}	<4.3	4.5	<4.3	4.4	4.5

Table 2.11: Results generated for acids **2.83a-e**

As the 2-pyridyl threonine compound **2.83e** was similar in potency to acid **2.83a**, this did not explain the difference in hWB potency observed between their esters **2.72a** and **2.72e**, respectively. To investigate whether a differential hCE-1 hydrolysis profile was driving this difference, **2.72a** and **2.72e** were tested within the specific activity assay using recombinant hCE-1 enzyme. Indeed, these compounds were found to have very different hydrolysis rates (Figure 2.26), mirroring the whole blood enhancements observed for these esters.

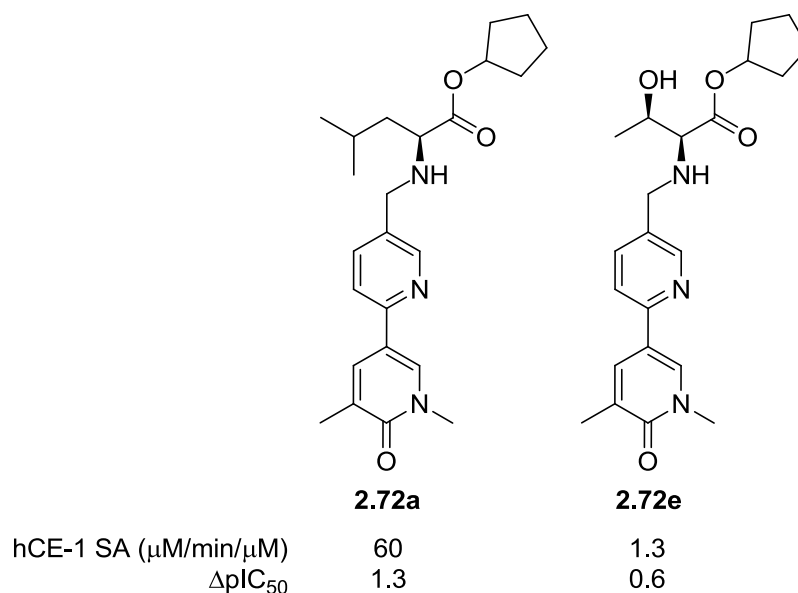
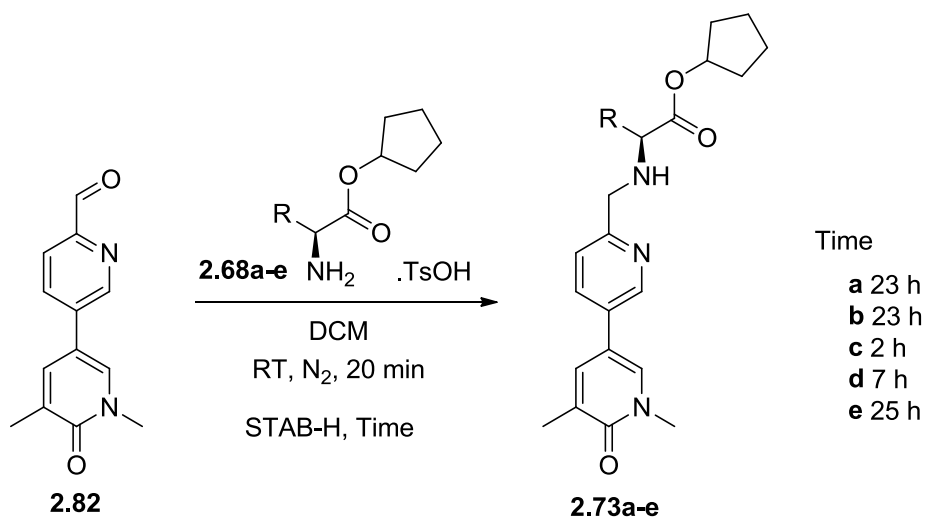


Figure 2.26: Differential hCE-1 SA for compounds 2.72a and 2.72e

Interestingly, the difference in hCE-1 hydrolysis rate and ΔpIC_{50} between **2.72a** and **2.72e** must be caused by the amino acid side chain. Threonine is more sterically encumbered with branching at the 3-position of the amino acid ester. This branching is lacking in the case of leucine, branched at the 4-position, more distal from the carbonyl.

These data suggested, for the first time in this programme of work, that hWB potency is correlated directly with hCE-1 rate of hydrolysis. This ability to modulate the hydrolysis rate and therefore the ΔpIC_{50} may be advantageous in future, considering the previously mentioned expression of hCE-1 within both target cells (monocytes and macrophages) and the undesired site: the liver. To investigate whether the 3-pyridyl isomer would offer a differentiated profile in relation to ΔpIC_{50} , reductive aminations were carried out, without triethylamine additive (Scheme 2.26), to synthesise the analogous compounds.



Scheme 2.26: Reductive aminations using aldehyde 2.82

Compounds **2.73a-e** were synthesised in moderate to good yield, allowing promising initial data to be collected for these compounds (Table 2.12). The biochemical potencies of the serine **2.73d** and threonine **2.73e** compounds (pIC_{50} of 5.6 and 5.5, respectively) were equipotent to lead compound **2.58e**. Furthermore, the alanine compound **2.73c** had a higher Brd4 BD1 potency than the other examples (Table 2.12). In terms of $ChromLogD_{7.4}$, the leucine **2.73a** and valine **2.73b** derivatives, although more lipophilic, are equipotent, biochemically, to the hydroxyl compounds.

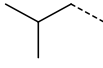
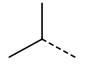
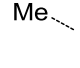
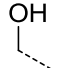
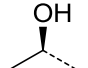
R					
	2.73a	2.73b	2.73c	2.73d	2.73e
Yield (%)	46	60	66	56	47
ChromLogD_{7.4}	6.1	5.6	3.7	2.5	3.1
Brd4 BD1 pIC_{50}	5.4	5.4	6.0	5.6	5.5
hWB_{DPU} (MCP-1) pIC_{50}	6.6	5.6	5.7	5.6	6.4
ΔpIC_{50}	1.2	0.2	-0.3	0.0	0.9

Table 2.12: Results for 3-pyridyl esters 2.73a-e

In this 3-pyridyl set of compounds, the leucine derivative **2.73a** demonstrated a similar ΔpIC_{50} as observed with the 2-pyridyl derivative **2.72a**. Disappointingly, **2.73b-d** showed little or no enhancement. Initially, the whole blood assay of compound **2.73e** failed, with large variations in potency observed. Encouragingly, when re-tested, compound **2.73e** had an excellent potency profile, which was

comparable to the phenyl compound **2.58e**. This was an excellent result considering the much reduced ChromLogD_{7.4} value of 3.1.

Hydrolysis of esters **2.73a-e** using the conditions highlighted in Scheme 2.25 gave acids **2.84a-e** in good yields. The yields and biochemical potencies are shown in Table 2.13. Acids **2.84a-e** all demonstrated low Brd4 BD1 potencies, although only compound **2.84c** was more than a log unit less potent than the corresponding ester.

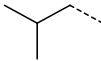
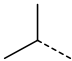
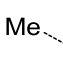
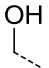
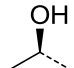
R					
	2.84a	2.84b	2.84c	2.84d	2.84e
Yield (%)	78	89	65 (sodium salt)	35 (sodium salt)	86
Brd4 BD1 pIC₅₀	4.5	4.5	≤4.4*	4.5	4.5

Table 2.13: Yields and biochemical potencies of 2.84a-e
*2.84c: pIC₅₀ <4.3 on 1 of 2 test occasions

The hCE-1 hydrolysis rates of the two threonine pyridyl derivatives **2.72e** and **2.73e** are compared in Figure 2.27. Compound **2.73e** was shown to have the higher hydrolysis rate and consequently an improved Δ pIC₅₀ compared to **2.72e**. From modelling the placement of **2.72e** in the hCE-1 binding pocket, it is hypothesised the polarity in the 2-position is less well tolerated due to a number of backbone carbonyls within the same region (Figure 2.28), which could lead to electronic repulsion and result in a lower affinity for the enzyme. The down-stream effect could be the differentiated profile between **2.72e** and **2.73e**, where the nitrogen is in a different position and would be placed differently within the enzyme pocket.

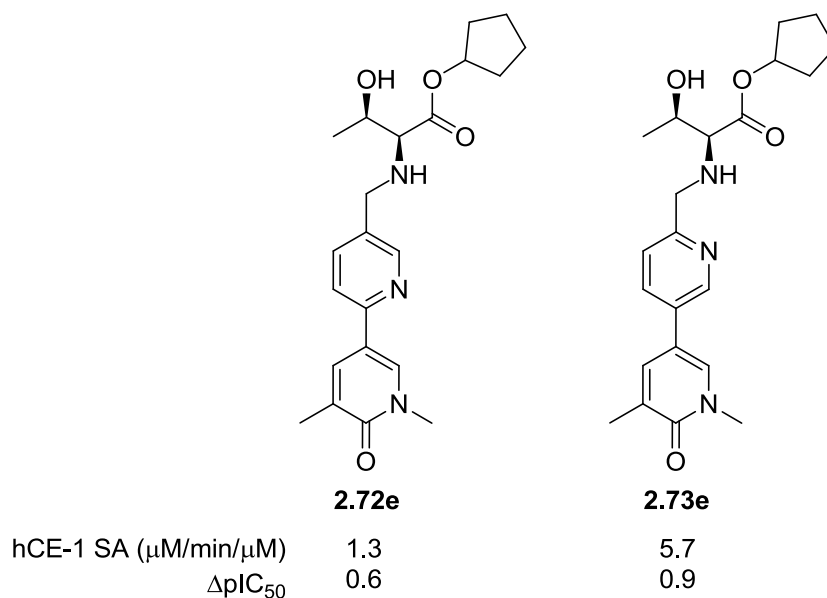


Figure 2.27: Comparison of the hydrolysis rates of the 2- and 3-pyridyl compounds, 2.72e and 2.73e

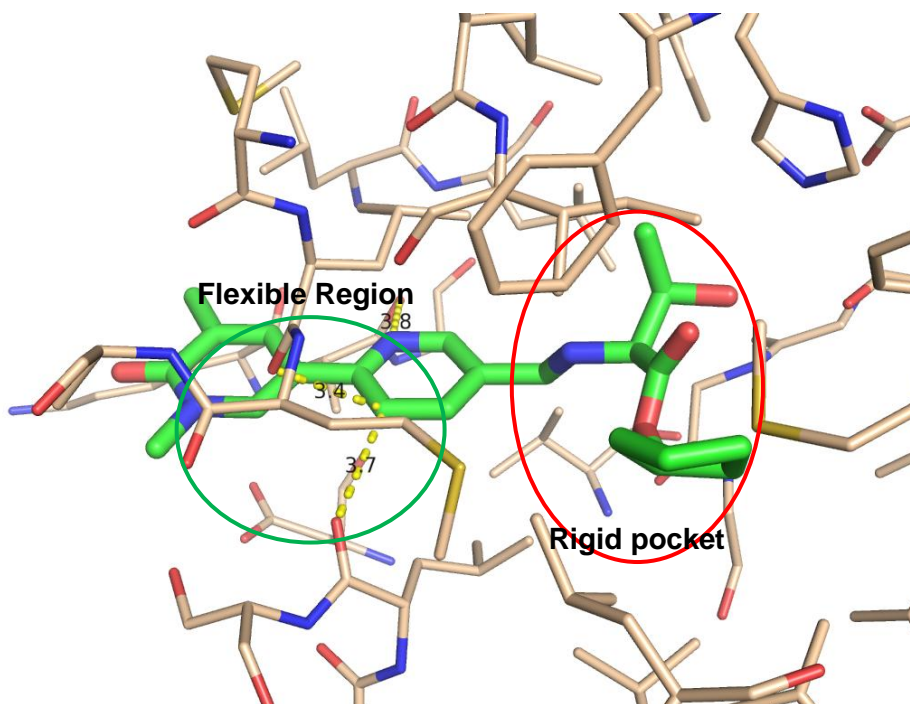


Figure 2.28: Compound 2.72e modelled within hCE-1 with distances to backbone carbonyls highlighted

To summarise, the 2- and 3-pyridyl isomers can be successfully incorporated to reduce the $\text{ChromLogD}_{7.4}$ of the initial lead compound (**2.58e**), as shown in Figure 2.29. Furthermore, the Brd4 BD1 and whole blood potencies are maintained from the phenyl to the 3-pyridyl compound **2.73e**, an excellent result considering the reduced $\text{ChromLogD}_{7.4}$. Further, taken together, this set of compounds have

demonstrated for the first time the importance of the hCE-1 hydrolysis rate as related to the observed ΔpIC_{50} . Generally, a higher ΔpIC_{50} results from a higher rate of turnover by the enzyme, which is important knowledge in the design of future inhibitors.

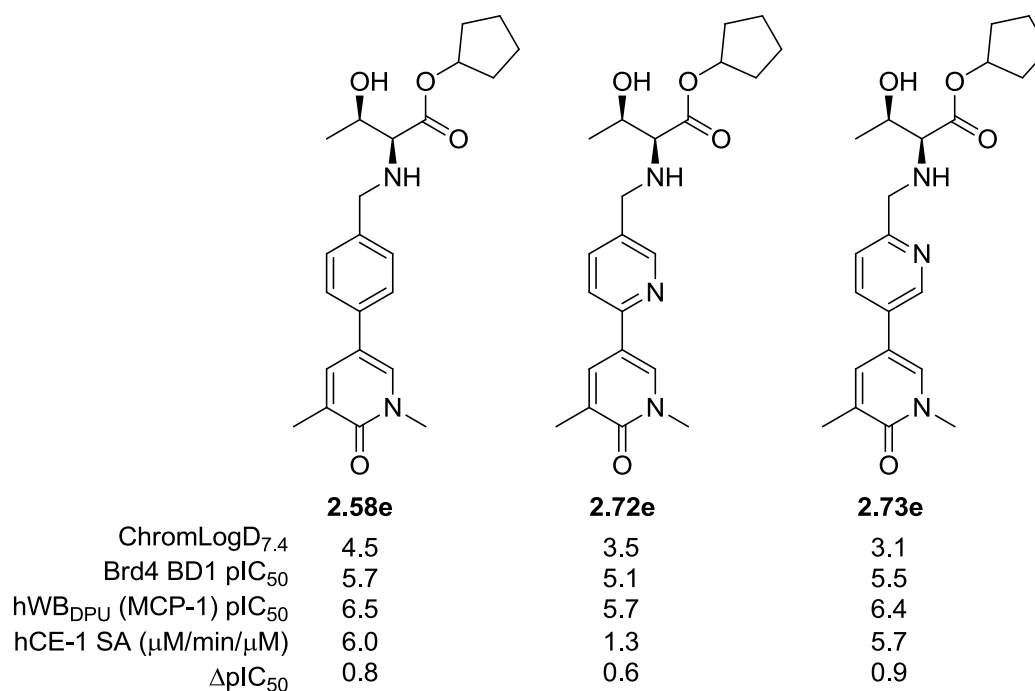


Figure 2.29: Comparison of pyridyl compounds, 2.72e and 2.73e, with compound 2.58e

2.4.3 Properties of Initial ESM-functionalised BET Inhibitor 2.58e

These encouraging results were the subject of further study elsewhere within our laboratory. Within the programme of work described in this thesis, optimisation of the phenyl derivative was continued and is described in the next section. However, to fully understand the areas for further optimisation an expanded profile for compound **2.58e** is described in Table 2.14.

It was found that the threonine ESM, as incorporated in compound **2.58e**, was most optimal due to the compound's good levels of potency in LPS stimulated whole blood coupled with the positive effect the hydroxyl group has on modulating lipophilicity, as measured by ChromLogD_{7.4} (Table 2.14). The reasonable level of lipophilicity, combined with the three-dimensional nature of the ESM, is translated into solubility of nearly 1 mg/mL seen within the pharmacologically relevant fasted state simulated intestinal fluid (FaSSIF) assay. This assay simulates the fluid found

within the gastrointestinal tract. The solubility is important here to ensure the compound would be adequately dissolved prior to being absorbed across the gut wall.

	TPP (Ester)	Fragment 2.2	Ester 2.58e	Acid 2.59e
Brd4 BD1 pIC ₅₀		5.5	5.7	4.6
hWB _{DPU} (MCP-1) pIC ₅₀	≥7.0	5.2	6.5	-
ΔpIC ₅₀	≥1.0	-0.3	0.8	-
Brd9 pIC ₅₀ (fold selectivity*)	(≥30)	-	6.0 (x2)**	5.3 (x5)**
hCE-1 SA (μM / min / μM)	<1	-	6.0	-
ChromLogD _{7.4}	≤4.0	3.6	4.5	-0.1
PFI	≤6.0	5.6	6.5	1.9
HLM IVC (-/+ benzil) (mL / min / g tissue)	<2 (- benzil)	-	28 / 5.4	-
Solubility (μg / mL)	>100	-	974	111
AMP (nm / s)	>100	-	510	<10

Table 2.14: Compound properties compared to TPP (*over Brd4 BD1)
(**Fold selectivity = $10^{(\text{Brd9 pIC}_{50} - \text{Brd4 BD1 pIC}_{50})}$)

From Table 2.14, the advantages of lead compound **2.58e** can be further highlighted. Firstly, compound **2.58e** has a reasonable potency (pIC₅₀) of 5.7 within the Brd4 BD1 biochemical assay. Using the ESM targeted approach, the aim is for the ester to be hydrolysed selectively within cells of the myeloid lineage, that is, those expressing human carboxylesterase 1 (hCE-1). Therefore, it was expected that a local high concentration of the ester and acid within the target cell type would enhance the observed biological effect. Pleasingly, compound **2.58e** demonstrated an enhanced potency within the human whole blood assay (hWB) measuring the inhibition of the release of Monocyte Chemoattractant Protein-1 (MCP-1) by monocytes, a progenitor of the macrophage.

Conversely, with a non-targeted medicinal chemistry programme, plasma protein binding within the blood reduces the effective concentration of compound available to enter the cell. A diminished biological effect would then be observed. Therefore, the enhanced potency observed within the cellular assay suggests the ESM mechanism is at work, delivering the active compound to the site of action in greater quantities. This is illustrated by comparing the biochemical and cellular potencies of non-targeted fragment **2.2** with ESM functionalised **2.58e**. As can be seen in Table

2.14, the biochemical potencies of **2.2** and **2.58e**, within the Brd4 BD1 assay, are similar. On the contrary, the ESM functionalised molecule **2.58e** is more than a log unit more potent in the whole blood.

To further verify the hydrolysis of ester **2.58e** within macrophages, a cell retention assay was carried out using compound **2.58e**.²⁴⁵ Initially, a no cell control was carried out, in which, the cellular supernatant was treated with 10 nMoles of **2.58e**. After 24 hours, the compound remained intact as measured by LCMS/MS (Table 2.15). However, 1% of the acid was observed in this no cell control experiment. This may be due to an impurity in the sample or minimal degradation of the ester in this control experiment. This result was not expected to interfere with the assay, with the acid hypothesised to be generated at a higher rate by the isolated macrophage.

	Ester (2.58e)	Acid (2.59e)
Quantity after 24 h (nMoles)	9.20	0.12

Table 2.15: Supernatant stability of 2.61e in no-cell control experiment

Following the control experiment, macrophage cells were treated with 10 nmoles of the cyclopentyl ester **2.58e**. At various timepoints, the supernatant, bathing the cells, was removed and the remaining cells washed and lysed. At each time point the quantities of ester and the acid (produced by intracellular hCE-1-mediated hydrolysis) in the cell lysate and supernatant were quantified by mass spectrometry (Figure 2.30).

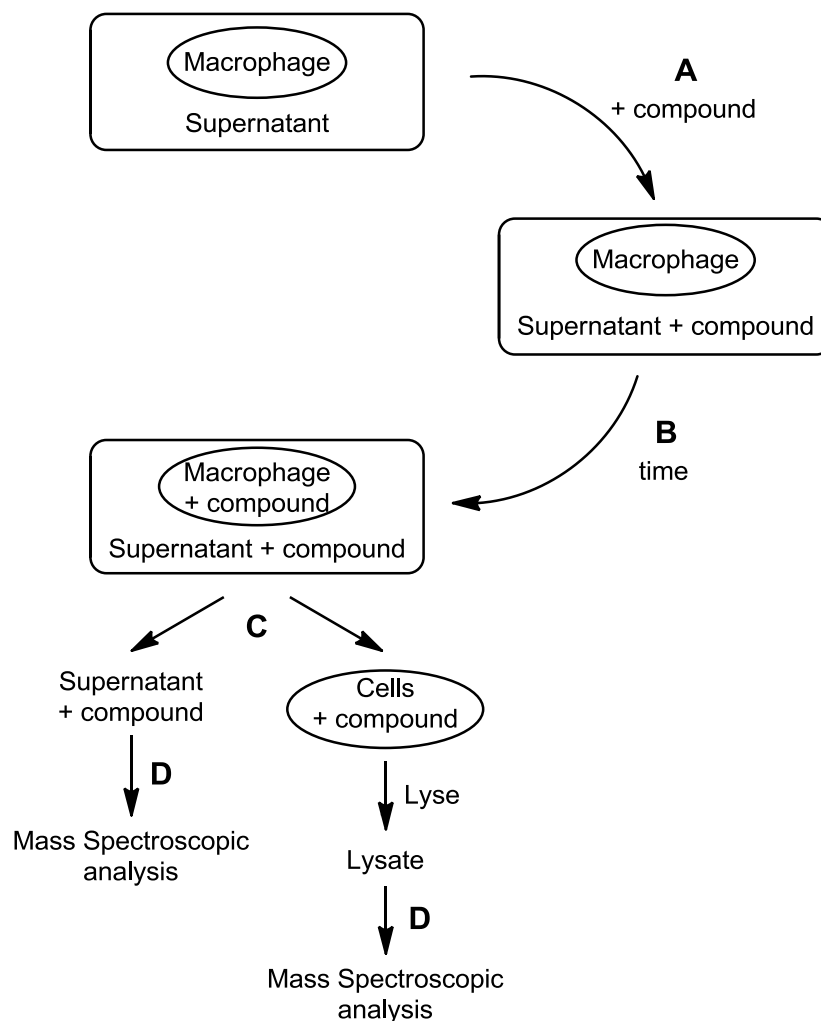
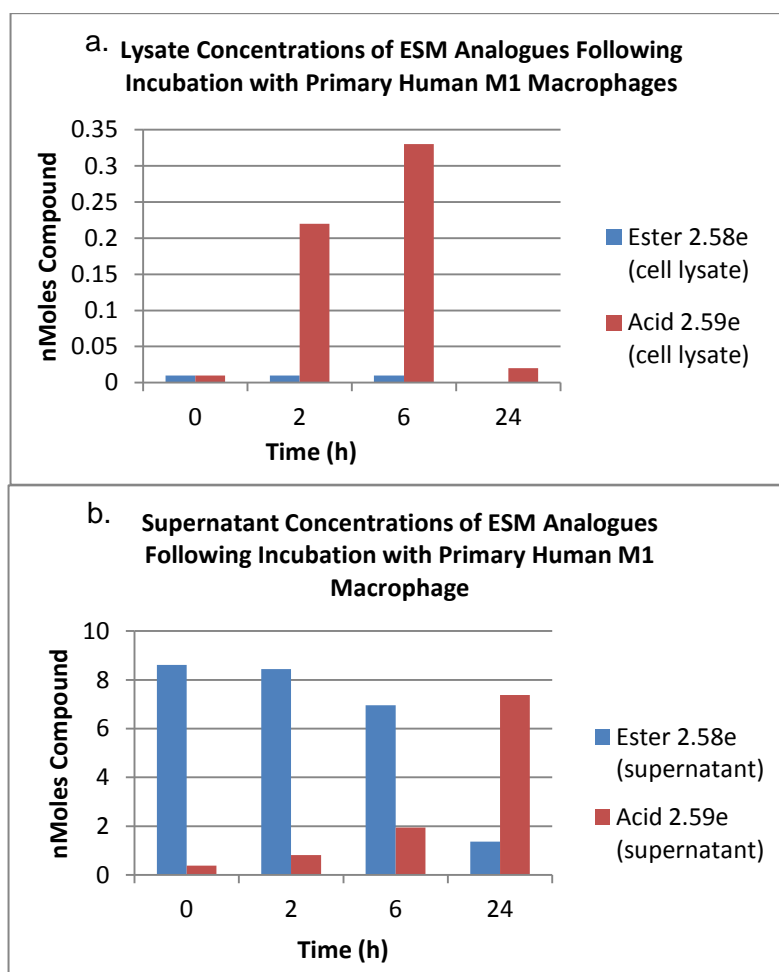


Figure 2.30: Flow diagram of macrophage retention assay

The data from this cell retention assay are shown within Graph 2.4a (lysate) and Graph 2.4b (supernatant). The quantity of acid within the supernatant was seen to increase over the 24 hour period, correlating with a decrease in ester. From the control experiment, the ester was shown to be stable in the supernatant, therefore the acid, produced intracellularly, is excreted from the cell. Therefore, hydrolysis of the ester, within the cells, was observed. The quantities of ester and acid in the lysate are shown in Graph 2.4a. As can be seen, the threonine ester remains at low concentrations throughout the time course, however, the acid is rapidly generated, peaking at 0.33 nMoles at 6 hours. At this time point, the cell contains approximately 30 times more acid than ester, confirming that the acid has been successfully delivered to the target cell. This is likely to be the cause of the enhanced cellular potency observed within the whole blood assay. Between the 6 and 24 hour time

point, loss of the acid across the membrane overtakes hydrolysis, resulting in depletion of the acid within the cells.



Graph 2.4: Cell retention assay results²⁴⁵

Interrogating these data further, the quantities of ester and acid within these target cell types can be compared to the potency values of the respective molecules. Using the calculations shown in Appendix 1, it can be shown that the 0.33 nmoles of acid at the six hour time point (Graph 2.4a) correlates to a concentration of 2.6 mM within these macrophage cells. With an IC_{50} of 25 μ M, for acid **2.59e**, the concentration within the cell is 100-fold higher than the IC_{50} and, therefore, around 10-fold higher than the IC_{90} .

Additionally, the ester was measured at 0.03 nmoles corresponding to a concentration of 0.24 mM, 10-fold lower than the acid. However, due to improved IC_{50} of 2.5 μ M for ester **2.58e**, the ester is also at concentrations 100-fold higher than the IC_{50} and approximately 10-fold higher than the IC_{90} .

Both these comparisons are important when considering the pharmacology of these compounds. With both the ester and acid at concentrations 10-fold higher than their IC₉₀ concentrations it ensures the compound is having the desired effect within these target cell types. These data also help to explain the enhanced potencies achieved within the human whole blood assay as very high levels of inhibition are being observed over a significant timecourse.

Whilst these data were very encouraging, there are a number of shortcomings associated with compound **2.58e**. Firstly, the ChromLogD_{7.4} of **2.58e** lies outside the target product profile (TPP). Lipophilicity is a good overall predictor of a compound's physical properties, such as solubility and permeability.²²³ Within our laboratory, lipophilicity is measured chromatographically, using ChromLogD_{7.4}. When lipophilicity is combined with the number of aromatic rings, the property forecast index (PFI) (Equation 2.3) is generated. A PFI of less than 6.0 is believed to lower the predicted chance of attrition as a compound moves through development.²²³ Unfortunately, compound **2.58e** has a higher than desired PFI, which would need to be modulated as part of this ongoing programme of work.

$$PFI = ChromLogD_{7.4} + Number\ of\ aromatic\ rings$$

Equation 2.3: Property Forecast Index (PFI)

Secondly, the biochemical and subsequent whole blood potency is lower than desired. It is required that compounds are not excessively potent, biochemically, in order to limit potential systemic effects driven by the ester within cells lacking hCE-1. However, an increase in the biochemical potency could translate into a higher whole blood potency. Improved potency here may be beneficial in the long term as it may reduce the potential dose of an eventual candidate molecule.

It is generally agreed, within the field of drug discovery, that high levels of selectivity for the target of interest is a very desirable profile,²⁴⁶ albeit that there is increasing belief that low activity at a number of related targets may have beneficial effects.²⁴⁷ However, with the limited knowledge available about the effects of inhibiting many of the non-BET bromodomain containing proteins, this would represent a higher risk strategy. Hence, selectivity towards the BET family of bromodomain containing proteins is the most desirable profile. In this regard, **2.58e** is equipotent at Brd9, a non-BET bromodomain, when compared to Brd4 BD1. In addition, the

corresponding acid, **2.59e**, is 5-fold more potent at Brd9 compared to Brd4 BD1, a profile that will be optimised in future iterations.

To understand the potential metabolic stability of compound **2.58e**, the *in vitro* clearance (IVC) of **2.58e** was tested within human liver microsomes (HLM). This assay gives information on the phase I metabolism of the compound.²⁴⁸ The assay when carried out in the absence of the carboxylesterase inhibitor, benzil, showed rapid clearance. However, the assay in the presence of benzil, removing the esterase component of metabolism, showed a more reasonable profile. Therefore, the ester in **2.58e** may be too labile or it may be that the linearity of **2.58e** as a molecule makes it a very efficient carboxylesterase substrate. As the carboxylesterase component of metabolism is high, only molecules with lower hCE-1 specific activities will be progressed into the IVC assay, with 6.0, as measured for compound **2.58e**, being too high (Table 2.14, Page 109).

In summary, to move forwards from compound **2.58e**, a range of properties were targeted for further optimisation, specifically, whole blood potency and lipophilicity.

2.5 Investigating Acid Potency

Having demonstrated the retention of the acid within primary human macrophages, it was hypothesised that the potency of the acid was an important contributor to the biological activity of this prodrug approach. However, to this point, the acid was significantly less potent than the parent ester, which would reduce the biological effect within the whole blood assay. Work within our laboratory on an alternative chemical series, using a benzimidazole core, delivered acids of potency closer to that of the parent ester.²³⁷ An example of this is shown in Figure 2.31. Ester **2.69** has a Brd4 BD1 potency of 6.1. Similarly, the corresponding acid, **2.71**, has a potency of 5.8, equipotent when considering the error of the assay. This translates into an excellent whole blood potency aided by a moderate hCE-1 activity.

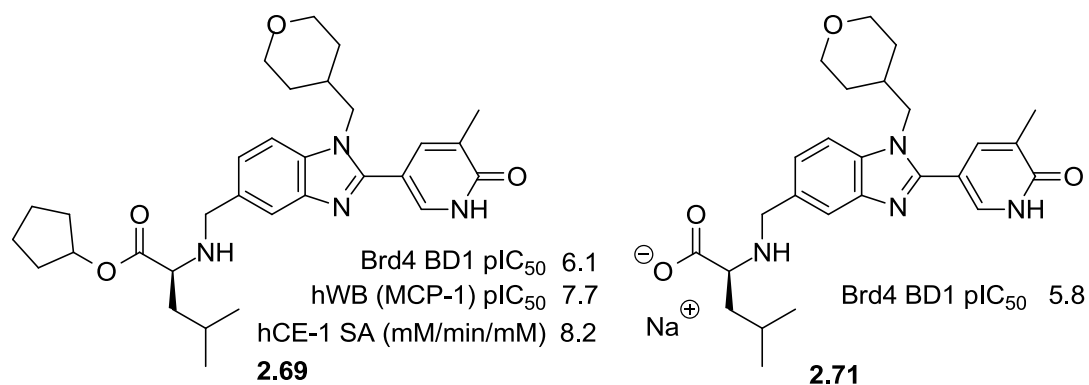


Figure 2.31: Equipotent ester and acid within the benzimidazole series²³⁷

The crystal structures within Brd4 BD1 of **2.69** and a computational model of compound **2.58e** within Brd4 BD1 were compared. With the pyridones occupying the acetyl lysine binding pocket, the overlay shows the greater extent to which the benzimidazole aromatic system protrudes through the ZA channel when compared to the phenyl ring of **2.58e** (Figure 2.32). Consequently, the carboxylic acid is also further from the protein. However, as the polar acid **2.59e** is closer to the lipophilic BET binding pocket, it was hypothesised that an adverse electrostatic interaction may exist, which results in a lower than desired acid potency.

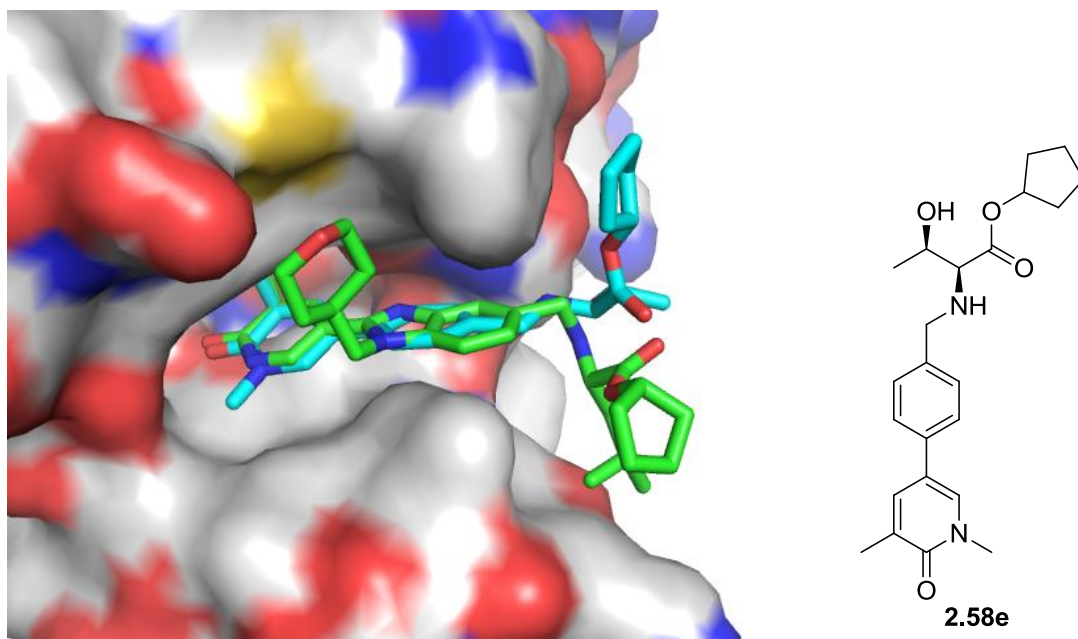


Figure 2.32: Overlay of phenyl (blue) (**2.58e**) and benzimidazole (green) (**2.69**) in Brd4 BD1, showing extension through ZA channel

In an attempt to mitigate this potential adverse interaction, it was hypothesised that extension of the linker between the phenyl ring and the ESM might improve the potency of the acid **2.59e**. Indeed, information from the patent literature from Chroma Therapeutics,¹⁹⁸ the originators of the ESM technology, suggests that the linker length is variable. A linker between the aryl ring and the ESM group of one to three atoms is suggested to be optimal. Therefore, analogues containing both a two and three atom linker were designed (Figure 2.33). As the ESM would extend further through the ZA channel, different amino acid esters could be used to again investigate the tolerability of the amino acid side chain towards the surface of the BET binding pocket.

Additional methylene groups could be added to furnish compounds **2.85** and **2.86** (Figure 2.33). The use of a three atom linker would also facilitate the incorporation of an aromatic ether, such as compound **2.87e**.

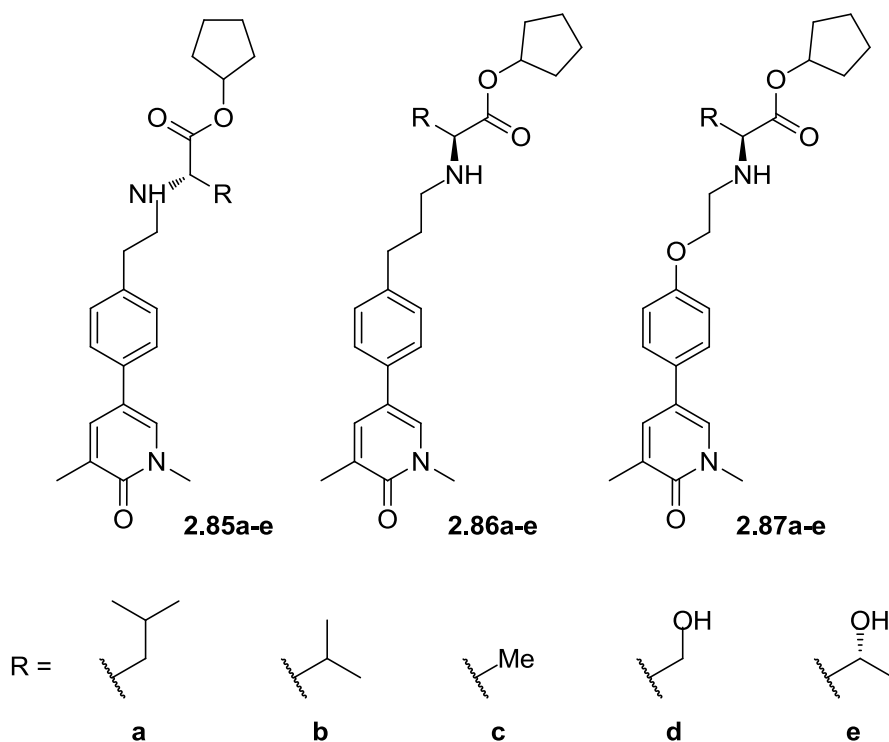


Figure 2.33: Proposed compounds investigating linker extension and ESM tolerability

Prior to commencing this body of work, the properties of such molecules were profiled, with the addition of one or two methylene units predicted to increase lipophilicity. However, perhaps counter-intuitively, the substitution of carbon for oxygen between **2.86e** and **2.87e** was predicted to moderately increase lipophilicity. In the cChromLogD_{7.4} model, the insertion of the more polar atom is likely to have

been counteracted by the reduced basicity of the nitrogen, resulting from the placement of a heteroatom β to the amine. The calculated pK_a values of the protonated amine support this reasoning (Figure 2.34).

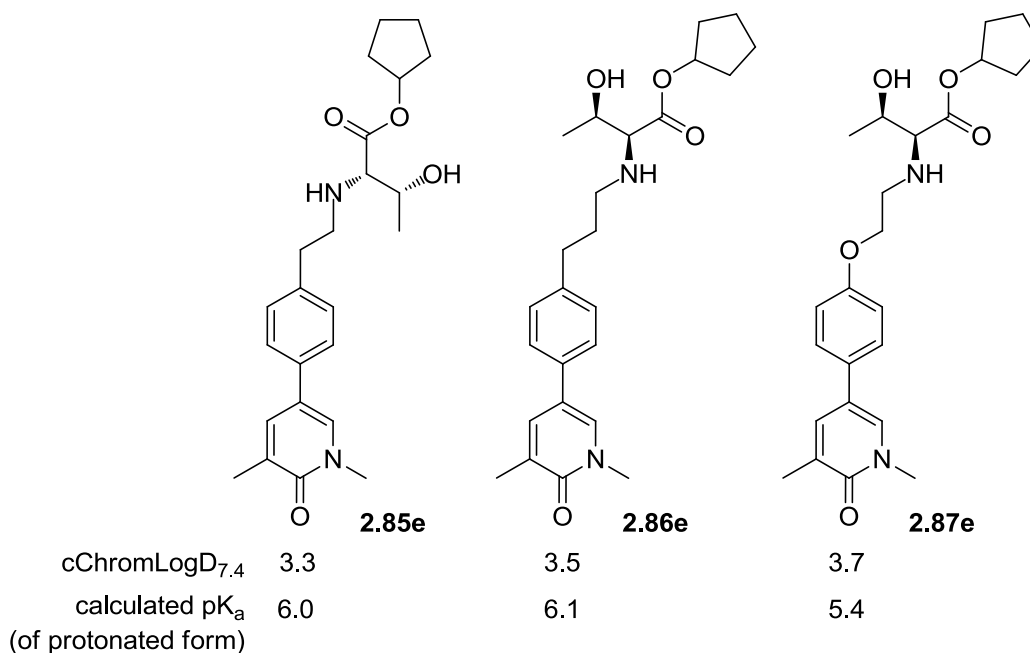
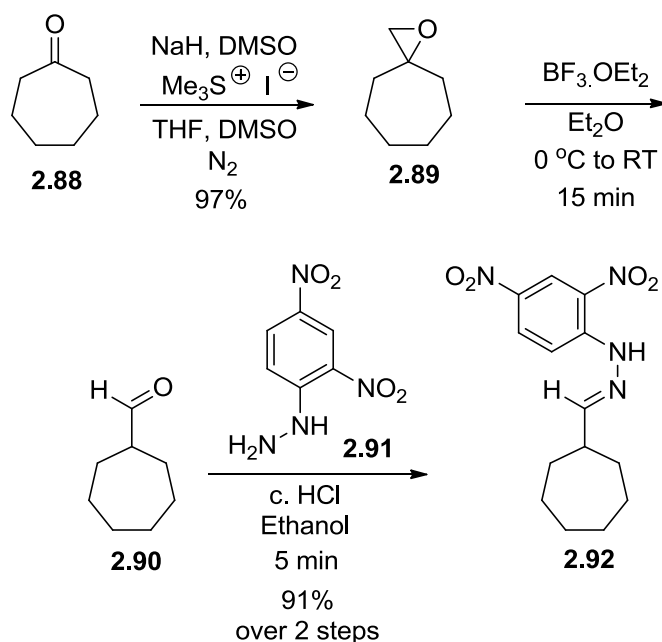


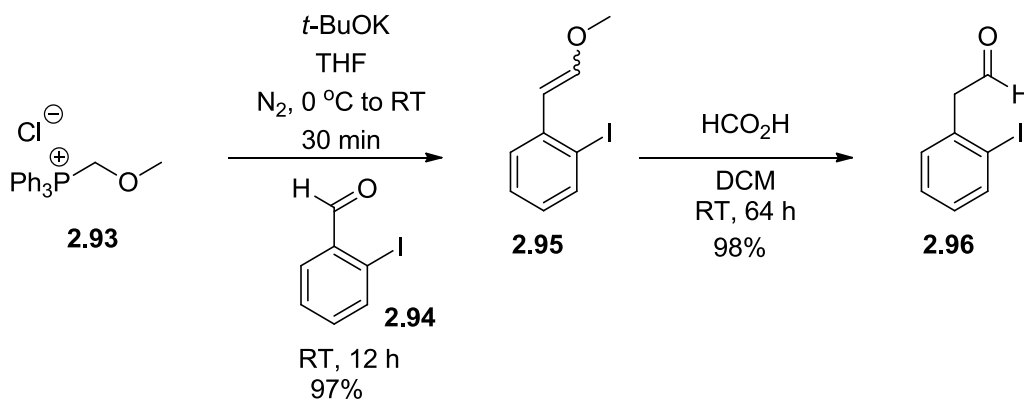
Figure 2.34: Exemplar compounds with calculated lipophilicities

To investigate synthetic routes to the singly homologated compound **2.85**, a literature search was undertaken. This search suggested that an aldehyde homologation could be performed using a method reported by Corey and Chaykovsky.²⁴⁹ They reported the formation of epoxide **2.89** from aldehyde **2.88**.²⁵⁰ Subsequent treatment of the epoxide with Lewis acid formed the homologated aldehyde **2.90**, which was trapped for characterisation as the hydrazone **2.92** (Scheme 2.27). The successful epoxidation of benzaldehyde to form styrene oxide, in 75% yield, was also described.



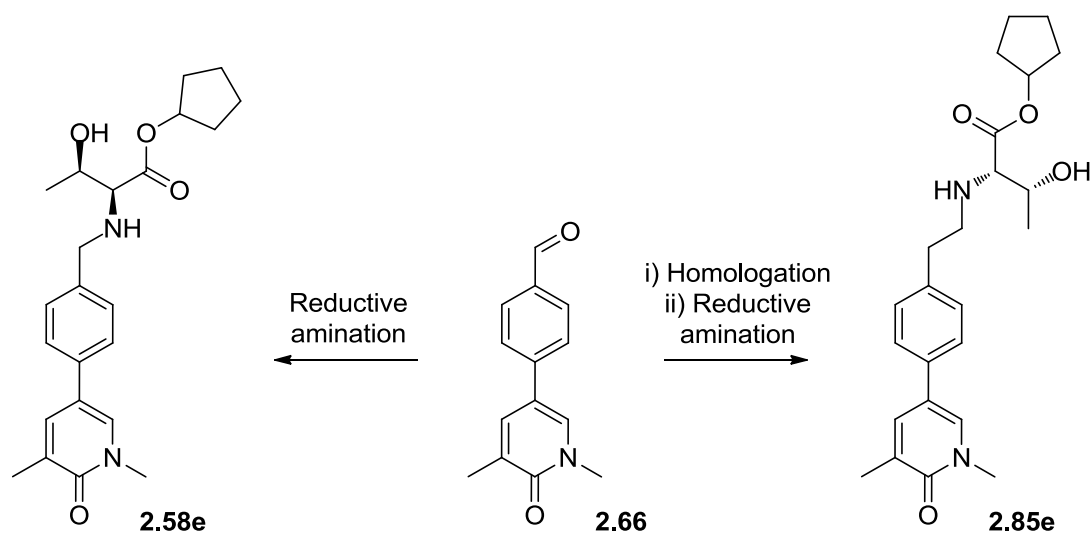
Scheme 2.27: Formation of epoxide 2.89 and subsequent rearrangement

An alternative strategy would be to use Wittig chemistry.²⁵¹ An example of this is the reaction of aldehyde **2.94** with the ylide derived from (methoxymethyl)triphenylphosphonium chloride (**2.93**) to form the enol ether **2.95** (Scheme 2.28). Treatment of the enol ether with formic acid yields the homologated aldehyde **2.96**.²⁵² The Corey-Chaykovsky method, however, was initially investigated to establish the stability of the homologated aldehyde.



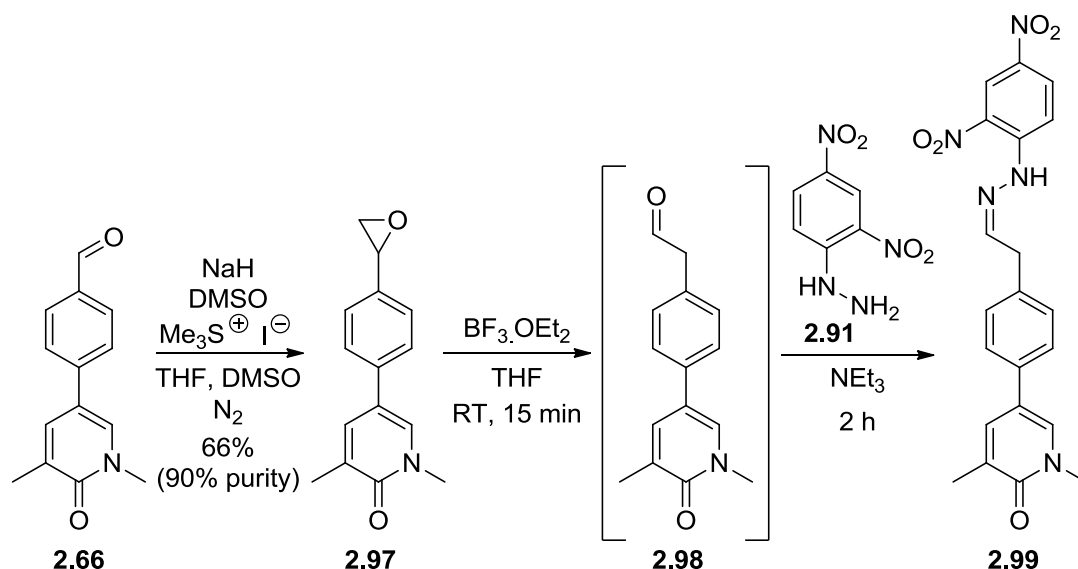
Scheme 2.28: Use of Wittig chemistry to form enol ether 2.96

Returning to lead compound **2.58e**, this was synthesised by reductive amination using the previously described key aldehyde intermediate **2.66**. With respect to the current targets, homologation prior to reductive amination was expected to yield the desired compound **2.85e** (Scheme 2.29).



Scheme 2.29: Strategy to synthesise homologated ESM compound 2.85e

To establish whether the reaction would be viable with aldehyde **2.66**, the epoxidation was attempted using the conditions detailed in the Corey-Chaykovsky paper (Scheme 2.30).²⁴⁹ Thus, the sulfonium ylide was prepared before aldehyde **2.66** was added. It was found that maintaining the temperature at -10°C ensured the stability of the product epoxide within the reaction mixture, preventing over reaction to the oxetane. An aqueous workup furnished the desired epoxide **2.97** in good yield and reasonable purity. Lewis acid-mediated rearrangement of the epoxide formed aldehyde **2.98**. Unfortunately, the homologated aldehyde was found to be challenging to isolate and handle. To ensure aldehyde **2.98** was being formed efficiently, dinitrophenylhydrazine **2.91** was used to trap the product as the hydrazone **2.99** without isolation of the intermediate aldehyde (Scheme 2.30). This was the procedure used within the seminal paper to isolate and characterise the aldehyde product.²⁴⁹ The desired hydrazone was observed by LCMS, although it proved unstable to normal phase silica chromatography.

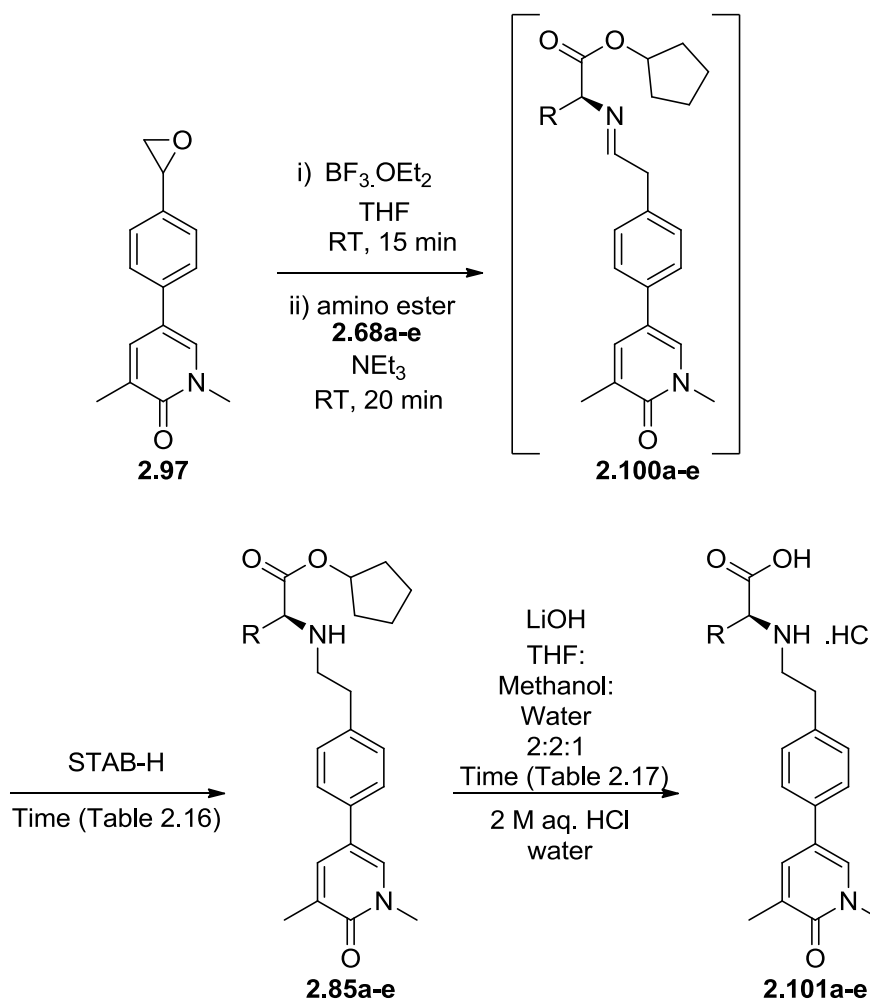


Scheme 2.30: Test of the mechanism on substrate 2.66

Although the hydrazone was not isolated in these pilot studies, its production *in situ* presented an opportunity. Addition of the amino acid ester to the pre-formed aldehyde may allow imine formation, thereby avoiding isolation of the seemingly unstable alkyl aldehyde. The resulting imine could then be reduced in the normal way, using sodium triacetoxyborohydride (Scheme 2.31).

To this end, reaction conditions were developed to facilitate this one-pot procedure. Initially, the epoxide was treated with Lewis acid to form the aldehyde, as before. The amine, along with triethylamine, to aid imine formation, were added. Monitoring the imine formation by LCMS, STAB-H was added at the appropriate time to form the desired product.

Returning to the synthetic targets, as the homologation would change the placement of the amino acid side chain within the BET binding pocket, different ESM analogues were targeted for synthesis. The five amino acid esters used in the optimisation of compound **2.58e**, were also used here: leucine, valine, alanine, serine and threonine. The products **2.85a-e** from these one-pot epoxide rearrangement and reductive aminations were isolated in moderate yields over the two steps (Scheme 2.31).



Scheme 2.31: Synthesis of two carbon linker compounds 2.85a-e from epoxide 2.97

These compounds were initially tested within the Brd4 BD1 biochemical assay and it was observed that all five derivatives were essentially equipotent (Table 2.16). The data illustrates that the BET pocket does not limit the size or polarity of the amino acid side chain of the homologated ester products. Interestingly, these homologated compounds **2.85a-e** are equipotent to lead compound **2.58e**. When compounds **2.85a-e** were tested within the human whole blood (hWB) assay, a range of potencies were observed. Pleasingly, the compound containing the threonine side chain had the highest cellular potency with a pIC_{50} of over 7, mirroring the effect seen with compound **2.58e**. The lipophilicities of these compounds also varied dramatically, with the hydroxyl containing amino acids showing the lowest lipophilicity. The two hydroxyl containing examples were tested within the hCE-1 specific activity assay. The serine derivative **2.85d** had a much higher turnover than

the more hindered threonine containing compound **2.85e**, however, the less rapidly hydrolysed **2.85e** was marginally more potent in the whole blood.

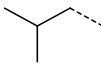
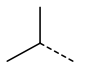
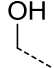
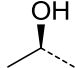
R			Me		
	2.85a	2.85b	2.85c	2.85d	2.85e
Yield (%)	18	11	21	29	30
Reaction Time (h)	2	3	2	3	4
Brd4 BD1 pIC ₅₀	5.6	5.8	5.7	5.8	5.8
hWB _{DPU} (MCP-1) pIC ₅₀	6.5	5.9	6.4	6.8	7.2
ΔpIC ₅₀	0.9	0.1	0.7	1.0	1.4
ChromLogD _{7.4}	7.3	7.0	5.0	3.6	4.6
hCE-1 SA (μM/min/μM)	-	-	-	61	20

Table 2.16: Yields and potencies for compounds **2.85a-e**

With the esters in hand, the corresponding acids **2.101a-e** were also generated in order to confirm whether homologation of the ESM would increase the acid's potency. The products from the hydrolysis were isolated in good yield as hydrochloride salts, ensuring good solubility in DMSO. Pleasingly, the acids were consistently more potent than the original lead acid **2.59e**, by around 0.5 log units (Table 2.17).

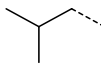
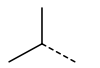
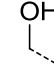
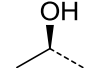
R			Me		
	2.101a	2.101b	2.101c	2.101d	2.101e
Yield	40	69	79	66	55
Reaction Time (h)	16	42	16	40	40
Brd4 BD1 pIC ₅₀	5.1	5.0	4.9	5.1	5.0

Table 2.17: yields and potencies of acids **2.101a-e**

To understand the increase in cellular potency, compounds **2.58e** and **2.85e** were compared side-by-side (Figure 2.35). As previously highlighted, the two esters are equipotent, therefore, other properties must be contributing to the observed increase in whole blood potency from 6.5 (**2.58e**) to 7.2 (**2.85e**). Previous experiments with compound **2.58e** have demonstrated increased local delivery of the acid within macrophages. Extending this observation to compound **2.85e**, a more potent acid would have a more pronounced inhibitory effect on BET function. Additionally, when

the homologated compound **2.85e** was tested within the recombinant hCE-1 assay, it was found to be more rapidly hydrolysed than compound **2.58e**. This could also have an effect on the whole blood potency as faster hydrolysis may lead to higher quantities of intracellular acid, leading to higher levels of BET inhibition. With this in mind, this was the first evidence, within this ESM strategy, supporting the combined importance of the acid potency and ester hydrolysis rate, in producing a cellular response.

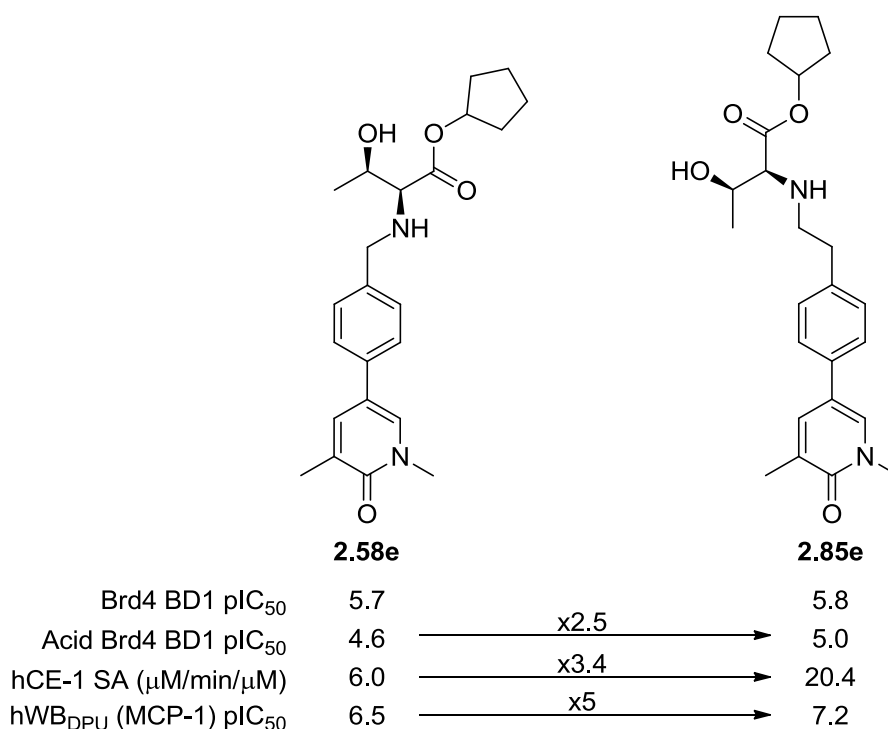


Figure 2.35: Comparison of 2.58e with its one carbon homologue 2.85e

The gain in potency of the acid in the biochemical assay, translating into an improved human whole blood potency, was a pleasing result as it supported the initial hypothesis. To investigate whether the number and nature of the atoms within the linker was optimal, two additional compounds, as previously mentioned, were designed: **2.86e**, utilising a propyl linker, and **2.87e** the oxyethyl analogue (Figure 2.36).

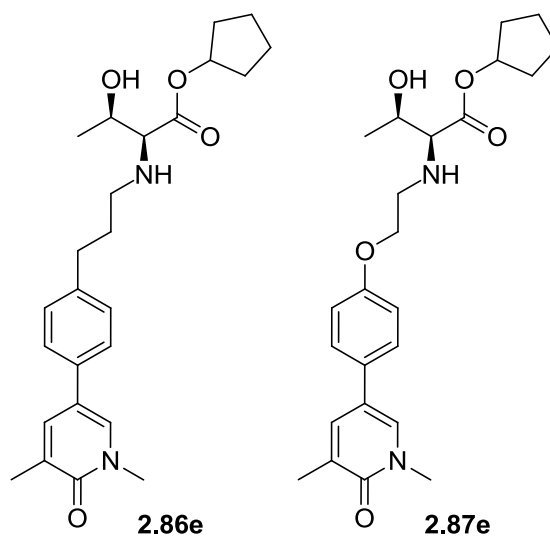
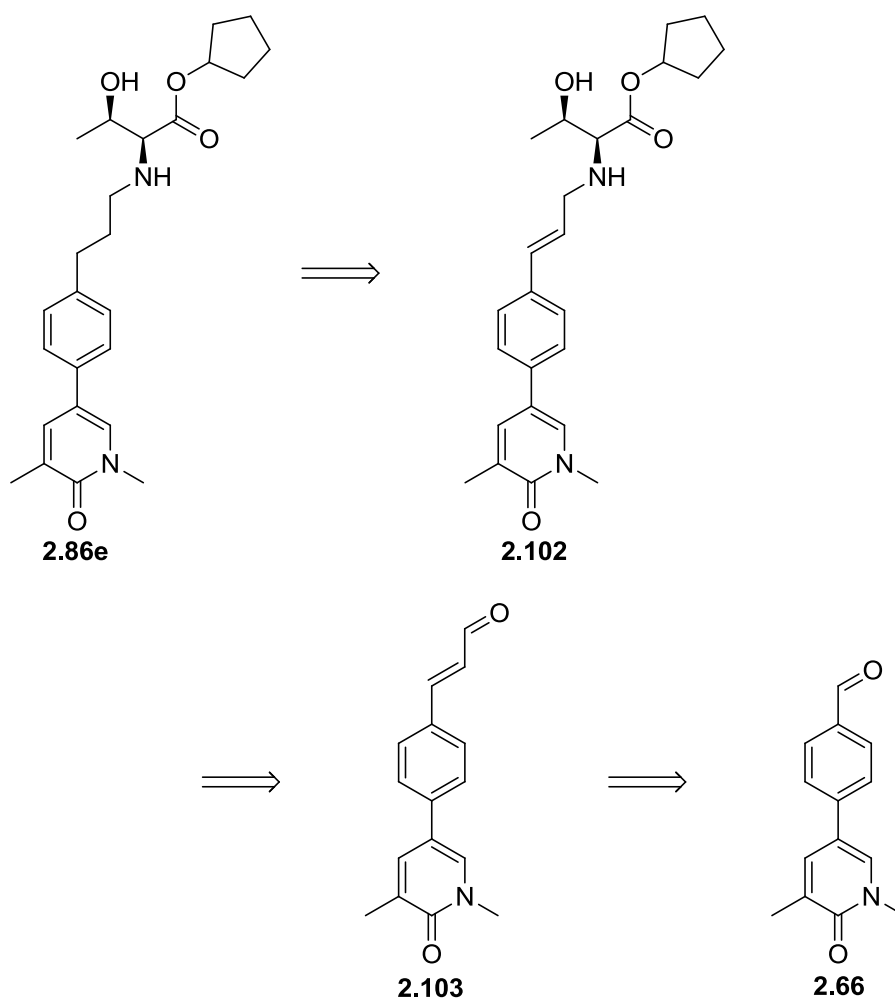


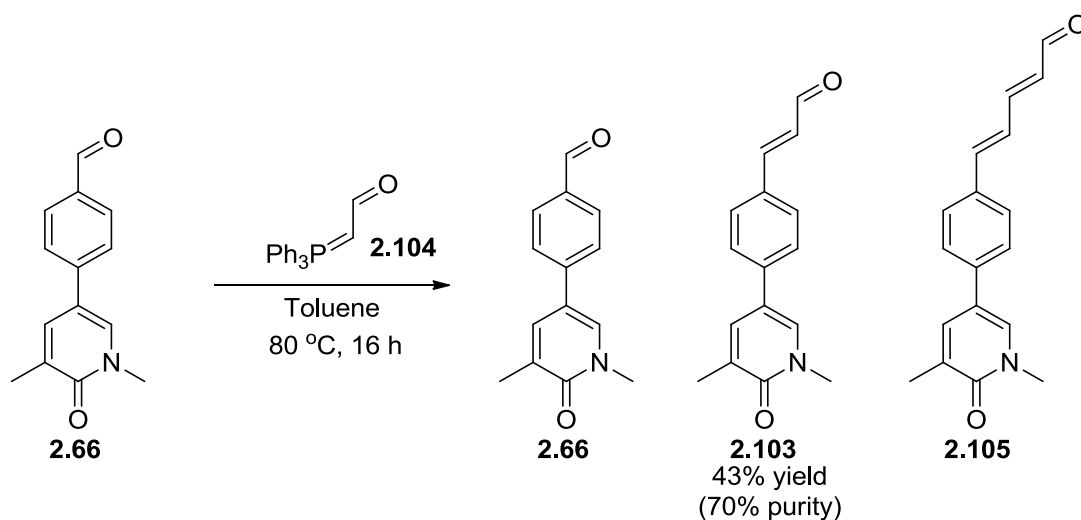
Figure 2.36: Proposed three atom linkers

Retrosynthetically (Scheme 2.32), it was envisaged that compound **2.86e** could be made from the corresponding alkene. The double bond could be disconnected to the aldehyde intermediate **2.103** and synthesised using Wittig chemistry in the forward direction.



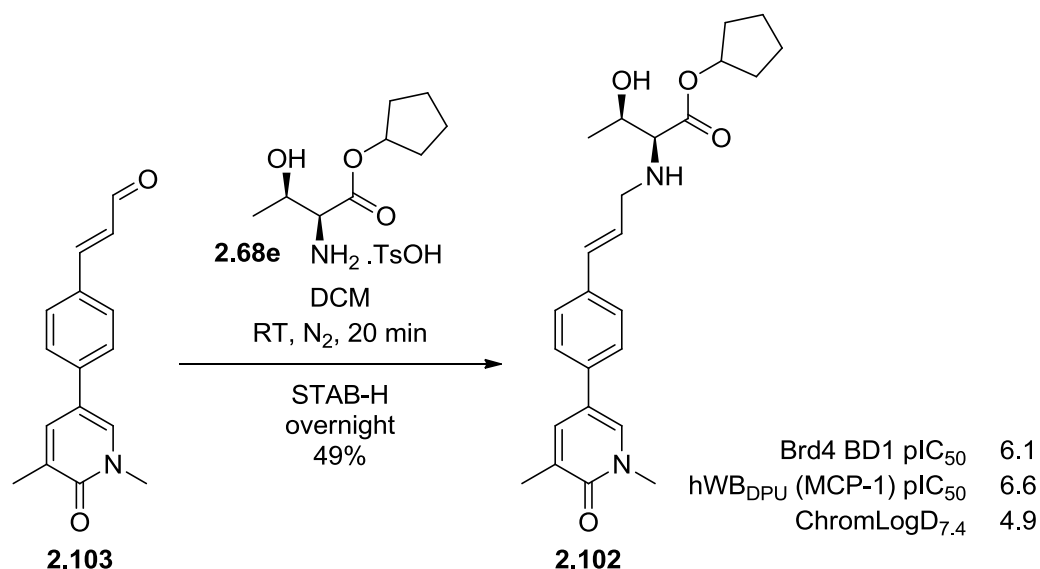
Scheme 2.32: Retrosynthetic analysis of compound 2.86e

From intermediate aldehyde **2.66**, it was found that a two carbon unit could, indeed, be inserted through addition of the commercially available (triphenylphosphoranylidene)acetaldehyde (**2.104**) via a Wittig reaction.²⁵³ This reaction, while furnishing the desired homologated product **2.103**, was challenging to control, with the desired product also being a substrate for the Wittig reagent (Scheme 2.33). Consequently, the product was contaminated with both starting material **2.66** and the double-addition by-product **2.105** (Scheme 2.33). The large coupling constant of 15.9 Hz, observed between the two alkenyl protons in the ¹H NMR spectrum confirmed the *trans* geometry of the product.

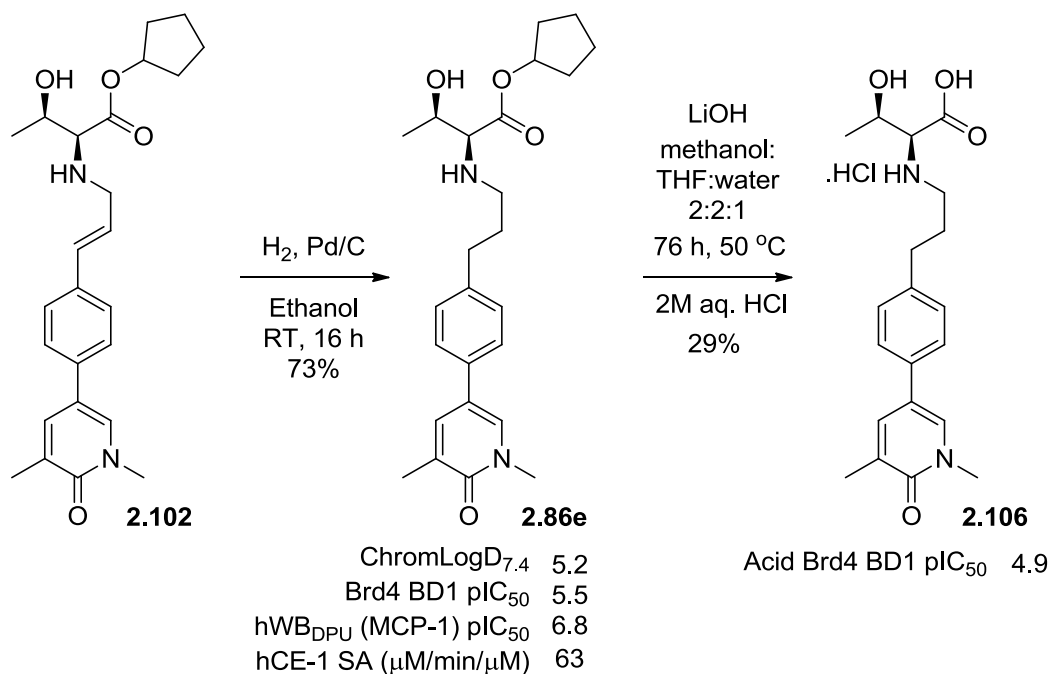


Scheme 2.33: Wittig two carbon homologation

The starting material **2.66**, product **2.103** and by-product **2.105** were found to have very similar chromatographic properties and, hence, column chromatography was unable to efficiently separate the mixture. Therefore, the material was used crude in the subsequent reductive amination reaction in the expectation that the ESM functionalised compound would be more soluble and separable. Maintaining the double bond within the molecule until after the reductive amination was expected to maintain the aldehyde's stability, through conjugation. Pleasingly, the ESM functionalised product **2.102** was subsequently isolated in reasonable yield (Scheme 2.34). In light of previous results with the one and two carbon linkers, it was decided at this point to focus on the threonine ESM as this motif provided the best balance between whole blood potency and physicochemical properties.

Scheme 2.34: Reductive amination with unsaturated aldehyde **2.103**

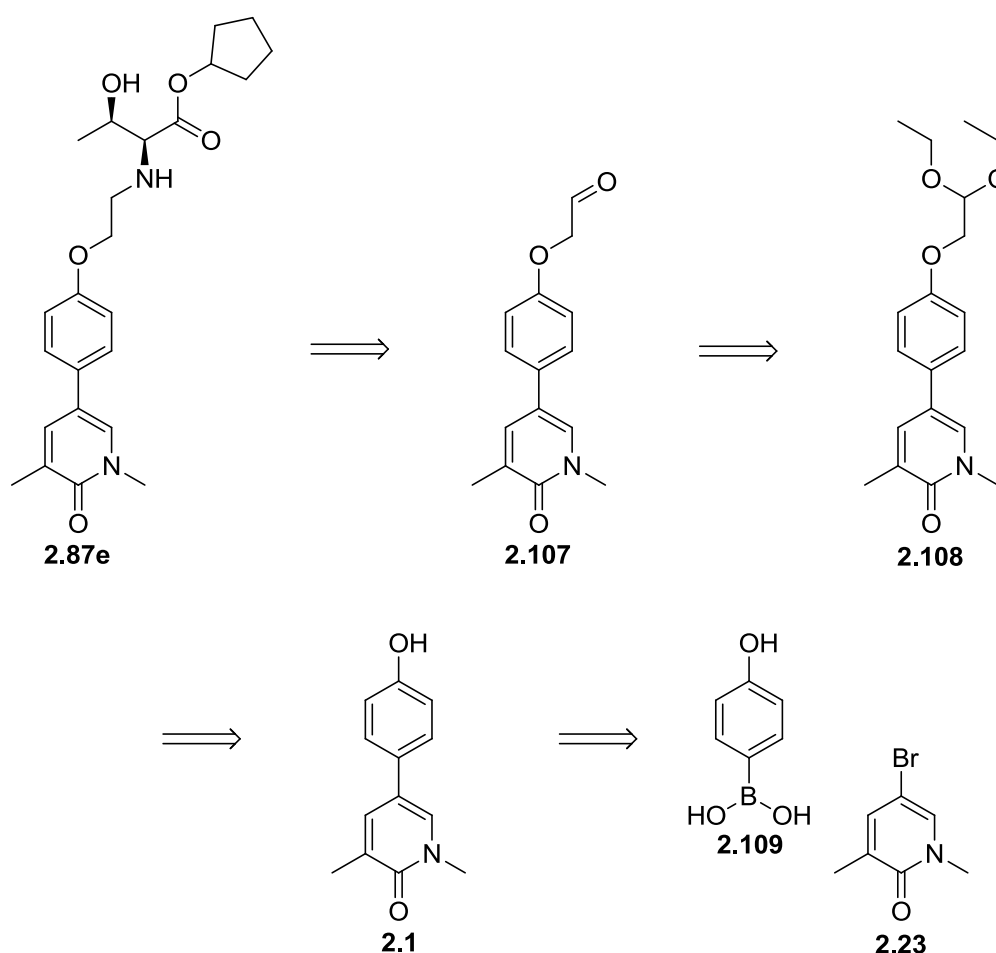
The product of this reductive amination was also tested within our *in vitro* assays to ascertain whether the unsaturated linker could be of use. While the biochemical potency was promising, the human whole blood assay showed only a modest increase, perhaps indicating the linker was not well tolerated by hCE-1. Hydrogenation of the alkene intermediate yielded the desired product **2.86e** in good yield (Scheme 2.35).



Scheme 2.35: Alkene hydrogenation and ester hydrolysis

The reduced product **2.86e** was tested in the initial set of screening assays (Scheme 2.35). Firstly, this compound was too lipophilic, with a ChromLogD_{7.4} in excess of 5. Also, **2.86e** had a lower than desired biochemical potency of 5.5, which might be explained by the flexibility of the three carbon linker which may introduce a number of compound conformations which are unfavourable for binding, thus reducing the potency. Having stated this, the human whole blood potency is very good. Again, this is potentially a combination of the biochemical potency of the acid, generated within the target cells, and the very rapid hydrolysis by hCE-1 of 63 µg/min/µg protein.

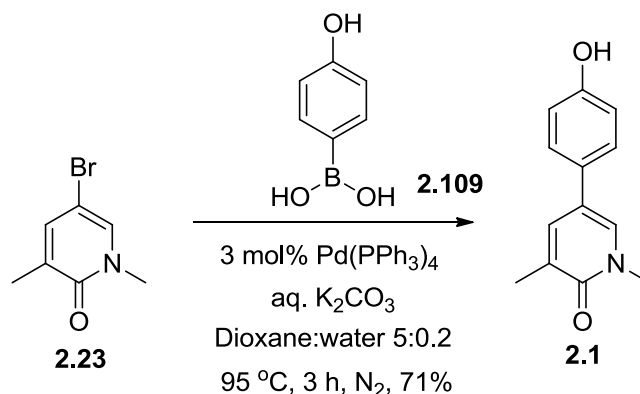
To reduce the lipophilicity of propyl-linked compound **2.86e**, the aromatic ether compound **2.87e** was proposed. Additionally, the ether linker was hypothesised to add a small amount of constraint to the linker, fixing a planar orientation with respect to the phenyl ring. To initiate this piece of work, a retrosynthetic analysis was undertaken (Scheme 2.36).



Scheme 2.36: Retrosynthesis of ether-linked ESM compound **2.87e**

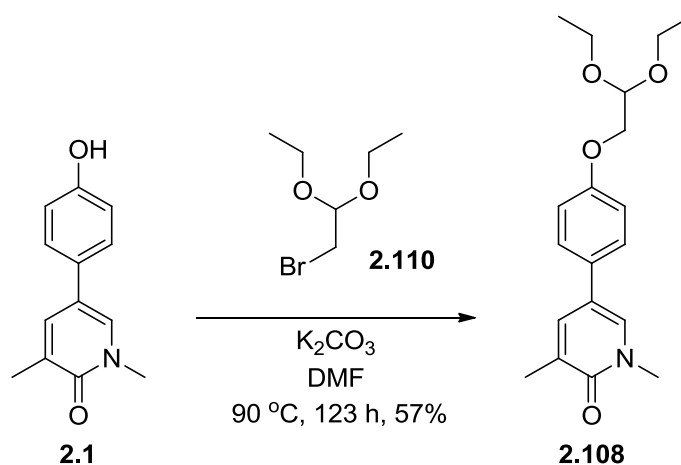
The target material could be disconnected to aldehyde **2.107**, itself formed from acetal **2.108**. The key disconnection of the aryl ether **2.108** back to phenol **2.1** was proposed. Phenol **2.1** could be disconnected to bromopyridone **2.23** and boronic acid **2.109**.

To begin the synthesis of **2.107**, a Suzuki cross coupling was carried out between bromopyridone **2.23** and commercially available phenol boronic acid **2.109** (Scheme 2.37). The desired product had poor solubility in dichloromethane, which was used to purify the product by trituration, isolating compound **2.1** in good yield.

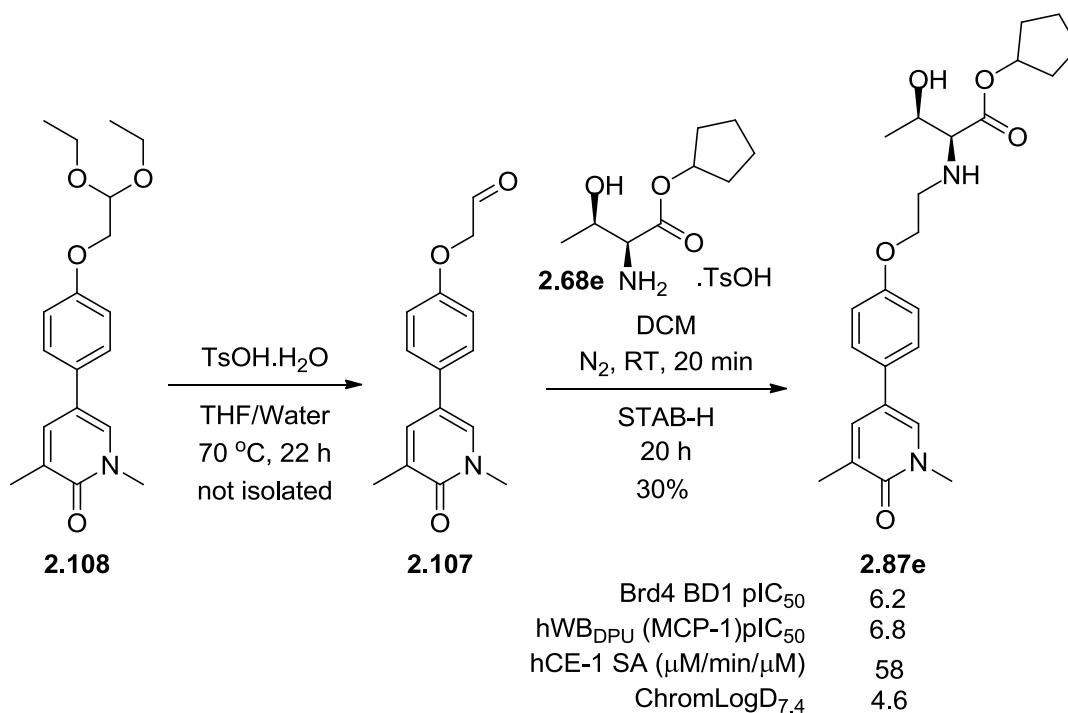


Scheme 2.37: Suzuki with 4-phenolboronic acid (2.109)

It was found in the literature that the additional two carbon unit could be installed through alkylation of the phenol using bromoacetal **2.110**.²⁵⁴ The initial attempt to synthesise intermediate **2.108** was carried out at reflux in acetone and was found to progress sluggishly. Dimethylformamide was used in a more successful reaction on the second attempt; the reaction continued to be slow, although did it progress to completion (Scheme 2.38).

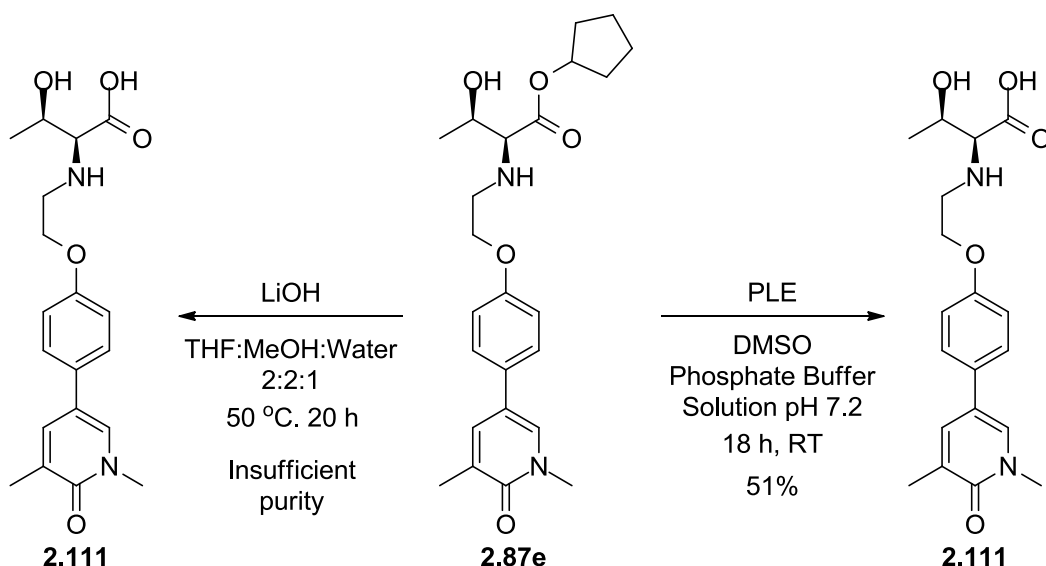
**Scheme 2.38: Insertion of two carbon acetal unit**

The conversion of the acetal to aldehyde **2.107** was achieved using catalytic tosic acid (Scheme 2.39).²⁵⁴ LCMS analysis showed the disappearance of the acetal and appearance of the aldehyde and the corresponding hydrate. As the amino esters were used as their tosic acid salts, the reaction was concentrated to dryness before the addition of the required reagents to achieve imine formation and subsequent reduction (Scheme 2.39). This furnished the final product **2.87e** in 30% yield, over two steps. The potency of 6.2 at Brd4 BD1 was pleasing, transitioning into 6.8 within the whole blood assay. As observed with the carbon-linked three atom linker, the hCE-1 hydrolysis rate was rapid, with a value of 58. To discover whether the acid potency was improved, the next step was to hydrolyse the ester.



Scheme 2.39: Conversion of acetal to aldehyde 2.107 and subsequent reductive amination

While two attempts were made to hydrolyse **2.87e**, using lithium hydroxide, the product was challenging to isolate in good purity. Recently, an esterase screen was undertaken within our laboratory, finding pig liver esterase (PLE) to hydrolyse these ester motifs in good yield and purity (Scheme 2.40).²⁵⁵ Hence, PLE was utilised to successfully make and isolate **2.111** in good yield and purity. Profiling within the Brd4 BD1 biochemical assay, this acid had a good level of potency of 5.5. However, no improvement was observed to narrow the potency difference between the ester and acid.



Scheme 2.40: Lithium hydroxide and PLE-mediated hydrolysis of 2.87e

As opposed to the values predicted by the *in silico* model of ChromLogD_{7.4}, the measured lipophilicity of the oxy-ethyl linked compound **2.87e** was lower than that of **2.86e**, the propyl-linked compound (Figure 2.37), as expected.

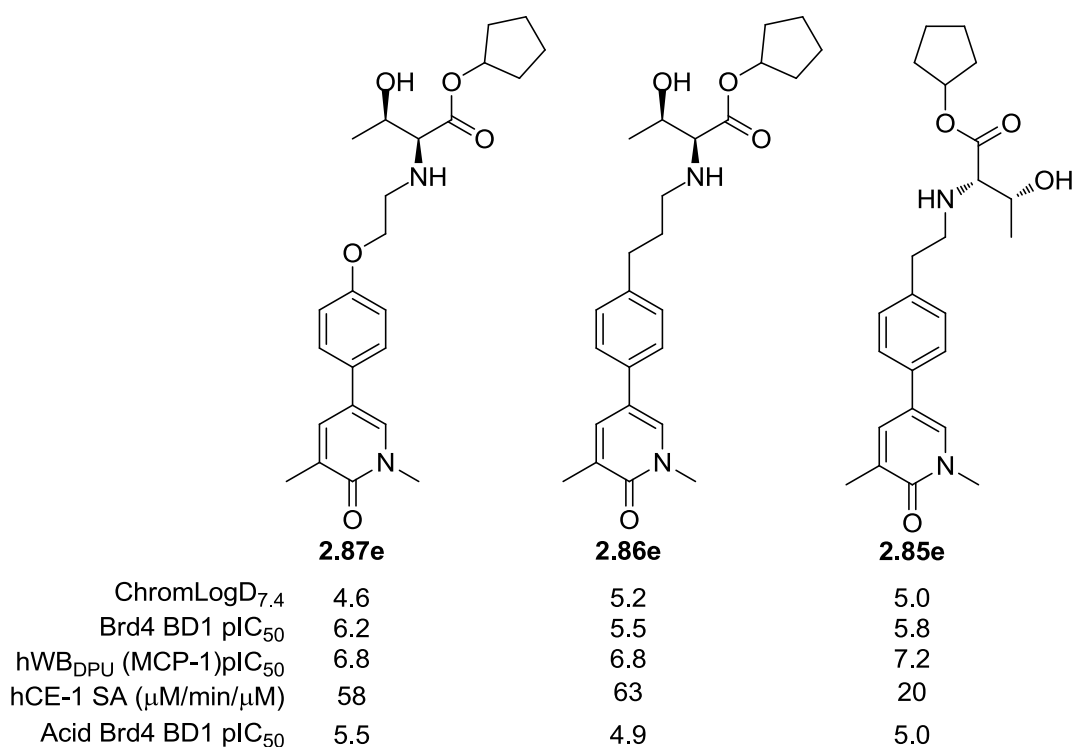


Figure 2.37: Comparison of three atom linkers with the two atom linker 2.85e

The Brd4 BD1 potency of the O-linked **2.87e** is higher than that of **2.86e**. This is probably due to the positioning of the sp² hybridised oxygen within the ZA channel. However, the initial fragment optimisation discounted the possibility of an edge-to-face interaction with the flanking tryptophan, comparing methyl (**2.18**) or methoxy group (**2.15**) with the fragment start point **2.2** (Figure 2.38). Instead, it was thought that the flatter ether is more favourable within the tight ZA channel. Additionally, the oxygen would add additional conformational constraint by limiting the rotation around the aryl-oxygen bond.

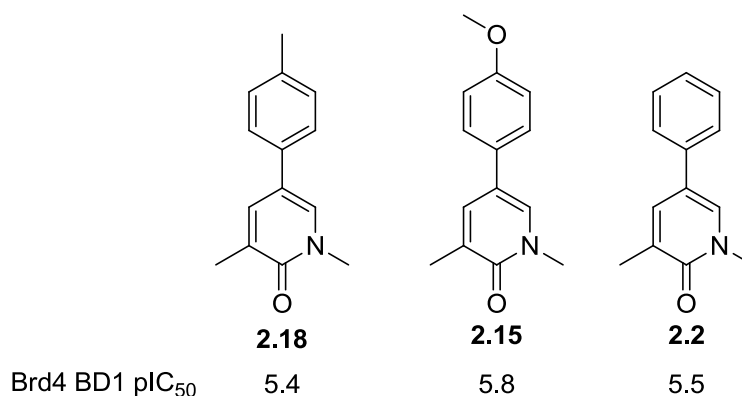


Figure 2.38: Baseline methyl and methoxy compounds

Overall, additional atoms within the linker to the ESM had the desired effect of reducing the apparent adverse interaction of the conjugate acid with the BET protein (Figure 2.37). Importantly, these compounds demonstrate the importance of the acid's potency to the desired human whole blood potency. Further, these initial results show that one additional atom is sufficient to remove part of the adverse interaction. However, further homologation has little impact on minimising the difference in potency between the ester and acid. Furthermore, throughout this study, the acid remains less potent than the ester. This could be associated with the more polar nature of the acid, compared with the ester, lacking some of the lipophilic interactions towards the surface of the BET protein.

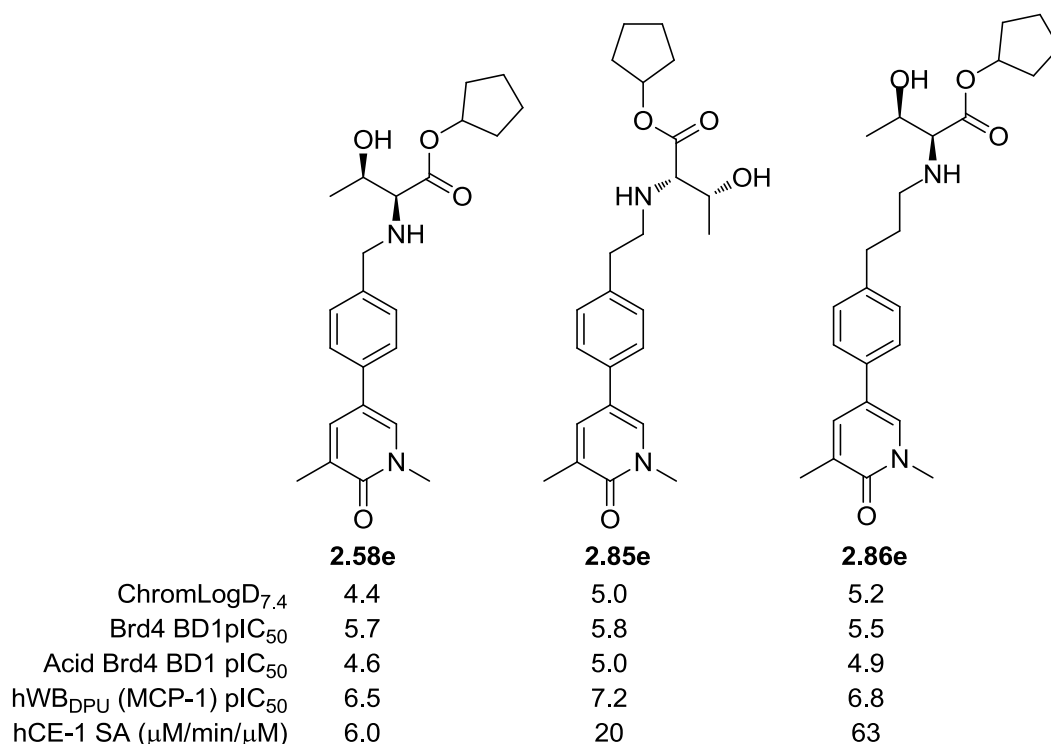


Figure 2.39: Comparison of one, two and three atom-linked compounds

As illustrated in Figure 2.39, increasing the linker length from one carbon to two or three carbons increases the potency of the acid while making the ester more readily hydrolysed by hCE-1. Meanwhile, the ester biochemical potency remains constant (Figure 2.39). The data show that it is the combination of the hCE-1 specific activity and the acid potency that are apparently key to the levels of whole blood potency.

With good biochemical potency and increased potency in the cellular assay, the two carbon-linked compound **2.85e** was chosen as the most efficient compound from this set. The lipophilicity of this compound, however, remained too high. Therefore, an alternative strategy to reduce the ChromLogD_{7.4} in this series was sought.

2.6 Alternative Methods to Reduce Lipophilicity

Modification of the ester component of the ESM has been successfully achieved within the previously mentioned benzimidazole series, where a tetrahydrofuranyl ester **2.112** has been incorporated in the place of the cyclopentyl ester **2.69** (Figure 2.40).²⁵⁶ A 1.7 unit decrease in lipophilicity was observed on incorporating the additional oxygen atom. Importantly, neither the biochemical nor the whole blood potencies are significantly affected by the change.

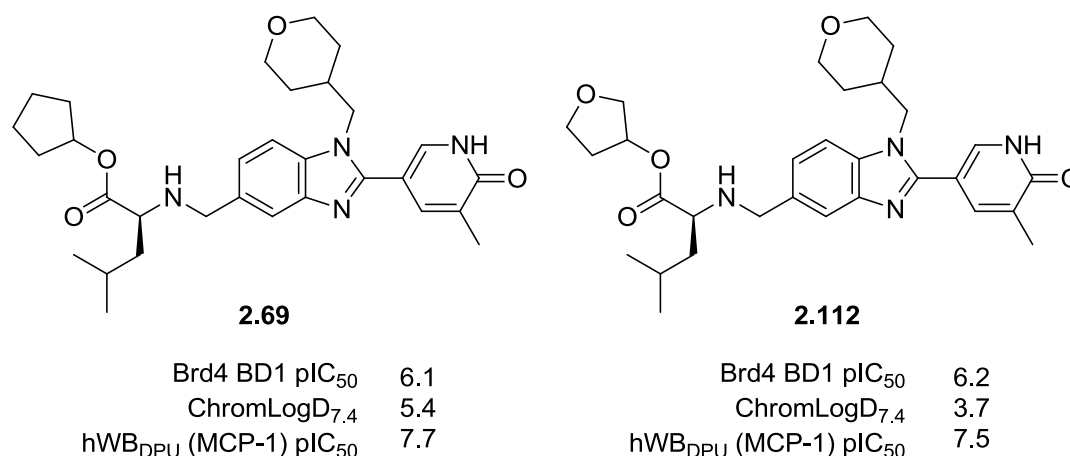


Figure 2.40: Substitution of cyclopentyl ester for tetrahydrofuranyl within the benzimidazole series

Separation of the THF isomers of **2.112** showed little difference between these stereoisomers, therefore, the more widely available *S*-enantiomer was utilised. Taking inspiration from this work, compound **2.85e**, could be modified to include the tetrahydrofuranyl ester. The calculated ChromLogD_{7.4} for compound **2.113** is predicted to be more than 1 log unit lower than compound **2.85e** (Figure 2.41).

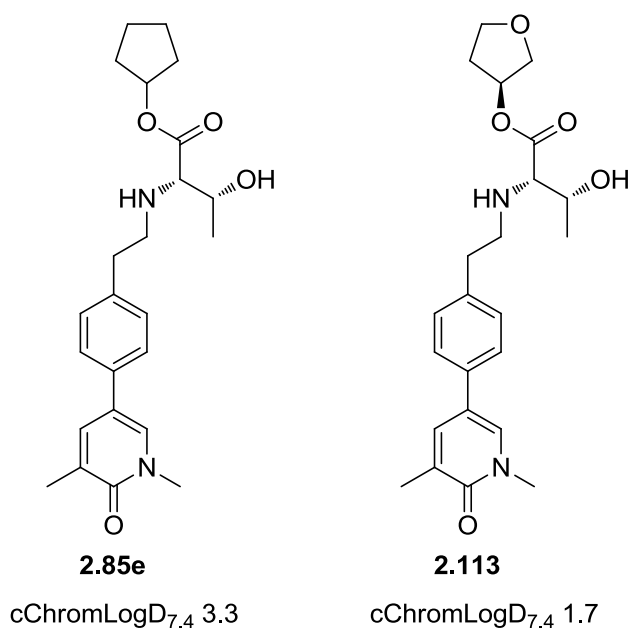
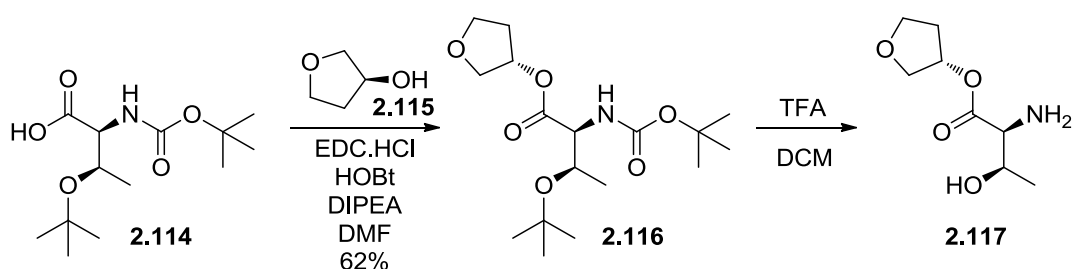


Figure 2.41: Calculated lipophilicities of cyclopentyl and tetrahydrofuran esters

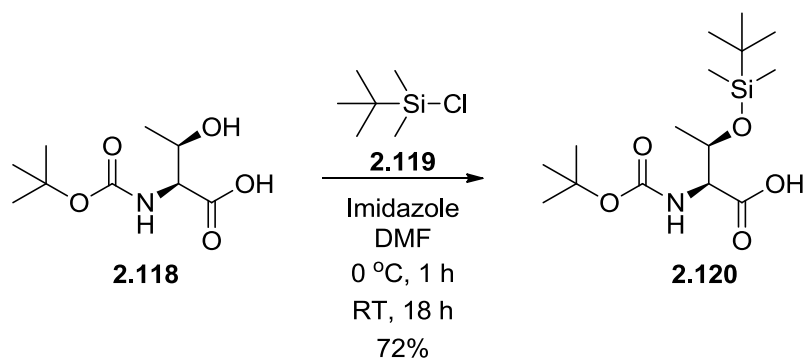
To synthesise compound **2.113**, the tetrahydrofuran threonine ester was required. The synthesis of the tetrahydrofuran leucine amino acid ester required for the synthesis of compound **2.112**, involved a Dean-Stark esterification. Unfortunately, it has been observed within our laboratory that the condensation of polar amino acids with polar alcohols, using this method, is less robust.²⁵⁷ An alternative was, therefore, required. Also within our laboratory, an initial attempt was made to synthesise this ester using doubly protected threonine **2.114** (Scheme 2.41).²⁴⁰ The initial esterification was successful, but the deprotection with TFA gave a product of insufficient purity for larger quantities.



Scheme 2.41: Attempted synthesis of threonine THF ester 2.117 from *t*-butyl analogue 2.114

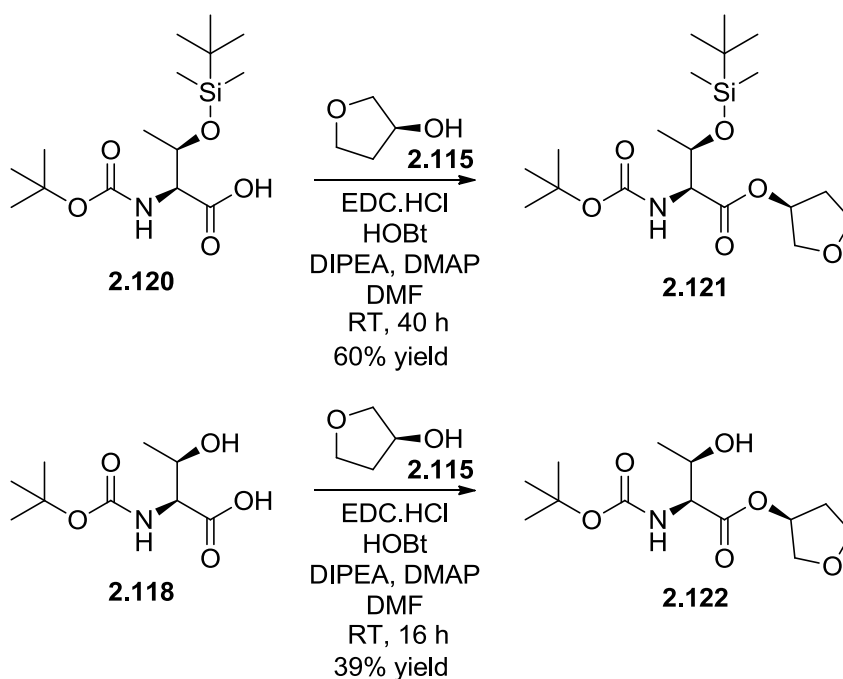
Accordingly, a more reliable method was required. The first step was to investigate the hydroxyl protecting group, as it was hypothesised that the threonine side chain would compete with the tetrahydrofuran alcohol in the esterification step. A literature search identified a mild procedure to protect the hydroxyl with a TBDMS group.²⁵⁸

This protection proceeded in good yield as shown in Scheme 2.42, and importantly, the subsequent removal would be facile under TBAF conditions.



Scheme 2.42: Silyl protection of Boc protected threonine

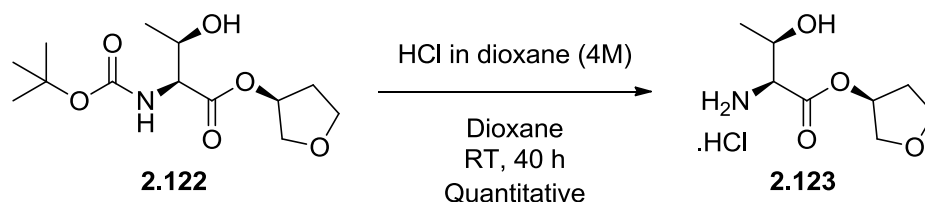
To test the benefits of the protecting group, two side-by-side reactions were carried out on a small scale. The first used the silyl protected product **2.120** from the previous reaction while the second used the Boc-threonine containing the free hydroxyl **2.118** (Scheme 2.43).



Scheme 2.43: Side-by-side comparison the esterification of 2.120 and 2.118

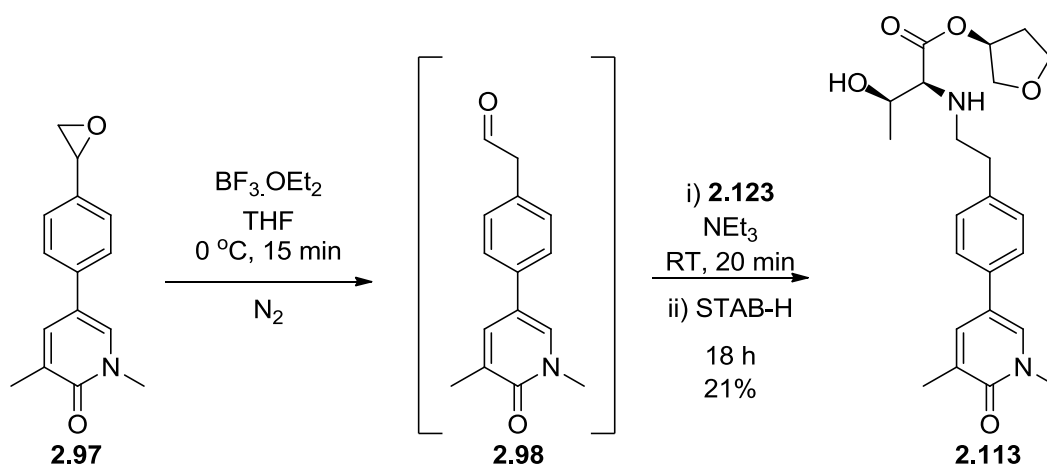
It was found that while the silyl protected ester **2.121** was formed in 60% isolated yield, the unprotected threonine side chain was not seen to interfere drastically, delivering a 39% isolated yield of **2.122**. Taking into account the protection and deprotection of the silyl group, it was decided to be unnecessary. A larger batch of

ester **2.122** was prepared and isolated in good purity (and with a similar yield of 41%). The Boc group was subsequently removed under acidic conditions forming the hydrochloride salt **2.123** on work-up, which was isolated in quantitative yield (Scheme 2.44).



Scheme 2.44: Deprotection of Boc group

This amino acid ester was subsequently used to form the desired product **2.113**. Again, the key epoxide **2.97** was treated with Lewis acid to effect the rearrangement before the addition of the newly synthesised amino acid ester, **2.123** (Scheme 2.45). The product was isolated in low yield over the two steps.



Scheme 2.45: Lewis acid rearrangement and reductive amination with amino acid ester 2.123

The next stage was to profile the compound to investigate whether modifying the ester had had the desired effect of reducing the lipophilicity, without affecting the other desirable properties of the molecule. Pleasingly, the ChromLogD_{7.4} was significantly reduced by two log units compared to compound **2.85e** (Figure 2.42, Table 2.18). It can also be highlighted that neither the biochemical nor the whole blood potencies were affected by the change, delivering a compound in excellent physicochemical space with excellent whole blood potency.

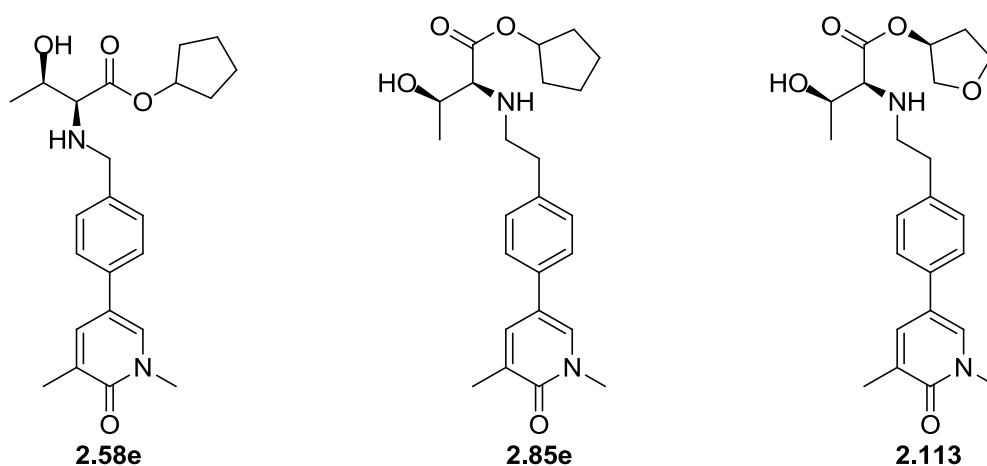


Figure 2.42: Comparison of THF and cyclopentyl esters

	TPP (Ester)	Compound 2.58e	Compound 2.85e	Compound 2.113
Brd4 BD1 pIC₅₀		5.7	5.8	5.6
Acid Brd4 BD1 pIC₅₀		4.6	5.0	5.0
hWB_{DPU} (MCP-1) pIC₅₀	≥7.0	6.5	7.2	7.1
ΔpIC₅₀	≥1.0	0.8	1.4	1.5
Brd9 pIC₅₀ (fold selectivity*)	(≥30)	6.0 (x2)	6.3 (x3)	6.3 (x5)
hCE-1 SA (μM/min/μM)	<1	6.0	20	13
ChromLogD_{7.4}	≤4.0	4.4	4.6	2.6
PFI	≤6.0	6.5	6.6	4.6
HLM IVC (-/+ benzil) (mL / min / g tissue)	<2 (- benzil)	28 / 5.4	26 / 9.4	- / -
Solubility (μg/mL)	>100	974 (FaSSIF)	147 (CLND)	154 (CLND)

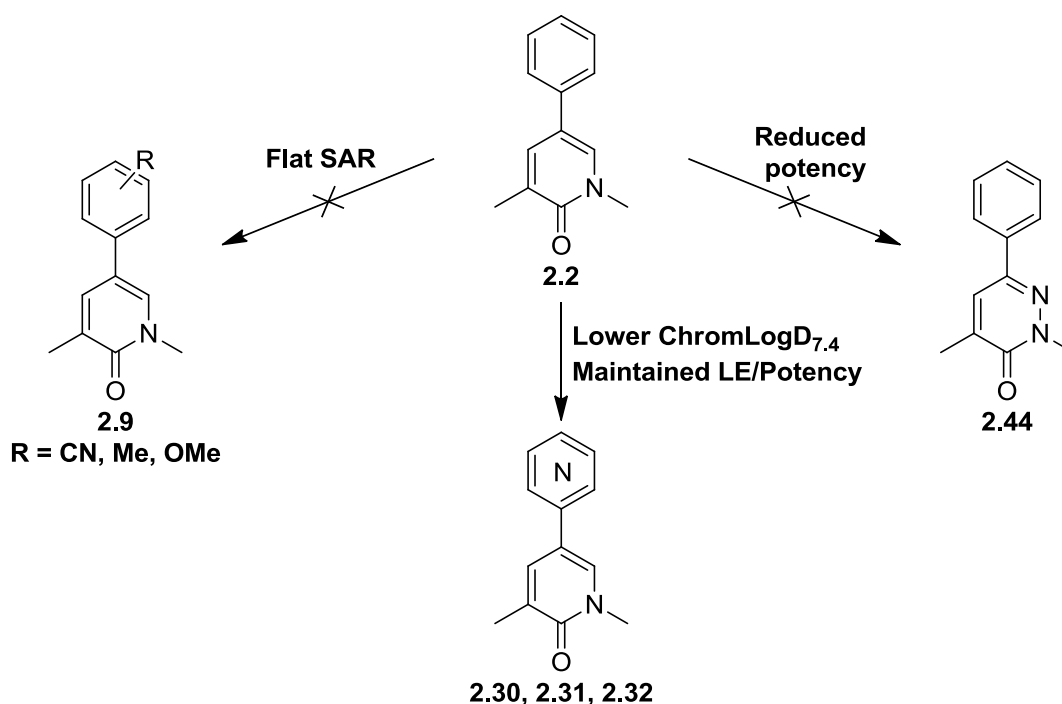
Table 2.18: Comparison of 2.113 with cyclopentyl ester 2.85e and start point 2.58e with the project TPP (*over Brd4 BD1)

Overall, the initial lead ESM-functionalised compound **2.58e** has been improved over a number of iterative steps to **2.113**. This compound was now in the desired area of the TPP for a number of key properties. An excellent whole blood potency of over 7 has been achieved by balancing the improved potency of the acid, combined with a higher hCE-1 specific activity. Similarly, by utilising the polar THF ester, the ChromLogD_{7.4} is comfortably within the TPP guidelines of less than 4 and the solubility of all three compounds was excellent. However, despite the lower

lipophilicity, the IVC was not measured due to the high hCE-1 value and the high clearance observed for compound **2.85e**. The obvious disadvantage with these compounds is the lack of selectivity over the representative non-BET bromodomain Brd9, a property of this chemotype which would require further optimisation.

2.7 Summary

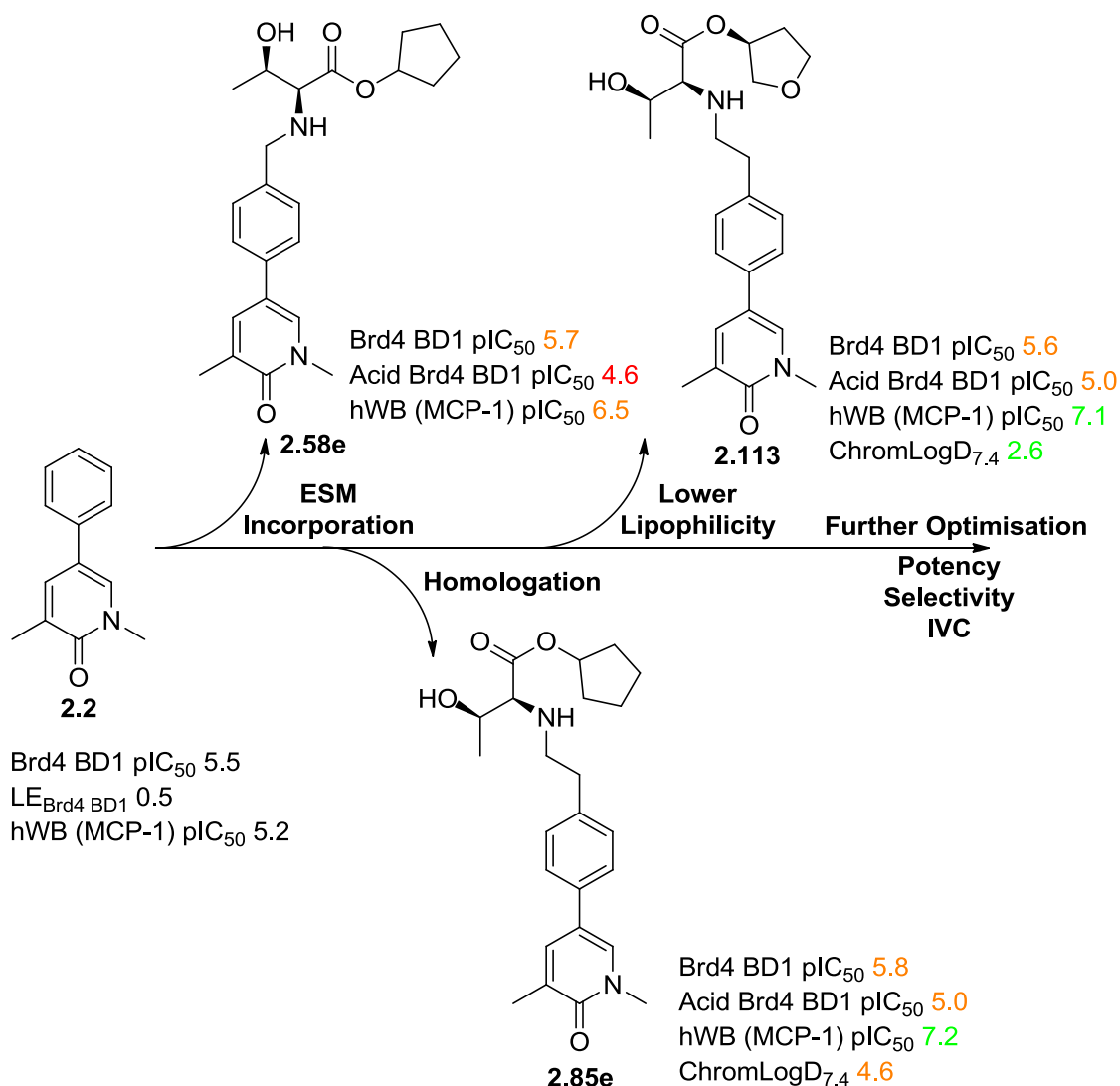
The initial focus of this programme of work was to select a ligand efficient fragment and to investigate the potential to further improve its efficiency prior to further functionalisation. Compound iterations investigated the electronics of the core phenyl ring as well as the ability to incorporate nitrogen atoms into the core and warhead to understand the ability to increase potency and reduce lipophilicity. While the SAR around the electronics study was flat, the use of a pyridyl core was found to be viable, reducing lipophilicity while maintaining biochemical potency (Scheme 2.46).



Scheme 2.46: Successful synthesis of modified fragment, 2.2, culminating in pyridyl examples 2.30, 2.31 and 2.32 being well tolerated

Following this optimisation, it was demonstrated that the ESM could be successfully added to a small ligand-efficient start point without loss of biochemical potency. Excitingly, the ESM-functionalised compound **2.58e** showed enhanced inhibition of

cytokine production within the hWB assay beyond the biochemical potency (Scheme 2.47).



Scheme 2.47: Key advancements through incorporation and optimisation of the ESM and linker

With this excellent result, a retention assay, using isolated macrophages, showed the ability to retain the acid within the target cell type in quantities 10-fold higher than that of the ester. The addition of the effect from the acid was hypothesised to be causing the enhancement in whole blood potency. However, the acid of **2.58e** was a log unit less potent within the hypothesised biochemical assay than the ester. As such, increasing the acid potency was thought to increase the whole blood potency. Synthesising homologated example **2.85e** maintained the ester potency while the acid potency was increased. For the first time, it was demonstrated that

the acid biochemical potency coupled with the hydrolysis rate by hCE-1 was key for the observed enhanced whole blood potency.

This section of the study concluded with compound **2.113**, which revealed the important contribution the ester plays in modulating the physicochemical properties. The THF ester of threonine ensured the template was well within the TPP, aiding other properties such as solubility.

However, having successfully optimised the addition of the ESM to fragment **2.2**, a number of properties require further optimisation: potency, selectivity, hCE-1 specific activity and IVC. Considering the lead compound **2.113** was more potent at the non-BET bromodomain Brd9, the selectivity must be changed towards BET by both increasing the Brd4 BD1 potency while optimising against Brd9. It is also hypothesised that reducing the high hCE-1 enzyme hydrolysis rate would be beneficial in reducing the hydrolysis-mediated liver metabolism. Efforts would also focus on reducing the overall metabolism within this assay.

3 BET Pharmacophore Optimisation

3.1 Non-BET Bromodomains

As previously described, only eight of the 61 known bromodomains reside within the BET family. Due to the increasing wealth of knowledge around the therapeutic potential of disrupting the BET bromodomain-histone recognition, the remainder can be grouped as non-BET bromodomains.²⁵⁹ The non-BET bromodomains can be seen within the phylogenetic tree shown in Figure 3.1.

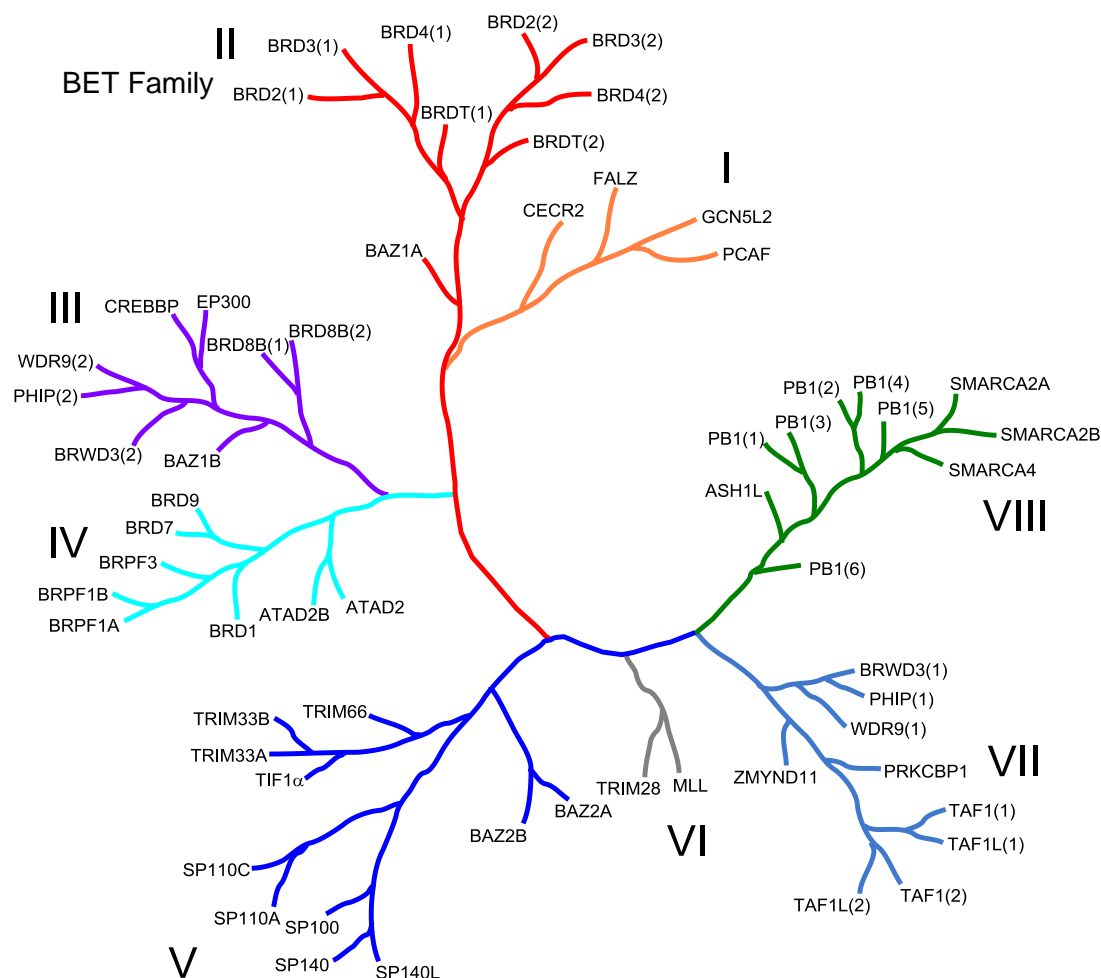


Figure 3.1: Phylogenetic tree with the BET family highlighted

Unfortunately, the biological function of the non-BET bromodomains is less well understood. Therefore, a number of research groups are focused on developing small molecule chemical probes for these lesser-understood bromodomains to elucidate their biological function. To highlight the successes in this area, two case studies will be used as examples of chemical probes with selectivity for just one or two of the 61 bromodomains.

3.1.1 Inhibitors of the non-BET Bromodomains

Firstly, in a collaboration between the SGC and the University of Oxford, scientists have developed the CREBBP/EP300 dual probe, SGC-CBP30 (**3.1**, Figure 3.2), a selective inhibitor of these family III bromodomains (Figure 3.1).²⁶⁰ As a nanomolar inhibitor of these ubiquitously expressed BCPs, the research groups were able to exploit differences between the remainder of the phylogenetic tree and these highly conserved bromodomains.

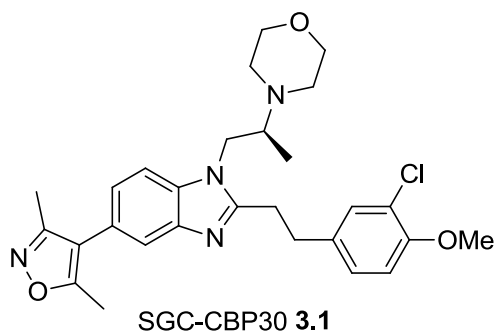


Figure 3.2: SGC-CBP **3.1**

Hay *et al.* initiated this work from fragment **3.2**, discovered from a hit-finding screen to be equipotent at Brd4 BD1 and CREBBP.²⁶¹ Structure-guided design led work towards substituting the 1- and 2-position of the benzimidazole to give compound **3.3** (Figure 3.3), 0.9 log units more potent at CREBBP than the initial fragment.²⁶²

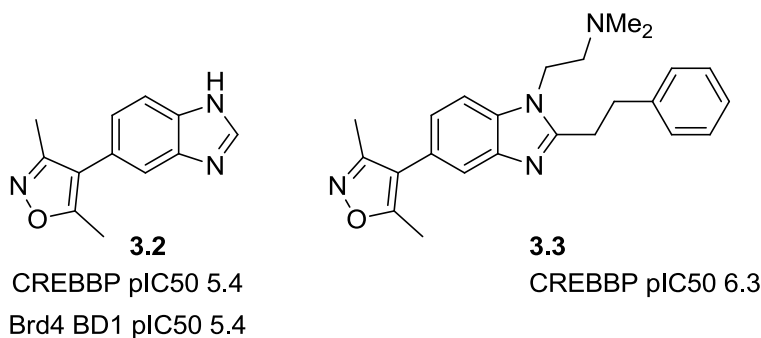


Figure 3.3: Fragment start point **3.2** and elaborated CREBBP selective compound **3.3**

Optimisation of the amine substituent initially produced compound **3.4**, which was seen to be only 3-fold selective against Brd4 BD1. X-ray crystallography demonstrated that different binding modes were observed in CREBBP and Brd4 BD1. Hence, the electronics of the phenyl ring were optimised towards example **3.5** (Figure 3.4), with electron-rich aryls favoured due to a π -stacking interaction with an arginine residue, shown with the X-ray crystal structure of SGC-CBP30 (**3.1**) in

CREBBP (Figure 3.5). Finally, constraining the flexible ethyl linkers was attempted to favour binding to CREBBP. This was successfully achieved, producing the chemical probe SGC-CBP30 **3.1**, with K_d values of 21 and 31 nM for CREBBP and EP300, respectively, whilst 40-fold selective against Brd4 BD1 (Figure 3.4).²⁶²

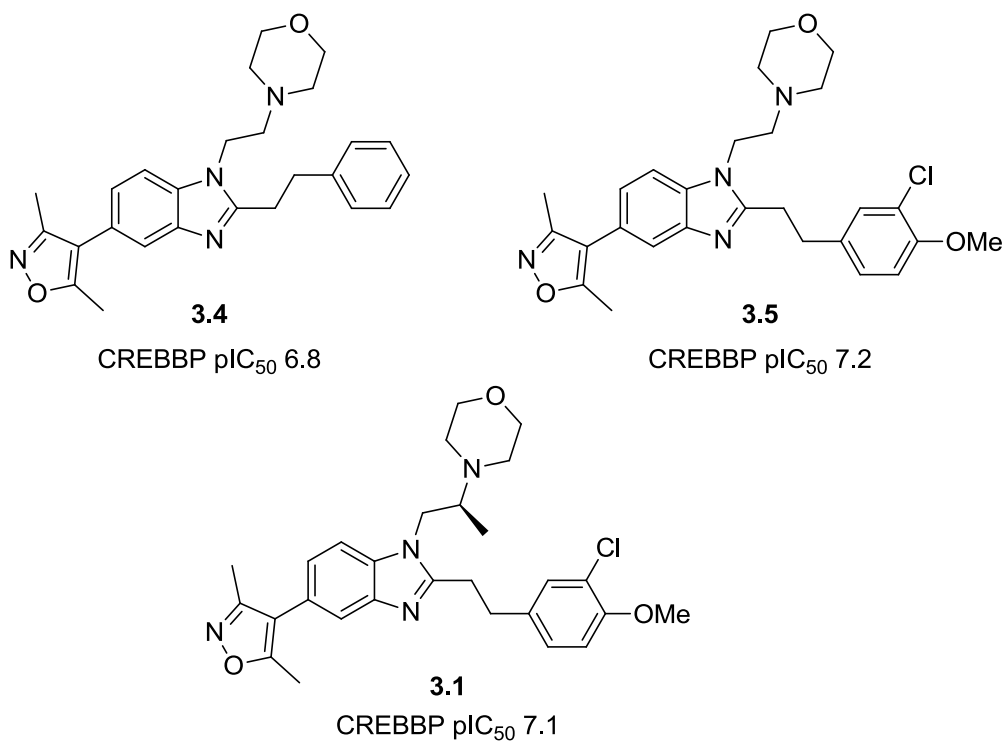


Figure 3.4: Progression of optimisation towards SGC-CBP30 **3.1**

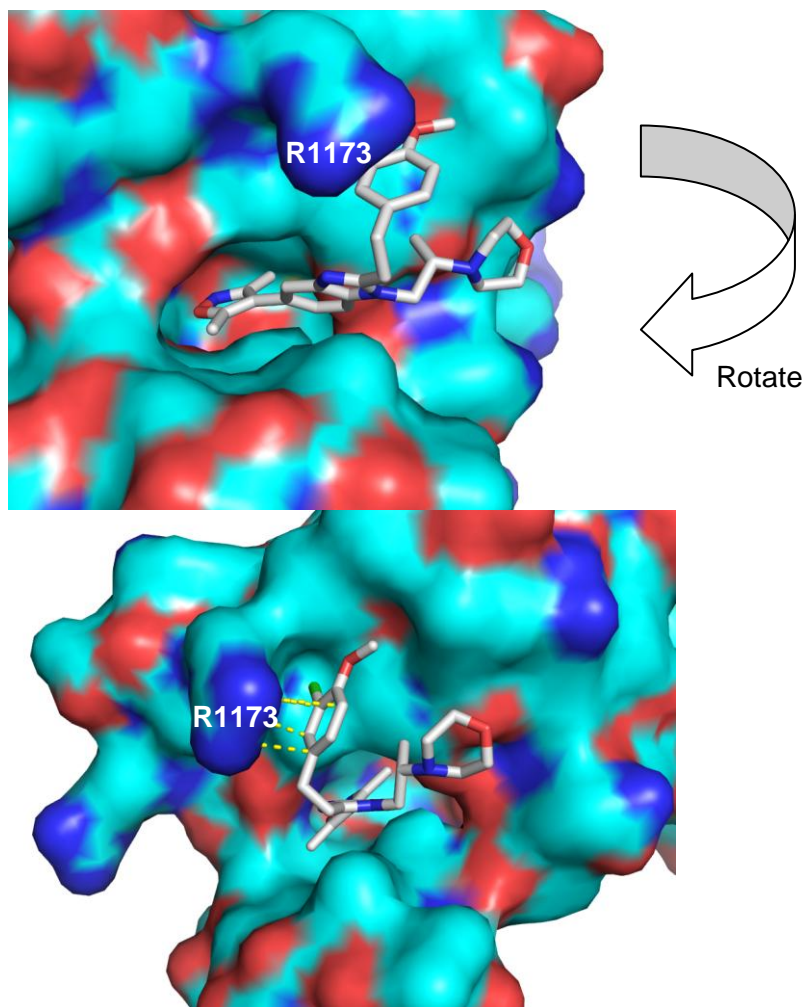


Figure 3.5: X-ray of SGC-CBP30 (3.1) in CREBBP bromodomain with rotated view highlighting π -stacking in yellow

While SGC-CBP30 was only published by Hay *et al.* in 2014, the chemical probe is being used to investigate potential therapeutic uses of a CREBBP/EP300 inhibitor. Recently, Hammitzsch and co-workers at the Botnar Research Institute have demonstrated the differentiated profile of SGC-CBP30 compared to the BET inhibitor (+)-JQ-1 in the down-regulation of pro-inflammatory cytokines.²⁶³ Further, Hammitzsch *et al.* undertook pre-clinical studies using cells from patients with the chronic arthritic conditions ankylosing spondylitis and psoriatic arthritis, demonstrating the potential for CBP-30 to down-regulate IL-17A. This finding is important considering an anti-IL-17A antibody, secikinumab, has been developed for the treatment of ankylosing spondylitis and had been shown to be efficacious. Therefore, drugging CREBBP/EP300 may offer a potential small-molecule strategy to treating this disease.

In comparison, a collaboration between GSK and the University of Strathclyde produced the Brd9 chemical probe, I-BRD9.²⁶⁴ This work started from the selective hit molecule **3.6** (Figure 3.6). It was discovered that secondary amides (**3.7**) introduced a key hydrogen bond donor, which increased the potency at Brd9, but also narrowed the selectivity over the BET bromodomains.

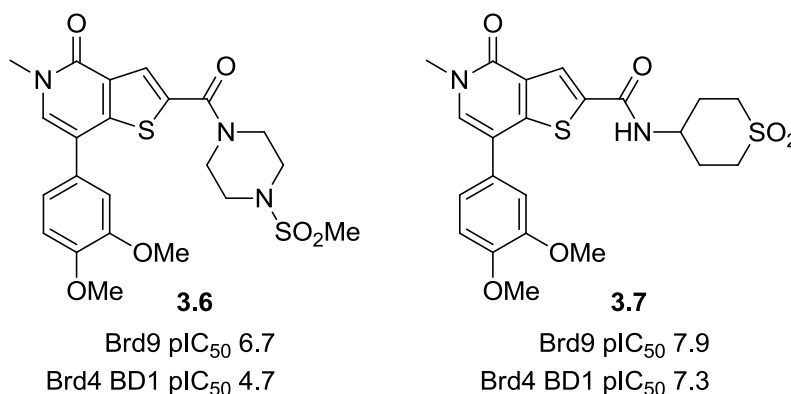


Figure 3.6: Hit molecule 3.6 and secondary amide 3.7

Similar to the strategy towards the development of SGC-CBP30, small structural differences were used to introduce selectivity for Brd9 over BET, during the optimisation towards I-BRD9. A large improvement was the introduction of the amidine, **3.8** (Figure 3.8).²⁶⁴ This group was able to make a hydrogen bond to the Brd9 protein (Figure 3.7), whilst improving selectivity by being placed in a lipophilic pocket within Brd4 BD1.

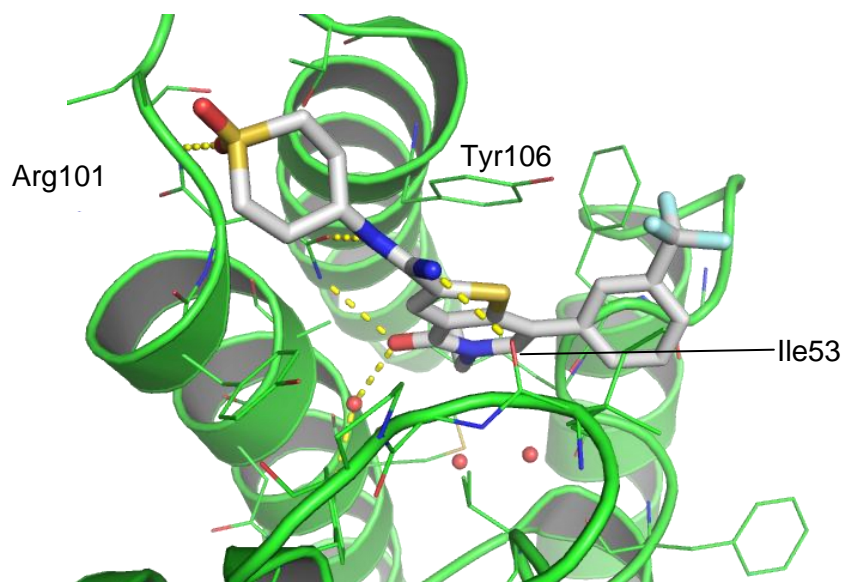


Figure 3.7: I-BRD9 (3.9) within Brd9
(Protein Data Bank: pdb 4uiw)

Further modifications to the aryl ring and introduction of the *N*-ethyl group facilitated the formation of a Brd9 selective chemical probe I-BRD9 (**3.9**) with 700-fold selectivity over BET (Figure 3.8). Additionally, 200-fold selectivity over the closest bromodomain, Brd7 and >70-fold selectivity against the remainder of the phylogenetic tree gave I-BRD9 an excellent profile.

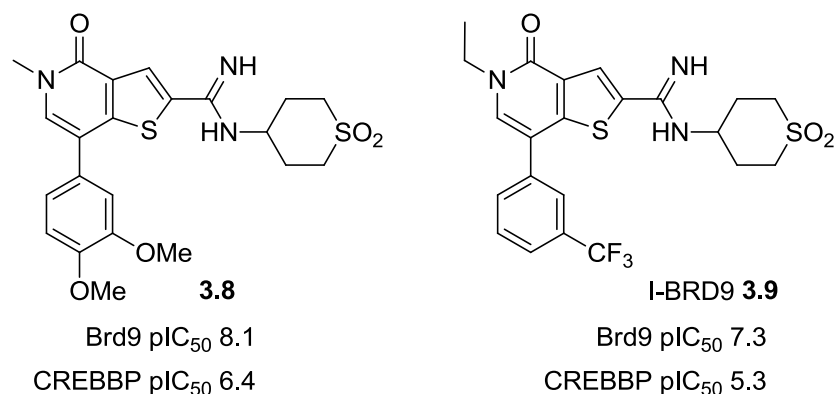


Figure 3.8: Amidine 3.8 and the chemical probe I-BRD9 (3.9)

Both SGC-CBP30 (**3.1**) and I-BRD9 (**3.9**) are excellent examples of utilising structure-based design to produce selective bromodomain inhibitors. However, due to the current yet to be uncovered effects of inhibiting the non-BET bromodomains, and from the point of view of this programme of work, any risks associated with targeting them can be mitigated by designing compounds that are selective for the BET family. Considering the successes detailed above in generating selective chemical probes for individual non-BET bromodomains, the inverse must be possible, that is using structure-based design to introduce selectivity for the BET family of bromodomains.

3.2 Introducing Selectivity for BET over the non-BET Bromodomains

Revisiting the lead compound and its acid, it can be seen that the ester **2.113** has moderate potency against Brd4 BD1 with a lower potency of 5.0 for the corresponding acid **2.101e** (Figure 3.9). However, at this stage, both the ester and acid were more potent within the Brd9 assay, which was undesirable. In order to introduce selectivity over the broader bromodomain family, it is important to

understand how the BET family of bromodomains differ from the non-BET bromodomains.

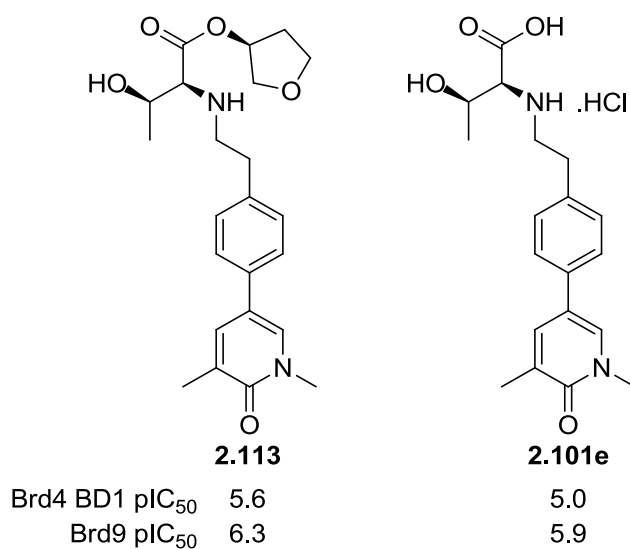


Figure 3.9: Lead compound 2.113 and acid 2.101e

Returning to the bromodomain binding pocket, there are three important regions of the BET family of proteins that can be interacted with when inhibiting the binding of acetylated lysine. Firstly and importantly, is the acetyl-lysine binding pocket. Within BET, the key binding interaction is a through water interaction to tyrosine Y97 with an additional hydrogen bond to the conserved asparagine residue (N140) (Figure 3.10).²⁰⁶

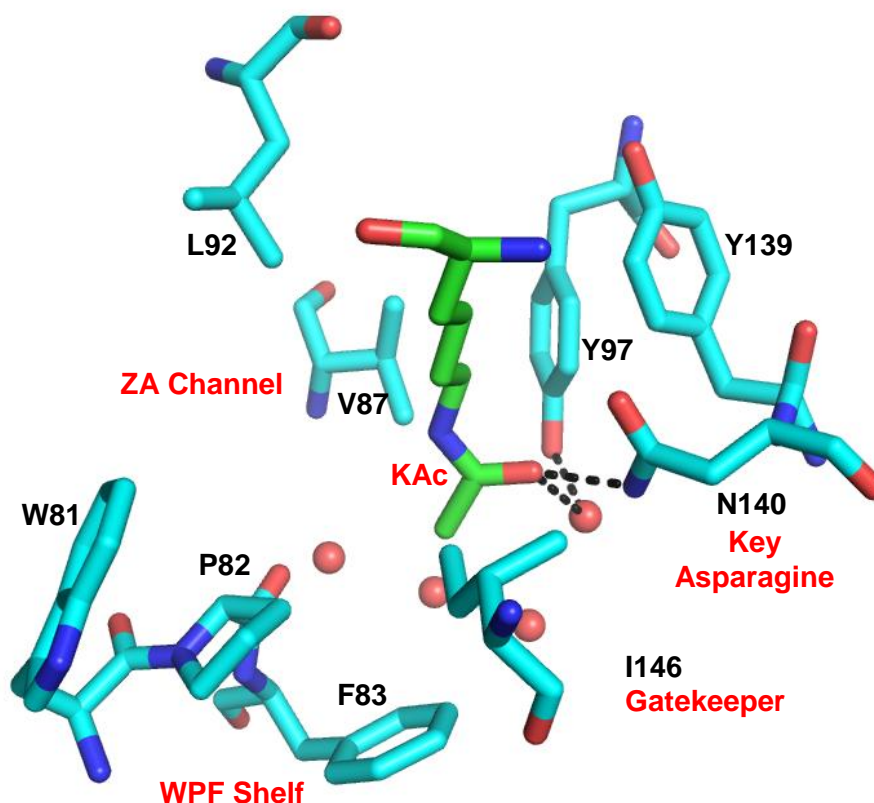


Figure 3.10: Key acetyl-lysine (AcK) binding residues in Brd4 BD1

A key feature of the BET family of bromodomains is the WPF shelf, so named for the amino acids it contains: tryptophan (W) 81, proline (P) 82 and phenylalanine (F) 83, respectively, as illustrated, for example, within Brd4 BD1 (Figure 3.10). This stack of residues defines the lipophilic nature of this WPF shelf region. However, whether the shelf region is open and accessible is defined by the gate-keeper residue. For Brd4 BD1, this is the amino acid isoleucine (I146), which maintains an open conformation, thus allowing molecules to interact with the WPF shelf region (Figure 3.11a).

In contrast, a number of the non-BET bromodomains contain a much larger gatekeeper residue, as seen, for example, within the Brd9 bromodomain. As illustrated in Figure 3.11b, the gatekeeper in Brd9 is the larger amino acid, tyrosine (Y106). This blocks the would-be shelf region and, as a result, affects the size and shape of the binding pocket compared to Brd4 BD1 (Figure 3.11a). Based on the structural similarities and differences shared by Brd9 and the BET family, Brd9 was selected as a representative bromodomain with which to gauge selectivity.

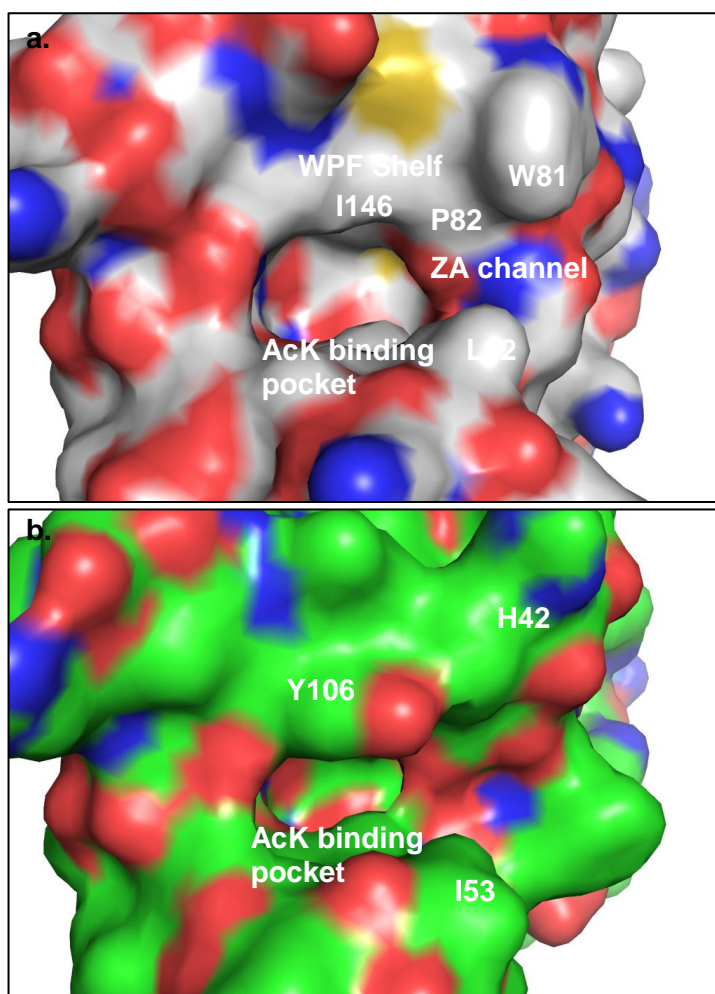


Figure 3.11: Comparison of the Brd4 BD1 (a) and Brd9 (b) binding pockets

On the other side of the WPF stack is the ZA channel (Figure 3.11a). This is flanked by the proline (P82) and tryptophan (W81) of the WPF stack on one side and a leucine (L92) on the other. To put this information into perspective, the exemplar compound **2.101c**, crystallised within Brd4 BD1, is informative (Figure 3.12). As previously discussed, the pyridone acts as the acetyl-lysine mimetic, with the phenyl entering the ZA channel positioned nicely between W81 and L92. The amino acid then extends through the ZA channel into solvent. However, this molecule does not exploit the potential potency gains associated with occupying the WPF shelf and the improved selectivity that could be introduced by clashing with the gatekeeper residues of other non-BET bromodomains.²⁶⁵ This is demonstrated in the potencies observed at Brd4 BD1 and Brd9 (Figure 3.12). Thus, it was hypothesised that given the linear nature of **2.101c** and lead compound **2.113**, the structure did not exploit the differences in the binding pocket between Brd9 and the BET family, particularly around the WPF shelf. Indeed, within Brd4 BD1, the X-ray crystal structure

demonstrates the ESM extending through the ZA channel, which in Brd9 is more open. Therefore, this more open ZA channel region within Brd9 may be the reason for the higher potency within Brd9 for this linear compound. Therefore, the addition of functionality to interact with the WPF shelf region in BET and clash with the gatekeeper within Brd9 was proposed as a promising strategy for further optimisation.

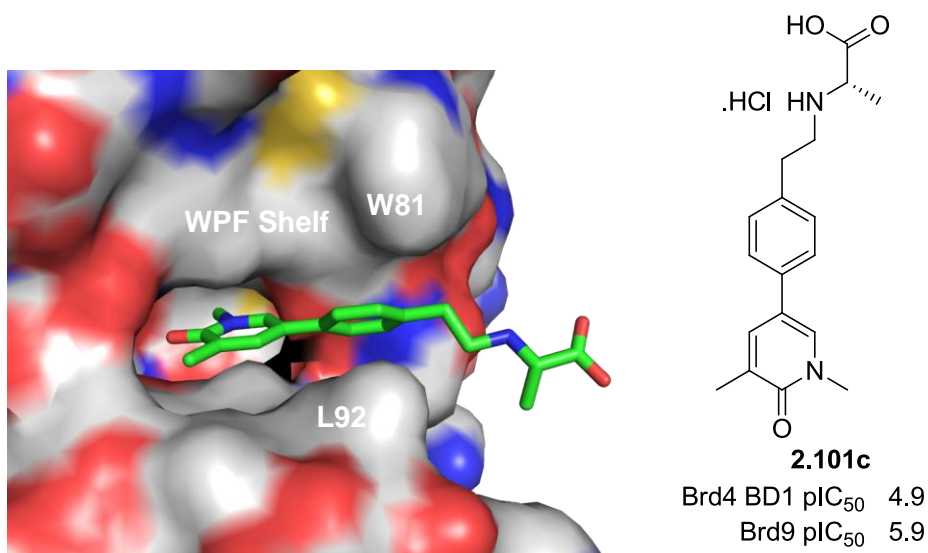


Figure 3.12: compound 2.101c crystallised in Brd4 BD1

3.2.1 Investigating Selectivity by Targeting the WPF Shelf

Binding with the lipophilic WPF shelf region occurs primarily through hydrophobic interactions, due to the lipophilic properties of the amino acid residues forming this area.²⁶⁶ Introducing a group to interact with the WPF shelf in BET was, therefore, hypothesised to improve the biochemical potency of this series at the BET bromodomains. This would also potentially improve the specificity for binding to BET due to steric clashes within the differently shaped binding pockets of non-BET bromodomains, such as Brd9.

The small ligand efficient cyclopropylmethyl group was chosen due to its previous successful use in other bromodomain studies, utilising the dimethylisoxazole acetyl-lysine mimetic (Figure 3.13).⁸⁶ Additionally, functionality containing π -character is known to make good lipophilic contacts with the WPF shelf, therefore cyclopropane was chosen due to its small size, and partial π -character.²⁶⁷ At this point, it was

decided that incorporation of additional aryl rings would be avoided in order to maintain a good PFI. Hence, the cyclopropane is a viable alternative.

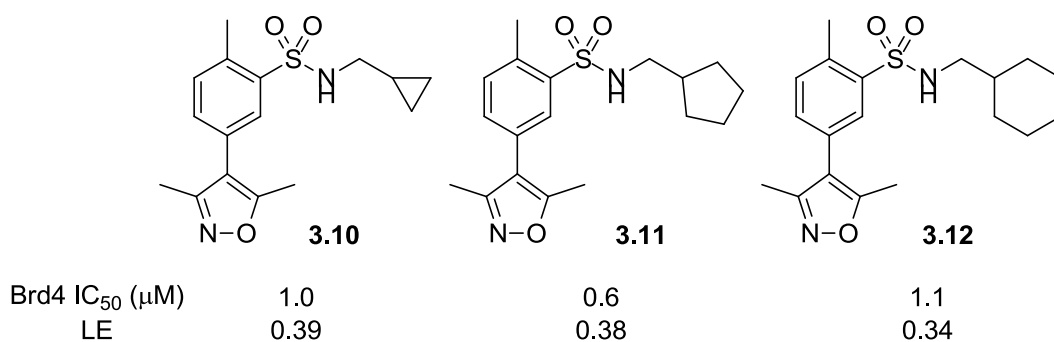


Figure 3.13: Varied WPF shelf groups

To ensure the most optimal vector for accessing the WPF shelf was selected, two initial compounds were proposed; incorporating the cyclopropylmethyl group in the *ortho*- and *meta*-positions (**3.13** and **3.14**) (Figure 3.14).

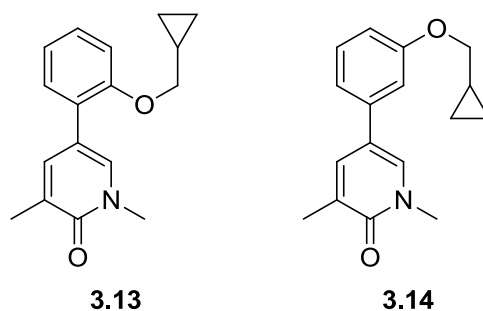
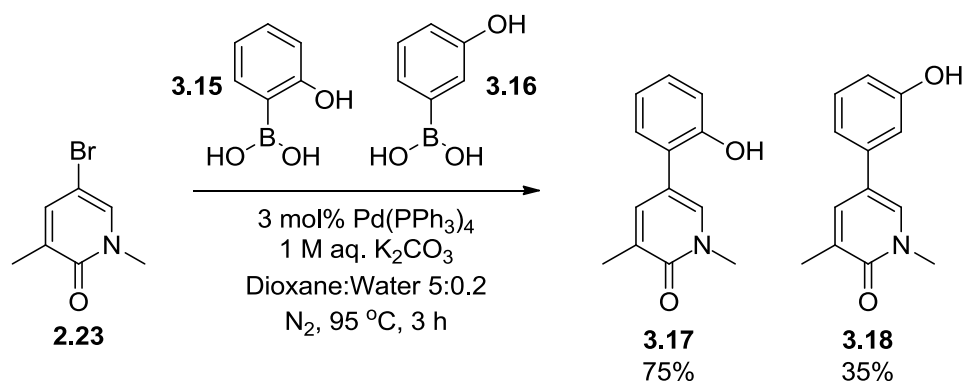
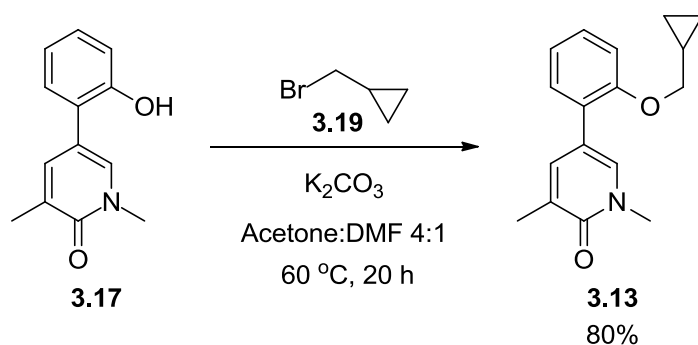
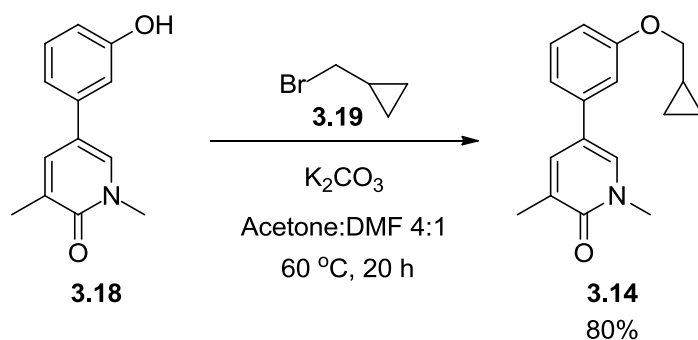


Figure 3.14: *Ortho*- and *meta*-substituted phenyl

To synthesise the proposed compounds, the previously used intermediate, bromopyridone **2.23**, was used in Suzuki cross couplings with phenol boronic acids **3.15** and **3.16** (Scheme 3.1). The resulting compounds were observed to have poor solubility in common organic solvents which, in the case of the *meta*-derivative, impacted the yield.

Scheme 3.1: Cross-coupling with boronic acids **3.15** and **3.16**

To complete the synthesis of these compounds, alkylations were undertaken using alkyl bromide **3.19**. In each case, the solubility of the phenol starting material hampered reaction progression. Therefore, an aliquot of DMF was used to aid the solubility, facilitating the reaction with the products **3.13** and **3.14** being isolated in excellent yields (Scheme 3.2 and Scheme 3.3, respectively).

Scheme 3.2: Alkylation of *ortho*-phenol **3.17**Scheme 3.3: Alkylation of *meta*-phenol **3.18**

Compounds **3.13** and **3.14** within the Brd4 BD1 biochemical assay were equipotent, leading to identical ligand efficiencies. However, the profiles within the Brd9 assay were very different (Table 3.1), with a log unit difference between the two

compounds. Also, as anticipated, introducing this cyclopropylmethyl group gave compounds with ChromLogD_{7.4} values of greater than 5.0.

	<i>ortho</i> (3.13)	<i>meta</i> (3.14)
Brd4 BD1 pIC₅₀	6.3	6.1
Brd9 pIC₅₀	4.6	5.7
LE_{BD1}	0.43	0.42
ChromLogD_{7.4}	5.2	5.1

Table 3.1: Properties of compounds 3.13 and 3.14

To understand the difference in potencies at Brd9 and to ensure the cyclopropyl was engaging the BET WPF shelf an X-ray crystal structure was obtained in Brd4 BD1 for each compound.

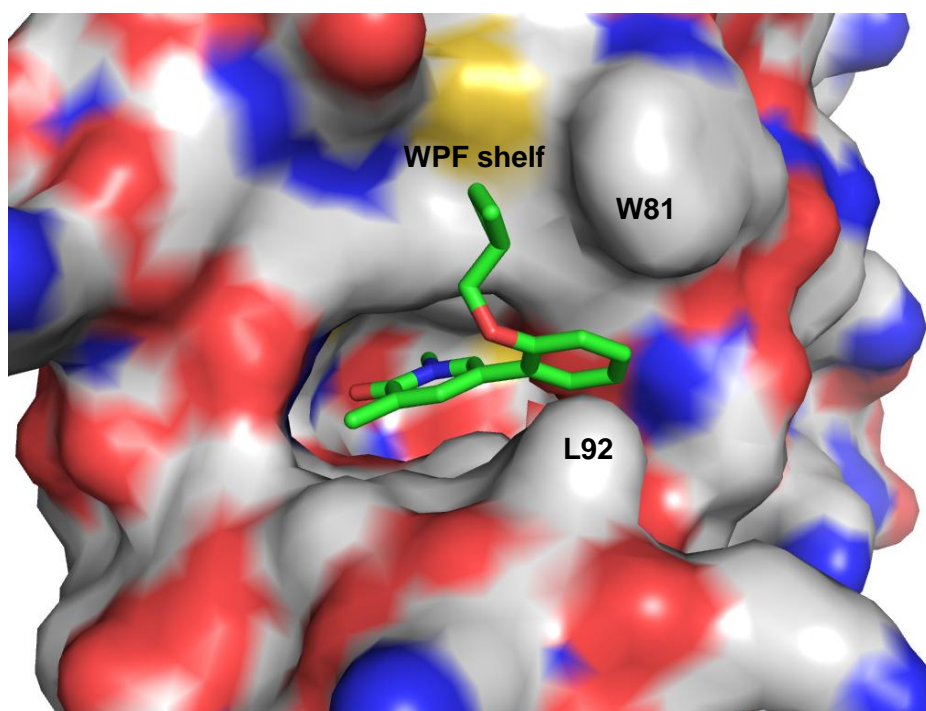


Figure 3.15: Compound 3.13 within Brd4 BD1, interacting with the WPF shelf

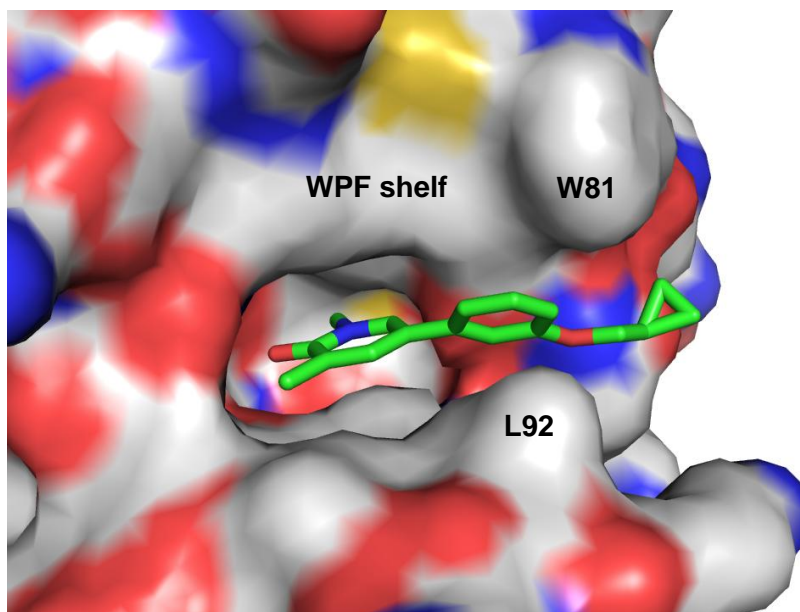


Figure 3.16: Compound 3.14 within Brd4 BD1, extending through the ZA channel

As can be seen from Figure 3.15, the cyclopropyl group is positioned towards the WPF shelf. In contrast, the substitution from the *meta*-position directs the cyclopropyl group through the ZA channel (Figure 3.16). However, as observed from the data in Table 3.1, the positioning of the cyclopropylmethyl group on the WPF shelf or through the ZA channel is similarly favourable. Additionally, these crystal data may inform as to why the *ortho*-substituted compound **3.13** is more selective than **3.14**. To visualise this, compound **3.13** was overlaid with the protein surface of Brd9. As can be seen in Figure 3.17, a major steric clash would be caused by this conformation, demonstrating that the tyrosine gatekeeper would impede the cyclopropyl group's access to the shelf. Thus, based on the biochemical data and subsequent X-ray and modelling data, the vector from the phenyl ring was shown to have an important impact on the selectivity for Brd4 BD1 over Brd9. While additional potency was not gained with **3.13** accessing the WPF shelf, compared to **3.14**, the introduction of selectivity was an excellent result providing a foundation for further optimisation. However, as previously stated, molecules including the cyclopropylmethylene group had displayed excessive lipophilicity for further development so alternatives were sought.

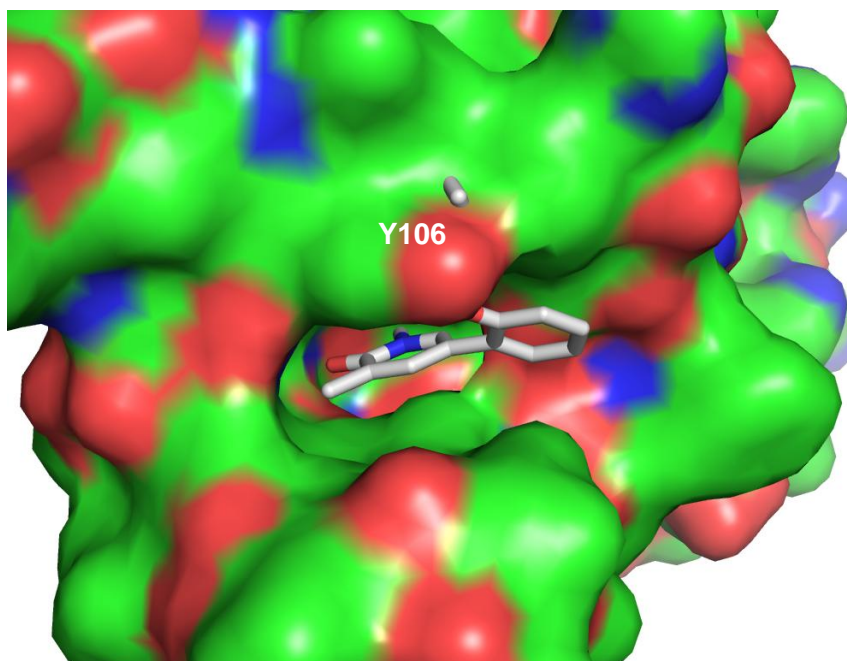


Figure 3.17: Compound 3.13 overlaid in Brd9, where access to the shelf region is blocked by Y106

To gain access to the shelf using a less lipophilic group, inspiration was taken from an associated BET BD1 project underway within our laboratory.²⁴¹ The furanopyridone template used in this associated programme is similar to the truncated pyridone **3.21** used within this work (Figure 3.18). As part of this related BD1 work, an ether linkage was used to branch from the pyridyl ring, directing groups towards the WPF shelf, demonstrated by **3.20a**, crystallised within Brd4 BD1 (Figure 3.19).²⁴¹

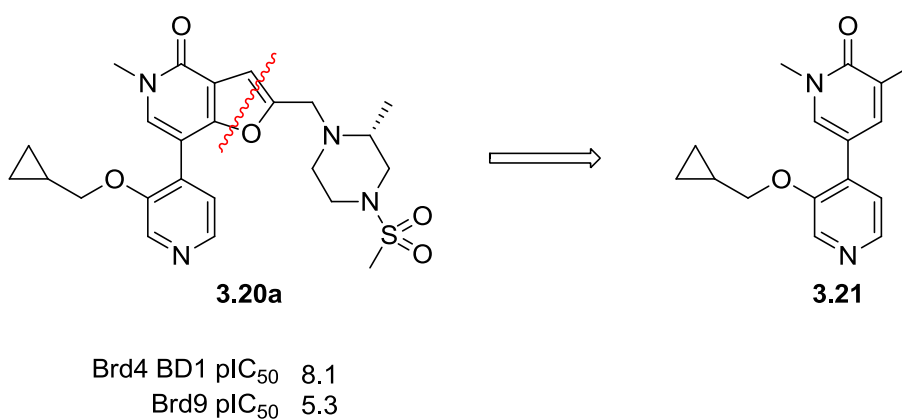


Figure 3.18: Furopyridone template

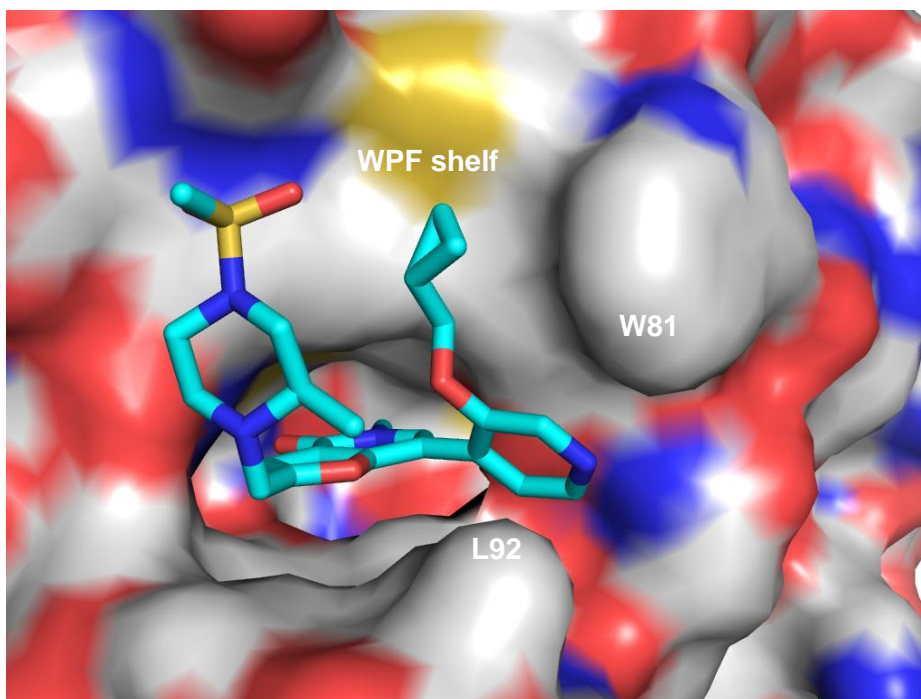


Figure 3.19: Compound 3.20a crystallised within Brd4 BD1²⁴¹

The cyclopropyl methyl group is shown to make lipophilic interactions with the WPF shelf (Figure 3.19). Furthermore, the BET family binding preference of this compound is excellent, with more than 600-fold selectivity over Brd9 (Figure 3.18). Having stated this, not all of this exquisite selectivity is due to the presence of the cyclopropylmethyl group; indeed, different WPF shelf groups within this template (Figure 3.20) deliver varying degrees of selectivity over Brd9 (Table 3.2).

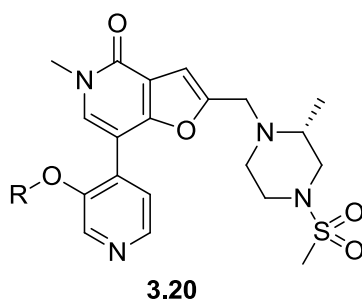


Figure 3.20: Compound 3.20 with variable R group, highlighted in Table 2.8²⁴¹

Compared to the cyclopropylmethane example **3.20a**, the alternative groups used to occupy the WPF shelf have lower ChromLogD_{7.4} values (Table 3.2). Furthermore and for example, compound **3.20c** demonstrates excellent potency and good levels of selectivity for such a small group. Increasing the size to **3.20d**, the biochemical potency decreases, but the selectivity is much improved. The tetrahydrofuran

containing examples **3.20e** and **3.20f** gave similar levels of Brd4 BD1 potency while delivering excellent selectivities over Brd9.

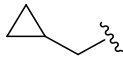
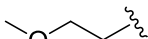
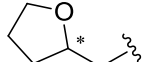
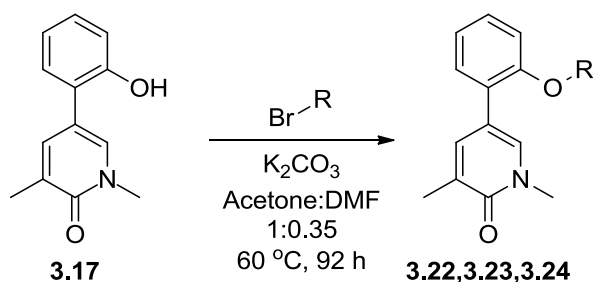
R (3.20)	Brd4 BD1 pIC ₅₀	Brd9 pIC ₅₀	Fold Selectivity*	ChromLogD _{7.4}	
	a	8.1	5.3	631	2.7
	b	7.4	4.5	794	1.9
	c	7.9	5.8	100	2.3
	d	7.4	4.6	631	2.1
	e	7.4	<4.3	>1250	2.3
	f	7.3	4.6	501	2.1

Table 3.2: Brd4 BD1 potency, selectivity and lipophilicity of 3.20 including different shelf groups²⁴¹ (*Selectivity for Brd4 BD1 over Brd9)

Returning to this programme of work, to find a more suitable group with which to occupy the WPF shelf, an exploratory study was undertaken on the core BET pharmacophore. It was hypothesised that outcomes from this study would then translate across to ESM-functionalised compounds. Three baseline compounds were proposed using ethyl **3.22**, methoxyethyl **3.23** and methylene-THF **3.24**. These initial baseline compounds were synthesised through a reaction with the appropriate alkyl bromide to yield the desired products in good to excellent yield (Scheme 3.4, Table 3.3).



Scheme 3.4: Synthesis of baseline compounds 3.22, 3.23 and 3.24

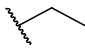
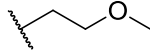
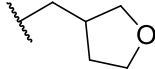
R			
	3.22	3.23	3.24*
Yield (%)	75	85	58
Brd4 BD1 pIC ₅₀ (LE)	5.7 (0.43)	5.9 (0.40)	6.3 (0.39)
Brd9 pIC ₅₀	5.1	4.7	4.9
Fold Selectivity**	x4	x16	x25
ChromLogD _{7.4}	4.3	3.6	3.7

Table 3.3: Baseline compounds (*racemate) (**Selectivity for Brd4 BD1 over Brd9)

As the size of the group occupying the WPF shelf increases, so does the potency (Table 3.3). To put these results in perspective, compound **3.22** with a pIC₅₀ at Brd4 BD1 of 5.7 is equipotent with initial fragment **2.2** (Figure 3.21) which had a pIC₅₀ of 5.5 (Figure 3.21), thus **3.22** is believed to be not making an interaction with the shelf. Compounds **3.23** and **3.24**, on the other hand, have improved Brd4 BD1 potencies and similar LE values. In terms of selectivity, the methoxyethyl group, in compound **3.23**, gives the lowest Brd9 potency, although the THF example has the best selectivity of 1.4 log units, corresponding to 25-fold selectivity. Overall, on the balance of data, the methoxyethyl group was selected for further investigation due to its reasonable selectivity and good LE from this low molecular weight group.

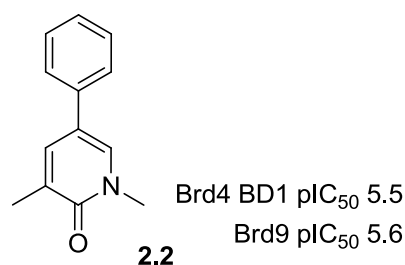


Figure 3.21: Baseline compound 2.2

As an initial investigation, the selectivity of baseline compound **3.23** was thought to be sufficient to combine this methoxyethyl group with the lead ESM-functionalised compound **2.113**. The aim was to combine the enhanced whole blood and low lipophilicity of ESM-functionalised **2.113** along with the emergence of selectivity achieved with compound **3.23** (Figure 3.22).

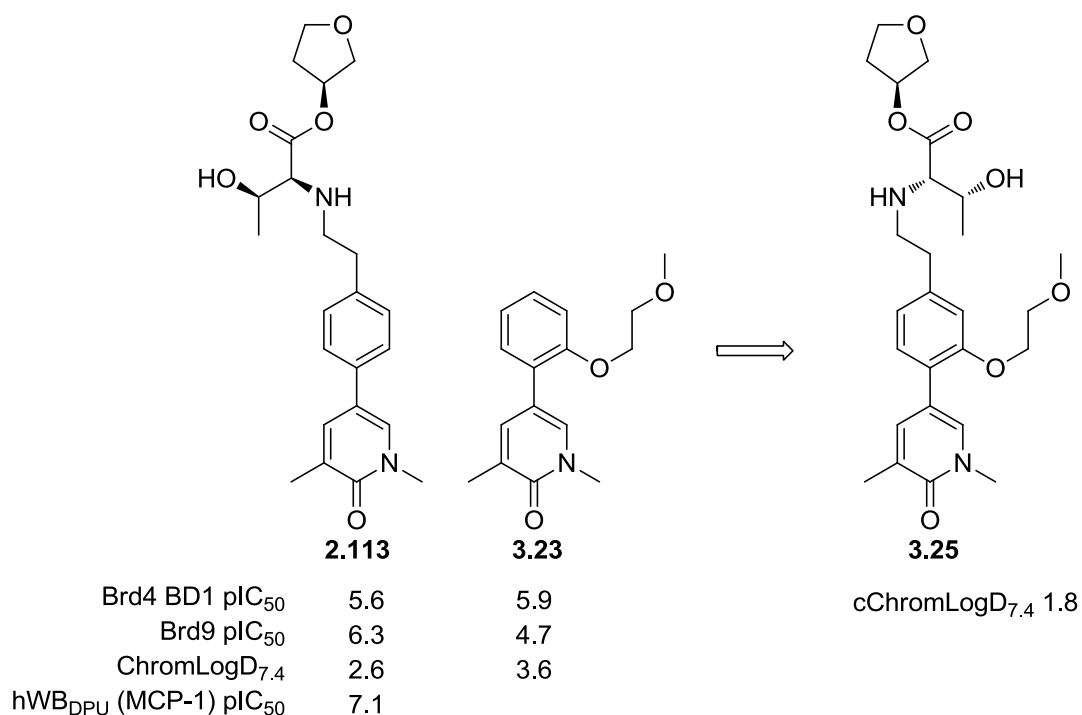
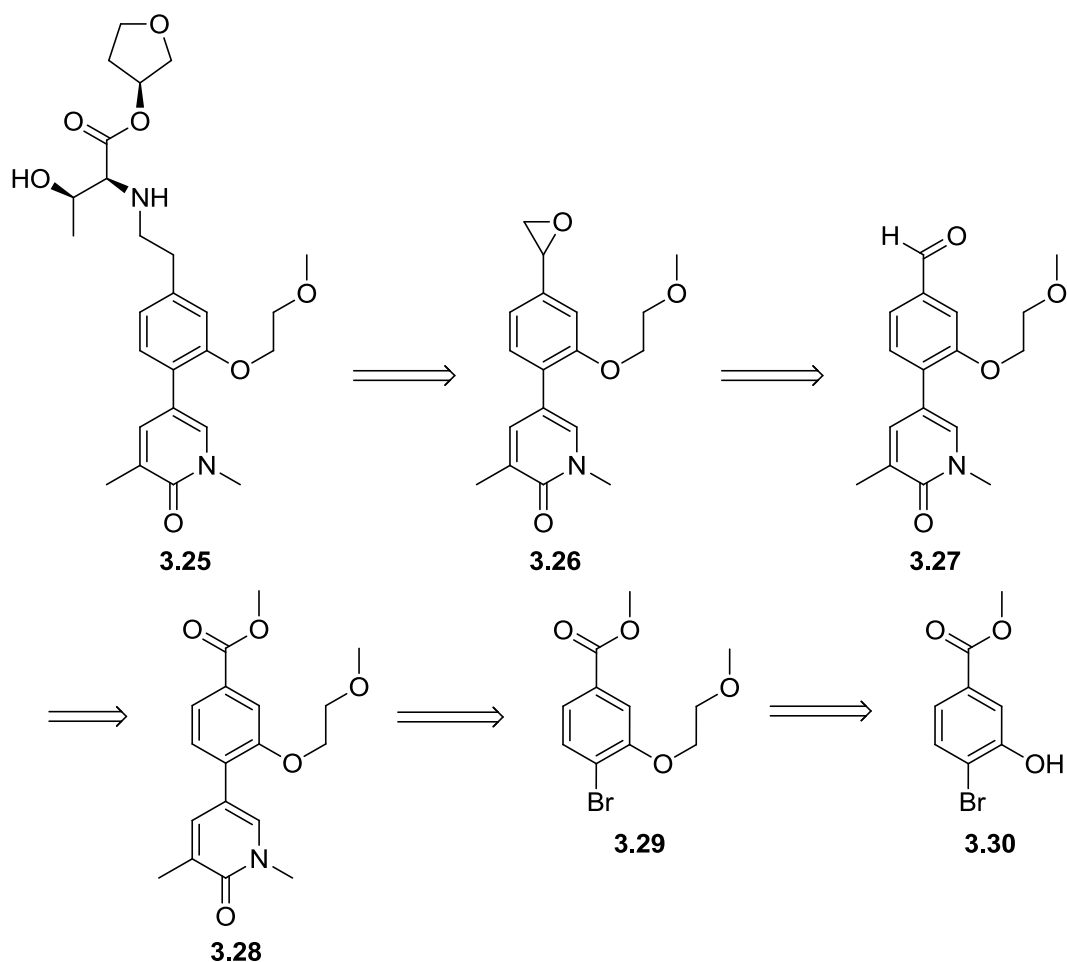


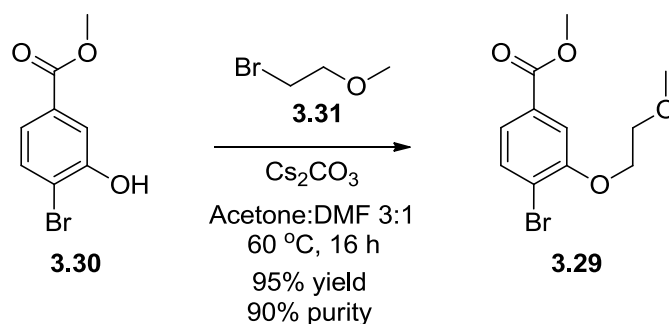
Figure 3.22: Combination of homologated compound 2.113 and baseline compound 3.23

Planning out the retrosynthesis of compound **3.25**, the amino acid ester could be disconnected to the homologated aldehyde formed by epoxide **3.26** rearrangement (Scheme 3.5). The epoxide could be formed from aldehyde **3.27**. Functional group interconversion could return to ester **3.28** and disconnection of the aryl ring could access readily available bromo ester **3.30**.



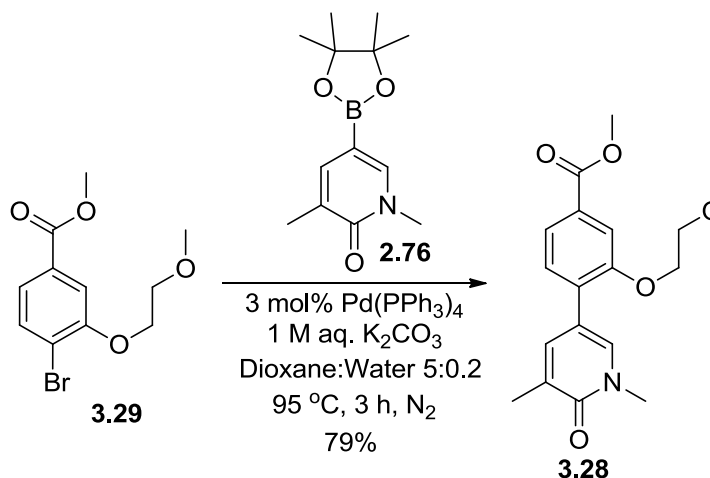
Scheme 3.5: Full retrosynthesis of desired compound 3.25

To begin this synthesis, alkylation of the bromophenol ester **3.30** was carried out using caesium carbonate as the base (Scheme 3.6). The reaction proceeded cleanly with a shorter reaction time and fewer equivalents of alkylating agent being required, compared to previous examples using potassium carbonate. Satisfyingly, an aqueous workup gave the product in good purity and excellent yield.



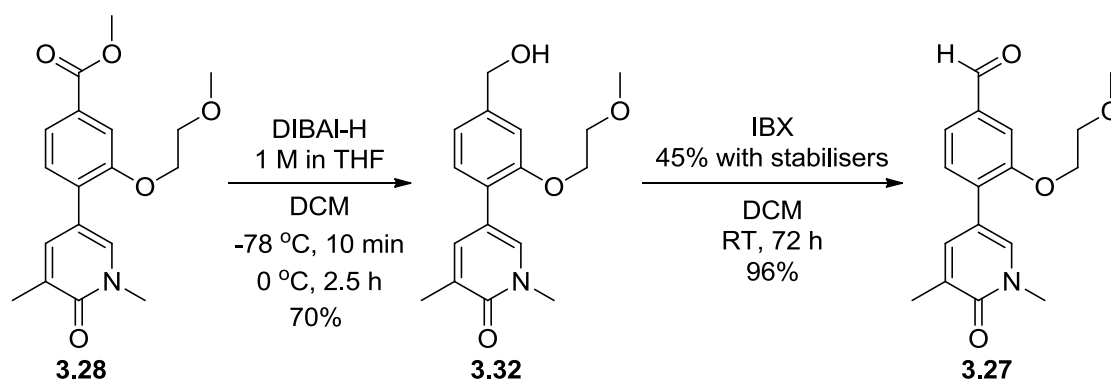
Scheme 3.6: Alkylation of phenol ester 3.30

The next step was to cross-couple aryl bromide **3.29** to the pyridone boronic ester **2.76**. This was achieved using a Suzuki-Miyaura cross-coupling reaction (Scheme 3.7), providing product **3.28** in good yield.



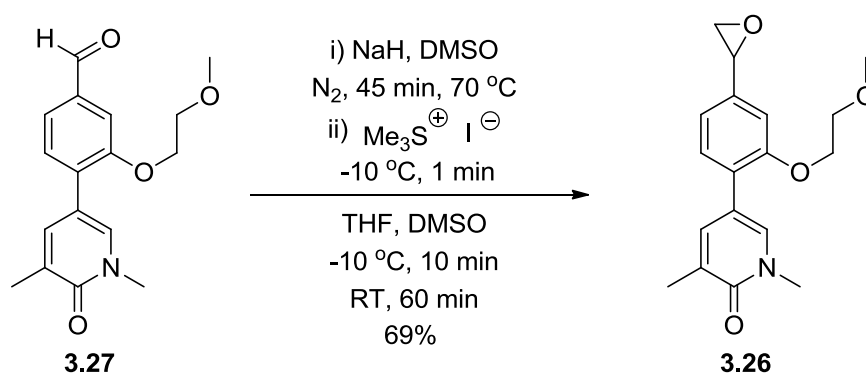
Scheme 3.7: Suzuki cross-coupling of bromo-intermediate 3.29 with pyridone boronic ester 2.76

With the ester in hand, conversion to the corresponding aldehyde was required. While DIBAL-H was used for the reduction, the alcohol prevailed while monitoring the reaction. Therefore, the ester was converted completely to the alcohol **3.32** before oxidation back to the aldehyde **3.27**. While the use of IBX was slow, the yield and purity after a basic aqueous work-up was excellent (Scheme 3.8).

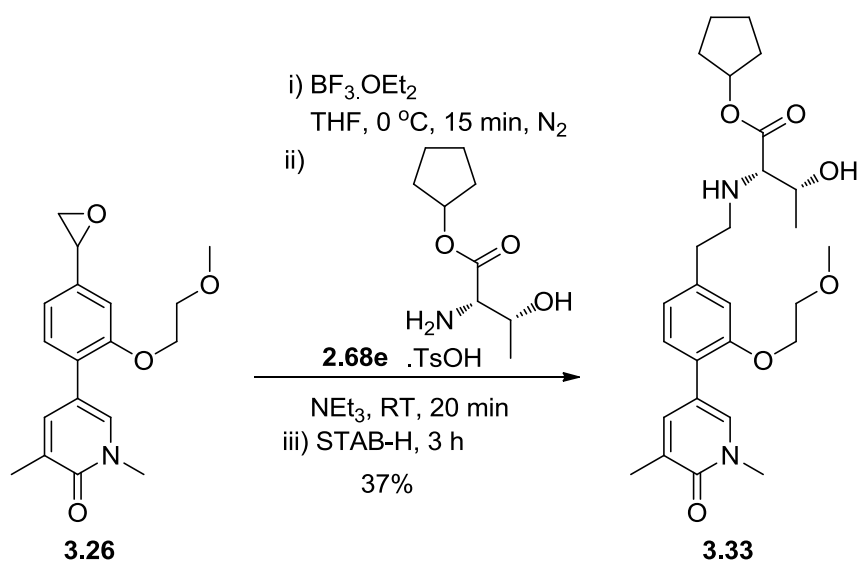


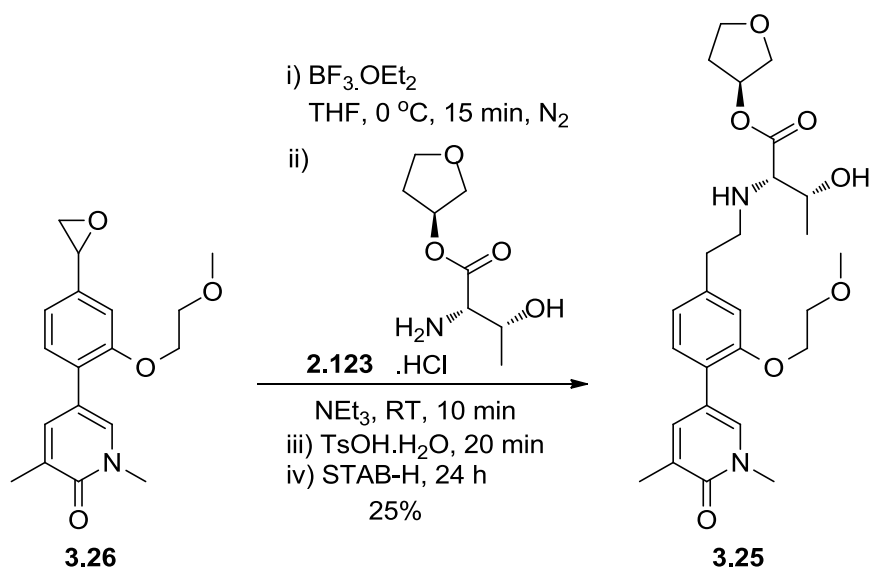
Scheme 3.8: Reduction and oxidation of ester 3.28

To homologate aldehyde **3.27**, the procedure by Corey and Chaykovsky was again utilised.²⁴⁹ The precursor epoxide was formed by reacting the aldehyde with the preformed sulfonium ylide. The reaction proceeded in reasonable yield (Scheme 3.9).

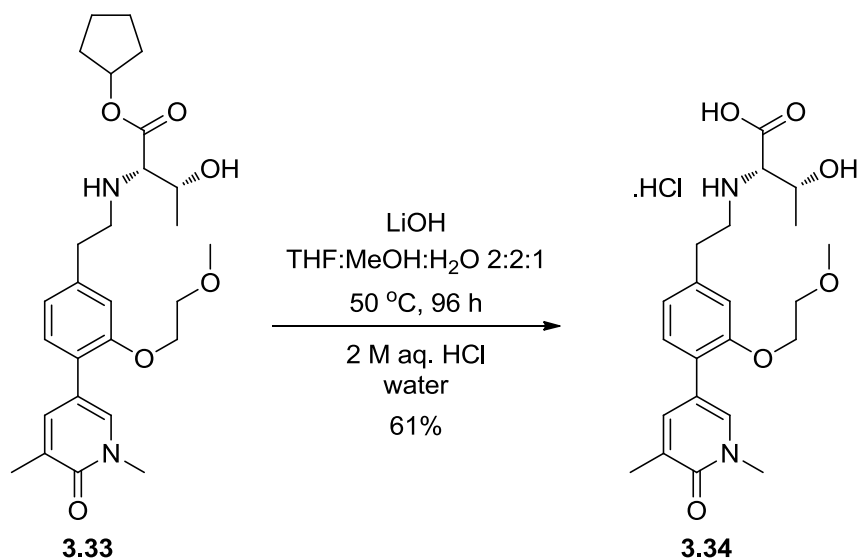
Scheme 3.9: Epoxidation of aldehyde **3.27**

With the key epoxide intermediate **3.26** in hand, the synthesis was completed using the previously discussed one-pot epoxide rearrangement and reductive amination protocol. The ESM-functionalised compounds **3.33** and **3.25** were prepared using the initial cyclopentyl threoninate **2.68e** (Scheme 3.10) and the (*S*)-tetrahydrofuryl threoninate **2.123** (Scheme 3.11), with the desired products being formed in 37% and 25% yield, respectively. The addition of tosic acid into the latter reaction had a beneficial effect on solubilising the amino acid ester.

Scheme 3.10: Epoxide opening and reductive amination of **3.26** with **2.68e**

Scheme 3.11: Epoxide opening and reductive amination of **3.26** with **2.123**

As a larger quantity of the cyclopentyl ester **3.33** was initially made due to the higher yield, it was this ester which was hydrolysed to the acid **3.34**, using lithium hydroxide (Scheme 3.12). As with previous examples, compound **3.34** was isolated as the hydrochloride salt.

Scheme 3.12: Hydrolysis of cyclopentyl ester **3.33**

During the synthesis of this ESM-functionalised molecule, the ester **3.28** and alcohol **3.32** intermediates were tested for biochemical potency. This was to understand whether these intermediates were a good predictor of potency and selectivity prior to

completion of the synthesis (Figure 3.23). The potencies at Brd4 BD1 are 10-fold higher than at Brd9. Accordingly, these constituted promising initial results.

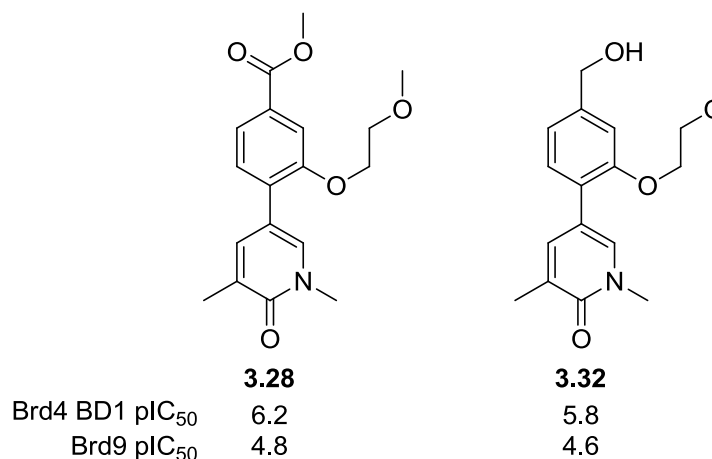


Figure 3.23: Potencies of ester and alcohol intermediates

It was then important to investigate how these initial insights into potency translated to the final compounds (Figure 3.24, Table 3.4). Both of these ESM-functionalised compounds, **3.33** and **3.25**, had good Brd4 BD1 biochemical potencies. This also translated into an excellent whole blood potency, with both esters having a potency of 7.4 in this assay. As expected, the cyclopentyl ester is more lipophilic than desired. In contrast, the tetrahydrofuryl ester's lipophilicity is within the TPP, with a ChromLogD_{7.4} of 2.9, again emphasising the dramatic contribution of the THF to the physicochemical properties of this series. Unfortunately, on testing the cyclopentyl ester and the acid, the window of selectivity between Brd4 BD1 and Brd9 is less than 1 log unit. As such, the intermediate ester **3.28** and alcohol **3.32** proved to be a poor model for the selectivity of ESM-functionalised final products, although the THF ester does demonstrate a moderate 15-fold window of selectivity over Brd9. This may be due to differences in the outer area of the Brd9 binding site where the cyclopentyl ester is making more optimal lipophilic interaction with the Brd9 surface. In general, this bias for Brd4 BD1 over Brd9 is a significant improvement, considering compound **2.113**, lacking the methoxyethyl group, was more potent at Brd9. However, compounds **3.33**, **3.25** and **3.34** remain outside the desired levels of selectivity sought as part of this programme.

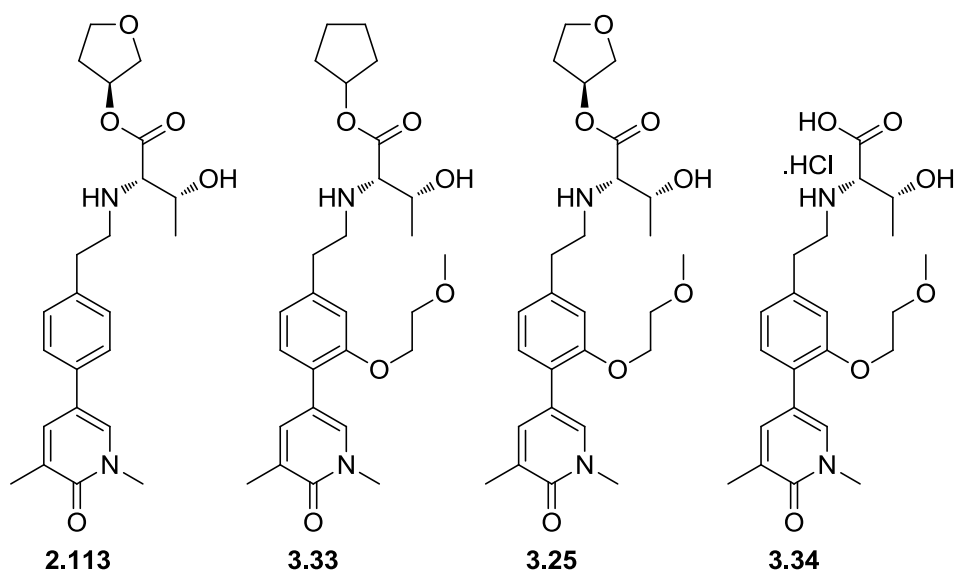


Figure 3.24: Comparison of cyclopentyl and THF esters

	2.113	3.33	3.25	3.34
Brd4 BD1 pIC₅₀	5.6	6.4	6.0	5.3
Brd9 pIC₅₀	6.3	5.5	4.8	4.8
hWB_{DPU} (MCP-1) pIC₅₀	7.1	7.4	7.4	-
ChromLogD_{7.4}	2.6	4.7	2.9	0.4

Table 3.4: Comparison of cyclopentyl and THF esters

To understand the limited window of selectivity observed within this series, compound **3.25** was submitted for X-ray crystallography within Brd4 BD1. As seen in Figure 3.25, unfortunately, the methoxyethyl group is not positioned on or towards the WPF shelf, as had been hypothesised from previous structural and biochemical potency data. As it can be seen from the similar biochemical potencies at each bromodomain, there is apparently no significant steric interaction with the tyrosine gatekeeper in Brd9. The orientation is instead into solvent, away from the WPF shelf and, subsequently, the tyrosine within Brd9, providing rationalisation for the observed minimal level of selectivity over Brd9.

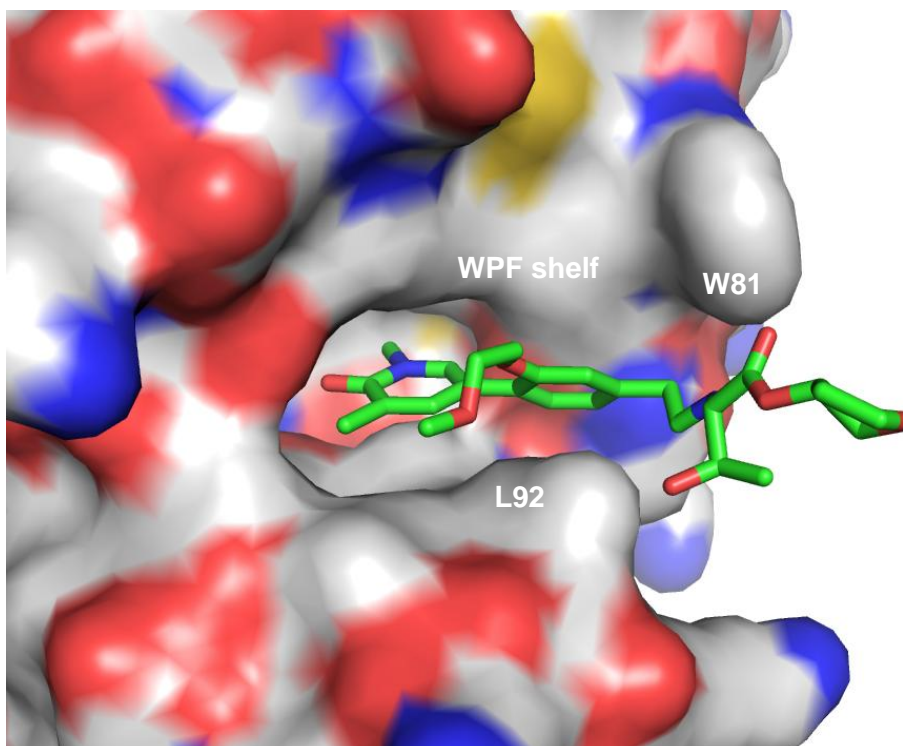


Figure 3.25: Crystal structure of 3.25 in Brd4 BD1

Despite this issue with selectivity, compound **3.25** represented the most advanced compound to date within this template. Therefore, to discover any other areas requiring optimisation, it was important that additional profiling, along the screening cascade (Figure 1.59, Page 61), be carried out. Compound **3.25**, at this point, was also compared to the TPP and, for reference, to an advanced compound within the benzimidazole (BI) series **1.81** (Table 3.5, Figure 3.26).²³³

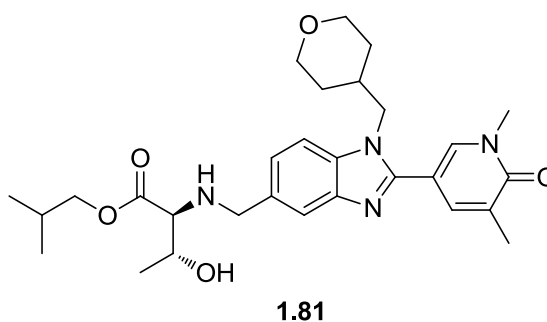


Figure 3.26: Lead compound within the benzimidazole series²³³

	TPP	Ester 3.25	Acid 3.34	Benzimidazole 1.81
Brd4 BD1 pIC₅₀		6.0	5.3	7.2
hWB_{DPU} (MCP-1) pIC₅₀	> 7.0	7.4	-	8.4
ΔpIC₅₀	≥ 1.0	1.4	-	1.2
hCE-1 SA (μM/min/μM)	< 1.0	0.68	-	0.44
Brd9 pIC₅₀ Selectivity*	> 30-fold	15-fold	3-fold	> 30-fold

Table 3.5: Biochemical, whole blood and hCE-1 results compared to 1.81 and the TPP
(* Selectivity for Brd4 BD1 over Brd9)

Lead compound **3.25** is around a log unit less potent within the Brd4 BD1 and whole blood assay compared to benzimidazole **1.81**. However, both of these compounds are within the TPP. The hCE-1 specific activities are at an acceptable level, which aids the excellent ΔpIC₅₀ achieved for both compounds. As previously mentioned, the area where compound **3.25** is weaker is selectivity against the non-BET bromodomains. While the ester **3.25** has 15-fold selectivity the acid showed a limited 3-fold bias over Brd9. The benzimidazole, containing the larger THP group to interact with the shelf, is more than 30-fold selective over Brd9.

	TPP	Ester 3.25	Acid 3.34	Benzimidazole 1.81
ChromLogD_{7.4}	< 4.0	2.9	0.4	3.6
PFI	< 6.0	4.9	2.4	6.6
CLND solubility (μg / mL)	> 100	128	150	> 950 (FaSSIF)
AMP (nm / s)	> 100	155	< 3	122
HSA (%)	< 90	46	-	44
MWt	< 550	489	455	524

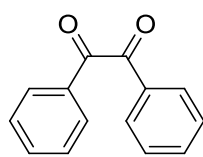
Table 3.6: Comparison of 3.25 with BI 1.81

The physical properties of lead compound **3.25** are also important to understand, with a view of progressing a suitable compound further through the screening cascade (Table 3.6). Firstly, the ChromLogD_{7.4} is improved compared with benzimidazole **1.81**. Furthermore, due to the fewer aromatic rings in compound **3.25**, the PFI is also comfortably within the TPP. However, both compounds demonstrate excellent physical properties such as solubility, permeability and human serum albumin binding. This may also be due to the molecular weight being within the TPP, ensuring the compound is not excessively large. Interestingly, the acid **3.34** has a low artificial membrane permeability (AMP), ideal for retaining the

acid intracellularly to achieve the desired local high concentration, having been produced within the target cell types.

With excellent results within the biochemical and whole blood assays and the physical properties within the TPP, the next stage was to understand the rate of metabolism of **3.25**. This is particularly important when using an ester in a prodrug strategy because the liver contains a number of esterases including hCE-1.²⁶⁸ Due to hCE-1 expression within the liver, a portion of the ester will be hydrolysed. Therefore, it is important to minimise hydrolysis and other phase I metabolism pathways in the liver, in order for the prodrug to get to the target myeloid cells in the systemic compartment.

To investigate the likely metabolism of **3.25** and related compounds, isolated human liver microsomes (HLM), vesicles, containing the liver's phase I metabolising enzymes, were used to test the *in vitro* clearance of **3.25**. While this *in vitro* clearance assay is a good method of gaining that initial insight, human liver microsomes contain esterases including, importantly, hCE-1. In order to investigate the underlying non-esterase driven metabolism, a carboxylesterase inhibitor, benzil (**3.35**), was used to block that layer of metabolism (Figure 3.27).²⁶⁹ The experiment was carried out in both the absence and presence of benzil. In the absence of benzil, the result is the sum of oxidative metabolism and ester hydrolysis. However, in the presence of benzil, the esterase contribution is removed, giving the underlying P450 metabolism. Overall, this allowed the relative contribution of these two forms of metabolism to be separated.²⁷⁰ Pleasingly, compound **3.25** had reasonable metabolic profile, with an expected reduction in metabolism on the addition of benzil.



3.35

Figure 3.27: structure of carboxylesterase inhibitor benzil 3.35

	TPP	Ester 3.25	Benzimidazole 1.81
<i>In vitro</i> clearance (mL / min / g tissue)	< 5 (-benzil)	3.2	4.9
	< 1.5 (+benzil)	1.8	2.1
Cyno plasma t_{1/2} (min)	> 240	>240	23

Table 3.7: IVC and Cyno plasma stability of 3.25 and 1.81

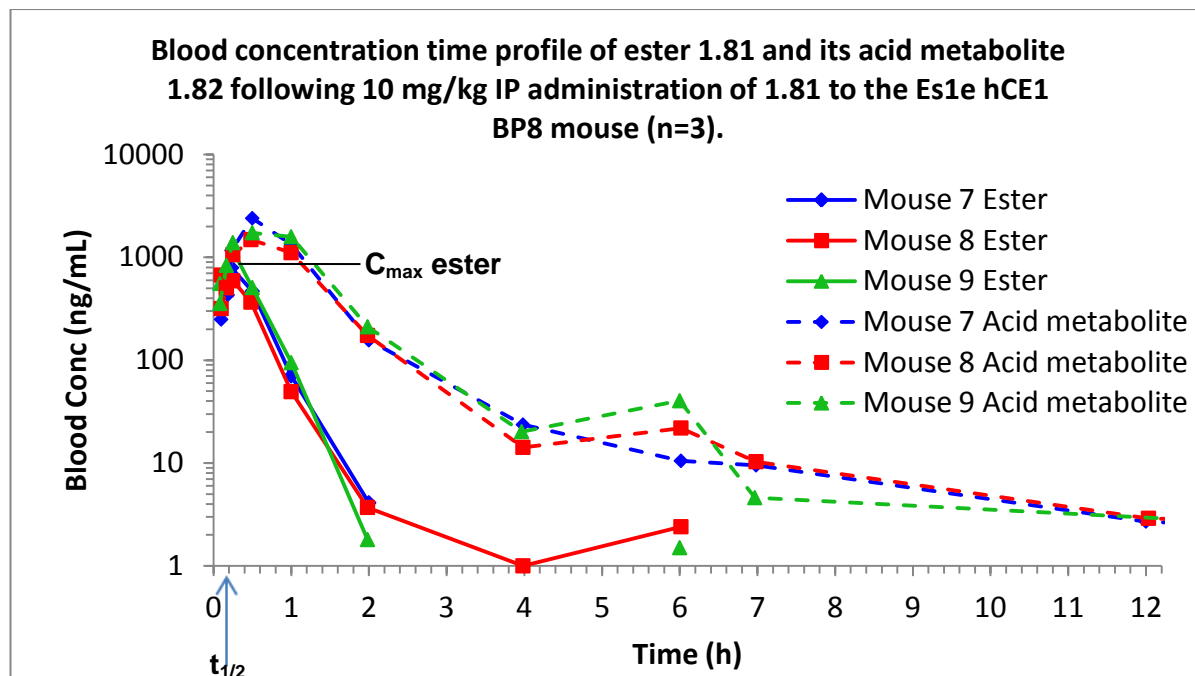
Additionally, it is important to ensure the compound is stable within the blood of pre-clinically relevant animal species. Different animal species have different forms of carboxylesterase 1 and differences in where these enzymes are expressed. Cynomolgus monkey has the most closely related form to human, with 92.9 % homology.²⁰³ Compound **3.25** was found to be stable within cynomolgus monkey blood plasma, with a half life of more than 240 minutes (Table 3.7). With an excellent improvement compared to benzimidazole **1.81**, compound **3.25** was the first compound found to be stable within this assay.

Translating this excellent *in vitro* data to an *in vivo* study was carried out using an Es1e hCE-1 transgenic mouse species. The Es1e mouse species is deficient in mouse blood esterases, Es1, which are equivalent to carboxylesterase 1.²⁷¹ Additionally, the *hCE-1* gene was inserted into the mouse genome along with the human CD68 promoter region, which restricts expression of this heterologous gene to the macrophage.²⁷² Overall, this aids the stability of the compound in circulation and ensures the acid will be generated in the cells of interest, in contrast to wild type mice.

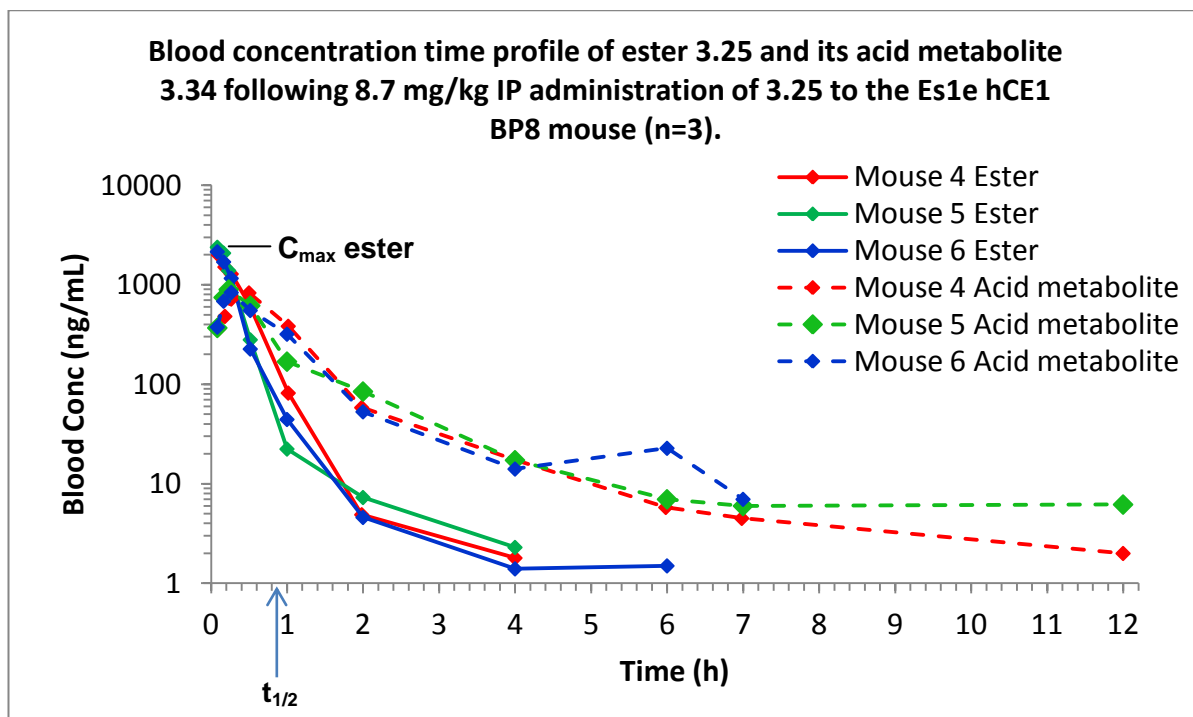
Previously, benzimidazole **1.81** was tested within this *in vivo* mouse study. It was seen that the maximum blood concentration, C_{max}, of compound **1.81** was 875 ng/mL, which was combined with a very short half life of 0.2 hours (Graph 3.1). These two properties help to define how long the compound is exposed to the circulation and therefore the extent to which it is free to distribute throughout the body. The total compound exposure, defined by the area under the curve (AUC), for **1.81** was 460 ng.h/mL, which is low and in line with the short half life. The low exposure to this ester can be rationalised by the *in vitro* Es1e mouse blood half life data. Compound **1.81** had a half life of just 20 min within this assay, suggesting a high rate of hydrolysis and low stability in Es1e transgenic mouse blood (Table 3.8). Combining this *in vitro* blood stability data along with the additional liver metabolism within the *in vivo* model may help to rationalise the very short half life.

	3.25	1.81
In vitro Es1e blood half life (min)	79	20

Table 3.8: Stability of 3.25 and 1.81 in transgenic mouse blood

Graph 3.1: *In vivo* PK data for compound 1.81 and its acid 1.82

On the other hand, lead compound **3.25** had a much improved C_{max} of 2178 ng/mL with an extended half life of 0.9 hours (Graph 3.2). This *in vivo* half life is again, shorter than the *in vitro* Es1e mouse blood half life, rationalised by the additional liver metabolism *in vivo*. The overall profile would give good exposure of the compound over a reasonable time. This can be seen by comparing the AUC to compound **1.81** with the improved AUC of 748 ng.h/mL for compound **3.25**. The body would be exposed to more compound over a longer period.



Graph 3.2: *In vivo* PK data for compound 3.25 and its acid 3.34

Overall, the pharmacokinetic profile for compound **3.25** is very encouraging. This initial experiment enabled the IVC data to be used as a benchmark for further compound profiling and set a bench mark for the potential to move into further *in vivo* studies with more selective compounds.

Given the positive *in vivo* data, the series was more broadly investigated within our laboratory, following on from the pyridyl investigation, described previously, and on the basis of the work described in this section, fully-elaborated pyridyl derivatives were also explored elsewhere in our laboratory.²⁷³ The pyridyl derivative **3.36** also had an interesting *in vitro* profile (Figure 3.28) as the ester had good Brd4 BD1 biochemical potency, although a smaller enhancement of potency was observed into the whole blood assay due to the low hCE-1 activity. Also, the *in vitro* clearance was reasonably low, although not as low as lead compound **3.25**.

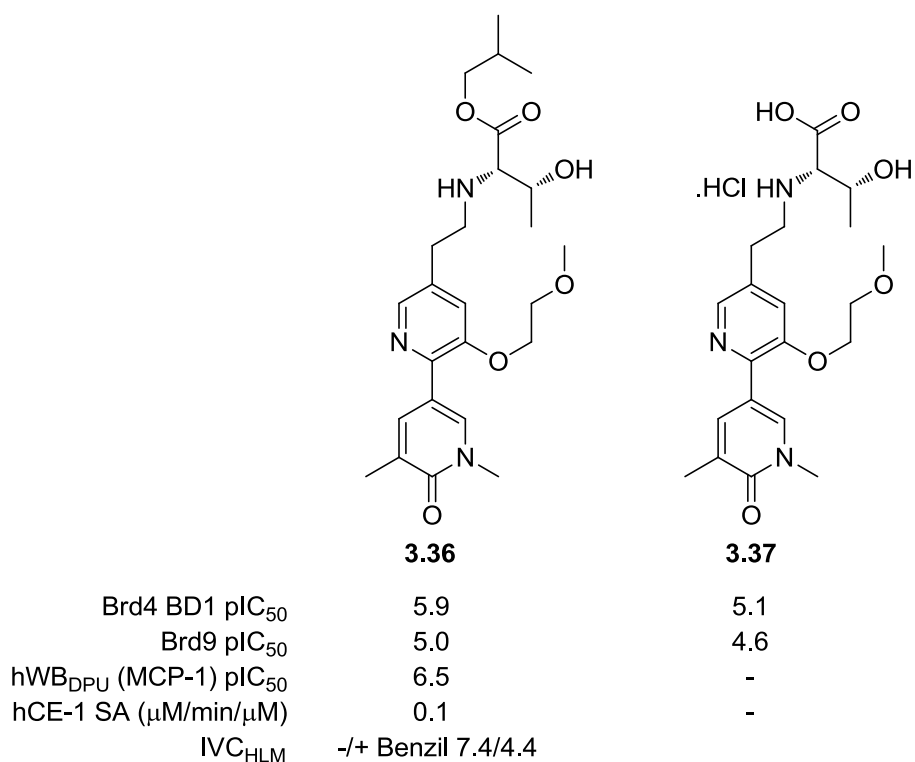


Figure 3.28: Pyridyl derivative 2.43 and acid 2.44

To investigate the broader selectivity profile of these compounds, ester **3.36** and acid **3.37** were sent externally to be tested against a broad range of bromodomains, with the data obtained shown in Figure 3.29, with an enlarged blank diagram available in Appendix 2.

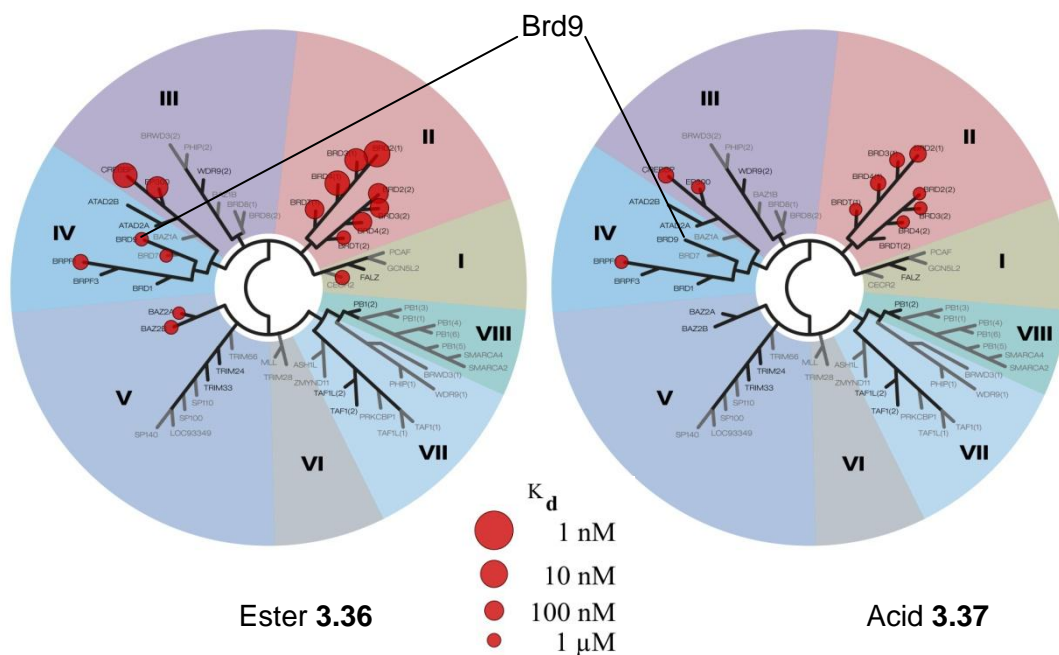


Figure 3.29: BROMOscan™ results for 3.36 and 3.37²⁷⁴

The BROMOscan™ method offered by DiscoverRx uses DNA-tagged bromodomain proteins and solid-supported ligands (Figure 3.30). On introducing the test inhibitor, the bromodomain is displaced from the ligand, and on reaching equilibrium, the bromodomain-inhibitor complex is washed away. The remaining DNA-tagged bromodomain bound to the solid-supported ligand is measured by quantitative polymerase chain reaction (qPCR) and a fluorescently labelled antisense strand of DNA.

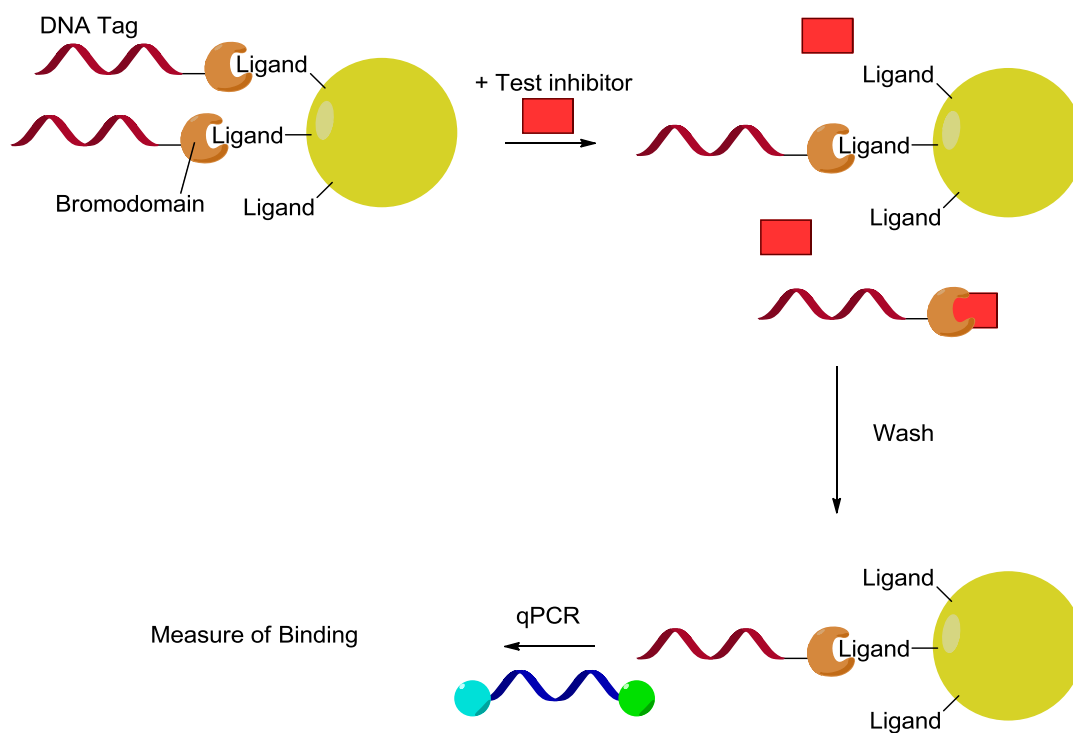


Figure 3.30: BROMOscan™ technology

The BROMOscan™ results, from the pyridyl derivatives **3.36** and **3.37**, were very encouraging, highlighting the bromodomains the compound had potency against (Figure 3.29). Results indicated activity at CREBBP, EP300 and BRPF1 in addition to the BET bromodomain containing proteins. Therefore, this revealed a potential selectivity challenge. Conversely, there is only limited activity at Brd9 for acid **3.37**. The non-BET protein CREBBP contains a bromodomain that has a very similar binding pocket to the BET bromodomains, making the lack of selectivity understandable.⁶⁷ Indeed, EP300 is closely related to CREBBP and compounds that interact with CREBBP typically interact with EP300, such as SGC-CBP30.²⁵⁹ BRPF1, on the other hand, has a very different binding pocket to the BET family, but similar to Brd9 due to the presence of the large phenylalanine gatekeeper.

Surprisingly, Brd9 was only moderately highlighted for **3.36** within the BROMOscan™ assay despite having biochemical activity in our laboratory. It was important to delineate how the selectivity profile for **3.25** and **3.34** compared to **3.36** and **3.37**. Firstly, the ester and acid pair (**3.36** and **3.37**) were tested in the CREBBP assay within our laboratory (Figure 3.31). The ester is less selective over CREBBP than it is over Brd9, thus supporting the BROMOscan™ results.

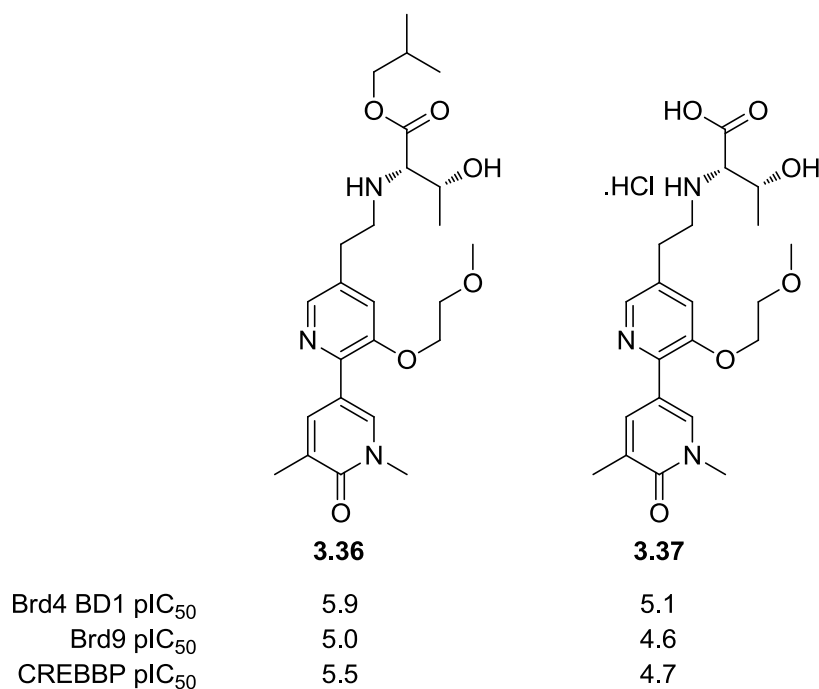


Figure 3.31: Ester **3.36** and acid **3.37** tested in the assays within our laboratory²⁷³

Returning to the series under investigation within this programme, compound **3.25** and its acid **3.34** were, subsequently, tested within the CREBBP assay within our laboratory and compared to the pyridyl ester **3.36** and acid **3.37**. These molecules predictably showed similar potencies at CREBBP as they did at Brd4 BD1 (Figure 3.32), thus supporting a structure activity relationship at both CREBBP and Brd9 compared to **3.36** and **3.37**.

As previously shown in X-ray crystal structures of **3.25** and **3.34** within Brd4 BD1, the methoxyethyl group was not orientated towards the WPF shelf, as hypothesised. Therefore, it was important to investigate why the methoxyethyl group was insufficient in order to further optimise the structure.

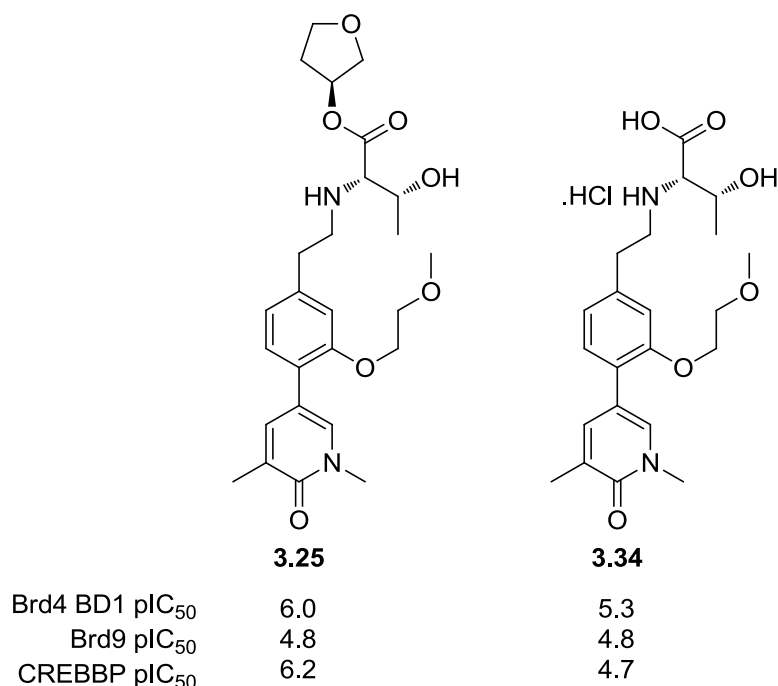


Figure 3.32: Comparison of BET and CREBBP potencies

To understand why the methoxyethyl was not engaging the WPF shelf, as highlighted in the previous crystal structure, an analysis of the small molecule X-ray database was initiated.^{275,276} This confirmed that for unbranched aromatic ethers the *anti*-conformation was the most likely geometry (Figure 3.34). This conformational bias caused the methoxyethyl group to be positioned away from the WPF shelf, as previously observed. It was hypothesised from modelling the crystal structure that a dihedral angle of between 60 and 80° may be required to position the group towards the WPF shelf (Figure 3.33), highlighted in green in Figure 3.34. However, this does not complete the picture. Recalling previously discussed data, the intermediate compounds which were tested in Brd4 BD1 and Brd9 were also tested within the CREBBP assay (Figure 3.35). These examples were 10-fold selective over CREBBP, as well as Brd9.

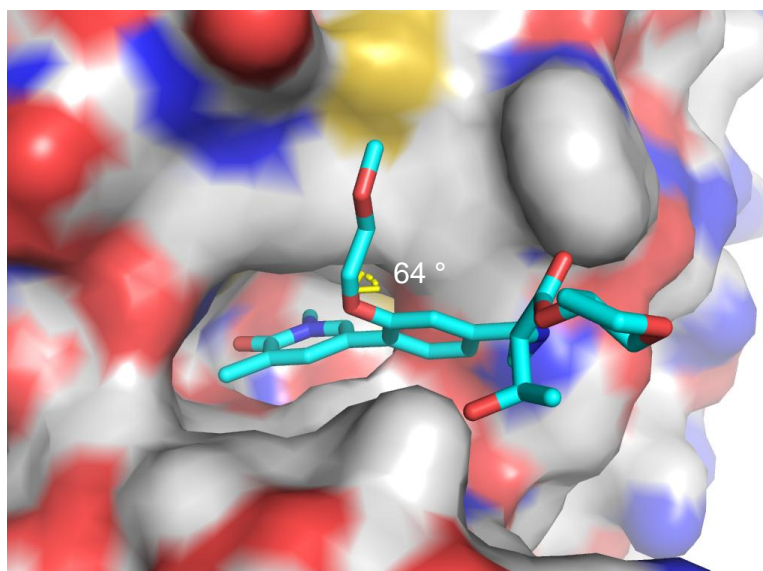


Figure 3.33: Computational model of the desired angle towards WPF shelf

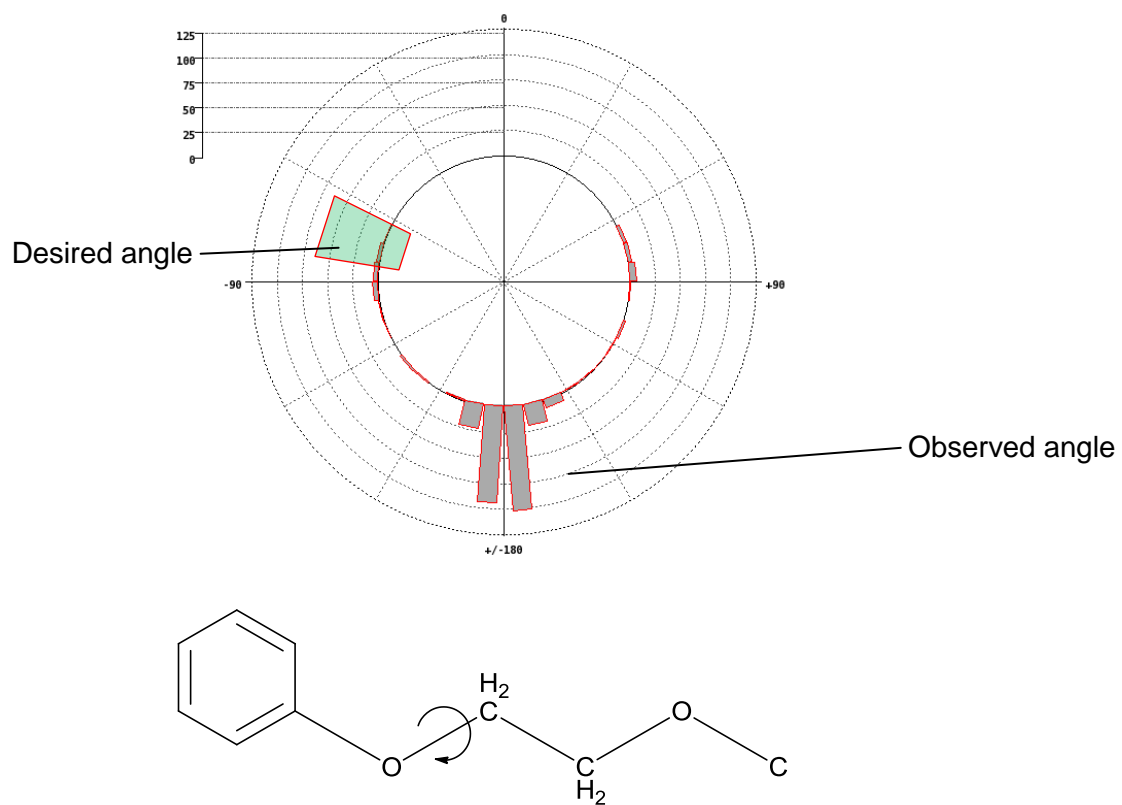


Figure 3.34: Dihedral angle around aromatic ether bond highlighted^{275,276}

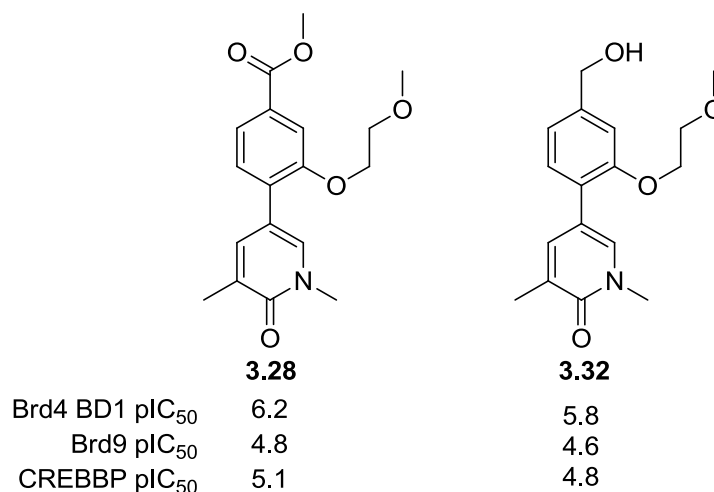


Figure 3.35: Selective intermediates retested at CREBBP

So the question remained, why is this small selectivity window diminished on addition of the ESM? Looking at the differences between the BET binding pocket and those of Brd9 and CREBBP, it can be seen that the ZA channel is flanked by smaller amino acids in Brd9 and CREBBP (Figure 3.36). The ZA channel may be more accommodating to the ESM within these non-BET bromodomains, even with the homologated linker. Accordingly, returning to a three atom linker may aid selectivity by further removing the bulk of the ESM away from the ZA channel, a tight region of the BET protein.

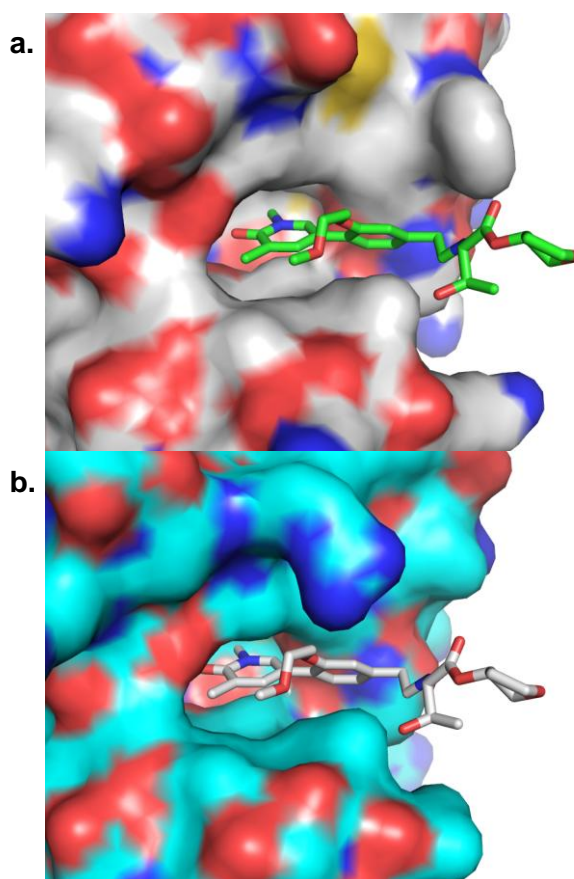


Figure 3.36: Crystal structure of (a) 3.25 in Brd4 BD1 compared to (b) an overlay of 3.25 in CREBBP

The methoxyethyl group, intended to interact with the WPF shelf is very linear. It was hypothesised that a strategy that would more effectively direct a desirable unit towards the BET WPF shelf might lead to a more selective and more potent compound. It was important to take learnings from within our laboratory to investigate whether such an approach could be transitioned into this template. Firstly, within the benzimidazole series, a large group such as a tetrahydropyran is utilised to occupy the shelf.²³³ An example is shown in Figure 3.37. It can be seen that, within this template, moving from the methoxyethyl **3.38** to the tetrahydropyran **1.81** improves the BET potency and, thus, improves the selectivity from 15-fold to 100-fold over CREBBP (Figure 3.37).

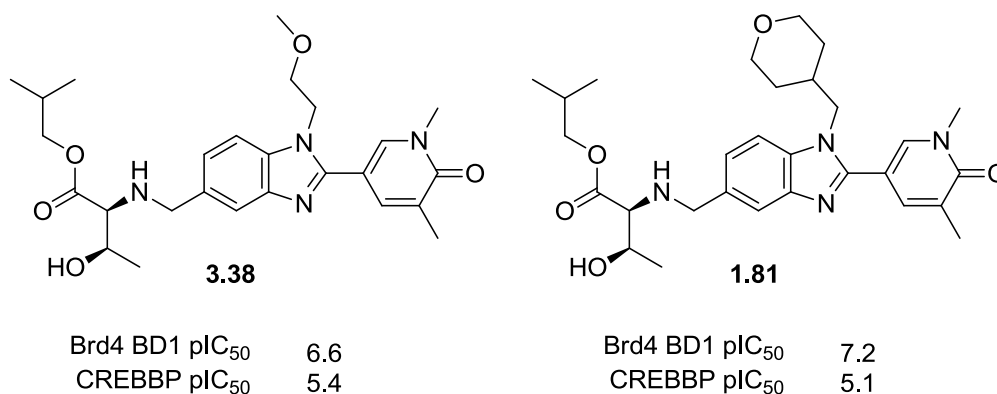


Figure 3.37: Comparison of methoxyethyl and THP within BI template

Alternatively, it was hypothesised that addition of constraint may change the dihedral angle around the ether bond. This theory was again supported by small molecule X-ray data (Figure 3.38).^{275,276} Addition of a methyl group changes the dihedral angle preference from 180° to 90°. Each enantiomer would favour either plus or minus 90°, where only one enantiomer is shown in Figure 3.38. This is closer to the angle hypothesised to be favourable to access the WPF shelf.

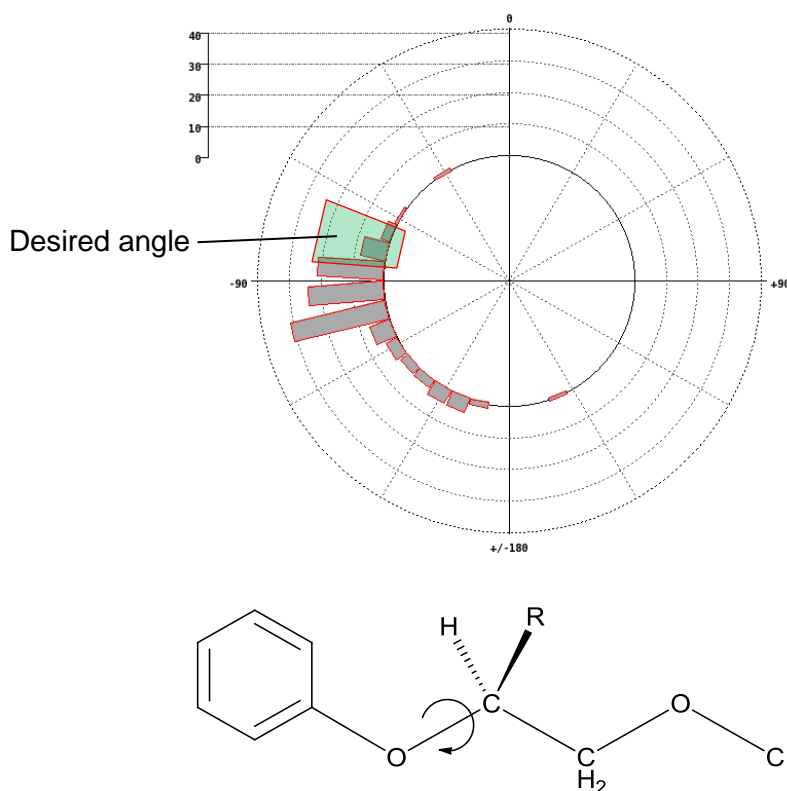
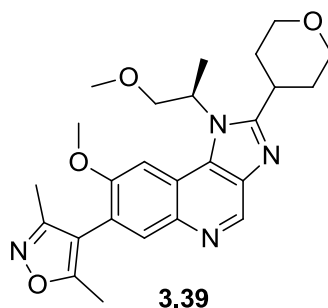


Figure 3.38: Change in the dihedral angle by introducing a group in the α -position

This was further supported by another BET inhibitor from our laboratory, compound **3.39**.²³³ This *R*-enantiomer was found to efficiently interact with the WPF shelf (Figure 3.39). Although the vector for accessing the shelf was very different, the potential for using this strategy of chiral constraint was reasonable and, indeed, had recent precedence within our laboratory.



Brd4 BD1 pIC ₅₀	7.4
CREBBP pIC ₅₀	5.0

Figure 3.39: BET inhibitor utilising chiral constraint to access the WPF shelf

To summarise this discussion and to interrogate the hypotheses presented, the following compounds were designed (Figure 3.40). Compound **3.40** was designed to mimic the successful tetrahydropyran shelf group used within the benzimidazole series. The second strategy involved analogues containing the α -methyl as a chiral constraint, such as **3.41**, analogous to BET inhibitor **3.39**.

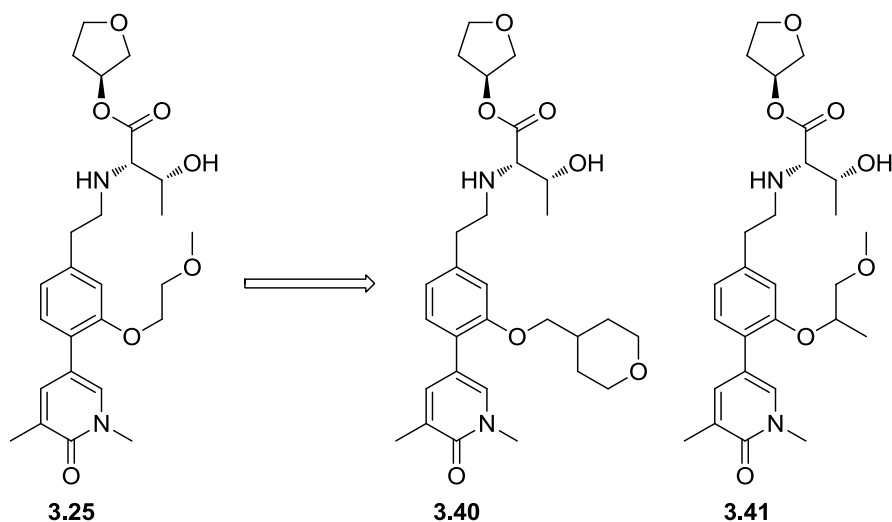
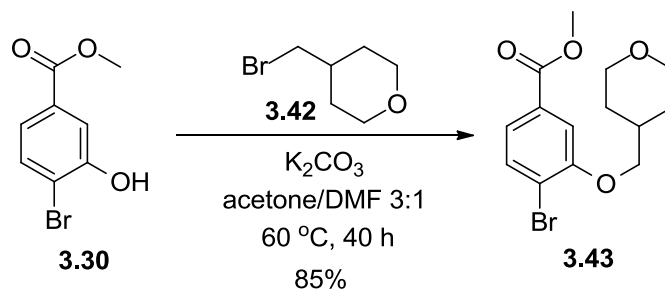


Figure 3.40: Proposed modifications of 3.25

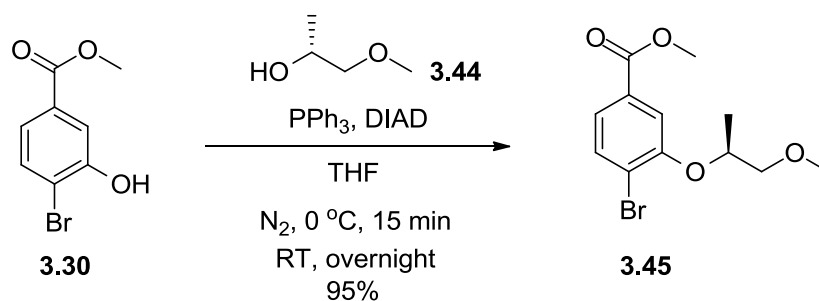
In comparison to lead compound **3.25**, a similar synthetic strategy was used for **3.40** and **3.41**. However, for the two isomers of **3.41**, this group was inserted using Mitsunobu methods,²⁷⁷ using the chiral alcohols as single enantiomers.

The first step in the synthesis of compound **3.40** was the alkylation of phenol **3.30** under basic conditions (Scheme 3.13). As with previous alkylations, the product was isolated in good yield.



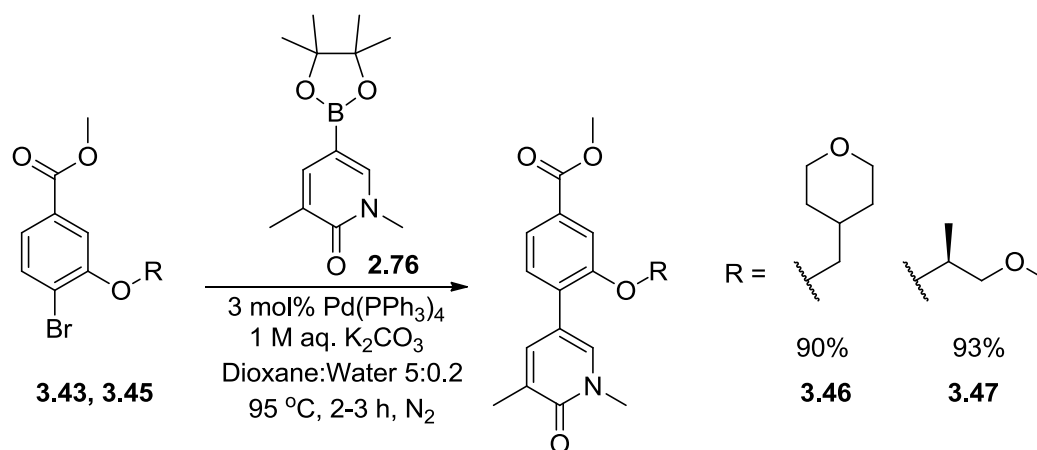
Scheme 3.13: Alkylation of phenol ester 3.30

A single enantiomer of the chiral α -methyl ether, as mentioned previously, was synthesised using a Mitsunobu reaction (Scheme 3.14). The reaction proceeded with 100% conversion. Pleasingly, the product from the reaction was more lipophilic than the triphenylphosphine oxide by-product. This resulted in an efficient isolation of the desired products, by chromatography, and with good levels of purity.



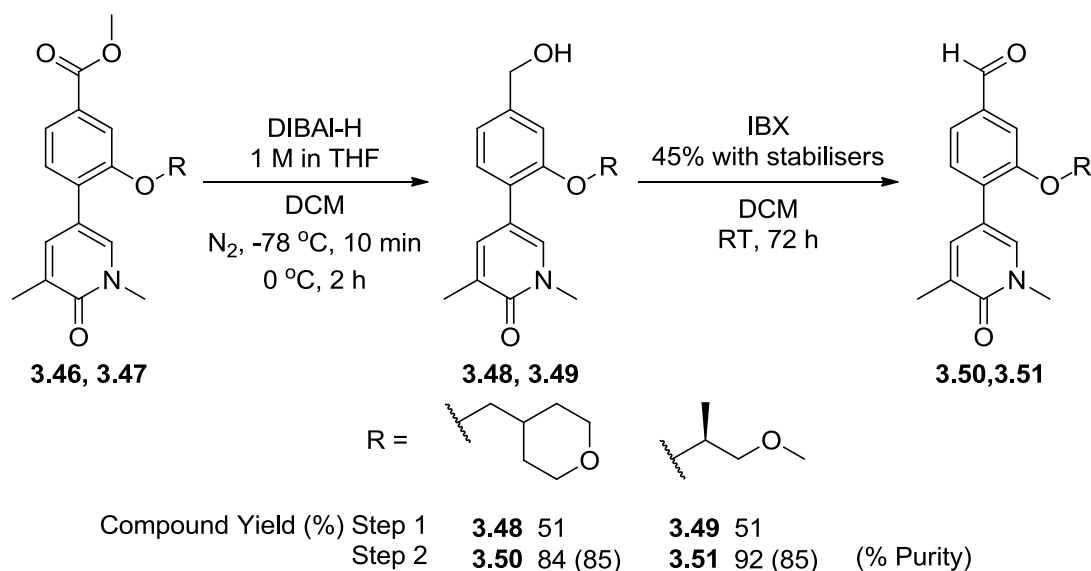
Scheme 3.14: Alkylation using Mitsunobu chemistry

With these ethers (**3.43** and **3.45**) in hand, the syntheses converge to a common route. The next stage was the Suzuki cross-coupling (Scheme 3.15). As with previous examples, the reaction was very robust and provided the desired products in excellent yield.



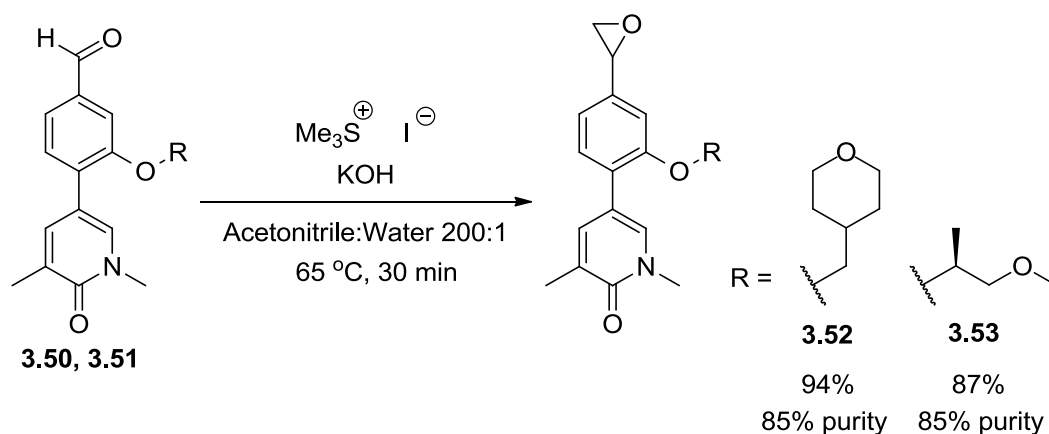
Scheme 3.15: Cross-coupling with boronic ester 2.76

To convert the esters into the desired aldehydes, a DIBAL-H reduction was first carried out before an oxidation using stabilised IBX (Scheme 3.16). Moderate yields were obtained from the reduction. The oxidation delivered excellent yields and the product purity levels achieved after aqueous workup in each case.



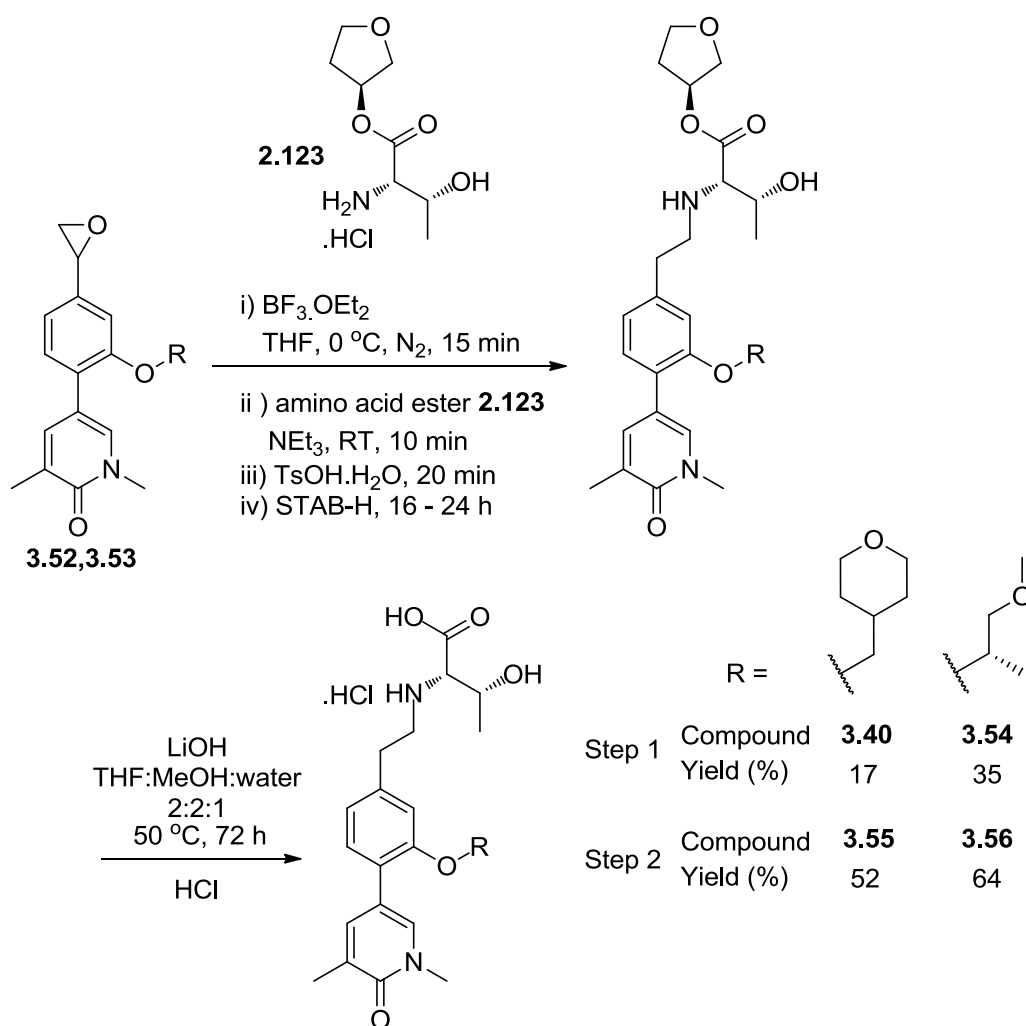
Scheme 3.16: Reduction and oxidation of esters 3.46 and 3.47

Within our laboratory, alternative epoxidation conditions were found to affect the next desired transformation.²⁷⁸ The procedure was much simplified over the original, using potassium hydroxide in wet acetonitrile.²⁷⁹ These modified conditions were attempted using aldehydes **3.50** and **3.51** (Scheme 3.17). In addition to the ease of the experimental procedure, the yields were also excellent.



Scheme 3.17: Epoxidation using new conditions

With epoxides **3.52** and **3.53** in hand, they were individually treated with a Lewis acid to form the homologated aldehydes *in situ*. The amino acid ester **2.123** was added to form the imine before reduction formed the desired product in moderate yields (Scheme 3.18). Compounds **3.40** and **3.54** were hydrolysed with lithium hydroxide and the corresponding acids isolated as the hydrochloride salt, each in moderate yield.



Scheme 3.18: Epoxide opening and reductive amination

The two final compounds synthesised here, with the additional compound **3.57**, the diastereoisomer of compound **3.54**, prepared elsewhere within our laboratory,²⁸⁰ were profiled within our assays (Figure 3.41). To highlight any improvements over lead compound **3.25**, they were compared side-by-side.

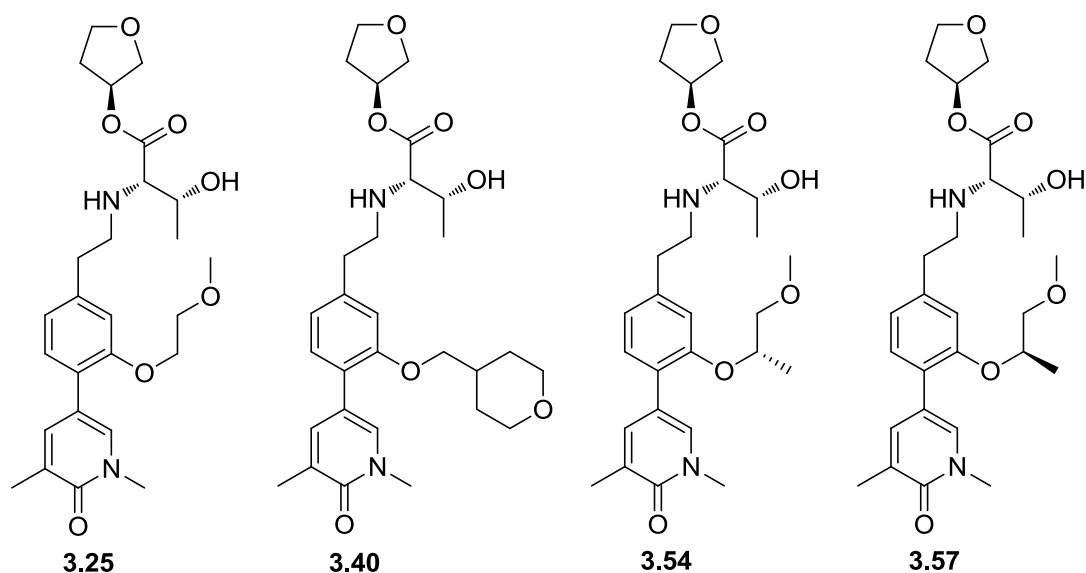


Figure 3.41: Final set of synthesised compounds

Firstly, compound **3.40** containing the larger THP group, was compared to lead compound **3.25** (Figure 3.42, Table 3.9). As hypothesised, this large THP imparted a 0.5 log unit increase in potency at Brd4 BD1 compared to lead compound **3.25**. Pleasingly, this larger group conferred some additional bias over CREBBP, with 1.2 log unit difference in pIC_{50} . However, the selectivity window was smaller than the desired 30-fold.

During the time between the synthesis of the lead compound **3.25** and these more elaborate WPF shelf group containing compounds, the human whole blood (hWB) assay, which was originally run within our laboratory (hWB_{DPU}), was transferred to an alternative laboratory (hWB_{BSci}). It was consistently seen that the results from this new assay were 0.5 log unit less potent than the original assay within our laboratory. The lead compound **3.25** was one of the first compounds to have been tested within both assays. This frame shift in potency was true for lead **3.25**, with the new value of 6.9 represented in Table 3.9. This is highlighted to allow like-for-like comparison to the newly synthesised compounds. Unfortunately, the increased Brd4 BD1 potency associated with **3.40** did not translate into the cellular assay. The ΔpIC_{50} , using the new BSci hWB assay, showed an excellent 0.9 log unit enhancement for lead compound **3.25**, whereas the THP derivative **3.40** showed only a 0.4 log unit increase. Initially, this was hypothesised to be caused by a lower hCE-1 hydrolysis rate. However, subsequent data showed the THP analogue was hydrolysed at a higher rate. The reason for the reduced whole blood enhancement is unknown,

although the higher molecular weight and greater molecular volume of **3.40**, may impair its cellular permeability, despite having a good measured AMP of 130 nm/s. Pleasingly, however, this larger THP group adds only half a log unit of lipophilicity, demonstrating that this template is capable of accommodating additional lipophilicity in this area.

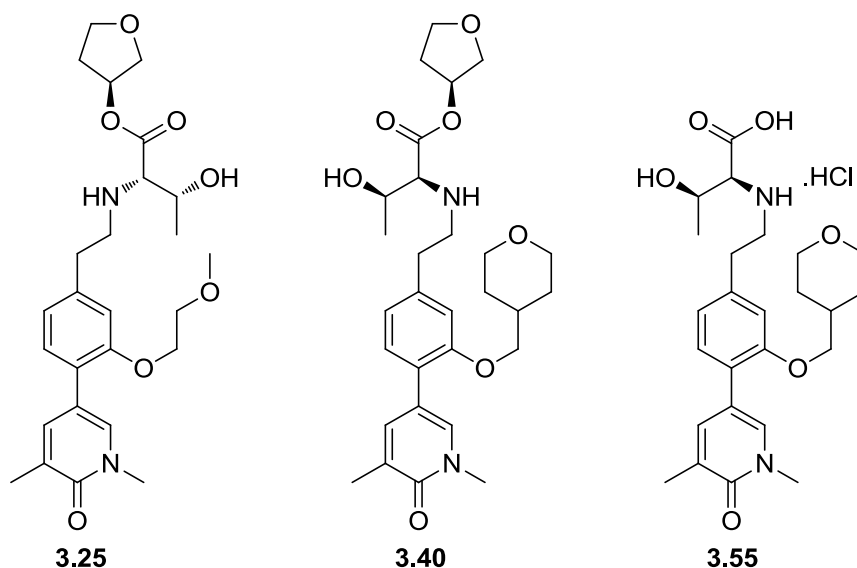


Figure 3.42: Compound 3.40 and its acid 3.55 compared to lead molecule 3.25

	3.25	3.40	3.55
Brd4 BD1 pIC₅₀	6.0	6.5	5.8
CREBBP pIC₅₀ (fold selectivity^{**})	6.2	5.3 (16 fold)	≤4.7 (12-fold)*
hWB_{BSci} (MCP-1) pIC₅₀	6.9	6.9	-
hWB_{DPU} (MCP-1) pIC₅₀	7.4	-	-
ΔpIC₅₀ BSci	0.9	0.4	-
hCE-1 SA (μM/min/μM)	0.68	3.1	-
ChromLogD_{7.4}	2.9	3.4	1.1
PFI	4.9	5.4	3.1

Table 3.9: Comparison of THP 3.40 with 3.25

*(3.55 inactive on 1 of 4 test occasions) (**Selectivity for Brd4 BD1 over CREBBP)

Increasing the size of the group occupying the WPF shelf increases the biochemical potency and selectivity. However, the size of this molecule may be adversely affecting the whole blood potency, through reduced permeability with a molecular weight of 528.

The alternative, potentially more efficient, strategy to occupy the WPF shelf was to add chiral constraint to the methoxyethyl chain of **3.25**. As such, the next pair of compounds tested within our assays were the α -methyl compounds **3.54** and **3.57**²⁸⁰ (Figure 3.43). As previously stated, the methyl group was hypothesised to twist the chain out of the preferred linear conformation observed with **3.25**, making the interaction with the shelf more likely.

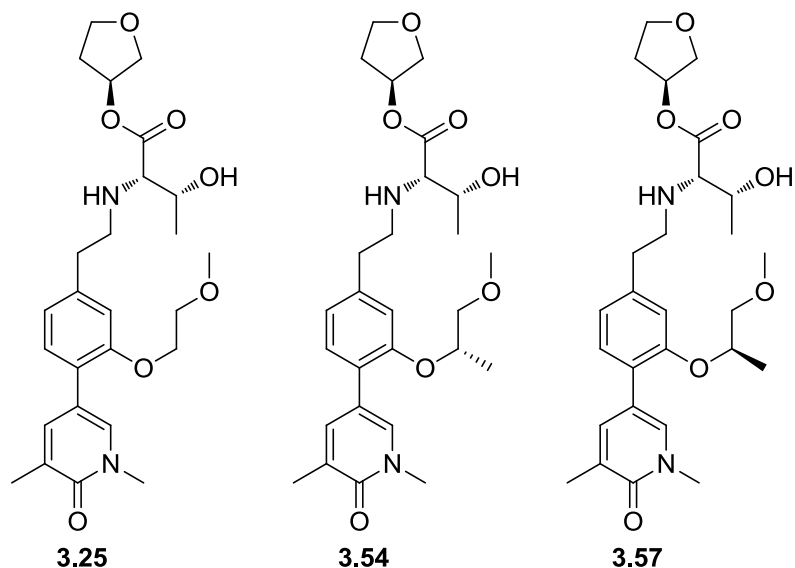


Figure 3.43: Diastereomers **3.54** and **3.57** compared to **3.25**

When the Brd4 BD1 potency of these two diastereomers are compared, binding of the (*S*)-diastereoisomer **3.54** as the ester is preferred, with a 0.6 higher potency compared to the (*R*)-**3.57** (Table 3.10). Unfortunately, this effect is mirrored within the CREBBP assay, where the (*S*)-diastereoisomer is 1.0 log units more potent than the (*R*)-isomer.

	Lead	<i>(S)</i> - α -methyl		<i>(R)</i> - α -methyl	
	3.25	Ester 3.54	Acid 3.56	Ester 3.57	Acid 3.58
Brd4 BD1 pIC₅₀	6.0	6.6	5.9	6.0	5.6
CREBBP pIC₅₀	6.2	5.8	5.0	5.0	≤4.7*

Table 3.10: Biochemical potencies within Brd4 BD1 and CREBBP
(**3.58** inactive on 1 of 4 test occasions)

To understand this result, the binding mode of **3.54** was investigated. Initially, X-ray crystal data in Brd4 BD1 was attempted to be collected for (*S*)- α -methyl **3.54**, to confirm how the compound interacts with the BET binding pocket. However, this

was unsuccessful for compound **3.54**. As such, in order to get an indication on how this group may be positioned, the compound was modelled with Brd4 BD1²⁸¹ in order to understand the selectivity profile and in an attempt to aid the next iteration of compound design. As the ESM protrudes into solvent, the modelling was carried out on the core molecule **3.59**. The results from the modelling suggested that it was not the ether of compound **3.59** that interacted with the shelf, but the α -methyl (Figure 3.44).

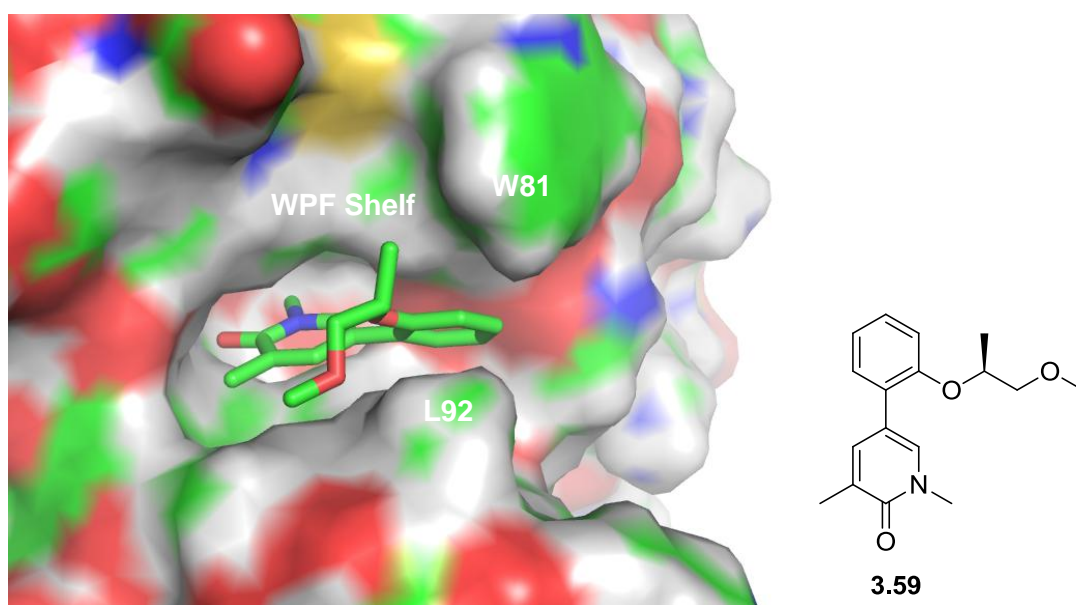


Figure 3.44: α -methyl compound 3.59 modelled in Brd4 BD1

Using this model, the cause of the differences in biochemical potencies between the two diastereoisomers while maintaining similar selectivity profiles, was hypothesised by interrogating the differences between the Brd4 BD1 and CREBBP binding sites. Similar interactions of the α -methyl group with the WPF shelf region, which is structurally different between Brd4 BD1 and CREBBP (Figure 3.45) would give a similar selectivity profile. However, the opposite side of the pocket, defined by leucine 92 (L92) in Brd4 BD1 is conserved within CREBBP. Therefore, less favourable interactions towards the structurally similar area of the protein would affect the biochemical potencies at both bromodomains.

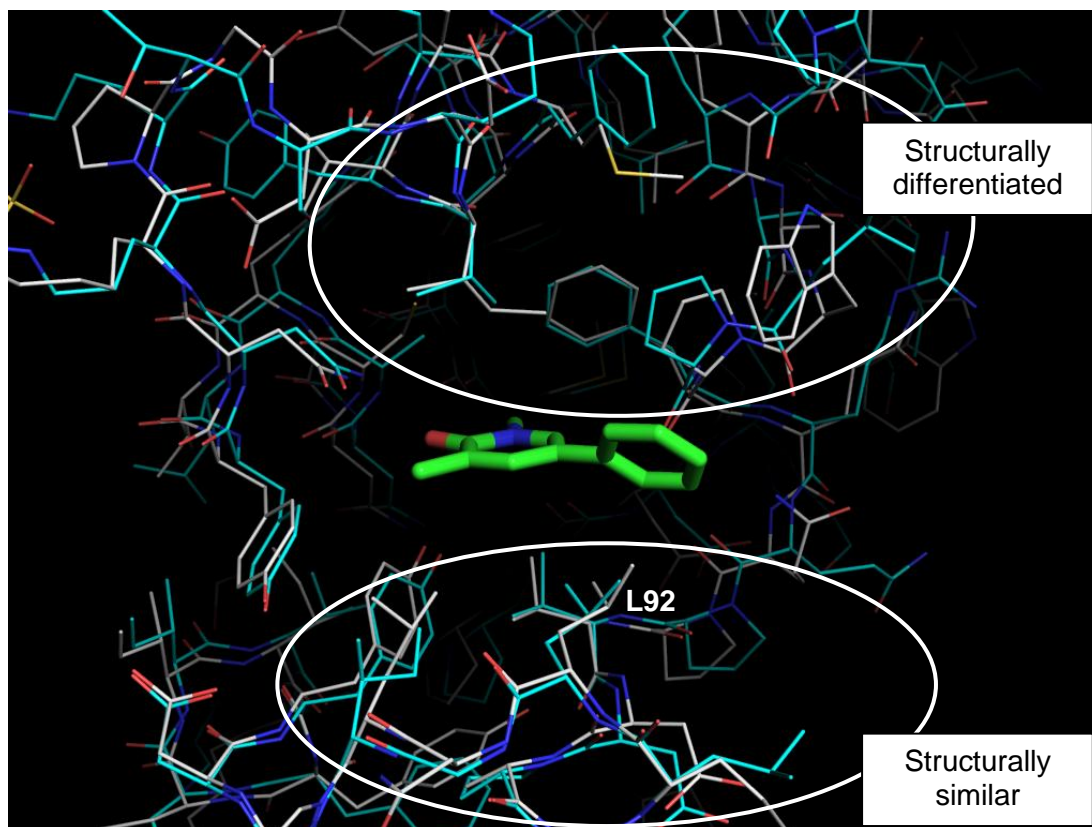


Figure 3.45: Differences between the Brd4 BD1 (green) and CREBBP (blue) binding pockets

Despite this, as shown in Table 3.11, an excellent 10-fold selectivity for BET over CREBBP was introduced. Also, pleasingly, the two corresponding acids showed the same selectivity windows as the esters. Further, the Brd4 BD1 biochemical potencies translated into a log unit ΔpIC_{50} into human whole blood. This effect was observed for both compounds, despite being tested in the downward frame shifted BSci assay. As expected, this high whole blood potency could be attributed to higher hCE-1 specific activity, relative to lead compound **3.25**. This increased specific activity produces a higher concentration of acid within the target cells. Finally, using the THF ester, the ChromLogD_{7.4} remained within the TPP, consistent with a number of previously synthesised examples.

	Lead	(S)- α -methyl		(R)- α -methyl	
	3.25	Ester 3.54	Acid 3.56	Ester 3.57	Acid 3.58
Brd4 BD1 pIC ₅₀	6.0	6.6	5.9	6.0	5.6
CREBBP pIC ₅₀	6.2	5.8	5.0	5.0	≤4.7*
hWB _{BSci} (MCP-1) pIC ₅₀	6.9	7.7	-	7.0	-
Δ pIC ₅₀	0.9	1.1	-	1.0	-
hCE-1 SA (μ M/min/ μ M)	0.68	2.4	-	1.9	-
ChromLogD _{7.4}	2.9	3.2	1.0	3.5	0.9
PFI	4.9	5.2	3.0	5.5	2.9

Table 3.11: Comparison of chiral constraint compounds with 3.25
*(3.58 inactive on 1 of 4 test occasions)

In an attempt to mechanically force the ether group to make good interactions with the WPF shelf, elsewhere in our laboratory the ESM functionalised molecule containing a symmetrical dimethoxypropyl group **3.60** was synthesised (Figure 3.46).²⁸² The crystal structure of the methoxyethyl compound **3.25** (Figure 3.25, Page 168) showed the methoxyethyl group did not interact with the Brd4 BD1 WPF shelf. Therefore, it was hypothesised that if the compound with one methoxyethyl group did not interact with the shelf region, then a compound containing an equivalent of two of these groups would be forced to direct one towards the shelf region. Additionally, the symmetrical nature alleviated the need to use chiral starting materials or chiral chromatography. Indeed, the compound was 0.9 log units more potent than compound **3.25** at Brd4 BD1 and demonstrated 1.3 log unit window of selectivity. The whole blood potency was excellent with the hCE-1 activity within the desired space. This compound **3.60**, along with the (S)- α -methyl **3.54** and the THP **3.40**, demonstrate that some selectivity can be gained through the judicious addition of more atoms.

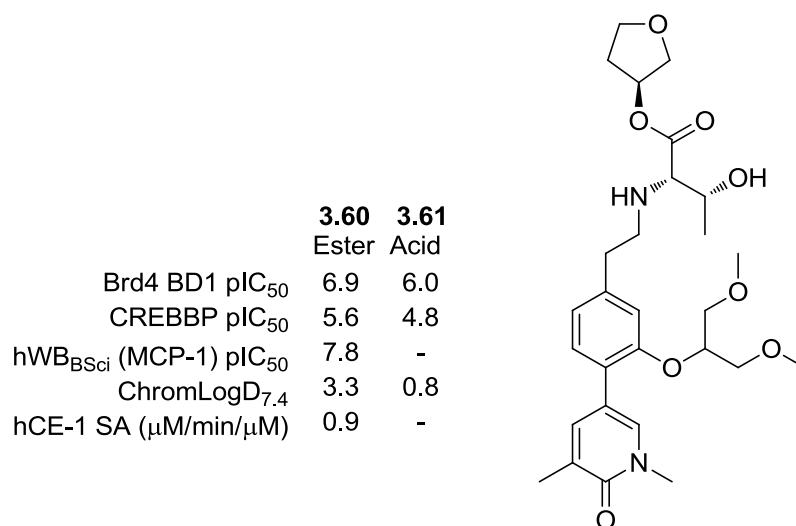


Figure 3.46: Dimethoxy compound 3.60 and acid 3.61

While dimethoxypropyl ester **3.60** was unable to be crystallised within Brd4 BD1, the corresponding dimethoxypropyl acid **3.61**, was also submitted for X-ray crystallography, successfully.²¹⁰ The structure of **3.61** within Brd4 BD1 is shown in Figure 3.47 and correlates well with the computational model. One of the ethers interacts with the WPF shelf, while the other is, apparently, redundant.

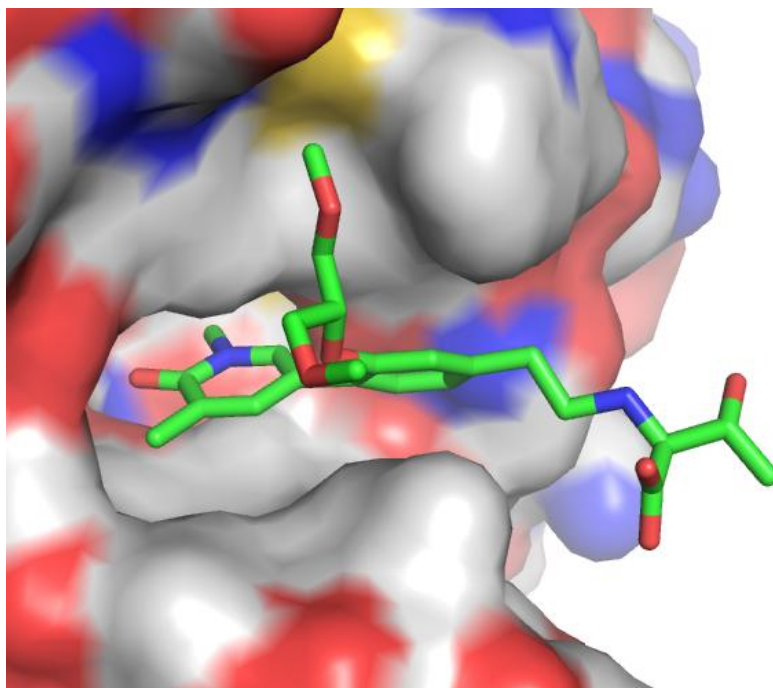


Figure 3.47: X-ray crystal structure of dimethoxypropyl acid 3.61 in Brd4 BD1²¹⁰

Summarising, the linear methoxyethyl group was inadequate to form the desired interactions with the WPF shelf to gain additional potency at Brd4 BD1 and

selectivity over exemplar non-BET bromodomain, Brd9, preferring a conformation that placed the methoxyethyl group into solvent. Having discovered through crystallography within Brd4 BD1 that the methoxyethyl chain was not interacting with the shelf region, compounds were designed to mitigate this. Both the bulky THP group and the α -methyl examples were made to occupy the shelf. While both compounds were more potent than the methoxyethyl compound, the α -methyl **3.54** gave the most balanced compound with good potency at Brd4 BD1 and 10-fold selectivity over the closely related CREBBP bromodomain. The human whole blood potency was excellent, although this may have been aided by the relatively high hCE-1 specific activity. Compound **3.60**, more potent at Brd4 BD1 and with a lower hCE-1 hydrolysis, was equipotent with **3.54** within the whole blood assay.

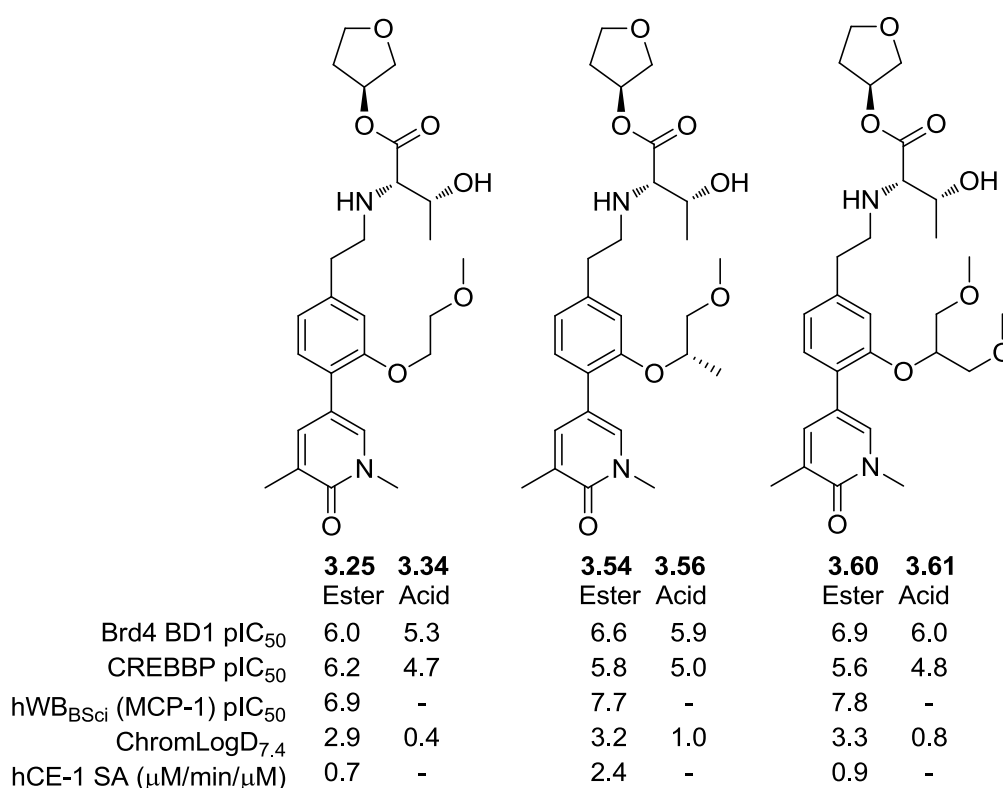


Figure 3.48: Comparison of **3.25**, **3.54** and **3.60**

Considering the 25-fold selectivity for Brd4 BD1 over CREBBP observed with compound **3.60**, it was proposed that rational design would enable a more efficient use of atoms to further improve the profiles of these compounds.

3.3 Interrogating the WPF Shelf Group

Pleasingly, the introduction of the α -methyl substituent had the desired effect of increasing potency at BET and delivering potency within the human whole blood assay, as well as introducing 10-fold selectivity against the CREBBP non-BET bromodomain. However, the TPP set out at the beginning of this work gives the aim of 30-fold selectivity. To further improve the selectivity, the degree of branching along the WPF shelf group was interrogated to more fully understand the requirements for selectivity. Modifications such as those in Figure 3.49 were proposed: larger α -substituents, introduction of a β -substituent and bulkier terminal ethers.

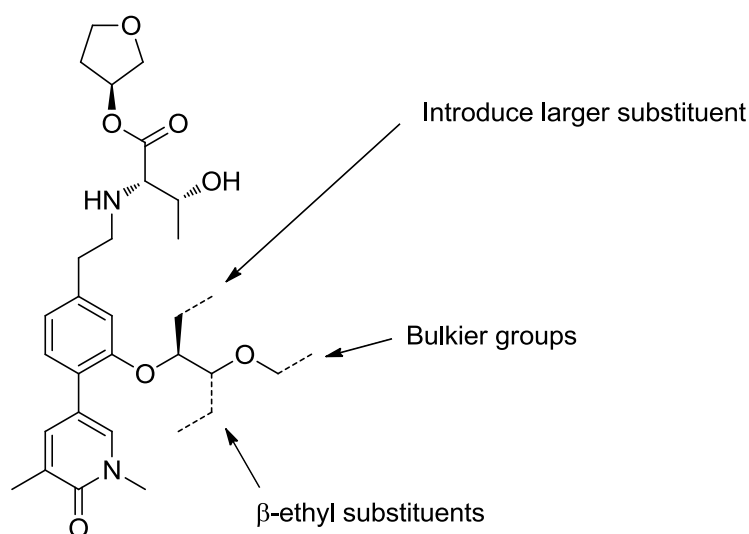


Figure 3.49: Proposed alterations to lead compound 3.54

3.3.1 Branching

To further interrogate this linear system, a branching study was proposed, with the synthetic targets outlined in Figure 3.50. Firstly, the α -ethyl compound would be made, having had the excellent result with the α -methyl substitution and the subsequent modelling. Secondly, the β -ethyl example would investigate whether the constraint is in the optimal position. Lastly, the bulkier ether is hypothesised to make the ether less favourable to extend away from the protein due to the additional lipophilicity and hence be more favourable to overcome the conformational barrier to interact with the WPF shelf region.

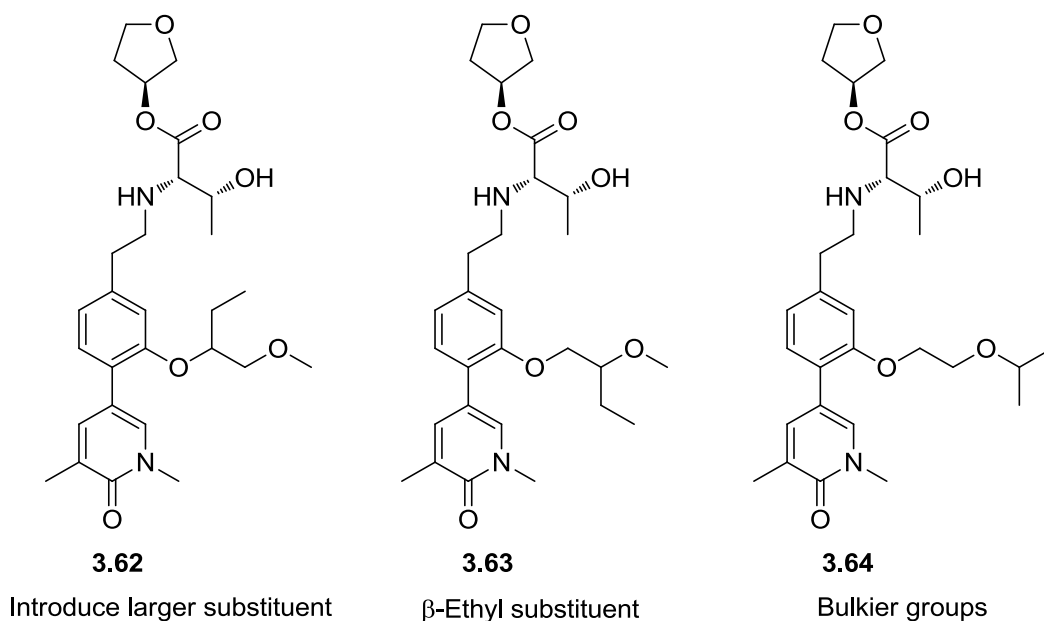
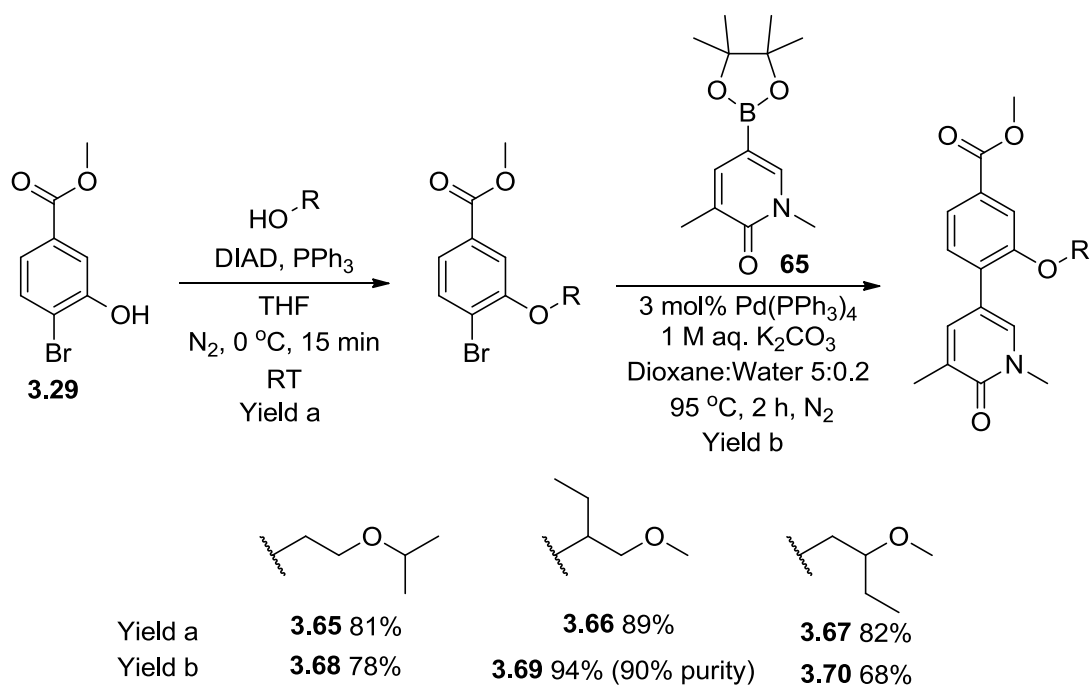


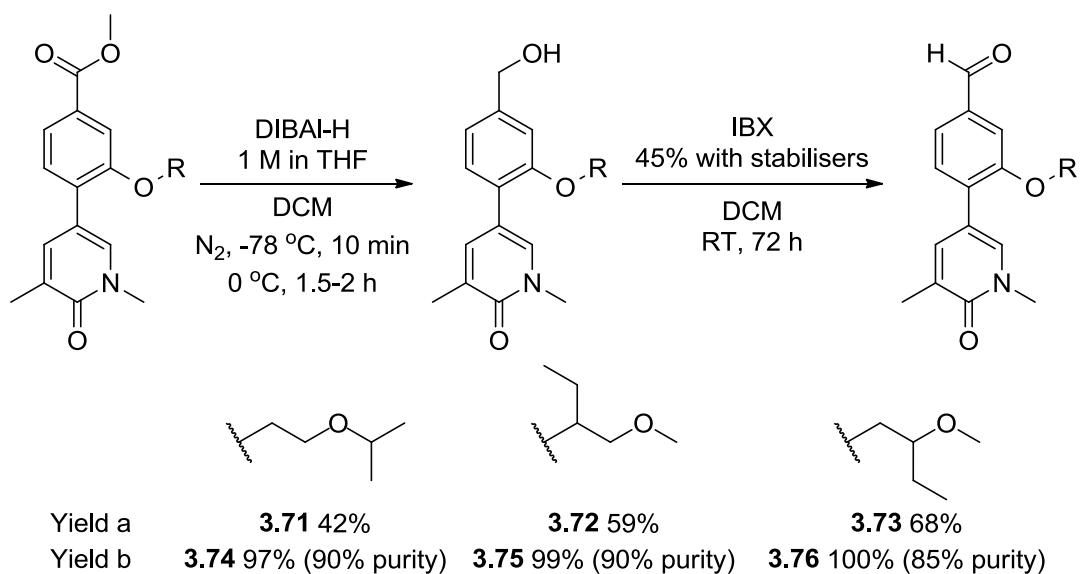
Figure 3.50: Proposed compounds 3.62, 3.63 and 3.64

The synthetic strategy to prepare these compounds would be similar to the previous examples, utilising the commercially available alcohols. Accordingly, the concurrent synthesis of compounds **3.62**, **3.63** and **3.64** was undertaken. The Mitsunobu reaction was successfully utilised to introduce the respective ethers in excellent yields. The subsequent Suzuki cross-coupling reactions, with boronic ester **2.76**, proceeded in good to excellent yield to furnish intermediates **3.68**, **3.69** and **3.70** (Scheme 3.19).



Scheme 3.19: Mitsunobu reaction and Suzuki cross-coupling

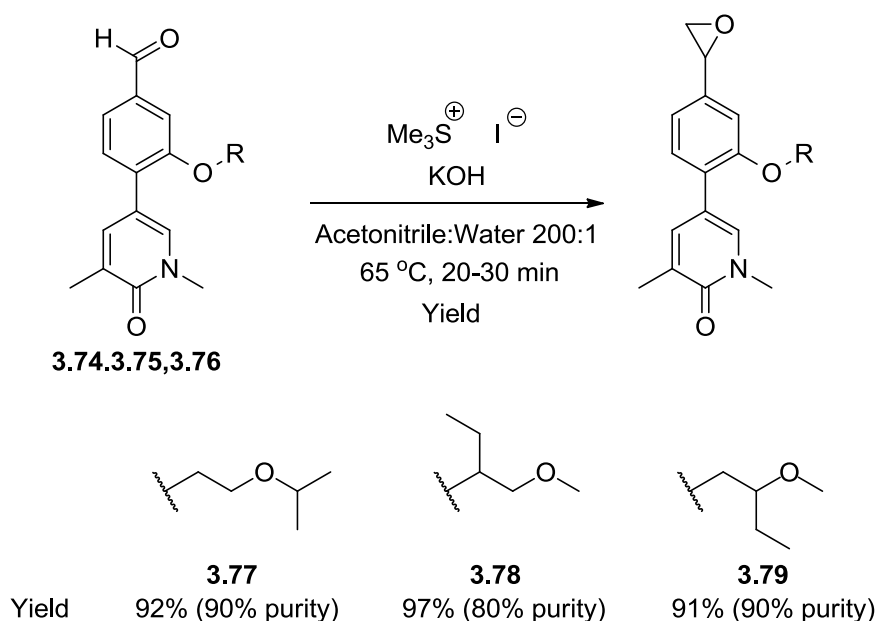
As with previously synthesised examples, the oxidation state of the ester was first reduced using DIBAL-H, in moderate to good yield. Secondly, oxidation to the desired aldehydes with IBX proceeded in excellent yields (Scheme 2.20).



Scheme 3.20: Reduction of esters 3.68-3.70 and subsequent oxidation to aldehydes 3.74-3.76

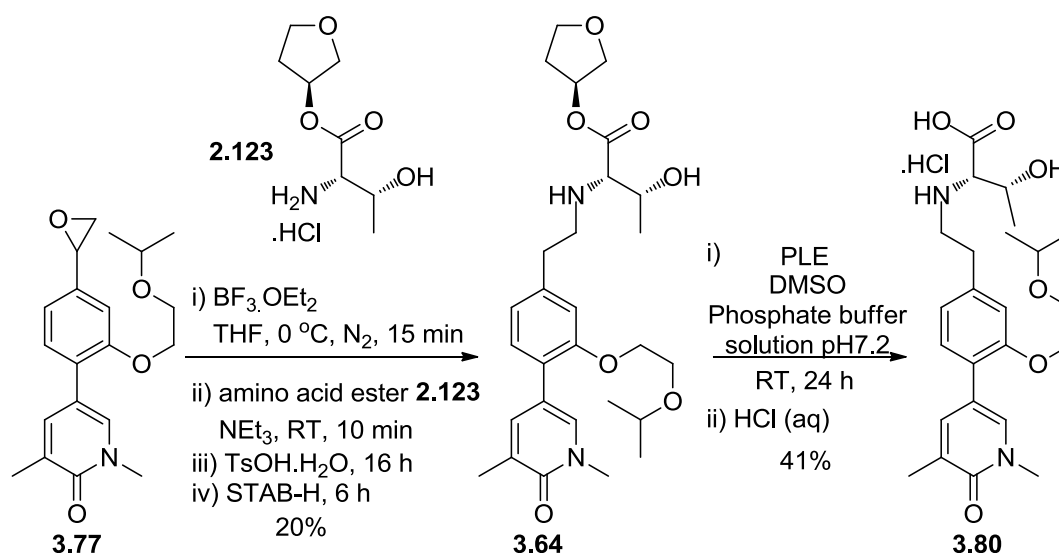
With the desired aldehydes in hand, the Corey-Chaykovsky chemistry introduced the additional methylene unit. Again, using the simpler procedure with potassium

hydroxide gave epoxides **3.77-3.79** in excellent yields and good purities (Scheme 3.21).



Scheme 3.21: Corey-Chaykovsky epoxidation

The resulting epoxides were individually subjected to the one-pot epoxide rearrangement and reductive amination. Firstly, the isopropoxyethyl example **3.77** was used. Using the threonine THF amino acid ester **2.123**, the product **3.64** was synthesised in a modest 20% yield over the two steps (Scheme 2.22). A portion of **3.64** was hydrolysed using the PLE conditions in moderate yield.



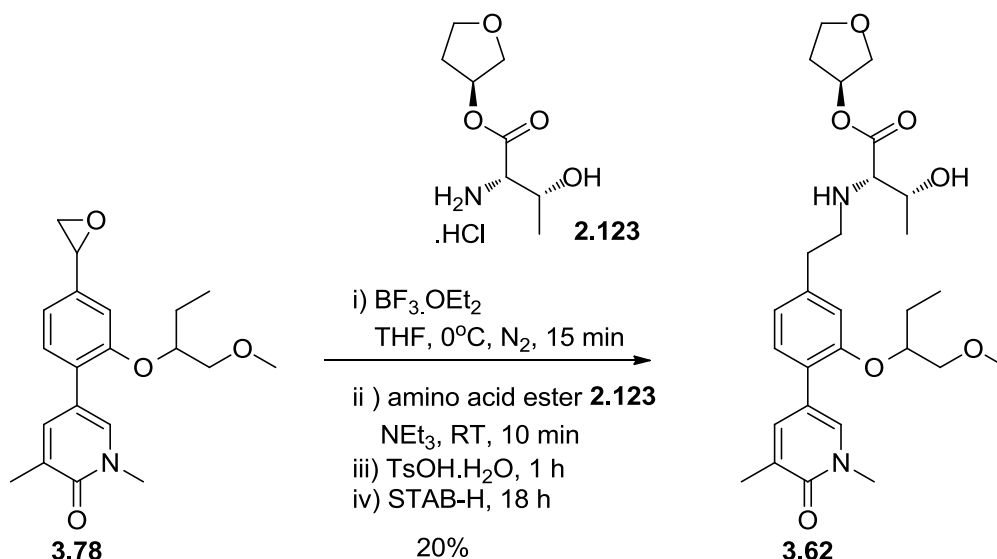
Scheme 3.22: Epoxide rearrangement-reductive amination and subsequent ester hydrolysis of compound 3.77

Compound **3.64** was tested within the biological assays for Brd4 BD1 and CREBBP (Table 3.12). Unfortunately, this compound had a BET biochemical potency of 6.1, half a log unit less than the lead compound **3.54**. Additionally, with a potency of 5.4 at CREBBP, the selectivity has reduced to 5-fold, suggesting that the lipophilic isopropyl group does not make efficient interactions with the WPF shelf. Additionally, the potency within the hWB assay was lower than desired, while the ChromLogD_{7.4} was also increased.

	3.64	3.80
Brd4 BD1 pIC₅₀	6.1	5.5
hWB_{BSci} (MCP-1) pIC₅₀	6.4	-
CREBBP pIC₅₀ (Selectivity*)	5.4 (5-fold)	-
ChromLogD_{7.4} / PFI	3.6 / 5.6	0.9 / 2.9

Table 3.12: Properties of ester 3.64 (*Selectivity for Brd4 BD1 over CREBBP)

The epoxides containing the α - and β -substituted racemic ethers were also used to form the corresponding ESM-functionalised compounds **3.62** and **3.63**. Firstly, a 20% yield was obtained from this one-pot reaction to obtain **3.62** (Scheme 3.23). Due to the use of the racemic alcohol starting material, the product from this reaction was an inseparable 1:1 mixture of diastereoisomers. However, the potency of this mixture of isomers was very promising. The BET potency showed a slight increase to 6.9, while the CREBBP potency was maintained at 5.6, improving the selectivity. The compound was tested within the human whole blood assay and maintained the log unit increase in potency into this assay (7.9).



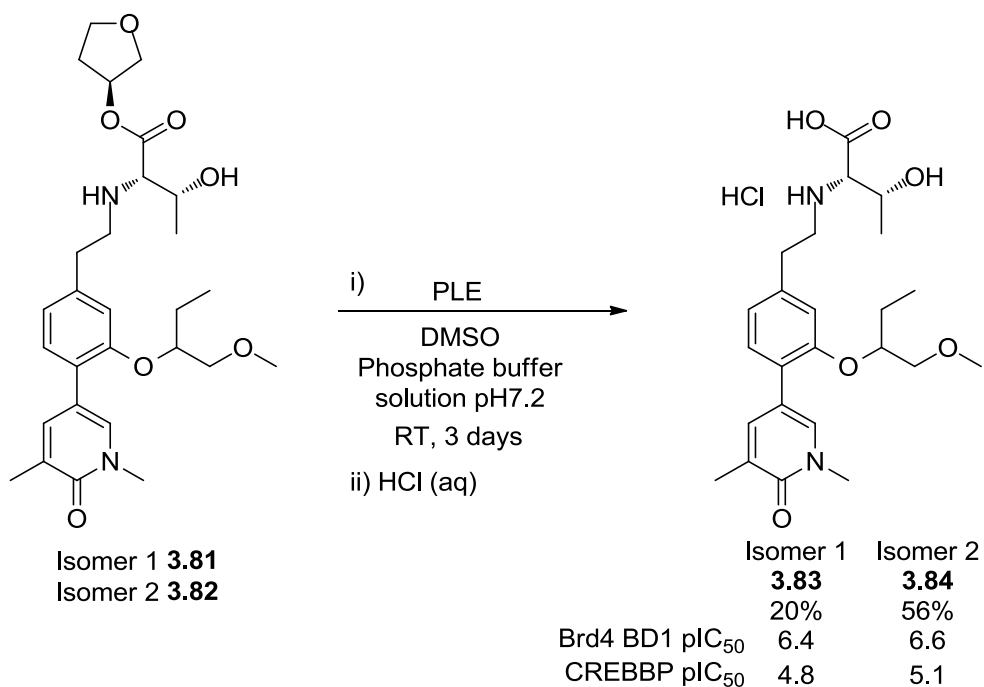
Scheme 3.23: Epoxide rearrangement and reductive amination to form diastereomeric mixture 3.62

To resolve the isomers, chiral chromatography was used.²⁸³ Good quantities of the two isomers (**3.81**, **3.82**) were isolated and the properties are highlighted in Table 3.13. The results from the biochemical assays were very pleasing. The excellent potency at Brd4 BD1 was maintained compared to the lead compound **3.54**. Additionally, the potency at CREBBP was maintained for isomer 2 (**3.82**), while a reduction was seen for isomer 1 (**3.81**). In both examples, the selectivity over this bromodomain was increased, with this additional carbon unit. Therefore, the α -ethyl must be in the correct orientation for isomer 1 to make more efficient interactions to Brd4 BD1 than CREBBP. However, the $\text{ChromLogD}_{7.4}$ was measured as 3.7 for both isomers, approaching the upper limit of <4 within the TPP. The IVC has also increased, thought to be a result of the higher lipophilicity.

	Isomer 1 (3.81)	Isomer 2 (3.82)
Brd4 BD1 pIC₅₀	6.7	7.0
hWB_{BSci} (MCP-1) pIC₅₀	7.7	8.1
CREBBP pIC₅₀ (Selectivity*)	5.2 (30-fold)	5.8 (16-fold)
ChromLogD_{7.4} / PFI	3.7 / 5.7	3.7 / 5.7
HLM IVC (- / + benzil)	11.5 / 5.5	18.1 / 6.6

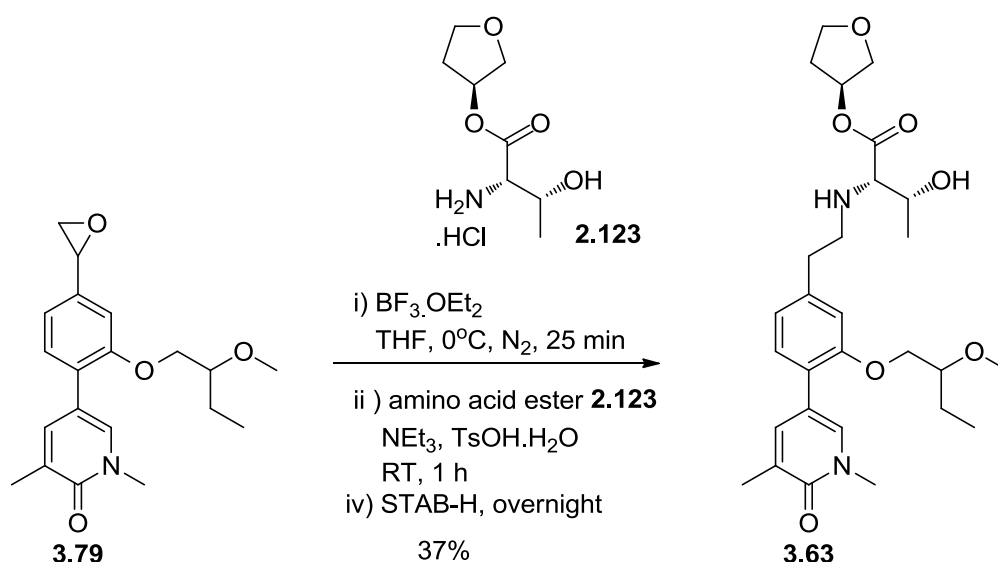
Table 3.13: Properties of separated diastereoisomers 3.81 and 3.82 (*Selectivity for Brd4 BD1 over CREBBP)

Pleasingly, the potency within the whole blood assay was excellent for both isomers, demonstrating a log unit enhancement from the biochemical into this cellular assay. To gain a full understanding of this profile, the two esters isomer 1 (**3.81**) and isomer 2 (**3.82**) were hydrolysed using the PLE conditions, with the resulting acids isolated in poor to moderate yields (Scheme 3.24). Interestingly and pleasingly, the acids of both isomer 1 and isomer 2 have a minimal decrease in potency between the ester and acid. Isomer 2 (**3.82**) also maintains the level of selectivity as the acid.



Scheme 3.24: Esterase-mediated hydrolysis of esters **3.81** and **3.82**

With the esters and acids of the α -ethyl isomer in hand, attention turned back to the β -ethyl regioisomer. The epoxide rearrangement and reductive amination proceeded well with a moderate yield (Scheme 3.25). Again, initial indications towards the potency of this compound were obtained as the diastereomeric mixture. At this stage, the β -ethyl regioisomer **3.63** was equipotent to compound **3.81** and **3.82**. The selectivity was also promising, with a CREBBP potency of 5.3, corresponding to an excellent 30-fold selectivity. Additionally, this compound maintained the excellent potency within the hWB assay (7.5).



Scheme 3.25: Epoxide rearrangement and reductive amination of β -ethyl example 3.79

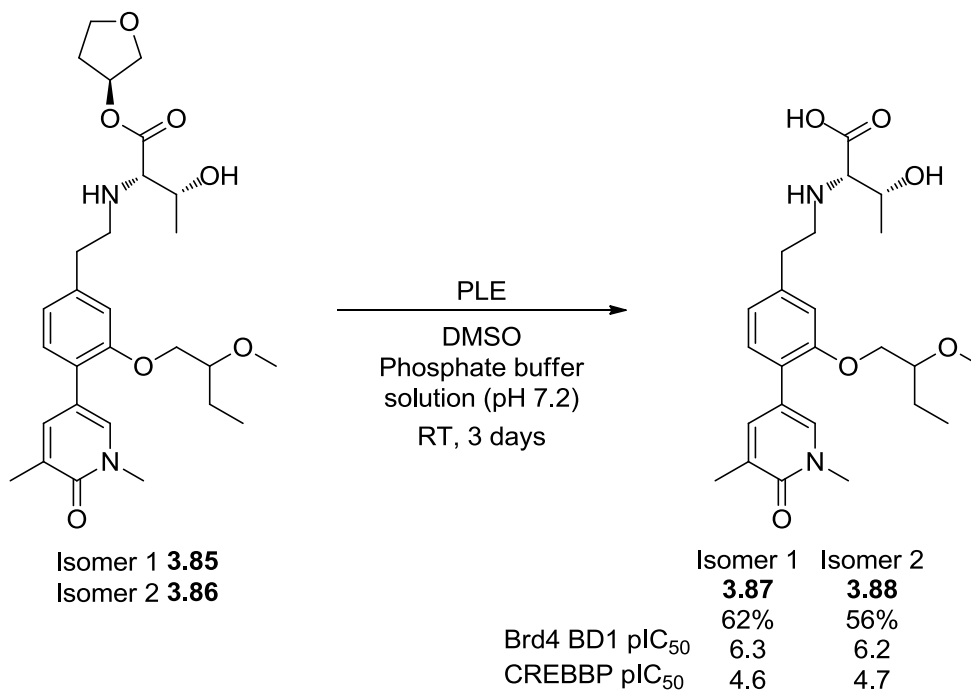
The diastereomers were separated by chiral chromatography²⁸³ and were subsequently tested within the relevant assays with the properties shown in Table 3.14. Both isomers have excellent biochemical potencies coupled with good levels of selectivity. However, the hWB potencies showed minimal enhancement relative to the biochemical potencies. Additionally, as observed with **3.81** and **3.82**, the lipophilicity and corresponding PFI are higher than desired, translating into high IVC values.

	Isomer 1 (3.85)	Isomer 2 (3.86)
Brd4 BD1 pIC₅₀	6.9	6.8
hWB_{BSci} (MCP-1) pIC₅₀	7.2	7.0
CREBBP pIC₅₀ (Selectivity*)	5.3 (40-fold)	5.4 (25-fold)
ChromLogD_{7.4} / PFI	4.1 / 6.1	4.1 / 6.1
HLM IVC (- / + benzil)	5.8 / 3.4	6.4 / 3.5

Table 3.14: Properties of separated β -ethyl isomers 3.85 and 3.86 (*Selectivity for Brd4 BD1 over CREBBP)

Interestingly, and in contrast to the α -ethyl compounds, **3.81** and **3.82**, the individual isomers **3.85** and **3.86** were equipotent at CREBBP. With the separated diastereoisomers in hand, and to understand the relatively low whole blood potencies, the esters were hydrolysed with PLE (Scheme 3.26). The yield of the initial transformation and purification were excellent. However, on attempting to form the hydrochloride salt, a small portion of the *O*-demethylated ether was observed.

The compound was re-purified and tested within the biological assays as the free base. Pleasingly, the acids of this regioisomer were equipotent to the α -ethyl derivatives, **3.83** and **3.84**. Similarly, the two diastereoisomers were indistinguishable in potency.



Scheme 3.26: Esterase-mediated hydrolysis of ester isomers 3.85 and 3.86

Compared to the lead compound **3.54**, the addition of bulk at the terminal position was detrimental to potency at Brd4 BD1, selectivity over CREBBP and potency within the hWB assay, demonstrating the importance of substitution of the ethyl chain in occupying the WPF shelf. On the other hand, both the α - and β -substituted compounds gave pleasing improvements in potency and selectivity (Figure 3.51), although the human whole blood potencies of the β -ethyl compounds were disappointing. Additionally, the measured ChromLogD_{7.4} values of these branched compounds were higher than desired. This high lipophilicity was thought to be causing the increase in the *in vitro* clearance, to an unacceptable level.

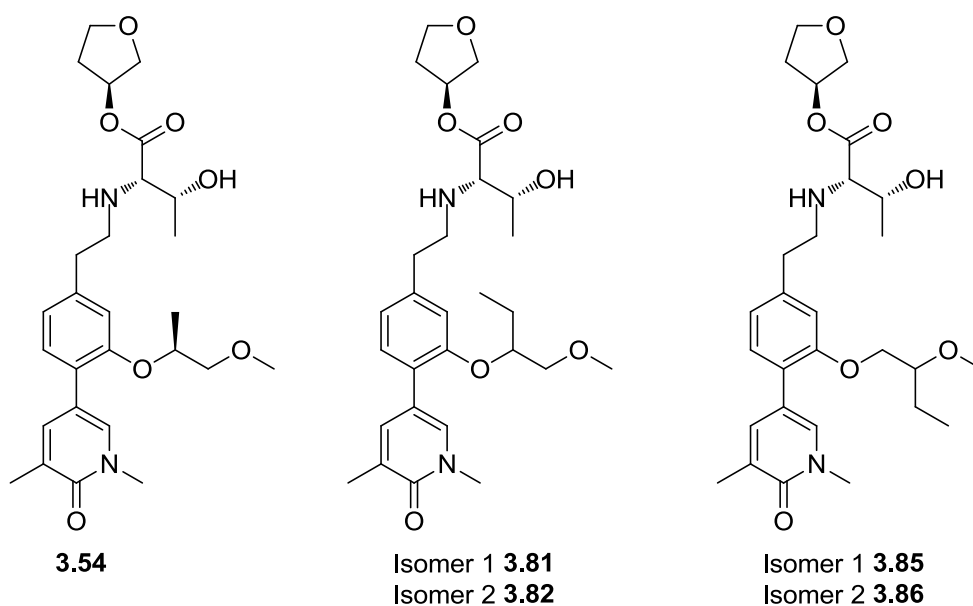


Figure 3.51: Comparison of α - and β -ethyl compounds with previous lead compound 3.54

Returning to the model of α -methyl fragment **3.59** within Brd4 BD1 (Figure 3.52), the ethyl group was thought to be making a more efficient interaction with the shelf, whereas, the methoxy was either making lipophilic interactions with the opposite face of the protein or directed into solvent.

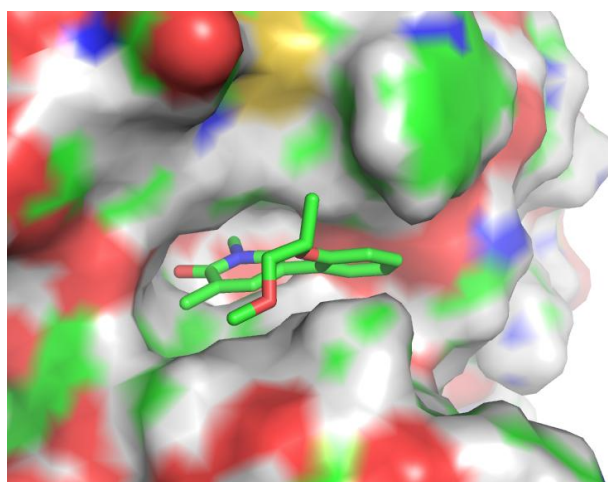


Figure 3.52: Computational model of truncated α -methyl 3.59 within Brd4 BD1

Consequently, it was hypothesised that synthesising the compounds lacking the methyl ether may help to confirm the binding mode around the WPF shelf as being associated with the alkyl or ether chain. Additionally, unmasking the alcohol would reduce the compound's lipophilicity and hence may improve the *in vitro* clearance. Further, if the methyl ether is directed into solvent, the more polar alcohol would be

favoured. As such, the following two compounds were proposed (**3.89** and **3.90**) (Figure 3.53).

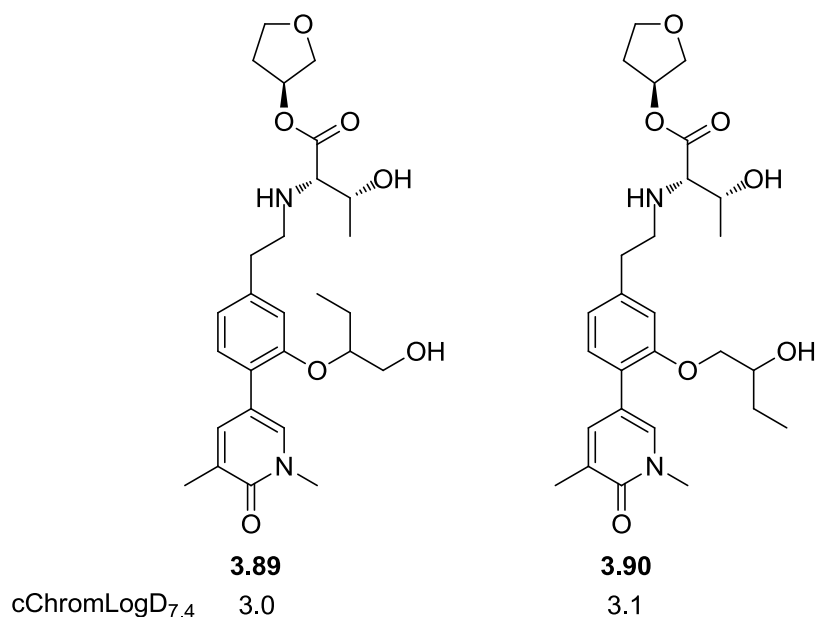
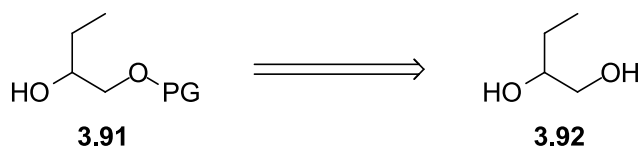


Figure 3.53: Compounds revealing the alcohol functionality

3.3.2 Demethylation

The robust chemistry developed for the synthesis of previous examples was used to synthesise the two new targets. However, a protecting group strategy was required due to the selectivity issues foreseen in using the diol starting material.

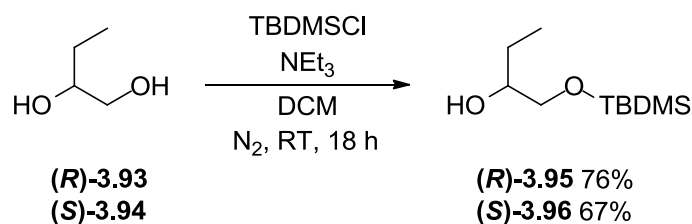
Firstly, the chemistry towards the α -ethyl example **3.89** was investigated. A strategy to protect the less sterically encumbered primary alcohol **3.91** was envisaged as shown in Scheme 3.27. This would enable the free alcohol to react under the Mitsunobu conditions while the desired alcohol is protected preventing oxidation, by IBX, later in the synthesis.



Scheme 3.27: Protection strategy for diol **3.92**

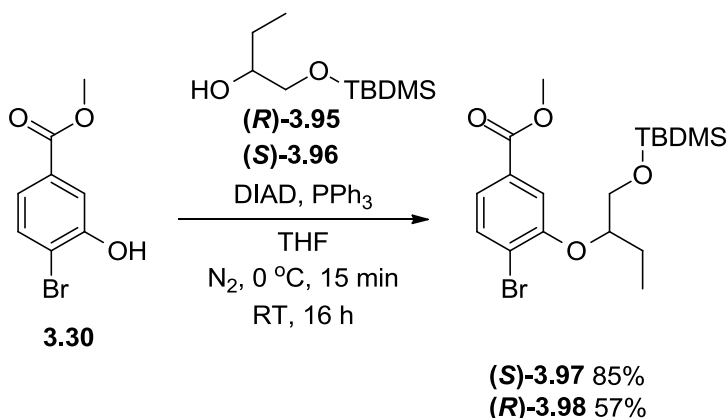
A literature search provided an efficient procedure for the selective silyl protection of the primary alcohol, as required, in an 84% yield.²⁸⁴ This one-step procedure to the

alcohol required for the Mitsunobu reaction made the use of the single enantiomers viable within this strategy. The procedure proved effective with a good yield obtained for each enantiomer (Scheme 3.28).



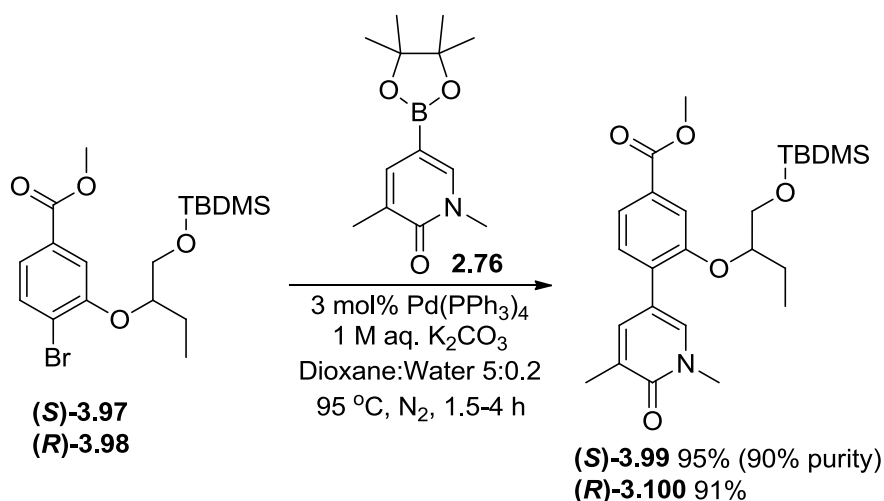
Scheme 3.28: Selective protection of the primary alcohol

With the successful formation of the mono-protected diols **(R)-3.95** and **(S)-3.96**, confirmed by NMR spectroscopy, the intermediates were progressed into the Mitsunobu reaction (Scheme 3.29). The reactions proceeded well with each enantiomer. **(S)-3.97** was isolated in excellent yield, while the purification of **(R)-3.98**, co-eluting with reaction by-products, limited the yield.



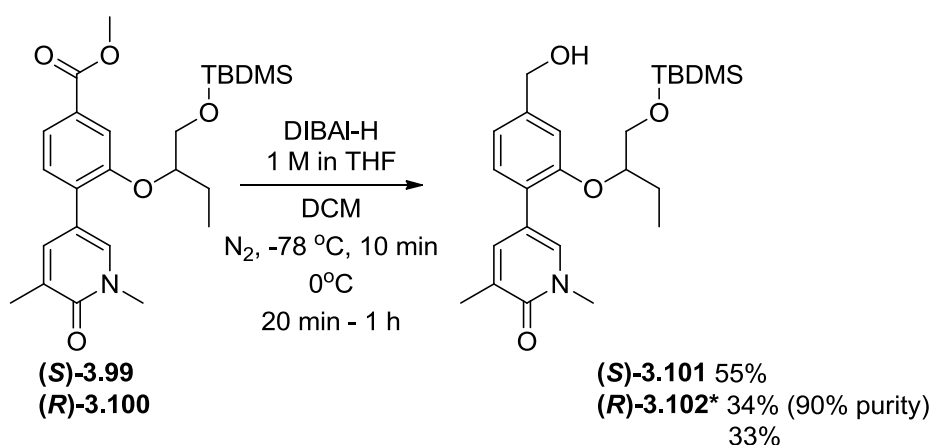
Scheme 3.29: Mitsunobu etherification with protected alcohols 3.95 and 3.96

The resulting Suzuki cross-coupling to insert the pyridone acetyl-lysine mimetic proved to be very efficient (Scheme 3.30). Both enantiomers were isolated in excellent yields.

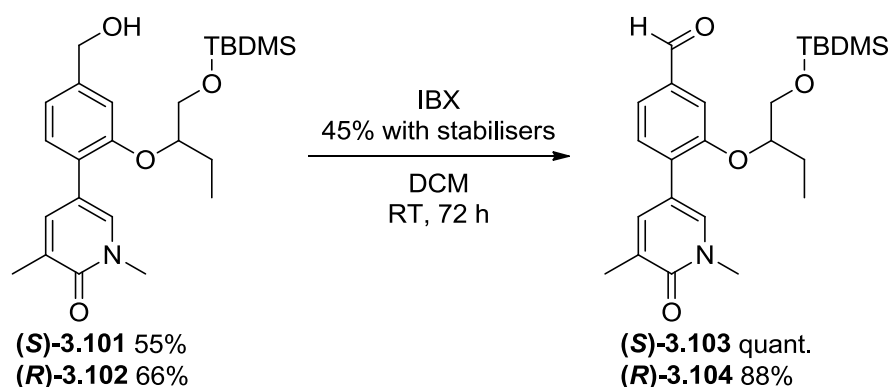


Scheme 3.30: Efficient Suzuki cross-couplings

Subsequent reduction of the ester gave the desired alcohols in moderate yields (Scheme 3.31). The time for this robust reaction could be reduced to as short as 20 minutes.

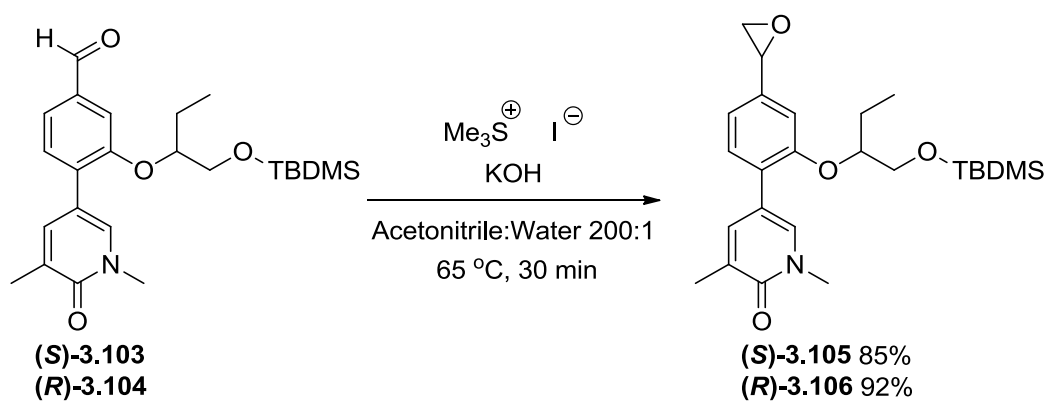
Scheme 3.31: Reduction of ester 3.99 and 3.100
(**(R)*-3.102 isolated in two batches)

As with previous examples, the IBX oxidation was very efficient (Scheme 3.32). Excellent yields were obtained setting up the homologation steps.



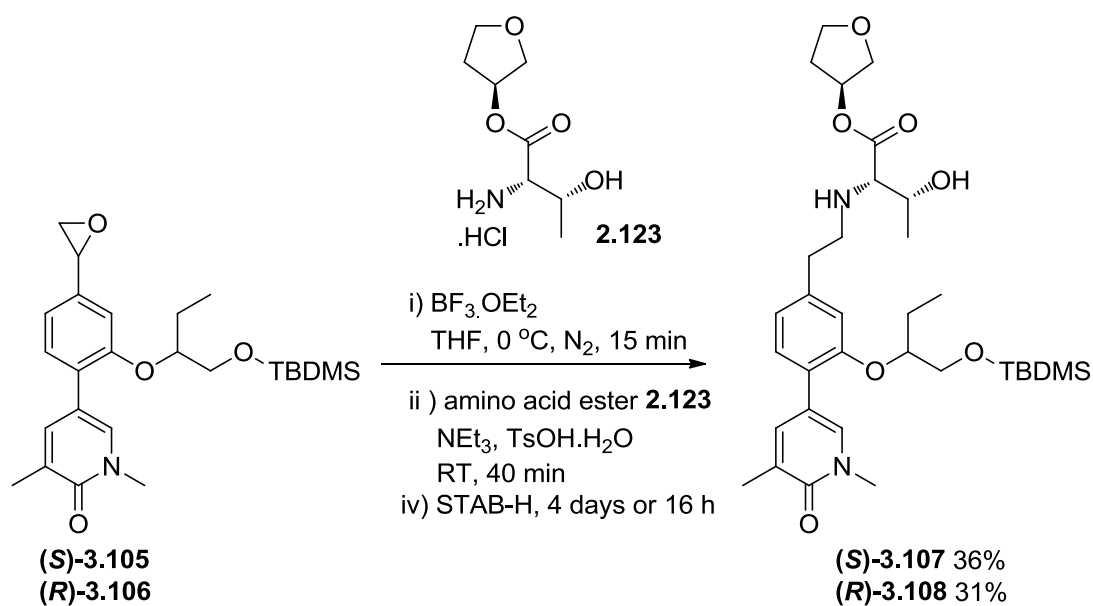
Scheme 3.32: Oxidation of alcohols 3.101 and 3.102

The epoxidation using the efficient hydroxide conditions were excellent (Scheme 3.33). The epoxide was isolated in excellent purity following aqueous workup, setting up the reductive amination.



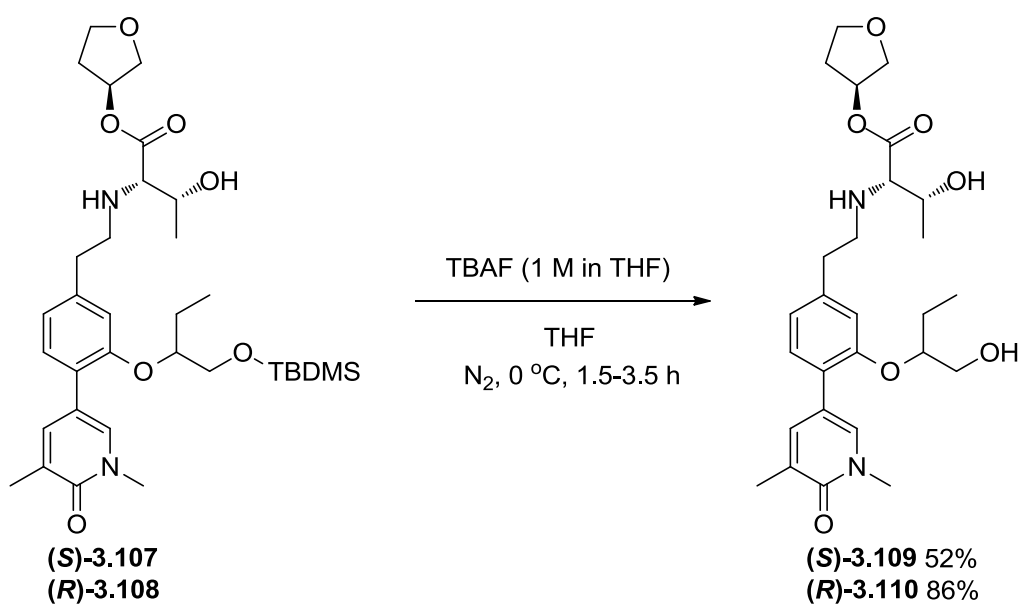
Scheme 3.33: Epoxidation of aldehydes 3.103 and 3.104

With the two epoxides in hand, the resulting epoxide rearrangement and reductive aminations were carried out (Scheme 3.34). Pleasingly, the desired products were obtained in over 30% yield across two steps.



Scheme 3.34: Epoxide rearrangement and reductive amination

The final step to the desired products was to remove the silyl protecting group. This was achieved using TBAF over a short reaction time (Scheme 3.35). The two products were isolated in moderate to good yield. With these two key compounds in hand, biological data was obtained.



Scheme 3.35: Silyl deprotection using TBAF

Firstly, the Brd4 BD1 potencies were measured, demonstrating **(S)-3.109** to be more potent than **(R)-3.110** (Table 3.15). Additionally, **(S)-3.109** is much more potent

within the whole blood assay with an excellent potency of 8.1. This is represented within the IVC assay lacking the esterase inhibitor. **(S)**-3.109, with a higher value of 5.7, suggests a faster hydrolysis rate for this isomer. However, both compounds show a reduction in underlying P450-mediated IVC compared to the methyl ether **3.81** and **3.82**. Additionally, the 25-fold selectivity over CREBBP constitutes a good result for **(S)**-3.109.

	(S) -3.109	(R) -3.110
Brd4 BD1 pIC₅₀	6.9	6.5
hWB_{BSci} (MCP-1) pIC₅₀	8.0	7.3
CREBBP pIC₅₀ (Selectivity)	5.5 (25-fold)	5.4 (12-fold)
ChromLogD_{7.4} / PFI	3.0 / 5.0	3.0 / 5.0
HLM IVC (- / + benzil)	5.7 / 1.4	3.4 / 1.6

Table 3.15: Properties of isomers 3.109 and 3.110 (*Selectivity for Brd4 BD1 over CREBBP)

Comparing these results to the methyl ether compounds **3.81** and **3.82** (Figure 3.54), **(S)**-3.109 has a very good profile. While maintaining potency and selectivity, both the lipophilicity and IVC have improved.

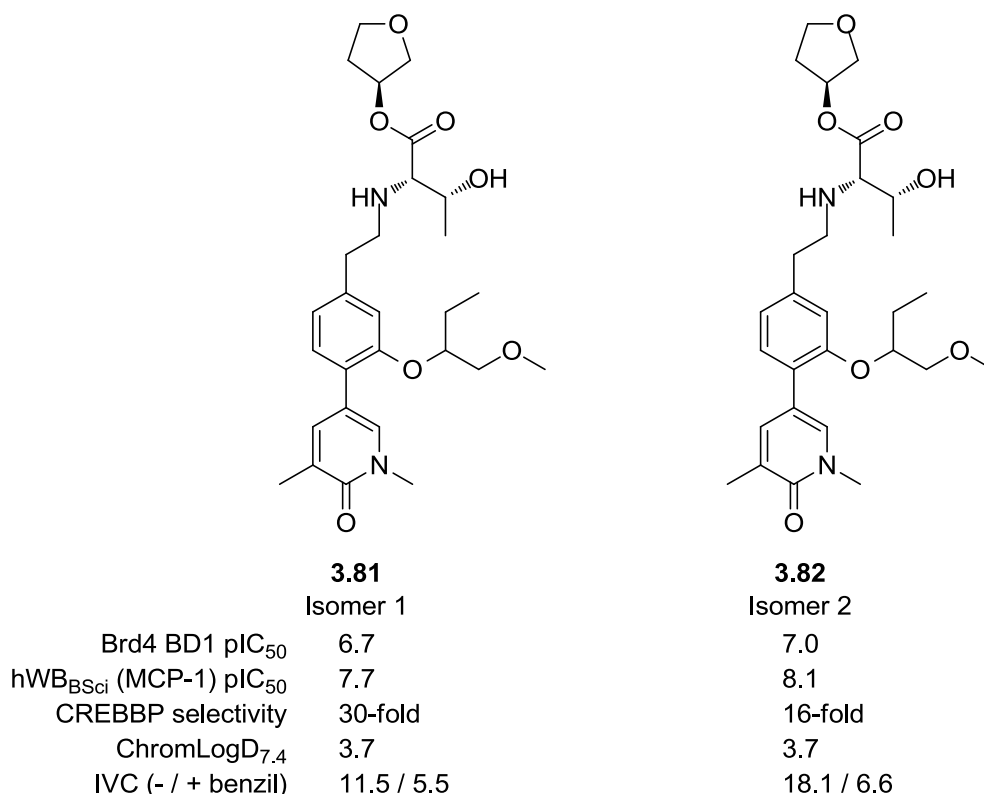


Figure 3.54: Methyl ether isomers 3.81 and 3.82 for comparison to 3.109 and 3.110

With **(S)**-**3.109** demonstrating excellent potency and selectivity, maintained from the methyl ether variants **3.81** and **3.82**, an X-ray crystal structure of **(S)**-**3.109** within Brd4 BD1 was obtained to confirm how this compound was interacting with the WPF shelf (Figure 3.55). Interestingly, as suggested by previous modelling, it was the ethyl chain interacting with the WPF shelf, while the alcohol interacts with the water surrounding the protein. This helps to explain why no loss of potency was observed by removing the pendant methyl group.

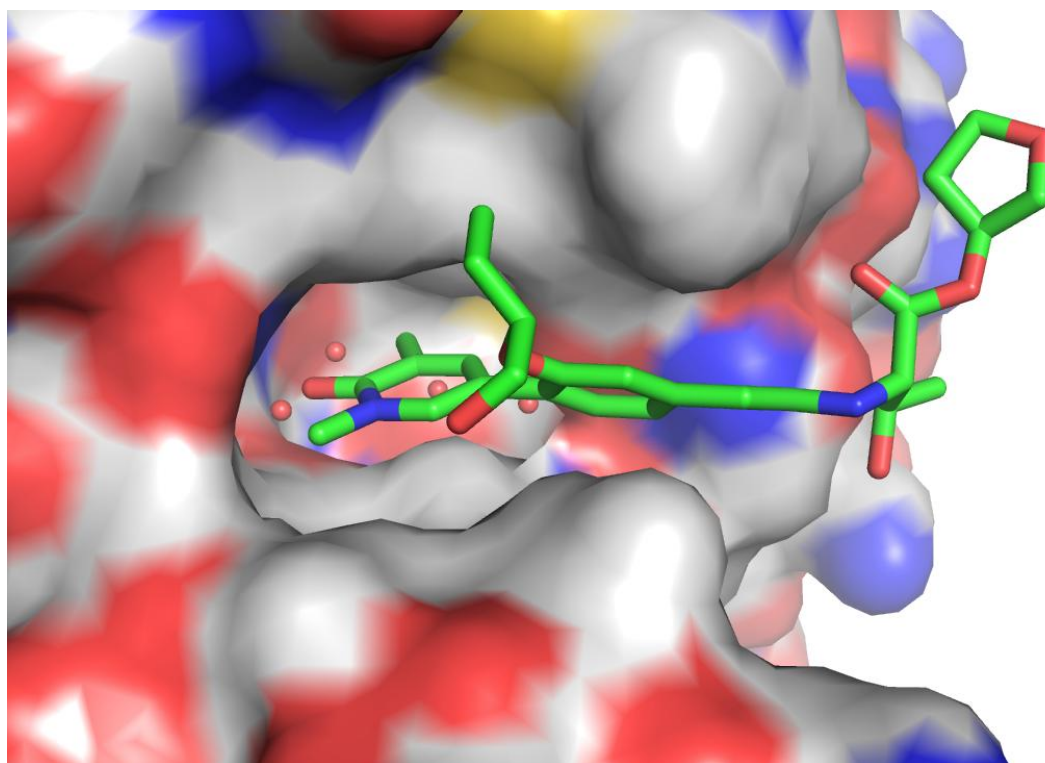
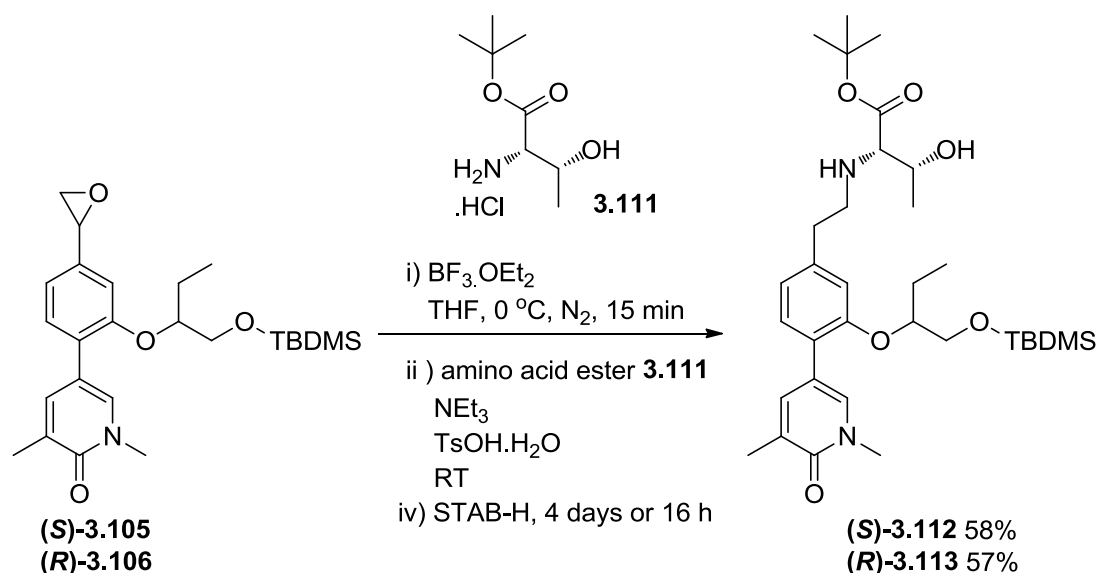
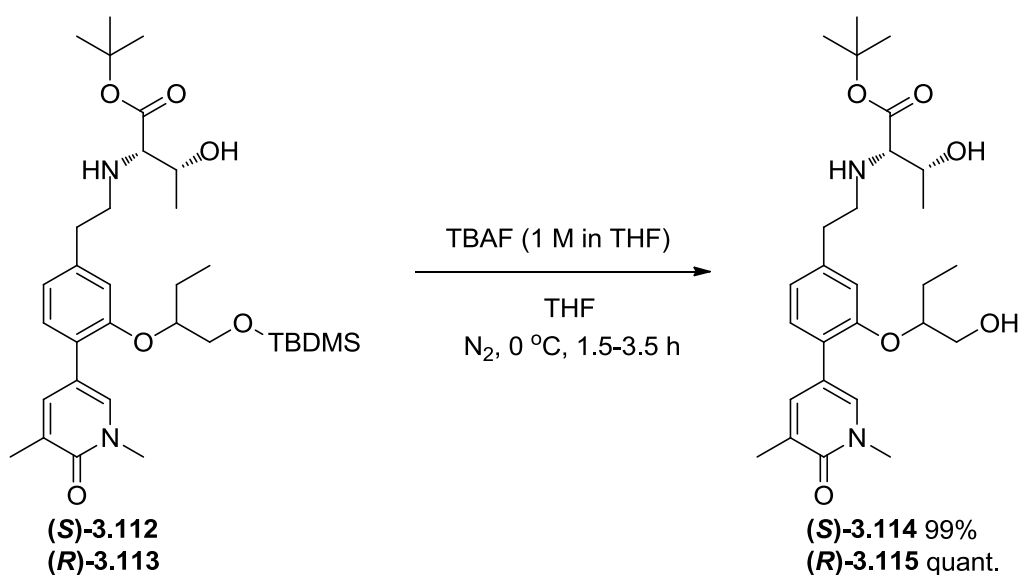


Figure 3.55: X-ray crystal structure of **3.109** in Brd4 BD1

Having understood how compound **3.109** binds to Brd4 BD1 and with a profile so near to the TPP, the ESM mechanism of compounds **(S)**-**3.109** and **(R)**-**3.110** were further investigated. To achieve this, the bulky *t*-butyl ester, which is chemically unable to be hydrolysed by hCE-1, was prepared as a control compound. Accordingly, the *t*-butyl ester was synthesised as shown in Scheme 3.36 using the commercially available *t*-butyl threoninate. This amino acid ester gave an excellent yield over the two steps, the best observed for this developed procedure.

Scheme 3.36: Reductive amination using threonine, *t*-butyl ester **3.111**

The silyl protected compounds **(S)-3.112** and **(R)-3.113** were treated with TBAF (Scheme 3.37). After additional portions of TBAF were added, the two reactions proceeded well. This allowed the two examples to be isolated in excellent yields.



Scheme 3.37: Silyl deprotection using TBAF

In order to further interrogate the contribution of the ESM mechanism through the *t*-butyl esters, both the biochemical and human whole blood potencies were collected. As illustrated in Table 3.16, comparing the THF esters to the *t*-butyl esters, the mutual pairs are biochemically equivalent at Brd4 BD1. However, the whole blood potencies in a pair wise fashion are markedly different. As expected, and previously

seen, the THF esters show a large enhancement of potency of between 0.8 and 1.1 log units between the biochemical and whole blood assays. As hypothesised, the *t*-butyl esters are 0.7 log units less potent than the hydrolysable esters. However, the challenging result was the 0.2 to 0.6 log unit enhanced potency still observed by the *t*-butyl esters.

	(S)-3.109	<i>t</i> -Bu (S)-3.114	(R)-3.110	<i>t</i> -Bu (R)-3.115
Brd4 BD1 pIC ₅₀	6.9	6.7	6.5	6.4
hWB _{BSci} (MCP-1) pIC ₅₀	8.0	7.3	7.3	6.6
ΔpIC ₅₀	1.1	0.6	0.8	0.2

Table 3.16: Comparison of THF and *t*-butyl esters

One way to rationalise this result was to hypothesise that the lipophilic basic amine, within these structures is causing accumulation within the acidic cellular compartments, organelles, such as the liposomes.^{285,286} However, this rationale does not explain a similar case within our laboratory within an orthogonal template (Figure 3.56).²⁸⁷

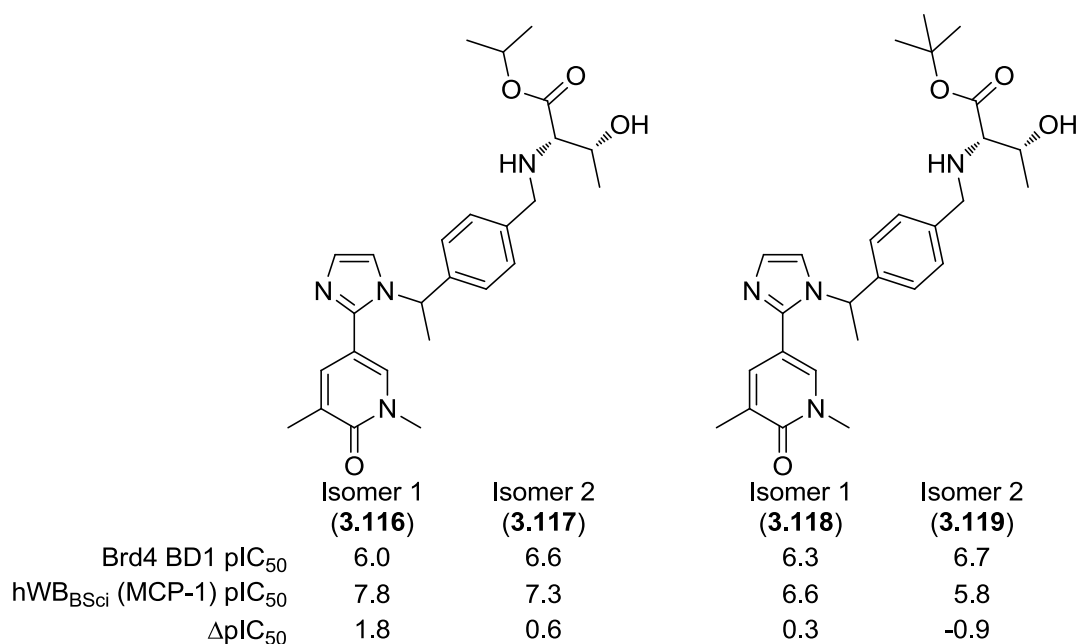
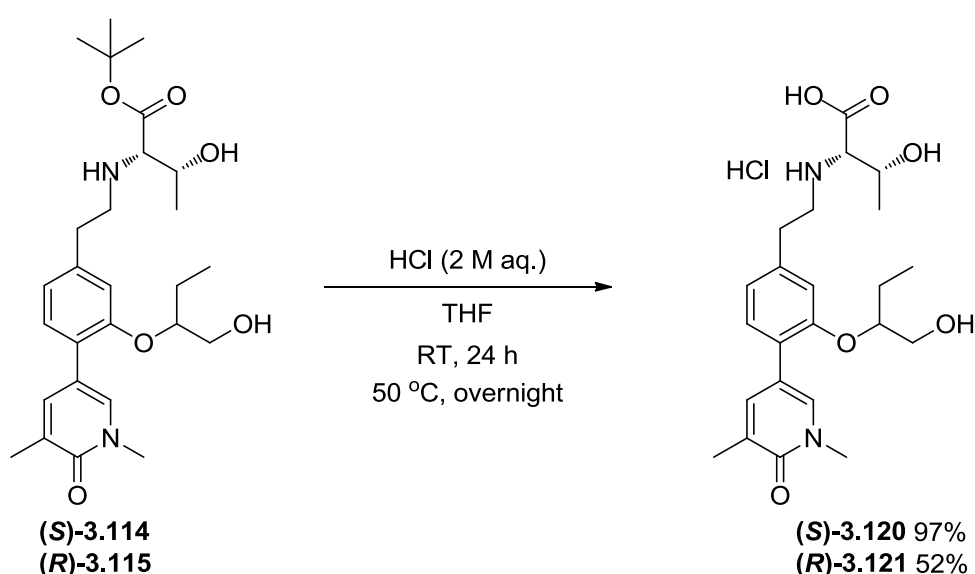


Figure 3.56: Example of enhanced *t*-butyl ester potency elsewhere within our laboratory²⁸⁷

Modifying only the stereochemistry of the bridging linker, a dramatic change is observed in the ΔpIC₅₀, the difference between the whole blood and biochemical assays. The *iso*-propyl ester **3.116**, hydrolysable by hCE-1, demonstrates a large ΔpIC₅₀. However, similarly to **3.114** and **3.115**, above, the non-hydrolysable *t*-butyl

ester **3.118** was, unexpectedly, more potent in the hWB assay than the Brd4 BD1 assay, although the ΔpIC_{50} for **3.118** was not as large as for the hCE-1 labile *iso*-propyl ester **3.116** (ΔpIC_{50} 1.8). Interestingly, the *t*-butyl esters with the higher whole blood potencies (**3.114** and **3.118**) are of the same stereochemistry as the more potent hydrolysable ester isomers (**3.109** and **3.116**).

Having made the *t*-butyl esters, it was more efficient to use these esters to produce the desired acids. Aqueous hydrochloric acid was expected to cleave the esters at room temperature, however, only small quantities of the desired products were observed by LCMS. Hence, the reactions were heated to 50 °C overnight, in which time the reactions had progressed to completion (Scheme 3.38).



Scheme 3.38: *t*-Butyl ester cleavage with aqueous acid

The biochemical potencies of the acids were obtained and the results presented in Table 3.17. While the reduced potencies of the acids were still observed relative to the parent ester, acid **(S)-3.120** showed a potency of 6.4, a reduction of just 0.5 log units. **(R)-3.121** demonstrated a lower acid potency of 5.9, although only 0.6 lower than the ester. The lower acid potency for **(R)-3.121** may help to explain the lower whole blood potency of the corresponding ester. Additionally, **(R)-3.121** has a CREBBP potency of 5.1, mirroring the low selectivity of its ester. Pleasingly, however, **(S)-3.120** has an excellent selectivity of 40-fold with a CREBBP potency of 4.8, important due to the high concentrations formed within the target cell-types.

(S)-3.120

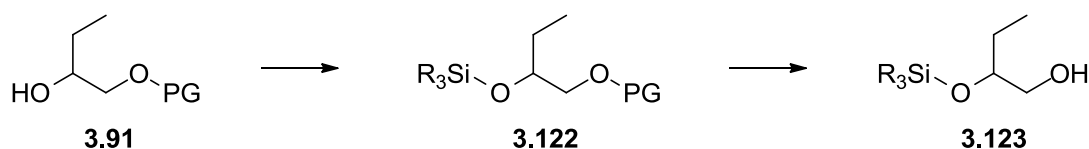
(R)-3.121

Brd4 BD1 pIC₅₀	6.4	5.9
CREBBP pIC₅₀ (Selectivity*)	4.8 (40-fold)	5.1 (6-fold)

Table 3.17: Potencies and selectivities of acids 3.120 and 3.121 (*Selectivity for Brd4 BD1 over CREBBP)

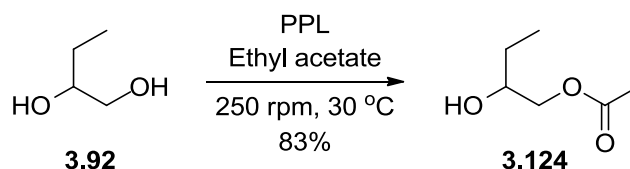
With these excellent results in hand, the focus turned to the alternative regioisomer, compound **3.90**. The challenge with this synthesis was the need to protect the secondary alcohol. Having observed the ease in silylating the primary alcohol a different strategy was therefore explored.

With the observed efficiency of removing the silyl group in the previous synthesis, the silyl group was once again pursued as part of this strategy. Ideally, the strategy would facilitate the selective protection of the primary alcohol, allowing the silyl protection of the secondary unit, before cleavage of the first group (Scheme 3.39).



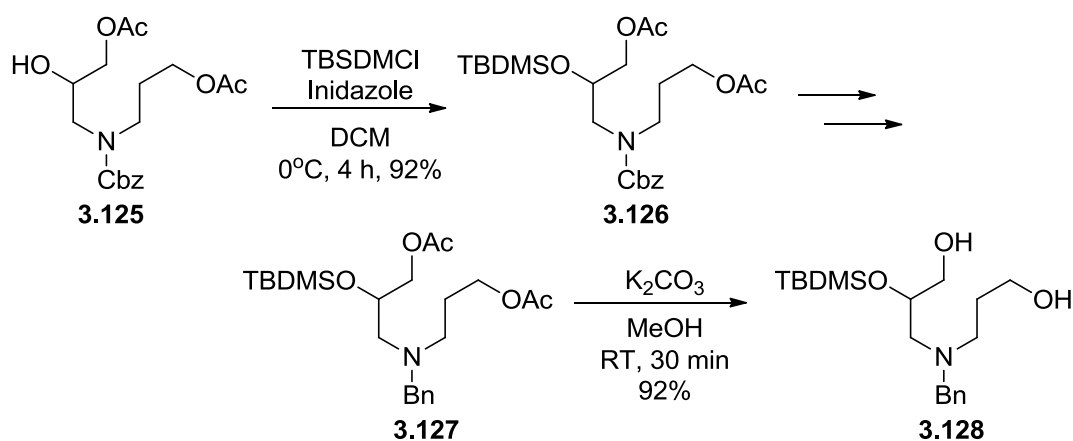
Scheme 3.39: Desired protecting group strategy

A literature search around the protection of such diols revealed the ability to perform a selective acetylation using an enzyme such as porcine pancreatic lipase (PPL). Pleasingly, the paper, by Cesti *et al.* described a procedure using the desired substrate for this synthesis (Scheme 3.40).²⁸⁸



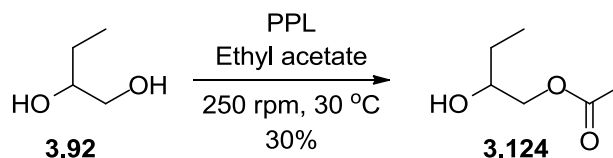
Scheme 3.40: Literature enzymatic transesterification on desired substrate 3.92

Evidence for the ability to introduce the silyl group and maintain its integrity within this 1,2-diol system was sought. A procedure reported by Kumar *et al.* described the efficient silyl protection of alcohol **3.125** with a TBDMS group (Scheme 3.41).²⁸⁹ After swapping the nitrogen protecting group, catalytic potassium carbonate in methanol was used to remove the acetyl groups in excellent yield.



Scheme 3.41: Literature precedence for silylation of mono-protected diol and subsequent cleavage of the acetyl protecting groups

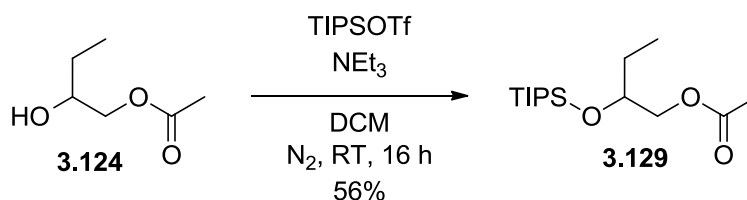
With literature precedence confirmed, the synthetic route was initiated. However, due to the involved nature of this protecting group strategy, the racemic starting material was used. The first step, as previously alluded to, involved the transesterification of ethyl acetate with the alcohol starting material, using PPL. The first attempt utilised the procedure as reported (Scheme 3.42).²⁸⁸ While the product was isolated, the reaction had not progressed to completion under these conditions.



Scheme 3.42: Acetate protection of primary alcohol 3.92

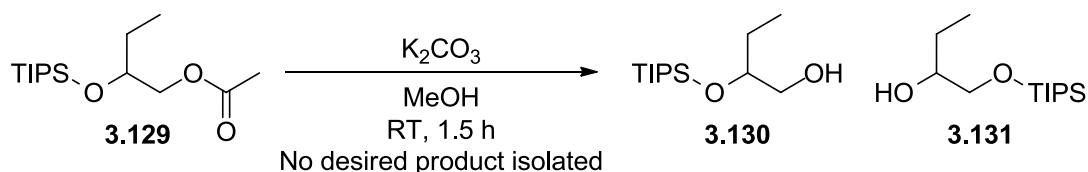
However, due to the successful formation of product, an approximately 10 g scale batch was undertaken. Considering the low yield from the previous attempt, the reaction was stirred for 47 hours, which gave an improved yield of 59%, an ample quantity for route progression.

The next step was to protect the secondary alcohol, with the more sterically encumbered TIPS protecting group being used (Scheme 3.43). The yield for this step was moderate as the lipophilic product showed some co-elution with the TIPS alcohol by-product.



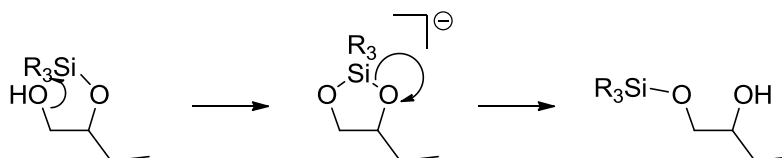
Scheme 3.43: Silyl protection of secondary alcohol 2.128

The next step was to hydrolyse the ester, which was initially tested on a 50 mg scale (Scheme 3.44). The procedure took longer than suggested for this substrate with an additional portion of potassium carbonate required to progress the reaction to completion.



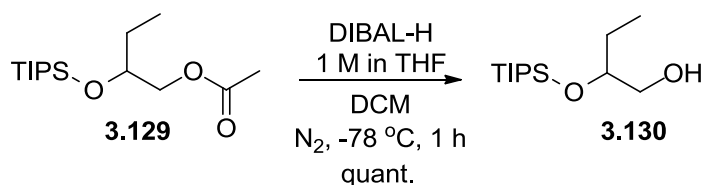
Scheme 3.44: Attempted ester hydrolysis using catalytic potassium carbonate

Unfortunately, when attempting to purify the product, it became apparent that during the reaction the silyl group had migrated to the primary alcohol **3.131**. This reactivity can be foreseen with a 5-membered intermediate (Scheme 3.45).



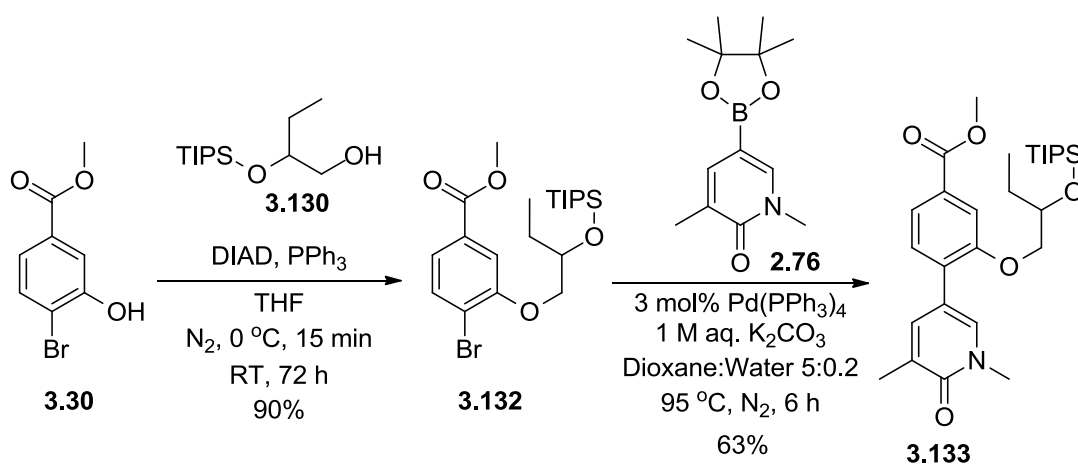
Scheme 3.45: Silyl rearrangement mechanism

An alternative strategy was therefore required to cleave this ester. It was thought that using DIBAL-H with its bulky alkyl groups may hinder silyl migration. This was indeed found to be the case, by ensuring the reaction was kept at -78 °C, no migration was observed. Pleasingly, this reduction proceeded in quantitative yield (Scheme 3.46)



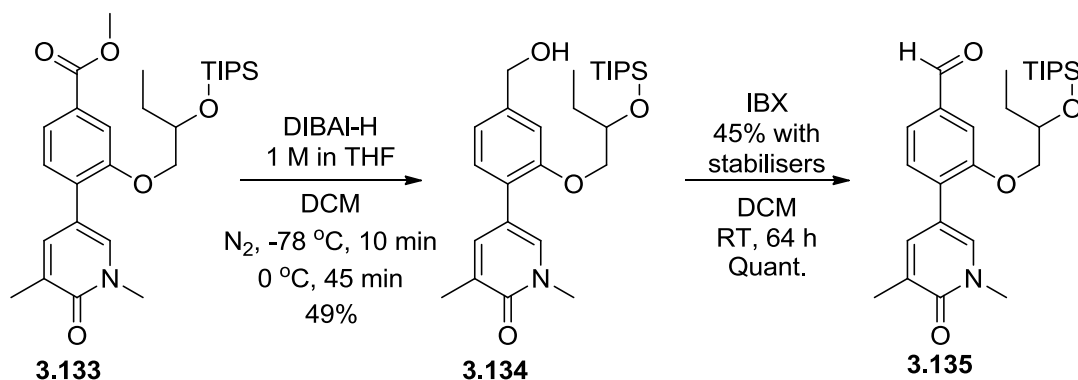
Scheme 3.46: Successful acetate deprotection using DIBAL-H

Having successfully made the required alcohol intermediate, the procedure follows the previously used chemistries (Scheme 3.47). The alcohol was coupled to phenol **3.30** to form ether **3.132** in excellent yield. The subsequent Suzuki reaction to introduce the pyridone warhead progressed in good yield to form intermediate **3.133**.



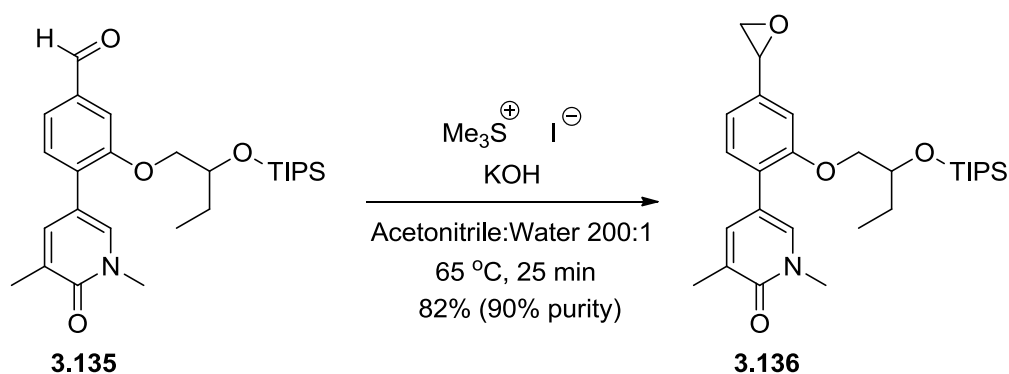
Scheme 3.47: Mitsunobu and subsequent Suzuki coupling

Subsequently, the oxidation state was altered, first by reduction to the alcohol using DIBAL-H in moderate yield (Scheme 3.48). Oxidation of alcohol **2.134** to the aldehyde using IBX proceeded in quantitative yield.



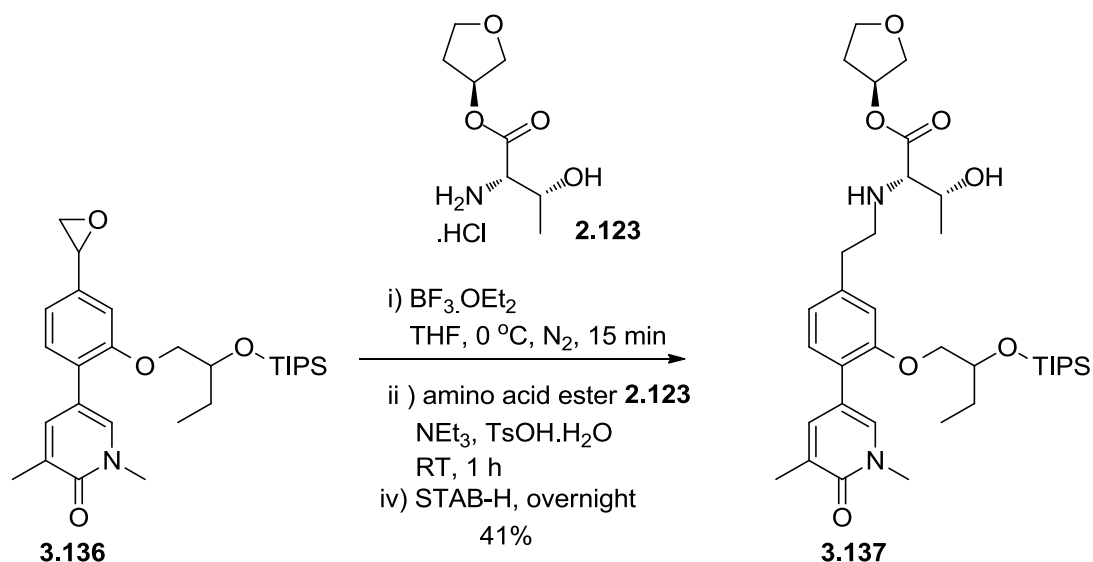
Scheme 3.48: Reduction of ester 3.133 and oxidation to aldehyde 3.135

With aldehyde **3.135** in hand, the material was progressed into the Corey-Chaykovsky epoxidation. The corresponding epoxide was formed in good yield and reasonable purity after aqueous workup (Scheme 3.49).



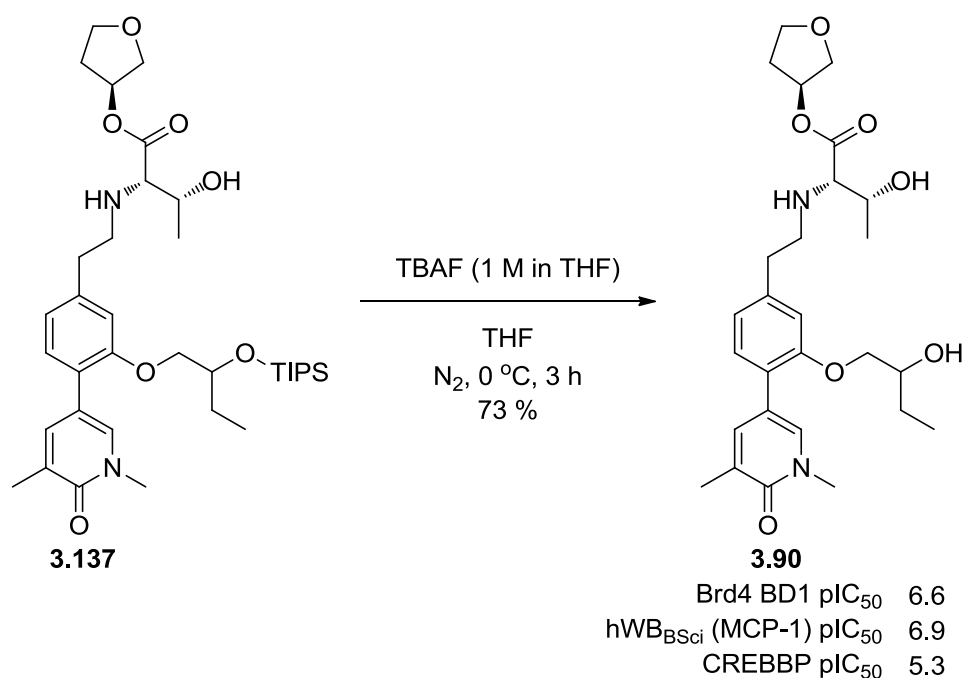
Scheme 3.49: Corey-Chaykovsky epoxidation

The epoxide **3.136** was subjected to the one-pot procedure to form the homologated aldehyde *in situ* before the reductive amination was undertaken (Scheme 3.50). The product was isolated as a mixture of diastereoisomers in 41% yield over these two steps.



Scheme 3.50: Epoxide rearrangement and reductive amination to form 3.137

To progress to the target material the silyl group was removed using the TBAF conditions used previously. Again, a very efficient reaction was observed, with a good isolated yield (Scheme 3.51). The product from this reaction, despite consisting of a mixture of diastereoisomers, was tested within the key assays. While the biochemical potency was good, the whole blood potency was less than expected, with a pIC_{50} of 6.9. This correlates to only a small enhancement of 0.3 log units. However, a 20-fold selectivity over CREBBP is good for this mixture.



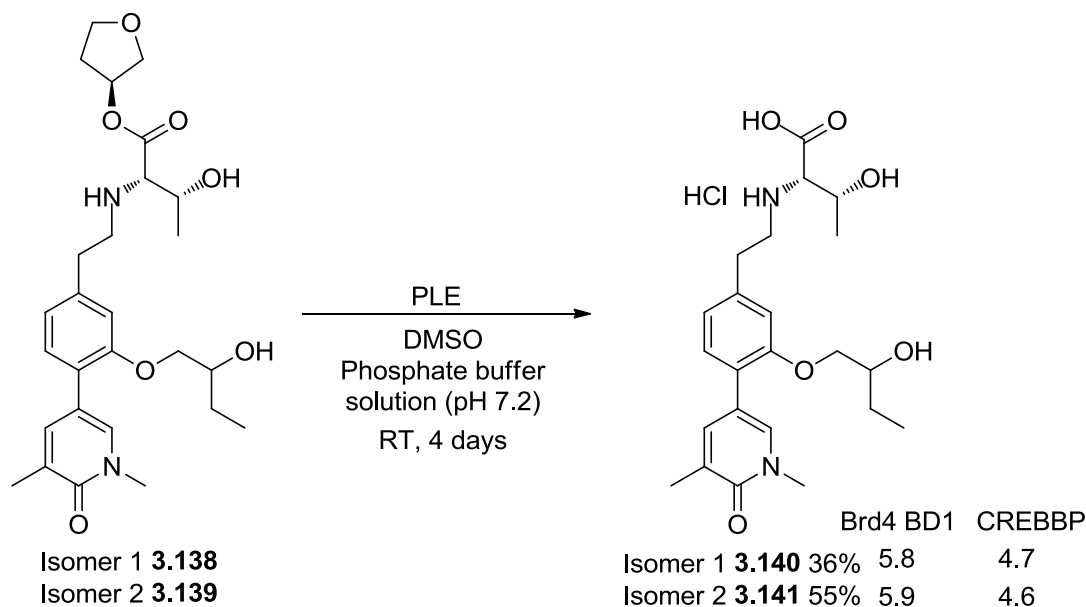
Scheme 3.51: Silyl deprotection using TBAF

To understand the properties of the individual diastereoisomers, the mixture was separated by chiral chromatography.²⁸³ This yielded the compounds, which were tested within the key assays and compared to the mixture (Table 3.18). Unfortunately, both isomer 1 (**3.138**) and isomer 2 (**3.139**) proved to be equipotent with the mixture **3.90** within the Brd4 BD1 biochemical assay. Pleasingly, the whole blood potency for isomer 2 demonstrated a 0.6 log unit enhancement relative to the biochemical potency at Brd4 BD1. In addition, a reasonable 20-fold selectivity was observed versus CREBBP. These selectivities were towards the 30-fold required within the TPP. As observed with the mixture, the ChromLogD_{7.4} and PFI were within an excellent area. The IVC values were also excellent with low values both with and without benzil. However, in lieu of an hCE-1 assay at this time, looking at the difference between the plus and minus benzil values gives an estimate of the esterase-mediated metabolism. The higher value for **3.139** may be aiding the whole blood potency compared to **3.138**. However, it is also important to investigate the contribution from the acid biochemical potencies.

	3.90	Isomer 1 3.138	Isomer 2 3.139
Brd4 BD1 pIC₅₀	6.6	6.5	6.5
hWB_{BSci} (MCP-1) pIC₅₀	6.9	6.6	7.1
CREBBP pIC₅₀ (Selectivity*)	5.3 (20-fold)	5.3 (15-fold)	5.2 (20-fold)
ChromLogD_{7.4} / PFI	2.8 / 4.8	2.9 / 4.9	2.7 / 4.7
HLM IVC (- / + benzil)	- / -	2.0 / 1.2	2.2 / 1.0
Esterase-mediated Metabolism	-	0.8	1.2
AMP (nm / s)	-	110	97

Table 3.18: Properties of isolated isomers 3.138 and 3.139 compared to mixture 3.90
(*Selectivity for Brd4 BD1 over CREBBP)

To ensure it was not the acid potency adversely affecting the whole blood potency, the corresponding acids were generated using the previously highlighted esterase procedure (Scheme 3.52). The resulting acids were isolated, as the hydrochloride salts in low to moderate yields. Pleasingly, the acids **3.140** and **3.141** had reasonable potencies within the Brd4 BD1 assay, 5.8 and 5.9, respectively. Therefore, as the esters (**3.138** and **3.139**) and acids (**3.140** and **3.141**) have good levels of biochemical potency, as well as having membrane permeability, a lower rate of generation of the acid may be the limiting factor, affecting the whole blood potency.

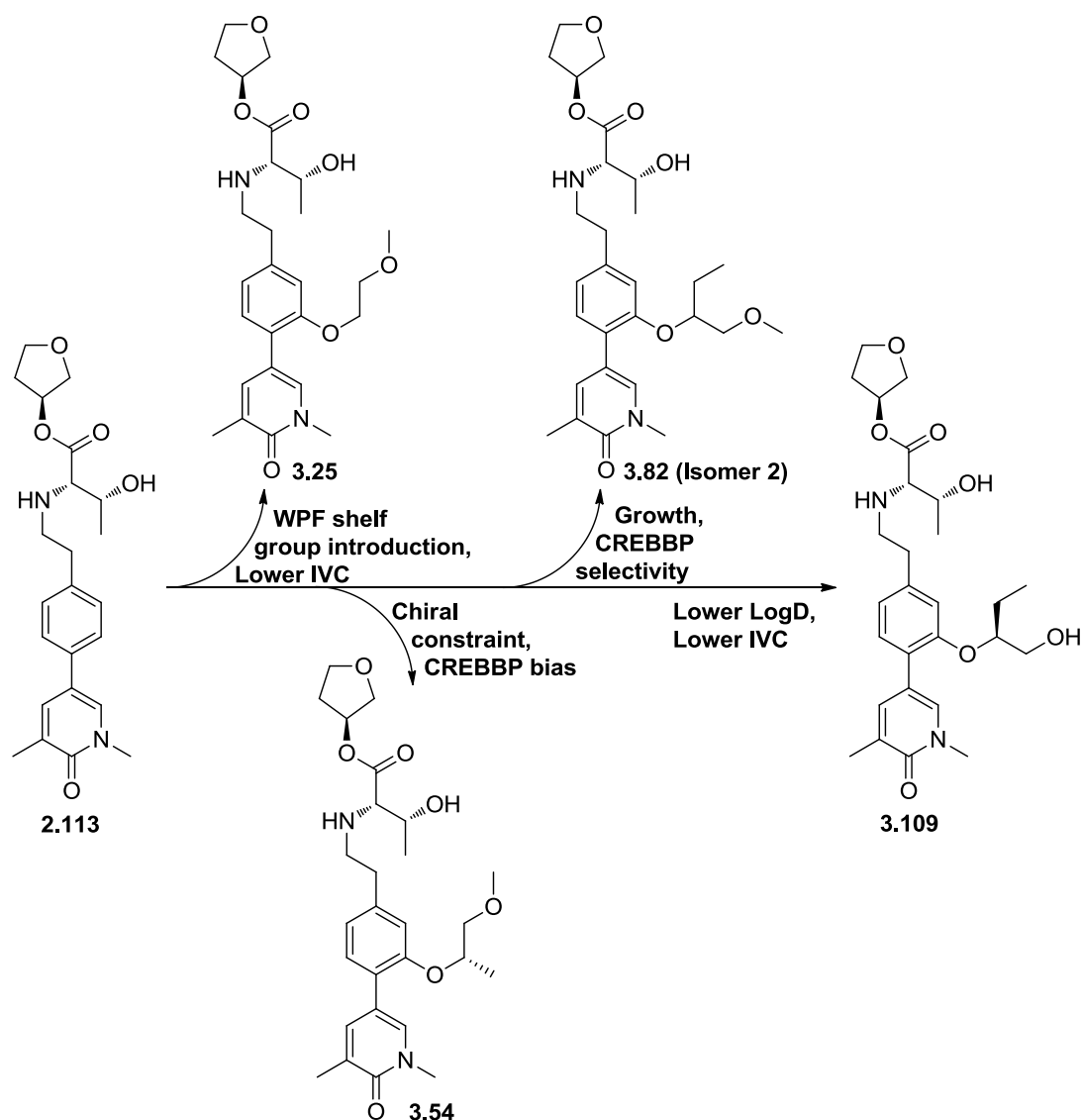


Scheme 3.52: Esterase-mediated hydrolysis of esters 3.138 and 3.139

Overall, the hypothesis of revealing the hydroxyl functionality had the desired effect of reducing the ChromLogD_{7.4} of the template, by up to a log unit. The effect of this lower LogD_{7.4} was observed with a reduction in the IVC, bringing these compounds back within the TPP.

3.4 Summary

Excellent progress has been made, improving the potency and selectivity, and reducing the *in vitro* clearance of this template, as set out at the fore. This was achieved through the inclusion and optimisation of an aliphatic group to interact with the WPF shelf region. Modern medicinal chemistry techniques, such as structure-based design, molecular modelling, physicochemical property profiling and external affinity profiling, were used to guide these steps. Significant progress was made in relation to understanding the template and the structural features required to introduce potency and selectivity. This knowledge was gained and used during the iterative steps in the optimisation of the initial lead compound **2.113** towards compound **3.109**, highlighted in Scheme 3.53.



Scheme 3.53: Key advancements made in this body of work

The key areas of optimisation at the onset of this work were to introduce additional potency and selectivity, over the non-BET bromodomains, relative to compound **2.113**. Taking learnings from the literature, it appeared that occupying the WPF shelf region could be important in both these factors.

The first advancement was the introduction of the methoxyethyl group to form **3.25**. Unfortunately, minimal potency gains were observed at Brd4 BD1 for compound **3.25**, compared to compound **2.113**. Additionally, this compound was also equipotent against CREBBP, a non-BET bromodomain with a structurally similar binding pocket. However, compound **3.25** including the THF ester was within the right physicochemical space for the TPP, coupled with an excellent whole blood

potency. The hCE-1 activity had also been reduced to a more reasonable level. Consequently, the *in vitro* clearance reflected this reduced hCE-1 activity, with moderate values generated, predicting an acceptable level of liver metabolism. Additionally, as a developability assay, the *in vitro* stability of compounds were tested within blood or plasma from different species. Compound **3.25** was found to be one of the first to have a half life of more than 240 minutes in cynomolgus monkey plasma. This reconfirmed this species for potential future *in vivo* pharmacokinetic (PK) studies. Due to the excellent properties of compound **3.25**, particularly the blood stability and IVC results, the compound was utilised as an *in vivo* tool molecule and progressed into a transgenic mouse *in vivo* PK study. The results showed a good PK profile, demonstrating reasonable stability and excellent maximum concentration of the ester.

As the crystal structure of **3.25** showed little interaction of the methoxyethyl with the WPF shelf within Brd4 BD1, compound **3.54** was designed to alter the conformation of the WPF shelf group and hence introduce selectivity over the CREBBP bromodomain. Pleasingly, compound **3.54** was able to demonstrate selectivity could be achieved within this series. Its small side chain was similar to the larger dimethoxypropyl compound **3.60** (Figure 3.46), although, the α -methyl compound was able to achieve similar levels of selectivity from a smaller group. Further optimisation of this WPF shelf group was undertaken altering the size and positioning of substitution. In this regard, growing from α -methyl to α -ethyl improved both potency and selectivity, although in detriment to the ChromLogD_{7.4}. The α -ethyl alcohol side chain present within **3.109** was found to have an excellent balance of selectivity over CREBBP while maintaining the ChromLogD_{7.4}, found to be important in minimising the *in vitro* clearance.

During this body of work, CREBBP has been a challenging bromodomain to achieve selectivity over. To gain some understanding of the broader selectivity profile, the lead compound **3.109** and the corresponding acid **3.120** were tested against a wide range of bromodomains offered externally by DiscoverRx within their BROMOscan™ assays (Figure 3.57). Both compounds, as expected, had similar affinities for all of the BET family of bromodomains due to the high sequence homology. Also, as observed within our laboratory, the lowest selectivity was against the CREBBP bromodomain, 10-fold and 20-fold for **3.109** and **3.120**, respectively. EP300, closely related to CREBBP, also shows less than 30-fold selectivity for compound **3.109**.

Selectivities against all the other bromodomains tested were more than 30-fold versus Brd4 BD1, as defined within the TPP.

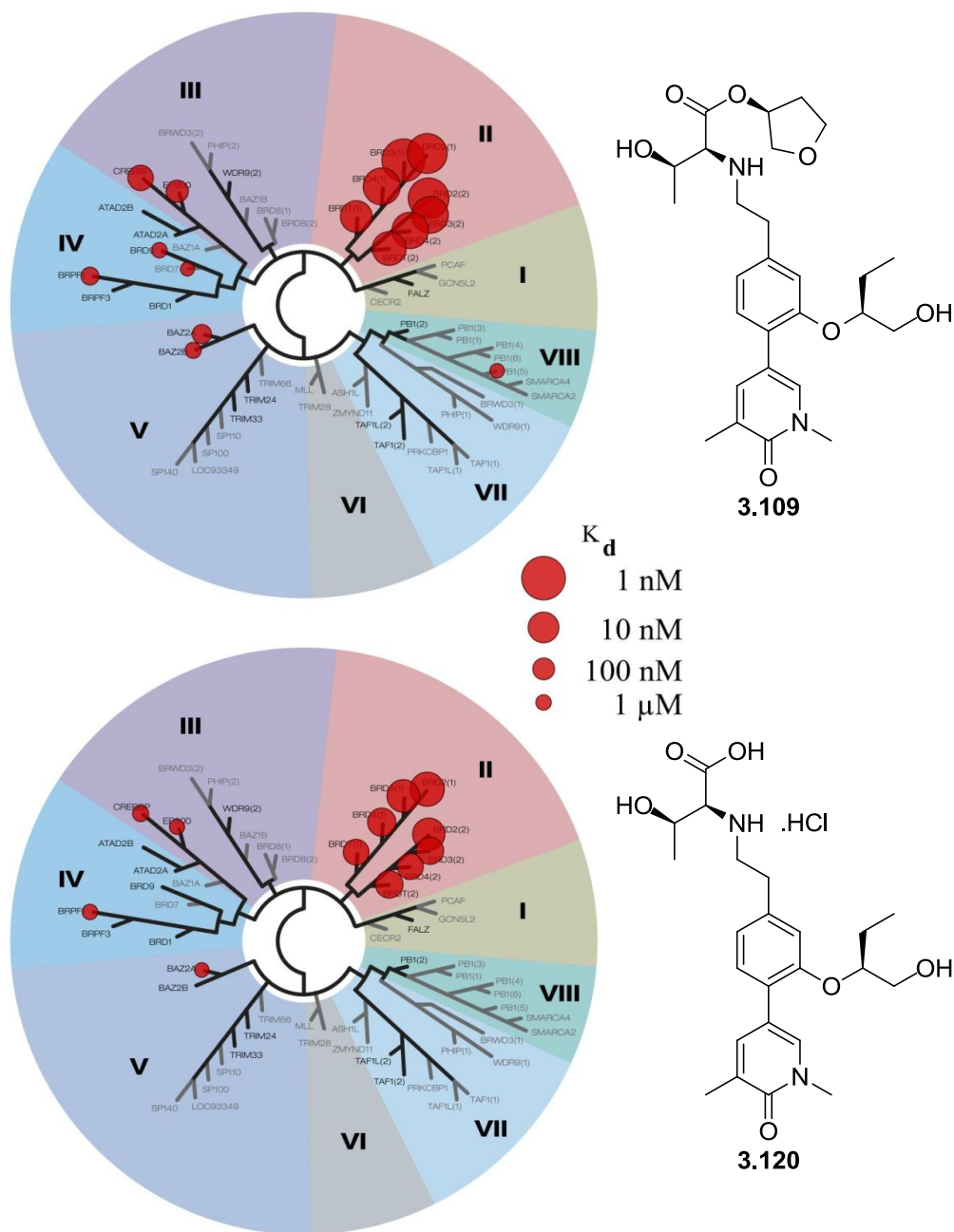


Figure 3.57: BROMOscan results for 3.109 and its acid 3.120²⁷⁴

Another important part of the TPP was the physicochemical properties (Figure 3.58, Table 3.19). Throughout the work within this thesis, the $\text{LogD}_{7.4}$ of the synthesised molecules has been closely monitored. In this regard, compound **3.109** had an excellent $\text{ChromLogD}_{7.4}$ of 3.0. Including the aromatic rings, the PFI can be examined. Actively maintaining the aromatic ring count to two, throughout this work,

has ensured the PFI has stayed within the TPP. As such, the low $\text{LogD}_{7.4}$ and high levels of sp^3 character, translated into good levels of solubility within the CLND solubility assay.

During the optimisation process, the correlation between $\text{LogD}_{7.4}$ and IVC was observed. This helped to guide the synthesis of compound **3.109** of low lipophilicity and subsequent low values within the IVC assay. Including the esterase inhibitor, benzil, the IVC for **3.109**, is excellent, and within the TPP, although the higher levels observed without benzil could be attributed to a high esterase hydrolysis rate. Pleasingly, compound **3.109** was also observed to be stable within the cyno plasma stability assay, even when this was prolonged to more than 12 hours.

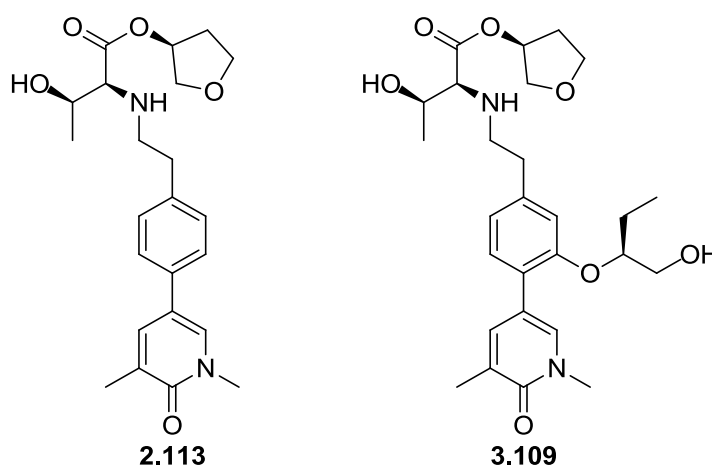


Figure 3.58: Lead compounds at the start (2.113) and end (3.109) of this optimisation

	TPP	Compound 2.113	Compound 3.109
Brd4 BD1 pIC₅₀		5.6	6.9
Acid Brd4 BD1 pIC₅₀		5.0	6.4
hWB_{BSci} (MCP-1) pIC₅₀	≥7.0	7.1	8.0
ΔpIC₅₀	≥1.0	1.5	1.1
Non-BET Selectivity	(≥30)	0	≥ x25
hCE-1 SA (μM/min/μM)	<1	13	-
ChromLogD_{7.4}	≤4.0	2.6	3.0
PFI	≤6.0	4.6	5.0
HLM IVC (-/+ benzil) (mL / min / g tissue)	<5 (- benzil) / <1.5 (+ benzil)	- / -	5.7 / 1.4
Solubility (μg/mL)	>100	154	182
Cyno Plasma Stability t_{1/2} (min)	>240	-	>745

Table 3.19: Comparison of 2.113 and 3.109

In direct comparison with the TPP, compound **3.109** was much improved compared to the lead compound **2.113** developed and applied at the start of this optimisation. This novel series demonstrated excellent potential for further development within our laboratories.

4 Conclusions and Further Work

Having taken a ligand efficient starting fragment, this thesis had demonstrated and explored how to optimise and grow the fragment into fully-elaborated ESM-functionalised BET inhibitors with excellent biological and physicochemical properties. Throughout this process, a number of modern synthetic and medicinal chemistry techniques have been used.

Initially, work focused on further improving the potency of the fragment without loss of ligand efficiency. Unfortunately, the electronics of the phenyl ring were found to not to beneficially affect binding. Pleasingly, however, the pyridyl replacements **2.30** and **2.31** maintained ligand efficiency while decreasing the lipophilicity (Figure 4.1).

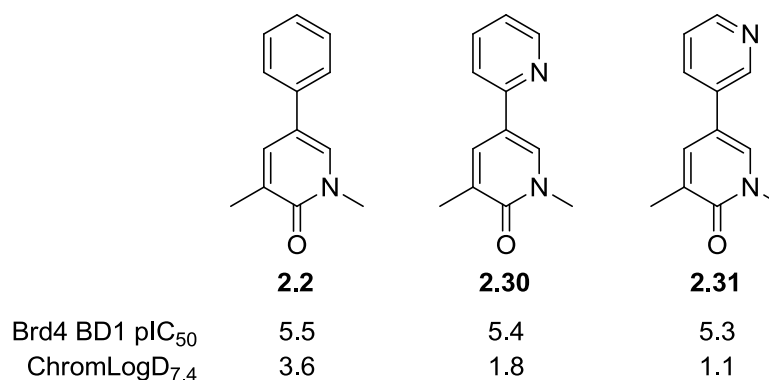


Figure 4.1: Successful fragment optimisation

On incorporation of the ESM to **2.2**, **2.30** and **2.31**, the enhancement of potency from the biochemical to whole blood assay (Δ pIC₅₀) was immediately observed utilising the threonine-based ESM (Figure 4.2). The mechanism, at work, was proven through the testing of **2.58e** within the macrophage cell retention assay, where the acid was observed at quantities 10-fold higher than the ester intracellularly. The resulting high acid concentrations within these target cells prompted investigations into increasing the acid biochemical potency. Pleasingly, homologation of the ESM, based on hypotheses generated by structure-based design techniques, to move it away from the lipophilic BET protein, generated compound **2.85e**, which improved the acid potency while maintaining the ester potency. This concurrent increase in acid biochemical potency and Δ pIC₅₀ showed for the first time the key role of the acid in increasing the “ESM effect”. In addition, it was also demonstrated for the first time how increased hydrolysis rates and therefore acid production also contributes to higher Δ pIC₅₀ values. In addition, it was demonstrated that the THF ester of threonine could be successfully incorporated (**2.113**) to reduce the lipophilicity of the template without detriment to the biochemical or whole blood potencies.

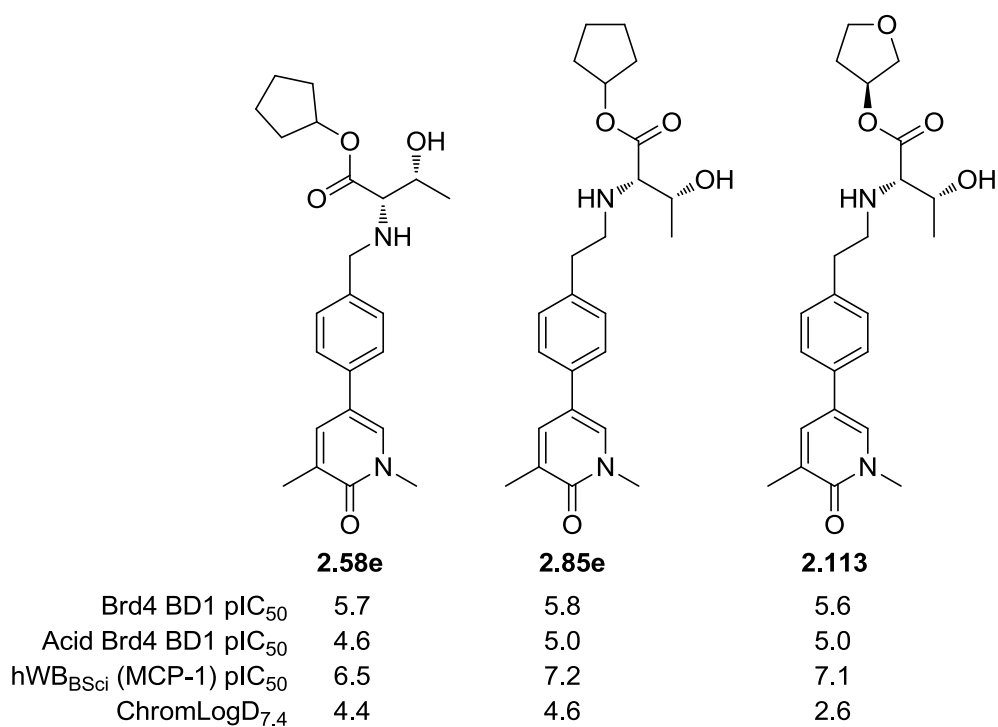
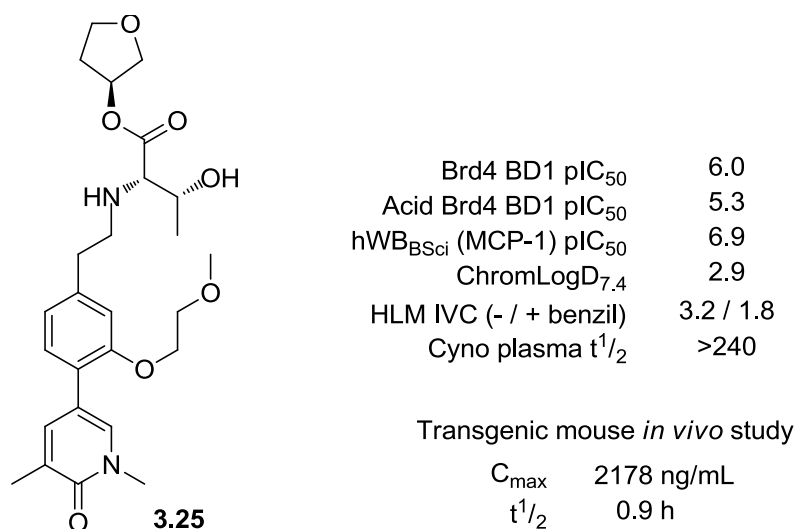
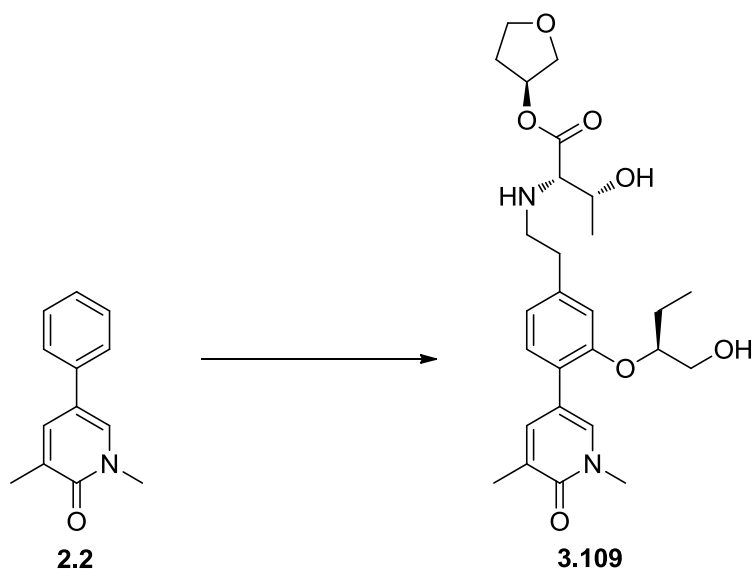


Figure 4.2: ESM incorporation and optimisation

The latter section of this thesis described the optimisation of potency, selectivity and *in vitro* clearance. Addition of the methoxyethyl group to give **3.25** (Figure 4.3) was hypothesised to increase potency and selectivity, although only modest improvements were made. Further profiling of fully elaborated example **3.25** demonstrated the physicochemical properties and corresponding IVC were excellent. Therefore, the compound was investigated for *in vitro* blood stability. Pleasingly, this compound was the first to demonstrate stability within cyno blood plasma, important for future pre-clinical experiments for the project. Due to the excellent results, **3.25** was progressed into the transgenic mouse pharmacokinetic study, in which the compound had a suitable profile and could be used as a standard for *in vitro* profiling for future compounds.

Figure 4.3: Fully elaborated compound, **3.25**

However, **3.25** was equipotent at the non-BET bromodomain CREBBP. Therefore, structure-based design and use of chiral constraint enabled stepwise optimisations to the saturated WPF shelf group. The synthesis and profiling of **3.109** confirmed the strategy of minimising aromatic ring count and using saturated systems to interact with the WPF shelf and gain potency and selectivity.



Scheme 4.1: Fragment growth and optimisation within this thesis

	2.2	3.109
Brd4 BD1 pIC₅₀	5.5	6.9
Acid Brd4 BD1 pIC₅₀	-	6.4
hWB_{BSci} (MCP-1) pIC₅₀	5.2	8.0
ΔpIC₅₀	-0.3	1.1
Non-BET Selectivity	0	≥ x25
ChromLogD_{7.4} / PFI	3.6 / 5.6	3.0 / 5.0
HLM IVC (-/+ benzil)	-	5.7 / 1.4
Solubility (µg / mL)	59	182
AMP (nm / s)	890	120
MWt	199	503
HSA (%)	82	44

Table 4.1: Comparison of the properties of 2.2 and 3.109

Overall, the biochemical potency of initial fragment **2.2** was improved throughout this body of work. However, due to the “ESM effect”, the human whole blood potency was extensively optimised by 630-fold to exquisitely potent compound **3.109**. Additionally, the selectivity over selected members of non-BET bromodomain families was at least 25-fold. In terms of physicochemical properties, the ChromLogD_{7.4} of **3.109** was improved compared to fragment **2.2** and inclusion of only two aromatic rings, therefore, maintained an excellent PFI. These excellent properties combined to provide a highly acceptable outcome within the IVC assay, with the esterase-mediated metabolism only marginally over the TPP.

Pleasingly, due to the well-rounded profile of **3.109**, the novel series developed within this body of work was transitioned into lead optimisation by a group of chemists within our laboratory due to the excellent properties shown by the final compound **3.109**. Therefore, work will continue on this template, within our laboratory, to further increase the selectivity and further narrow the potency gap between the ester and the acid. These further optimisations aim towards a candidate molecule to safely treat immune-mediated diseases such as RA.

Importantly, this work has demonstrated, throughout this thesis, the non-essential nature of aromatic groups to introduce selectivity for BET over the non-BET bromodomains. Rational design, aided by X-ray crystallography and computational modelling, guided the optimisation to improved selectivities.

Future Work

To progress these compounds within lead optimisation, it would be beneficial to further investigate the structure around the WPF shelf group. Considering the ethyl interacts with the WPF shelf region, further larger examples may further improve the biochemical profile while increasing steric bulk to reduce the hydrolysis rate (Figure 4.4).

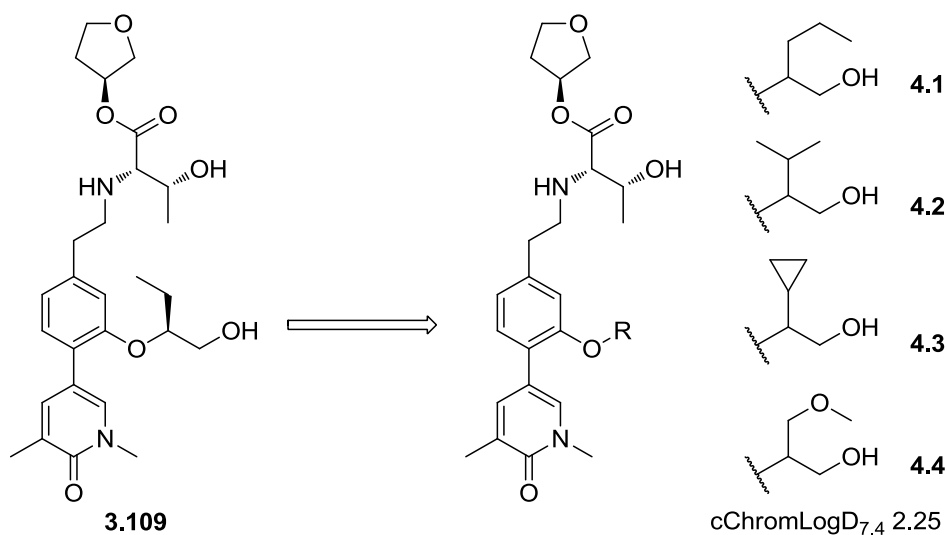


Figure 4.4: Potential examples of future groups for the WPF shelf

Out with the scope of this work, recent literature has suggested aryl rings placed optimally on the WPF shelf can give an improved selectivity profile. Specifically, scientists at Abbott Laboratories demonstrated exemplar compound **4.5** as a nanomolar inhibitor of Brd4 BD1 (Figure 4.5).²⁹⁰ Additionally, scientists at Quantical Pharmaceuticals synthesised the corresponding pyridone example **4.6** (Figure 4.5).²⁹¹ This example had an IC₅₀ of less than 0.5 μM at Brd4 with additional evidence of cellular activity of less than 0.5 μM.

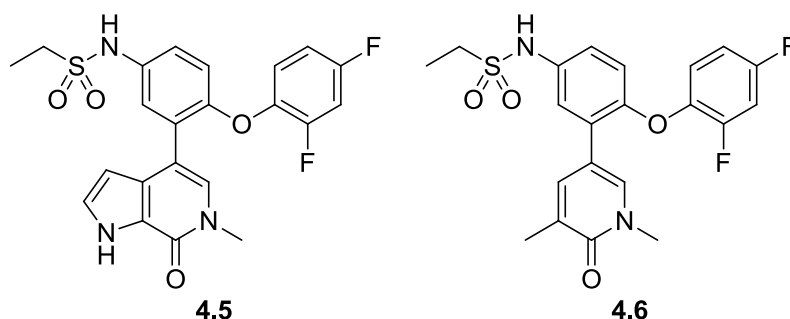


Figure 4.5: Aryl ether shelf group from Abbott and Quantical

Therefore, this strategy could be used with ESM-functionalised BET inhibitors (Figure 4.6). While this would likely increase the $\text{LogD}_{7.4}$ and PFI, the benefits for potency and selectivity may be worth investigating.

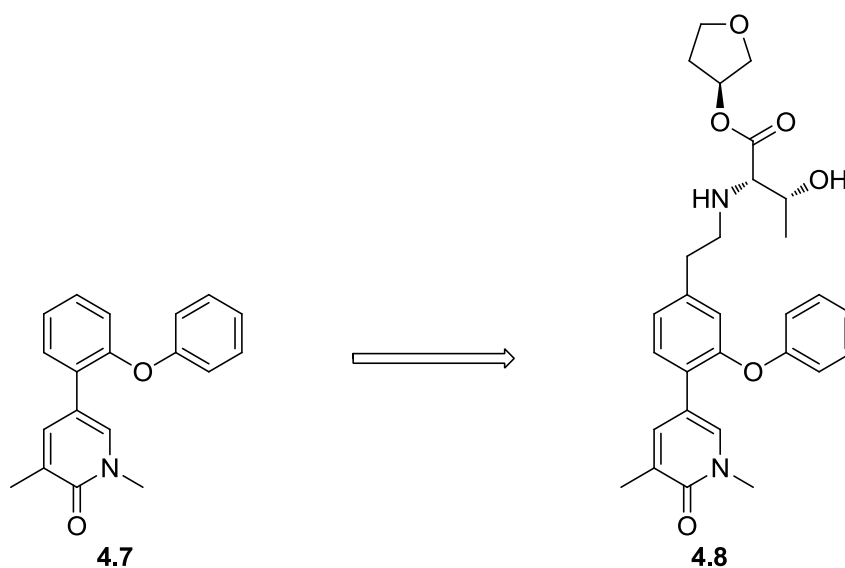


Figure 4.6: Aryl ethers combined with the ESM

5 Experimental

5.1 General Experimental Details

The names of the compounds cited herein have been obtained using ChemDraw Ultra 12.0.

LCMS Methodology

Method using formic acid modifier – “LCMS (formic acid)”

LC conditions:

The UPLC analysis was conducted on an Acquity UPLC BEH C₁₈ column (50 mm x 2.1 mm, i.d. 1.7 µm packing diameter) at 40 °C. The solvents employed were: A = 0.1% v/v solution of formic acid in water; B = 0.1% v/v solution of formic acid in acetonitrile. The gradient (A:B) employed was from 97:3 to 3:97 over 2 min. The UV detection was a summed signal from wavelength of 210 nm to 350 nm.

MS conditions:

The mass spectrometry was conducted on a Waters ZQ mass spectrometer, with an ionisation mode of alternate-scan positive and negative electrospray. The scan range was 100 to 1000 AMU, the scan time was 0.27 sec and the inter-scan delay was 0.10 sec.

Method using ammonium bicarbonate modifier – “LCMS (high pH)”

LC conditions:

The UPLC analysis was conducted on an Acquity UPLC BEH C₁₈ column (50 mm x 2.1 mm, i.d. 1.7 µm packing diameter) at 40 °C. The solvents employed were: A = ammonium hydrogen carbonate in water adjusted to pH 10 with ammonia solution; B = acetonitrile. The gradient (A:B) employed was from 99:1 to 0:100 over 2 min. The UV detection was a summed signal from wavelength of 210 nm to 350 nm.

MS conditions:

The mass spectrometry was conducted on a Waters ZQ mass spectrometer, with an ionisation mode of alternate-scan positive and negative electrospray. The scan range was 100 to 1000 AMU, the scan time was 0.27 sec and the inter-scan delay was 0.10 sec.

High Resolution Mass Spectrometry

Chromatography and analysis conditions:

An Agilent 1100 Liquid Chromatograph equipped with a model G1367A autosampler, a model G1312A binary pump and a HP1100 model G1315B diode array detector was used. The method used was generic for all experiments. All separations were achieved using a C₁₈ reversed phase column (100 x 2.1 mm, 3 µm particle size) or equivalent. Gradient elution was carried out with the mobile phases as (A) water containing 0.1% (v/v) TFA and (B) acetonitrile containing 0.1% (v/v) TFA. The conditions for the gradient elution were initially 0% B, increasing linearly to 95% B over 8 min, remaining at 95% B for 0.5 min, then decreasing linearly to 0% B over 0.1 min, followed by an equilibration period of 1.49 min prior to the next injection. The flow rate was 1 mL/min, split to source and the temperature controlled at 40 °C with an injection volume of between 2 to 5 µL.

Mass Spectrometry conditions:

Positive ion mass spectra were acquired using a Thermo LTQ–Orbitrap FT mass spectrometer, equipped with a ESI interface, over a mass range of 100 – 1100 Da, with a scan time of 1 sec. The elemental composition was calculated using Xcalibur software and processed using RemoteAnalyzer (Spectral Works Ltd) for the [M+H]⁺ and the mass error quoted as ppm.

MDAP Methodology

Method using formic acid modifier – “MDAP (formic acid)”

LC conditions:

The HPLC analysis was conducted on either a Sunfire C₁₈ column (100 mm x 19 mm, i.d 5 µm packing diameter) or a Sunfire C₁₈ column (150 mm x 30 mm, i.d. 5 µm packing diameter) at ambient temperature. The solvents employed were: A =

0.1% v/v solution of formic acid in water; B = 0.1% v/v solution of formic acid in acetonitrile. The purification was run as a gradient (A:B) over either 15 min or 25 min, with a flow rate of 20 mL/min (100 mm x 19 mm, i.d 5 µm packing diameter) or 40 mL/min (150 mm x 30 mm, i.d. 5 µm packing diameter). The UV detection was a summed signal from wavelength of 210 nm to 350 nm.

MS conditions:

The mass spectrometry was conducted on a Waters ZQ mass spectrometer, with an ionisation mode of alternate-scan positive and negative electrospray. The scan range was 100 to 1000 AMU, the scan time was 0.50 secs and the inter-scan delay was 0.20 sec.

Method using ammonium bicarbonate modifier – “MDAP (high pH)”

LC conditions:

The HPLC analysis was conducted on either an Xbridge C₁₈ column (100 mm x 19 mm, i.d 5 µm packing diameter) or an Xbridge C₁₈ column (100 mm x 30 mm, i.d. 5 µm packing diameter) at ambient temperature. The solvents employed were: A = 10 mM ammonium bicarbonate in water, adjusted to pH 10 with ammonia solution; B = acetonitrile. The purification was run as a gradient (A:B) over either 15 min or 25 min, with a flow rate of 20 ml/min (100 mm x 19 mm, i.d 5 µm packing diameter) or 40 mL/min (150 mm x 30 mm, i.d. 5 µm packing diameter). The UV detection was a summed signal from wavelength of 210 nm to 350 nm.

MS conditions:

The mass spectrometry was conducted on a Waters ZQ mass spectrometer, with an ionisation mode of alternate-scan positive and negative electrospray. The scan range was 100 to 1000 AMU, the scan time was 0.50 sec and the inter-scan delay was 0.20 sec.

NMR Spectroscopy

Unless otherwise specified, ^1H and ^{13}C NMR spectra were recorded using a Bruker DPX400 spectrometer at 400 MHz and 101 MHz, respectively, or using a Bruker Avance 500 spectrometer at 500 MHz and 126 MHz, respectively. Chemical shifts are given in ppm (δ) relative to tetramethylsilane (TMS) as an internal standard. Chemical shifts are given to the nearest 0.01 ppm (^1H NMR) or 0.1 ppm (^{13}C NMR) and coupling constants are given to the nearest 0.1 Hz. NMR spectra are recorded at room temperature unless otherwise stated.

Infrared Spectroscopy

Infra-red (IR) spectra were recorded using a Perkin Elmer Spectrum One FT-IR spectrometer, and key well-defined peaks were recorded in cm^{-1} .

Optical Rotation

Optical rotation measurements were recorded using a Jasco P-1030 polarimeter. The concentration was recorded in g/ml, path length in mm, and temperature in $^{\circ}\text{C}$.

Melting Point

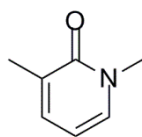
Melting point measurements were recorded using a Stuart SMP10 melting point apparatus.

Compound Purity

The purity of compounds tested in *in vitro* and *in vivo* assays was greater than 95% using interpretation of a combination of LCMS and ^1H NMR data, unless stated otherwise.

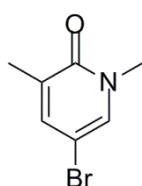
5.2 Experimental

1,3-Dimethylpyridin-2(1H)-one, 2.24²⁹²



A round bottom flask was charged with 3-methylpyridin-2(1H)-one (5 g, 45.8 mmol), acetone (50 mL), potassium carbonate (12.7 g, 92 mmol) and methyl iodide (10 mL, 160 mmol). A condenser was fitted and the mixture warmed to 35 °C under a blanket of nitrogen overnight. LCMS analysis showed conversion to the desired product. The insolubles were removed by filtration and the solids washed with acetone (20 mL) before the filtrate was concentrated *in vacuo* to give 1,3-dimethylpyridin-2(1H)-one (6.12 g, crude material used in next reaction) as a waxy pale yellow solid. LCMS (formic acid): *rt* = 0.45, *MH*⁺ 123.9. ¹H NMR δ (400 MHz, CD₃OD) ppm: 7.50 (1H, dd, *J*=6.8, 1.2 Hz), 7.38-7.42 (1H, m), 6.30 (1H, t, *J*=6.8 Hz), 3.58 (3H, s), 2.13 (3H, s).

5-Bromo-1,3-dimethylpyridin-2(1H)-one, 2.23²⁹²



A round bottom flask was charged with 1,3-dimethylpyridin-2(1H)-one (5.9 g), tetrahydrofuran (90 mL) and cooled to 0 °C. NBS (8.95 g, 50.3 mmol) was added portionwise over 20 min, before the reaction mixture was allowed to warm to RT. The slurry was stirred at room temperature for 16 h. The reaction was cooled to 0 °C and quenched through slow addition of 10% sodium thiosulfate solution (50 mL). The mixture was diluted with ethyl acetate and partitioned with saturated aqueous sodium bicarbonate. The layers were mixed and separated before the organics were washed with brine, passed through a hydrophobic frit and concentrated *in vacuo* to give a pink solid. The sample was dissolved in DCM and loaded onto three 100 g SNAP silica columns. The crude material on silica was purified in 3 portions by Biotage SP4 using a gradient of 0-40% ethyl acetate in cyclohexane over 15 CV. The appropriate fractions were combined and evaporated *in vacuo* to give the required product 5-bromo-1,3-dimethylpyridin-2(1H)-one (6.15 g, 30.4 mmol, 66% yield (over 2 steps)) as a white solid. *R_f* = 0.21, 50% ethyl acetate in cyclohexane. LCMS (formic acid): *rt* = 0.66 min, *MH*⁺ 202.0, 204.0. ¹H NMR δ (400 MHz, CDCl₃) ppm: 7.31-7.28 (1H, m), 7.26-7.24 (1H, m), 3.53 (3H, s), 2.15 (3H, s). ¹³C NMR δ (CDCl₃): 160.2 (C=O), 139.5 (C-H), 135.3 (C-H), 131.4 (C-C), 97.3 (C-Br), 37.8 (N-CH₃), 18.2 (C-CH₃). IR (neat): 3065, 1649, 1590, 1421. Melting Point: 105-108 °C.

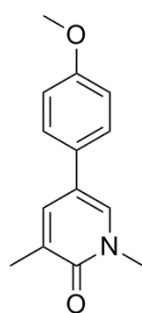
HRMS (ESI) exact mass calculated for C₇H₉⁷⁹BrNO [M+H]⁺ m/z 201.9862, found m/z 201.9860.

General procedure for dimethylpyridinone Suzuki cross coupling with boronic acids

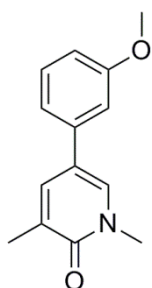
To a solution of 5-bromo-1,3-dimethylpyridin-2(1H)-one (a) (1 equivalent) and boronic acid (b) (1.5 equivalents) in 1,4-dioxane (c) and water (d) stirred under nitrogen at RT was added palladium tetrakis triphenylphosphene (e) (0.03 equivalents) and 1 M aqueous potassium carbonate (f). The reaction mixture was stirred at 95 °C for 3 hours. The desired mass ion was observed by LCMS. After cooling to room temperature, the reaction mixture was diluted with water (10 mL) and extracted with ethyl acetate (2 x 10 mL). The organics were combined and the solvent removed under reduced pressure. The resulting gum was dissolved in DMSO (2 mL) and purified by open access mass directed autoprep on Sunfire C18 column using gradient (g) acetonitrile water with a formic acid modifier. The solvent was evaporated *in vacuo* to give the required product (h).

Table 2.2, Page 76

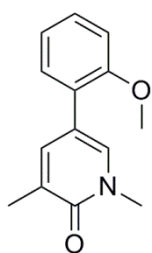
5-(4-Methoxyphenyl)-1,3-dimethylpyridin-2(1H)-one, 2.15



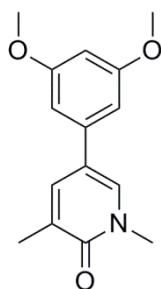
(a) 75 mg, 0.37 mmol, (b) ((4-methoxyphenyl)boronic acid, 85 mg, 0.56 mmol, (c) 3 mL, (d) 0.12 mL, (e) 123 mg, 0.01 mmol, (f) 1.1 mL, 1.1 mmol, (g) 15-55%, (h) 5-(4-methoxyphenyl)-1,3-dimethylpyridin-2(1H)-one (62 mg, 0.27 mmol, 73% yield) as a white solid. LCMS (formic acid): rt = 0.83 min, MH⁺ 230.1. ¹H NMR δ(400 MHz, CDCl₃) ppm: 7.48 - 7.45 (1H, m), 7.35 - 7.29 (3H, m), 6.96 - 6.91 (2H, m), 3.84 (3H, s), 3.62 (3H, s), 2.22 (3H, s).

5-(3-Methoxyphenyl)-1,3-dimethylpyridin-2(1H)-one, 2.14

(a) 100 mg, 0.50 mmol, (b) (3-methoxyphenyl)boronic acid, 113 mg, 0.74 mmol, (c) 4 mL, (d) 0.16 mL, (e) 17 mg, 0.015 mmol, (f) 1.5 mL, 1.5 mmol, (g) 15-55%, (h) 5-(3-methoxyphenyl)-1,3-dimethylpyridin-2(1H)-one (98 mg, 0.39 mmol, 78% yield) as a clear gum, which crystallised to give a white solid on standing. LCMS (formic acid): $t_r = 0.85$ min ($MH^+ = 230.2$). 1H NMR δ (400 MHz, $CDCl_3$) ppm 7.54-7.50 (1H, m) 7.40 (1H, d, $J=2.3$ Hz) 7.34 (1H, t, $J=8.0$ Hz) 7.03-6.99 (1H, m) 6.95 (1H, t, $J=2.0$ Hz) 6.90-6.85 (1H, m) 3.88 (3H, s) 3.65 (3H, s) 2.25 (3H, s). ^{13}C NMR δ (101 MHz, $CDCl_3$) ppm: 162.8 (C=O), 160.1 (C-O), 138.4 (C-C), 136.6 (CH), 133.1 (CH), 130.0 (CH), 129.6 (C-C), 119.5 (C-C), 118.3 (CH), 112.3 (CH), 111.8 (CH), 55.3 (O-CH₃), 38.0 (N-CH₃), 17.4 (C-CH₃). IR (neat): 1651, 1592, 1227. Melting point: 108-113 °C. HRMS (ESI) exact mass calculated for $C_{14}H_{16}NO_2$ $[M+H]^+$ m/z 230.1176, found m/z 230.1171.

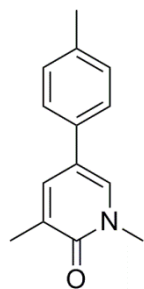
5-(2-Methoxyphenyl)-1,3-dimethylpyridin-2(1H)-one, 2.13

(a) 75 mg, 0.37 mmol, (b) ((2-methoxyphenyl)boronic acid, 85 mg, 0.56 mmol, (c) 3 mL, (d) 0.12 mL, (e) 13 mg, 0.01 mmol, (f) 1.1 mL, 1.1 mmol, (g) 15-55%, (h) 5-(2-methoxyphenyl)-1,3-dimethylpyridin-2(1H)-one (57 mg, 0.25 mmol, 67% yield) as a white solid. LCMS (formic acid): $t_r = 0.85$ min, $MH^+ 230.1$. 1H NMR δ (400 MHz, $CDCl_3$) ppm: 7.46 - 7.43 (1H, m), 7.37 (1H, d, $J=2.3$ Hz), 7.32-7.27 (1H, m), 7.22 (1H, dd, $J=7.6, 1.8$ Hz), 7.00 (1H, dt, $J=7.6, 1.0$ Hz), 6.97-6.94 (1H, m), 3.84 (3H, s), 3.60 (3H, s), 2.20 (3H, s).

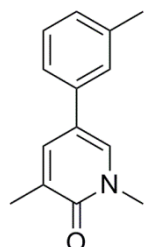
5-(3,5-Dimethoxyphenyl)-1,3-dimethylpyridin-2(1H)-one, 2.27

(a) 75 mg, 0.37 mmol, (b) 3,5-dimethoxyphenyl)boronic acid (101 mg, 0.56 mmol), (c) 3 mL, (d) 0.12 mL, (e) 13 mg, 0.01 mmol, (f) 1.1 mL, 1.1 mmol, (g) 15-55%, (h) 5-(3,5-dimethoxyphenyl)-1,3-dimethylpyridin-2(1H)-one (64 mg, 0.25 mmol, 67% yield) as an off-white solid. LCMS (formic acid): $t_r = 0.87$ min, $MH^+ 260.2$. 1H NMR δ (400 MHz, $CDCl_3$) ppm: 7.49 - 7.47 (1H, m), 7.39 - 7.36 (1H, m), 6.53 (2H, d, $J=2.0$ Hz), 6.42 (1H, t, $J=2.0$ Hz), 3.83 (6H, s), 3.62 (3H, s), 2.22 (3H, s).

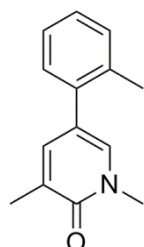
Table 2.3, Page 76

1,3-Dimethyl-5-(*p*-tolyl)pyridin-2(1H)-one, 2.18

(a) 75 mg, 0.37 mmol, (b) *p*-tolylboronic acid (76 mg, 0.56 mmol), (c) 3 mL, (d) 0.12 mL, (e) 13 mg, 0.01 mmol, (f) 1.1 mL, 1.1 mmol, (g) 30-85%, (h) 1,3-dimethyl-5-(*p*-tolyl)pyridin-2(1H)-one (61 mg, 0.27 mmol, 73% yield) as a white solid. LCMS (formic acid): *rt* = 0.94 min, *MH*⁺ = 214.1. ¹H NMR δ (400 MHz, CDCl₃) ppm: 7.48 - 7.48 (1H, m), 7.35 (1H, d, *J*=2.4 Hz), 7.32 - 7.27 (2H, m), 7.23 - 7.19 (2H, m), 3.62 (3H, s), 2.37 (3H, s), 2.22 (3H, s).

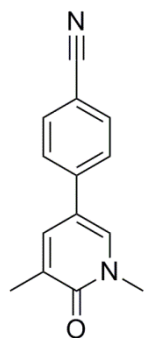
1,3-Dimethyl-5-(*m*-tolyl)pyridin-2(1H)-one, 2.17

(a) 75 mg, 0.37 mmol, (b) *m*-tolylboronic acid (76 mg, 0.56 mmol), (c) 3 mL, (d) 0.12 mL, (e) 13 mg, 0.01 mmol, (f) 1.1 mL, 1.1 mmol, (g) 30-85%, (h) 1,3-dimethyl-5-(*m*-tolyl)pyridin-2(1H)-one (69 mg, 0.30 mmol, 80% yield) as a white solid. LCMS (formic acid): *rt* = 0.94 min, *MH*⁺ = 214.1. ¹H NMR δ (400 MHz, CDCl₃) ppm: 7.52 - 7.50 (1H, m), 7.37 (1H, d, *J*=2.4 Hz), 7.29 (1H, t, *J*=7.6 Hz), 7.24 - 7.18 (2H, m), 7.13 (1H, d, *J*=7.6 Hz), 3.63 (3H, s), 2.40 (3H, s), 2.23 (3H, s).

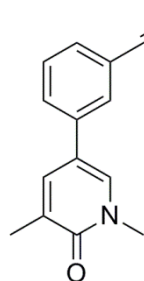
1,3-Dimethyl-5-(*o*-tolyl)pyridin-2(1H)-one, 2.16

(a) 75 mg, 0.37 mmol, (b) *o*-tolylboronic acid (76 mg, 0.557 mmol), (c) 3 mL, (d) 0.12 mL, (e) 13 mg, 0.01 mmol, (f) 1.1 mL, 1.1 mmol, (g) 30-85%, (h) 1,3-dimethyl-5-(*o*-tolyl)pyridin-2(1H)-one (61, mg, 0.26 mmol, 71% yield) as a white solid. LCMS (formic acid): *rt* = 0.91 min, *MH*⁺ = 214.1. ¹H NMR δ (400 MHz, CDCl₃) ppm: 7.18 - 7.26 (4H, m), 7.13 - 7.17 (1H, m), 7.11 (1H, d, *J*=2.2 Hz), 3.60 (3H, s), 2.29 (3H, s), 2.20 (3H, s).

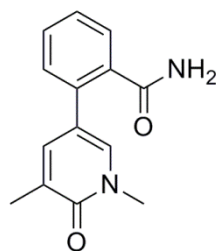
Table 2.4, Page 78

4-(1,5-Dimethyl-6-oxo-1,6-dihydropyridin-3-yl)benzonitrile, 2.21

(a) 75 mg, 0.37 mmol, (b) (4-cyanophenyl)boronic acid (82 mg, 0.56 mmol), (c) 3 mL, (d) 0.12 mL, (e) 13 mg, 0.01 mmol, (f) 1.1 mL, 1.1 mmol, (g) 15-55%, (h) 4-(1,5-dimethyl-6-oxo-1,6-dihydropyridin-3-yl)benzonitrile (34 mg, 0.15 mmol, 40% yield) as a white solid. LCMS (formic acid): rt = 0.77 min, MH⁺ 225.1. ¹H NMR δ(400 MHz, CDCl₃) ppm: 7.71 - 7.67 (2H, m), 7.54 - 7.48 (3H, m), 7.46 (1H, d, J=2.4 Hz), 3.65 (3H, s), 2.24 (3H, s).

3-(1,5-Dimethyl-6-oxo-1,6-dihydropyridin-3-yl)benzonitrile, 2.20

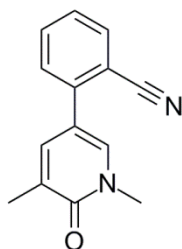
(a) 75 mg, 0.37 mmol, (b) (3-cyanophenyl)boronic acid (82 mg, 0.56 mmol), (c) 3 mL, (d) 0.12 mL, (e) 13 mg, 0.01 mmol, (f) 1.1 mL, 1.1 mmol, (g) 15-55%, (h) 3-(1,5-dimethyl-6-oxo-1,6-dihydropyridin-3-yl)benzonitrile (65 mg, 0.29 mmol, 77% yield) as a white solid. LCMS (formic acid): rt = 0.79 min, MH⁺ = 225.1. ¹H NMR δ(400 MHz, CDCl₃) ppm: 7.71 - 7.68 (1H, m), 7.66 - 7.62 (1H, m), 7.61 - 7.57 (1H, m), 7.52 (1H, t, J=7.8 Hz), 7.48 - 7.45 (1H, m), 7.41 (1H, d, J=2.7 Hz), 3.64 (3H, s), 2.24 (3H, s).

Unexpected formation of 2-(1,5-dimethyl-6-oxo-1,6-dihydropyridin-3-yl)benzamide 2.29

To a round bottomed flask was added 5-bromo-1,3-dimethylpyridin-2(1H)-one (75 mg, 0.37 mmol), (2-cyanophenyl)boronic acid (82 mg, 0.56 mmol), 1,4-dioxane (3 mL) and water (0.12 mL). The resulting mixture was stirred under nitrogen at RT. Palladium tetrakis triphenylphosphine (13 mg, 0.01 mmol) and 1 M aqueous potassium carbonate (1.11 mL, 1.11 mmol) were added and the reaction mixture was stirred at 95 °C for 3 h. After cooling to room temperature, the reaction mixture was diluted with water (10 mL) and extracted with ethyl acetate (2 x 10 mL). The organics were combined and the solvent removed under reduced pressure. The resulting crude material was dissolved in DMSO (2 mL) and purified in 2 batches by open access mass directed

autoprep on Sunfire C18 column using 5-30% acetonitrile water with a formic acid modifier. The solvent was evaporated *in vacuo* to give 2-(1,5-dimethyl-6-oxo-1,6-dihydropyridin-3-yl)benzamide with formic acid impurity. The crude product was dissolved in methanol and loaded onto an amino propyl ion exchange column. The product was eluted with methanol and the solvent removed under reduced pressure to yield 2-(1,5-dimethyl-6-oxo-1,6-dihydropyridin-3-yl)benzamide (14 mg, 0.06 mmol, 16% yield) as a white solid. LCMS (formic acid): *rt* = 0.54, MH^+ 243.1. 1H NMR δ (400 MHz, $CDCl_3$) ppm: 7.65 (1H, dd, $J=7.7, 1.1$ Hz), 7.4 (1H, dt, $J=7.6, 1.5$ Hz), 7.40 (1H, dt, $J=7.6, 1.2$ Hz), 7.35 - 7.31 (2H, m), 7.30 (1H, dd, $J=7.7, 0.9$ Hz), 5.73 (1H, br. s), 5.61 (1H, br. s), 3.59 (3H, s), 2.19 (3H, s).

2-(1,5-Dimethyl-6-oxo-1,6-dihydropyridin-3-yl)benzonitrile 2.19



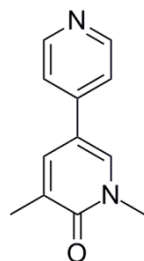
A round bottom flask was charged with 5-bromo-1,3-dimethylpyridin-2(1H)-one (100 mg, 0.50 mmol), (2-cyanophenyl)boronic acid (87 mg, 0.59 mmol), potassium carbonate (342 mg, 2.47 mmol), toluene (2.5 mL) and ethanol (2.5 mL). To the stirred mixture was added palladium tetrakis triphenylphosphine (29 mg, 0.025 mmol) and the system degassed with nitrogen. The vessel was heated to reflux at 90 °C for 3 hours under a blanket of nitrogen. LCMS analysis after this time showed the desired mass ion ($MH^+ = 225.1$) at *rt* = 0.76 min, whilst also indicating the formation of the undesired amide **91**. The mixture was cooled to room temperature. The reaction mixture was filtered through celite, before the volatiles were removed *in vacuo* to give an orange solid. The solid was dissolved in a 1:1 ethyl acetate/water mixture (20 mL). The layers were mixed and separated before the organics were washed with brine (10 mL), passed through a hydrophobic frit and concentrated *in vacuo* to give an orange oil. The sample were dissolved in DMSO (1 mL) and the solid filtered, washed with methanol and dried to yield 2-(1,5-dimethyl-6-oxo-1,6-dihydropyridin-3-yl)benzonitrile (7 mg). The remaining sample was purified by open access mass directed autoprep on Sunfire C18 column using 15-55% acetonitrile water with a formic acid modifier. The solvent was evaporated *in vacuo* to give the required product 2-(1,5-dimethyl-6-oxo-1,6-dihydropyridin-3-yl)benzonitrile (22 mg). The two pure samples were combined in an overall yield of 29 mg (0.13 mmol, 26% yield). LCMS (formic acid): *rt* = 0.76, MH^+ 225.1. 1H NMR δ (400 MHz, $CDCl_3$) ppm:

7.74 (1H, dd, $J=8.1, 1.2$ Hz), 7.62 (1H, dd, $J=7.7, 1.3$ Hz), 7.49 (1H, d, $J=2.7$ Hz), 7.45 - 7.39 (3H, m), 3.64 (3H, s), 2.23 (3H, s). IR (neat): 2220, 1660, 1612, 759.

General procedure for pyridyl Suzuki couplings

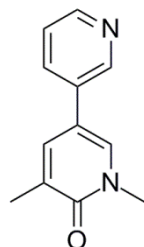
To a round bottom flask was added 5-bromo-1,3-dimethylpyridin-2(1H)-one (75 mg, 0.37 mmol), pyridyl/pyrimidyl boronic acid (a) in 1,4-dioxane (3 mL) and water (0.12 mL) stirred under nitrogen at RT was added palladium tetrakis triphenylphosphene (12.9 mg, 0.01 mmol) and 1 M aqueous potassium carbonate (1.1 mL, 1.1 mmol). The reaction mixture was stirred at 95 °C for 3 h. After cooling to room temperature, the reaction mixture was filtered through celite eluting with ethyl acetate. The resulting diluted with water (10 mL) and extracted with ethyl acetate (3 x 10 mL). The organics were combined, dried by passing through a hydrophobic frit and the solvent was removed under reduced pressure. The resulting light brown solid was dissolved in DMSO (2 mL) and purified by mass directed autoprep on Sunfire C18 column using gradient (b) acetonitrile water with a formic acid modifier. The solvent was evaporated *in vacuo* to give the required product (c).

1,5-Dimethyl-[3,4'-bipyridin]-6(1H)-one, 2.32

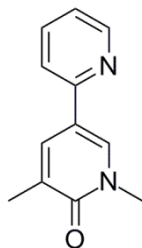


(a) pyridin-4-ylboronic acid (68 mg, 0.56 mmol), (b) 5-30%, (c) 1,5-dimethyl-[3,4'-bipyridin]-6(1H)-one (19 mg, 0.10 mmol, 26% yield) as a white solid. LCMS (formic acid): $rt = 0.35$, $MH^+ 201.1$. 1H NMR δ (400 MHz, $CDCl_3$) ppm: 8.65 - 8.59 (2H, m), 7.58 - 7.56 (1H, m), 7.56 - 7.54 (1H, m), 7.41 - 7.37 (2H, m), 3.66 (3H, s), 2.25 (3H, s).

1,5-Dimethyl-[3,3'-bipyridin]-6(1H)-one, 2.31



(a) Pyridin-3-ylboronic acid (68 mg, 0.56 mmol), (b) 5-30%, (c) 1,5-dimethyl-[3,3'-bipyridin]-6(1H)-one (43 mg, 0.22 mmol, 58% yield) as a white solid. LCMS (formic acid): $rt = 0.37$, $MH^+ 201.1$. 1H NMR δ (400 MHz, $CDCl_3$) ppm: 8.74 - 8.68 (1H, m), 8.60 - 8.54 (1H, m), 7.77 - 7.71 (1H, m), 7.51 - 7.46 (1H, m), 7.45 - 7.41 (1H, m), 7.40 - 7.33 (1H, m), 3.65 (3H, s), 2.25 (3H, s).

Attempted synthesis of 1',5'-Dimethyl-[2,3'-bipyridin]-6'(1'H)-one, 2.30

To a round bottom flask was added 5-bromo-1,3-dimethylpyridin-2(1H)-one (75 mg, 0.37 mmol), 4-methyl-2,6-dioxo-8-(pyridin-2-yl)hexahydro-[1,3,2]oxazaborolo[2,3-b][1,3,2]oxazaborol-4-ium-8-uide (130 mg, 0.56 mmol), 1,4-dioxane (3 mL) and water (0.12 mL). To the mixture, stirred under nitrogen at RT, was added tetrakis(triphenylphosphene)palladium(0) (12.9 mg, 0.01 mmol) and potassium carbonate (1.1 mL, 1.1 mmol). The reaction mixture was stirred at 95 °C for 3 h. No product was observed by LCMS analysis and therefore the reaction was abandoned.

Synthesis of 1',5'-dimethyl-[2,3'-bipyridin]-6'(1'H)-one, 2.30 (Table 2.8)**Conditions A**

To a carousel tube was added 5-bromo-1,3-dimethylpyridin-2(1H)-one (103 mg, 0.51 mmol), 2-(4,4,5,5-tetramethyl-1,3,2-dioxaborolan-2-yl)pyridine (209 mg, 1.02 mmol), copper(I) chloride (50.5 mg, 0.51 mmol), palladium(II) acetate (5.7 mg, 0.03 mmol), dicyclohexyl(2',6'-dimethoxy-[1,1'-biphenyl]-2-yl)phosphine (S-phos) (41.9 mg, 0.10 mmol) and cesium carbonate (664 mg, 2.04 mmol). *N,N*-Dimethylformamide (5.1 ml) was added and the tube flushed with nitrogen. The reaction mixture was heated to 100 °C for 2 h. LCMS analysis showed reaction complete. The reaction mixture was cooled to room temperature and quenched with saturated aqueous ammonium chloride (10 mL). The aqueous phase was extracted with ethyl acetate (3 x 15 mL). The combined organic phases were washed with saturated aqueous ammonium chloride (2 x 10 mL) and brine (10 mL). The organics were dried by passing through a hydrophobic frit and the solvent removed under reduced pressure. The resulting yellow gum was dissolved in DCM (2 mL) and loaded onto a 10 g SNAP silica column. The crude material on silica was purified by Biotage SP4 using a gradient of 50 - 100% ethyl acetate in cyclohexane over 20 CV. Fractions containing pure product were collected and the solvent removed *in vacuo* to yield 1',5'-dimethyl-[2,3'-bipyridin]-6'(1'H)-one (77 mg, 0.37 mmol, 72% yield) as an off-white solid. LCMS (formic acid): rt = 0.48 min, MH⁺ 201.1. ¹H NMR δ(400 MHz, CDCl₃) ppm: 8.59 (1H, d, J=4.2 Hz), 8.04 (1H, s), 7.85 - 7.80 (1H, m), 7.75 -

7.68 (1H, m), 7.51 (1H, d, J=8.1 Hz), 7.20 - 7.14 (1H, m), 3.68 - 3.64 (3H, m), 2.25 (3H, s).

Conditions B

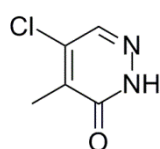
To a carousel tube was added 5-bromo-1,3-dimethylpyridin-2(1H)-one (103 mg, 0.51 mmol), chloro(2-dicyclohexylphosphino-2',4',6'-triisopropyl-1,1'-biphenyl)[2-(2-aminoethyl)phenyl]-palladium(II) (XphosPdcycle) (18.8 mg, 0.03 mmol) and 6-methyl-2-(pyridin-2-yl)-1,3,6,2-dioxazaborocane-4,8-dione (179 mg, 0.77 mmol) and the tube flushed with nitrogen. To the tube was added *N,N*-dimethylformamide (4 mL), diethanolamine (49 μ L, 0.51 mmol), potassium phosphate (541 mg, 2.55 mmol) and copper(II) acetate (46.3 mg, 0.26 mmol). The resulting mixture was stirred at 100 °C for 24 h. Despite the reaction having not progressed to completion, the reaction was slowly cooled to room temperature over a period of 30 min. To the mixture was added 2 M aqueous HCl (5 mL) and the mixture shaken. To the flask was then added 2 M aqueous NaOH (5 mL) and the mixture again shaken. Diethyl ether (10 mL) was added, the phases separated and the organics collected. The aqueous was extracted with a further 2 portions of diethyl ether (10 mL). The organics were combined, washed with brine (5 mL) and dried by passing through a hydrophobic frit. The resulting residue was dissolved in DCM (2 mL) and loaded onto a 10 g SNAP silica column. The material was purified by Biotage SP4 using a gradient of 50 - 100% ethyl acetate in cyclohexane over 25 CV. The solvent was then swapped to 0 - 5% methanol in DCM, however, no desired product was isolated. Fractions containing starting material were collected and the solvent removed *in vacuo* to yield 5-bromo-1,3-dimethylpyridin-2(1H)-one (37 mg, 0.18 mmol, 36% recovery) as a cream solid.

Conditions C

To a carousel tube was added 5-bromo-1,3-dimethylpyridin-2(1H)-one (103 mg, 0.51 mmol), 2-(4,4,5,5-tetramethyl-1,3,2-dioxaborolan-2-yl)pyridine (209 mg, 1.02 mmol), cesium carbonate (664 mg, 2.04 mmol), copper(I) chloride (50.5 mg, 0.51 mmol), palladium(II) acetate (5.7 mg, 0.03 mmol) and DPPF (28.3 mg, 0.05 mmol). *N,N*-Dimethylformamide (5.1 ml) was added, the tube purged with nitrogen and the resulting mixture stirred at 100 °C for 2 h. The reaction was cooled to room temperature and diluted with ethyl acetate (50 mL). The organics were washed with water (2 x 25 mL), dried by passing through a hydrophobic frit and the solvent

removed *in vacuo*. The crude brown gum was dissolved in DCM (3 mL) and loaded onto a 10 g SNAP silica column. The crude material on silica was purified by Biotage SP4 using a gradient of 50 - 100% ethyl acetate in cyclohexane over 20 CV. Pure fractions were collected and the solvent removed *in vacuo* to yield 1',5'-dimethyl-[2,3'-bipyridin]-6'(1'H)-one (63 mg, 0.31 mmol, 61% yield) as an off-white solid. $R_f = 0.15$, 100% ethyl acetate. LCMS (formic acid): $rt = 0.48$ min, MH^+ 201.1. 1H NMR δ (400 MHz, $CDCl_3$) ppm: 8.59 (1H, d, $J=4.2$ Hz), 8.04 (1H, s), 7.85 - 7.80 (1H, m), 7.75 - 7.68 (1H, m), 7.51 (1H, d, $J=8.1$ Hz), 7.20 - 7.14 (1H, m), 3.68 - 3.64 (3H, m), 2.25 (3H, s). ^{13}C NMR δ (101 MHz, $CDCl_3$) ppm: 163.2 (C=O), 153.9 (C-N), 149.6 (C-H), 136.9 (C-H), 135.0 (CH-N), 134.9 (CH-C), 129.2 (C-C), 121.6 (C-H), 118.4 (C-H), 117.9 (C-C), 38.2 (N- CH_3), 17.5 (C- CH_3). IR (neat): 1650, 1584, 1564, 1470, 1441, 1421, 777. HRMS (ESI) exact mass calculated for $C_{12}H_{13}N_2O$ $[M+H]^+$ m/z 201.1022, found m/z 201.1019. Melting point: 105 - 107 °C.

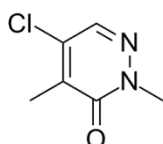
5-Chloro-4-methylpyridazin-3(2H)-one, 2.42



A suspension of 4,5-dichloropyridazin-3(2H)-one (5 g, 30.3 mmol) in dry tetrahydrofuran (100 mL) under nitrogen was cooled to 1 °C in an ice/water bath. Methylmagnesium bromide in diethyl ether (3 M, 30.3 ml, 91 mmol) was added dropwise over 20 mins. A strong exotherm was observed during addition of the first equivalent which was controlled by slow addition of the reagent to the reaction mixture and addition of salt to the ice bath to maintain a temperature below 5 °C. The temperature was easily maintained at <3 °C for the second and third equivalents during which time the reaction turned a deep orange colour. The resulting solution was stirred in the ice/water bath for 10 mins. The solution was then allowed to warm to room temperature and stirred under nitrogen for 5 hours. The reaction mixture was cooled to 0 °C and saturated aqueous ammonium chloride solution (50 mL) was added slowly over 10 mins. Ethyl acetate (100 mL) and 2 M aqueous hydrochloric acid (100 mL) were added, the mixture shaken, and the organic layer removed. The aqueous layer was washed with ethyl acetate (50 mL) and all organic layers were combined, dried using a hydrophobic frit and evaporated under reduced pressure. The resulting orange solid was triturated and then sonicated in diethyl ether (200 mL). The solid was removed by filtration and discarded. The filtrate was evaporated under reduced pressure to yield 5-chloro-4-methylpyridazin-3(2H)-one (3.6 g, 19.9 mmol, 66% yield, 80% purity) as an orange solid. LCMS (formic acid): $rt = 0.50$, MH^+ 144.9, 146.9. 1H NMR

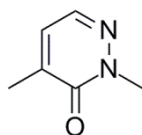
δ (400 MHz, CDCl_3) ppm: 12.08 (1H, br. s.), 7.77 (1H, s), 2.28 (3H, s). ^{13}C NMR δ (101 MHz, CDCl_3): 162.2 (C=O), 138.0 (CH), 137.9, 137.6, 12.9 (C- CH_3). IR (neat): 2976, 1633. HRMS (ESI) exact mass calculated for $\text{C}_5\text{H}_6^{35}\text{ClN}_2\text{O}$ [M+H] $^+$ m/z 145.0163, found m/z 145.0159.

5-Chloro-2,4-dimethylpyridazin-3(2H)-one, 2.43



A round bottom flask was charged with 5-chloro-4-methylpyridazin-3(2H)-one (3.5 g, 24.2 mmol), acetone (27 mL), potassium carbonate (6.69 g, 48.4 mmol) and methyl iodide (5.30 mL, 85 mmol). A condenser was fitted and the mixture warmed to 35 °C under a blanket of nitrogen overnight. The reaction mixture was allowed to cool to room temperature and partitioned between DCM (3 x 250 mL) and water (250 mL). The organic layers were combined, dried using a hydrophobic frit and evaporated under reduced pressure. The resulting solid was dissolved in DCM and loaded onto 2 x 100 g SNAP silica columns. The crude material on silica was purified by Biotage SP4 using a gradient of 0 – 30% ethyl acetate in cyclohexane over 20 CV. Pure fractions were combined and the solvent removed under reduced pressure to form 5-chloro-2,4-dimethylpyridazin-3(2H)-one (2.52 g, 15.6 mmol, 64% yield) as a light brown solid. R_f = 0.29, 25% ethyl acetate in cyclohexane. LCMS (formic acid): r_t = 0.64, MH $^+$ 158.9, 160.9. ^1H NMR δ (400 MHz, CDCl_3) ppm: 7.68 (1H, s), 3.76 (3H, s), 2.27 (3H, s). ^{13}C NMR δ (101 MHz, CDCl_3) ppm: 160.5 (C=O), 136.7 (C-Cl), 136.2 (C-C), 136.1 (C-H), 40.3 (CH_3), 13.5 (CH_3). IR (neat) 1634, 1015. Melting point: 72-76 °C. HRMS (ESI) exact mass calculated for $\text{C}_6\text{H}_8^{35}\text{ClN}_2\text{O}$ [M+H] $^+$ m/z 159.0320, found m/z 159.0318.

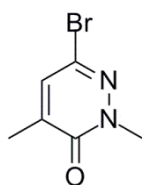
2,4-Dimethylpyridazin-3(2H)-one, 2.45



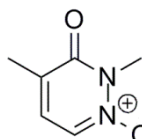
To a solution of 5-chloro-2,4-dimethylpyridazin-3(2H)-one (246 mg, 1.55 mmol) in ethanol (10 mL) was added palladium on carbon (100 mg, 0.94 mmol). The reaction mixture was placed under a hydrogen atmosphere and stirred at RT for 1 h. LCMS analysis after this time showed the reaction was incomplete. The reaction was stirred further under hydrogen for 16 hours. LCMS analysis showed the reaction had proceeded further, but not to

completion. The reaction mixture was kept under a flow of nitrogen while being filtered through celite, and the celite washed with ethanol (30 mL). The product was collected and the solvent removed under reduced pressure. The resulting yellow residue was dissolved in DCM (2 mL) and loaded onto silica. The crude product on silica was purified by Biotage SP4 SNAP 10g silica (Si) using a gradient of 20 - 70% ethyl acetate in cyclohexane over 15 CV. The appropriate fractions were combined and evaporated *in vacuo* to give the required product 2,4-dimethylpyridazin-3(2H)-one (38 mg, 0.29 mmol, 19% yield) as a light brown solid. R_f = 0.28, 50% ethyl acetate in cyclohexane. LCMS (formic acid): rt = 0.41, MH⁺ 124.9. ¹H NMR δ(400 MHz, CDCl₃) ppm: 7.63 (1H, d, *J*=4.0 Hz), 7.02 - 7.07 (1H, m), 3.79 (3H, s), 2.21 (3H, d, *J*=1.0 Hz). ¹³C NMR δ(CDCl₃, 101MHz) ppm: 161.9 (C-O), 140.1 (C-C), 135.7 (C-H), 128.6 (C-H), 40.2 (N-CH₃), 16.7 (C-CH₃). IR (CDCl₃) 1644, 1600. HRMS (ESI) exact mass calculated for C₆H₉N₂O [M+H]⁺ m/z 125.0709, found m/z 125.0709.

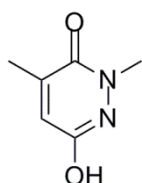
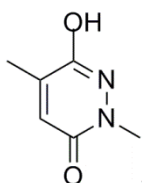
Attempted synthesis of 6-bromo-2,4-dimethylpyridazin-3(2H)-one, 2.46



A round bottom flask was charged with 2,4-dimethylpyridazin-3(2H)-one (40 mg, 0.32 mmol), tetrahydrofuran (1 mL) and cooled to 0 °C. NBS (60 mg, 0.34 mmol) was added portionwise over 20 min, before the reaction mixture was allowed to warm to RT. The slurry was stirred at room temperature for 16 h. LCMS analysis, after this time showed no conversion to the desired product. The reaction mixture was re-cooled to 0 °C before another equivalent of NBS (60 mg, 0.32 mmol) was added. LCMS analysis again showed no evidence of the desired reaction. The reaction was quenched through slow addition of 10% sodium thiosulfate solution (1 mL). The mixture was diluted with ethyl acetate (2 mL) and partitioned with saturated sodium bicarbonate (2 mL). The layers were mixed and separated before the organics were washed with brine (1 mL), passed through a hydrophobic frit and concentrated *in vacuo* to give a pink solid. The sample was diluted with DCM (2 mL) and loaded onto a 10 g SNAP silica column. The crude material on silica was purified by Biotage SP4 using a gradient of 20 - 80% ethyl acetate in cyclohexane over 20 CV. The appropriate fractions were combined and evaporated *in vacuo*, however, the NMR analysis showed no trace of starting material. The reaction was abandoned.

Attempted synthesis of 2,4-dimethyl-3-oxo-2,3-dihydropyridazine 1-oxide, 2.47

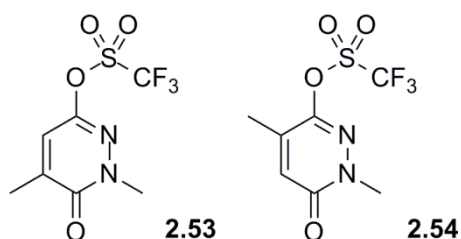
To a solution of 2,4-dimethylpyridazin-3(2H)-one (50 mg, 0.36 mmol) in DCM (2.5 mL) stirred under nitrogen at RT was added *m*-CPBA (75 mg, 0.44 mmol) portionwise during 1 min. The reaction mixture was stirred at RT for 16 h. LCMS analysis showed no trace of the desired product. The sample was loaded in methanol and purified by SPE on a 5 g aminopropyl column using methanol. However, no starting material was re-isolated. The reaction was abandoned.

6-Hydroxy-2,4-dimethylpyridazin-3(2H)-one, 2.51 and 6-hydroxy-2,5-dimethylpyridazin-3(2H)-one, 2.52²³¹**2.51****2.52**

Hydrochloric acid (4.1 mL, 48.2 mmol), methylhydrazine (2.29 mL, 43.4 mmol) and water (10 mL) were added to a round bottomed flask and heated to 100 °C. 3-Methylfuran-2,5-dione (3.9 mL, 43.4 mmol) was added and the solution refluxed for 4 h. The reaction mixture was cooled to room temperature, diluted with water (10 mL) and the solvent removed under reduced pressure. A first crystallisation from boiling water yielded 6-hydroxy-2,5-dimethylpyridazin-3(2H)-one **2.52** (2.37 g, 16.7 mmol, 39% yield) as a white solid. *R*_f = 0.21, 100% ethyl acetate. LCMS (formic acid): *rt* = 0.36, *MH*⁺ 140.9. ¹H NMR δ(400 MHz, CD₃OD) ppm: 6.77 (1 H, d, *J* = 1.2 Hz), 3.59 (3 H, s), 2.16 (4 H, d, *J* = 1.2 Hz). ¹³C NMR δ(101 MHz, CD₃OD) ppm: 160.4 (C=O), 153.6 (C-O), 138.7 (C-C), 128.6 (C-H), 38.0 (N-CH₃), 14.8 (C-CH₃).

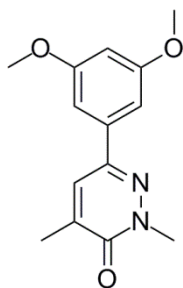
The resulting filtrate was collected, the water removed under reduced pressure and the resulting yellow solid was recrystallised from water to yield 6-hydroxy-2,4-dimethylpyridazin-3(2H)-one **2.51** (1.6 g, 9.13 mmol, 21% yield, 83% purity) as an off-white solid. *R*_f = 0.34, 100% ethyl acetate. LCMS (formic acid): *rt* = 0.36, *MH*⁺ 140.9. ¹H NMR δ(400 MHz, CD₃OD) ppm 7.00 - 6.96 (1H, m), 3.62 (3H, s), 2.17 (3H, d, *J* = 1.0 Hz). ¹³C NMR δ(101 MHz, CD₃OD) ppm: 160.4 (C=O), 153.4 (C-O), 142.3 (C-C), 123.6 (C-H), 38.7 (N-CH₃), 15.5 (C-CH₃).

1,5-Dimethyl-6-oxo-1,6-dihydropyridazin-3-yl trifluoromethanesulfonate, 2.53
and 1,4-dimethyl-6-oxo-1,6-dihydropyridazin-3-yl trifluoromethanesulfonate,
2.54

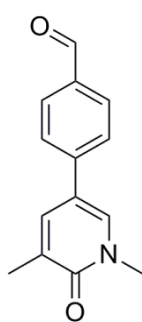


To a solution of a mixture of 6-hydroxy-2,4-dimethylpyridazin-3(2H)-one **2.51** and 6-hydroxy-2,5-dimethylpyridazin-3(2H)-one **2.52** (5:1) (200 mg, 1.43 mmol) and DMAP (349 mg, 2.85 mmol) in DCM (5 mL) stirred under nitrogen at -20 °C was added neat triflic anhydride (0.24 mL, 1.44 mmol) dropwise during 5 min. The reaction mixture was stirred at -20 °C for 15 min. After this time, the reaction mixture was diluted with DCM (10 mL), washed once with hydrochloric acid (1 M, 4 mL) and the organic layer collected, dried using a hydrophobic frit and the solvent removed *in vacuo*. The crude product was dissolved in DCM (1 mL) and loaded onto a 25 g SNAP silica column. The crude material on silica was purified by Biotage SP4 using a gradient of 50 - 85% acetone in ethyl acetate over 20 CV. Fractions containing crude product were collected, the solvent removed under reduced pressure. The resulting liquid was loaded onto a 10 g SNAP silica column. The crude material on silica was purified by Biotage SP4 using a gradient of 20 - 75% ethyl acetate in cyclohexane over 16 CV. The appropriate fractions were combined and evaporated *in vacuo* to give the required products 1,5-dimethyl-6-oxo-1,6-dihydropyridazin-3-yl trifluoromethanesulfonate **2.53** (233 mg, 0.86 mmol, 60% yield). $R_f = 0.41$, 50% ethyl acetate in cyclohexane. LCMS (high pH): $r_t = 0.96$, MH^+ 272.8. 1H NMR δ (400 MHz, $CDCl_3$) ppm: 7.06 (1H, d, $J=1.3$ Hz), 3.74 (3H, s), 2.28 (3H, d, $J=1.3$ Hz). ^{13}F NMR δ (376 MHz, $CDCl_3$) ppm: -72.5 (3F, s).

1,4-Dimethyl-6-oxo-1,6-dihydropyridazin-3-yl trifluoromethanesulfonate **2.54** (35 mg, 0.13 mmol, 9% yield). $R_f = 0.25$, 50% ethyl acetate in cyclohexane. LCMS (high pH): $r_t = 0.94$, MH^+ 273.0. 1H NMR δ (400 MHz, $CDCl_3$) ppm: 6.86 (1H, d, $J=1.3$ Hz), 3.70 (3H, s), 2.26 (3H, d, $J=1.3$ Hz). ^{13}F NMR δ (376 MHz, $CDCl_3$) ppm: -72.4 (3F, s).

6-(3,5-Dimethoxyphenyl)-2,4-dimethylpyridazin-3(2H)-one, 2.40

To a solution of 1,5-dimethyl-6-oxo-1,6-dihydropyridazin-3-yl trifluoromethanesulfonate (50 mg, 0.18 mmol) and (3,5-dimethoxyphenyl)boronic acid (40 mg, 0.22 mmol) in 1,4-dioxane (1 mL) and water (40 μ L) stirred under nitrogen at RT was added palladium tetrakis triphenylphosphine (6.4 mg, 5.51 μ mol) and 1 M aqueous potassium carbonate (0.55 mL, 0.55 mmol). The reaction mixture was stirred at 95 $^{\circ}$ C for 3 h. After cooling to room temperature, the reaction mixture was filtered through celite, diluted with water (10 mL) and extracted with ethyl acetate (2 x 10 mL). The organics were combined, dried using a hydrophobic frit and the solvent removed under reduced pressure. The sample was dissolved in DMSO (1 mL) and purified by mass directed autoprep on Sunfire C18 column using 30-85% acetonitrile water with a formic acid modifier. The solvent was evaporated *in vacuo* to give the crude product. The resulting white solid was dissolved in DCM (2 mL) and loaded onto a pasteur pipette silica column. The crude material on silica was purified using a gradient of 25 - 75% ethyl acetate-cyclohexane. Fractions containing pure product were evaporated *in vacuo* to give the required product 6-(3,5-dimethoxyphenyl)-2,4-dimethylpyridazin-3(2H)-one (10 mg, 0.04 mmol, 21% yield) as a white solid. R_f = 0.52, 100% ethyl acetate. LCMS (formic acid): r_t = 0.91, MH^+ 261.1. 1H NMR δ (400 MHz, $CDCl_3$) ppm: 7.49 (1H, d, J =1.2 Hz), 6.90 (2H, d, J =2.4 Hz), 6.51 (1H, t, J =2.2 Hz), 3.87 (3H, s), 3.85 (6H, s), 2.28 (3H, d, J =1.0 Hz). ^{13}C NMR δ (101 MHz, $CDCl_3$) ppm: 161.3 (C=O), 161.2 (2xC-O), 143.8 (C=N), 139.9 (C-C), 137.1 (C-C), 127.7 (CH), 104.2 (2xCH), 101.1 (CH), 55.5 (2 x O-CH₃), 40.6 (N-CH₃), 17.1 (C-CH₃).

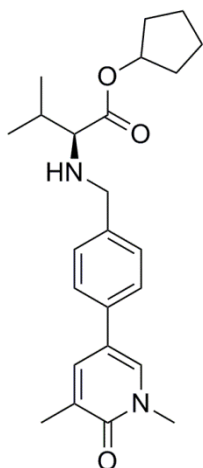
4-(1,5-Dimethyl-6-oxo-1,6-dihydropyridin-3-yl)benzaldehyde, 2.66

To a solution of 5-bromo-1,3-dimethylpyridin-2(1H)-one (2.9 g, 14.4 mmol) and 4-(4,4,5,5-tetramethyl-1,3,2-dioxaborolan-2-yl)benzaldehyde (5.0 g, 21.5 mmol) in 1,4-dioxane (90 mL) and water (3.6 mL) stirred under nitrogen at RT was added palladium tetrakis triphenylphosphine (498 mg, 0.43 mmol) and 1 M aqueous potassium carbonate (43.1 mL, 43.1 mmol). The reaction mixture was stirred at 95 $^{\circ}$ C for 3 h. After cooling to room temperature, the reaction mixture

was diluted with water (75 mL) and the precipitate filtered and dried under vacuum. The resulting solid was dissolved in methanol (100 mL) and passed through celite. The resulting solution was dried *in vacuo* to yield the required product 4-(1,5-dimethyl-6-oxo-1,6-dihydropyridin-3-yl)benzaldehyde (1.4 g, 5.85 mmol, 41% yield) as a light grey solid. After leaving to stand overnight, a second crop of solid was filtered from the mother liquors, and the resulting solid dissolved in methanol, passed through a celite column and the solvent removed under reduced pressure. The product was contaminated with triphenylphosphine oxide. The solid was suspended in ethyl acetate, filtered and washed with further ethyl acetate to yield 4-(1,5-dimethyl-6-oxo-1,6-dihydropyridin-3-yl)benzaldehyde (1.2 g, 4.75 mmol, 33% yield) as a light grey solid. These batches were combined to give the product 4-(1,5-dimethyl-6-oxo-1,6-dihydropyridin-3-yl)benzaldehyde (2.6 g, 10.6 mmol, 74% yield). LCMS (formic acid): *rt* = 0.73, *MH*⁺ 228.1. ¹H NMR δ (400 MHz, CDCl₃) ppm: 10.03 (1H, s), 7.95 - 7.89 (2H, m), 7.61 - 7.57 (2H, m), 7.56 (1H, dd, *J*=2.4, 1.2 Hz), 7.52 (1H, d, *J*=2.4 Hz), 3.66 (3H, s), 2.25 (3H, s). ¹³C NMR δ (101 MHz, CDCl₃) ppm: 191.4 (CHO), 162.7 (C=O), 142.8 (C-C), 135.8 (C-CH), 135.0 (C-CHO), 134.1 (N-CH), 130.5 (2 x CH), 130.2 (C-CH₃), 126.0 (2 x CH), 118.1 (C-C), 38.2 (N-CH₃), 17.4 (C-CH₃) IR (CDCl₃): 1703, 1652, 1599.

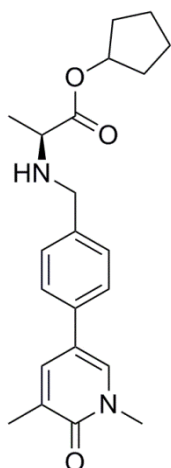
General reductive amination procedure of benzaldehyde, 2.66

To a carousel tube was added 4-(1,5-dimethyl-6-oxo-1,6-dihydropyridin-3-yl)benzaldehyde (50 mg, 0.22 mmol) and an amino ester (a) along with DCM (4 mL) and the resulting suspension stirred under nitrogen for 20 min. Sodium triacetoxyborohydride (93 mg, 0.44 mmol) was added and the reaction mixture stirred under nitrogen at room temperature for 17 h. The reaction mixture was diluted with DCM (10 mL), the mixture washed with saturated aqueous sodium hydrogen carbonate solution (10 mL) and the layers separated. The aqueous was extracted with DCM (3 x 10 mL) and the organics combined, dried by passing through a hydrophobic frit and the solvent removed under reduced pressure. The crude product was dissolved in DMSO (2 x 1 mL) and purified by mass directed autoprep on Sunfire C18 column using gradient (b) acetonitrile water with a formic acid modifier. The solvent was evaporated *in vacuo* to give the crude product. The product was dried in the vacuum oven for 72 hours to yield product (c).

(S)-Cyclopentyl 2-((4-(1,5-dimethyl-6-oxo-1,6-dihydropyridin-3-yl)benzyl)amino)-3-methylbutanoate, 2.58b

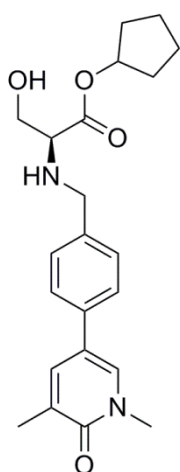
(a) (S)-Cyclopentyl 2-amino-3-methylbutanoate 4-methylbenzenesulfonate (157 mg, 0.44 mmol), (b) 15-55%, (c) (S)-cyclopentyl 2-((4-(1,5-dimethyl-6-oxo-1,6-dihydropyridin-3-yl)benzyl)amino)-3-methylbutanoate, impure due to co-elution on MDAP with the reduced aldehyde by-product. The crude material was dissolved in DCM (1 mL) and loaded onto a 10 g SNAP silica column. The crude material on silica was purified by Biotage SP4 using a gradient of 50 - 100% ethyl acetate in cyclohexane over 15 CV. The appropriate fractions were combined and evaporated *in vacuo* to give the required product (S)-cyclopentyl 2-((4-(1,5-dimethyl-6-oxo-1,6-dihydropyridin-3-yl)benzyl)amino)-3-methylbutanoate (39 mg, 0.10 mmol, 45% yield) as a clear gum. $R_f = 0.20$, 100% ethyl acetate. LCMS (formic acid): $rt = 0.80$, MH^+ 397.3. 1H NMR δ (400 MHz, $CDCl_3$) ppm: 7.52 - 7.48 (1H, m), 7.40 - 7.32 (5H, m), 5.28 - 5.20 (1H, m), 3.85 (1H, d, $J=13.1$ Hz), 3.62 (3H, s), 3.60 (1H, d, $J=13.4$ Hz), 2.95 (1H, d, $J=6.1$ Hz), 2.23 (3H, s), 1.97 - 1.82 (3H, m), 1.81 - 1.66 (4H, m), 1.66 - 1.56 (2H, m), 0.96 (3H, d, $J=6.8$ Hz) (3H, d, $J=6.8$ Hz). ^{13}C NMR δ (101 MHz, $CDCl_3$) ppm: 175.0 (COO), 162.7 (C=O), 139.3 (C-C), 136.7 (C-CH), 135.6 (C-C), 132.8 (N-CH), 129.6 (C- CH_3), 128.9 (2 x CH), 125.7 (2 x CH), 119.5 (C-C), 77.3 (C-O), 66.5 (CH), 52.1 (N- CH_2), 38.1 (N- CH_3), 32.8 (2 x CH_2), 31.7 (CH- $(CH_3)_2$), 23.68 (CH_2), 23.65 (CH_2), 19.3 (CH- CH_3), 18.6 (CH- CH_3), 17.4 (C- CH_3). IR ($CDCl_3$): 2961, 1722, 1656, 1603, 1191, 1151, 833. HRMS (ESI) exact mass calculated for $C_{24}H_{33}N_2O_3$ $[M+H]^+$ m/z 397.2486, found m/z 397.2480.

(S)-Cyclopentyl 2-((4-(1,5-dimethyl-6-oxo-1,6-dihydropyridin-3-yl)benzyl)amino)propanoate, 2.58c

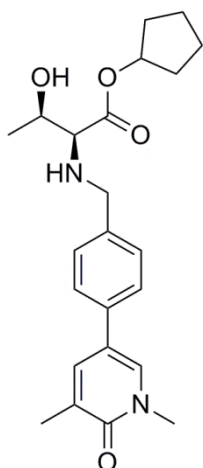


(a) (S)-Cyclopentyl 2-aminopropanoate 4-methylbenzenesulfonate (145 mg, 0.44 mmol), (b) 15-55%, (c) (S)-cyclopentyl 2-((4-(1,5-dimethyl-6-oxo-1,6-dihydropyridin-3-yl)benzyl)amino)propanoate (59 mg, 0.16 mmol, 73% yield) as a clear gum. LCMS (formic acid): $r_t = 0.70$ min, $MH^+ 369.3$. 1H NMR δ (400 MHz, $CDCl_3$) ppm: 7.51 - 7.49 (1H, m), 7.39 - 7.34 (5H, m), 5.26 - 5.21 (1H, m), 3.83 (1H, d, $J=13.0$ Hz), 3.68 (1H, d, $J=12.7$ Hz), 3.62 (3H, s), 3.33 (1H, q, $J=7.0$ Hz), 2.23 (3H, s), 1.94 - 1.83 (2H, m), 1.80 - 1.62 (6H, m), 1.30 (3H, d, $J=7.1$ Hz).

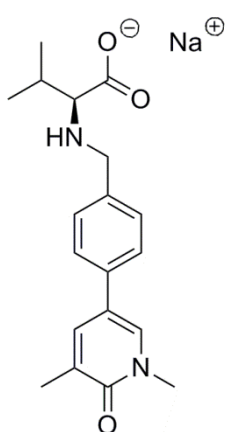
(S)-Cyclopentyl 2-((4-(1,5-dimethyl-6-oxo-1,6-dihydropyridin-3-yl)benzyl)amino)-3-hydroxypropanoate, 2.58d



(a) (S)-Cyclopentyl 2-amino-3-hydroxypropanoate 4-methylbenzenesulfonate (152 mg, 0.44 mmol), (b) 15-55%, (c) (S)-cyclopentyl 2-((4-(1,5-dimethyl-6-oxo-1,6-dihydropyridin-3-yl)benzyl)amino)-3-hydroxypropanoate (70 mg, 0.18 mmol, 83% yield) as a clear gum. LCMS (formic acid): $r_t = 0.64$, $MH^+ 385.2$. 1H NMR δ (400 MHz, $CDCl_3$) ppm: 7.51 - 7.49 (1H, m), 7.39 - 7.36 (5H, m), 5.27 - 5.22 (1H, m), 3.92 (1H, d, $J=13.2$ Hz), 3.82 - 3.74 (2H, m), 3.65 - 3.58 (4H, m), 3.40 (1H, dd, $J=6.5, 4.5$ Hz), 2.23 (3H, s), 1.90 - 1.84 (2H, m), 1.75 - 1.58 (6H, m).

(2S,3R)-Cyclopentyl 2-((4-(1,5-dimethyl-6-oxo-1,6-dihydropyridin-3-yl)benzyl)amino)-3-hydroxybutanoate, 2.58e

(a) (2S,3R)-Cyclopentyl 2-amino-3-hydroxybutanoate 4-methylbenzenesulfonate (158 mg, 0.44 mmol), (b) 15-55%, (c) (2S,3R)-cyclopentyl 2-((4-(1,5-dimethyl-6-oxo-1,6-dihydropyridin-3-yl)benzyl)amino)-3-hydroxybutanoate (67 mg, 0.17 mmol, 76% yield) as a clear gum. LCMS (formic acid): $rt = 0.68$, $MH^+ 399.2$. 1H NMR δ (400 MHz, $CDCl_3$) ppm: 7.51 - 7.48 (1H, m), 7.40 - 7.32 (5H, m), 5.25 - 5.19 (1H, m), 3.86 (1H, d, $J=13.0$ Hz), 3.70 (1H, d, $J=13.0$ Hz), 3.66 (1H, dd, $J=7.6, 6.4$ Hz), 3.63 (3H, s), 2.97 (1H, d, $J=7.8$ Hz), 2.23 (3H, s), 1.92 - 1.53 (8H, m), 1.21 (3H, d, $J=6.4$ Hz).

(S)-2-((4-(1,5-Dimethyl-6-oxo-1,6-dihydropyridin-3-yl)benzyl)amino)-3-methylbutanoate, sodium salt, 2.59b

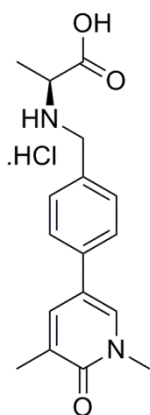
A round bottom flask was charged with (S)-cyclopentyl 2-((4-(1,5-dimethyl-6-oxo-1,6-dihydropyridin-3-yl)benzyl)amino)-3-methylbutanoate (65 mg, 0.16 mmol), tetrahydrofuran (3 mL), methanol (3 mL) and water (1.5 mL). To the stirred solution was added lithium hydroxide (23.6 mg, 0.98 mmol), a condenser fitted and the mixture warmed to 50 °C for 70 h. After this time, the reaction mixture was cooled to room temperature and acetic acid (1 mL) was added before the volatiles were removed *in vacuo* to give a light yellow oil. The oil was dissolved in DMSO (2 mL) and solubilised by addition of a few drops of 2 M sodium hydroxide and purified by mass directed autoprep on Xbridge column using 5-30% acetonitrile water with an ammonium carbonate modifier. The fraction containing product was collected and the solvent was evaporated *in vacuo* to give a white solid. It was suspended in tetrahydrofuran (4 mL) and 2 M aqueous HCl solution (1 mL) was added. The cloudy solution was blown down a stream of nitrogen to form a white solid. However, the HCl salt was not observed by NMR. A portion of this product (S)-2-((4-(1,5-dimethyl-6-oxo-1,6-dihydropyridin-3-yl)benzyl)amino)-3-methylbutanoic acid (4.3 mg, 0.01 mmol, 8% yield) was set aside. The remaining material (31 mg,

0.09 mmol) was slurried in a DCM:methanol:tetrahydrofuran solution (4.5 ml 1:1:1) prior to the addition of sodium hydroxide (2 M) (47 μ L, 0.09 mmol). The resultant solution was stirred for 5 minutes prior to blow down and drying in the vacuum oven to give (S)-2-((4-(1,5-dimethyl-6-oxo-1,6-dihydropyridin-3-yl)benzyl)amino)-3-methylbutanoate, sodium salt (29 mg, 0.08 mmol, 51% yield) as a white solid. LCMS (formic acid): rt = 0.48 min, MH+ 329.3. ^1H NMR δ (400 MHz, DMSO- d_6) ppm: 7.99 (1H, d, $J=2.5$ Hz), 7.75 - 7.73 (1H, m), 7.54 (2H, d, $J=8.3$ Hz), 7.39 (2H, d, $J=8.1$ Hz), 3.89 (1H, d, $J=13.7$), 3.65 (1H, d, $J=13.7$), 3.52 (3H, s), 2.83 (1H, d, $J=5.4$ Hz), 2.08 (3H, s), 1.96 - 1.87 (1H, m), 0.90 (6H, dd, $J=6.4, 5.4$ Hz).

General procedure for ester hydrolysis of 2.58c-e

To a carousel tube was added an ester (a), tetrahydrofuran (2 mL), methanol (2 mL) and water (1 mL). To the stirred solution was added lithium hydroxide (5.5 mg, 0.23 mmol), and the mixture warmed to 50 $^{\circ}\text{C}$ overnight. The reaction mixture was cooled to room temperature and acetic acid (1 mL) was added before the volatiles were removed *in vacuo* to give the crude product as a light yellow oil. The resulting oil was dissolved in DMSO (1 mL) and purified by mass directed autoprep on Xbridge column using gradient (b) acetonitrile water with an ammonium carbonate modifier. The fractions containing the desired products were collected and the solvent was evaporated *in vacuo* to give the crude products as white solids. The solids were suspended in tetrahydrofuran and 2 M aqueous HCl solution (1 mL) was added. The clear solution was blown down a stream of nitrogen to give the required product (b).

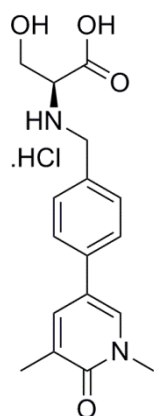
(S)-2-((4-(1,5-Dimethyl-6-oxo-1,6-dihydropyridin-3-yl)benzyl)amino)propanoic acid, hydrochloride, 2.59c



(a) (S)-Cyclopentyl 2-((4-(1,5-dimethyl-6-oxo-1,6-dihydropyridin-3-yl)benzyl)amino) propanoate (40 mg, 0.11 mmol), (b) 5-30%, (c) (S)-2-((4-(1,5-dimethyl-6-oxo-1,6-dihydropyridin-3-yl)benzyl)amino) propanoic acid, hydrochloride (33 mg, 0.10 mmol, 88% yield) as a white solid. LCMS (formic acid): rt = 0.44 min, MH+ 301.2. ^1H NMR δ (400 MHz, DMSO- d_6) ppm: 9.87 (1H, br. s.), 9.44 (1H, br. s.), 8.07 (1H, d, $J=2.5$ Hz), 7.78 (1H, dd, $J=2.5, 1.0$ Hz), 7.68 - 7.63 (2H, m), 7.61 - 7.56 (2H, m), 4.22 - 4.11 (2H, m), 4.02 - 3.91 (1H, m), 3.53 (3H,

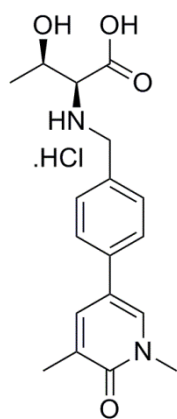
s), 2.09 (3H, s), 1.53 (3H, d, $J=7.3$ Hz). ^{13}C NMR δ (101 MHz, DMSO- d_6) ppm: 171.3 (COOH), 162.1 (C=O), 137.4 (C-C), 136.1 (C-CH), 135.2 (N-CH), 131.2 (2 x CH), 130.4 (C-C), 128.3 (C-CH $_3$), 125.6 (2 x CH), 116.8 (C-C), 54.6 (N-CH), 48.6 (NCH $_2$), 37.7 (N-CH $_3$), 17.5 (C-CH $_3$), 15.0 (CHCH $_3$). IR (neat): 2732, 1734, 1648. Melting point: 249 – 256 °C (decomposition). HRMS (ESI) exact mass calculated for C $_{17}$ H $_{21}$ N $_2$ O $_3$ [M+H] $^+$ m/z 301.1547, found m/z 301.1548.

(S)-2-((4-(1,5-Dimethyl-6-oxo-1,6-dihydropyridin-3-yl)benzyl)amino)-3-hydroxypropanoic acid, hydrochloride, 2.59d



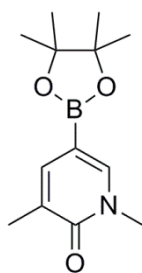
(a) (S)-Cyclopentyl 2-((4-(1,5-dimethyl-6-oxo-1,6-dihydropyridin-3-yl)benzyl)amino)-3-hydroxypropanoate (40 mg, 0.10 mmol), (b) 5-30%, (c) (S)-2-((4-(1,5-dimethyl-6-oxo-1,6-dihydropyridin-3-yl)benzyl)amino)-3-hydroxypropanoic acid, hydrochloride (26 mg, 0.07 mmol, 67% yield) as white solid. LCMS (formic acid): rt = 0.42 min, MH- 315.4. ^1H NMR δ (400 MHz, DMSO- d_6) ppm: 9.53 (1H, br. s.), 9.41 (1H, br. s.), 8.06 (1H, d, $J=2.5$ Hz), 7.78 (1H, dd, $J=2.5, 1.0$ Hz), 7.67 - 7.62 (2H, m), 7.59 - 7.54 (2H, m), 4.23 (2H, br. s.), 3.99 - 3.87 (3H, m), 3.53 (3H, s), 2.09 (3H, s).

(2S,3R)-2-((4-(1,5-Dimethyl-6-oxo-1,6-dihydropyridin-3-yl)benzyl)amino)-3-hydroxybutanoic acid, hydrochloride, 2.59e



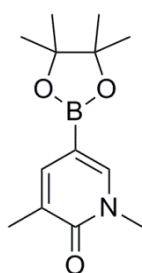
(a) (2S,3R)-Cyclopentyl 2-((4-(1,5-dimethyl-6-oxo-1,6-dihydropyridin-3-yl)benzyl) amino)-3-hydroxybutanoate (40 mg, 0.10 mmol), (b) 5-30%, (c) (2S,3R)-2-((4-(1,5-dimethyl-6-oxo-1,6-dihydropyridin-3-yl)benzyl)amino)-3-hydroxybutanoic acid, hydrochloride (28 mg, 0.08 mmol, 69% yield) as a white solid. LCMS (formic acid): rt = 0.43 min, MH+ 331.2. ^1H NMR δ (400 MHz, DMSO- d_6) ppm: 9.36 (2H, br. s.), 8.07 (1H, d, $J=2.5$ Hz), 7.80 - 7.76 (1H, m), 7.65 (2H, m, $J=8.3$ Hz), 7.55 (2H, m, $J=8.3$ Hz), 4.22 (2H, br. s.), 4.14 - 4.05 (1H, m), 3.55 - 3.51 (4H, m), 2.09 (3H, s), 1.21 (3H, d, $J=6.6$ Hz).

1,3-Dimethyl-5-(4,4,5,5-tetramethyl-1,3,2-dioxaborolan-2-yl)pyridin-2(1H)-one, 2.76



A round bottom flask was charged with 5-bromo-1,3-dimethylpyridin-2(1H)-one (500 mg, 2.48 mmol), 2-methyltetrahydrofuran (20 mL), PdCl₂(dppf) (91 mg, 0.12 mmol), potassium acetate (607 mg, 6.19 mmol) and bis(pinacolato)diboron (943 mg, 3.71 mmol). The mixture was de-gassed with nitrogen and warmed to 80 °C under a blanket of nitrogen overnight before being cooled to room temperature. The crude reaction mixture was passed through celite (ethyl acetate as eluant). The filtrate was concentrated *in vacuo* to give a brown gum. The sample was dissolved in DCM (3 mL) and loaded onto a 100 g SNAP silica column. The crude material on silica was purified by Biotage SP4 using a gradient of 0 - 60% ethyl acetate-cyclohexane over 20 CV. The appropriate fractions were combined and evaporated *in vacuo* to give the crude product 1,3-dimethyl-5-(4,4,5,5-tetramethyl-1,3,2-dioxaborolan-2-yl)pyridin-2(1H)-one (320 mg, 0.77 mmol, 31% yield) as a yellow solid. The compound was determined to be approximately 60% pure by NMR (pinacol related impurities). R_f = 0.19, 25% ethyl acetate in cyclohexane. LCMS (formic acid): rt = 0.91, MH⁺ 250.1. ¹H NMR δ(400 MHz, CDCl₃) ppm: 7.66 - 7.64 (1H, m), 7.49 - 7.47 (1H, m), 3.55 (3H, s), 2.13 (3H, s), 1.31 (12H, s).

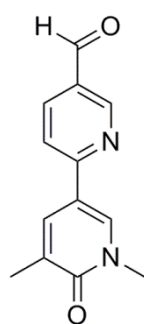
1,3-Dimethyl-5-(4,4,5,5-tetramethyl-1,3,2-dioxaborolan-2-yl)pyridin-2(1H)-one, 2.76



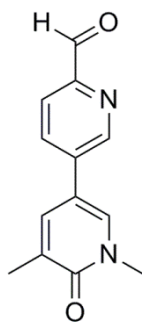
To a solution of 5-bromo-1,3-dimethylpyridin-2(1H)-one (1.5 g, 7.4 mmol) in 1,4-dioxane (18 mL) stirred under nitrogen was added triethylamine (6.2 mL, 44 mmol), 4,4,5,5-tetramethyl-1,3,2-dioxaborolane (6.4 mL, 44 mmol) and palladium tetrakis triphenylphosphine (0.85 g, 0.74 mmol). The reaction mixture was stirred at 100 °C under a blanket of N₂ for 2 h. After this time, the starting material had been completely consumed and the product observed by LCMS at 0.90 min (MH⁺ 250.3). The reaction mixture was cooled to room temperature before quenching with isopropanol (30 mL). This was initially added dropwise in response to the gas evolution with an ice bath used to control the exotherm. The resulting suspension was filtered through celite (isopropanol as

eluant). The filtrate was concentrated *in vacuo* to give a yellow oil. The sample was loaded in DCM (6 mL) onto two 100 g SNAP silica columns and purified by Biotage SP4 using a gradient of 0 – 60% ethyl acetate in cyclohexane over 20 CV. The appropriate fractions were combined and evaporated *in vacuo* to give the crude product, 1,3-dimethyl-5-(4,4,5,5-tetramethyl-1,3,2-dioxaborolan-2-yl)pyridin-2(1H)-one (2.1 g, 6.8 mmol, 92% yield, 80% purity) as a white solid. LCMS (formic acid): *rt* = 0.91 min, *MH*⁺ 250.1. ¹H NMR δ (400 MHz, CDCl₃) ppm: 7.65 (1H, d, *J*=1.5 Hz), 7.49 - 7.46 (1H, m), 3.55 (3H, s), 2.13 (3H, s), 1.31 (12H, s).

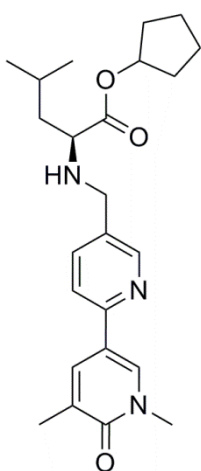
1',5'-Dimethyl-6'-oxo-1',6'-dihydro-[2,3'-bipyridine]-5-carbaldehyde, 2.74



To a solution of 6-bromonicotinaldehyde (185 mg, 1.00 mmol) and 1,3-dimethyl-5-(4,4,5,5-tetramethyl-1,3,2-dioxaborolan-2-yl)pyridin-2(1H)-one (600 mg, 1.45 mmol) in 1,4-dioxane (5.5 mL) and water (0.2 mL) stirred under nitrogen at RT was added palladium tetrakis triphenylphosphine (34.5 mg, 0.03 mmol) and 1 M aqueous potassium carbonate (3 mL, 2.98 mmol). The reaction mixture was stirred at 95 °C for 3 h. After cooling to room temperature, the reaction mixture was filtered through celite and the column washed with ethyl acetate. The reaction mixture was diluted with water (10 mL) and extracted with ethyl acetate (2 x 15 mL). The combined organics were washed with brine (10 mL) and the solvent was removed under reduced pressure. The resulting brown solid was dissolved in DCM (2 mL) and loaded onto a 10 g SNAP silica column. The crude material on silica was purified by Biotage SP4 using a gradient of 50 - 100% ethyl acetate in cyclohexane over 30 CV. Fractions containing the desired product were evaporated *in vacuo* to yield the desired product 1',5'-dimethyl-6'-oxo-1',6'-dihydro-[2,3'-bipyridine]-5-carbaldehyde (180 mg, 0.78 mmol, 78% yield) as a light yellow solid. *R_f* = 0.20, 100% ethyl acetate. LCMS (formic acid): *rt* = 0.62 min, *MH*⁺ 229.3. ¹H NMR δ (400 MHz, DMSO-*d*₆) ppm: 10.08 (1H, s), 9.05 (1H, d, *J*=2.0 Hz), 8.63 (1H, d, *J*=2.5 Hz), 8.25 (1H, dd, *J*=8.5, 2.1 Hz), 8.22 - 8.16 (1H, m), 8.03 (1H, d, *J*=8.3 Hz), 3.58 (3H, s), 2.12 (3H, s). ¹³C NMR δ (126 MHz, DMSO-*d*₆) ppm: 192.1 (CHO), 162.6 (C=O), 158.5 (C-C), 152.2 (N-CH), 138.8 (C-CH), 137.3 (CH), 135.0 (CH), 129.5 (C-CHO), 128.0 (C-CH₃), 118.8 (CH), 115.7 (C-C), 38.1 (N-CH₃), 17.5 (C-CH₃). IR (neat): 2841, 2734, 1704, 1645. HRMS (ESI) exact mass calculated for C₁₃H₁₃N₂O₂ [*M+H*]⁺ *m/z* 229.0972, found *m/z* 229.0966.

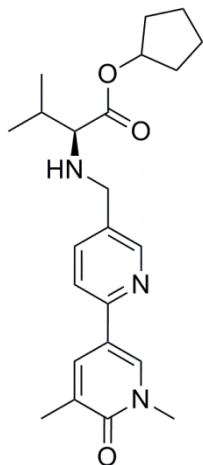
1',5'-Dimethyl-6'-oxo-1',6'-dihydro-[3,3'-bipyridine]-6-carbaldehyde, 2.82

To a solution of 5-bromo-1,3-dimethylpyridin-2(1H)-one (0.58 g, 2.87 mmol) and 5-(4,4,5,5-tetramethyl-1,3,2-dioxaborolan-2-yl) picolinaldehyde (1.0 g, 4.29 mmol) in 1,4-dioxane (18 mL) and water (0.7 mL) stirred under nitrogen at RT was added palladium tetrakis triphenylphosphine (0.1 g, 0.086 mmol) and 1 M aqueous potassium carbonate (8.6 mL, 8.6 mmol). The reaction mixture was stirred at 95°C for 3 h. After this time, LCMS analysis indicated the reaction had not progressed to completion. An additional portion of palladium tetrakis triphenylphosphine (59 mg, 0.051 mmol) was added and the reaction stirred for 18 h. After cooling to room temperature, the reaction mixture was filtered through celite (ethyl acetate as eluent). The resulting solution was diluted with water (25 mL) and extracted with ethyl acetate (3 x 40 mL). The combined organics were washed with brine (10 mL) and the solvent was removed under reduced pressure. The resulting brown solid was dissolved in methanol (10 mL) and silica added. The mixture was evaporated to dryness and loaded onto a 25 g SNAP silica column. The crude material on silica was purified by Biotage SP4 using a gradient of 25 - 100 % ethyl acetate in cyclohexane over 15 CV. The solvent system was changed to 0 - 10 % methanol in DCM over 19 CV. Fractions containing product were collected and the solvent removed *in vacuo* to yield the desired product, 1',5'-dimethyl-6'-oxo-1',6'-dihydro-[3,3'-bipyridine]-6-carbaldehyde (219 mg, 0.77 mmol, 27 % yield, 80 % purity) as a yellow solid. LCMS (High pH): rt = 0.62 min, MH⁺ 229.3. ¹H NMR δ(400 MHz, DMSO-d₆) ppm: 9.99 (1H, s), 9.09 (1H, d, *J*=1.7 Hz), 8.34 (1H, d, *J*=2.7 Hz), 8.24 (1H, dd, *J*=8.1, 2.0 Hz), 7.96 (1H, d, *J*=8.3 Hz), 7.93 (1H, dd, *J*=2.6, 1.1 Hz), 3.55 (3H, s), 2.11 (3H, s).

(S)-Cyclopentyl 2-(((1',5'-dimethyl-6'-oxo-1',6'-dihydro-[2,3'-bipyridin]-5-yl)methyl)amino)-4-methylpentanoate, 2.72a

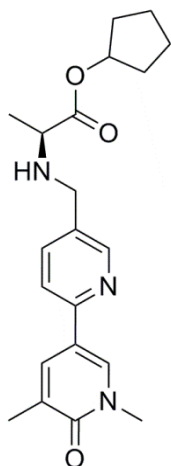
1',5'-Dimethyl-6'-oxo-1',6'-dihydro-[2,3'-bipyridine]-5-carbaldehyde (49 mg, 0.215 mmol) and (S)-cyclopentyl 2-amino-4-methylpentanoate, 4-methylbenzene sulfonic acid salt (160 mg, 0.43 mmol) were dissolved in DCM (4 mL). Triethylamine (75 μ L, 0.54 mmol), followed by sodium triacetoxyborohydride (91 mg, 0.43 mmol) were added to the reaction mixture and stirred at room temperature for 16 h. LCMS analysis showed slow reaction progression, therefore the mixture was warmed to 40 $^{\circ}$ C and an additional portion of sodium triacetoxyborohydride (91 mg, 0.43 mmol) was added and stirred for 4 h. After this time, DCM (15 mL) was added to the flask and the mixture was partitioned with saturated sodium bicarbonate (15 mL). The layers were separated and the aqueous phase extracted with DCM (15 mL). The organic phases were combined, dried over magnesium sulfate and the solvent removed. The residue was loaded onto a 10 g SNAP silica column. The crude material on silica was purified by Biotage SP4 using a gradient of 0 - 5% methanol in DCM. Appropriate fractions were combined and solvent removed under reduced pressure to give (S)-cyclopentyl 2-(((1',5'-dimethyl-6'-oxo-1',6'-dihydro-[2,3'-bipyridin]-5-yl)methyl)amino)-4-methyl pentanoate (51 mg, 0.12 mmol, 58% yield) as white wax. R_f = 0.25, (5% methanol in DCM). LCMS (formic acid): t_r = 0.80 min, MH^+ 412.4. 1H NMR δ (400 MHz, $CDCl_3$) ppm: 8.53 (1H, br. s), 8.04 (1H, br. s.), 7.84 (1H, br. s.), 7.73 (1H, d, $J=7.8$ Hz), 7.48 (1H, d, $J=7.8$ Hz), 5.26 (1H, br. s.), 3.86 (1H, d, $J=13.1$ Hz), 3.74 - 3.58 (4H, m), 3.24 (1H, t, $J=6.9$ Hz), 2.26 (3H, s), 2.03 - 1.86 (2H, m), 1.86 - 1.59 (7H, m), 1.59 - 1.37 (2H, m), 1.05 - 0.80 (6H, m). ^{13}C NMR δ (101 MHz, $CDCl_3$) ppm: 175.6 (COO), 163.1 (C=O), 152.8 (C-C), 149.6 (CH), 137.0 (CH), 135.0 (N-CH), 134.8 (C-CH), 133.4 (C-C), 129.2 (C- CH_2 N), 118.1 (CH), 117.8 (C-C), 75.9 (O-CH), 59.3 (N-CH), 49.1 (N- CH_2), 42.8 (CH_2), 38.2 (N- CH_3), 32.8 (CH_2), 32.7 (CH_2), 24.9 (CH-(CH_3) $_2$), 23.7 (CH_2), 23.72 (CH_2), 22.68 (CH- CH_3), 22.3 (CH- CH_3), 17.4 (C- CH_3). IR (neat): 2956, 1724, 1655. HRMS (ESI) exact mass calculated for $C_{24}H_{34}N_3O_3$ $[M+H]^+$ m/z 412.2595, found m/z 412.2587.

(S)-Cyclopentyl 2-(((1',5'-dimethyl-6'-oxo-1',6'-dihydro-[2,3'-bipyridin]-5-yl)methyl)amino)-3-methylbutanoate, 2.72b

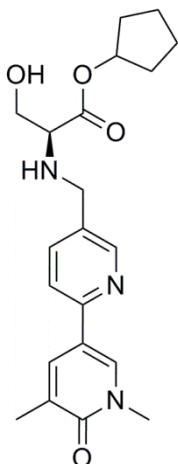


To a carousel tube was added 1',5'-dimethyl-6'-oxo-1',6'-dihydro-[2,3'-bipyridine]-5-carbaldehyde (60 mg, 0.26 mmol) and (S)-cyclopentyl 2-amino-3-methylbutanoate 4-methylbenzene sulfonate (188 mg, 0.53 mmol) along with DCM (5 mL) and the resulting suspension stirred under nitrogen for 20 min. Sodium triacetoxyborohydride (139 mg, 0.66 mmol) was added and the reaction mixture stirred under nitrogen at room temperature for 2 h. LCMS analysis showed the reaction to be incomplete. Therefore an additional portion of sodium triacetoxyborohydride (70 mg, 0.33 mmol) was added and the mixture stirred for 1 h.

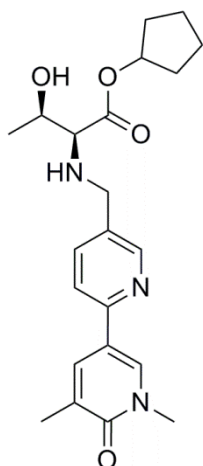
Again, the reaction had not reached completion. An additional portion of sodium triacetoxyborohydride (10 mg, 0.05 mmol) was added and the mixture stirred for 72 h. After this time, the reaction mixture was diluted with DCM (10 mL), the mixture washed with saturated aqueous sodium hydrogen carbonate solution (10 mL) and the layers separated. The aqueous was extracted with DCM (3 x 10 mL) and the organics combined, dried by passing through a hydrophobic frit and the solvent removed under reduced pressure. The crude products were each dissolved in DMSO (2 x 1 mL) and purified by mass directed autoprep on an Xbridge column using 30-85% acetonitrile water with an ammonium carbonate modifier. The solvent was evaporated *in vacuo* to give the required product (S)-cyclopentyl 2-(((1',5'-dimethyl-6'-oxo-1',6'-dihydro-[2,3'-bipyridin]-5-yl)methyl) amino)-3-methyl butanoate (68 mg, 0.17 mmol, 64% yield) as a clear gum. LCMS (formic acid): rt = 0.74 min, MH⁺ 398.2. ¹H NMR δ(400 MHz, CDCl₃) ppm: 8.55 - 8.47 (1H, m), 8.05 - 8.00 (1H, m), 7.82 (1H, d, J=1.0 Hz), 7.72 (1H, dd, J=8.1, 1.7 Hz), 7.46 (1H, d, J=8.1 Hz), 5.29 - 5.21 (1H, m), 3.87 (1H, d, J=13.4 Hz), 3.65 (3H, s), 3.59 (1H, d, J=13.4 Hz), 2.92 (1H, d, J=5.9 Hz), 2.24 (3H, s), 1.98 - 1.85 (3H, m), 1.77 - 1.57 (6H, m), 0.94 (6H, d, J=6.8 Hz). ¹³C NMR δ(101 MHz, CDCl₃) ppm: 174.8 (COO), 163.1 (C=O), 152.7 (C-C), 149.6 (CH), 137.0 (CH), 135.0 (C-CH), 134.8 (N-CH), 133.6 (C-CH₂), 129.2 (C-CH₃), 118.1 (CH), 117.8 (C-C), 77.4 (C-O), 66.4 (NH-CH), 49.5 (NH-CH₂), 38.2 (N-CH₃), 32.79 (CH₂), 32.77 (CH₂), 31.7 (CH-(CH₃)₂), 23.7 (CH₂), 23.6 (CH₂), 19.4 (CH-CH₃), 18.4 (CH-CH₃), 17.4 (C-CH₃). IR (CDCl₃): 1721, 1654, 1597, 2961. HRMS (ESI) exact mass calculated for C₂₃H₃₂N₃O₃ [M+H]⁺ m/z 398.2438, found m/z 398.2445.

(S)-Cyclopentyl 2-(((1',5'-dimethyl-6'-oxo-1',6'-dihydro-[2,3'-bipyridin]-5-yl)methyl)amino)propanoate, 2.72c

1',5'-Dimethyl-6'-oxo-1',6'-dihydro-[2,3'-bipyridine]-5-carbaldehyde (49 mg, 0.22 mmol) and (S)-cyclopentyl 2-aminopropanoate, 4-methylbenzenesulphonic acid salt (141 mg, 0.43 mmol) were dissolved in DCM (4 mL). Triethylamine (75 μ L, 0.54 mmol), followed by sodium triacetoxyborohydride (91 mg, 0.43 mmol) were added to the reaction mixture and left stirred at room temperature for 14 h. LCMS analysis showed slow reaction progression, therefore the mixture was warmed to 40 °C and an additional portion of sodium triacetoxyborohydride (91 mg, 0.43 mmol) was added and stirred for 6 h. An additional portion of (S)-cyclopentyl 2-aminopropanoate, 4-methylbenzenesulphonic acid salt (141 mg, 0.43 mmol) and subsequently sodium triacetoxyborohydride (91 mg, 0.429 mmol) were added and stirred at 40 °C for 2 days. After this time, DCM (15 mL) was added to the flask and the mixture was partitioned with saturated sodium bicarbonate (15 mL). The layers were separated and the aqueous phase extracted with DCM (15 mL). The organic phases were combined, dried over magnesium sulfate and the solvent removed. The residue was loaded onto a 10 g SNAP silica column. The crude material on silica was purified by Biotage SP4 using a gradient of 0 - 5% methanol in DCM. Appropriate fractions were combined and solvent removed under reduced pressure to give impure material. The crude material was dissolved in 1:1 methanol:DMSO (0.8 mL) and purified by mass directed autoprep on an Xbridge column using 5-30% acetonitrile water with an ammonium carbonate modifier. Appropriate fractions were combined and the solvent removed to give (S)-cyclopentyl 2-(((1',5'-dimethyl-6'-oxo-1',6'-dihydro-[2,3'-bipyridin]-5-yl)methyl)amino)propanoate (28 mg, 0.08 mmol, 35% yield) as a white solid. LCMS (formic acid): rt = 0.61 min, MH⁺ 370.4. ¹H NMR δ (400 MHz, Methanol-d₄) ppm: 8.50 (1H, d, *J*=1.7 Hz), 8.22 (1H, d, *J*=2.2 Hz), 8.07 - 8.02 (1H, m), 7.82 (1H, dd, *J*=8.2, 2.1 Hz), 7.70 (1H, d, *J*=8.1 Hz), 5.21 - 5.15 (1H, m), 3.82 (1H, d, *J*=13.4 Hz), 3.72 (1H, d, *J*=13.2 Hz), 3.66 (3H, s), 3.37 - 3.32 (1H, m), 2.20 (3H, s), 1.93 - 1.83 (2H, m), 1.80 - 1.58 (6H, m), 1.30 (3H, d, *J*=6.8 Hz).

(S)-Cyclopentyl 2-(((1',5'-dimethyl-6'-oxo-1',6'-dihydro-[2,3'-bipyridin]-5-yl)methyl)amino)-3-hydroxypropanoate, 2.72d

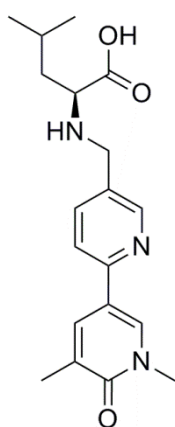
To a carousel tube was added 1',5'-dimethyl-6'-oxo-1',6'-dihydro-[2,3'-bipyridine]-5-carbaldehyde (71 mg, 0.31 mmol) and (S)-cyclopentyl 2-amino-3-hydroxy propanoate 4-methyl benzenesulfonate (215 mg, 0.62 mmol) along with DCM (6 mL) and the resulting suspension stirred under nitrogen for 20 min. Sodium triacetoxyborohydride (165 mg, 0.78 mmol) was added and the reaction mixture stirred under nitrogen at room temperature for 2 h. LCMS analysis showed the reaction to be incomplete. Therefore an additional portion of sodium triacetoxyborohydride (55 mg, 0.26 mmol) was added and the mixture stirred for 1 h. An additional portion of sodium triacetoxyborohydride (10 mg, 0.05 mmol) was added and the mixture stirred for 72 h. After this time, the reaction mixture was diluted with DCM (10 mL), the mixture washed with saturated aqueous sodium hydrogen carbonate solution (10 mL) and the layers separated. The aqueous phase was extracted with DCM (3 x 10 mL) and the organics combined, dried by passing through a hydrophobic frit and the solvent removed under reduced pressure. The crude products were each dissolved in DMSO (2 x 1 mL) and purified by mass directed autoprep on an Xbridge column using 15-55% acetonitrile water with an ammonium carbonate modifier. The solvent was evaporated *in vacuo* to give the required product (S)-cyclopentyl 2-(((1',5'-dimethyl-6'-oxo-1',6'-dihydro-[2,3'-bipyridin]-5-yl)methyl)amino)-3-hydroxypropanoate (46 mg, 0.12 mmol, 37% yield) as a clear gum. LCMS (formic acid): *rt* = 0.59 min, *MH*⁺ 386.1. ¹H NMR δ (400 MHz, CDCl₃) ppm: 8.51 (1H, d, *J*=1.7 Hz), 8.02 (1H, d, *J*=2.4 Hz), 7.81 (1H, dd, *J*=2.4, 1.0 Hz), 7.71 (1H, dd, *J*=8.1, 2.2 Hz), 7.48 (1H, d, *J*=8.3 Hz), 5.27 - 5.21 (1H, m), 3.93 (1H, d, *J*=13.2 Hz), 3.82 - 3.71 (2H, m), 3.67 - 3.59 (4H, m), 3.37 (1H, dd, *J*=6.4, 4.4 Hz), 2.24 (3H, s), 1.94 - 1.84 (2H, m), 1.77 - 1.57 (6H, m). ¹³C NMR δ (101 MHz, CDCl₃) ppm 172.6 (COO), 163.1 (C=O), 153.0 (C-C), 149.5 (CH), 137.0 (CH), 134.9 (2 x C: C-CH, N-CH), 132.8 (C-CH₂), 129.2 (C-CH₃), 118.2 (CH), 117.7 (C-C), 78.4 (C-O), 62.7 (CH₂-OH), 62.0 (NH-CH), 49.2 (NH-CH₂), 38.3 (N-CH₃), 32.8 (CH₂), 32.7 (CH₂), 23.71 (CH₂), 23.67 (CH₂), 17.5 (C-CH₃). IR (CDCl₃): 3332, 2956, 1725, 1651, 1594. HRMS (ESI) exact mass calculated for C₂₁H₂₈N₃O₄ [*M*+*H*]⁺ *m/z* 386.2074, found *m/z* 386.2075.

(2S,3R)-Cyclopentyl 2-(((1',5'-dimethyl-6'-oxo-1',6'-dihydro-[2,3'-bipyridin]-5-yl)methyl)amino)-3-hydroxybutanoate, 2.72e

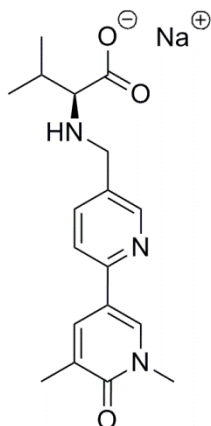
1',5'-Dimethyl-6'-oxo-1',6'-dihydro-[2,3'-bipyridine]-5-carbaldehyde (49 mg, 0.215 mmol) and (2S,3R)-cyclopentyl 2-amino-3-hydroxybutanoate, 4-methylbenzenesulfonic acid salt (154 mg, 0.43 mmol) were dissolved in DCM (4 mL). Triethylamine (75 μ L, 0.54 mmol), followed by sodium triacetoxyborohydride (91 mg, 0.43 mmol) were added to the reaction mixture and left stirred at room temperature for 14 h. LCMS analysis showed slow reaction progression, thereby the mixture was warmed to 40 °C and an additional portion of sodium triacetoxyborohydride (91 mg, 0.43 mmol) was added and stirred for 6 h. An additional portion of (2S,3R)-cyclopentyl 2-amino-3-hydroxybutanoate, 4-methylbenzenesulfonic acid salt (154 mg, 0.43 mmol) and subsequently sodium triacetoxyborohydride (91 mg, 0.43 mmol) were added and left at 40 °C for 2 days. After this time, DCM (15 mL) was added to the flask and the mixture was partitioned with saturated sodium bicarbonate (15 mL). The layers were separated and the aqueous phase extracted with DCM (15 mL). The organic phases were combined, dried over magnesium sulfate and the solvent removed. The residue was loaded onto a 10 g SNAP silica column. The crude material on silica was purified by Biotage SP4 using a gradient of 0 - 5% methanol in DCM. Appropriate fractions were combined and solvent removed under reduced pressure to give the crude product. The crude material was dissolved in 1:1 methanol:DMSO (0.8 mL) and purified by mass directed autoprep on an Xbridge column using 5-30% acetonitrile water with an ammonium carbonate modifier. Appropriate fractions were combined and the solvent removed to give (2S,3R)-cyclopentyl 2-(((1',5'-dimethyl-6'-oxo-1',6'-dihydro-[2,3'-bipyridin]-5-yl)methyl)amino)-3-hydroxybutanoate (12 mg, 0.03 mmol, 14% yield) as a purple solid. R_f = 0.27, (5% methanol in DCM). LCMS (formic acid): r_t = 0.64 min, MH^+ 400.4. 1H NMR δ (400 MHz, Methanol- d_4) ppm: 8.51 (1H, d, J =1.7 Hz), 8.22 (1H, d, J =2.4 Hz), 8.03 - 8.07 (1H, m), 7.84 (1H, dd, J =8.1, 2.2 Hz), 7.70 (1H, d, J =8.3 Hz), 5.20 - 5.13 (1H, m), 3.94 - 3.83 (2H, m), 3.71 (1H, d, J =13.7 Hz), 3.67 (3H, s), 3.05 (1H, d, J =5.4 Hz), 2.20 (3H, s), 1.92 - 1.80 (2H, m), 1.78 - 1.57 (6H, m), 1.20 (3H, d, J =6.4 Hz). ^{13}C NMR δ (101 MHz, Methanol- d_4) ppm: 173.2 (COO), 163.4 (C=O), 152.5 (C-C), 149.1 (CH), 137.6 (CH), 136.2 (N-CH), 135.6 (C-CH), 133.8 (C-CH₃), 128.1 (C-CH₂N), 118.9 (CH), 118.8 (C-C), 77.9 (O-CH), 68.0 (CH-OH), 66.6 (N-CH), 48.9 (N-

CH₂), 37.3 (N-CH₃), 32.24 (CH₂), 32.17 (CH₂), 23.23 (CH₂), 23.20 (CH₂), 18.84 (CH-CH₃), 15.93 (C-CH₃). IR (neat): 3343, 2968, 1722, 1651. HRMS (ESI) exact mass calculated for C₂₂H₃₀N₃O₄ [M+H]⁺ m/z 400.2231, found m/z 400.2228.

(S)-2-(((1',5'-Dimethyl-6'-oxo-1',6'-dihydro-[2,3'-bipyridin]-5-yl)methyl)amino)-4-methyl pentanoic acid, 2.83a

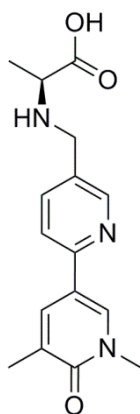


To a carousel tube was charged (S)-cyclopentyl 2-(((1',5'-dimethyl-6'-oxo-1',6'-dihydro-[2,3'-bipyridin]-5-yl)methyl)amino)-4-methyl pentanoate (20 mg, 0.05 mmol), tetrahydrofuran (0.75 mL), methanol (0.75 mL) and water (0.24 mL). To the stirred solution was added lithium hydroxide (6 mg, 0.24 mmol) and the mixture stirred at RT for 14 h. After this time, the reaction mixture was cooled to room temperature and the solvent was removed under reduced pressure. The residue was dissolved in 400 μ L of DMSO and 400 μ L methanol and purified by mass directed autoprep on an Xbridge column using 5-30% acetonitrile water with an ammonium carbonate modifier. The fractions containing the desired products were collected and the solvent was evaporated *in vacuo* to give (S)-2-(((1',5'-dimethyl-6'-oxo-1',6'-dihydro-[2,3'-bipyridin]-5-yl)methyl)amino)-4-methylpentanoic acid (12 mg, 0.04 mmol, 72% yield) as a white solid. LCMS (high pH): rt = 0.54 min, MH⁺ 344.4. ¹H NMR δ (400 MHz, Methanol-*d*₄) ppm: 8.67 - 8.63 (1H, m), 8.34 - 8.29 (1H, m), 8.10 (1H, br. s.), 7.94 (1H, dd, *J*=8.1, 1.7 Hz), 7.80 (1H, d, *J*=8.3 Hz), 4.59 (1H, br. s.), 4.16 (1H, d, *J*=13.2 Hz), 4.07 (1H, d, *J*=13.2 Hz), 3.67 (3H, s), 3.46 (1H, t, *J*=7.1 Hz), 2.20 (3H, s), 1.89 - 1.79 (1H, m), 1.78 - 1.68 (1 H, m), 1.62 - 1.51 (1H, m), 0.99 (3H, d, *J*=6.4 Hz), 0.94 (3H, d, *J*=6.6 Hz).

(S)-2-(((1',5'-Dimethyl-6'-oxo-1',6'-dihydro-[2,3'-bipyridin]-5-yl)methyl)amino)-3-methyl butanoate, sodium salt, 2.83b

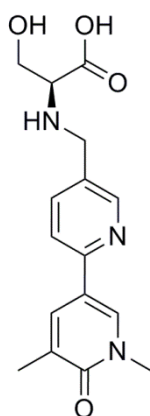
To a carousel tube was charged (S)-cyclopentyl 2-(((1',5'-dimethyl-6'-oxo-1',6'-dihydro-[2,3'-bipyridin]-5-yl)methyl)amino)-3-methylbutanoate (50 mg, 0.13 mmol), tetrahydrofuran (2 mL), methanol (2 mL) and water (1 mL). To the stirred solution was added lithium hydroxide (12 mg, 0.50 mmol) and the mixture stirred at 50 °C for 3 h. An additional portion of lithium hydroxide (15 mg, 0.63 mmol) was added and stirred for an additional 6 h. After this time, the reaction mixture was cooled to room temperature and acetic acid (1 mL) added before the volatiles were removed *in vacuo* to give a yellow oil. The resulting oil was dissolved in DMSO (1 mL) and purified by mass directed autoprep on an Xbridge column using 5-30% acetonitrile water with an ammonium carbonate modifier. The fractions containing the desired products were collected and the solvent was evaporated *in vacuo* to give the crude product (17 mg, 0.05 mmol). The material was slurried in a DCM/MeOH/THF solution (3 mL 1:1:1) prior to the addition of sodium hydroxide (2 M) (26 μ L, 0.05 mmol). The resultant solution was stirred for 5 minutes prior to blow down and drying in the vacuum oven to yield (S)-2-(((1',5'-dimethyl-6'-oxo-1',6'-dihydro-[2,3'-bipyridin]-5-yl)methyl)amino)-3-methyl butanoate, sodium salt (32 mg, 0.09 mmol, 71% yield) as a white solid. LCMS (high pH): *rt* = 0.49 min, MH⁺ 330.2. ¹H NMR δ (400 MHz, DMSO-*d*₆) ppm: 8.46 (1H, s), 8.36 (1H, d, *J*=2.4 Hz), 8.06 (1H, dd, *J*=2.4, 1.0 Hz), 7.76 - 7.70 (2H, m), 3.76 (1H, d, *J*=13.7 Hz), 3.54 (3H, s), 3.49 (1H, d, *J*=13.7 Hz), 2.46 (1H, d, *J*=4.6 Hz), 2.09 (3H, s), 1.83 (1H, dq, *J*=11.8, 6.8 Hz), 0.85 (3H, d, *J*=6.8 Hz), 0.80 (3H, d, *J*=6.8 Hz). ¹³C NMR δ (126 MHz, DMSO-*d*₆) ppm: 176.6 (COO), 162.5 (C=O), 152.0 (C-C), 149.4 (CH), 137.1 (CH), 136.2 (NCH), 135.3 (C-CH), 135.1 (C-CH₂), 127.7 (C-CH₃), 118.2 (CH), 116.9 (C-C), 68.8 (NCH), 50.4 (NCH₂), 37.9 (NCH₃), 31.5 (CH-CH₃), 20.9 (CH-CH₃), 19.0 (CH-CH₃), 17.6 (C-CH₃). IR (neat): 3381, 2956, 1651, 1571. HRMS (ESI) exact mass calculated for C₁₈H₂₄N₃O₃ [M+H]⁺ *m/z* 330.1812, found *m/z* 330.1818 (for parent neutral compound). Melting Point: 316 - 335 °C (decomp.).

(S)-2-(((1',5'-Dimethyl-6'-oxo-1',6'-dihydro-[2,3'-bipyridin]-5-yl)methyl)amino)propanoic acid, 2.83c



To a carousel tube was charged (S)-cyclopentyl 2-(((1',5'-dimethyl-6'-oxo-1',6'-dihydro-[2,3'-bipyridin]-5-yl)methyl)amino) propanoate (12 mg, 0.03 mmol), tetrahydrofuran (0.75 mL), methanol (0.75 mL) and water (0.16 mL). To the stirred solution was added lithium hydroxide (4 mg, 0.16 mmol), and the mixture stirred at RT for 14 h. After this time, the reaction mixture was cooled to room temperature and the solvent was removed under reduced pressure. The residue was dissolved in 400 μ L of DMSO and 400 μ L methanol and purified by mass directed autoprep on an Xbridge column using 5-30% acetonitrile water with an ammonium carbonate modifier. The fractions containing the desired products were collected and the solvent was evaporated *in vacuo* to give (S)-2-(((1',5'-dimethyl-6'-oxo-1',6'-dihydro-[2,3'-bipyridin]-5-yl)methyl)amino)propanoic acid (8 mg, 0.03 mmol, 82% yield) as a white solid. LCMS (high pH): rt = 0.43 min, MH⁺ 302.4. ¹H NMR δ (400 MHz, Methanol-*d*₄) ppm: 8.57 - 8.54 (1H, m), 8.26 - 8.23 (1H, m), 8.07 (1H, s), 7.87 (1H, dd, *J*=8.2, 2.1 Hz), 7.72 (1H, d, *J*=8.3 Hz), 3.86 (1H, d, *J*=13.0 Hz), 3.71 - 3.65 (4H, m), 3.17 (1H, q, *J*=7.1 Hz), 2.20 (3H, s), 1.29 (3H, d, *J*=7.1 Hz).

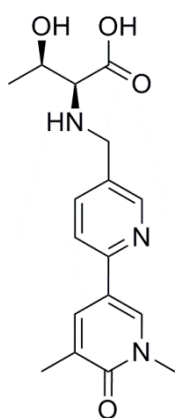
(S)-2-(((1',5'-Dimethyl-6'-oxo-1',6'-dihydro-[2,3'-bipyridin]-5-yl)methyl)amino)-3-hydroxy propanoic acid, 2.83d



To a carousel tube was charged (S)-cyclopentyl 2-(((1',5'-dimethyl-6'-oxo-1',6'-dihydro-[2,3'-bipyridin]-5-yl)methyl)amino)-3-hydroxy propanoate (50 mg, 0.13 mmol), tetrahydrofuran (3 mL), methanol (3 mL) and water (1.5 mL). To the stirred solution was added lithium hydroxide (12 mg, 0.52 mmol) and the mixture stirred at 50 °C for 16 h. After this time, the reaction mixture was cooled to room temperature and the solvent was removed under a stream of nitrogen. The solid was suspended in methanol and acetic acid added dropwise forming a cloudy suspension. The material was re-basified dropwise with 2 M NaOH until complete dissolution was achieved. The solvent was again removed under a stream of nitrogen. The resulting oil was dissolved in DMSO (1 mL) and purified by mass directed autoprep on an Xbridge column using 5 to 30%

acetonitrile water with an ammonium carbonate modifier. The fractions containing the desired products were collected and the solvent was evaporated *in vacuo* to give the desired product (S)-2-(((1',5'-dimethyl-6'-oxo-1',6'-dihydro-[2,3'-bipyridin]-5-yl)methyl)amino)-3-hydroxypropanoic acid (33 mg, 0.10 mmol, 76% yield) as a white solid. LCMS (high pH): rt = 0.41 min, MH+ 318.2. ¹H NMR δ(400 MHz, Methanol-*d*₄) ppm: 8.70 (1H, d, *J*=2.0 Hz), 8.35 (1H, d, *J*=2.4 Hz), 8.13 (1H, dd, *J*=2.3, 1.1 Hz), 8.01 (1H, dd, *J*=8.3, 2.2 Hz), 7.84 (1H, d, *J*=8.1 Hz), 4.38 - 4.28 (2H, m), 4.05 (1H, dd, *J*=12.0, 3.9 Hz), 3.92 (1H, dd, *J*=12.0, 7.1 Hz), 3.69 (3H, s), 3.64 (1H, dd, *J*=7.1, 3.9 Hz), 2.23 (3H, s). HRMS (ESI) exact mass calculated for C₁₆H₂₀N₃O₄ [M+H]⁺ m/z 318.1448, found m/z 318.1452.

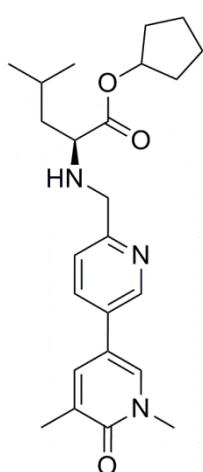
(2S,3R)-2-(((1',5'-Dimethyl-6'-oxo-1',6'-dihydro-[2,3'-bipyridin]-5-yl)methyl)amino)-3-hydroxybutanoic acid, 2.83e



To a carousel tube was charged (2S,3R)-cyclopentyl 2-(((1',5'-dimethyl-6'-oxo-1',6'-dihydro-[2,3'-bipyridin]-5-yl)methyl) amino)-3-hydroxybutanoate (24 mg, 0.06 mmol), tetrahydrofuran (1.5 mL), methanol (1.5 mL) and water (0.75 mL). To the stirred solution was added lithium hydroxide (5.8 mg, 0.24 mmol) and the mixture stirred at 50 °C for 16 h. After this time, the reaction mixture was cooled to room temperature and acetic acid (0.5 mL) was added before the volatiles were removed *in vacuo* to give a clear oil. The resulting oil was dissolved in DMSO (1 mL) and purified by mass directed autoprep on an Xbridge column using 5-30% acetonitrile water with an ammonium carbonate modifier. The fractions containing the desired products were collected and the solvent was evaporated *in vacuo* to give the crude product as a white solid. The crude material (20 mg, 0.06 mmol) was slurried in a DCM/MeOH/THF solution (3 ml 1:1:1) prior to the addition of sodium hydroxide (2 M) (30 μL, 0.06 mmol). The resultant solution was stirred for 5 minutes prior to blow down in a stream on nitrogen and drying in the vacuum oven to yield the crude product in insufficient purity. The material was dissolved in DMSO (1 mL) and purified by mass directed autoprep on an Xbridge column using 5-30% acetonitrile water with an ammonium carbonate modifier. The solvent was evaporated *in vacuo* to yield the desired product (2S,3R)-2-(((1',5'-dimethyl-6'-oxo-1',6'-dihydro-[2,3'-bipyridin]-5-yl)methyl)amino)-3-hydroxy butanoic acid (15 mg, 0.04 mmol, 72% yield) as a white

solid. LCMS (High pH): rt = 0.43 min, MH+ 332.2. ¹H NMR δ(400 MHz, Methanol-*d*₄) ppm: 8.58 (1H, d, *J*=1.8 Hz), 8.24 (1H, d, *J*=2.3 Hz), 8.09 - 8.06 (1H, m), 7.91 (1H, dd, *J*=8.2, 2.1 Hz), 7.72 (1H, d, *J*=8.3 Hz), 3.97 (1H, d, *J*=13.4 Hz), 3.81 (1H, quin, *J*=6.4 Hz), 3.75 (1H, d, *J*=13.4 Hz), 3.69 (3H, s), 2.96 (1H, d, *J*=6.3 Hz), 2.22 (3H, s), 1.23 (3H, d, *J*=6.3 Hz). ¹³C NMR δ(101 MHz, Methanol-*d*₄) ppm: 178.2 (COO), 163.5 (C=O), 152.5 (C-C), 149.2 (CH), 137.7 (CH), 136.2 (NCH), 135.6 (C-CH), 133.7 (C-CH₂), 128.1 (C-CH₃), 118.93 (CH), 118.87 (C-C), 69.3 (CHOH), 68.3 (NHCH), 48.9 (N-CH₂), 37.3 (N-CH₃), 18.8 (CHCH₃), 15.9 (C-CH₃). IR (neat): 2971, 1658, 1598. HRMS (ESI) exact mass calculated for C₁₇H₂₂N₃O₄ [M+H]⁺ m/z 332.1605, found m/z 332.1606.

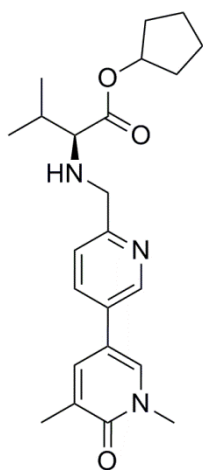
(S)-Cyclopentyl 2-(((1',5'-dimethyl-6'-oxo-1',6'-dihydro-[3,3'-bipyridin]-6-yl)methyl)amino)-4-methylpentanoate, 2.73a



To a carousel tube was added 1',5'-dimethyl-6'-oxo-1',6'-dihydro-[3,3'-bipyridine]-6-carbaldehyde (73 mg, 0.26 mmol) and (S)-cyclopentyl 2-amino-4-methylpentanoate, 4-methylbenzene sulfonic acid salt (260 mg, 0.70 mmol) along with DCM (6 mL) and the resulting suspension stirred under nitrogen for 20 min. Sodium triacetoxyborohydride (163 mg, 0.77 mmol) was added and the reaction mixture stirred under nitrogen at RT for 2 h. An additional portion of sodium triacetoxyborohydride (100 mg, 0.52 mmol) was added and the reaction stirred for 5 h then left to stand overnight. After this time, the reaction mixture was diluted with DCM (20 mL), the mixture washed with saturated aqueous sodium hydrogen carbonate solution (20 mL) and the layers separated. The aqueous was extracted with DCM (3 x 20 mL) and the organics combined, dried by passing through a hydrophobic frit and the solvent removed under reduced pressure. The crude products were each dissolved in DMSO (2 x 1 mL) and purified by mass directed autoprep on an Xbridge column using 30-85% acetonitrile water with an ammonium carbonate modifier. The solvent was evaporated *in vacuo* to give the required product (S)-cyclopentyl 2-(((1',5'-dimethyl-6'-oxo-1',6'-dihydro-[3,3'-bipyridin]-6-yl)methyl)amino)-4-methyl pentanoate (66 mg, 0.16 mmol, 46% yield) as a yellow gum. LCMS (high pH): rt = 1.15 min, MH+ 412.2. ¹H NMR δ(400 MHz, CDCl₃) ppm 8.60 (1H, d, *J*=2.0 Hz), 7.67 (1H, dd, *J*=8.1, 2.3 Hz), 7.45 (1H, dd, *J*=2.4, 1.1 Hz), 7.42 - 7.37 (2H, m), 5.26 - 5.19

(1H, m), 3.98 (1H, d, $J=14.1$ Hz), 3.81 (1H, d, $J=14.1$ Hz), 3.64 (3H, s), 3.30 (1H, t, $J=7.2$ Hz), 2.24 (3H, s), 1.90 - 1.82 (2H, m), 1.81 - 1.58 (7H, m), 1.52 (2H, t, $J=7.2$ Hz), 0.94 (3H, d, $J=6.6$ Hz), 0.89 (3H, d, $J=6.6$ Hz). ^{13}C NMR δ (101 MHz, CDCl_3) ppm: 175.4 (COO), 162.7 (C=O), 158.5 (C- CH_2N), 146.3 (CH), 136.0 (CH), 133.6 (CH), 133.2 (CHNMe), 130.9 (C-C), 130.3 (C- CH_3), 122.0 (CH), 116.3 (C-C), 77.4 (C-O), 59.8 (N-CH), 53.1 (N- CH_2), 42.8 (CH- CH_2), 38.1 (N- CH_3), 32.8 (CH_2), 32.7 (CH_2), 25.0 (CH(CH_3) $_2$), 23.70 (CH_2), 23.67 (CH_2), 22.7 (CH_3), 22.5 (CH_3), 17.4 (C- CH_3). IR (CDCl_3): 2955, 1722, 1654, 1191, 1157. HRMS (ESI) exact mass calculated for $\text{C}_{24}\text{H}_{34}\text{N}_3\text{O}_3$ [M+H] $^+$ m/z 412.2595, found m/z 412.2590.

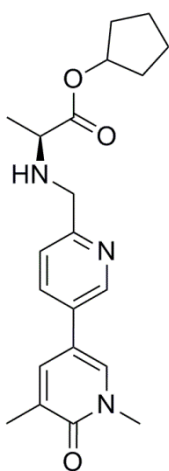
(S)-Cyclopentyl 2-(((1',5'-dimethyl-6'-oxo-1',6'-dihydro-[3,3'-bipyridin]-6-yl)methyl)amino)-3-methylbutanoate, 2.73b



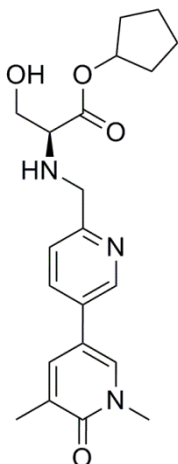
To a carousel tube was added 1',5'-dimethyl-6'-oxo-1',6'-dihydro-[3,3'-bipyridine]-6-carbaldehyde (73 mg, 0.26 mmol) and (S)-cyclopentyl 2-amino-3-methylbutanoate 4-methylbenzene sulfonate (251 mg, 0.70 mmol) along with DCM (6 mL) and the resulting suspension stirred under nitrogen for 20 min. Sodium triacetoxyborohydride (163 mg, 0.77 mmol) was added and the reaction mixture stirred under nitrogen at RT for 2 h. An additional portion of sodium triacetoxyborohydride (100 mg, 0.52 mmol) was added as required and the reactions stirred for 5 h then left to stand overnight. After this time, the reaction mixture was diluted with DCM (20 mL), the mixture washed with saturated aqueous sodium hydrogen carbonate solution (20 mL) and the layers separated. The aqueous was extracted with DCM (3 x 20 mL) and the organics combined, dried by passing through a hydrophobic frit and the solvent removed under reduced pressure. The crude product was each dissolved in DMSO (2 x 1 mL) and purified by mass directed autoprep on an Xbridge column using 30-85% acetonitrile water with an ammonium carbonate modifier. The solvent was evaporated *in vacuo* to give the required product (S)-cyclopentyl 2-(((1',5'-dimethyl-6'-oxo-1',6'-dihydro-[3,3'-bipyridin]-6-yl)methyl)amino)-3-methylbutanoate (83 mg, 0.21 mmol, 60% yield) as a yellow gum. LCMS (high pH): rt = 1.09 min, MH $^+$ 398.2. ^1H NMR δ (400 MHz, CDCl_3) ppm: 8.60 (1H, d, $J=2.0$ Hz), 7.67 (1H, dd, $J=8.2, 2.3$ Hz), 7.48 - 7.42 (2H, m), 7.39 (1H, d, $J=2.4$ Hz), 5.26 - 5.20 (1H, m), 4.00 (1H, d, $J=14.4$ Hz), 3.78 (1H, d, $J=14.4$ Hz),

3.64 (3H, s), 3.02 (1H, d, $J=5.9$ Hz), 2.24 (3H, s), 2.03 - 1.93 (1H, m), 1.93 - 1.80 (2H, m), 1.79 - 1.65 (4H, m), 1.65 - 1.54 (2H, m), 0.98 (6H, 2 x d (overlapping), $J=6.8$ Hz). HRMS (ESI) exact mass calculated for $C_{23}H_{32}N_3O_3$ $[M+H]^+$ m/z 398.2438, found m/z 398.2440.

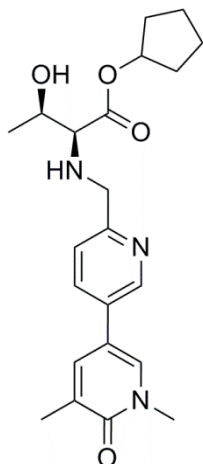
(S)-Cyclopentyl 2-(((1',5'-dimethyl-6'-oxo-1',6'-dihydro-[3,3'-bipyridin]-6-yl)methyl)amino)propanoate, 2.73c



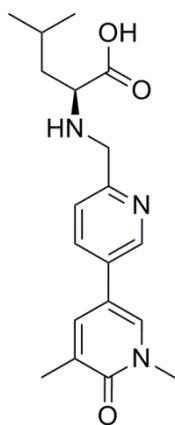
To a carousel tube was added 1',5'-dimethyl-6'-oxo-1',6'-dihydro-[3,3'-bipyridine]-6-carbaldehyde (73 mg, 0.26 mmol) and (S)-cyclopentyl 2-aminopropanoate 4-methylbenzenesulfonate (169 mg, 0.51 mmol) along with DCM (6 mL) and the resulting suspension stirred under nitrogen for 20 min. Sodium triacetoxyborohydride (163 mg, 0.77 mmol) was added and the reaction mixture stirred under nitrogen at RT for 2 h. After this time, the reaction mixture was diluted with DCM (20 mL), the mixture washed with saturated aqueous sodium hydrogen carbonate solution (20 mL) and the layers separated. The aqueous was extracted with DCM (3 x 20 mL) and the organics combined, dried by passing through a hydrophobic frit and the solvent removed under reduced pressure. The crude product was dissolved in DMSO (2 x 1 mL) and purified by mass directed autoprep on Xbridge column using 15-55% acetonitrile water with an ammonium carbonate modifier. The solvent was evaporated *in vacuo* to give the required product (S)-cyclopentyl 2-(((1',5'-dimethyl-6'-oxo-1',6'-dihydro-[3,3'-bipyridin]-6-yl)methyl)amino) propanoate (64 mg, 0.17 mmol, 66% yield) as a yellow gum. LCMS (High pH): $rt = 0.90$ min, MH^+ 370.4. 1H NMR δ (400 MHz, $CDCl_3$) ppm: 8.61 (1H, d, $J=1.7$ Hz), 7.67 (1H, dd, $J=8.1, 2.4$ Hz), 7.46 (1H, dd, $J=2.6, 1.1$ Hz), 7.41 - 7.36 (2H, m), 5.27 - 5.18 (1H, m), 3.98 (1H, d, $J=14.2$ Hz), 3.84 (1H, d, $J=14.2$ Hz), 3.64 (3H, s), 3.39 (1H, q, $J=7.1$ Hz), 2.24 (3H, s), 1.95 - 1.78 (2H, m), 1.78 - 1.56 (6H, m), 1.35 (3H, d, $J=6.8$ Hz). ^{13}C NMR δ (126 MHz, $CDCl_3$) ppm: 175.2 (COO), 162.7 (C=O), 158.2 (C- CH_2N), 146.5 (CH), 136.1 (C-CH), 133.7 (CH), 133.2 (N-CH), 131.0 (C-C), 130.3 (C- CH_3), 122.1 (CH), 116.3 (C-C), 77.6 (C-O), 56.4 (NH-CH), 52.9 (N- CH_2), 38.2 (N- CH_3), 32.8 (CH_2), 32.7 (CH_2), 23.74 (CH_2), 23.71 (CH_2), 19.1 (CH- CH_3), 17.5 (C- CH_3). HRMS (ESI) exact mass calculated for $C_{21}H_{28}N_3O_3$ $[M+H]^+$ m/z 370.2125, found m/z 370.2124. IR (neat): 3317, 2968, 1724, 1656, 1608.

(S)-Cyclopentyl 2-(((1',5'-dimethyl-6'-oxo-1',6'-dihydro-[3,3'-bipyridin]-6-yl)methyl)amino)-3-hydroxypropanoate 2.73d

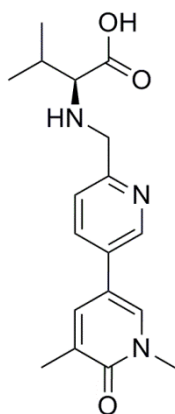
To a carousel tube was added 1',5'-dimethyl-6'-oxo-1',6'-dihydro-[3,3'-bipyridine]-6-carbaldehyde (73 mg, 0.26 mmol) and (S)-cyclopentyl 2-amino-3-hydroxypropanoate 4-methylbenzene sulfonate (177 mg, 0.51 mmol) along with DCM (6 mL) and the resulting suspension stirred under nitrogen for 20 min. Sodium triacetoxyborohydride (163 mg, 0.77 mmol) was added and the reaction mixture stirred under nitrogen at RT for 2 h. An additional portion of sodium triacetoxyborohydride (100 mg, 0.52 mmol) was added as required and the reactions stirred for 5 h. After this time, the reaction mixture was diluted with DCM (20 mL), the mixture washed with saturated aqueous sodium hydrogen carbonate solution (20 mL) and the layers separated. The aqueous phase was extracted with DCM (3 x 20 mL) and the organics combined, dried by passing through a hydrophobic frit and the solvent removed under reduced pressure. The crude product was dissolved in DMSO (2 x 1 mL) and purified by mass directed autoprep on an Xbridge column using 15-55% acetonitrile water with an ammonium carbonate modifier. The solvent was evaporated *in vacuo* to give the required product (S)-cyclopentyl 2-(((1',5'-dimethyl-6'-oxo-1',6'-dihydro-[3,3'-bipyridin]-6-yl)methyl)amino)-3-hydroxypropanoate (58 mg, 0.14 mmol, 56% yield) as a yellow gum. LCMS (High pH): *rt* = 0.76 min, *MH*⁺ 386.4. ¹H NMR δ(400 MHz, CDCl₃) ppm: 8.63 (1H, d, *J*=2.2 Hz), 7.69 (1H, dd, *J*=8.1, 2.4 Hz), 7.46 (1H, dd, *J*=2.4, 1.2 Hz), 7.41 (1H, d, *J*=2.4 Hz), 7.35 (1H, d, *J*=8.1 Hz), 5.28 - 5.21 (1H, m), 4.10 (1H, d, *J*=14.7 Hz), 3.94 (1H, d, *J*=14.7 Hz), 3.84 (1H, dd, *J*=11.1, 4.3 Hz), 3.70 (1H, dd, *J*=11.0, 6.4 Hz), 3.64 (3H, s), 3.48 (1H, dd, *J*=6.2, 4.3 Hz), 2.24 (3H, s), 1.93 - 1.82 (2H, m), 1.75 - 1.67 (4H, m), 1.65 - 1.56 (2H, m).

(2S,3R)-Cyclopentyl 2-(((1',5'-dimethyl-6'-oxo-1',6'-dihydro-[3,3'-bipyridin]-6-yl)methyl) amino)-3-hydroxybutanoate, 2.73e

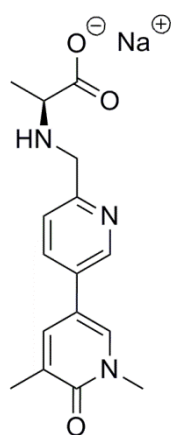
To a carousel tube was added 1',5'-dimethyl-6'-oxo-1',6'-dihydro-[3,3'-bipyridine]-6-carbaldehyde (73 mg, 0.26 mmol) and (2S,3R)-cyclopentyl 2-amino-3-hydroxybutanoate 4-methylbenzene sulfonate (184 mg, 0.51 mmol) along with DCM (6 mL) and the resulting suspension stirred under nitrogen for 20 min. Sodium triacetoxyborohydride (163 mg, 0.77 mmol) was added and the reaction mixture stirred under nitrogen at RT for 2 h. An additional portion of sodium triacetoxyborohydride (100 mg, 0.52 mmol) was added and the reactions stirred for 5 h. A third portion of sodium triacetoxyborohydride (100 mg, 0.52 mmol) was added and stirred for 18 h. After this time, the reaction mixture was diluted with DCM (20 mL), the mixture washed with saturated aqueous sodium hydrogen carbonate solution (20 mL) and the layers separated. The aqueous was extracted with DCM (3 x 20 mL) and the organics combined, dried by passing through a hydrophobic frit and the solvent removed under reduced pressure. The crude product was dissolved in DMSO (2 x 1 mL) and purified by mass directed autoprep on an Xbridge column using 15-55% acetonitrile water with an ammonium carbonate modifier. The solvent was evaporated *in vacuo* to give the required product (2S,3R)-cyclopentyl 2-(((1',5'-dimethyl-6'-oxo-1',6'-dihydro-[3,3'-bipyridin]-6-yl)methyl)amino)-3-hydroxybutanoate (48 mg, 0.12 mmol, 47% yield) as a light yellow gum. LCMS (high pH): rt = 0.83 min, MH⁺ 400.4. ¹H NMR δ(400 MHz, CDCl₃) ppm: 8.62 (1H, d, J=2.0 Hz), 7.69 (1H, dd, J=8.1, 2.4 Hz), 7.46 (1H, dd, J=2.3, 1.1 Hz), 7.40 (1H, d, J=2.4 Hz), 7.36 (1H, d, J=8.1 Hz), 5.25 - 5.17 (1H, m), 4.04 (1H, d, J=14.4 Hz), 3.89 (1H, d, J=14.4 Hz), 3.78 - 3.70 (1H, m), 3.64 (3H, s), 3.04 (1H, d, J=7.6 Hz), 2.24 (3H, s), 1.92 - 1.81 (2H, m), 1.77 - 1.58 (6H, m), 1.22 (3H, d, J=6.1 Hz). ¹³C NMR d(101 MHz, CDCl₃) ppm: 173.1 (COO), 162.7 (C=O), 157.7 (C-CH₂), 146.4 (NCH), 136.0 (C-C), 133.8 (CH), 133.2 (CH), 131.3 (CH), 130.4 (C-CH₃), 122.2 (CH), 116.1 (C-C), 78.1 (OCH), 68.1 (CHOH), 67.9 (NCH), 53.4 (NCH₂), 38.2 (N-CH₃), 32.73 (CH₂), 32.69 (CH₂), 23.7 (CH₂), 23.6 (CH₂), 19.4 (COHCH₃), 17.4 (C-CH₃). HRMS (ESI) exact mass calculated for C₂₂H₃₀N₃O₄ [M+H]⁺ m/z 400.2231, found m/z 400.2226. IR (neat): 3348, 2968, 1722, 1654, 1606.

(S)-2-(((1',5'-Dimethyl-6'-oxo-1',6'-dihydro-[3,3'-bipyridin]-6-yl)methyl)amino)-4-methyl pentanoic acid, 2.84a

To a carousel tube was added (S)-cyclopentyl 2-(((1',5'-dimethyl-6'-oxo-1',6'-dihydro-[3,3'-bipyridin]-6-yl)methyl)amino)-4-methyl pentanoate (45 mg, 0.11 mmol), tetrahydrofuran (2 mL), methanol (2 mL) and water (1 mL). To the stirred solution was added lithium hydroxide (10.5 mg, 0.44 mmol) a condenser fitted and the mixture warmed to 50 °C for 3 h. The reaction mixture was cooled to room temperature and acetic acid (0.5 ml) was added before the volatiles were removed *in vacuo* to give a yellow oil. The resulting oil was dissolved in DMSO (1 mL) and purified by mass directed autoprep on an Xbridge column using 5 to 30% acetonitrile water with an ammonium carbonate modifier. The fractions containing the desired products were collected and the solvent was evaporated *in vacuo* to give the required product (S)-2-(((1',5'-dimethyl-6'-oxo-1',6'-dihydro-[3,3'-bipyridin]-6-yl)methyl) amino)-4-methylpentanoic acid (30 mg, 0.09 mmol, 78% yield) as a white solid. LCMS (high pH): rt = 0.53 min, MH⁺ 344.3. ¹H NMR δ(400 MHz, Methanol-*d*₄) ppm: 8.77 (1H, d, *J*=2.0 Hz), 7.98 (1H, dd, *J*=8.1, 2.0 Hz), 7.94 (1H, d, *J*=2.0 Hz), 7.77 (1H, s), 7.50 (1H, d, *J*=8.1 Hz), 4.28 (1H, d, *J*=14.7 Hz), 4.20 (1H, d, *J*=14.7 Hz), 3.65 (3H, s), 3.50 (1H, t, *J*=7.1 Hz), 2.19 (3H, s), 1.96 - 1.86 (1H, m), 1.80 - 1.70 (1H, m), 1.70 - 1.59 (1H, m), 0.99 (3H, d, *J*=6.6 Hz), 0.95 (3H, d, *J*=6.6 Hz). ¹³C NMR δ(101 MHz, Methanol-*d*₄) ppm: 174.7 (COO), 163.1 (C=O), 152.1 (C-CH₂N), 146.0 (N-CH), 136.6 (CH), 134.7 (CH), 134.2 (CH), 132.1 (C-C), 129.0 (C-CH₃), 122.8 (CH), 116.5 (C-C), 61.4 (NCH), 50.2 (NCH₂), 40.6 (NCH-CH₂), 37.1 (N-CH₃), 24.7 (CH-(CH₃)₂), 21.6 (CH-CH₃), 21.5 (CH-CH₃), 15.9 (C-CH₃). IR (neat): 2955, 1655, 1593. HRMS (ESI) exact mass calculated for C₁₉H₂₆N₃O₃ [M+H]⁺ m/z 344.1969, found m/z 344.1971.

(S)-2-(((1',5'-Dimethyl-6'-oxo-1',6'-dihydro-[3,3'-bipyridin]-6-yl)methyl)amino)-3-methyl butanoic acid, 2.84b

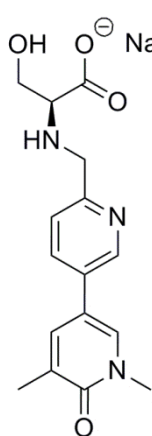
To a carousel tube was charged (S)-cyclopentyl 2-(((1',5'-dimethyl-6'-oxo-1',6'-dihydro-[3,3'-bipyridin]-6-yl)methyl)amino)-3-methyl butanoate (57 mg, 0.143 mmol), tetrahydrofuran (2 mL), methanol (2 mL) and water (1 mL). To the stirred solution was added lithium hydroxide (27.5 mg, 1.15 mmol) and the mixture warmed to 50 °C for 3 h. The reaction mixture was cooled to room temperature and acetic acid (0.5 ml) was added before the volatiles were removed *in vacuo* to give a yellow oil. The resulting oil was dissolved in DMSO (1 ml) and purified by mass directed autoprep on an Xbridge column using 5-30% acetonitrile water with an ammonium carbonate modifier. The fractions containing the desired products were collected and the solvent was evaporated *in vacuo* to give the required product (S)-2-(((1',5'-dimethyl-6'-oxo-1',6'-dihydro-[3,3'-bipyridin]-6-yl)methyl) amino)-3-methylbutanoic acid (43 mg, 0.13 mmol, 89% yield) as an off-white solid. LCMS (high pH): rt = 0.49 min, MH⁺ 330.3. ¹H NMR δ(400 MHz, Methanol-*d*₄) ppm: 8.80 (1H, d, *J*=2.2 Hz), 8.00 (1H, dd, *J*=8.2, 2.3 Hz), 7.96 (1H, d, *J*=2.2 Hz), 7.81 - 7.76 (1H, m), 7.50 (1H, d, *J*=8.1 Hz), 4.37 (1H, d, *J*=14.7 Hz), 4.28 (1H, d, *J*=14.9 Hz), 3.65 (3H, s), 3.40 (1H, d, *J*=4.2 Hz), 2.33 - 2.22 (1H, m), 2.20 (3H, s), 1.10 (6H, 2 x d (overlapping), *J*=7.3 Hz). HRMS (ESI) exact mass calculated for C₁₈H₂₄N₃O₃ [M+H]⁺ m/z 330.1812, found m/z 330.1815.

(S)-2-(((1',5'-Dimethyl-6'-oxo-1',6'-dihydro-[3,3'-bipyridin]-6-yl)methyl)amino) propanoate, sodium salt, 2.84c

To a carousel tube was charged (S)-cyclopentyl 2-(((1',5'-dimethyl-6'-oxo-1',6'-dihydro-[3,3'-bipyridin]-6-yl)methyl)amino) propanoate (30 mg, 0.08 mmol), tetrahydrofuran (2 mL), methanol (2 mL) and water (1 mL). To the stirred solution was added lithium hydroxide (7.8 mg, 0.33 mmol) and the mixture warmed to 50 °C for 3 h. The reaction mixture was cooled to room temperature and acetic acid (0.5 mL) was added before the volatiles were removed *in vacuo* to give a yellow oil. The resulting oil was dissolved in DMSO (1 mL) and purified by mass directed autoprep on an Xbridge column using

5-30% acetonitrile water with an ammonium carbonate modifier. The fractions containing the desired products were collected and the solvent was evaporated *in vacuo* to give the crude product (15 mg, 0.05 mmol). This material was slurried in a DCM/methanol/tetrahydrofuran solution (1.5 mL, 1:1:1) prior to the addition of sodium hydroxide (2 M) (25 μ L, 0.05 mmol). The resultant solution was stirred for 5 minutes prior to blow down and drying in the vacuum oven to yield (S)-2-(((1',5'-dimethyl-6'-oxo-1',6'-dihydro-[3,3'-bipyridin]-6-yl)methyl)amino) propanoate, sodium salt (18 mg, 0.05 mmol, 65% yield) as a white gum. LCMS (high pH): rt = 0.42 min, MH⁺ 302.1. ¹H NMR δ (400 MHz, DMSO-*d*₆) ppm: 8.68 (1H, d, *J*=2.2 Hz), 8.05 (1H, d, *J*=2.4 Hz), 7.90 (1H, dd, *J*=8.1, 2.4 Hz), 7.78 - 7.71 (1H, m), 7.44 (1H, d, *J*=8.3 Hz), 3.82 - 3.75 (1H, m), 3.68 (1H, d, *J*=13.0 Hz), 3.52 (3H, s), 2.80 - 2.71 (1H, m), 2.08 (3H, s), 1.07 (3H, d, *J*=6.8 Hz). HRMS (ESI) exact mass calculated for C₁₆H₂₀N₃O₃ [M+H]⁺ m/z 302.1499, found m/z 302.1498 (for parent neutral compound).

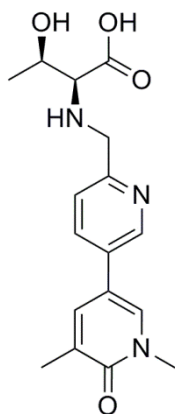
(S)-2-(((1',5'-Dimethyl-6'-oxo-1',6'-dihydro-[3,3'-bipyridin]-6-yl)methyl)amino)-3-hydroxy propanoate, sodium salt, 2.84d



To a round bottomed flask was added (S)-cyclopentyl 2-(((1',5'-dimethyl-6'-oxo-1',6'-dihydro-[3,3'-bipyridin]-6-yl)methyl)amino)-3-hydroxypropanoate (20 mg, 0.052 mmol), tetrahydrofuran (1 mL), methanol (1 mL) and water (0.5 mL). To the stirred solution was added lithium hydroxide (5.0 mg, 0.21 mmol), an air condenser fitted and the mixture warmed to 50 °C for 3 hours. An additional portion of lithium hydroxide (15 mg, 0.40 mmol) was added and stirred for 16 h. The reaction mixture was cooled to room temperature and the solvent removed under a stream of nitrogen. The yellow gum was dissolved in methanol (0.5 mL). To the resulting cloudy solution was added acetic acid, forming a precipitate. Sodium hydroxide (2 M) was added to effect dissolution before the volatiles were removed *in vacuo* to give a yellow oil. The resulting oil was dissolved in 1:1 MeOH:DMSO (1 mL) and purified by mass directed autoprep on an Xbridge column using 5-30% acetonitrile water with an ammonium carbonate modifier. The fractions containing the desired product were collected and the solvent was evaporated *in vacuo* to give the crude product as a white solid. The solid was suspended in methanol (3 mL) and a drop of sodium

hydroxide (2 M) was added to form a clear solution. The solution was filtered and the solvent removed under a stream of nitrogen to yield (*S*)-2-(((1',5'-dimethyl-6'-oxo-1',6'-dihydro-[3,3'-bipyridin]-6-yl)methyl)amino)-3-hydroxypropanoate, sodium salt (6.5 mg, 0.018 mmol, 35% yield) as a white solid. LCMS (high pH): *rt* = 0.40 min, *MH*⁺ 318.2. ¹H NMR δ (400 MHz, Methanol-*d*₄) ppm: 8.71 - 8.65 (1H, m), 8.00 - 7.91 (2H, m), 7.80 (1H, br. s.), 7.57 (1H, d, *J*=8.1 Hz), 4.06 (1H, d, *J*=14.2 Hz), 3.89 (1H, d, *J*=14.2 Hz), 3.84 - 3.77 (1H, m), 3.74 - 3.65 (4H, m), 3.21 (1H, t, *J*=5.5 Hz), 2.22 (3H, s). HRMS (ESI) exact mass calculated for C₁₆H₂₀N₃O₄ [*M*+*H*]⁺ *m/z* 318.1448, found *m/z* 318.1451 (for parent neutral compound).

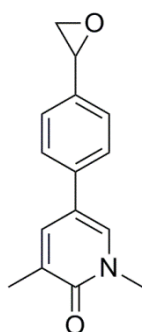
(2*S*,3*R*)-2-(((1',5'-Dimethyl-6'-oxo-1',6'-dihydro-[3,3'-bipyridin]-6-yl)methyl)amino)-3-hydroxybutanoic acid, 2.84e



To a carousel tube was charged (*2S,3R*)-cyclopentyl 2-(((1',5'-dimethyl-6'-oxo-1',6'-dihydro-[3,3'-bipyridin]-6-yl)methyl)amino)-3-hydroxybutanoate (65 mg, 0.16 mmol), tetrahydrofuran (2 mL), methanol (2 mL) and water (1 mL). To the stirred solution was added lithium hydroxide (15.6 mg, 0.65 mmol), a condenser fitted and the mixture warmed to 50 °C for 3 h. The reaction mixture was cooled to room temperature and acetic acid (0.5 mL) was added before the volatiles were removed *in vacuo* to give a yellow oil. The resulting oil was dissolved in DMSO (1 mL) and purified by mass directed autoprep on an Xbridge column using 5-30% acetonitrile water with an ammonium carbonate modifier. The fractions containing the desired products were collected and the solvent was evaporated *in vacuo* to give the required product (*2S,3R*)-2-(((1',5'-dimethyl-6'-oxo-1',6'-dihydro-[3,3'-bipyridin]-6-yl)methyl) amino)-3-hydroxybutanoic acid (49 mg, 0.14 mmol, 86% yield) as a white solid. LCMS (high pH): *rt* = 0.42 min, *MH*⁺ 332.2. ¹H NMR δ (400 MHz, Methanol-*d*₄) ppm: 8.84 (1H, d, *J*=1.8 Hz), 8.04 (1H, dd, *J*=8.1, 2.5 Hz), 7.98 (1H, d, *J*=2.3 Hz), 7.81 (1H, dd, *J*=2.4, 1.1 Hz), 7.52 (1H, d, *J*=8.1 Hz), 4.47 (1H, d, *J*=14.9 Hz), 4.38 (1H, d, *J*=14.9 Hz), 4.14 - 4.06 (1H, m), 3.68 (3H, s), 3.40 (1H, d, *J*=7.1 Hz), 2.22 (3H, s), 1.39 (3H, d, *J*=6.3 Hz). ¹³C NMR δ (101 MHz, Methanol-*d*₄) ppm: 170.5 (COO), 163.1 (C=O), 150.1 (C-CH₂N), 146.1 (N-CH), 136.6 (CH), 134.8 (CH), 134.3 (CH), 132.5 (C-C), 129.0 (C-CH₃), 122.9 (CH), 116.4 (C-C), 68.6 (CHOH), 66.2 (NCH), 49.8 (N-CH₂), 37.1 (N-CH₃), 20.0 (CH-CH₃), 15.8 (C-CH₃). IR (neat): 2975, 1657, 1597. HRMS

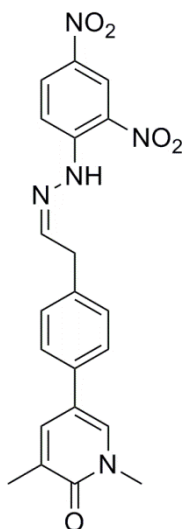
(ESI) exact mass calculated for $C_{17}H_{22}N_3O_4$ $[M+H]^+$ m/z 332.1605, found m/z 332.1611.

1,3-Dimethyl-5-(4-(oxiran-2-yl)phenyl)pyridin-2(1H)-one, 2.97



Sodium hydride (46 mg, 1.15 mmol) was weighed into a dry three-necked, round-bottomed flask including a stirrer bar and rubber septums. A reflux condenser was fitted and the system was placed under nitrogen by evacuating and filling with nitrogen several times. Dry DMSO (0.4 mL, 5.64 mmol) was introduced via hypodermic syringe and the mixture is heated with stirring to 70 °C for 45 min, yielding an orange solution. The solution was cooled to room temperature, diluted with tetrahydrofuran (0.5 mL) (to prevent freezing) and then cooled in a salt-ice bath. With stirring, a solution of trimethylsulfonium iodide (184 mg, 0.9 mmol) in dimethyl sulfoxide (0.67 mL) was added over a period of about 2 min. After the addition of the salt was complete, the mixture was stirred for 1 min longer before adding 4-(1,5-dimethyl-6-oxo-1,6-dihydropyridin-3-yl)benzaldehyde (193 mg, 0.85 mmol), dissolved in dimethyl sulfoxide (1 mL) and tetrahydrofuran (2 mL), at a moderately rapid rate. Stirring was continued at salt-ice temperature for 10 minutes and then for 60 min with the bath removed. The reaction mixture was diluted with water (10 mL) and the product extracted with diethyl ether (5 x 15 mL). The combined organics were washed with water (10 mL), dried by passing through a hydrophobic frit and the solvent removed *in vacuo* to yield the desired product 1,3-dimethyl-5-(4-(oxiran-2-yl)phenyl)pyridin-2(1H)-one (214 mg, 0.75 mmol, 66% yield, 90% purity) as an off-white solid. R_f = 0.40, 100% ethyl acetate. LCMS (high pH): rt = 0.80 min, MH^+ = 242.1. 1H NMR δ (400 MHz, DMSO- d_6) ppm: 8.01 (1H, d, $J=2.4$ Hz), 7.73 - 7.77 (1H, m), 7.57 (2H, d, $J=8.3$ Hz), 7.33 (2H, d, $J=8.3$ Hz), 3.95 (1H, dd, $J=3.9, 2.7$ Hz), 3.52 (3H, s), 3.14 (1H, dd, $J=5.4, 4.2$ Hz), 2.89 (1H, dd, $J=5.4, 2.4$ Hz), 2.08 (3H, s). IR (neat): 1650, 829.

Attempted synthesis of **5-(4-(2-(2-(2,4-dinitrophenyl)hydrazono)ethyl)phenyl)-1,3-dimethylpyridin-2(1H)-one, 2.99**



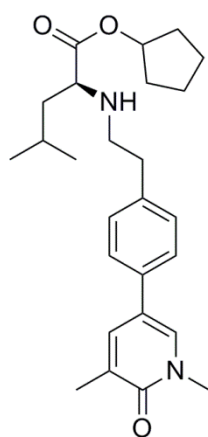
To a solution of 1,3-dimethyl-5-(4-(oxiran-2-yl)phenyl)pyridin-2(1H)-one (80 mg, 0.33 mmol) in tetrahydrofuran (2 mL) cooled in an ice bath was added boron trifluoride diethyl etherate (20 μ L, 0.17 mmol). The reaction mixture was stirred at RT for 15 min. After this time, 2,4-dinitrophenylhydrazine, hydrochloride (156 mg, 0.66 mmol) and triethylamine (0.14 mL, 0.99 mmol) were added. The mixture was stirred for 2 h. After this time, the desired mass ion (MH^+ 422.2) was observed at $rt = 1.16$ min. The solvent was removed *in vacuo* and to the resulting solid was added a 1:1 mixture of ethyl acetate:water (30 mL). The layers were separated and the aqueous washed with ethyl acetate (2 x 20 mL). The combined organics were washed with brine (10 mL), dried by passing through a hydrophobic frit and the solvent removed under reduced pressure. The resulting solid was dissolved in DCM (4 mL) and loaded onto a 25 g SNAP silica column. The crude material on silica was purified using a Biotage SP4 using a gradient of 0 - 50% ethyl acetate in cyclohexane. No desired product was isolated.

General procedure for synthesis of homologated ESM compounds 2.85a-e

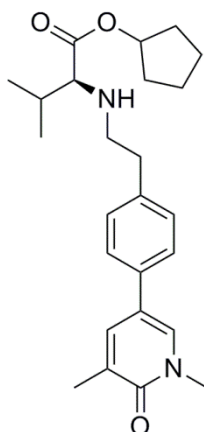
To a round bottomed flask was added 1,3-dimethyl-5-(4-(oxiran-2-yl)phenyl)pyridin-2(1H)-one (a) and the flask flushed with nitrogen before dissolution in tetrahydrofuran (7.5 mL). To the solution, cooled in an ice bath, was added boron trifluoride diethyl etherate (b). The reaction mixture was stirred at RT for 15 min. After this time, an amino ester (c) and triethylamine (d) were added. The mixture was stirred for 20 min before sodium triacetoxyborohydride (e) was added and the mixture stirred for 2 h. If the reaction was incomplete, additional portions of sodium triacetoxyborohydride (f) were added and stirred for an additional time (g). After this time, the reaction mixture was diluted with DCM (30 mL), the mixture washed with saturated aqueous sodium hydrogen carbonate solution (30 mL) and the layers separated. The aqueous was extracted with DCM (3 x 30 mL) and the organics combined, dried by passing through a hydrophobic frit and the solvent removed under reduced pressure. The resulting gum was dissolved in DCM (2 mL) and

loaded onto a 10 g SNAP silica column. The crude material on silica was purified using a Biotage SP4 using a gradient of 0 - 10% 2 M methanolic ammonia in DCM. Fractions containing product were collected and the solvent removed *in vacuo*. The samples were dissolved in DMSO and purified by mass directed autoprep on an Xbridge column using gradient (h) acetonitrile water with an ammonium carbonate modifier. The solvent was evaporated *in vacuo* to yield the desired product (i).

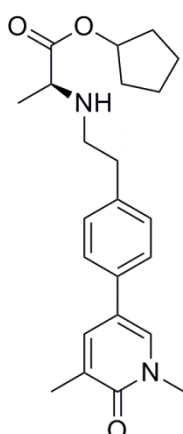
(S)-Cyclopentyl 2-((4-(1,5-dimethyl-6-oxo-1,6-dihydropyridin-3-yl)phenethyl) amino)-4-methylpentanoate, 2.85a



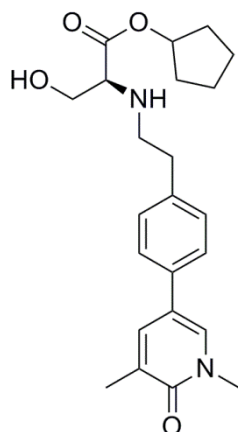
(a) 80 mg, 0.33 mmol, (b) 20 μ L, 0.17 mmol, (c) (S)-cyclopentyl 2-amino-4-methylpentanoate 4-methylbenzenesulfonate (246 mg, 0.66 mmol), (d) 0.14 mL, 1.00 mmol, (e) 141 mg, 0.66 mmol, (h) 50-99%, (i) (S)-cyclopentyl 2-((4-(1,5-dimethyl-6-oxo-1,6-dihydropyridin-3-yl)phenethyl) amino)-4-methylpentanoate (25 mg, 0.06 mmol, 18% yield) as a yellow solid. LCMS (high pH): rt = 1.33 min, MH⁺ 425.5. ¹H NMR δ (400 MHz, CDCl₃) ppm: 7.49 (1H, dd, *J*=2.5, 1.3 Hz), 7.35 (1H, d, *J*=2.3 Hz), 7.32 (2H, d, *J*=8.3 Hz), 7.24 (2H, d, *J*=8.1 Hz), 5.23 - 5.17 (1H, m), 3.62 (3H, s), 3.24 (1H, t, *J*=7.3 Hz), 2.90 - 2.79 (2H, m), 2.79 - 2.70 (2H, m), 2.22 (3H, s), 1.92 - 1.78 (2H, m), 1.75 - 1.58 (7H, m), 1.48 - 1.38 (2H, m), 0.92 (3H, d, *J*=6.6 Hz), 0.89 (3H, d, *J*=6.6 Hz). ¹³C NMR δ (126 MHz, CDCl₃) ppm: 175.4 (COO), 162.7 (C=O), 138.8 (C-CH₂), 136.7 (C-CH), 134.8 (C-C), 132.8 (N-CH), 129.6 (C-CH₃), 129.3 (2xCH), 125.9 (2xCH), 119.6 (C-C), 77.4 (O-CH), 60.1 (N-CH), 49.2 (N-CH₂), 42.7 (CH₂), 38.1 (N-CH₃), 36.0 (C-CH₂), 32.8 (CH₂), 32.7 (CH₂), 25.0 (CH(CH₃)₂), 23.68 (CH₂), 23.65 (CH₂), 22.7 (CH-CH₃), 22.4 (CH-CH₃), 17.5 (C-CH₃). HRMS (ESI) exact mass calculated for C₂₆H₃₇N₂O₃ [M+H]⁺ m/z 425.2799, found m/z 425.2784.

(S)-Cyclopentyl 2-((4-(1,5-dimethyl-6-oxo-1,6-dihydropyridin-3-yl)phenethyl)amino)-3-methylbutanoate, 2.85b

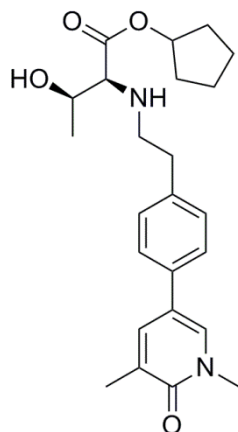
(a) 150 mg, 0.62 mmol, (b) 38 μ L, 0.31 mmol, (c) (S)-cyclopentyl 2-amino-3-methylbutanoate 4-methylbenzenesulfonate (444 mg, 1.24 mmol), (d) 0.26 mL, 1.87 mmol, (e) 329 mg, 1.55 mmol, (f) 10 mg, 0.05 mmol (g) 1 h, (h) 50-99%, (i) (S)-cyclopentyl 2-((4-(1,5-dimethyl-6-oxo-1,6-dihydropyridin-3-yl)phenethyl)amino)-3-methyl butanoate (30 mg, 0.07 mmol, 11% yield) as a clear gum. LCMS (high pH): rt = 1.29 min, MH+ 411.5. 1 H NMR d(400 MHz, CDCl₃) ppm: 7.49 (1H, dd, $J=2.4, 1.2$ Hz), 7.36 (1H, d, $J=2.4$ Hz), 7.34 - 7.30 (2H, m), 7.26 - 7.22 (2H, m), 5.25 - 5.18 (1H, m), 3.62 (3H, s), 2.96 (1H, d, $J=6.1$ Hz), 2.92 - 2.65 (4H, m), 2.22 (3H, s), 1.94 - 1.78 (3H, m), 1.76 - 1.54 (6H, m), 0.92 (3H, d, $J=6.8$ Hz), 0.93 (3H, d, $J=6.8$ Hz). HRMS (ESI) exact mass calculated for C₂₅H₃₅N₂O₃ [M+H]⁺ m/z 411.2642, found m/z 411.2642.

(S)-Cyclopentyl 2-((4-(1,5-dimethyl-6-oxo-1,6-dihydropyridin-3-yl)phenethyl)amino)propanoate, 2.85c

(a) 80 mg, 0.33 mmol, (b) 20 μ L, 0.17 mmol, (c) (S)-cyclopentyl 2-aminopropanoate 4-methylbenzenesulfonate (218 mg, 0.66 mmol), (d) 0.14 mL, 1.00 mmol, (e) 141 mg, 0.66 mmol, (h) 30-85%, (i) (S)-cyclopentyl 2-((4-(1,5-dimethyl-6-oxo-1,6-dihydropyridin-3-yl)phenethyl)amino)propanoate (26 mg, 0.068 mmol, 21% yield) as a yellow gum. LCMS (high pH): rt = 1.07 min, MH+ 383.4. 1 H NMR δ (400 MHz, CDCl₃) ppm: 7.51 - 7.47 (1H, m), 7.36 (1H, d, $J=2.4$ Hz), 7.33 (2H, d, $J=8.1$ Hz), 7.25 (2H, d, $J=8.1$ Hz), 5.22 - 5.16 (1H, m), 3.62 (3H, s), 3.32 (1H, q, $J=7.1$ Hz), 2.92 - 2.83 (2H, m), 2.83 - 2.74 (2H, m), 2.22 (3H, s), 1.92 - 1.75 (2H, m), 1.75 - 1.55 (6H, m), 1.27 (3H, d, $J=7.1$ Hz). 13 C NMR δ (101 MHz, CDCl₃) ppm: 175.4 (COO), 162.7 (C=O), 138.8 (C-C), 136.7 (N-CH), 134.8 (C-C), 132.8 (C-CH), 129.6 (C-CH₃), 129.3 (2xCH), 125.9 (2xCH), 119.6 (C-C), 77.4 (C-O), 56.7 (N-CH), 49.0 (CH₂), 38.1 (N-CH₃), 36.2 (CH₂), 32.71 (CH₂), 32.68 (CH₂), 23.70 (CH₂), 23.69 (CH₂), 19.0 (CHCH₃), 17.4 (C-CH₃). IR (CDCl₃): 2965, 1727, 1652. HRMS (ESI) exact mass calculated for C₂₃H₃₁N₂O₃ [M+H]⁺ m/z 383.2329, found m/z 383.2327.

(S)-Cyclopentyl 2-((4-(1,5-dimethyl-6-oxo-1,6-dihydropyridin-3-yl)phenethyl)amino)-3-hydroxypropanoate, 2.85d

(a) 300 mg, 1.24 mmol, (b) 76 μ L, 0.62 mmol, (c) (S)-cyclopentyl 2-amino-3-hydroxypropanoate 4-methylbenzene sulfonate (859 mg, 2.49 mmol), (d) (0.52 mL, 3.73 mmol), (e) 659 mg, 3.11 mmol, (f) 45 mg, 0.21 mmol (g) 1 h. (h) 30-85%, (i) (S)-cyclopentyl 2-((4-(1,5-dimethyl-6-oxo-1,6-dihydropyridin-3-yl)phenethyl)amino)-3-hydroxy propanoate (153 mg, 0.37 mmol, 29% yield) as a yellow gum. LCMS (high pH): rt = 0.91 min, MH⁺ 399.4. ¹H NMR δ (400 MHz, CDCl₃) ppm: 7.49 (1H, dd, *J*=2.4, 1.0 Hz), 7.36 (1H, d, *J*=2.7 Hz), 7.35 - 7.32 (2H, m), 7.26 - 7.22 (2H, m), 5.25 - 5.18 (1H, m), 3.74 (1H, dd, *J*=10.6, 4.5 Hz), 3.62 (3H, s), 3.53 (1H, dd, *J*=10.6, 6.7 Hz), 3.34 (1H, dd, *J*=6.7, 4.5 Hz), 3.05 - 2.97 (1H, m), 2.90 - 2.75 (3H, m), 2.22 (3H, s), 1.92 - 1.81 (2H, m), 1.74 - 1.56 (6H, m). HRMS (ESI) exact mass calculated for C₂₃H₃₁N₂O₄ [M+H]⁺ m/z 399.2278, found m/z 399.2276.

(2S,3R)-Cyclopentyl 2-((4-(1,5-dimethyl-6-oxo-1,6-dihydropyridin-3-yl)phenethyl)amino)-3-hydroxybutanoate, 2.85e

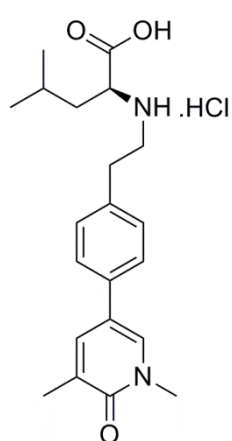
(a) 300 mg, 1.24 mmol, (b) 76 μ L, 0.62 mmol, (c) (2S,3R)-cyclopentyl 2-amino-3-hydroxybutanoate 4-methylbenzene sulfonate (894 mg, 2.49 mmol), (d) (0.52 mL, 3.73 mmol), (e) 659 mg, 3.11 mmol, (f) 250 mg, 1.18 mmol, 260 mg, 1.23 mmol, 260 mg, 1.23 mmol (g) 1 h, 30 min, 30 min, (h) 30 to 85%, (i) (2S,3R)-Cyclopentyl 2-((4-(1,5-dimethyl-6-oxo-1,6-dihydropyridin-3-yl)phenethyl)amino)-3-hydroxybutanoate (152 mg, 0.37 mmol, 30% yield) as a clear gum. LCMS (high pH): rt = 1.02 min, MH⁺ 413.5. ¹H NMR δ (400 MHz, CDCl₃) ppm: 7.49 (1H, dd, *J*=2.4, 1.2 Hz), 7.36 (1H, d, *J*=2.4 Hz), 7.35 - 7.31 (2H, m), 7.25 - 7.20 (2H, m), 5.25 - 5.20 (1H, m), 3.62 (3H, s), 3.61 - 3.54 (1H, m), 3.03 - 2.95 (1H, m), 2.92 (1H, d, *J*=8.1 Hz), 2.87 - 2.81 (1H, m), 2.81 - 2.72 (2H, m), 2.22 (3H, s), 1.93 - 1.81 (2H, m), 1.75 - 1.55 (6H, m), 1.19 (3H, d, *J*=6.1 Hz). ¹³C NMR δ (101 MHz, CDCl₃) ppm: 173.3 (COO), 162.7 (C=O), 138.5 (C-CH₂), 136.6 (N-CH), 134.9 (C-C), 132.8 (C-CH), 129.6 (C-CH₃), 129.3 (2 x CH), 125.9 (2 x CH), 119.5 (C-C), 78.0 (C-O), 68.3 (NH-CH), 67.8 (CH-OH), 49.7 (CH₂), 38.0 (N-CH₃), 36.2 (CH₂), 32.73 (CH₂),

32.69 (CH₂), 23.7 (CH₂), 23.6 (CH₂), 19.3 (CH-CH₃), 17.4 (C-CH₃). IR (CDCl₃): 3380, 2967, 1724, 1652, 1595. HRMS (ESI) exact mass calculated for C₂₄H₃₃N₂O₄ [M+H]⁺ m/z 413.2435, found m/z 413.2434.

General procedure for hydrolysis to homologated acids 2.101a-e

A carousel tube was charged with (a), tetrahydrofuran (1 mL), methanol (1 mL) and water (0.5 mL). To the stirred solution was added lithium hydroxide (b), a condenser fitted and the mixture warmed to 50 °C overnight. If the reaction after this time was incomplete, a further portion of lithium hydroxide (c) was added and stirred for additional time (d). The reaction mixture was cooled to room temperature and acetic acid (0.25 mL) was added before the volatiles were removed *in vacuo* to give a yellow oil. The resulting oil was dissolved in DMSO (1 mL) and purified by mass directed autoprep on an Xbridge column using gradient (e) acetonitrile water with an ammonium carbonate modifier. The fractions containing the desired products were collected and the solvent was evaporated *in vacuo* to give the crude product as a white solid, which was further dried by vacuum oven. The solid was suspended in tetrahydrofuran and 2 M aqueous HCl solution (0.5 mL) was added. The clear solution was blown down a stream of nitrogen to yield the desired product (f).

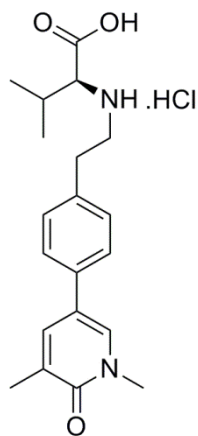
(S)-2-((4-(1,5-Dimethyl-6-oxo-1,6-dihydropyridin-3-yl)phenethyl)amino)-4-methyl pentanoic acid, hydrochloride, 2.101a



(a) (S)-Cyclopentyl 2-((4-(1,5-dimethyl-6-oxo-1,6-dihydropyridin-3-yl)phenethyl) amino)-4-methylpentanoate (20 mg, 0.05 mmol), (b) 2.4 mg, 0.10 mmol, (e) 5-30%, (f) (S)-2-((4-(1,5-dimethyl-6-oxo-1,6-dihydropyridin-3-yl)phenethyl)amino)-4-methylpentanoic acid, hydrochloride (7.4 mg, 0.02 mmol, 40% yield) as a white solid. LCMS (formic acid): rt = 0.59 min, MH⁺ 357.3. ¹H NMR δ(400 MHz, DMSO-*d*₆) ppm: 9.45 (1H, br. s.), 9.28 (1H, br. s.), 7.99 (1H, d, *J*=2.4 Hz), 7.76 - 7.71 (1H, m), 7.55 (2H, d, *J*=8.3 Hz), 7.30 (2H, d, *J*=8.1 Hz), 3.95 - 3.87 (1H, m), 3.52 (3H, s), 3.28 - 3.11 (2H, m), 3.09 - 2.93 (2H, m), 2.09 (3H, s), 1.86 - 1.67 (3H, m), 0.93 (6H, d, *J*=5.9 Hz). ¹³C NMR δ(151 MHz, DMSO-*d*₆) ppm: 170.5 (COO), 161.5 (C=O), 135.6 (C-CH), 135.3 (C-CH₂), 134.8 (C-C), 134.2 (N-CH), 129.0 (2 x CH), 127.7 (C-CH₃), 125.3 (2 x CH), 116.7 (C-C), 57.7 (CH-NH₂), 46.5 (CH₂), 37.8 (CH₂), 37.1 (N-

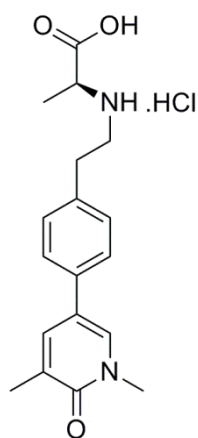
CH₃), 31.1 (CH₂), 24.2 (CH(CH₃)₂), 22.8 (CH₃), 21.3 (CH₃), 17.0 (C-CH₃). HRMS (ESI) exact mass calculated for C₂₁H₂₉N₂O₃ [M+H]⁺ m/z 357.2173, found m/z 357.2166 (for parent neutral compound).

(S)-2-((4-(1,5-Dimethyl-6-oxo-1,6-dihydropyridin-3-yl)phenethyl)amino)-3-methyl butanoic acid, hydrochloride, 2.101b



(a) (S)-Cyclopentyl 2-((4-(1,5-dimethyl-6-oxo-1,6-dihydropyridin-3-yl)phenethyl) amino)-3-methylbutanoate (17 mg, 0.04 mmol), (b) 2.1 mg, 0.09 mmol, (c) 12 mg, 0.50 mmol, 12 mg, 0.50 mmol, 6 mg, 0.25 mmol, (d) 4 h, 16 h, 6 h, (e) 5-30%, (f) (S)-2-((4-(1,5-dimethyl-6-oxo-1,6-dihydropyridin-3-yl)phenethyl)amino)-3-methyl butanoic acid, hydrochloride (11 mg, 0.028 mmol, 69% yield) as a white solid. LCMS (high pH): rt = 0.55 min, MH⁺ 343.3. ¹H NMR δ(400 MHz, DMSO-*d*₆) ppm: 9.13 (2H, br. s.), 7.98 (1H, d, *J*=2.5 Hz), 7.75 - 7.71 (1H, m), 7.55 (2H, d, *J*=8.2 Hz), 7.29 (2H, d, *J*=8.2 Hz), 3.95 - 3.89 (1H, m), 3.52 (3H, s), 3.25 - 3.10 (2H, m), 3.10 - 2.94 (2H, m), 2.42 - 2.32 (1H, m), 2.08 (3H, s), 1.07 (3H, d, *J*=7.1 Hz), 0.99 (3H, d, *J*=6.9 Hz). ¹³C NMR δ(126 MHz, CDCl₃) ppm: 169.4 (COOH), 161.6 (C=O), 135.7 (N-CH), 135.4 (C-CH₂), 134.9 (C-C), 134.3 (CH), 129.1 (2 x CH), 127.8 (C-CH₃), 125.4 (2 x CH), 116.7 (C-C), 64.5 (N-CH), 47.5 (N-CH₂), 37.2 (N-CH₃), 31.0 (CH₂), 28.3 (CH-(CH₃)₂), 19.3 (CH-CH₃), 17.1 (C-CH₃), 16.9 (CH-CH₃). IR (neat): 2734, 1721, 1644, 1514, 1546. HRMS (ESI) exact mass calculated for C₂₀H₂₇N₂O₃ [M+H]⁺ m/z 343.2016, found m/z 343.2016 (for parent neutral compound).

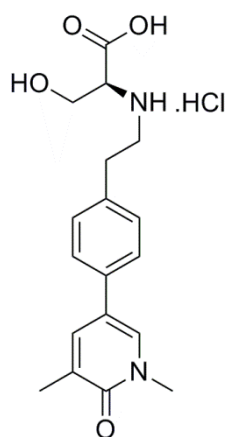
(S)-2-((4-(1,5-Dimethyl-6-oxo-1,6-dihydropyridin-3-yl)phenethyl)amino) propanoic acid, hydrochloride, 2.101c



(a) (S)-Cyclopentyl 2-((4-(1,5-dimethyl-6-oxo-1,6-dihydropyridin-3-yl)phenethyl) amino)propanoate (20 mg, 0.05 mmol), (b) 2.6 mg, 0.11 mmol, (e) 5-30%, (f) (S)-2-((4-(1,5-dimethyl-6-oxo-1,6-dihydropyridin-3-yl)phenethyl)amino)propanoic acid, hydrochloride (15 mg, 0.04 mmol, 79% yield) as a white solid. LCMS (formic acid): rt = 0.48 min, MH⁺ 315.1. ¹H NMR δ(400 MHz, DMSO-*d*₆) ppm: 9.59 (1H, br. s.), 9.22 (1H, br. s.), 7.99 (1H, d, *J*=2.4 Hz), 7.74 (1H, dd, *J*=2.4, 1.0 Hz), 7.55 (2H, d, *J*=8.3 Hz), 7.31 (2H, d, *J*=8.3 Hz), 4.09 - 3.99 (1H, m), 3.52 (3H, s), 3.28 - 3.10 (2H, m),

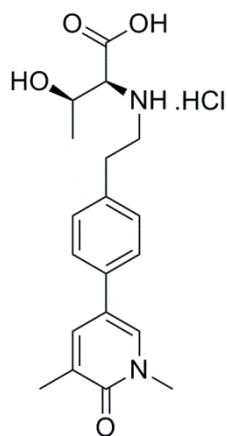
3.06 - 2.98 (2H, m), 2.08 (3H, s), 1.50 (3H, d, $J=7.1$ Hz). ^{13}C NMR δ (151 MHz, DMSO- d_6) ppm: 170.9 (COOH), 161.5 (C=O), 135.6 (C-CH), 135.4 (C-CH₂), 134.8 (C-C), 134.2 (N-CH), 129.0 (2 x CH), 127.7 (C-CH₃), 125.3 (2 x CH), 116.7 (C-C), 54.3 (N-CH), 45.8 (CH₂), 37.1 (N-CH₃), 31.1 (CH₂), 17.0 (C-CH₃), 14.2 (CH-CH₃). IR (neat): 3415, 2732, 1732, 1650, 821. HRMS (ESI) exact mass calculated for C₁₈H₂₃N₂O₃ [M+H]⁺ m/z 315.1703, found m/z 315.1701 (for parent neutral compound). Melting Point: 245 - 255 (decomposed).

(S)-2-((4-(1,5-Dimethyl-6-oxo-1,6-dihydropyridin-3-yl)phenethyl)amino)-3-hydroxypropanoic acid, hydrochloride, 2.101d



(a) (S)-Cyclopentyl 2-((4-(1,5-dimethyl-6-oxo-1,6-dihydropyridin-3-yl)phenethyl) amino)-3-hydroxypropanoate (48 mg, 0.12 mmol), (b) 6.1 mg, 0.26 mmol, (c) 12 mg, 0.51 mmol, 12 mg, 0.51 mmol, 3 mg, 0.18 mmol, (d) 4 h, 4 h, 16 h, (e) 5-30%, (f) (S)-2-((4-(1,5-dimethyl-6-oxo-1,6-dihydropyridin-3-yl)phenethyl) amino)-3-hydroxy propanoic acid, hydrochloride (30 mg, 0.08 mmol, 66% yield) as a white solid. LCMS (high pH): rt = 0.49 min, MH⁺ 331.3. ^1H NMR δ (400 MHz, DMSO- d_6) ppm: 9.24 (1H, br. s.), 9.16 (1H, br. s.), 7.97 (1H, d, $J=2.4$ Hz), 7.72 (1H, d, $J=1.5$ Hz), 7.57 - 7.52 (2H, m), 7.31 - 7.26 (2H, m), 4.12 - 4.07 (1H, m), 3.99 (1H, dd, $J=12.2, 2.9$ Hz), 3.91 (2H, dd, $J=12.0, 3.4$ Hz), 3.52 (3H, s), 3.29 - 3.14 (2H, m), 3.08 - 2.99 (2H, m), 2.08 (3H, s).

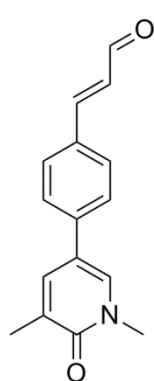
(2S,3R)-2-((4-(1,5-Dimethyl-6-oxo-1,6-dihydropyridin-3-yl)phenethyl)amino)-3-hydroxybutanoic acid, hydrochloride, 2.101e



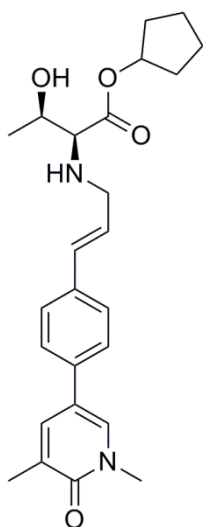
(a) (2S,3R)-Cyclopentyl 2-((4-(1,5-dimethyl-6-oxo-1,6-dihydro pyridin-3-yl)phenethyl)amino)-3-hydroxybutanoate (50 mg, 0.12 mmol), (b) 6.1 mg, 0.26 mmol, (c) 12 mg, 0.51 mmol, 12 mg, 0.51 mmol, 3 mg, 0.18 mmol, (d) 4 h, 4 h, 16 h, (e) 5-30%, (f) (2S,3R)-2-((4-(1,5-dimethyl-6-oxo-1,6-dihydropyridin-3-yl) phenethyl)amino)-3-hydroxybutanoic acid, hydrochloride (26 mg, 0.07 mmol, 55% yield) as a white solid. LCMS (high pH): rt = 0.51 min, MH⁺ 345.3. ^1H NMR δ (400 MHz, DMSO- d_6) ppm: 9.07 (1H, br. s.), 8.97 (1H, br. s.), 7.97 (1H, d, $J=2.4$ Hz), 7.72 (1H, dd, 2.5, 1.0 Hz), 7.56 - 7.52 (2H, m), 7.30 - 7.26 (2H, m), 4.14 (1H, quin, $J=6.2$ Hz),

3.90 - 3.84 (1H, m), 3.52 (3H, s), 3.30 - 3.12 (2H, m), 3.12 - 2.93 (2H, m), 2.08 (3H, s), 1.29 (3H, d, $J=6.6$ Hz). ^{13}C NMR δ (126 MHz, $\text{DMSO}-d_6$) ppm: 169.4 (COOH), 162.1 (C=O), 136.2 (N-CH), 136.0 (C-CH₂), 135.3 (C-C), 134.8 (C-CH), 129.6 (2xCH), 128.2 (C-CH₃), 125.9 (2xCH), 117.2 (C-C), 65.7 (CHOH), 65.4 (N-CH), 48.3 (N-CH₂), 37.7 (N-CH₃), 31.4 (C-CH₂), 21.1 (COH-CH₃), 17.6 (C-CH₃). IR (neat): 2745, 1717, 1650, 1513, 1548. HRMS (ESI) exact mass calculated for $\text{C}_{19}\text{H}_{25}\text{N}_2\text{O}_4$ $[\text{M}+\text{H}]^+$ m/z 345.1809, found m/z 345.1809 (for parent neutral compound). Melting point: 219 - 233 (decomp).

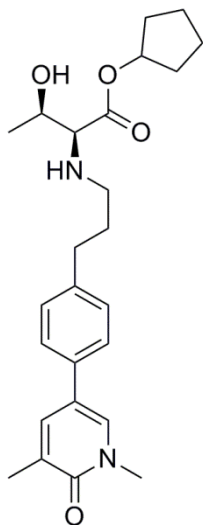
(E)-3-(4-(1,5-Dimethyl-6-oxo-1,6-dihydropyridin-3-yl)phenyl)acrylaldehyde, 2.103



A solution of 4-(1,5-dimethyl-6-oxo-1,6-dihydropyridin-3-yl)benzaldehyde (200 mg, 0.88 mmol) and 2-(triphenylphosphoranylidene)acetaldehyde (321 mg, 1.06 mmol) in toluene (7 mL) was stirred at 80 °C for 16 h. The reaction was cooled to room temperature before the solvent was removed *in vacuo*. The resulting brown solid was dissolved in DCM (10 mL) and loaded onto a 25 g SNAP silica column. The crude material on silica was purified by Biotage SP4 using a gradient of 50 - 100% ethyl acetate in cyclohexane over 20 CV. Fractions containing the desired product were collected and the solvent removed under reduced pressure to yield the desired product (*E*)-3-(4-(1,5-dimethyl-6-oxo-1,6-dihydropyridin-3-yl)phenyl)acrylaldehyde (138 mg, 0.38 mmol, 43% yield) (70% purity, contaminated with 4-(1,5-dimethyl-6-oxo-1,6-dihydropyridin-3-yl)benzaldehyde **2.66** and (2,4)-5-(4-(1,5-dimethyl-6-oxo-1,6-dihydropyridin-3-yl)phenyl)penta-2,4-dienal **2.105** as a yellow solid. LCMS (formic acid): r_t = 0.78 min, MH^+ 254.1. ^1H NMR δ (400 MHz, CDCl_3) ppm: (key resonances from crude spectra) 9.72 (1H, d, $J=7.6$ Hz), 6.74 (1H, dd, $J=15.9, 7.6$ Hz).

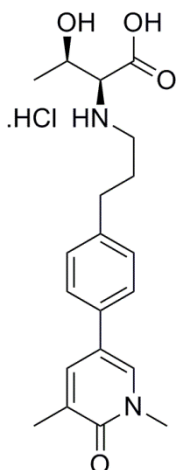
(2S,3R)-Cyclopentyl 2-(((E)-3-(4-(1,5-dimethyl-6-oxo-1,6-dihydropyridin-3-yl)phenyl)allyl)amino)-3-hydroxybutanoate, 2.102

To a round bottomed flask was added (*E*)-3-(4-(1,5-dimethyl-6-oxo-1,6-dihydropyridin-3-yl)phenyl)acrylaldehyde (130 mg, 0.51 mmol) and (2*S*,3*R*)-cyclopentyl 2-amino-3-hydroxybutanoate, 4-methylbenzenesulfonic acid salt (369 mg, 1.03 mmol) along with DCM (10 mL) and the resulting suspension stirred under nitrogen for 20 min. Sodium triacetoxyborohydride (326 mg, 1.54 mmol) was added and the reaction mixture stirred under nitrogen at room temperature overnight. After this time, the reaction mixture was diluted with DCM (30 mL), the mixture washed with saturated aqueous sodium hydrogen carbonate solution (25 mL) and the layers separated. The aqueous phase was extracted with DCM (2 x 30 mL) and the organics combined, dried by passing through a hydrophobic frit and the solvent removed under reduced pressure. The crude product was dissolved in DMSO (2 x 1 mL) and purified by mass directed autoprep on Xbridge column using 30-85% acetonitrile water with an ammonium carbonate modifier. The solvent was evaporated *in vacuo* to give the required product (2*S*,3*R*)-cyclopentyl 2-(((*E*)-3-(4-(1,5-dimethyl-6-oxo-1,6-dihydropyridin-3-yl)phenyl)allyl)amino)-3-hydroxybutanoate (113 mg, 0.25 mmol, 49% yield) as a yellow gum. LCMS (high pH): *rt* = 1.04 min, MH⁺ 425.4. ¹H NMR δ(400 MHz, CDCl₃) ppm: 7.51 (1H, dd, *J*=2.4, 1.2 Hz), 7.42 - 7.33 (5H, m), 6.51 (1H, d, *J*=15.9 Hz), 6.22 (1H, dt, *J*=15.7, 6.4 Hz), 5.24 - 5.19 (1H, m), 3.67 - 3.64 (1H, m), 3.63 (3H, s), 3.46 (1H, ddd, *J*=13.9, 6.9, 1.2 Hz), 3.37 (1H, ddd, *J*=13.9, 6.1, 1.5 Hz), 2.97 (1H, d, *J*=7.8 Hz), 2.23 (3H, s), 1.91 - 1.77 (2H, m), 1.75 - 1.54 (6H, m), 1.22 (3H, d, *J*=6.4 Hz). HRMS (ESI) exact mass calculated for C₂₅H₃₃N₂O₄ [M+H]⁺ *m/z* 425.2435, found *m/z* 425.2436.

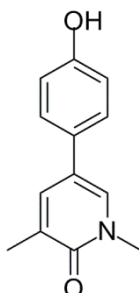
(2S,3R)-Cyclopentyl 2-(((E)-3-(4-(1,5-dimethyl-6-oxo-1,6-dihydropyridin-3-yl)phenyl)propyl)amino)-3-hydroxybutanoate, 2.86e

To a solution of (2S,3R)-cyclopentyl 2-(((E)-3-(4-(1,5-dimethyl-6-oxo-1,6-dihydropyridin-3-yl)phenyl)allyl)amino)-3-hydroxybutanoate (78 mg, 0.18 mmol) in ethanol (5 mL) under nitrogen at RT was added 10% palladium on carbon (50% water) (8 mg, 75 μ mol). The reaction mixture was placed under a hydrogen atmosphere and stirred at RT for 16 h. LCMS analysis showed the reaction to have gone to completion. The reaction mixture was kept under a flow of nitrogen while being filtered through celite, and the celite washed with ethanol (30 mL). The crude product was collected and the solvent removed under reduced pressure.

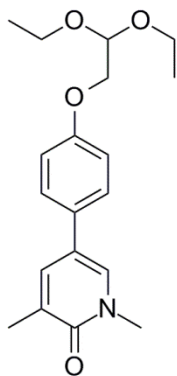
The sample was dissolved in DMSO (1 mL) and purified by mass directed autoprep on an Xbridge column using 30-85% acetonitrile water with an ammonium carbonate modifier. The solvent was evaporated *in vacuo* to give the required product (2S,3R)-cyclopentyl 2-(((E)-3-(4-(1,5-dimethyl-6-oxo-1,6-dihydropyridin-3-yl)phenyl)propyl) amino)-3-hydroxybutanoate (58 mg, 0.13 mmol, 73% yield) as a clear gum. LCMS (high pH): rt = 1.08 min, MH⁺ 427.4. ¹H NMR δ (400 MHz, CDCl₃) ppm: 7.49 (1H, dd, *J*=2.6, 1.1 Hz), 7.36 (1H, d, *J*=2.4 Hz), 7.34 - 7.30 (2H, m), 7.23 - 7.19 (2H, m, *J*=8.3 Hz), 5.26 - 5.20 (1H, m), 3.63 - 3.55 (4H, m), 2.88 (1H, d, *J*=7.8 Hz), 2.77 - 2.66 (3H, m), 2.51 (1H, dt, *J*=11.6, 7.2 Hz), 2.22 (3H, s), 1.92 - 1.76 (3H, m), 1.76 - 1.57 (7H, m), 1.21 (3H, d, *J*=6.1 Hz). ¹³C NMR δ (101 MHz, CDCl₃) ppm: 173.6 (COO), 162.7 (C=O), 140.8 (C-CH₂), 136.7 (N-CH), 134.5 (C-C), 132.7 (C-CH), 129.6 (C-CH₃), 129.0 (2 x CH), 125.8 (2 x CH), 119.6 (C-C), 78.1 (C-O), 68.3 (N-CH), 67.8 (CHOH), 48.0 (N-CH₂), 38.0 (N-CH₃), 32.9 (C-CH₂), 32.8 (CH₂), 32.7 (CH₂), 31.8 (CH₂), 23.7 (CH₂), 23.6 (CH₂), 19.4 (CH-CH₃), 17.4 (C-CH₃). IR (CDCl₃): 3368, 2937, 1723, 1653. HRMS (ESI) exact mass calculated for C₂₅H₃₅N₂O₄ [M+H]⁺ m/z 427.2591, found m/z 427.2593.

(2S,3R)-2-((3-(4-(1,5-Dimethyl-6-oxo-1,6-dihydropyridin-3-yl)phenyl)propyl)amino)-3-hydroxybutanoic acid, hydrochloride, 2.106

A carousel tube was charged with (2S,3R)-cyclopentyl 2-((3-(4-(1,5-dimethyl-6-oxo-1,6-dihydropyridin-3-yl)phenyl)propyl)amino)-3-hydroxybutanoate (34 mg, 0.08 mmol), tetrahydrofuran (1 mL), methanol (1 mL) and water (0.5 mL). To the stirred solution was added lithium hydroxide (5.7 mg, 0.24 mmol), a condenser fitted and the mixture warmed to 50 °C for 72 h. After this time, the reactions were incomplete. To the reaction was added lithium hydroxide (10 mg, 0.42 mmol) and the reaction stirred for 4 h. The reaction mixture was cooled to room temperature and the solvent removed *in vacuo* to give a yellow oil. The resulting oil was dissolved in DMSO (1 mL) and purified by mass directed autoprep on Xbridge column using 5-30% acetonitrile water with an ammonium carbonate modifier. The fractions containing the desired products were collected and the solvent was evaporated *in vacuo* to give the crude product as a white solid, which was further dried by vacuum oven. The solid was suspended in tetrahydrofuran and 2 M aqueous HCl solution (1 mL) was added. The clear solution was blown down a stream of nitrogen to yield (2S,3R)-2-((3-(4-(1,5-dimethyl-6-oxo-1,6-dihydropyridin-3-yl)phenyl)propyl)amino)-3-hydroxy butanoic acid, hydrochloride (9 mg, 0.02 mmol, 29% yield) as a pale brown solid. LCMS (high pH): *rt* = 0.56 min, *MH*⁺ 359.2. ¹H NMR δ (400 MHz, DMSO-*d*₆) ppm: 8.90 (1H, br. s.), 8.65 (1H, br. s.), 7.95 (1H, d, *J*=2.7 Hz), 7.74 - 7.70 (1H, m), 7.51 (2H, d, *J*=8.3 Hz), 7.25 (2H, d, *J*=8.1 Hz), 4.08 (1H, t, *J*=6.0 Hz), 3.84 - 3.78 (2H, m), 3.51 (3H, s), 3.05 - 2.90 (2H, m), 2.68 - 2.66 (1H, m), 2.63 (1H, d, *J*=7.1 Hz), 2.08 (3H, s), 2.05 - 1.86 (2H, m), 1.25 (3H, d, *J*=6.4 Hz).

5-(4-Hydroxyphenyl)-1,3-dimethylpyridin-2(1H)-one, 2.1

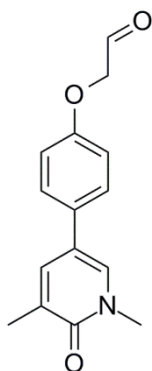
To a solution of 5-bromo-1,3-dimethylpyridin-2(1H)-one (1.95 g, 9.65 mmol) and (4-hydroxyphenyl)boronic acid (2.0 g, 14.5 mmol) in 1,4-dioxane (53 ml) and water (2.1 ml) stirred under nitrogen at RT was added palladium tetrakis triphenylphosphine (335 mg, 0.29 mmol) and 1 M aqueous potassium carbonate (29 ml, 29 mmol). The reaction mixture was stirred at 95 °C for 3 h. After cooling to room temperature, the reaction mixture was diluted with water (75 mL) and ethyl acetate (25 mL), the layers separated and the organics collected. The aqueous phase was further extracted with ethyl acetate (2 x 90 mL) and the organics combined. A portion of product remained in the aqueous layer. The aqueous was acidified with 2 M aqueous HCl and further extracted with ethyl acetate (2 x 90 mL). The organics were combined, passed through celite, dried by passing through a hydrophobic frit and the solvent removed under reduced pressure. To the resulting brown gum was added DCM and the resulting solid filtered and washed with further DCM to yield 5-(4-hydroxyphenyl)-1,3-dimethylpyridin-2(1H)-one (1.49 g, 6.85 mmol, 71% yield) as a light brown solid. LCMS (formic acid): rt = 0.62 min, MH⁺ 216.1. ¹H NMR δ(400 MHz, Methanol-*d*₄) ppm: 7.72 - 7.69 (2H, m), 7.38 - 7.33 (2H, m), 6.87 - 6.82 (2H, m), 3.65 (3H, s), 2.20 (3H, s). ¹³C NMR δ(101 MHz, Methanol-*d*₄) ppm: 162.9 (C=O), 156.8 (C-O), 137.7 (C-H), 132.8 (C-H), 128.1 (C-C), 127.7 (C-C), 126.7 (2 x CH), 121.2 (C-CH₃), 115.4 (2 x CH), 37.0 (N-CH₃), 15.9 (C-CH₃). IR (neat): 3103, 1650, 1228, 831. Melting point: 225 - 227 °C.

5-(4-(2,2-Diethoxyethoxy)phenyl)-1,3-dimethylpyridin-2(1H)-one, 2.108

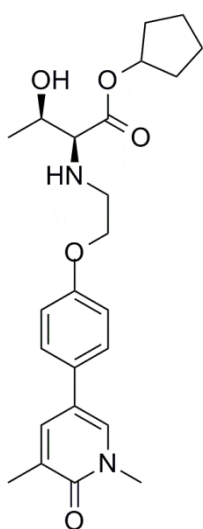
To a solution of 5-(4-hydroxyphenyl)-1,3-dimethylpyridin-2(1H)-one (500 mg, 2.32 mmol) in *N,N*-dimethylformamide (23 mL) was added solid potassium carbonate (482 mg, 3.48 mmol) followed by 2-bromo-1,1-diethoxyethane (454 μL, 3.02 mmol). The reaction mixture was stirred at 90 °C for 20 h. LCMS analysis confirmed the reaction to be incomplete. Therefore, an additional portion of 2-bromo-1,1-diethoxyethane (0.454 mL, 3.02 mmol) was added and the reaction stirred for 96 h. The reaction had proceeded to near completion. An additional portion of 2-bromo-1,1-diethoxyethane (0.454 mL, 3.02 mmol) and stirred for 7 h. The solvent was removed under reduced pressure and the

resulting gum dissolved in ethyl acetate (30 mL) and washed with saturated aqueous sodium bicarbonate (3 x 30 mL). The combined organics were dried by passing through a hydrophobic frit and the solvent removed *in vacuo*. The resulting pale brown solid was dissolved in DCM (3 mL) and loaded onto a 25 g SNAP silica column and purified by Biotage SP4 using a gradient of 0 - 12.5% ethanol in ethyl acetate. Fractions containing the desired product were collected and the solvent removed under reduced pressure to yield 5-(4-(2,2-diethoxyethoxy)phenyl)-1,3-dimethylpyridin-2(1H)-one (435 mg, 1.31 mmol, 57% yield) as a pale yellow gum. LCMS (high pH): *rt* = 1.04 min, *MH*⁺ 332.3. ¹H NMR δ (400 MHz, CDCl₃) ppm: 7.47 (1H, dd, *J*=2.4, 1.2 Hz), 7.34 - 7.28 (3H, m), 6.99 - 6.94 (2H, m), 4.85 (1H, t, *J*=5.1 Hz), 4.03 (2H, d, *J*=5.1 Hz), 3.83 - 3.63 (4H, m), 3.62 (3H, s), 2.22 (3H, s), 1.26 (6H, t, *J*=7.1 Hz).

2-(4-(1,5-Dimethyl-6-oxo-1,6-dihydropyridin-3-yl)phenoxy)acetaldehyde, 2.107

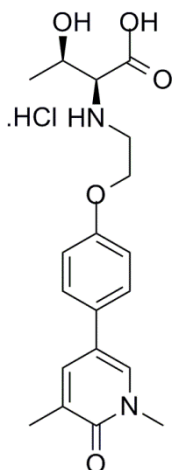


To a solution of 5-(4-(2,2-diethoxyethoxy)phenyl)-1,3-dimethylpyridin-2(1H)-one (210 mg, 0.63 mmol) in tetrahydrofuran (3 mL) and water (0.1 mL) was added *p*-toluenesulfonic acid monohydrate (5.3 mg, 0.028 mmol). The reaction mixture was stirred at 70 °C for 22 h. After this time, the reaction was cooled and concentrated to yield the crude product 2-(4-(1,5-dimethyl-6-oxo-1,6-dihydropyridin-3-yl)phenoxy)acetaldehyde which was used directly in the next step.

(2S,3R)-Cyclopentyl 2-((2-(4-(1,5-dimethyl-6-oxo-1,6-dihydropyridin-3-yl)phenoxy)ethyl)amino)-3-hydroxybutanoate, 2.87e

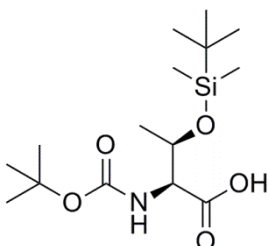
To a round bottomed flask was added 2-(4-(1,5-dimethyl-6-oxo-1,6-dihydropyridin-3-yl)phenoxy)acetaldehyde (160 mg, 0.62 mmol) and (2S,3R)-cyclopentyl 2-amino-3-hydroxybutanoate, 4-methylbenzenesulfonic acid salt (447 mg, 1.24 mmol) along with DCM (15 mL) and the resulting suspension stirred under nitrogen for 20 min. Sodium triacetoxyborohydride (395 mg, 1.87 mmol) was added and the reaction mixture stirred under nitrogen at room temperature for 18 h. After this time, the reaction was incomplete. An additional portion of sodium triacetoxyborohydride (100 mg, 0.47 mmol) was added and stirred for 1 h. Again the reaction was incomplete so an additional portion of sodium triacetoxyborohydride (100 mg, 0.47 mmol) was added and stirred for 1 h. After this time, the reaction mixture was diluted with DCM (30 mL), the mixture washed with saturated aqueous sodium hydrogen carbonate solution (25 mL) and the layers separated. The aqueous was extracted with DCM (2 x 30 mL) and the organics combined, dried by passing through a hydrophobic frit and the solvent removed under reduced pressure. The crude product was dissolved in 1:1 methanol:dimethylsulfoxide (3 x 1 mL) and purified by mass directed autoprep on an Xbridge column using 30-85% acetonitrile water with an ammonium carbonate modifier. The solvent was evaporated *in vacuo* to give the required product (2S,3R)-cyclopentyl 2-((2-(4-(1,5-dimethyl-6-oxo-1,6-dihydropyridin-3-yl)phenoxy)ethyl)amino)-3-hydroxybutanoate (80 mg, 0.19 mmol, 30% yield) as a clear gum. LCMS (high pH): rt = 1.01 min, 429.4. ¹H NMR δ(400 MHz, CDCl₃) ppm: 7.46 (1H, dd, *J*=2.4, 1.2 Hz), 7.34 - 7.29 (3H, m), 6.95 - 6.90 (2H, m), 5.25 - 5.19 (1H, m), 4.06 (2H, dd, *J*=5.6, 4.6 Hz), 3.70 - 3.63 (1H, m), 3.62 (3H, s), 3.19 - 3.11 (1H, m), 3.00 (1H, d, *J*=7.6 Hz), 2.89 (1H, dt, *J*=12.7, 4.4 Hz), 2.22 (3H, s), 1.92 - 1.82 (2H, m), 1.78 - 1.57 (6H, m), 1.23 (3H, d, *J*=6.4 Hz). ¹³C NMR δ(101 MHz, CDCl₃) ppm: 173.1 (COO), 162.6 (C=O), 158.0 (C-O), 136.7 (C-CH), 132.3 (N-CH), 129.8 (C-C), 129.5 (C-CH₃), 127.0 (2 x CH), 119.4 (C-C), 115.0 (2 x CH), 78.2 (CH-O), 68.4 (N-CH), 67.9 (CH-OH), 67.8 (O-CH₂), 47.8 (CH₂), 38.0 (N-CH₃), 32.7 (2 x CH₂), 23.7 (CH₂), 23.6 (CH₂), 19.4 (CH-CH₃), 17.4 (C-CH₃). IR (CDCl₃): 3357, 2967, 1725, 1654, 1247. HRMS (ESI) exact mass calculated for C₂₄H₃₃N₂O₅ [M+H]⁺ m/z 429.2384, found m/z 429.2386. [α_D]^{24.6°C}_λ(c 0.5, CDCl₃): +19.6 °.

(2S,3R)-2-((2-(4-(1,5-Dimethyl-6-oxo-1,6-dihydropyridin-3-yl)phenoxy)ethyl)amino)-3-hydroxybutanoic acid, hydrochloride, 2.111



A solution of (2S,3R)-cyclopentyl 2-((2-(4-(1,5-dimethyl-6-oxo-1,6-dihydropyridin-3-yl) phenoxy)ethyl)amino)-3-hydroxybutanoate (25 mg, 0.058 mmol) in DMSO (0.25 mL) was added to a solution of pig liver esterase (lyophilized solid) (10 mg), in phosphate buffer solution pH 7.2 (0.5 mL). The mixture was stirred at room temperature for 18 hours. Methanol was added, whereupon a thick suspension occurred. The solid was removed by filtration and the resulting solution blown down under a stream of nitrogen. Methanol was added to make the solution up to 1 mL, and the sample was purified by mass directed autoprep on Xbridge column using 5-30% acetonitrile water with an ammonium carbonate modifier. The solvent was evaporated *in vacuo* and further dried in a vacuum oven for 1 week. To the resulting white solid was added water (0.5 mL) and 2 M aqueous HCl added dropwise. The solvent was evaporated under a stream of nitrogen to yield the desired product (2S,3R)-2-((2-(4-(1,5-dimethyl-6-oxo-1,6-dihydropyridin-3-yl)phenoxy)ethyl)amino)-3-hydroxybutanoic acid, hydrochloride (12.3 mg, 0.029 mmol, 51% yield) as a light brown solid. LCMS (high pH): rt = 0.51 min, MH⁺ 361.4. ¹H NMR δ(400 MHz, DMSO-*d*₆) ppm: 9.19 (2H, br. s.), 7.90 (1H, d, *J*=2.4 Hz), 7.68 (1H, dd, *J*=2.4, 1.0 Hz), 7.57 - 7.48 (2H, m), 7.05 - 6.98 (2H, m), 4.34 (2H, t, *J*=5.1 Hz), 4.15 (1H, quin, *J*=6.2 Hz), 3.97 - 3.88 (1H, m), 3.56 - 3.38 (5H, m), 2.08 (3H, s), 1.29 (3H, d, *J*=6.6 Hz).

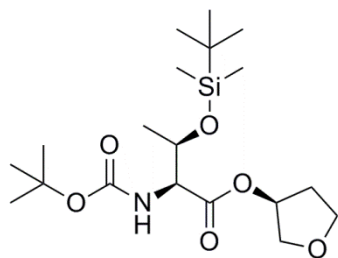
(2S,3R)-2-((*tert*-Butoxycarbonyl)amino)-3-((*tert*-butyldimethylsilyl)oxy)butanoic acid, 2.120



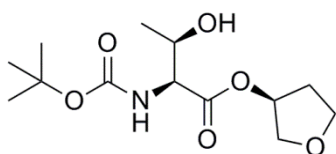
To a solution of (2S,3R)-2-((*tert*-butoxycarbonyl)amino)-3-hydroxybutanoic acid (1.0 g, 4.56 mmol) in *N,N*-dimethylformamide (9 mL) stirred at 0 °C was added *tert*-butyldimethylchlorosilane (0.89 g, 5.93 mmol) followed by imidazole (0.93 g, 13.7 mmol) and the mixture was stirred at 0 °C for 1 h. The reaction was warmed to RT and stirred for an additional 18 h. After this time, the reaction mixture was diluted diethyl ether (40 mL) and 1 M aqueous HCl (40 mL). The organic layer was separated and the aqueous extracted with diethyl ether (2 x 40 mL). The organic layers were combined, dried by passing

through a hydrophobic frit and the solvent removed *in vacuo*. The crude oil was diluted with DCM (3 mL) and loaded onto a 50 g SNAP silica column. The crude material on silica was purified by Biotage SP4 using a gradient of 10 - 75% ethyl acetate in cyclohexane over 17 CV. Fractions containing the desired product were collected and the solvent removed under reduced pressure to yield the desired product (2*S*,3*R*)-2-((*tert*-butoxycarbonyl)amino)-3-((*tert*-butyldimethylsilyl)oxy)butanoic acid (1.1 g, 3.30 mmol, 72% yield) as a clear oil, which formed a white solid on scraping. ¹H NMR δ(400 MHz, CDCl₃) ppm: 5.23 (1H, d, *J*=8.3 Hz), 4.44 (1H, d, *J*=4.5 Hz), 4.26 (1H, d, *J*=7.6 Hz), 1.46 (9H, s), 1.21 (3H, d, *J*=6.1 Hz), 0.87 (9H, s), 0.11 - 0.04 (6H, m). ¹³C NMR δ(101 MHz, CDCl₃) ppm: 175.2 (COOH), 156.0 (CO), 80.1 (OC(CH₃)₃), 68.6 (CO), 59.0 (CNH), 28.3 (OC(CH₃)₃), 25.6 (SiC(CH₃)₃), 19.9 (SiC(CH₃)₃), 17.8 (CH₃), -4.6 (SiCH₃), -5.2 (SiCH₃). HRMS (ESI) exact mass calculated for C₁₅H₃₂NO₅Si [M+H]⁺ *m/z* 334.2044, found *m/z* 334.2054.

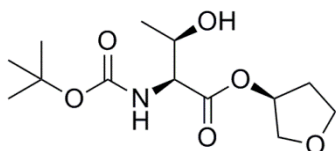
(2*S*,3*R*)-(S)-Tetrahydrofuran-3-yl 2-((*tert*-butoxycarbonyl)amino)-3-((*tert*-butyldimethylsilyl)oxy)butanoate, 2.121



To a solution of (2*S*,3*R*)-2-((*tert*-butoxycarbonyl)amino)-3-((*tert*-butyldimethyl silyl)oxy)butanoic acid (76 mg, 0.23 mmol) in *N,N*-dimethylformamide (0.5 mL) was added diisopropylethylamine (80 μL, 0.46 mmol), 1-hydroxybenzotriazole hydrate (42 mg, 0.27 mmol), *N*-(3-dimethylaminopropyl)-*N*-ethylcarbodiimide hydrochloride (52 mg, 0.27 mmol), DMAP (2.8 mg, 0.023 mmol) and (*S*)-tetrahydrofuran-3-ol (183 μL, 2.28 mmol). The reaction mixture was stirred at RT for 16 h and left to stand for 24 h. The reaction mixture was partitioned between ethyl acetate (2.5 mL) and saturated sodium hydrogen carbonate (2.5 mL). The organic phase was separated, washed with 2 M HCl (2 mL), water (2 mL) and brine (2 mL). The organic phase was dried and evaporated to give the crude product (2*S*,3*R*)-(S)-tetrahydrofuran-3-yl 2-((*tert*-butoxycarbonyl)amino)-3-((*tert*-butyldimethylsilyl)oxy)butanoate (55 mg, 0.14 mmol, 60% yield) as a colourless oil. ¹H NMR δ(400 MHz, CDCl₃) ppm 5.32 (1H, br. s.), 5.17 (1H, d, *J*=9.8 Hz), 4.42 (1H, q, *J*=5.8 Hz), 4.18 (1H, d, *J*=9.8 Hz), 3.95 - 3.78 (4H, m), 2.25 - 2.11 (1H, m), 2.11 - 1.98 (1H, m), 1.48 (9H, s), 1.22 (3H, d, *J*=6.1 Hz), 0.86 (9H, s), 0.06 (3H, s), 0.01 (3H, s).

(2S,3R)-(S)-Tetrahydrofuran-3-yl 2-((*tert*-butoxycarbonyl)amino)-3-hydroxybutanoate, 2.122

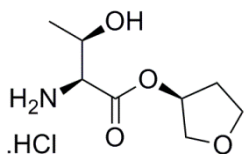
To a solution of (2S,3R)-2-((*tert*-butoxycarbonyl)amino)-3-hydroxybutanoic acid (50 mg, 0.23 mmol) in *N,N*-dimethylformamide (0.5 mL) was added diisopropylethylamine (80 μ L, 0.46 mmol), 1-hydroxybenzotriazole hydrate (42 mg, 0.27 mmol), *N*-(3-dimethylaminopropyl)-*N'*-ethylcarbodiimide hydrochloride (53 mg, 0.27 mmol), DMAP (2.8 mg, 0.023 mmol) and (*S*)-tetrahydrofuran-3-ol (183 μ L, 2.28 mmol). The reaction mixture was stirred at RT for 16 h. The reaction mixture was partitioned between ethyl acetate (2.5 mL) and saturated sodium hydrogen carbonate (2.5 mL). The organic phase was separated, washed with 2 M HCl (2 mL), water (2 mL) and brine (2 mL). The organic phase was dried and evaporated to give the crude product (2S,3R)-(S)-tetrahydrofuran-3-yl 2-((*tert*-butoxycarbonyl) amino)-3-hydroxybutanoate (26 mg, 0.09 mmol, 39% yield) as a clear gum. $^1\text{H NMR}$ δ (500 MHz, CDCl_3) ppm: 5.38 (1H, t, $J=5.4$ Hz), 5.29 (1H, d, $J=7.7$ Hz), 4.36 - 4.27 (1H, m), 4.23 (1H, d, $J=8.5$ Hz), 3.98 - 3.81 (4H, m), 2.25 - 2.13 (1H, m), 2.10 - 2.01 (1H, m), 1.64 (1H, br. s), 1.46 (9H, s), 1.26 (3H, d, $J=6.6$ Hz).

Larger scale synthesis of (2S,3R)-(S)-Tetrahydrofuran-3-yl 2-((*tert*-butoxycarbonyl)amino)-3-hydroxybutanoate, 2.122

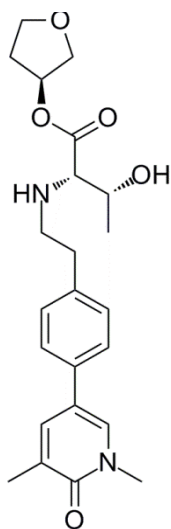
To a solution of (2S,3R)-2-((*tert*-butoxycarbonyl)amino)-3-hydroxybutanoic acid (5 g, 22.8 mmol) in *N,N*-dimethylformamide (22.5 mL) was added diisopropylethylamine (7.97 mL, 45.6 mmol), 1-hydroxybenzotriazole hydrate (4.19 g, 27.4 mmol), *N*-(3-dimethylaminopropyl)-*N'*-ethylcarbodiimide hydrochloride (5.25 g, 27.4 mmol), DMAP (0.28 g, 2.26 mmol) and (*S*)-tetrahydrofuran-3-ol (18.3 mL, 228 mmol). The reaction mixture was stirred at RT for 72 h. The reaction mixture was partitioned between ethyl acetate (200 mL) and saturated aqueous sodium hydrogen carbonate (200 mL). The organic phase was separated, washed with 2 M aqueous HCl (160 mL), water (160 mL) and brine (160 mL). The organic phase was dried and evaporated to give the crude product as a clear oil. The oil was dissolved in DCM (2 mL) and loaded onto 2 x 100 g SNAP silica column. The crude material on silica was purified by Biotage SP4 using a gradient of 10 - 50% ethyl acetate in cyclohexane over 24 CV. Fractions containing

pure product were collected and the solvent removed under reduced pressure and further dried under high vacuum overnight to yield (2*S*,3*R*)-(S)-tetrahydrofuran-3-yl 2-((tert-butoxy carbonyl)amino)-3-hydroxybutanoate (2.81 g, 9.42 mmol, 41% yield) as a clear gum. ¹H NMR δ(500 MHz, CDCl₃) ppm: 5.38 (1H, t, *J*=5.4 Hz), 5.29 (1H, d, *J*=7.7 Hz), 4.36 - 4.27 (1H, m), 4.23 (1H, d, *J*=8.5 Hz), 3.98 - 3.81 (4H, m), 2.25 - 2.13 (1H, m), 2.10 - 2.01 (1H, m), 1.64 (1H, br. s), 1.46 (9H, s), 1.26 (3H, d, *J*=6.6 Hz).

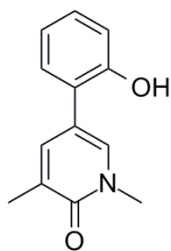
(2*S*,3*R*)-(S)-Tetrahydrofuran-3-yl 2-amino-3-hydroxybutanoate, hydrochloride, 2.123



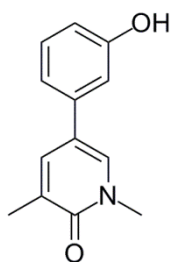
To a solution of (2*S*,3*R*)-(S)-tetrahydrofuran-3-yl 2-((tert-butoxycarbonyl)amino)-3-hydroxybutanoate (570 mg, 1.97 mmol) in 1,4-dioxane (5.5 mL) at RT was added hydrochloric acid (4 M in dioxane) (1.97 mL, 7.88 mmol). The reaction mixture was stirred at RT for 16 h. The reaction (monitored by TLC) showed conversion, but not to completion. An additional portion of hydrochloric acid (4 M in dioxane) (1.97 mL, 7.88 mmol) was added and stirred for 6 h. Hydrochloric acid (4 M in dioxane) (1.97 mL, 7.88 mmol) was again added, stirred for 2 h and left to stand for 16 h. A small sample was taken, the solvent removed under a stream of nitrogen and analysed by ¹H NMR. With exception to a signal associated with 1,4-dioxane, the compound was consistent with the desired product. The solvent was removed *in vacuo* and the product further dried in the vacuum oven to yield (2*S*,3*R*)-(S)-tetrahydrofuran-3-yl 2-amino-3-hydroxybutanoate, hydrochloride (470 mg, 1.979 mmol, 100% yield) as a yellow gum. ¹H NMR δ(400 MHz, DMSO-*d*₆) ppm: 8.46 (3H, br. s.), 5.66 (1H, br. s.), 5.35 (1H, td, *J*=4.2, 2.3 Hz), 4.17 - 4.08 (1H, m), 3.89 (1H, d, *J*=3.8 Hz), 3.85 - 3.69 (4H, m), 2.24 - 2.13 (1H, m), 2.00 - 1.91 (1H, m), 1.22 (3H, d, *J*=6.6 Hz). ¹³C NMR δ(101 MHz, DMSO-*d*₆) ppm: 168.3 (COO), 77.0 (C-O), 72.4 (OCH₂), 66.7 (OCH₂), 65.5 (CH-OH), 58.3 (N-CH), 32.6 (CH₂), 20.5 (CH₃). IR (neat): 3335, 2877, 1740.

(2S,3R)-(S)-Tetrahydrofuran-3-yl 2-((4-(1,5-dimethyl-6-oxo-1,6-dihydropyridin-3-yl)phenethyl)amino)-3-hydroxybutanoate, 2.113

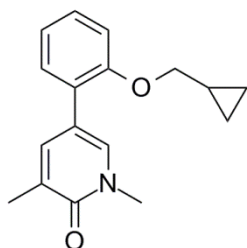
To a round bottomed flask was added 1,3-dimethyl-5-(4-(oxiran-2-yl)phenyl)pyridin-2(1H)-one (100 mg, 0.41 mmol) and the flask flushed with nitrogen before dissolution in tetrahydrofuran (2.5 mL). To the solution, cooled in an ice bath, was added boron trifluoride diethyl etherate (25 μ L, 0.21 mmol). The reaction mixture was stirred at 0 $^{\circ}$ C for 15 min. After this time, (2S,3R)-(S)-tetrahydrofuran-3-yl 2-amino-3-hydroxybutanoate, hydrochloride (187 mg, 0.83 mmol) and triethylamine (173 μ L, 1.24 mmol) were added. The mixture was warmed to RT and stirred for 20 min. After this time, sodium triacetoxyborohydride (220 mg, 1.04 mmol) was added and the mixture stirred for 2 h. After this time, an additional portion of sodium triacetoxyborohydride (100 mg, 0.47 mmol) was added and the reaction stirred for a further 16 h. The reaction mixture was diluted with DCM (10 mL), the mixture washed with saturated aqueous sodium hydrogen carbonate solution (10 mL) and the layers separated. The aqueous was extracted with DCM (3 x 10 mL) and the organics combined, dried by passing through a hydrophobic frit and the solvent removed under reduced pressure. The resulting gum was dissolved in DMSO (2 x 1 mL) and purified by mass directed autoprep on an Xbridge column using 15 to 55% acetonitrile water with an ammonium carbonate modifier. The solvent was evaporated *in vacuo* to yield (2S,3R)-(S)-tetrahydrofuran-3-yl 2-((4-(1,5-dimethyl-6-oxo-1,6-dihydropyridin-3-yl)phenethyl)amino)-3-hydroxybutanoate (36 mg, 0.09 mmol, 21% yield) as a yellow gum. LCMS (high pH): rt = 0.79 min, MH⁺ 415.4. ¹H NMR δ (400 MHz, CDCl₃) ppm: 7.49 (1H, dd, *J*=2.4, 1.2 Hz), 7.36 (1H, d, *J*=2.2 Hz), 7.34 (2H, d, *J*=8.3 Hz), 7.23 (2H, d, *J*=8.1 Hz), 5.37 - 5.32 (1H, m), 3.93 - 3.84 (3H, m), 3.79 - 3.75 (1H, m), 3.64 - 3.59 (4H, m), 3.03 - 2.96 (2H, m), 2.88 - 2.73 (3H, m), 2.26 - 2.15 (4H, m), 2.03 - 1.95 (1H, m), 1.20 (3H, d, *J*=6.4 Hz). ¹³C NMR δ (101 MHz, CDCl₃) ppm: 173.4 (COO), 162.7 (C=O), 138.4 (C-CH₂), 136.6 (N-CH), 135.0 (C-C), 132.8 (C-CH), 129.6 (C-CH₃), 129.3 (2 x CH), 125.9 (2 x CH), 119.4 (C-C), 75.7 (O-CH), 73.0 (CH₂), 68.1 (N-CH), 67.8 (CH-OH), 66.9 (CH₂), 49.7 (N-CH₂), 38.1 (N-CH₃), 36.2 (C-CH₂), 32.8 (CH₂), 19.4 (CH-CH₃), 17.4 (C-CH₃). IR (CDCl₃): 3366, 2930, 1729, 1653, 1107. HRMS (ESI) exact mass calculated for C₂₃H₃₁N₂O₅ [M+H]⁺ m/z 415.2227, found m/z 415.2234. $[\alpha]_D^{24.7^{\circ}}$ (c 0.5, CDCl₃): -5.2 $^{\circ}$

5-(2-Hydroxyphenyl)-1,3-dimethylpyridin-2(1H)-one, 3.17

To a solution of 5-bromo-1,3-dimethylpyridin-2(1H)-one (0.5 g, 2.48 mmol) and (2-hydroxyphenyl)boronic acid (512 mg, 3.71 mmol) in 1,4-dioxane (13.6 mL) and water (0.54 mL) stirred under nitrogen at RT was added palladium tetrakis triphenylphosphine (86 mg, 0.07 mmol) and potassium carbonate (7.4 ml, 7.4 mmol). The reaction mixture was stirred at 95 °C for 3 h. After cooling to room temperature, the reaction mixture was filtered through celite, diluted with water (25 mL), the layers separated and the organics collected. The aqueous phase was further extracted with ethyl acetate (2 x 30 mL). The organics were combined, dried by passing through a hydrophobic frit and the solvent removed under reduced pressure. The resulting brown gum was dissolved in DCM (5 mL) and the resulting solid filtered to yield 5-(2-hydroxyphenyl)-1,3-dimethylpyridin-2(1H)-one (50 mg, 0.23 mmol, 9% yield) of crude light brown solid. The filtrate was loaded onto a 100 g silica column. The crude material on silica was purified by Biotage SP4 using a gradient of 25-100% ethyl acetate in cyclohexane. Fractions containing pure product were collected and the solvent removed under reduced pressure to yield 5-(2-hydroxyphenyl)-1,3-dimethylpyridin-2(1H)-one (370 mg, 1.63 mmol, 66% yield) as a light yellow solid. $R_f = 0.04$, 50% ethyl acetate in cyclohexane. LCMS (formic acid): $rt = 0.70$ min, $MH^+ 216.1$. 1H NMR δ (400 MHz, $CDCl_3$) ppm: 7.44 (1H, dd, $J=2.3, 1.1$ Hz), 7.39 (1H, d, $J=2.2$ Hz), 7.25 - 7.19 (1H, m), 7.17 (1H, dd, $J=7.8, 1.7$ Hz), 6.99 - 6.94 (2H, m), 5.87 (1H, s), 3.60 (3H, s), 2.20 (3H, s). ^{13}C NMR δ (101 MHz, $CDCl_3$) ppm: 162.7 (C=O), 153.2 (C-O), 138.9 (C-CH), 135.3 (N-CH), 129.8 (CH), 129.2 (C- CH_3), 129.1 (CH), 123.9 (C-C), 120.9 (CH), 116.6 (CH), 116.4 (C-C), 38.2 (N- CH_3), 17.3 (C- CH_3). IR (neat) 2949, 1641, 1289, 753. Melting Point: 172 - 175 °C. (75% overall yield).

5-(3-Hydroxyphenyl)-1,3-dimethylpyridin-2(1H)-one, 3.18

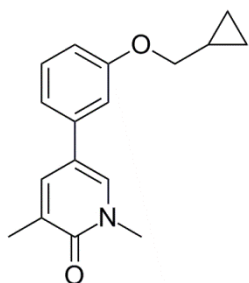
To a solution of 5-bromo-1,3-dimethylpyridin-2(1H)-one (0.98 g, 4.85 mmol) and (3-hydroxyphenyl)boronic acid (1.00 g, 7.28 mmol) in 1,4-dioxane (27 mL) and water (1.1 mL) stirred under nitrogen at RT was added palladium tetrakis triphenylphosphine (0.17 g, 0.15 mmol) and 1 M aqueous potassium carbonate (15 mL, 14.6 mmol). The reaction mixture was stirred at 95 °C for 3 h. After cooling to room temperature, the reaction mixture was filtered through celite, diluted with water (50 mL) and extracted with ethyl acetate (2 x 30 mL). The organics were combined, dried by passing through a hydrophobic frit and the solvent removed under reduced pressure. The resulting brown gum was dissolved in DCM (20 mL) and the resulting solid filtered to yield 1 g of crude light brown solid. The solid was incompletely dissolved in methanol, sonicated and the solid filtered to yield 5-(3-hydroxyphenyl)-1,3-dimethylpyridin-2(1H)-one (226 mg, 1.03 mmol, 21% yield) as a yellow solid. The resulting filtrate was dried *in vacuo* and recrystallised from methanol to yield 5-(3-hydroxyphenyl)-1,3-dimethylpyridin-2(1H)-one (150 mg, 0.70 mmol, 14% yield) as a grey solid. LCMS (formic acid): rt = 0.66, MH⁺ 216.1. ¹H NMR δ(400 MHz, DMSO-*d*₆) ppm: 9.44 (1H, s), 7.90 (1H, d, *J*=2.4 Hz), 7.64 (1H, dd, *J*=2.6, 1.1 Hz), 7.22 - 7.16 (1H, m), 6.98 - 6.94 (1H, m), 6.91 (1H, t, *J*=2.1 Hz), 6.71 - 6.67 (1H, m), 3.50 (3H, s), 2.07 (3H, s). ¹³C NMR δ(101 MHz, DMSO-*d*₆) ppm: 162.1 (C=O), 158.3 (C-O), 138.2 (C-C), 136.3 (C-H), 134.8 (C-H), 130.3 (C-H), 128.1 (C-C), 117.8 (C-C), 116.5 (C-H), 114.2 (C-H), 112.6 (C-H), 37.7 (N-CH₃), 17.5 (C-CH₃). IR (neat): 3157, 1648, 1237, 861, 764. Melting point: 242 - 246 °C. (35% overall yield).

5-(2-(Cyclopropylmethoxy)phenyl)-1,3-dimethylpyridin-2(1H)-one, 3.13

To a solution of 5-(2-hydroxyphenyl)-1,3-dimethylpyridin-2(1H)-one (50 mg, 0.23 mmol) in acetone (2 mL) and *N,N*-dimethylformamide (0.5 mL) was added solid potassium carbonate (48 mg, 0.35 mmol) followed by (bromomethyl)cyclopropane (24 μL, 0.24 mmol). The reaction mixture was stirred at 60 °C for 20 h. The reaction mixture was cooled to room temperature, the acetone removed under reduced pressure and the liquid dissolved in 1:1 ethyl acetate:water (20 mL), the layers separated and the

organics collected. The aqueous was washed further with ethyl acetate (2x10 mL), and the combined organics were washed with brine, dried by passing through a hydrophobic frit, and the solvent removed *in vacuo*. The sample was dissolved in DMSO (1 mL) and purified by mass directed autoprep on Sunfire C18 column using 30-85% acetonitrile water with a formic acid modifier. The solvent was evaporated *in vacuo* to give the required product 5-(2-(cyclopropylmethoxy)phenyl)-1,3-dimethylpyridin-2(1H)-one (50 mg, 0.19 mmol, 80% yield) as a clear gum. LCMS (formic acid): *rt* = 1.03, *MH*⁺ 270.2. ¹H NMR δ (400 MHz, CDCl₃) ppm: 7.55 (1H, dd, *J*=2.4, 1.2 Hz), 7.52 (1H, d, *J*=2.4 Hz), 7.29 - 7.21 (2H, m), 6.99 (1H, dt, *J*=7.3, 1.0 Hz), 6.94 - 6.88 (1H, m), 3.85 (2H, d, *J*=6.8 Hz), 3.62 (3H, s), 2.21 (3H, s), 1.28 - 1.18 (1H, m), 0.65 - 0.56 (2H, m), 0.35 - 0.29 (2H, m). ¹³C NMR δ (101 MHz, CDCl₃) ppm: 162.7 (C=O), 155.8 (C-O), 139.4 (C-H), 135.4 (C-H), 129.3 (C-H), 128.6 (C-H), 128.1 (C-C), 126.1 (C-C), 121.1 (C-H), 116.9 (C-C), 112.9 (C-H), 73.0 (C-O), 38.1 (N-CH₃), 17.3 (C-CH₃), 10.3 (CH), 3.0 (2 x CH₂). IR (CDCl₃): 3074, 3006, 1654, 1238, 1006, 752. HRMS (ESI) exact mass calculated for C₁₇H₂₀NO₂ [M+H]⁺ *m/z* 270.1489, found *m/z* 270.1484.

5-(3-(Cyclopropylmethoxy)phenyl)-1,3-dimethylpyridin-2(1H)-one, 3.14

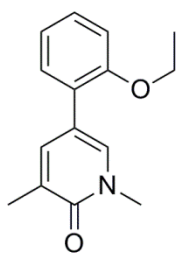


To a solution of 5-(3-hydroxyphenyl)-1,3-dimethylpyridin-2(1H)-one (75 mg, 0.35 mmol) in acetone (3 mL) was added solid potassium carbonate (72 mg, 0.52 mmol) followed by (bromomethyl)cyclopropane (35 μ L, 0.37 mmol). The reaction mixture was stirred at 60 °C for 20 h. The reaction had proceeded by 3% by LCMS, so *N,N*-dimethylformamide (1 mL) was added to solubilise the starting material. After a further 2 hours, the reaction had not progressed to completion, so an extra portion of (bromomethyl)cyclopropane (35 μ L, 0.37 mmol) was added and the mixture stirred overnight. The reaction mixture was cooled to room temperature, the acetone removed under reduced pressure and the liquid dissolved in 1:1 ethyl acetate:water (20 mL), the layers separated and the organics collected. The aqueous was washed further with ethyl acetate (2 x 10 mL), and the combined organics were washed with brine, dried by passing through a hydrophobic frit, and the solvent removed *in vacuo*. The resulting solid was dissolved in DCM (2 mL) and loaded onto a 10 g SNAP silica column. The crude material on silica was purified by Biotage SP4 using

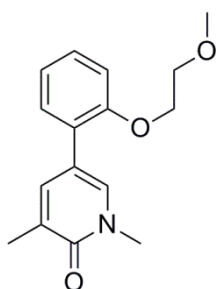
a gradient of 25 – 75% ethyl acetate-cyclohexane over 16 CV. Pure fractions were combined and the solvent removed under reduced pressure to yield 5-(3-(cyclopropylmethoxy)phenyl)-1,3-dimethylpyridin-2(1H)-one (77 mg, 0.28 mmol, 80% yield) as a crystalline white solid. $R_f = 0.21$, 75% ethyl acetate in cyclohexane. LCMS (formic acid): $rt = 1.03$, $MH^+ 270.1$. 1H NMR δ (400 MHz, $CDCl_3$) ppm: 7.51 - 7.48 (1H, m), 7.38 (1H, d, $J=2.4$ Hz), 7.30 (1H, t, $J=7.9$ Hz), 7.00 - 6.96 (1H, m), 6.94 (1H, t, $J=2.1$ Hz), 6.87 - 6.81 (1H, m), 3.85 (2H, d, $J=7.1$ Hz), 3.62 (3H, s), 2.22 (3H, s), 1.34 - 1.24 (1H, m), 0.70 - 0.63 (2H, m), 0.40 - 0.34 (2H, m). ^{13}C NMR δ (101 MHz, $CDCl_3$) ppm: 162.8 (C=O), 159.6 (C-O), 138.3 (C-C), 136.6 (C-H), 133.0 (C-H), 130.0 (C-H), 129.6 (C-C), 119.5 (C-C), 118.1 (C-H), 112.9 (C-H), 112.5 (C-H), 72.9 (O- CH_2), 38.1 (N- CH_3), 17.4 (C- CH_3), 10.3 (C-H), 3.2 (2x CH_2). IR (neat) 3077, 3002, 1651, 1224, 1004. Melting point: 91-93 °C. HRMS (ESI) exact mass calculated for $C_{17}H_{20}NO_2$ $[M+H]^+$ m/z 270.1489, found m/z 270.1480.

General procedure for phenol alkylation

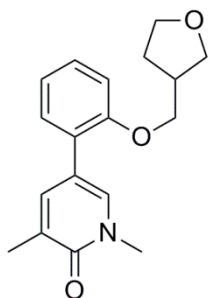
To a round bottomed flask was added 5-(2-hydroxyphenyl)-1,3-dimethylpyridin-2(1H)-one (50 mg, 0.23 mmol), acetone (2 mL) and *N,N*-dimethylformamide (0.7 mL). To the stirred mixture was added solid potassium carbonate (48 mg, 0.35 mmol) followed by an alkyl bromide (a). The reaction mixture was stirred at 60 °C for 20 h. After this time the reactions were incomplete. An additional portion of alkyl bromide (b) was added to each reaction and the mixture stirred for an additional 72 h. The reactions were cooled to room temperature, the solvent removed under reduced pressure and the liquid dissolved in 1:1 ethyl acetate:water (20 mL). The layers were separated and the organics collected. The aqueous was washed further with ethyl acetate (2 x 10 mL), and the combined organics were washed with brine, dried by passing through a hydrophobic frit, and the solvent removed *in vacuo*. The resulting solids were dissolved in DMSO (1 mL) and purified by mass directed autoprep on Sunfire C18 column using gradient (c) acetonitrile water with a formic acid modifier. The solvent was evaporated *in vacuo* to give the required product (d).

5-(2-Ethoxyphenyl)-1,3-dimethylpyridin-2(1H)-one, 3.22

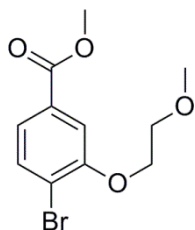
(a) Bromoethane (19 μL , 0.26 mmol), (b) bromoethane (10 μL , 0.14 mmol), (c) 30-85%, (d) 5-(2-ethoxyphenyl)-1,3-dimethylpyridin-2(1H)-one (43 mg, 0.175 mmol, 75% yield) as a white solid. LCMS (formic acid): $t_r = 0.95$ min, MH^+ 244.1. ^1H NMR δ (400 MHz, CDCl_3) ppm: 7.51 - 7.48 (1H, m), 7.44 (1H, d, $J=2.2$ Hz), 7.30 - 7.21 (2H, m), 6.98 (1H, td, $J=7.5, 1.1$ Hz), 6.94 (1H, d, $J=8.1$ Hz), 4.06 (2H, q, $J=6.8$ Hz), 3.61 (3H, s), 2.21 (3H, s), 1.39 (3H, t, $J=7.0$ Hz). ^{13}C NMR δ (101 MHz, CDCl_3) ppm: 162.6 (C=O), 155.8 (C-O), 139.1 (C-CH), 135.2 (N-CH), 129.5 (CH), 128.6 (CH), 128.2 (C- CH_3), 126.1 (C-C), 121.0 (CH), 116.7 (C-C), 112.5 (CH), 64.0 (O- CH_2), 37.9 (N- CH_3), 17.3 (C- CH_3), 14.8 (CH_2CH_3). IR (neat): 2978, 1649, 1235, 1124, 746. HRMS (ESI) exact mass calculated for $\text{C}_{15}\text{H}_{18}\text{NO}_2$ [$\text{M}+\text{H}$] $^+$ m/z 244.1332, found m/z 244.1330. Melting point: 79 – 81 $^\circ\text{C}$.

5-(2-(2-Methoxyethoxy)phenyl)-1,3-dimethylpyridin-2(1H)-one 3.23

(a) 1-Bromo-2-methoxyethane (24 μL , 0.26 mmol), (b) 1-bromo-2-methoxyethane (22 μL , 0.23 mmol), (c) 5-55%, (d) 5-(2-(2-methoxyethoxy)phenyl)-1,3-dimethylpyridin-2(1H)-one (55 mg, 0.20 mmol, 85% yield) as a white solid. LCMS (formic acid): $t_r = 0.86$ min, MH^+ 274.0. ^1H NMR δ (400 MHz, CDCl_3) ppm: 7.57 (1H, d, $J=2.2$ Hz), 7.54 (1H, dd, $J=2.3, 1.1$ Hz), 7.29 - 7.23 (2H, m), 7.04 - 6.98 (1H, m), 6.97 - 6.92 (1H, m), 4.16 - 4.11 (2H, m), 3.74 - 3.69 (2H, m), 3.60 (3H, s), 3.42 (3H, s), 2.21 (3H, s). ^{13}C NMR δ (101 MHz, CDCl_3) ppm: 162.7 (C=O), 155.6 (C-O), 139.0 (C-CH), 135.7 (N-CH), 129.3 (CH), 128.5 (CH), 128.2 (C- CH_3), 126.3 (C-C), 121.5 (CH), 116.3 (C-C), 112.8 (CH), 71.1 (O- CH_2), 67.9 (O- CH_2), 59.1 (O- CH_3), 38.0 (N- CH_3), 17.3 (C- CH_3). IR (CDCl_3): 1654, 1243, 1127, 753. HRMS (ESI) exact mass calculated for $\text{C}_{16}\text{H}_{20}\text{NO}_3$ [$\text{M}+\text{H}$] $^+$ m/z 274.1438, found m/z 274.1440. Melting point: 102 - 105 $^\circ\text{C}$.

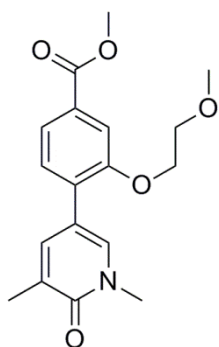
1,3-Dimethyl-5-(2-((tetrahydrofuran-3-yl)methoxy)phenyl)pyridin-2(1H)-one**3.24**

(a) 3-(Bromomethyl)tetrahydrofuran (28 μL , 0.26 mmol), (b) 3-(bromomethyl)tetrahydrofuran (0.1 mL, 0.91 mmol), (c) 5-55%, (d) 1,3-dimethyl-5-(2-((tetrahydrofuran-3-yl)methoxy)phenyl)pyridin-2(1H)-one (41 mg, 0.14 mmol, 58% yield) as a clear gum. LCMS (formic acid): rt = 0.89 min, MH⁺ 300.0. ¹H NMR δ (400 MHz, CDCl₃) ppm: 7.46 (1H, dd, $J=2.4, 1.1$ Hz), 7.38 (1H, d, $J=2.3$ Hz), 7.30 - 7.21 (2H, m), 7.00 (1H, td, $J=7.5, 1.0$ Hz), 6.95 - 6.91 (1H, m), 3.99 - 3.82 (4H, m), 3.79 - 3.72 (1H, m), 3.66 (1H, dd, $J=8.7, 5.4$ Hz), 3.61 (3H, s), 2.75 - 2.63 (1H, m), 2.20 (3H, s), 2.12 - 2.01 (1H, m), 1.75 - 1.65 (1H, m). ¹³C NMR δ (101 MHz, CDCl₃) ppm: 162.6 (C=O), 155.6 (C-O), 139.1 (C-CH), 135.1 (N-CH), 129.5 (CH), 128.7 (CH), 128.2 (C-CH₃), 126.2 (C-C), 121.3 (CH), 116.5 (C-C), 112.3 (CH), 70.7 (OCH₂), 70.2 (OCH₂), 67.8 (OCH₂), 38.9 (CH), 37.9 (N-CH₃), 29.0 (CH₂), 17.3 (C-CH₃). IR (CDCl₃): 1655, 1238, 754. HRMS (ESI) exact mass calculated for C₁₈H₂₂NO₃ [M+H]⁺ m/z 300.1594, found m/z 300.1598.

Methyl 4-bromo-3-(2-methoxyethoxy)benzoate, 3.29

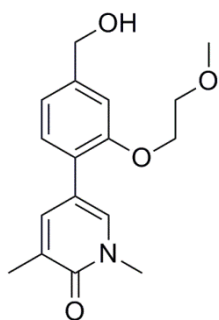
To a solution of methyl 4-bromo-3-hydroxybenzoate (4 g, 17.3 mmol) in acetone (128 ml) and *N,N*-dimethylformamide (43 ml) stirred at RT was added solid caesium carbonate (8.5 g, 26 mmol) followed by 1-bromo-2-methoxyethane (2.4 ml, 26 mmol). The reaction mixture was stirred at 60 °C for 2 h. After this time LCMS analysis showed only a small presence of starting material. The reaction was stirred for a further 14 h to ensure reaction completion. The reaction was cooled to room temperature, the solvent removed under reduced pressure and the liquid dissolved in 1:1 ethyl acetate:water (400 mL). The layers were separated and the organics collected. The aqueous was washed further with ethyl acetate (2 x 150 mL), and the combined organics were washed with brine, dried by passing through a hydrophobic frit and the solvent removed *in vacuo* to yield methyl 4-bromo-3-(2-methoxyethoxy)benzoate (5.3 g, 16.50 mmol, 95% yield) (90% purity) as a light yellow oil. LCMS (formic acid): rt = 1.07 min, MH⁺ 288.9, 290.9. ¹H NMR δ (400 MHz, CDCl₃) ppm: 7.61 (1H, d, $J=8.1$ Hz), 7.57 (1H, d, $J=1.7$ Hz), 7.51 (1H, dd, $J=8.1, 1.7$ Hz), 4.26 - 4.22 (2H, m), 3.91 (3H, s), 3.85 - 3.81 (2H, m), 3.49 (3H, s).

Methyl 4-(1,5-dimethyl-6-oxo-1,6-dihydropyridin-3-yl)-3-(2-methoxyethoxy)benzoate, 3.28



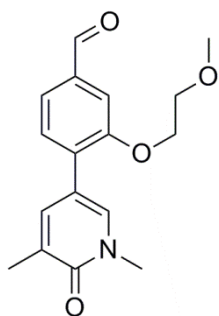
To a solution of methyl 4-bromo-3-(2-methoxyethoxy)benzoate (0.65 g, 2.25 mmol) and 1,3-dimethyl-5-(4,4,5,5-tetramethyl-1,3,2-dioxaborolan-2-yl)pyridin-2(1H)-one (1.2 g, 3.37 mmol) in 1,4-dioxane (12 mL) and water (0.5 mL) stirred under nitrogen at RT was added palladium tetrakis triphenylphosphine (78 mg, 67 μ mol) and 1 M potassium carbonate (aq) (6.7 mL, 6.7 mmol). The reaction mixture was stirred at 95 °C for 3 h. After cooling to room temperature, the reaction mixture was diluted with water (40 mL) and extracted with ethyl acetate (3 x 40 mL). The combined organics were extracted with brine (20 mL). The organics were combined, dried by passing through a hydrophobic frit and the solvent was removed under reduced pressure. The resulting pink solid was dissolved in DCM (5 mL) and loaded onto a 50 g SNAP silica column. The crude material on silica was purified by Biotage SP4 using a gradient of 50 - 100% ethyl acetate in cyclohexane over 26 CV. Fractions containing the desired product were evaporated *in vacuo* to yield the desired product methyl 4-(1,5-dimethyl-6-oxo-1,6-dihydropyridin-3-yl)-3-(2-methoxyethoxy)benzoate (585 mg, 1.77 mmol, 79% yield) as a white solid. R_f = 0.17 (100% ethyl acetate). LCMS (formic acid): rt = 0.88 min, MH^+ 332.0. 1H NMR δ (400 MHz, $CDCl_3$) ppm: 7.71 (1H, d, J =2.5 Hz), 7.69 (1H, dd, J =7.8, 1.5 Hz), 7.60 (1H, d, J =1.5 Hz), 7.55 (1H, dd, J =2.4, 1.1 Hz), 7.33 (1H, d, J =8.1 Hz), 4.24 - 4.18 (2H, m), 3.93 (3H, s), 3.77 - 3.72 (2H, m), 3.61 (3H, s), 3.43 (3H, s), 2.21 (3H, s). ^{13}C NMR δ (101 MHz, $CDCl_3$) ppm: 166.6 (COO), 162.6 (C=O), 155.4 (C-O), 138.3 (CH), 136.5 (CH), 130.9 (C-C), 129.9 (C-C), 128.9 (CH), 128.5 (C- CH_3), 122.8 (CH), 115.1 (C-C), 113.4 (CH), 70.9 (O CH_2), 68.0 (O CH_2), 59.1 (O CH_3), 52.2 (COO CH_3), 38.0 (N- CH_3), 17.3 (C- CH_3). IR ($CDCl_3$): 1716, 1657, 1232, 1124. HRMS (ESI) exact mass calculated for $C_{18}H_{22}NO_5$ [$M+H$] $^+$ m/z 332.1493, found m/z 332.1499.

5-(4-(Hydroxymethyl)-2-(2-methoxyethoxy)phenyl)-1,3-dimethylpyridin-2(1H)-one, 3.32



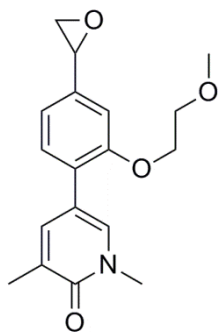
To a solution of methyl 4-(1,5-dimethyl-6-oxo-1,6-dihydropyridin-3-yl)-3-(2-methoxyethoxy)benzoate (700 mg, 2.11 mmol) in DCM (10 mL) stirred under nitrogen and cooled to $-78\text{ }^{\circ}\text{C}$ was added a solution of DIBAL-H (1 M) in tetrahydrofuran (5.3 mL, 5.3 mmol) dropwise during 1 min. After 10 min, the reaction mixture was warmed to $0\text{ }^{\circ}\text{C}$ and stirred for 2 h. After this time, LCMS analysis indicated the reaction to be incomplete. An additional aliquot of DIBAL-H (1 M) in tetrahydrofuran (0.5 mL, 0.5 mmol) was added and stirred for an additional 30 min. After this time, the reaction was quenched with 10% aq. citric acid (20 mL) and the mixture stirred at $25\text{ }^{\circ}\text{C}$ for 1 h, then left to stand overnight. The layers were separated and the aqueous layer was extracted with DCM (2 x 30 mL) and the combined organics were washed with brine (10 mL), dried and concentrated *in vacuo* to provide crude product. The resulting solid was dissolved in DCM (3 mL) and loaded onto a 25 g SNAP silica column. The crude material on silica was purified by Biotage SP4 using a gradient of 0 - 10% methanol in DCM for 21 CV. The fractions containing product were collected and the solvent removed under reduced pressure to yield the desired product 5-(4-(hydroxymethyl)-2-(2-methoxyethoxy)phenyl)-1,3-dimethylpyridin-2(1H)-one (460 mg, 1.49 mmol, 70% yield) as a white solid. $R_f = 0.21$ (10% methanol in DCM). LCMS (formic acid): $rt = 0.65$ min, MH^+ 304.0. $^1\text{H NMR } \delta(400\text{ MHz, CDCl}_3)$ ppm: 7.53 (1H, d, $J=2.3$ Hz), 7.49 (1H, dd, $J=2.3, 1.0$ Hz), 7.19 (1H, d, $J=7.6$ Hz), 6.97 (1H, s), 6.96 - 6.92 (1H, m), 4.69 (2H, d, $J=5.8$ Hz), 4.17 - 4.10 (2H, m), 3.74 - 3.69 (2H, m), 3.56 (3H, s), 3.42 (3H, s), 2.65 (1H, t, $J=5.9$ Hz), 2.17 (3H, s). $^{13}\text{C NMR } \delta(101\text{ MHz, CDCl}_3)$ ppm: 162.6 (C=O), 155.6 (C-O), 141.9 (C-CH₂OH), 139.0 (C-CH), 135.7 (N-CH), 129.2 (CH), 128.1 (C-CH₃), 125.2 (C-C), 119.7 (CH), 116.2 (C-C), 111.2 (CH), 71.0 (O-CH₂), 67.8 (O-CH₂), 64.9 (CH₂OH), 59.1 (O-CH₃), 37.9 (N-CH₃), 17.3 (C-CH₃). IR (CDCl₃): 3358, 2924, 2881, 1650. HRMS (ESI) exact mass calculated for C₁₇H₂₂NO₄ [M+H]⁺ m/z 304.1543, found m/z 304.1549.

4-(1,5-Dimethyl-6-oxo-1,6-dihydropyridin-3-yl)-3-(2-methoxyethoxy) benzaldehyde, 3.27



To a solution of 5-(4-(hydroxymethyl)-2-(2-methoxyethoxy) phenyl)-1,3-dimethylpyridin-2(1H)-one (455 mg, 1.50 mmol) in DCM (27 mL) was added 45% iodoxybenzoic acid (stabilised by benzoic acid and isophthalic acid) (1.12 g, 1.80 mmol), portionwise. The reaction mixture was stirred at room temperature for 72 h. LCMS analysis indicated no starting material remained. The reaction mixture was partitioned between DCM (3 x 30 mL) and saturated aqueous sodium bicarbonate solution (30 mL). The organic layers were combined, washed with saturated aqueous sodium bicarbonate solution (30 mL), dried using a hydrophobic frit and evaporated under reduced pressure to give the crude product 4-(1,5-dimethyl-6-oxo-1,6-dihydropyridin-3-yl)-3-(2-methoxyethoxy) benzaldehyde (513 mg, 1.45 mmol, 96% yield) (85% purity) as a white solid. LCMS (formic acid): rt = 0.78 min, MH⁺ 302.0. ¹H NMR δ(400 MHz, Methanol-*d*₄) ppm: 9.97 (1H, s), 7.99 - 7.95 (1H, m), 7.80 (1H, s), 7.60 - 7.55 (3H, m), 4.30 - 4.24 (2H, m), 3.81 - 3.76 (2H, m), 3.66 (3H, s), 3.44 (3H, s), 2.19 (3H, s). HRMS (ESI) exact mass calculated for C₁₇H₂₀NO₄ [M+H]⁺ m/z 302.1387, found m/z 302.1394.

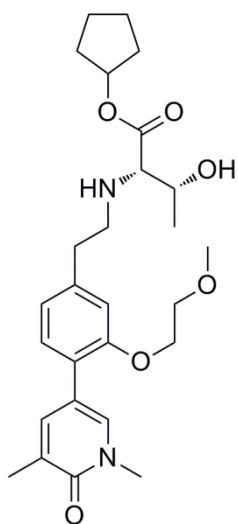
5-(2-(2-Methoxyethoxy)-4-(oxiran-2-yl)phenyl)-1,3-dimethylpyridin-2(1H)-one, 3.26



Sodium hydride (80 mg, 2.00 mmol) was weighed into a dry two-necked, round-bottomed flask including stirrer bar and rubber septum. A reflux condenser was fitted and the system was placed under nitrogen by evacuating and filling with nitrogen several times. Dry DMSO (0.70 mL, 9.80 mmol) was introduced via hypodermic syringe and the mixture was heated with stirring to 70 °C for 45 min, yielding a yellow solution. The solution was cooled to room temperature, diluted with tetrahydrofuran (0.9 mL) (to prevent freezing), and then cooled to -10 °C in a salt-ice bath. With stirring, a solution of trimethylsulfonium iodide (318 mg, 1.56 mmol) in dimethylsulfoxide (1.2 mL) was added over a period of 2 min. After the addition of the salt was complete, the mixture was stirred for 1 min longer before adding 4-(1,5-dimethyl-6-oxo-1,6-dihydropyridin-3-yl)-3-(2-methoxyethoxy)benzaldehyde (510 mg, 1.439 mmol), as a suspension in

dimethylsulfoxide (2.8 mL) and tetrahydrofuran (4.5 mL), at a moderately rapid rate. Stirring was continued at salt-ice temperature (-10 °C) for 10 minutes and then for 60 min with the bath removed. The reaction mixture was diluted with water (20 mL) and the product extracted with diethyl ether (5 x 30 mL). The combined organics were washed with water (10 mL), dried by passing through a hydrophobic frit and the solvent removed *in vacuo*. The compound was thoroughly dried under high vacuum to yield the desired product 5-(2-(2-methoxyethoxy)-4-(oxiran-2-yl)phenyl)-1,3-dimethylpyridin-2(1H)-one (438 mg, 1.389 mmol, 69% yield) as a yellow gum. LCMS (high pH): *rt* = 0.83 min, *MH*⁺ 316.2. ¹H NMR δ (400 MHz, DMSO-*d*₆) ppm: 7.80 (1H, d, *J*=2.2 Hz), 7.63 - 7.59 (1H, m), 7.31 (1H, d, *J*=7.8 Hz), 6.99 - 6.96 (1H, m), 6.94 (1H, dd, *J*=7.8, 1.5 Hz), 4.19 - 4.08 (2H, m), 3.93 (1H, dd, *J*=4.0, 2.6 Hz), 3.66 (2H, t, *J*=4.5 Hz), 3.48 (3H, s), 3.31 (3H, s), 3.12 (1H, dd, *J*=5.4, 4.2 Hz), 2.89 (1H, dd, *J*=5.5, 2.6 Hz), 2.04 (3H, s). IR (neat): 1651, 1244, 963, 826.

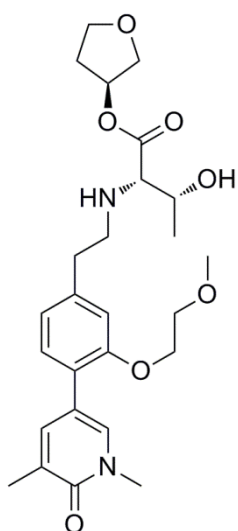
(2*S*,3*R*)-Cyclopentyl 2-((4-(1,5-dimethyl-6-oxo-1,6-dihydropyridin-3-yl)-3-(2-methoxy ethoxy)phenethyl)amino)-3-hydroxybutanoate, 3.33



To a round bottomed flask was added 5-(2-(2-methoxyethoxy)-4-(oxiran-2-yl)phenyl)-1,3-dimethylpyridin-2(1H)-one (200 mg, 0.63 mmol) and the flask flushed with nitrogen before dissolution in tetrahydrofuran (4 mL). To the solution, cooled in an ice bath, was added boron trifluoride diethyl etherate (39 μ L, 0.32 mmol). The reaction mixture was stirred at 0 °C for 15 min. After this time, (2*S*,3*R*)-cyclopentyl 2-amino-3-hydroxy butanoate, 4-methylbenzenesulfonic acid salt (456 mg, 1.27 mmol) and triethylamine (0.27 mL, 1.90 mmol) were added. The mixture was warmed to RT and stirred for 20 min. After this time, sodium triacetoxyborohydride (336 mg, 1.59 mmol) was added and the mixture stirred for 2 h. Additional portion of sodium triacetoxyborohydride (200 mg, 0.94 mmol) was required and the mixture stirred for 1 h. The reaction mixture was diluted with DCM (40 mL), the mixture washed with saturated aqueous sodium hydrogen carbonate solution (40 mL) and the layers separated. The aqueous was extracted with DCM (3 x 40 mL) and the organics combined, dried by passing through a hydrophobic frit and the solvent removed under reduced pressure. The sample was dissolved in DMSO (3 x 1 mL) and purified by mass directed autoprep on an Xbridge column using 30 to 85%

acetonitrile water with an ammonium carbonate modifier. The solvent was evaporated *in vacuo* to yield (2*S*,3*R*)-cyclopentyl 2-((4-(1,5-dimethyl-6-oxo-1,6-dihydropyridin-3-yl)-3-(2-methoxyethoxy)phenethyl) amino)-3-hydroxy butanoate (115 mg, 0.24 mmol, 37% yield) as a light yellow gum. LCMS (high pH): *rt* = 1.04 min, MH⁺ 487.4. ¹H NMR δ(400 MHz, CDCl₃) ppm: 7.54 (1H, d, *J*=2.2 Hz), 7.53 - 7.49 (1H, m), 7.18 (1H, d, *J*=7.6 Hz), 6.84 (1H, dd, *J*=7.8, 1.5 Hz), 6.77 (1H, d, 1.5 Hz), 5.26 - 5.19 (1H, m), 4.15 - 4.09 (2H, m), 3.73 - 3.69 (2H, m), 3.61 - 3.53 (4H, m), 3.42 (3H, s), 3.01 - 2.96 (1H, m), 2.92 (1H, d, *J*=7.8 Hz), 2.84 - 2.70 (3H, m), 2.20 (3H, s), 1.92 - 1.82 (2H, m), 1.74 - 1.56 (8H, m), 1.20 (3H, d, *J*=6.1 Hz). ¹³C NMR δ(101 MHz, CDCl₃) ppm: 173.3 (COO), 162.6 (C=O), 155.6 (C-O), 140.2 (C-CH₂), 138.9 (C-CH), 135.6 (N-CH), 129.3 (CH), 128.1 (C-CH₃), 124.4 (C-C), 121.6 (CH), 116.1 (C-C), 113.3 (CH), 78.1 (C-O), 71.1 (CH₂), 68.4 (N-CH), 68.0 (CH₂), 67.8 (CH-OH), 59.1 (O-CH₃), 49.7 (N-CH₂), 37.9 (N-CH₃), 36.6 (C-CH₂), 32.8 (CH₂), 32.7 (CH₂), 23.7 (CH₂), 23.6 (CH₂), 19.4 (CH-CH₃), 17.3 (C-CH₃). IR (CDCl₃): 3334, 2932, 1725, 1654, 1127, 1253. HRMS (ESI) exact mass calculated for C₂₇H₃₉N₂O₆ [M+H]⁺ *m/z* 487.2803, found *m/z* 487.2800. [α]_D^{24.2°C} (c 0.5, CDCl₃): -9.2 °.

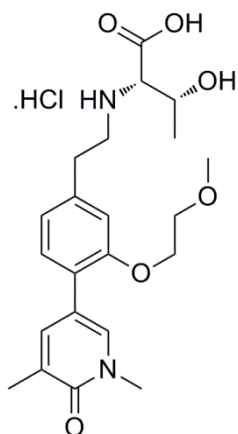
(2*S*,3*R*)-(S)-Tetrahydrofuran-3-yl 2-((4-(1,5-dimethyl-6-oxo-1,6-dihydropyridin-3-yl)-3-(2-methoxyethoxy)phenethyl)amino)-3-hydroxybutanoate, 3.25



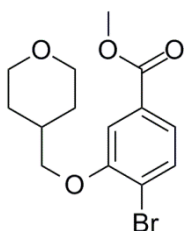
To a round bottomed flask was added 5-(2-(2-methoxyethoxy)-4-(oxiran-2-yl)phenyl)-1,3-dimethylpyridin-2(1H)-one (414 mg, 1.12 mmol) and the flask flushed with nitrogen before dissolution in tetrahydrofuran (9 mL). To the solution, cooled in an ice bath, was added boron trifluoride diethyl etherate (69 μL, 0.56 mmol). The reaction mixture was stirred at 0 °C for 15 min. After this time, (2*S*,3*R*)-(S)-tetrahydrofuran-3-yl 2-amino-3-hydroxybutanoate, hydrochloride (450 mg, 1.99 mmol) and triethylamine (0.47 mL, 3.35 mmol) were added and the mixture warmed to RT. The mixture was stirred for 10 min. The amino ester salt was poorly soluble within the reaction mixture.

Therefore, a portion of *p*-toluenesulfonic acid monohydrate (200 mg, 1.05 mmol) was added to aid salt solubility. The mixture was stirred for a further 20 min. After this time, sodium triacetoxyborohydride (946 mg, 4.46 mmol) was added and the mixture stirred for 24 h. The reaction mixture was diluted with DCM (60 mL), the mixture washed with saturated aqueous sodium hydrogen carbonate solution (60

mL) and the layers separated. The aqueous was extracted with DCM (3 x 60 mL) and the organics combined, dried by passing through a hydrophobic frit and the solvent removed under reduced pressure. The crude gum was dissolved in DCM (3 mL) and loaded onto a 25 g SNAP silica column. The crude material on silica was purified by Biotage SP4 using a gradient of 0 - 25% ethanol in ethyl acetate over 24 CV. Fractions containing the desired product were collected and the solvent removed *in vacuo* to yield a yellow gum. The crude material was dissolved in 1:1 methanol:dimethylsulfoxide (3 mL) and purified by mass directed autoprep on Xbridge column using 15-55% acetonitrile water with an ammonium carbonate modifier. The solvent was evaporated *in vacuo* to yield (2*S*,3*R*)-(S)-tetrahydrofuran-3-yl 2-((4-(1,5-dimethyl-6-oxo-1,6-dihydropyridin-3-yl)-3-(2-methoxyethoxy)phenethyl)amino)-3-hydroxy butanoate (138 mg, 0.28 mmol, 25% yield) as a light yellow gum. $R_f = 0.32$, 25% ethanol in ethyl acetate. LCMS (high pH): $t_r = 0.81$ min, MH^+ 489.4. 1H NMR δ (400 MHz, $CDCl_3$) ppm: 7.55 (1H, d, $J=2.2$ Hz), 7.53 - 7.49 (1H, m), 7.18 (1H, d, $J=7.6$ Hz), 6.84 (1H, dd, $J=7.8, 1.5$ Hz), 6.78 (1H, d, 1.3 Hz), 5.38 - 5.32 (1H, m), 4.12 (2H, dd, $J=5.3, 3.8$ Hz), 3.94 - 3.81 (3H, m), 3.77 (1H, d, $J=10.5$ Hz), 3.73 - 3.69 (2H, m), 3.66 - 3.58 (4H, m), 3.42 (3H, s), 3.02 - 2.97 (2H, m), 2.87 - 2.71 (3H, m), 2.26 - 2.14 (4H, m), 2.03 - 1.95 (1H, m), 1.21 (3H, d, $J=6.4$ Hz). ^{13}C NMR δ (101 MHz, $CDCl_3$) ppm: 173.4 (COO), 162.6 (C=O), 155.7 (C-O), 140.1 (C- CH_2), 138.9 (C-CH), 135.6 (N-CH), 129.3 (CH), 128.1 (C- CH_3), 124.4 (C-C), 121.6 (CH), 116.0 (C-C), 113.3 (CH), 75.7 (C-O), 73.0 (CH_2), 71.1 (O- CH_2), 68.1 (N-CH), 68.0 (O- CH_2), 67.8 (CH-OH), 66.9 (CH_2), 59.1 (O- CH_3), 49.7 (N- CH_2), 37.9 (N- CH_3), 36.6 (C- CH_2), 32.8 (CH_2), 19.5 (CH- CH_3), 17.3 (C- CH_3). IR ($CDCl_3$): 3348, 2928, 1728, 1652, 1125. HRMS (ESI) exact mass calculated for $C_{26}H_{37}N_2O_7$ $[M+H]^+$ m/z 489.2595, found m/z 489.2589. $[\alpha_D]^{22.5^\circ}_\lambda(c 1, CDCl_3)$: -14.4°.

(2S,3R)-2-((4-(1,5-Dimethyl-6-oxo-1,6-dihydropyridin-3-yl)-3-(2-methoxyethoxy)phenethyl)amino)-3-hydroxybutanoic acid, hydrochloride, 3.34

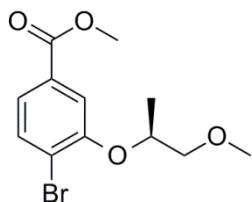
A carousel tube was charged with (2S,3R)-cyclopentyl 2-((4-(1,5-dimethyl-6-oxo-1,6-dihydropyridin-3-yl)-3-(2-methoxyethoxy)phenethyl)amino)-3-hydroxybutanoate (50 mg, 0.10 mmol), tetrahydrofuran (2 mL), methanol (2 mL) and water (1 mL). To the stirred solution was added lithium hydroxide (9.8 mg, 0.41 mmol) and the mixture warmed to 50 °C for 96 h. The reaction mixture was cooled to room temperature and the volatiles were removed under a stream of nitrogen to give a yellow oil. The resulting oil was dissolved in 1:1 MeOH:DMSO (1 ml) and purified by mass directed autoprep on an Xbridge column using 5-30% acetonitrile water with an ammonium carbonate modifier. The fractions containing the desired product were collected and the solvent was evaporated *in vacuo* to give the crude product as a white solid, which was further dried by vacuum oven. The solid was suspended in water (0.5 mL) and 2 M aqueous HCl solution (0.2 mL) was added. The clear solution was blown down a stream of nitrogen to yield (2S,3R)-2-((4-(1,5-dimethyl-6-oxo-1,6-dihydropyridin-3-yl)-3-(2-methoxyethoxy)phenethyl)amino)-3-hydroxybutanoic acid, hydrochloride (30 mg, 0.06 mmol, 61% yield) as an off-white solid. LCMS (high pH): *rt* = 0.51 min, *MH*⁺ 419.4. ¹H NMR δ (400 MHz, DMSO-*d*₆) ppm: 9.05 (1H, br. s.), 8.88 (1H, br. s.), 7.77 (1H, d, *J*=2.2 Hz), 7.62 - 7.58 (1H, m), 7.28 (1H, d, *J*=7.6 Hz), 6.96 (1H, d, *J*=1.2 Hz), 6.87 (1H, dd, *J*=7.8, 1.2 Hz), 4.18 - 4.11 (3H, m), 3.88 - 3.83 (1H, m), 3.69 - 3.64 (2H, m), 3.48 (3H, s), 3.32 (3H, s), 3.30 - 3.13 (2H, m), 3.11 - 2.91 (2H, m), 2.04 (3H, s), 1.29 (3H, d, *J*=6.4 Hz).

Methyl 4-bromo-3-((tetrahydro-2H-pyran-4-yl)methoxy)benzoate, 3.43

To a solution of methyl 4-bromo-3-hydroxybenzoate (2 g, 8.66 mmol) in acetone (64.9 mL) and *N,N*-dimethylformamide (21.6 mL) stirred at RT was added solid potassium carbonate (1.80 g, 12.98 mmol) followed by 4-(bromomethyl)tetrahydro-2H-pyran (2.33 g, 12.98 mmol). The reaction mixture was stirred at 60 °C for 16 h. After this time, the reaction was incomplete. An additional 1 eq. of 4-(bromomethyl)tetrahydro-2H-pyran (1.53 g, 8.65 mmol) was added and stirred for 24 h. The reaction was cooled to room temperature, the solvent removed under

reduced pressure and the liquid dissolved in 1:1 ethyl acetate:water (200 mL). The layers were separated and the organics collected. The aqueous was washed further with ethyl acetate (2 x 100 mL), and the combined organics were washed with brine, dried by passing through a hydrophobic frit, and the solvent removed *in vacuo* to yield the crude product as a yellow viscous liquid. The crude material was diluted with DCM (4 mL) and loaded onto a 100 g SNAP silica column. The crude material on silica was purified by Biotage SP4 using a gradient of 0 - 40% ethyl acetate in cyclohexane. Fractions containing pure product were collected and the solvent removed under reduced pressure to yield methyl 4-bromo-3-((tetrahydro-2H-pyran-4-yl)methoxy)benzoate (2.45 g, 7.37 mmol, 85% yield) as a light yellow oil. Rf = 0.28, 25% ethyl acetate in cyclohexane. LCMS (formic acid): rt = 1.17 min, MH+ 329.0, 331.1. ¹H NMR δ(400 MHz, CDCl₃) ppm: 7.62 - 7.58 (1H, m), 7.53 - 7.48 (2H, m), 4.04 (2H, dd, J=11.0, 3.4 Hz), 3.95 - 3.90 (5H, m), 3.47 (2H, td, J=11.7, 2.0 Hz), 2.22 - 2.09 (1H, m), 1.86 - 1.78 (2H, m), 1.59 - 1.46 (2H, m). ¹³C NMR δ(101 MHz, CDCl₃) ppm: 166.4 (COO), 155.3 (C-O), 133.3 (C-H), 130.5 (C-COO), 122.8 (C-H), 118.0 (C-Br), 113.4 (C-H), 73.7 (O-CH₂), 67.6 (2 x O-CH₂), 52.4 (O-CH₃), 35.1 (CH), 29.6 (2 x CH₂). IR (CDCl₃): 2947, 2857, 1727, 1288, 1233, 1111, 1092, 875, 854. HRMS (ESI) exact mass calculated for C₁₄H₁₈⁷⁹BrO₄ [M+H]⁺ m/z 329.0383, found m/z 329.0387.

(S)-Methyl 4-bromo-3-((1-methoxypropan-2-yl)oxy)benzoate, 3.45



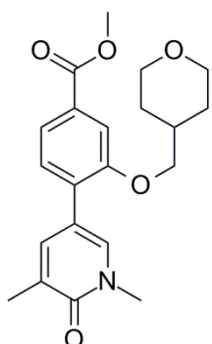
Diisopropyl azodicarboxylate (3.16 mL, 16.2 mmol) was added dropwise over 2 min to a stirred solution of methyl 4-bromo-3-hydroxybenzoate (2.5 g, 10.8 mmol), triphenylphosphine (4.26 g, 16.2 mmol) and (*R*)-1-methoxypropan-2-ol (1.27 mL, 13.0 mmol) in tetrahydrofuran (75 mL) at 0 °C under N₂. Following stirring at 0 °C for 15 min, the cooling bath was removed and resulting solution was stirred at RT overnight. After this time, the volatiles were removed under reduced pressure and the mixture was diluted with ethyl acetate (175 ml) then partitioned with NaHCO₃ (150 ml). The aqueous layer was extracted with ethyl acetate (2 x 175 mL). The combined organics were washed with brine (50 mL), dried by passing through a hydrophobic frit and the volatiles were removed under reduce pressure. The crude product was dissolved in DCM (8 mL) and loaded onto two 100 g SNAP silica columns. The crude material on silica was purified by Biotage SP4 using a gradient of 0 - 30% ethyl acetate in cyclohexane over 15 CV. Fractions containing product

were collected and the volatiles were removed under reduce pressure to yield (S)-methyl 4-bromo-3-((1-methoxypropan-2-yl)oxy)benzoate (3.18 g, 10.3 mmol, 95% yield) as a clear liquid. LCMS (formic acid): rt = 1.26 min, MH⁺ 302.8, 304.9. ¹H NMR δ(400 MHz, CDCl₃) ppm: 7.63 (1H, d, J=2.0 Hz), 7.60 (1H, d, J=8.3 Hz), 7.50 (1H, dd, J=8.2, 1.8 Hz), 4.69 - 4.60 (1H, m), 3.91 (3H, s), 3.66 (1H, dd, J=10.5, 6.1 Hz), 3.55 (1H, dd, J=10.3, 4.4 Hz), 3.43 (3H, s), 1.37 (3H, d, J=6.4 Hz). ¹³C NMR δ(101 MHz, CDCl₃) ppm: 166.4 (COO), 154.7 (C-O), 133.4 (CH), 130.4 (C-C), 123.1 (CH), 119.4 (C-Br), 116.2 (CH), 75.8 (O-CH₂), 75.5 (OCH), 59.5 (COOCH₃), 52.3 (O-CH₃), 16.9 (CH-CH₃). HRMS (ESI) exact mass calculated for C₁₂H₁₆⁷⁹BrO₄ [M+H]⁺ m/z 303.0226, found m/z 303.0234. [α_D]^{22.5°C}_λ(c 1, CDCl₃): +8.5 °.

General experimental procedure for Suzuki cross coupling

To a solution of aryl bromide (a) and 1,3-dimethyl-5-(4,4,5,5-tetramethyl-1,3,2-dioxaborolan-2-yl)pyridin-2(1H)-one (b) in 1,4-dioxane (c) and water (d) stirred under nitrogen at RT was added palladium tetrakis triphenylphosphine (e) and 1 M aqueous potassium carbonate (f). The reaction mixture was stirred at 95 °C for time (g). After cooling to room temperature, the reaction mixture was diluted with water (100 mL) and extracted with ethyl acetate (3 x 100 mL). The combined organics were extracted with brine (50 mL). The organics were dried by passing through a hydrophobic frit and the solvent was removed under reduced pressure. The crude oil was dissolved in DCM (5 mL) and loaded onto a 100 g SNAP silica column. The crude material on silica was purified by Biotage SP4 using gradient (h). Fractions containing the desired product were evaporated *in vacuo* to yield the desired product (i).

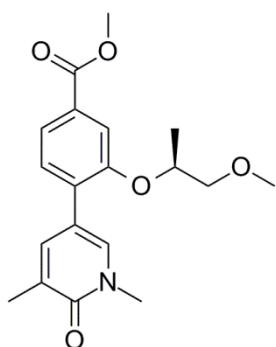
Methyl 4-(1,5-dimethyl-6-oxo-1,6-dihydropyridin-3-yl)-3-((tetrahydro-2H-pyran-4-yl) methoxy)benzoate, 3.46



(a) Methyl 4-bromo-3-((tetrahydro-2H-pyran-4-yl)methoxy)benzoate (2.28 g, 6.93 mmol), (b) 2.59 g, 10.39 mmol, (c) 38 mL, (d) 1.5 mL, (e) 0.24 g, 0.21 mmol, (f) 20.8 mL, 20.8 mmol, (g) 3 h, (h) 0 - 5% ethanol in ethyl acetate, (i) methyl 4-(1,5-dimethyl-6-oxo-1,6-dihydropyridin-3-yl)-3-((tetrahydro-2H-pyran-4-yl) methoxy)benzoate (2.43 g, 6.22 mmol, 90% yield) as a yellow solid. R_f = 0.31, 5% ethanol in ethyl acetate. LCMS (formic acid):

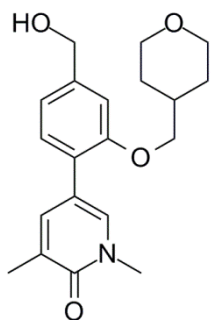
rt = 1.00 min, MH+ 372.1. ^1H NMR δ (400 MHz, CDCl_3) ppm: 7.68 (1H, dd, $J=7.9$, 1.6 Hz), 7.58 (1H, d, $J=1.5$ Hz), 7.50 - 7.47 (1H, m), 7.46 (1H, d, $J=2.2$ Hz), 7.30 (1H, d, $J=7.8$ Hz), 4.01 (2H, dd, $J=11.2$, 3.4 Hz), 3.94 (3H, s), 3.90 (2H, d, $J=6.4$ Hz), 3.61 (3H, s), 3.42 (2H, td, $J=11.8$, 2.1 Hz), 2.20 (3H, s), 2.11 - 2.00 (1H, m), 1.68 (2H, dd, $J=12.8$, 1.8 Hz), 1.47 (2H, qd, $J=12.2$, 4.6 Hz). ^{13}C NMR δ (101 MHz, CDCl_3) ppm: 166.7 (COOR), 162.6 (C=O), 155.6 (C-O), 138.6 (C-CH), 135.6 (N-CH), 130.8 (C-COOR), 130.2 (C-C), 129.1 (CH), 128.4 (C- CH_3), 122.5 (CH), 115.6 (C-C), 112.9 (CH), 73.2 (O- CH_2), 67.5 (2 x O- CH_2), 52.3 (COO CH_3), 38.0 (N- CH_3), 35.2 (CH), 29.8 (2 x CH_2), 17.2 (C- CH_3). IR (CDCl_3): 1718, 1654, 1289, 1229. HRMS (ESI) exact mass calculated for $\text{C}_{21}\text{H}_{26}\text{NO}_5$ [M+H] $^+$ m/z 372.1805, found m/z 372.1809. Melting point: 126 – 127 °C

(S)-Methyl 4-(1,5-dimethyl-6-oxo-1,6-dihydropyridin-3-yl)-3-((1-methoxypropan-2-yl)oxy)benzoate, 3.47

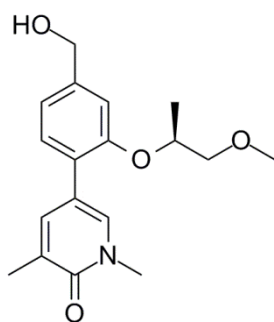


(a) (S)-Methyl 4-bromo-3-((1-methoxypropan-2-yl)oxy)benzoate (3.03 g, 9.00 mmol), (b) 2.87 g, 11.5 mmol, (c) 49 mL, (d) 2.0 mL, (e) 0.31 g, 0.27 mmol, (f) 27.0 mL, 27.0 mmol, (g) 2 h, (h) 0 - 7.5% ethanol in ethyl acetate, (i) (S)-methyl 4-(1,5-dimethyl-6-oxo-1,6-dihydropyridin-3-yl)-3-((1-methoxypropan-2-yl)oxy)benzoate (3.04 g, 8.36 mmol, 93% yield) as an off-white solid. LCMS (formic acid): rt = 0.93 min, MH+ 346.3. ^1H NMR δ (400 MHz, CDCl_3) ppm: 7.62 - 7.70 (3H, m), 7.54 (1H, dd, $J=2.4$, 1.2 Hz), 7.31 (1H, d, $J=7.8$ Hz), 4.69 - 4.61 (1H, m), 3.93 (3H, s), 3.61 (3H, s), 3.56 (1H, dd, $J=10.6$, 6.0 Hz), 3.49 (1H, dd, $J=10.4$, 3.8 Hz), 3.39 (3H, s), 2.21 (3H, s), 1.31 (3H, d, $J=6.4$ Hz). ^{13}C NMR δ (101 MHz, CDCl_3) ppm: 166.7 (COOR), 162.6 (C=O), 154.6 (C-O), 138.5 (C-CH), 136.3 (N-CH), 131.7 (C-C), 129.9 (C-C), 129.2 (CH), 128.4 (C- CH_3), 122.6 (CH), 115.5 (C-C), 115.1 (CH), 75.7 (CH $_2$ -O), 73.9 (CH-O), 59.2 (O- CH_3), 52.2 (COO CH_3), 38.0 (N- CH_3), 17.3 (C- CH_3), 16.6 (CH CH_3). IR (CDCl_3): 1717, 1653, 1598. HRMS (ESI) exact mass calculated for $\text{C}_{19}\text{H}_{24}\text{NO}_5$ [M+H] $^+$ m/z 346.1649, found m/z 346.1649. Melting point: 98 – 99 °C. $[\alpha_D]^{22.5^\circ}_\lambda(c\ 1, \text{CDCl}_3)$: +53.6°.

5-(4-(Hydroxymethyl)-2-((tetrahydro-2H-pyran-4-yl)methoxy)phenyl)-1,3-dimethylpyridin-2(1H)-one, 3.48



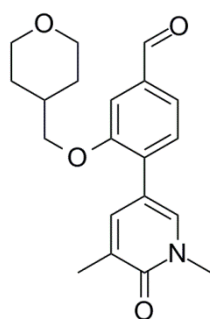
To a solution of methyl 4-(1,5-dimethyl-6-oxo-1,6-dihydropyridin-3-yl)-3-((tetrahydro-2H-pyran-4-yl)methoxy)benzoate (2.4 g, 6.46 mmol) in DCM (32 mL) stirred under nitrogen and cooled to -78 °C in a dry ice-acetone bath was added a 1 M solution of DIBAL-H in tetrahydrofuran (19.4 mL, 19.4 mmol) dropwise during 3 min and stirred for 10 min. After this time, the reaction mixture was warmed to 0 °C and stirred for 2 h. After this time, the reaction was quenched with 10% aq. citric acid (70 mL) and the mixture stirred at 25 °C for 2 h. The layers were separated and the aqueous layer was extracted with DCM (2 x 100 mL) and the combined organics were washed with brine (10 mL), dried and concentrated *in vacuo* to provide crude product. The resulting solid was dissolved in DCM (3 mL) and loaded onto a 25 g SNAP silica column. The crude material on silica was purified by Biotage SP4 using a gradient of 0 - 15% ethanol in ethyl acetate for 21 CV. The fractions containing product were collected and the solvent removed under reduced pressure to yield the desired product 5-(4-(hydroxymethyl)-2-((tetrahydro-2H-pyran-4-yl)methoxy)phenyl)-1,3-dimethylpyridin-2(1H)-one (1.19 g, 3.29 mmol, 51% yield) as a white waxy solid. LCMS (formic acid): *rt* = 0.70 min, *MH*⁺ 344.3. ¹H NMR δ (400 MHz, CDCl₃) ppm: 7.45 (1H, dd, *J*=2.3, 1.1 Hz), 7.36 (1H, d, *J*=2.2 Hz), 7.21 (1H, d, *J*=7.6 Hz), 7.00 - 6.95 (2H, m), 4.71 (2H, d, *J*=5.9 Hz), 4.00 (2H, dd, *J*=11.0, 3.4 Hz), 3.85 (2H, d, *J*=6.6 Hz), 3.59 (3H, s), 3.41 (2H, td, *J*=11.8, 2.1 Hz), 2.19 (3H, s), 1.97 - 2.09 (1H, m), 1.87 (1H, t, *J*=5.9 Hz), 1.70 - 1.64 (2H, m), 1.50 - 1.38 (2H, m). ¹³C NMR δ (101 MHz, CDCl₃) ppm: 162.7 (C=O), 156.0 (C-O), 141.9 (C-CH₂OH), 139.2 (N-CH), 135.0 (C-CH), 129.5 (CH), 128.2 (C-CH₃), 125.4 (C-C), 119.3 (CH), 116.4 (C-C), 110.7 (CH), 73.0 (OCH₂), 67.5 (2 x O-CH₂), 65.1 (CH₂-OH), 37.9 (N-CH₃), 35.3 (CH), 29.8 (2 x CH₂), 17.2 (C-CH₃). IR(neat): 3345, 2936, 1647, 1277, 1145, 1026, 822. HRMS (ESI) exact mass calculated for C₂₀H₂₆NO₄ [M+H]⁺ *m/z* 344.1856, found *m/z* 344.1857. Melting point: 178 – 180 °C.

(S)-5-(4-(Hydroxymethyl)-2-((1-methoxypropan-2-yl)oxy)phenyl)-1,3-dimethylpyridin-2(1H)-one, 3.49

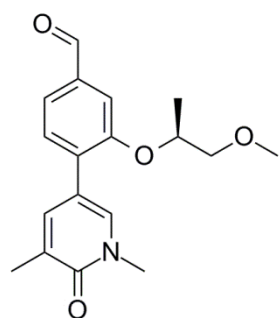
To a solution of (S)-methyl 4-(1,5-dimethyl-6-oxo-1,6-dihydropyridin-3-yl)-3-((1-methoxypropan-2-yl)oxy)benzoate (2.97 g, 8.60 mmol) in DCM (42 mL) stirred under nitrogen and cooled -78 °C in an dry ice-acetone bath was added a 1 M solution of DIBAL-H in tetrahydrofuran (25.8 mL, 25.8 mmol) dropwise during 3 min. After this time, the reaction was stirred for 10 min before the reaction mixture was warmed to 0 °C and stirred for an additional for 2 h. After this time, the reaction was quenched with 10% aq. citric acid (80 mL) and the mixture stirred at 25 °C for 2 h. The layers were separated and the aqueous layer was extracted with DCM (2 x 110 mL) and the combined organics were washed with brine (30 mL), dried and concentrated *in vacuo* to provide crude product. The resulting solid was dissolved in DCM (3 mL) and loaded onto a 25 g SNAP silica column. The crude material on silica was purified by Biotage SP4 using a gradient of 0 - 15% ethanol in ethyl acetate for 21 CV. The fractions containing product were collected and the solvent removed under reduced pressure to yield the desired product (S)-5-(4-(hydroxymethyl)-2-((1-methoxypropan-2-yl)oxy)phenyl)-1,3-dimethylpyridin-2(1H)-one (1.43 g, 4.42 mmol, 51% yield) as a white waxy solid. LCMS (formic acid): rt = 0.69 min, MH⁺ 318.2. ¹H NMR δ(400 MHz, CDCl₃) ppm: 7.53 - 7.49 (2H, m), 7.22 (1H, d, *J*=7.6 Hz), 7.03 - 7.01 (1H, m), 6.97 (1H, dd, *J*=7.8, 1.5 Hz), 4.69 (2H, d, *J*=5.9 Hz), 4.60 - 4.52 (1H, m), 3.59 (3H, s), 3.54 (1H, dd, *J*=10.3, 6.1 Hz), 3.45 (1H, dd, *J*=10.3, 3.9 Hz), 3.38 (3H, s), 2.20 (3H, s), 1.81 (1H, t, *J*=6.0 Hz), 1.28 (3H, d, *J*=6.4 Hz). ¹³C NMR δ(101 MHz, CDCl₃) ppm: 162.3 (C=O), 155.0 (C-O), 141.6 (C-CH₂OH), 139.0 (C-CH), 135.6 (N-CH), 129.6 (CH), 128.1 (C-CH₃), 126.4 (C-C), 119.7 (CH), 116.3 (C-C), 113.1 (CH), 75.9 (CH₂), 73.9 (CH), 65.1 (CH₂OH), 59.2 (O-CH₃), 37.9 (N-CH₃), 17.3 (C-CH₃), 16.8 (CH-CH₃). IR (neat): 3345, 2917, 1654, 1247, 1100, 1048, 825. HRMS (ESI) exact mass calculated for C₁₈H₂₄NO₄ [M+H]⁺ m/z 318.1700, found m/z 318.1699. Melting point: 132-133 °C. [α_D]^{22.8°C}_λ(c 1, CDCl₃): +49.0°.

General experimental for IBX oxidation

To a solution of alcohol (a) in DCM (b) was added 45% iodoxybenzoic acid (stabilised by benzoic acid and isophthalic acid) (c), portionwise. The reaction mixture was stirred at room temperature for 72 h. LCMS analysis indicated no starting material remained. The reaction mixture was partitioned between DCM (3 x 30 mL) and saturated aqueous sodium bicarbonate solution (30 mL). The organic layers were combined, washed with saturated aqueous sodium bicarbonate solution (30 ml), dried using a hydrophobic frit and evaporated under reduced pressure to give the crude product (d).

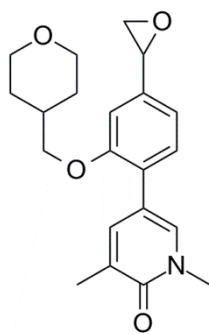
4-(1,5-Dimethyl-6-oxo-1,6-dihydropyridin-3-yl)-3-((tetrahydro-2H-pyran-4-yl) methoxy)benzaldehyde, 3.50


(a) 5-(4-(Hydroxymethyl)-2-((tetrahydro-2H-pyran-4-yl)methoxy) phenyl)-1,3-dimethyl pyridin-2(1H)-one (500 mg, 1.46 mmol), (b) 30 mL, (c) 1.18 g, 1.89 mmol, (d) 4-(1,5-dimethyl-6-oxo-1,6-dihydropyridin-3-yl)-3-((tetrahydro-2H-pyran-4-yl)methoxy) benzaldehyde (490 mg, 1.22 mmol, 84% yield, 85% purity) as a white solid. LCMS (formic acid): rt = 0.84 min, MH⁺ 342.3. ¹H NMR δ(400 MHz, Methanol-*d*₄) ppm: 9.98 (1H, s), 7.82 (1H, d, *J*=2.4 Hz), 7.72 (1H, dd, *J*=2.3, 1.1 Hz), 7.61 - 7.58 (1H, m), 7.58 - 7.57 (1H, m), 7.56 - 7.53 (1H, m), 4.03 - 3.95 (4H, m), 3.66 (3H, s), 3.47 (2H, td, *J*=11.8, 2.1 Hz), 2.19 (3H, s), 2.14 - 2.05 (1H, m), 1.75 - 1.69 (2H, m), 1.57 - 1.45 (2H, m).

(S)-4-(1,5-Dimethyl-6-oxo-1,6-dihydropyridin-3-yl)-3-((1-methoxypropan-2-yl) oxy)benzaldehyde, 3.51


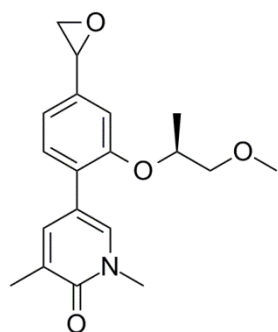
(a) (S)-5-(4-(Hydroxymethyl)-2-((1-methoxypropan-2-yl)oxy) phenyl)-1,3-dimethyl pyridin-2(1H)-one (500 mg, 1.58 mmol), (b) 30 mL, (c) 1.27 g, 2.05 mmol, (d) (S)-4-(1,5-dimethyl-6-oxo-1,6-dihydropyridin-3-yl)-3-((1-methoxypropan-2-yl)oxy)benzaldehyde (536 mg, 1.45 mmol, 92% yield, 85% purity) as a white solid. LCMS (formic acid): rt = 0.83 min, MH⁺ 316.2. ¹H NMR δ(400 MHz, Methanol-*d*₄) ppm: 9.97 (1H, s), 7.92 (1H, d, *J*=2.4 Hz), 7.80 - 7.76 (1H, m), 7.60 (1H, s), 7.58 - 7.55 (2H, m), 4.81 - 4.73 (1H, m), 3.66 (3H, s), 3.59 - 3.56 (2H, m), 3.39 (3H, s), 2.19 (3H, s), 1.33 (3H, d, *J*=6.4 Hz).

1,3-Dimethyl-5-(4-(oxiran-2-yl)-2-((tetrahydro-2H-pyran-4-yl)methoxy)phenyl)pyridin-2(1H)-one, 3.52



Powdered potassium hydroxide (411 mg, 7.32 mmol) was added in a single portion to a stirred suspension of 4-(1,5-dimethyl-6-oxo-1,6-dihydropyridin-3-yl)-3-((tetrahydro-2H-pyran-4-yl)methoxy)benzaldehyde (490 mg, 1.22 mmol) and trimethylsulfonium iodide (254 mg, 1.24 mmol) in acetonitrile (5.3 mL) and water (27 μ L) at RT. The resulting suspension was heated to 65 $^{\circ}$ C for 30 min and then allowed to cool to RT. The suspension was diluted with ethyl acetate (10 mL) and filtered through a hydrophobic frit. The filtrate was diluted with saturated aqueous NaHCO_3 (10 mL). The separated aqueous phase was extracted with ethyl acetate (2 x 10 mL), the combined organic phase was passed through a hydrophobic frit and the solvent evaporated under reduced pressure to yield 1,3-dimethyl-5-(4-(oxiran-2-yl)-2-((tetrahydro-2H-pyran-4-yl)methoxy)phenyl)pyridin-2(1H)-one (482 mg, 1.15 mmol, 94% yield, 85% purity) as a pale yellow oil. LCMS (High pH): rt = 0.91 min, MH^+ 356.3. ^1H NMR δ (400 MHz, CDCl_3) ppm: 7.46 (1H, dd, $J=2.3, 1.1$ Hz), 7.38 (1H, d, $J=2.4$ Hz), 7.23 (1H, d, $J=7.8$ Hz), 6.97 (1H, dd, $J=7.8, 1.5$ Hz), 6.83 (1H, d, $J=1.5$ Hz), 4.02 (2H, dd, $J=11.0, 3.7$ Hz), 3.90 (1H, dd, $J=3.9, 2.7$ Hz), 3.84 (2H, dd, $J=6.4, 1.5$ Hz), 3.62 (3H, s), 3.43 (2H, td, $J=11.9, 2.0$ Hz), 3.19 (1H, dd, $J=5.5, 4.0$ Hz), 2.81 (1H, dd, $J=5.5, 2.6$ Hz), 2.20 (3H, s), 2.06 - 1.98 (1H, m), 1.69 (2H, d, $J=12.5$ Hz), 1.52 - 1.39 (2H, m).

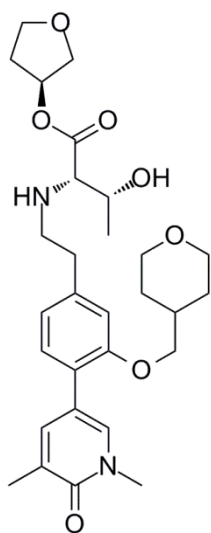
5-(2-(((S)-1-Methoxypropan-2-yl)oxy)-4-(oxiran-2-yl)phenyl)-1,3-dimethylpyridin-2(1H)-one, 3.53



Powdered potassium hydroxide (486 mg, 8.67 mmol) was added in a single portion to a stirred suspension of (S)-4-(1,5-dimethyl-6-oxo-1,6-dihydropyridin-3-yl)-3-((1-methoxypropan-2-yl)oxy)benzaldehyde (536 mg, 1.45 mmol) and trimethylsulfonium iodide (301 mg, 1.47 mmol) in acetonitrile (6.3 mL) and water (31.4 μ L) at RT. The resultant suspension was heated to 65 $^{\circ}$ C for 30 min and then allowed to cool to RT. The suspension was diluted with ethyl acetate (10 mL) and filtered through a hydrophobic frit. The filtrate was diluted with saturated aqueous NaHCO_3 (10 mL). The separated aqueous phase was extracted with EtOAc (2 x 10

mL), the combined organic phase was passed through a hydrophobic frit and the solvent evaporated under reduced pressure to yield 5-(2-(((S)-1-methoxypropan-2-yl)oxy)-4-(oxiran-2-yl)phenyl)-1,3-dimethylpyridin-2(1H)-one (488 mg, 1.26 mmol, 87% yield) (85% purity) as a pale yellow oil. LCMS (high pH): rt = 0.89 min, MH+ 330.2. ¹H NMR δ(400 MHz, CDCl₃) ppm: 7.54 - 7.48 (2H, m), 7.24 - 7.19 (1H, m), 6.94 (1H, dt, J=7.8, 2.0 Hz), 6.88 (1H, s), 4.59 - 4.50 (1H, m), 3.86 (1H, dd, J=4.0, 2.6 Hz), 3.59 (3H, s), 3.56 - 3.50 (1H, m), 3.47 - 3.42 (1H, m), 3.38 (3H, d, J=2.4 Hz), 3.16 (1H, ddd, J=5.6, 4.1, 1.3 Hz), 2.78 (1H, ddd, J=5.5, 2.6, 1.5 Hz), 2.20 (3H, s), 1.27 (3H, dd, J=6.1, 2.2 Hz).

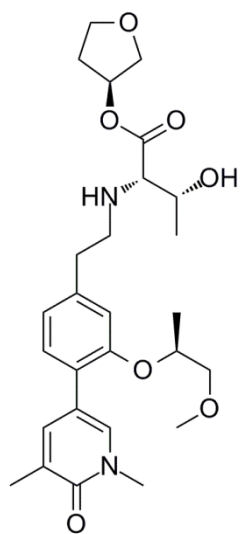
(2S,3R)-(S)-Tetrahydrofuran-3-yl 2-((4-(1,5-dimethyl-6-oxo-1,6-dihydropyridin-3-yl)-3-((tetrahydro-2H-pyran-4-yl)methoxy)phenethyl)amino)-3-hydroxybutanoate, 3.40



To a round bottomed flask was added 1,3-dimethyl-5-(4-(oxiran-2-yl)-2-((tetrahydro-2H-pyran-4-yl)methoxy)phenyl)pyridin-2(1H)-one (482 mg, 1.15 mmol) and the flask flushed with nitrogen before dissolution in tetrahydrofuran (10 mL). To the solution, cooled in an ice bath, was added boron trifluoride diethyl etherate (71 μL, 0.58 mmol). The reaction mixture was stirred at 0 °C for 15 min. After this time, (2S,3R)-(S)-tetrahydrofuran-3-yl 2-amino-3-hydroxybutanoate, hydrochloride (450 mg, 1.99 mmol) and triethylamine (0.48 mL, 3.46 mmol) were added and the mixture warmed to RT and stirred for 10 min. The amino acid ester salt was poorly soluble within the reaction mixture. Therefore, a portion of *p*-toluenesulfonic acid monohydrate (200 mg, 1.05 mmol) was added to aid salt solubility. The mixture was stirred for a further 20 min. After this time, sodium triacetoxyborohydride (977 mg, 4.61 mmol) was added and the mixture stirred for 16 h. The reaction mixture was diluted with DCM (75 mL), the mixture washed with saturated aqueous sodium hydrogen carbonate solution (75 mL) and the layers separated. The aqueous phase was extracted with DCM (3 x 75 mL) and the organics combined, dried by passing through a hydrophobic frit and the solvent removed under reduced pressure. The crude gum was dissolved in DCM (3 mL) and loaded onto a 25 g SNAP silica column. The crude material on silica was purified by Biotage SP4 using a gradient of 0 - 25% ethanol in ethyl acetate over 24 CV. Fractions containing the desired product were collected and the solvent removed *in*

vacuo to yield a yellow gum. The crude material was dissolved in 1:1 MeOH:DMSO (3 mL) and purified by mass directed autoprep on an Xbridge column using 15-55% acetonitrile water with an ammonium carbonate modifier. The solvent was evaporated *in vacuo* to yield (2*S*,3*R*)-(S)-tetrahydrofuran-3-yl 2-((4-(1,5-dimethyl-6-oxo-1,6-dihydro pyridin-3-yl)-3-((tetrahydro-2H-pyran-4-yl)methoxy)phenethyl) amino)-3-hydroxybutanoate (104 mg, 0.19 mmol, 17% yield) as a clear gum. R_f = 0.39, 25% ethanol in ethyl acetate. LCMS (high pH): r_t = 0.91 min, MH^+ 529.4. 1H NMR δ (400 MHz, $CDCl_3$) ppm: 7.47 - 7.43 (1H, m), 7.35 (1H, d, $J=2.2$ Hz), 7.15 (1H, d, $J=7.6$ Hz), 6.83 (1H, dd, $J=7.7, 1.3$ Hz), 6.76 (1H, d, $J=1.2$ Hz), 5.38 - 5.32 (1H, m), 4.00 (2H, dd, $J=11.4, 3.3$ Hz), 3.94 - 3.83 (3H, m), 3.82 (2H, d, $J=6.4$ Hz), 3.78 (1H, d, $J=10.8$ Hz), 3.68 - 3.57 (4H, m), 3.41 (2H, td, $J=11.8, 1.8$ Hz), 3.04 - 2.95 (2H, m), 2.89 - 2.72 (3H, m), 2.26 - 2.16 (4H, m), 2.07 - 1.95 (2H, m), 1.71 - 1.64 (2H, m), 1.50 - 1.38 (2H, m), 1.22 (3H, d, $J=6.4$ Hz).

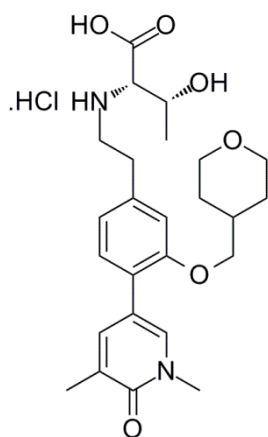
(2*S*,3*R*)-(S)-Tetrahydrofuran-3-yl 2-((4-(1,5-dimethyl-6-oxo-1,6-dihydropyridin-3-yl)-3-(((S)-1-methoxypropan-2-yl)oxy)phenethyl)amino)-3-hydroxybutanoate, 3.54



To a round bottomed flask was added 5-(2-(((S)-1-methoxypropan-2-yl)oxy)-4-(oxiran-2-yl)phenyl)-1,3-dimethyl pyridin-2(1H)-one (488 mg, 1.26 mmol) and the flask flushed with nitrogen before dissolution in tetrahydrofuran (10 mL). To the solution, cooled in an ice bath, was added boron trifluoride diethyl etherate (77 μ L, 0.63 mmol). The reaction mixture was stirred at 0 $^{\circ}$ C for 15 min. After this time, (2*S*,3*R*)-(S)-tetrahydrofuran-3-yl 2-amino-3-hydroxybutanoate, hydrochloride (450 mg, 1.99 mmol) and triethylamine (0.53 mL, 3.78 mmol) were added and the mixture warmed to RT and was stirred for 10 min. The amino ester salt was poorly soluble within the reaction mixture. Therefore, a portion of *p*-toluenesulfonic acid monohydrate (200 mg, 1.05 mmol) was added to aid salt solubility. The mixture was stirred for a further 20 min. After this time, sodium triacetoxyborohydride (1.07 g, 5.04 mmol) was added and the mixture stirred for 24 h. The reaction mixture was diluted with DCM (60 mL), the mixture washed with saturated aqueous sodium hydrogen carbonate solution (60 mL) and the layers separated. The aqueous was extracted with DCM (3 x 60 mL) and the organics combined, dried by passing

through a hydrophobic frit and the solvent removed under reduced pressure. The crude gum was dissolved in DCM (3 mL) and loaded onto a 25 g SNAP silica column. The crude material on silica was purified by Biotage SP4 using a gradient of 0 - 25% ethanol in ethyl acetate over 24 CV. Fractions containing the desired product were collected and the solvent removed *in vacuo* to yield a yellow gum. The crude material was dissolved in DMSO (3 mL) and purified by mass directed autoprep on an Xbridge column using 15-55% acetonitrile water with an ammonium carbonate modifier. The solvent was evaporated *in vacuo* to yield (2*S*,3*R*)-(S)-tetrahydrofuran-3-yl 2-((4-(1,5-dimethyl-6-oxo-1,6-dihydropyridin-3-yl)-3-(((S)-1-methoxypropan-2-yl)oxy)phenethyl)amino)-3-hydroxybutanoate (236 mg, 0.45 mmol, 35% yield) as a clear gum. $R_f = 0.37$, 25% ethanol in ethyl acetate. LCMS (high pH): $rt = 0.90$ min, $MH^+ 503.4$. 1H NMR δ (400 MHz, $CDCl_3$) ppm: 7.50 (2H, s), 7.16 (1H, d, $J=8.3$ Hz), 6.85 - 6.80 (2H, m), 5.37 - 5.32 (1H, m), 4.55 - 4.46 (1H, m), 3.94 - 3.82 (3H, m), 3.80 - 3.75 (1H, m), 3.67 - 3.57 (4H, m), 3.53 (1H, dd, $J=10.1, 6.2$ Hz), 3.44 (1H, dd, $J=10.3, 3.9$ Hz), 3.38 (3H, s), 3.04 - 2.93 (2H, m), 2.87 - 2.71 (3H, m), 2.27 - 2.16 (4H, m), 2.04 - 1.96 (1H, m), 1.27 (3H, d, $J=6.4$ Hz), 1.21 (3H, d, $J=6.4$ Hz).

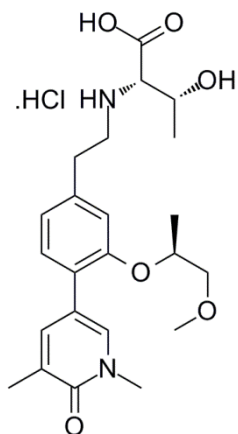
(2*S*,3*R*)-2-((4-(1,5-Dimethyl-6-oxo-1,6-dihydropyridin-3-yl)-3-((tetrahydro-2H-pyran-4-yl)methoxy)phenethyl)amino)-3-hydroxybutanoic acid, hydrochloride, 3.55



A carousel tube was charged with (2*S*,3*R*)-(S)-tetrahydrofuran-3-yl 2-((4-(1,5-dimethyl-6-oxo-1,6-dihydropyridin-3-yl)-3-((tetrahydro-2H-pyran-4-yl)methoxy)phenethyl)amino)-3-hydroxybutanoate (45 mg, 0.09 mmol), tetrahydrofuran (2 mL), methanol (2 mL) and water (1 mL). To the stirred solution was added lithium hydroxide (8.2 mg, 0.34 mmol) and the mixture warmed to 50 °C for 72 h. The reaction mixture was cooled to room temperature and the volatiles were removed under a stream of nitrogen to give a yellow oil. The resulting oil was dissolved in 1:1 MeOH:DMSO (1 mL) and purified by mass directed autoprep on an Xbridge column using 5 to 30% acetonitrile water with an ammonium carbonate modifier. The fractions containing the desired products were collected and the solvent was evaporated *in vacuo* to give the crude product as a white solid, which was further dried by vacuum oven. The solid was suspended

in water (0.5 mL) and 2 M aqueous HCl solution (0.2 mL) was added. The clear solution was blown down a stream of nitrogen and further dried by vacuum oven to yield (2*S*,3*R*)-2-((4-(1,5-dimethyl-6-oxo-1,6-dihydropyridin-3-yl)-3-((tetrahydro-2H-pyran-4-yl)methoxy) phenethyl)amino)-3-hydroxybutanoic acid, hydrochloride (21.8 mg, 0.044 mmol, 52% yield) as a white solid. LCMS (high pH): *rt* = 0.62 min, *MH*⁺ 459.2. ¹H NMR δ(400 MHz, DMSO-*d*₆) ppm 9.09 (1H, br. s.), 8.93 (1H, br. s.), 7.67 (1H, d, *J*=2.4 Hz), 7.51 (1H, s), 7.25 (1H, d, *J*=7.6 Hz), 6.94 (1H, s), 6.85 (1H, d, *J*=7.6 Hz), 4.18 - 4.10 (1H, m), 3.91 - 3.83 (5H, m), 3.48 (3H, s), 3.32 (2H, t, *J*=10.8 Hz), 3.28 - 3.13 (2H, m), 3.11 - 2.91 (2H, m), 2.06 - 1.92 (4H, m), 1.61 (2H, d, *J*=13.9 Hz), 1.41 - 1.32 (2H, m), 1.29 (3H, d, *J*=6.4 Hz).

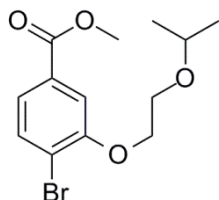
(2*S*,3*R*)-2-((4-(1,5-Dimethyl-6-oxo-1,6-dihydropyridin-3-yl)-3-(((*S*)-1-methoxypropan-2-yl)oxy)phenethyl)amino)-3-hydroxybutanoic acid, hydrochloride, 3.56



A carousel tube was charged with (2*S*,3*R*)-(*S*)-tetrahydrofuran-3-yl 2-((4-(1,5-dimethyl-6-oxo-1,6-dihydropyridin-3-yl)-3-(((*S*)-1-methoxypropan-2-yl)oxy)phenethyl)amino)-3-hydroxy butanoate (90 mg, 0.18 mmol), tetrahydrofuran (4 mL), methanol (4 mL) and water (2 mL). To the stirred solution was added lithium hydroxide (17 mg, 0.72 mmol) and the mixture warmed to 50 °C for 72 h. The reaction mixture was cooled to room temperature and the volatiles were removed under a stream of nitrogen to give a yellow oil. The resulting oil was dissolved in 1:1 MeOH:DMSO (1 mL) and purified by mass directed autoprep on an Xbridge column using 5 to 30% acetonitrile water with an ammonium carbonate modifier. The fractions containing the desired products were collected and the solvent was evaporated *in vacuo* to give the crude product as a white solid, which was further dried by vacuum oven. The solids were suspended in water (0.5 mL) and 2 M aqueous HCl solution (0.2 mL) was added. The clear solutions was blown down a stream of nitrogen and further dried by vacuum oven to yield (2*S*,3*R*)-2-((4-(1,5-dimethyl-6-oxo-1,6-dihydropyridin-3-yl)-3-(((*S*)-1-methoxypropan-2-yl)oxy)phenethyl) amino)-3-hydroxybutanoic acid, hydrochloride (53.6 mg, 0.11 mmol, 64% yield) as an off-white solid. LCMS (high pH): *rt* = 0.60 min, *MH*⁺ 433.1. ¹H NMR δ(400 MHz, DMSO-*d*₆) ppm: 9.08 (1H, br. s.), 9.02 (1H, br. s.), 7.72 (1H, d, *J*=2.4 Hz), 7.60 - 7.53 (1H, m), 7.25 (1H, d, *J*=7.8 Hz), 6.97 (1H, d, *J*=1.0 Hz), 6.85 (1H, dd, *J*=7.8, 1.2

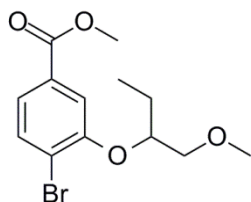
Hz), 4.67 - 4.59 (1H, m), 4.18 - 4.10 (1H, m), 3.86 (1H, d, $J=4.6$ Hz), 3.50 - 3.45 (5H, m), 3.29 (3H, s), 3.28 - 3.17 (2H, m), 3.10 - 2.93 (2H, m), 2.04 (3H, s), 1.29 (3H, d, $J=6.4$ Hz), 1.22 (3H, d, $J=6.1$ Hz).

Methyl 4-bromo-3-(2-isopropoxyethoxy)benzoate, 3.65



Diisopropyl azodicarboxylate (3.16 mL, 16.2 mmol) was added dropwise over 2 min to a stirred solution of methyl 4-bromo-3-hydroxybenzoate (2.5 g, 10.8 mmol), triphenylphosphine (4.26 g, 16.2 mmol) and 2-isopropoxyethanol (1.5 mL, 13.0 mmol) in tetrahydrofuran (75 mL) at 0 °C under N₂. Following stirring at 0 °C for 15 min, the cooling bath was removed and resulting solution was stirred at RT overnight. After this time, LCMS analysis indicated reaction completion. The volatiles were removed under reduced pressure and the mixture was diluted with ethyl acetate (175 mL) then partitioned with saturated aqueous NaHCO₃ (150 mL). The aqueous layer was extracted with ethyl acetate (2 x 175 mL). The combined organics were washed with brine (50 mL), dried by passing through a hydrophobic frit and the volatiles were removed under reduce pressure. The crude product was dissolved in DCM (5 mL) and loaded onto a 100 g SNAP silica column. The crude material on silica was purified by Biotage SP4 using a gradient of 0 - 30% ethyl acetate in cyclohexane over 18 CV. Fractions containing product were collected and the volatiles were removed under reduce pressure to yield methyl 4-bromo-3-(2-isopropoxyethoxy)benzoate (2.93 g, 8.78 mmol, 81% yield) as a clear liquid. LCMS (formic acid): *rt* = 1.29 min, *MH*⁺ 316.9, 318.9. ¹H NMR δ(400 MHz, CDCl₃) ppm: 7.62 - 7.57 (2H, m), 7.50 (1H, dd, $J=8.3, 1.7$ Hz), 4.25 - 4.19 (2H, m), 3.91 (3H, s), 3.88 - 3.82 (2H, m), 3.75 (1H, spt, $J=6.1$ Hz), 1.21 (6H, d, $J=6.1$ Hz).

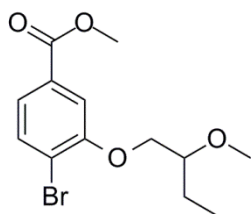
Methyl 4-bromo-3-((1-methoxybutan-2-yl)oxy)benzoate, 3.66



Diisopropyl azodicarboxylate (3.16 mL, 16.2 mmol) was added dropwise over 2 min to a stirred solution of methyl 4-bromo-3-hydroxybenzoate (2.5 g, 10.8 mmol), triphenylphosphine (4.26 g, 16.2 mmol) and 1-methoxybutan-2-ol (1.49 mL, 13.0 mmol) in tetrahydrofuran (75 mL) at 0 °C under N₂. Following stirring at 0 °C for 15 min, the cooling bath was removed and resulting solution was stirred at RT overnight. After this time, LCMS analysis indicated reaction completion. The

volatiles were removed under reduced pressure and the mixture was diluted with ethyl acetate (175 mL) then partitioned with saturated aqueous NaHCO₃ (150 mL). The aqueous layer was extracted with ethyl acetate (2 x 175 mL). The combined organics were washed with brine (50 mL), dried by passing through a hydrophobic frit and the volatiles were removed under reduce pressure. The crude product was dissolved in DCM (5 mL) and loaded onto a 100 g SNAP silica column. The crude material on silica was purified by Biotage SP4 using a gradient of 0 - 12% ethyl acetate in cyclohexane over 14 CV. Fractions containing product were collected and the volatiles were removed under reduce pressure to yield methyl 4-bromo-3-((1-methoxybutan-2-yl)oxy)benzoate (3.11 g, 9.61 mmol, 89% yield) as a clear liquid. LCMS (formic acid): rt = 1.32 min, MH⁺ 317.1, 319.0. ¹H NMR δ(400 MHz, CDCl₃) ppm: 7.66 (1H, d, *J*=2.0 Hz), 7.59 (1H, d, *J*=8.3 Hz), 7.48 (1H, dd, *J*=8.2, 1.8 Hz), 4.50 - 4.42 (1H, m), 3.91 (3H, s), 3.64 (1H, dd, *J*=10.5, 5.9 Hz), 3.58 (1H, dd, *J*=10.5, 4.4 Hz), 3.40 (3H, s), 1.83 - 1.73 (2H, m), 1.02 (3H, t, *J*=7.5 Hz). ¹³C NMR δ(101 MHz, CDCl₃) ppm: 166.4 (COO), 155.2 (C-O), 133.4 (CH), 130.4 (C-Br), 123.0 (CH), 119.2 (C-COO), 116.0 (CH), 80.6 (O-CH), 74.0 (O-CH₂), 59.4 (O-CH₃), 52.3 (COOCH₃), 24.4 (CH₂), 9.5 (CH₃). IR (neat): 2933, 2880, 1721, 1586, 1575, 1410, 1287, 1230, 1104.

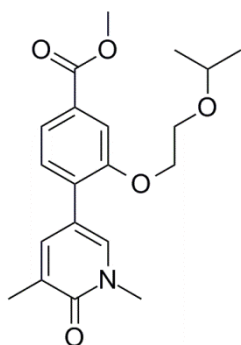
Methyl 4-bromo-3-(2-methoxybutoxy)benzoate, 3.67



Diisopropyl azodicarboxylate (3.16 mL, 16.2 mmol) was added dropwise over 2 min to a stirred solution of methyl 4-bromo-3-hydroxybenzoate (2.5 g, 10.8 mmol), triphenylphosphine (4.26 g, 16.2 mmol) and 2-methoxybutan-1-ol (1.45 mL, 13.0 mmol) in tetrahydrofuran (75 mL) at 0 °C under N₂. Following stirring at 0 °C for 15 min, the cooling bath was removed and resulting solution was stirred at RT for 4 days. The volatiles were removed under reduced pressure and the mixture was diluted with ethyl acetate (175 mL) then partitioned with saturated aqueous NaHCO₃ (150 mL). The aqueous layer was extracted with ethyl acetate (175 mL). The combined organics were washed with brine (50 mL), dried by passing through a hydrophobic frit and the volatiles were removed under reduce pressure. The crude product was diluted with cyclohexane (5 mL) and loaded onto a 100 g SNAP silica column. The crude material on silica was purified by Biotage SP4 using a gradient of 0 - 10% ethyl acetate in cyclohexane over 17 CV. Fractions containing product were collected and the volatiles were removed under reduce pressure to

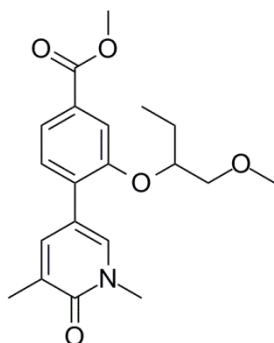
yield methyl 4-bromo-3-(2-methoxybutoxy)benzoate (2.83 g, 8.92 mmol, 82% yield) as a clear liquid, which formed a low melting solid on standing. LCMS (formic acid): rt = 1.31 min, MH+ 317.2, 319.0. ¹H NMR δ(400 MHz, CDCl₃) ppm: 7.60 (1H, d, *J*=8.3 Hz), 7.54 (1H, d, *J*=1.7 Hz), 7.51 (1H, dd, *J*=8.3, 1.7 Hz), 4.12 - 4.04 (2H, m), 3.92 (3H, s), 3.60 - 3.52 (4H, m), 1.78 - 1.60 (2H, m), 1.01 (3H, t, *J*=7.5 Hz). ¹³C NMR δ(101 MHz, CDCl₃) ppm: 166.4 (C=O), 155.4 (C-O), 133.3 (CH), 130.5 (C-COO), 122.9 (CH), 118.0 (C-Br), 113.5 (CH), 80.6 (OCH), 71.3 (OCH₂), 58.5 (OCH₃), 52.3 (CO₂CH₃), 24.5 (CH₂-CH₃), 9.6 (CH₂-CH₃). HRMS (ESI) exact mass calculated for C₁₃H₁₈⁷⁹BrO₄ [M+H]⁺ m/z 317.0383, found m/z 317.0384. IR (CDCl₃): 2936, 2879, 1722, 1290, 1237, 1104. Melting point: 37 – 38 °C.

Methyl 4-(1,5-dimethyl-6-oxo-1,6-dihydropyridin-3-yl)-3-(2-isopropoxyethoxy)benzoate 3.68

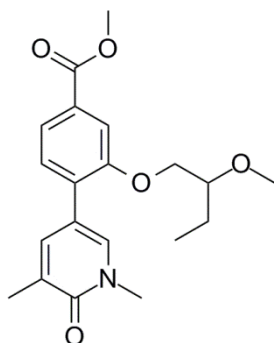


To a solution of methyl 4-bromo-3-(2-isopropoxyethoxy)benzoate (2.9 g, 9.14 mmol) and 1,3-dimethyl-5-(4,4,5,5-tetramethyl-1,3,2-dioxaborolan-2-yl)pyridin-2(1H)-one (2.92 g, 11.7 mmol) in 1,4-dioxane (50 mL) and water (2.0 mL) stirred under nitrogen at RT was added palladium tetrakis triphenylphosphine (0.32 g, 0.27 mmol) and 1 M potassium carbonate (aq) (27.4 mL, 27.4 mmol). The reaction mixture was stirred at 95 °C for 2 h. After cooling to room temperature, the reaction mixture was diluted with water (120 mL) and extracted with ethyl acetate (3 x 100 mL). The combined organics were extracted with brine (30 mL), dried by passing through a hydrophobic frit and the solvent was removed under reduced pressure. The resulting red oil was dissolved in DCM (5 mL) and loaded onto a 100 g SNAP silica column. The crude material on silica was purified by Biotage SP4 using a gradient of 0 - 5% ethanol in ethyl acetate over 12 CV. Fractions containing the desired product were evaporated *in vacuo* and further dried under high vacuum to yield the desired product methyl 4-(1,5-dimethyl-6-oxo-1,6-dihydropyridin-3-yl)-3-(2-isopropoxyethoxy)benzoate (2.7 g, 7.14 mmol, 78% yield) as a pale yellow solid. LCMS (formic acid): rt = 1.05 min, MH+ 360.0. ¹H NMR δ(400 MHz, CDCl₃) ppm: 7.68 (1H, dd, *J*=8.1, 1.5 Hz), 7.64 (1H, d, *J*=2.2 Hz), 7.61 (1H, d, *J*=1.5 Hz), 7.55 (1H, dd, *J*=2.4, 1.2 Hz), 7.32 (1H, d, *J*=7.8 Hz), 4.23 - 4.17 (2H, m), 3.93 (3H, s), 3.80 - 3.74 (2H, m), 3.69 - 3.60 (4H, m), 2.21 (3H, s), 1.18 (6H, d, *J*=6.1 Hz).

Methyl 4-(1,5-dimethyl-6-oxo-1,6-dihydropyridin-3-yl)-3-((1-methoxybutan-2-yl)oxy)benzoate, 3.69

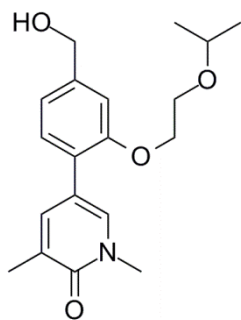


To a solution of methyl 4-bromo-3-((1-methoxybutan-2-yl)oxy)benzoate (3.0 g, 9.46 mmol) and 1,3-dimethyl-5-(4,4,5,5-tetramethyl-1,3,2-dioxaborolan-2-yl)pyridin-2(1H)-one (3.02 g, 12.1 mmol) in 1,4-dioxane (50 mL) and water (2.0 mL) stirred under nitrogen at RT was added palladium tetrakis triphenylphosphine (0.33 g, 0.28 mmol) and 1 M potassium carbonate (aq) (28.4 mL, 28.4 mmol). The reaction mixture was stirred at 95 °C for 2 h. After cooling to room temperature, the reaction mixture was diluted with water (120 mL) and extracted with ethyl acetate (3 x 100 mL). The combined organics were extracted with brine (30 mL). The organics were combined, dried by passing through a hydrophobic frit and the solvent was removed under reduced pressure. The resulting red oil was dissolved in DCM (5 mL) and loaded onto a 100 g SNAP silica column. The crude material on silica was purified by Biotage SP4 using a gradient of 0 - 5% ethanol in ethyl acetate over 12 CV. Fractions containing the desired product were evaporated *in vacuo* and further dried under high vacuum to yield the desired product methyl 4-(1,5-dimethyl-6-oxo-1,6-dihydropyridin-3-yl)-3-((1-methoxybutan-2-yl)oxy)benzoate (3.55 g, 8.89 mmol, 94% yield)(90% purity) as a yellow gum. LCMS (formic acid): *rt* = 1.07 min, *MH*⁺ 360.0. ¹H NMR δ (400 MHz, CDCl₃) ppm: 7.68 - 7.62 (3H, m), 7.54 (1H, dd, *J*=2.4, 1.0 Hz), 7.31 (1H, d, *J*=8.3 Hz), 4.50 - 4.42 (1H, m), 3.93 (3H, s), 3.61 (3H, s), 3.58 - 3.49 (2H, m), 3.36 (3H, s), 2.21 (3H, s), 1.73 (2H, quin, *J*=7.0 Hz), 0.96 (3H, t, *J*=7.5 Hz).

Methyl 4-(1,5-dimethyl-6-oxo-1,6-dihydropyridin-3-yl)-3-(2-methoxybutoxy)benzoate, 3.70

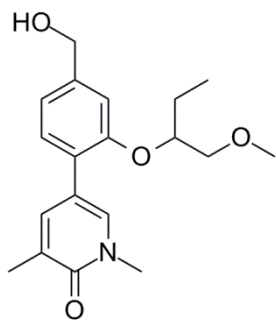
To a solution of methyl 4-bromo-3-(2-methoxybutoxy)benzoate (2.5 g, 7.88 mmol) and 1,3-dimethyl-5-(4,4,5,5-tetramethyl-1,3,2-dioxaborolan-2-yl)pyridin-2(1H)-one (2.51 g, 10.1 mmol) in 1,4-dioxane (50 mL) and water (2.0 mL) stirred under nitrogen at RT was added palladium tetrakis triphenylphosphine (0.27 g, 0.24 mmol) and 1 M potassium carbonate (aq) (23.7 mL, 23.7 mmol). The reaction mixture was stirred at 95 °C for 2 h. After cooling to room temperature, the reaction mixture was diluted with water (100 mL) and extracted with ethyl acetate (3 x 75 mL). The combined organics were washed with brine (50 mL), dried by passing through a hydrophobic frit and the solvent removed under reduced pressure. The resulting red oil was dissolved in DCM (5 mL) and loaded onto a 220 g RediSep silica column. The crude material on silica was purified by Biotage Isolera using a gradient of 75 - 100% ethyl acetate in cyclohexane over 15 CV. Fractions containing the desired product were evaporated *in vacuo* and further dried under high vacuum to yield the desired product methyl 4-(1,5-dimethyl-6-oxo-1,6-dihydropyridin-3-yl)-3-(2-methoxybutoxy)benzoate (1.98 g, 5.34 mmol, 68% yield) as a yellow gum. LCMS (formic acid): rt = 1.06 min, MH⁺ 360.2. ¹H NMR δ(400 MHz, CDCl₃) ppm: 7.68 (1H, dd, *J*=7.9, 1.6 Hz), 7.63 (1H, d, *J*=2.2 Hz), 7.59 (1H, d, *J*=1.5 Hz), 7.53 (1H, dd, *J*=2.4, 1.2 Hz), 7.32 (1H, d, *J*=8.1 Hz), 4.09 (1H, dd, *J*=10.0, 3.9 Hz), 4.04 (1H, dd, *J*=9.8, 5.4 Hz), 3.93 (3H, s), 3.61 (3H, s), 3.49 - 3.39 (4H, m), 2.21 (3H, s), 1.69 - 1.60 (2H, m), 0.97 (3H, t, *J*=7.5 Hz). ¹³C NMR δ(101 MHz, CDCl₃) ppm: 166.7 (COOR), 162.6 (C=O), 155.6 (C-O), 138.5 (C-CH), 136.2 (N-CH), 130.9 (C-C), 130.1 (C-C), 129.0 (CH), 128.4 (CCH₃), 122.6 (CH), 115.3 (C-COO), 113.0 (CH), 80.6 (OCH), 69.8 (O-CH₂), 57.6 (O-CH₃), 52.2 (COOCH₃), 37.9 (N-CH₃), 24.0 (CH₂CH₃), 17.2 (C-CH₃), 9.6 (CH₂CH₃). HRMS (ESI) exact mass calculated for C₂₀H₂₆NO₅ [M+H]⁺ m/z 360.1806, found m/z 360.1802. IR (neat): 2941, 1712, 1655, 1599, 1433, 1287, 1222.

5-(4-(Hydroxymethyl)-2-(2-isopropoxyethoxy)phenyl)-1,3-dimethylpyridin-2(1H)-one, 3.71

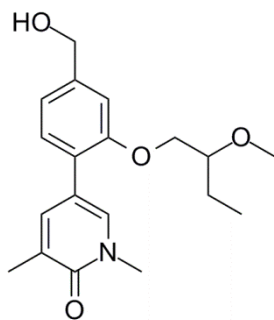


To a solution of methyl 4-(1,5-dimethyl-6-oxo-1,6-dihydropyridin-3-yl)-3-(2-isopropoxyethoxy)benzoate (1.39 g, 3.87 mmol) in DCM (19 mL) stirred under nitrogen and cooled to -78 °C in a dry ice-acetone bath was added a solution of 1 M DIBAL-H in tetrahydrofuran (11.6 mL, 11.6 mmol) dropwise during 3 min. The reaction mixture was stirred at 0 °C for 2 h. After this time, the reaction was quenched with 10% aqueous citric acid (35 mL) and the mixture stirred at 25 °C overnight. The layers were separated and the aqueous layer was extracted with DCM (2 x 60 mL) and the combined organics were washed with brine (15 mL), dried and concentrated *in vacuo* to provide crude product. The resulting solid was suspended in DCM (5 mL), filtered and further washed with DCM. The solid was dried under vacuum to yield the desired product 5-(4-(hydroxymethyl)-2-(2-isopropoxyethoxy)phenyl)-1,3-dimethylpyridin-2(1H)-one (538 mg, 1.62 mmol, 42% yield) as a white solid. LCMS (formic acid): rt = 0.79 min, MH⁺ 332.0. ¹H NMR δ(400 MHz, DMSO-*d*₆) ppm: 7.74 (1H, d, *J*=2.2 Hz), 7.59 (1H, dd, *J*=2.4, 1.2 Hz), 7.25 (1H, d, *J*=7.6 Hz), 7.02 (1H, s), 6.93 (1H, d, *J*=7.8 Hz), 5.18 (1H, t, *J*=5.7 Hz), 4.50 (2H, d, *J*=5.9 Hz), 4.08 (2H, dd, *J*=5.5, 3.8 Hz), 3.68 (2H, dd, *J*=5.4, 3.7 Hz), 3.60 (1H, spt, *J*=6.1 Hz), 3.48 (3H, s), 2.04 (3H, s), 1.08 (6H, d, *J*=6.1 Hz). ¹³C NMR δ(101 MHz, DMSO-*d*₆) ppm: 161.9 (C=O), 155.7 (C-O), 143.7 (C-CH₂), 139.1 (C-CH), 136.4 (N-CH), 129.3 (CH), 126.7 (C-CH₃), 124.3 (C-C), 119.2 (CH), 115.6 (C-C), 111.2 (CH), 71.5 (CH(CH₃)₂), 68.4 (CH₂), 66.3 (CH₂), 63.2 (CH₂OH), 37.6 (N-CH₃), 22.5 (CH(CH₃)₂), 17.5 (C-CH₃). HRMS (ESI) exact mass calculated for C₁₉H₂₆NO₄ [M+H]⁺ m/z 332.1856, found m/z 332.1852. IR (neat): 3333, 2966, 1652, 1578. Melting point: 151 – 153 °C

5-(4-(Hydroxymethyl)-2-((1-methoxybutan-2-yl)oxy)phenyl)-1,3-dimethylpyridin-2(1H)-one, 3.72

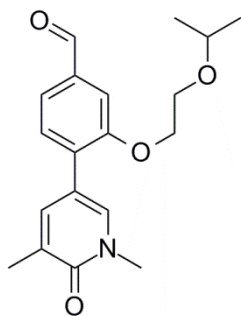


To a solution of methyl 4-(1,5-dimethyl-6-oxo-1,6-dihydropyridin-3-yl)-3-((1-methoxybutan-2-yl)oxy)benzoate (1.85 g, 5.15 mmol) in DCM (25 mL) stirred under nitrogen and cooled to -78 °C in an dry ice-acetone bath was added a solution of 1 M DIBAL-H in tetrahydrofuran (15.4 mL, 15.4 mmol) dropwise during 3 min. The reaction mixture was stirred at 0 °C for 1.5 h. After this time, a small quantity of starting material remained. An additional aliquot of 1 M DIBAL-H in tetrahydrofuran (2.5 mL, 2.5 mmol) was added and stirred for a further 30 min. The reaction was quenched with 10% aqueous citric acid (45 mL) and the mixture stirred at 25°C overnight. The layers were separated and the aqueous layer was extracted with DCM (2 x 60 mL). The combined organics were washed with brine (15 mL), dried and concentrated *in vacuo* to provide crude product. The resulting solid was dissolved in DCM (5 mL) and loaded onto a 50 g SNAP silica column. The crude material on silica was purified by Biotage SP4 using a gradient of 0 - 10% ethanol in ethyl acetate for 20 CV. The fractions containing product were collected and the solvent removed under reduced pressure to yield the desired product which was further dried under high vacuum to yield 5-(4-(hydroxymethyl)-2-((1-methoxybutan-2-yl)oxy)phenyl)-1,3-dimethylpyridin-2(1H)-one (1 g, 3.02 mmol, 59% yield) as a light brown solid. LCMS (formic acid): *rt* = 0.81 min, *MH*⁺ 332.1. ¹H NMR δ(400 MHz, CDCl₃) ppm: 7.53 - 7.47 (2H, m), 7.21 (1H, d, *J*=7.8 Hz), 7.03 (1H, s), 6.96 (1H, dd, *J*=7.6, 1.5 Hz), 4.73 - 4.66 (2H, m), 4.41 - 4.33 (1H, m), 3.59 (3H, s), 3.53 (1H, dd, *J*=10.3, 5.9 Hz), 3.48 (1H, dd, *J*=10.0, 4.2 Hz), 3.35 (3H, s), 2.19 (3H, s), 1.89 (1H, br. s.), 1.76 - 1.65 (2H, m), 0.94 (3H, t, *J*=7.5 Hz). ¹³C NMR δ(101 MHz, CDCl₃) ppm: 162.6 (C=O), 155.4 (C-O), 141.6 (C-CH₂OH), 139.1 (C-CH), 135.5 (N-CH), 129.6 (CH), 128.0 (C-CH₃), 126.4 (C-C), 119.6 (CH), 116.5 (C-C), 113.0 (CH), 79.0 (O-CH), 73.6 (O-CH₂), 65.1 (CH₂OH), 59.2 (O-CH₃), 37.9 (N-CH₃), 24.2 (CH₂), 17.3 (C-CH₃), 9.5 (CH₂-CH₃). IR (CDCl₃): 3310, 2892, 1652, 1581, 1429, 1249, 1110.

5-(4-(Hydroxymethyl)-2-(2-methoxybutoxy)phenyl)-1,3-dimethylpyridin-2(1H)-one, 3.73

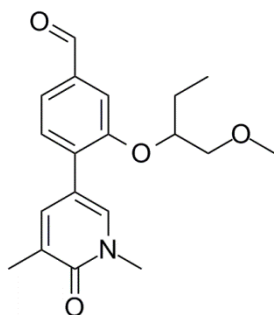
To a solution of methyl 4-(1,5-dimethyl-6-oxo-1,6-dihydropyridin-3-yl)-3-(2-methoxybutoxy)benzoate (1.54 g, 4.28 mmol) in DCM (20 mL) stirred under nitrogen and cooled to -78 °C in an dry ice-acetone bath was added a solution of 1 M DIBAL-H in tetrahydrofuran (12.9 mL, 12.9 mmol) dropwise during 3 min. The reaction mixture was stirred at 0 °C for 1 h. After this time, a small quantity of starting material remained. An additional aliquot of 1 M DIBAL-H in tetrahydrofuran (2.5 mL, 2.5 mmol) was added and stirred for a further 30 min at 0 °C. The reaction was quenched with 10 % aqueous citric acid (50 mL) and the mixture stirred at RT overnight. The layers were separated and the aqueous layer was extracted with DCM (2 x 50 mL). The combined organics were washed with brine (40 mL), dried and concentrated *in vacuo* to provide crude product. The resulting gum was dissolved in DCM (5 mL) and loaded onto a 50 g SNAP silica column. The crude material on silica was purified by Biotage SP4 using a gradient of 0 - 10% ethanol in ethyl acetate for 21 CV which eluted the product. The fractions containing product were collected and the solvent removed under reduced pressure to yield the desired product 5-(4-(hydroxymethyl)-2-(2-methoxybutoxy)phenyl)-1,3-dimethylpyridin-2(1H)-one (1.0 g, 2.93 mmol, 68% yield) as a white solid. LCMS (formic acid): rt = 0.81 min, MH⁺ 332.2. ¹H NMR δ(400 MHz, CDCl₃) ppm: 7.52 - 7.45 (2H, m), 7.21 (1H, d, *J*=7.6 Hz), 7.00 - 6.94 (2H, m), 4.71 (2H, d, *J*=5.9 Hz), 4.04 - 3.96 (2H, m), 3.59 (3H, s), 3.47 - 3.38 (4H, m), 2.19 (3H, s), 1.95 (1H, t, *J*=5.9 Hz), 1.67 - 1.58 (2H, m), 0.96 (3H, t, *J*=7.5 Hz). ¹³C NMR δ(101 MHz, CDCl₃) ppm: 162.6 (C=O), 155.9 (C-O), 141.9 (C-CH₂OH), 139.1 (C-CH), 135.5 (N-CH), 129.3 (CH), 128.1 (C-CH₃), 125.4 (C-C), 119.5 (CH), 116.2 (C-C), 110.9 (CH), 80.7 (O-CH), 69.7 (O-CH₂), 65.0 (CH₂OH), 57.6 (O-CH₃), 37.9 (N-CH₃), 24.0 (CH₂CH₃), 17.2 (C-CH₃), 9.5 (CH₂CH₃). HRMS (ESI) exact mass calculated for C₁₉H₂₆NO₄ [M+H]⁺ m/z 332.1856, found m/z 332.1858. IR (neat): 3318, 2931, 1650, 1576, 1432, 1252, 1087. Melting point: 92 – 94 °C

4-(1,5-Dimethyl-6-oxo-1,6-dihydropyridin-3-yl)-3-(2-isopropoxyethoxy)benzaldehyde, 3.74



To a solution of 5-(4-(hydroxymethyl)-2-(2-isopropoxyethoxy)phenyl)-1,3-dimethylpyridin-2(1H)-one (502 mg, 1.52 mmol) in DCM (30 mL) was added 45% iodoxybenzoic acid (stabilised by benzoic acid and isophthalic acid) (1.23 g, 1.97 mmol), portionwise. The reaction mixture was stirred at room temperature for 72 h. LCMS analysis indicated no starting material remained. The reaction mixture was partitioned between DCM (3 x 30 mL) and saturated aqueous sodium bicarbonate solution (30 mL). The organic layers were combined, washed with saturated aqueous sodium bicarbonate solution (30 mL), dried using a hydrophobic frit and the solvent evaporated under reduced pressure to give the crude product 4-(1,5-dimethyl-6-oxo-1,6-dihydropyridin-3-yl)-3-(2-isopropoxyethoxy)benzaldehyde (537 mg, 1.47 mmol, 97% yield, 90% purity) as a white solid. LCMS (formic acid): $t_r = 0.96$ min, MH^+ 330.1. 1H NMR δ (400 MHz, $CDCl_3$) ppm: 9.97 (1H, s), 7.68 (1H, d, $J=2.4$ Hz), 7.56 (1H, dd, $J=2.4, 1.2$ Hz), 7.50 (1H, dd, $J=7.8, 1.5$ Hz), 7.46 (1H, d, $J=1.2$ Hz), 7.43 (1H, d, $J=7.8$ Hz), 4.25 - 4.18 (2H, m), 3.81 - 3.75 (2H, m), 3.70 - 3.61 (4H, m), 2.22 (3H, s), 1.18 (6H, d, $J=6.1$ Hz).

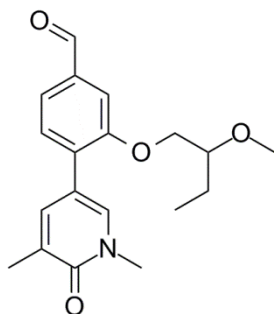
4-(1,5-Dimethyl-6-oxo-1,6-dihydropyridin-3-yl)-3-((1-methoxybutan-2-yl)oxy)benzaldehyde, 3.75



To a solution of 5-(4-(hydroxymethyl)-2-((1-methoxybutan-2-yl)oxy)phenyl)-1,3-dimethylpyridin-2(1H)-one (760 mg, 2.06 mmol) in DCM (45 mL) was added 45% iodoxybenzoic acid (stabilised by benzoic acid and isophthalic acid) (1.67 g, 2.68 mmol), portionwise. The reaction mixture was stirred at room temperature for 72 h. LCMS analysis indicated no starting material remained. The reaction mixture was partitioned between DCM (3 x 45 mL) and saturated aqueous sodium bicarbonate solution (50 mL). The organic layers were combined, washed with saturated aqueous sodium bicarbonate solution (30 mL), dried using a hydrophobic frit and the solvent evaporated under reduced pressure to give the crude product 4-(1,5-dimethyl-6-oxo-1,6-dihydropyridin-3-yl)-3-((1-methoxybutan-2-yl)oxy)benzaldehyde

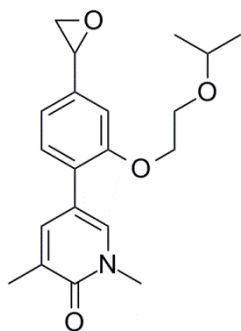
(750 mg, 2.05 mmol, 99% yield, 90% purity) as a pale yellow gum. LCMS (formic acid): rt = 0.98 min, MH+ 330.1. ¹H NMR δ(400 MHz, CDCl₃) ppm: 9.96 (1H, s), 7.68 (1H, d, *J*=2.4 Hz), 7.54 (1H, dd, *J*=2.4, 1.2 Hz), 7.53 - 7.45 (2H, m), 7.42 (1H, d, *J*=7.6 Hz), 4.54 - 4.45 (1H, m), 3.62 (3H, s), 3.59 - 3.52 (2H, m), 3.36 (3H, s), 2.21 (3H, s), 1.79 - 1.69 (2H, m), 0.96 (3H, t, *J*=7.6 Hz).

4-(1,5-Dimethyl-6-oxo-1,6-dihydropyridin-3-yl)-3-(2-methoxybutoxy) benzaldehyde, 3.76



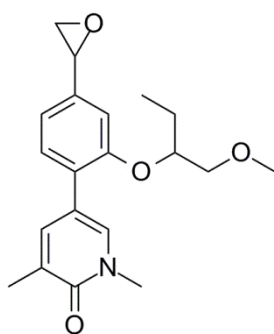
To a solution of 5-(4-(hydroxymethyl)-2-(2-methoxybutoxy) phenyl)-1,3-dimethylpyridin-2(1H)-one (900 mg, 2.44 mmol) in DCM (60 mL) was added 45% iodoxybenzoic acid (stabilised by benzoic acid and isophthalic acid) (2.20 g, 3.54 mmol), portionwise. The reaction mixture was stirred at room temperature for 72 h. LCMS analysis indicated no starting material remained. The reaction mixture was partitioned between DCM (3 x 45 mL) and saturated aqueous sodium bicarbonate solution (75 mL). The organic layers were combined, washed with saturated aqueous sodium bicarbonate solution (30 mL), dried using a hydrophobic frit and the solvent evaporated under reduced pressure to give the crude product 4-(1,5-dimethyl-6-oxo-1,6-dihydropyridin-3-yl)-3-(2-methoxybutoxy)benzaldehyde (0.96 g, 2.48 mmol, 100% yield, 85% purity) as a white solid. LCMS (formic acid): rt = 0.97 min, MH+ 330.1. ¹H NMR δ(400 MHz, CDCl₃) ppm: 9.97 (1H, s), 7.68 (1H, d, *J*=2.4 Hz), 7.54 (1H, d, *J*=1.2 Hz), 7.50 (1H, dd, *J*=7.8, 1.2 Hz), 7.47 - 7.40 (2H, m), 4.17 - 4.01 (2H, m), 3.62 (3H, s), 3.51 - 3.40 (4H, m), 2.21 (3H, s), 1.69 - 1.61 (2H, m), 0.97 (3H, t, *J*=7.5 Hz).

5-(2-(2-Isopropoxyethoxy)-4-(oxiran-2-yl)phenyl)-1,3-dimethylpyridin-2(1H)-one, 3.77



Powdered potassium hydroxide (484 mg, 8.62 mmol) was added in a single portion to a stirred suspension of 4-(1,5-dimethyl-6-oxo-1,6-dihydropyridin-3-yl)-3-(2-isopropoxyethoxy)benzaldehyde (526 mg, 1.44 mmol) and trimethylsulfonium iodide (299 mg, 1.47 mmol) in acetonitrile (6.25 mL) and water (31.2 μ L) at RT. The resultant suspension was heated to 65 $^{\circ}$ C for 30 min and then allowed to cool to RT. The suspension was diluted with ethyl acetate (10 mL) and filtered through a hydrophobic frit. The filtrate was diluted with saturated aqueous NaHCO_3 (10 mL). The separated aqueous phase was extracted with ethyl acetate (2 x 10 mL), the combined organic phase was passed through a hydrophobic frit and the solvent evaporated under reduced pressure to yield 5-(2-(2-isopropoxyethoxy)-4-(oxiran-2-yl)phenyl)-1,3-dimethylpyridin-2(1H)-one (504 mg, 1.32 mmol, 92% yield, 90% purity) as a pale yellow oil. LCMS (high pH): t_r = 1.01 min, MH^+ 344.3. ^1H NMR δ (400 MHz, CDCl_3) ppm: 7.50 (2H, s), 7.21 (1H, d, $J=7.8$ Hz), 6.95 (1H, dd, $J=7.7$, 1.3 Hz), 6.83 (1H, d, $J=1.0$ Hz), 4.16 - 4.08 (2H, m), 3.86 (1H, dd, $J=3.8$, 2.6 Hz), 3.76 - 3.70 (2H, m), 3.68 - 3.57 (4H, m), 3.16 (1H, dd, $J=5.6$, 4.2 Hz), 2.78 (1H, dd, $J=5.5$, 2.6 Hz), 2.20 (3H, s), 1.17 (6H, d, $J=6.1$ Hz).

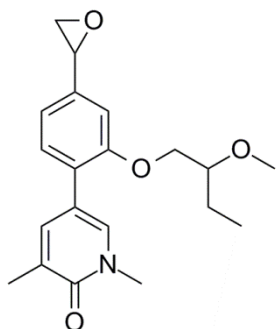
4-(1,5-Dimethyl-6-oxo-1,6-dihydropyridin-3-yl)-3-((1-methoxybutan-2-yl)oxy)benzaldehyde, 3.78



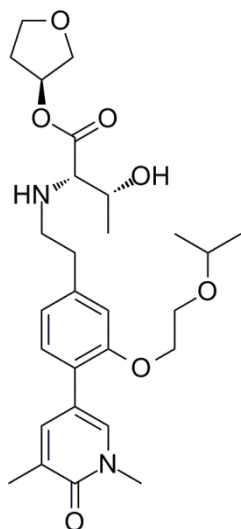
Powdered potassium hydroxide (515 mg, 9.18 mmol) was added in a single portion to a stirred suspension of 4-(1,5-dimethyl-6-oxo-1,6-dihydropyridin-3-yl)-3-((1-methoxybutan-2-yl)oxy)benzaldehyde (560 mg, 1.53 mmol) and trimethylsulfonium iodide (318 mg, 1.56 mmol) in acetonitrile (6.65 mL) and water (33.2 μ L) at RT. The resultant suspension was heated to 65 $^{\circ}$ C for 30 min and then allowed to cool to RT. The suspension was diluted with ethyl acetate (10 mL) and filtered through a hydrophobic frit. The filtrate was diluted with saturated aqueous NaHCO_3 (10 mL). The separated aqueous phase was extracted with ethyl acetate (2 x 10 mL), the combined organic phase was passed through a hydrophobic frit and

evaporated under reduced pressure to yield 5-(2-((1-methoxybutan-2-yl)oxy)-4-(oxiran-2-yl)phenyl)-1,3-dimethylpyridin-2(1H)-one (640 mg, 1.49 mmol, 97% yield, 80% purity) as a pale yellow oil. LCMS (high pH): rt = 1.03 min, MH⁺ 344.3. ¹H NMR δ(400 MHz, CDCl₃) ppm: 7.53 - 7.46 (2H, m), 7.21 (1H, d, J=7.6 Hz), 6.95 - 6.91 (1H, m), 6.90 (1H, s), 4.39 - 4.31 (1H, m), 3.86 (1H, dd, J=3.9, 2.7 Hz), 3.59 (3H, s), 3.55 - 3.45 (2H, m), 3.35 (3H, d, J=2.0 Hz), 3.16 (1H, dd, J=5.4, 4.2 Hz), 2.78 (1H, dd, J=5.5, 2.6 Hz), 2.19 (3H, s), 1.75 - 1.64 (2H, m), 0.93 (3H, td, J=7.5, 2.9 Hz).

5-(2-(2-Methoxybutoxy)-4-(oxiran-2-yl)phenyl)-1,3-dimethylpyridin-2(1H)-one, 3.79



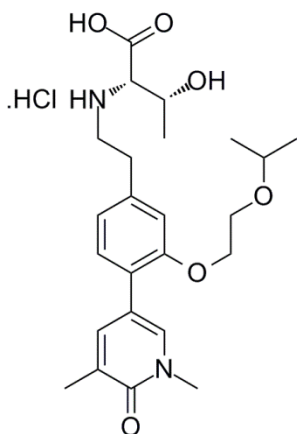
Powdered potassium hydroxide (608 mg, 10.8 mmol) was added in a single portion to a stirred suspension of 4-(1,5-dimethyl-6-oxo-1,6-dihydropyridin-3-yl)-3-(2-methoxybutoxy) benzaldehyde (700 mg, 1.81 mmol) and trimethylsulfonium iodide (376 mg, 1.84 mmol) in acetonitrile (7.85 mL) and water (39.2 mL) at RT. The resultant suspension was heated to 65 °C for 20 min and then allowed to cool to RT. The suspension was diluted with ethyl acetate (15 mL) and filtered through a hydrophobic frit. The filtrate was diluted with saturated aqueous NaHCO₃ (15 mL). The separated aqueous phase was extracted with ethyl acetate (2 x 15 mL), the combined organic phase was passed through a hydrophobic frit and evaporated under reduced pressure to yield 5-(2-(2-methoxybutoxy)-4-(oxiran-2-yl)phenyl)-1,3-dimethylpyridin-2(1H)-one (630 mg, 1.65 mmol, 91% yield, 90% purity) as a pale yellow oil which was further dried under high vacuum overnight. LCMS (high pH): rt = 1.01 min, MH⁺ 344.3. ¹H NMR δ(400 MHz, CDCl₃) ppm 7.51 - 7.48 (2H, s), 7.22 (1H, d, J=7.8 Hz), 6.95 (1H, dt, J=7.8, 1.3 Hz), 6.82 (1H, dd, J=3.2, 1.5 Hz), 4.03 - 3.94 (2H, m), 3.87 (1H, dd, J=4.0, 2.6 Hz), 3.60 (3H, s), 3.46 - 3.38 (4H, m), 3.16 (1H, dd, J=5.6, 4.2 Hz), 2.79 (1H, dd, J=5.6, 2.2 Hz), 2.19 (3H, s), 1.66 - 1.58 (2H, m), 0.98 - 0.93 (3H, m).

(2S,3R)-(S)-Tetrahydrofuran-3-yl 2-((4-(1,5-dimethyl-6-oxo-1,6-dihydropyridin-3-yl)-3-(2-isopropoxyethoxy)phenethyl)amino)-3-hydroxybutanoate, 3.64

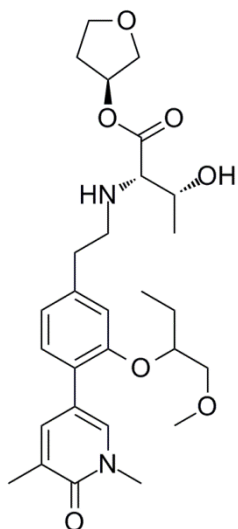
To a round bottomed flask was added 5-(2-(2-isopropoxyethoxy)-4-(oxiran-2-yl)phenyl)-1,3-dimethylpyridin-2(1H)-one (483 mg, 1.27 mmol) and the flask flushed with nitrogen before dissolution in tetrahydrofuran (10 mL). To the solution, cooled in an ice bath, was added boron trifluoride diethyl etherate (78 μ L, 0.63 mmol). The reaction mixture was stirred at 0 $^{\circ}$ C for 15 min. After this time, (2S,3R)-(S)-tetrahydrofuran-3-yl 2-amino-3-hydroxybutanoate, hydrochloride (359 mg, 1.59 mmol) and triethylamine (0.53 mL, 3.80 mmol) were added and the mixture warmed to RT and was stirred for 10 min. The amino ester salt was poorly soluble within the reaction mixture, therefore, a portion of *p*-toluenesulfonic acid monohydrate (200 mg, 1.05 mmol) was added to aid salt solubility. The mixture was stirred for a further 16 h. After this time, sodium triacetoxyborohydride (1.07 g, 5.06 mmol) was added and the mixture stirred for 6 h. The reaction mixture was diluted with DCM (60 mL), the mixture was washed with saturated aqueous sodium hydrogen carbonate solution (60 mL) and the layers separated. The aqueous was extracted with DCM (3 x 60 mL) and the organics combined, dried by passing through a hydrophobic frit and the solvent removed under reduced pressure. The crude gum was dissolved in DCM (3 mL) and loaded onto a 25 g SNAP silica column. The crude material on silica was purified by Biotage SP4 using a gradient of 0 - 25% ethanol in ethyl acetate over 24 CV. Fractions containing the desired product were collected and the solvent removed *in vacuo* to yield a yellow gum. The crude material was dissolved in 1:1 MeOH:DMSO (3 mL) and purified by mass directed autoprep on Xbridge column using 30 - 85% acetonitrile water with an ammonium carbonate modifier. The solvent was evaporated *in vacuo* to yield (2S,3R)-(S)-tetrahydrofuran-3-yl 2-((4-(1,5-dimethyl-6-oxo-1,6-dihydro pyridin-3-yl)-3-(2-isopropoxyethoxy)phenethyl)amino)-3-hydroxybutanoate (142 mg, 0.26 mmol, 20% yield) as a clear gum. LCMS (high pH): rt = 0.96 min, MH⁺ 517.5. ¹H NMR δ (400 MHz, CDCl₃) ppm: 7.52 - 7.49 (1H, m), 7.49 - 7.47 (1H, m), 7.16 (1H, d, *J*=7.8 Hz), 6.82 (1H, dd, *J*=7.7, 1.3 Hz), 6.77 (1H, d, *J*=1.5 Hz), 5.37 - 5.33 (1H, m), 4.14 - 4.08 (2H, m), 3.95 - 3.82 (3H, m), 3.77 (1H, d, *J*=10.8 Hz), 3.75 - 3.71 (2H, m), 3.68 - 3.58 (5H, m), 3.02 - 2.97 (2H, m), 2.87 - 2.70 (3H, m), 2.27 - 2.16 (4H, m), 2.04 -

1.95 (1H, m), 1.21 (3H, d, $J=6.1$ Hz), 1.17 (6H, d, $J=6.1$ Hz). $[\alpha_D]^{24.6^\circ}_\lambda(c\ 0.5, \text{CDCl}_3)$: -15.6°.

(2S,3R)-2-((4-(1,5-Dimethyl-6-oxo-1,6-dihydropyridin-3-yl)-3-(2-isopropoxyethoxy)phenethyl)amino)-3-hydroxybutanoic acid, hydrochloride, 3.80



A solution of (2S,3R)-(S)-tetrahydrofuran-3-yl 2-((4-(1,5-dimethyl-6-oxo-1,6-dihydropyridin-3-yl)-3-(2-isopropoxyethoxy)phenethyl)amino)-3-hydroxybutanoate (25 mg, 0.048 mmol) in dimethyl sulfoxide (0.25 mL) was added to a solution of pig liver esterase (lyophilized solid) (10 mg) in phosphate buffer solution pH 7.2 (0.5 mL). The mixture was stirred at room temperature for 24 h. Methanol was added, whereupon a thick suspension occurred. The solid was removed by filtration and the resulting solution blown down under a stream of nitrogen. 1:1 DMSO:methanol was added to make the solution up to 1 mL, the sample filtered and purified by mass directed autoprep on an Xbridge column using 15-55% acetonitrile water with an ammonium carbonate modifier. The solvent was evaporated *in vacuo* and further dried in a vacuum oven for 1 week. NMR analysis contained a large water peak, obscuring the characterisation. Therefore, to the resulting white solid was added water (0.5 mL) and 2 M aqueous HCl added dropwise. The solvent was evaporated under a stream of nitrogen to form the desired product (2S,3R)-2-((4-(1,5-dimethyl-6-oxo-1,6-dihydropyridin-3-yl)-3-(2-isopropoxyethoxy)phenethyl)amino)-3-hydroxy butanoic acid, hydrochloride (9.5 mg, 0.020 mmol, 41% yield) as an off-white solid. LCMS (high pH): $t_r = 0.63$ min, MH^+ 447.4. 1H NMR δ (400 MHz, DMSO- d_6) ppm: 9.03 (1H, br. s.), 8.86 (1H, br. s.), 7.72 (1H, d, $J=2.2$ Hz), 7.59 - 7.55 (1H, m), 7.26 (1H, d, $J=7.6$ Hz), 6.95 (1H, d, $J=1.2$ Hz), 6.86 (1H, dd, $J=7.8, 1.2$ Hz), 4.14 (1H, d, $J=6.1$ Hz), 4.10 (2H, dd, $J=5.3, 3.5$ Hz), 3.88 - 3.82 (1H, m), 3.68 (2H, dd, $J=5.1, 3.9$ Hz), 3.60 (1H, spt, $J=6.1$ Hz), 3.49 (3H, s), 3.32 - 3.14 (2H, m), 3.09 - 2.92 (2H, m), 2.04 (3H, s), 1.29 (3H, d, $J=6.6$ Hz), 1.08 (6H, d, $J=6.1$ Hz).

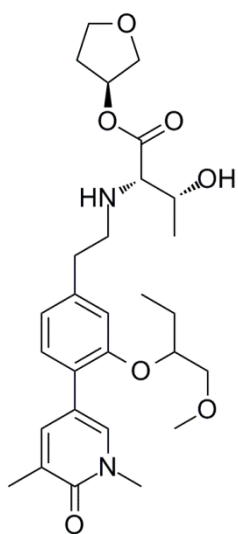
(2S,3R)-(S)-Tetrahydrofuran-3-yl 2-((4-(1,5-dimethyl-6-oxo-1,6-dihydropyridin-3-yl)-3-((1-methoxybutan-2-yl)oxy)phenethyl)amino)-3-hydroxybutanoate, 3.62

To a round bottomed flask was added 5-(2-((1-methoxybutan-2-yl)oxy)-4-(oxiran-2-yl)phenyl)-1,3-dimethylpyridin-2(1H)-one (530 mg, 1.31 mmol) and the flask flushed with nitrogen before dissolution in tetrahydrofuran (11 mL). To the solution, cooled in an ice bath, was added boron trifluoride diethyl etherate (81 μ L, 0.66 mmol). The reaction mixture was stirred at 0 °C for 15 min. After this time, (2S,3R)-(S)-tetrahydrofuran-3-yl 2-amino-3-hydroxybutanoate, hydrochloride (440 mg, 1.95 mmol) and triethylamine (0.55 mL, 3.94 mmol) were added and the mixture warmed to RT and was stirred for 10 min. The amino ester salt was poorly soluble within the reaction mixture, therefore, a portion of *p*-toluenesulfonic acid monohydrate (250 mg, 1.31 mmol) was added to aid salt solubility. The mixture was stirred for 1 h. After this time, sodium triacetoxyborohydride (1.11 g, 5.25 mmol) was added and the mixture stirred for 16 h. The reaction had not progressed to completion after this time, therefore, an additional portion of sodium triacetoxyborohydride (278 mg, 1.31 mmol) was added and stirred for 2 h. The reaction mixture was diluted with DCM (60 mL), the mixture washed with saturated aqueous sodium hydrogen carbonate solution (60 mL) and the layers separated. The aqueous was extracted with DCM (2 x 60 mL) and the organics combined, dried by passing through a hydrophobic frit and the solvent removed under reduced pressure. The crude gum was dissolved in DCM (3 mL) and loaded onto a 25 g SNAP silica column. The crude material on silica was purified by Biotage SP4 using a gradient of 0 - 20% ethanol in ethyl acetate over 25 CV. Fractions containing the desired product were collected and the solvent removed *in vacuo* to yield a yellow gum. The crude material was dissolved in 1:1 MeOH:DMSO (3 mL) and purified by mass directed autoprep on Xbridge column using 30 – 85% acetonitrile water with an ammonium carbonate modifier. The solvent was evaporated *in vacuo* to yield (2S,3R)-(S)-tetrahydrofuran-3-yl 2-((4-(1,5-dimethyl-6-oxo-1,6-dihydro pyridin-3-yl)-3-((1-methoxybutan-2-yl)oxy)phenethyl)amino)-3-hydroxybutanoate (139 mg, 0.26 mmol, 20% yield) as a pale yellow gum. LCMS (high pH): rt = 0.97 min, MH⁺ 517.5. ¹H NMR δ (400 MHz, CDCl₃) ppm: 7.51 - 7.47 (2H, m), 7.16 (1H, d, *J*=7.6 Hz), 6.86 - 6.79 (2H, m), 5.38 - 5.32 (1H, m), 4.37 - 4.29 (1H, m), 3.94 - 3.82 (3H, m), 3.80 - 3.75 (1H, m), 3.66 - 3.58 (4H, m), 3.52 (1H, dd,

$J=10.3, 5.6$ Hz), 3.47 (1H, dd, $J=10.3, 4.2$ Hz), 3.35 (3H, s), 3.01 - 2.93 (2H, m), 2.86 - 2.71 (3H, m), 2.26 - 2.16 (4H, m), 2.04 - 1.95 (1H, m), 1.73 - 1.64 (2H, m), 1.21 (3H, d, $J=6.4$ Hz), 0.93 (3H, t, $J=7.5$ Hz).

Chiral Separation of **(2*S*,3*R*)-(S)-Tetrahydrofuran-3-yl 2-((4-(1,5-dimethyl-6-oxo-1,6-dihydropyridin-3-yl)-3-((1-methoxybutan-2-yl)oxy)phenethyl)amino)-3-hydroxybutanoate, 3.62**

(2*S*,3*R*)-(S)-Tetrahydrofuran-3-yl 2-((4-(1,5-dimethyl-6-oxo-1,6-dihydropyridin-3-yl)-3-((1-methoxybutan-2-yl)oxy)phenethyl)amino)-3-hydroxybutanoate (Isomer 1), 3.81²⁸³

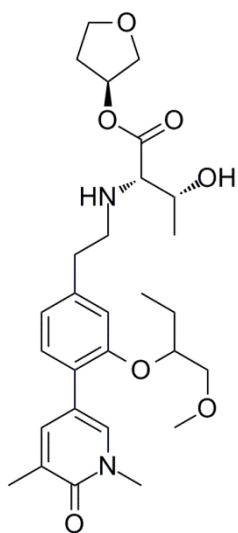


The mixture of diastereoisomers (2*S*,3*R*)-(S)-tetrahydrofuran-3-yl 2-((4-(1,5-dimethyl-6-oxo-1,6-dihydropyridin-3-yl)-3-((1-methoxybutan-2-yl)oxy)phenethyl) amino)-3-hydroxybutanoate (190 mg, 0.37 mmol) was separated by chiral HPLC. The HPLC purification was carried out on a Chiralpak AD-H column “ADH12143-01” (250 x 30 mm). The purification was run using 15% ethanol in heptane over 45 min, with a flow rate of 30 mL/min. The UV detection was at a wavelength of 215 nm. The first eluting isomer was collected, between 23 and 27 min. The fractions eluted between 27 and 30 min contained a mixture of isomers and were re-subjected to the HPLC conditions.

Combined fraction solutions from the first eluting isomer were evaporated to dryness under reduced pressure to yield (2*S*,3*R*)-(S)-tetrahydrofuran-3-yl 2-((4-(1,5-dimethyl-6-oxo-1,6-dihydropyridin-3-yl)-3-(2-methoxybutoxy) phenethyl)amino)-3-hydroxybutanoate Isomer 1 (77 mg, 0.15 mmol) as a clear gum. Chiral HPLC analysis: Chiralpak AD-H column “ADH0CE-PC014” (250 x 4.6mm) using 15% ethanol in heptane over 40 min, with a flow rate of 1.0 mL/min and a UV detection wavelength of 215 nm: $rt = 19.90$ min, analytical purity >99.5%. LCMS (high pH): $rt = 0.97$ min, MH^+ 517.5. 1H NMR δ (400 MHz, $CDCl_3$) ppm: 7.51 - 7.47 (2H, m), 7.16 (1H, d, $J=7.8$ Hz), 6.85 - 6.79 (2H, m), 5.39 - 5.32 (1H, m), 4.36 - 4.29 (1H, m), 3.94 - 3.81 (3H, m), 3.77 (1H, d, $J=10.5$ Hz), 3.66 - 3.58 (4H, m), 3.52 (1H, dd, $J=10.3, 5.6$ Hz), 3.47 (1H, dd, $J=10.0, 4.2$ Hz), 3.35 (3H, s), 3.03 - 2.93 (2H, m), 2.86 - 2.70 (3H, m), 2.27 - 2.15 (4H, m), 2.04 - 1.96 (1H, m), 1.74 - 1.65 (2H, m), 1.21 (3H, d, $J=6.4$ Hz), 0.93 (3H, t, $J=7.5$ Hz). ^{13}C NMR δ (126 MHz, $CDCl_3$) ppm: 173.0 (COO, HMBC),

162.6 (C=O), 155.3 (C-O), 139.8 (C-CH₂), 139.2 (C-CH), 135.4 (N-CH), 129.6 (CH), 128.0 (C-CH₃), 125.3 (C-C), 121.4 (CH), 116.5 (C-C), 115.2 (CH), 79.0 (O-CH), 75.8 (COOCH), 73.7 (OCH₂), 73.0 (OCH₂, THF), 68.1 (CHOH), 67.7 (CHNH), 66.9 (O-CH₂, THF), 59.2 (O-CH₃), 49.7 (N-CH₂), 37.9 (N-CH₃), 36.4 (CH₂), 32.8 (C-CH₂), 24.3 (CH₂CH₃), 19.5 (CHCH₃), 17.3 (C-CH₃), 9.5 (CH₂CH₃). HRMS (ESI) exact mass calculated for C₂₈H₄₁N₂O₇ [M+H]⁺ m/z 517.2908, found m/z 517.2902. IR (CDCl₃): 3382, 2928, 1730, 1654, 1106. $[\alpha_D]^{24.8^\circ C}_\lambda(c\ 0.5, CDCl_3)$: -20.6°.

(2*S*,3*R*)-(S)-Tetrahydrofuran-3-yl 2-((4-(1,5-dimethyl-6-oxo-1,6-dihydropyridin-3-yl)-3-((1-methoxybutan-2-yl)oxy)phenethyl)amino)-3-hydroxybutanoate (Isomer 2) 3.82²⁸³

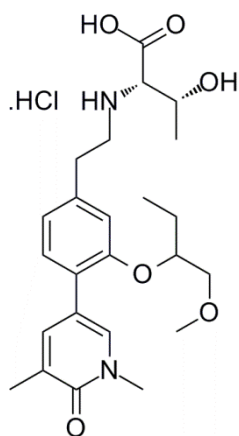


The mixture of diastereoisomers (2*S*,3*R*)-(S)-tetrahydrofuran-3-yl 2-((4-(1,5-dimethyl-6-oxo-1,6-dihydropyridin-3-yl)-3-((1-methoxybutan-2-yl)oxy)phenethyl) amino)-3-hydroxybutanoate (190 mg, 0.37 mmol) was separated by chiral HPLC. The HPLC purification was carried out on a Chiralpak AD-H column "ADH12143-01" (250 x 30 mm). The purification was run using 15% ethanol in heptane over 45 min, with a flow rate of 30 mL/min. The UV detection was at a wavelength of 215 nm. The first eluting isomer was collected, between 30 and 37 min. The fractions eluted between 27 and 30 min contained a mixture of isomers and were re-subjected to the HPLC conditions.

Combined fraction solutions from the first eluting isomer were evaporated to dryness under reduced pressure to yield (2*S*,3*R*)-(S)-tetrahydrofuran-3-yl 2-((4-(1,5-dimethyl-6-oxo-1,6-dihydropyridin-3-yl)-3-(2-methoxybutoxy) phenethyl)amino)-3-hydroxybutanoate Isomer 1 (89 mg, 0.17 mmol) as a clear gum. Chiral HPLC analysis: Chiralpak AD-H column "ADH0CE-PC014" (250 x 4.6mm) using 15% ethanol in heptane over 40 min, with a flow rate of 1.0 mL/min and a UV detection wavelength of 215 nm: rt = 23.00 min, analytical purity 96.8%. LCMS (high pH): rt = 0.97 min, MH⁺ 517.5. ¹H NMR δ(400 MHz, CDCl₃) ppm: 7.53 - 7.48 (2H, m), 7.18 (1H, d, *J*=7.8 Hz), 6.88 - 6.80 (2H, m), 5.40 - 5.33 (1H, m), 4.39 - 4.30 (1H, m), 3.97 - 3.83 (3H, m), 3.79 (1H, d, *J*=10.8 Hz), 3.70 - 3.60 (4H, m), 3.54 (1H, dd, *J*=10.3, 5.9 Hz), 3.49 (1H, dd, *J*=10.3, 4.2 Hz), 3.37 (3H, s), 3.07 - 2.92 (2H, m), 2.90 - 2.70 (3H, m), 2.29 - 2.16 (4H, m), 2.06 - 1.96 (1H, m), 1.75 - 1.66 (2H, m), 1.23 (3H, d, *J*=6.1 Hz),

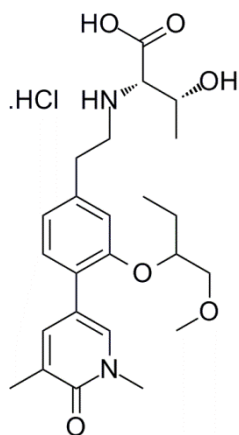
0.95 (3H, t, $J=7.5$ Hz). ^{13}C NMR δ (126 MHz, CDCl_3) ppm: 173.1 (COO, HMBC), 162.6 (C=O), 155.3 (C-O), 139.8 (C- CH_2 , HMBC) 139.2 (C-CH), 135.4 (N-CH), 129.6 (CH), 128.0 (C- CH_3), 125.3 (C-C), 121.4 (CH), 116.5 (C-C), 115.2 (CH), 79.1 (O-CH), 75.8 (COOCH), 73.7 (OCH_2), 73.0 (OCH_2 , THF), 68.1 (CHOH), 67.7 (CHNH), 66.9 (O- CH_2 , THF), 59.2 (O- CH_3), 49.8 (N- CH_2), 37.9 (N- CH_3), 36.4 (CH_2), 32.8 (C- CH_2), 24.3 (CH_2CH_3), 19.5 (CH CH_3), 17.3 (C- CH_3), 9.5 (CH_2CH_3). HRMS (ESI) exact mass calculated for $\text{C}_{28}\text{H}_{41}\text{N}_2\text{O}_7$ $[\text{M}+\text{H}]^+$ m/z 517.2908, found m/z 517.2911. IR (CDCl_3): 3374, 2933, 1730, 1653, 1104. $[\alpha_D]^{24.8^\circ}_\lambda(c\ 0.5, \text{CDCl}_3)$: -5.9° .

(2S,3R)-2-((4-(1,5-Dimethyl-6-oxo-1,6-dihydropyridin-3-yl)-3-((1-methoxybutan-2-yl)oxy)phenethyl)amino)-3-hydroxybutanoic acid, hydrochloride (Isomer 1), 3.83

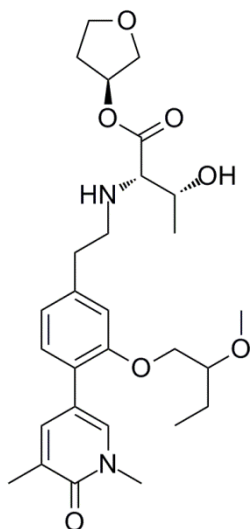


A solution of (2S,3R)-(S)-tetrahydrofuran-3-yl 2-((4-(1,5-dimethyl-6-oxo-1,6-dihydropyridin-3-yl)-3-((1-methoxybutan-2-yl)oxy)phenethyl)amino)-3-hydroxy butanoate (Isomer 1) (29 mg, 0.056 mmol) in dimethyl sulfoxide (0.25 mL) was added to a solution of pig liver esterase (lyophilized solid) (10 mg), in phosphate buffer solution pH 7.2 (0.5 mL). The mixture was stirred at room temperature for 3 days. Methanol was added, whereupon a thick suspension occurred. The solid was removed by filtration and the resulting solution blown down under a stream of nitrogen. Methanol was added to make the solution up to 1 ml, and purified by mass directed autoprep on Xbridge column using 15 – 55% acetonitrile water with an ammonium carbonate modifier. The solvent was evaporated *in vacuo* and further dried in a vacuum oven for 1 week. To the resulting white solid was added water (0.5 mL) and 2 M aqueous HCl added dropwise. The solvent was evaporated under a stream of nitrogen to yield the desired compound (2S,3R)-2-((4-(1,5-dimethyl-6-oxo-1,6-dihydropyridin-3-yl)-3-((1-methoxybutan-2-yl)oxy)phenethyl)amino)-3-hydroxybutanoic acid, hydrochloride (Isomer 1) (5.3 mg, 11.0 μmol , 20 % yield) as a clear gum. LCMS (high pH): $r_t = 0.62$ min, MH^+ 447.2. ^1H NMR δ (400 MHz, $\text{DMSO}-d_6$) ppm: 8.95 (2H, br. s.), 7.71 (1H, d, $J=2.2$ Hz), 7.59 - 7.53 (1H, m), 7.25 (1H, d, $J=7.8$ Hz), 6.97 (1H, d, $J=1.0$ Hz), 6.85 (1H, dd, $J=7.7, 1.1$ Hz), 5.79 (1H, br. s.), 4.47 (1H, quin, $J=5.3$ Hz), 4.13 (1H, quin, $J=6.2$ Hz), 3.86 (1H, d, $J=4.2$ Hz), 3.52 - 3.47 (5H, m), 3.28 (3H, s), 3.25 - 3.13 (2H, m), 3.08 - 2.90 (2H, m), 2.04 (3H, s), 1.71 - 1.58 (2H, m), 1.30 (3H, d, $J=6.6$ Hz), 0.89 (3H, t, $J=7.5$ Hz).

(2S,3R)-2-((4-(1,5-Dimethyl-6-oxo-1,6-dihydropyridin-3-yl)-3-((1-methoxybutan-2-yl)oxy)phenethyl)amino)-3-hydroxybutanoic acid, hydrochloride (Isomer 2), 3.84



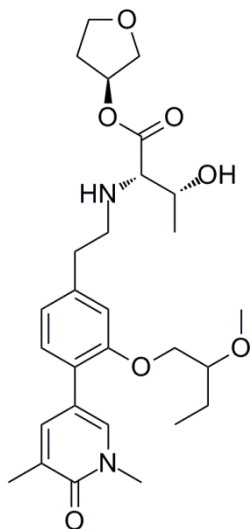
A solution of (2S,3R)-(S)-tetrahydrofuran-3-yl 2-((4-(1,5-dimethyl-6-oxo-1,6-dihydropyridin-3-yl)-3-((1-methoxybutan-2-yl)oxy)phenethyl)amino)-3-hydroxy butanoate (Isomer 2) (23 mg, 0.045 mmol) in dimethyl sulfoxide (0.25 mL) was added to a solution of pig liver esterase (lyophilized solid) (10 mg), in phosphate buffer solution pH 7.2 (0.5 mL). The mixture was stirred at room temperature for 3 days. Methanol was added, whereupon a thick suspension occurred. The solid was removed by filtration and the resulting solution blown down under a stream of nitrogen. Methanol was added to make the solution up to 1 mL, and purified by Mass Directed AutoPrep on Xbridge column using 15 – 55% acetonitrile water with an ammonium carbonate modifier. The solvent was evaporated *in vacuo* and further dried in a vacuum oven for 1 week. To the resulting white solid was added water (0.5 mL) and 2 M aqueous HCl added dropwise. The solvent was evaporated under a stream of nitrogen to yield the desired compound (2S,3R)-2-((4-(1,5-dimethyl-6-oxo-1,6-dihydropyridin-3-yl)-3-((1-methoxybutan-2-yl)oxy)phenethyl)amino)-3-hydroxybutanoic acid, hydrochloride (Isomer 2) (12.1 mg, 0.025 mmol, 56 % yield) as a clear gum. LCMS (high pH): rt = 0.62 min, MH⁺ 447.2. ¹H NMR δ(400 MHz, DMSO-*d*₆) ppm: 9.06 (1H, br. s.), 8.95 (1H, br. s.), 7.71 (1H, d, *J*=2.4 Hz), 7.60 - 7.53 (1H, m), 7.25 (1H, d, *J*=7.8 Hz), 6.98 (1H, s), 6.85 (1H, dd, *J*=7.7, 1.3 Hz), 4.47 (1H, quin, *J*=5.3 Hz), 4.14 (1H, quin, *J*=6.2 Hz), 3.87 (1H, d, *J*=4.4 Hz), 3.50 - 3.46 (5H, m), 3.31 - 3.15 (5H, m), 3.11 - 2.91 (2H, m), 2.04 (3H, s), 1.72 - 1.56 (2H, m), 1.30 (3H, d, *J*=6.4 Hz), 0.89 (3H, t, *J*=7.5 Hz).

(2S,3R)-(S)-Tetrahydrofuran-3-yl 2-((4-(1,5-dimethyl-6-oxo-1,6-dihydropyridin-3-yl)-3-(2-methoxybutoxy)phenethyl)amino)-3-hydroxybutanoate, 3.63

To a round bottomed flask was added a solution of 5-(2-(2-methoxybutoxy)-4-(oxiran-2-yl)phenyl)-1,3-dimethylpyridin-2(1H)-one (450 mg, 1.11 mmol) in tetrahydrofuran (9.3 mL). To the solution stirred under nitrogen and cooled in an ice bath, was added boron trifluoride diethyl etherate (0.068 mL, 0.56 mmol). The reaction mixture was stirred at 0 °C for 25 min. After this time, (2S,3R)-(S)-tetrahydrofuran-3-yl 2-amino-3-hydroxybutanoate, hydrochloride (377 mg, 1.67 mmol), triethylamine (0.47 mL, 3.34 mmol) and *p*-toluenesulfonic acid monohydrate (200 mg, 1.05 mmol) were added and the mixture warmed to RT. The mixture was stirred for 1 h. After this time, sodium triacetoxyborohydride (944 mg, 4.46 mmol) was added and the mixture stirred overnight. The reaction mixture was diluted with DCM (50 mL), the mixture washed with saturated aqueous sodium hydrogen carbonate solution (50 mL) and the layers separated. The aqueous layer was extracted with DCM (2 x 50 mL) and the organics combined, dried by passing through a hydrophobic frit and the solvent removed under reduced pressure. The crude gum was dissolved in DCM (3 mL) and loaded onto a 50 g SNAP silica column. The crude material on silica was purified by Biotage SP4 using a gradient of 0 - 20% ethanol in ethyl acetate over 25 CV. Fractions containing the desired product were collected and the solvent removed *in vacuo* to yield a yellow gum. The crude material was dissolved in 1:1 MeOH:DMSO (2 mL) and purified by mass directed autoprep on Xbridge column using 30 - 85% acetonitrile water with an ammonium carbonate modifier. The solvent was evaporated *in vacuo* to yield (2S,3R)-(S)-tetrahydrofuran-3-yl 2-((4-(1,5-dimethyl-6-oxo-1,6-dihydropyridin-3-yl)-3-(2-methoxybutoxy)phenethyl)amino)-3-hydroxybutanoate (210 mg, 0.41 mmol, 37% yield) as a clear gum. LCMS (high pH): rt = 0.97 min, MH⁺ 517.5. ¹H NMR δ(400 MHz, CDCl₃) ppm: 7.53 - 7.44 (2H, m), 7.16 (1H, d, *J*=7.8 Hz), 6.83 (1H, dd, *J*=7.7, 1.3 Hz), 6.77 (1H, d, *J*=1.2 Hz), 5.38 - 5.32 (1H, m), 3.98 (2H, d, *J*=4.9 Hz), 3.94 - 3.81 (3H, m), 3.80 - 3.74 (1H, m), 3.68 - 3.58 (4H, m), 3.46 - 3.39 (4H, m), 3.03 - 2.94 (2H, m), 2.88 - 2.71 (3H, m), 2.26 - 2.15 (4H, m), 2.04 - 1.95 (1H, m), 1.67 - 1.58 (2H, m), 1.21 (3H, d, *J*=6.1 Hz), 0.96 (3 H, t, *J*=7.5 Hz).

Chiral Separation of **(2S,3R)-(S)-Tetrahydrofuran-3-yl 2-((4-(1,5-dimethyl-6-oxo-1,6-dihydropyridin-3-yl)-3-(2-methoxybutoxy)phenethyl)amino)-3-hydroxybutanoate, 3.63**

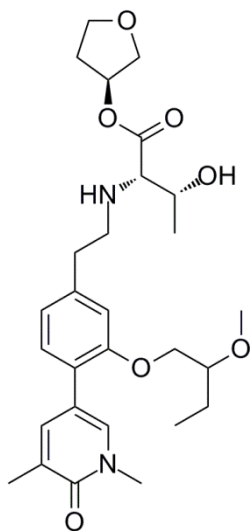
(2S,3R)-(S)-Tetrahydrofuran-3-yl 2-((4-(1,5-dimethyl-6-oxo-1,6-dihydropyridin-3-yl)-3-(2-methoxybutoxy)phenethyl)amino)-3-hydroxybutanoate (Isomer 1), 3.85²⁸³



The mixture of diastereoisomers (2S,3R)-(S)-tetrahydrofuran-3-yl 2-((4-(1,5-dimethyl-6-oxo-1,6-dihydropyridin-3-yl)-3-(2-methoxybutoxy)phenethyl)amino)-3-hydroxybutanoate (180 mg, 0.35 mmol) was separated by chiral HPLC. The HPLC purification was carried out on a Chiralcel OJ-H column "OJH10027-01" (250 x 30 mm, 5 μ m packing diameter). The purification was run using 15% ethanol in heptanes over 35 min, with a flow rate of 30 mL/min. The UV detection was at a wavelength of 215 nm. The first eluting isomer was collected, between 20 and 22.5 min. The fractions eluted between 22.5 and 25.5 min contained a mixture of isomers and were re-subjected to the HPLC conditions. Combined fraction solutions from the first eluting isomer were evaporated to dryness under reduced pressure to yield (2S,3R)-(S)-tetrahydrofuran-3-yl 2-((4-(1,5-dimethyl-6-oxo-1,6-dihydropyridin-3-yl)-3-(2-methoxybutoxy)phenethyl)amino)-3-hydroxybutanoate (Isomer 1) (81 mg, 0.16 mmol) as a clear gum. Chiral HPLC analysis: Chiralcel OJ-H column "OJH0CE-RK012" (250 x 4.6mm) using 20% ethanol in heptanes over 30 min, with a flow rate of 1.0 mL/min and a UV detection wavelength of 215 nm: t_r = 11.14 min, analytical purity 99.5%. LCMS (high pH): t_r = 0.96 min, MH^+ 517.4. 1H NMR δ (400 MHz, $CDCl_3$) ppm: 7.50 - 7.46 (2H, m), 7.16 (1H, d, $J=7.6$ Hz), 6.83 (1H, dd, $J=7.6, 1.5$ Hz), 6.77 (1H, d, $J=1.5$ Hz), 5.38 - 5.32 (1H, m), 3.98 (2H, d, $J=4.6$ Hz), 3.93 - 3.82 (3H, m), 3.80 - 3.75 (1H, m), 3.67 - 3.58 (4H, m), 3.46 - 3.39 (4H, m), 3.04 - 2.95 (2H, m), 2.86 - 2.73 (3H, m), 2.27 - 2.16 (4H, m), 2.04 - 1.96 (1H, m), 1.67 - 1.58 (2H, m), 1.21 (3H, d, $J=6.1$ Hz), 0.96 (3H, t, $J=7.6$ Hz). ^{13}C NMR δ (101 MHz, $CDCl_3$) ppm: 173.4 (COO), 162.6 (C=O), 155.8 (C-O), 140.2 (C- CH_2), 139.1 (C-CH), 135.4 (N-CH), 129.4 (CH), 128.1 (C- CH_3), 124.3 (C-C), 121.3 (CH), 116.3 (C-C), 112.9 (CH), 80.8 (O-CH), 75.7 (COOCH), 73.0 (O- CH_2 THF), 69.8 (O- CH_2), 68.1 (NH-CH), 67.8 (CH-OH), 66.9 (O- CH_2 THF), 57.7 (O- CH_3), 49.7 (N- CH_2), 37.9 (N- CH_3), 36.6 (C- CH_2), 32.8 (CH_2), 24.1

(CH₂CH₃), 19.5 (CH-CH₃), 17.2 (C-CH₃), 9.5 (CH₂CH₃). HRMS (ESI) exact mass calculated for C₂₈H₄₁N₂O₇ [M+H]⁺ m/z 517.2908, found m/z 517.2902. [α _D]^{24.4°C}_λ(c 0.5, CDCl₃): -13.3 °

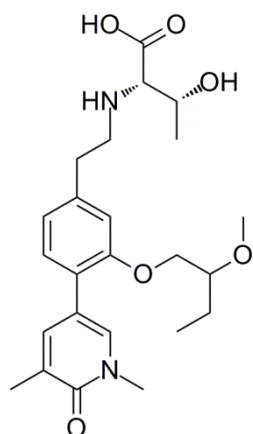
(2*S*,3*R*)-(S)-Tetrahydrofuran-3-yl 2-((4-(1,5-dimethyl-6-oxo-1,6-dihydropyridin-3-yl)-3-(2-methoxybutoxy)phenethyl)amino)-3-hydroxybutanoate (Isomer 2), 3.86²⁸³



The mixture of diastereoisomers (2*S*,3*R*)-(S)-tetrahydrofuran-3-yl 2-((4-(1,5-dimethyl-6-oxo-1,6-dihydropyridin-3-yl)-3-(2-methoxybutoxy)phenethyl)amino)-3-hydroxybutanoate (180 mg, 0.35 mmol) was separated by chiral HPLC. The HPLC purification was carried out on a Chiralcel OJ-H column “OJH10027-01” (250 x 30 mm, 5 μm packing diameter). The purification was run using 15% ethanol in heptanes over 35 min, with a flow rate of 30 mL/min. The UV detection was at a wavelength of 215 nm. The second eluting isomer was collected, between 25.5 and 30 min. The fractions eluted between 22.5 and 25.5 min contained a mixture of isomers and were re-subjected to the HPLC conditions. Combined fraction solutions from the second eluting isomer were evaporated to dryness under reduced pressure to yield (2*S*,3*R*)-(S)-tetrahydrofuran-3-yl 2-((4-(1,5-dimethyl-6-oxo-1,6-dihydro pyridin-3-yl)-3-(2-methoxybutoxy)phenethyl)amino)-3-hydroxybutanoate (Isomer 2) (68 mg, 0.13 mmol) as a clear gum. Chiral HPLC analysis: Chiralcel OJ-H column “OJH0CE-RK012” (250 x 4.6mm) using 20% ethanol in heptanes over 30 min, with a flow rate of 1.0 mL/min and a UV detection wavelength of 215 nm: rt = 12.96 min, analytical purity 97.3%. LCMS (high pH): rt = 0.96 min, MH⁺ 517.4. ¹H NMR δ(400 MHz, CDCl₃) ppm: 7.51 - 7.45 (2H, m), 7.16 (1H, d, *J*=7.6 Hz), 6.83 (1H, dd, *J*=7.6, 1.5 Hz), 6.77 (1H, d, *J*=1.2 Hz), 5.37 - 5.32 (1H, m), 3.98 (2H, d, *J*=4.9 Hz), 3.94 - 3.81 (3H, m), 3.80 - 3.75 (1H, m), 3.67 - 3.57 (4H, m), 3.46 - 3.39 (4H, m), 3.05 - 2.95 (2H, m), 2.89 - 2.72 (3H, m), 2.26 - 2.16 (4H, m), 2.03 - 1.95 (1H, m), 1.62 (2H, quin, *J*=7.0 Hz), 1.21 (3H, d, *J*=6.4 Hz), 0.96 (3H, t, *J*=7.5 Hz). ¹³C NMR δ(101 MHz, CDCl₃) ppm: 173.4 (COO), 162.6 (C=O), 155.8 (C-O), 140.2 (C-CH₂), 139.1 (C-CH), 135.4 (N-CH), 129.4 (CH), 128.1 (C-CH₃), 124.3 (C-C), 121.3 (CH), 116.3 (C-C), 112.9 (C-H), 80.8 (O-CH), 75.7 (COOCH), 73.0 (O-CH₂ THF), 69.8 (O-CH₂), 68.1

(NH-CH), 67.8 (CH-OH), 66.9 (O-CH₂ THF), 57.7 (O-CH₃), 49.7 (N-CH₂), 37.9 (N-CH₃), 36.6 (C-CH₂), 32.8 (CH₂), 24.1 (CH₂CH₃), 19.5 (CH-CH₃), 17.2 (C-CH₃), 9.5 (CH₂CH₃). HRMS (ESI) exact mass calculated for C₂₈H₄₁N₂O₇ [M+H]⁺ m/z 517.2908, found m/z 517.2896. $[\alpha_D]^{24.4^\circ C}_\lambda(c\ 0.5, CDCl_3)$: -2.8 °

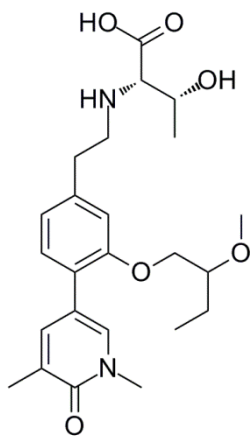
(2S,3R)-2-((4-(1,5-Dimethyl-6-oxo-1,6-dihydropyridin-3-yl)-3-(2-methoxybutoxy)phenethyl)amino)-3-hydroxybutanoic acid (Isomer 1), 3.87



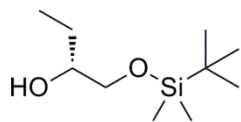
A solution of (2S,3R)-2-((4-(1,5-dimethyl-6-oxo-1,6-dihydropyridin-3-yl)-3-(2-methoxybutoxy)phenethyl)amino)-3-hydroxybutanoate (Isomer 1) (19 mg, 0.037 mmol) in dimethyl sulfoxide (0.5 mL) was added to a solution of pig liver esterase (lyophilized solid) (10 mg), in phosphate buffer solution pH 7.2 (1 mL). The mixture was stirred at room temperature for 3 days. Methanol was added, whereupon a thick suspension occurred. The solid was removed by filtration and the resulting solution blown down under a stream of nitrogen. Methanol was added to make the solution up to 1 mL and purified by mass directed autoprep on Xbridge column using 15 – 55% acetonitrile water with an ammonium carbonate modifier. The solvent was evaporated *in vacuo* and further dried in a vacuum oven for 1 week. To the resulting white solid was added water (0.5 mL) and 2 M aqueous HCl added dropwise. The solvent was evaporated under a stream of nitrogen to yield the product (contaminated with O-demethylated material ~10 %). The impure compound was dissolved in DMSO (1 mL) and purified by mass directed autoprep on Xbridge column using 15-55% acetonitrile water with an ammonium carbonate modifier. The solvent was evaporated *in vacuo* and further dried in a vacuum oven for 7 days to yield the desired product (2S,3R)-2-((4-(1,5-dimethyl-6-oxo-1,6-dihydropyridin-3-yl)-3-(2-methoxybutoxy)phenethyl)amino)-3-hydroxybutanoic acid (Isomer 1) (10.2 mg, 0.023 mmol, 62 % yield) as a white solid. LCMS (high pH): rt = 0.62 min, MH⁺ 447.4. ¹H NMR δ(400 MHz, DMSO-*d*₆) ppm: 7.72 (1H, d, *J*=2.2 Hz), 7.56 (1H, dd, *J*=2.4, 1.0 Hz), 7.24 (1H, d, *J*=7.8 Hz), 6.98 (1H, s), 6.86 (1H, dd, *J*=7.8, 1.2 Hz), 4.04 (1H, dd, *J*=10.3, 3.9 Hz), 3.97 (1H, dd, *J*=10.0, 5.4 Hz), 3.90 (1H, quin, *J*=6.1 Hz), 3.47 (3H, s), 3.45 - 3.39 (1H, m), 3.31 (3H, s), 3.16 - 3.05 (3H, m), 3.05 - 2.95

(1H, m), 2.94 - 2.84 (2H, m), 2.03 (3H, s), 1.62 - 1.48 (2H, m), 1.18 (3H, d, $J=6.4$ Hz), 0.90 (3H, t, $J=7.3$ Hz).

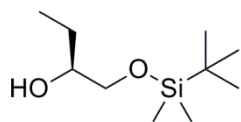
(2S,3R)-2-((4-(1,5-Dimethyl-6-oxo-1,6-dihydropyridin-3-yl)-3-(2-methoxybutoxy)phenethyl)amino)-3-hydroxybutanoic acid (Isomer 2), 3.88



A solution of (2S,3R)-(S)-tetrahydrofuran-3-yl 2-((4-(1,5-dimethyl-6-oxo-1,6-dihydropyridin-3-yl)-3-(2-methoxybutoxy)phenethyl)amino)-3-hydroxybutanoate (Isomer 2) (23 mg, 0.045 mmol) in dimethyl sulfoxide (0.5 mL) was added to a solution of pig liver esterase (lyophilized solid) (10 mg), in phosphate buffer solution pH 7.2 (1 mL). The mixture was stirred at room temperature for 3 days. Methanol was added, whereupon a thick suspension occurred. The solid was removed by filtration and the resulting solution blown down under a stream of nitrogen. Methanol was added to make the solution up to 1 mL and purified by mass directed autoprep on Xbridge column using 15-55% acetonitrile water with an ammonium carbonate modifier. The solvent was evaporated *in vacuo* and further dried in a vacuum oven for 1 week. To the resulting white solid was added water (0.5 mL) and 2 M aqueous HCl added dropwise. The solvent was evaporated under a stream of nitrogen to yield the product the desired product (contaminated with O-demethylated material ~10 %). The compound was dissolved in DMSO (1 mL) and purified by mass directed autoprep on Xbridge column using 15-55% acetonitrile water with an ammonium carbonate modifier. The solvent was evaporated *in vacuo* and further dried in a vacuum oven for 7 days to yield the desired product (2S,3R)-2-((4-(1,5-dimethyl-6-oxo-1,6-dihydropyridin-3-yl)-3-(2-methoxybutoxy)phenethyl)amino)-3-hydroxybutanoic acid (Isomer 2) (11.1 mg, 0.025 mmol, 56% yield) as a white solid. LCMS (high pH): $t_r = 0.62$ min, MH^+ 447.4. 1H NMR δ (400 MHz, DMSO- d_6) ppm: 7.73 (1H, d, $J=2.4$ Hz), 7.56 (1H, dd, $J=2.3, 1.1$ Hz), 7.24 (1H, d, $J=7.8$ Hz), 6.98 (1H, d, $J=1.0$ Hz), 6.86 (1H, dd, $J=7.8, 1.2$ Hz), 4.03 (1H, dd, $J=10.0, 3.9$ Hz), 3.97 (1H, dd, $J=10.3, 5.4$ Hz), 3.93 - 3.85 (1H, m), 3.47 (3H, s), 3.45 - 3.39 (2H, m), 3.31 (3H, s), 3.14 - 3.05 (2H, m), 3.04 - 2.96 (1H, m), 2.95 - 2.84 (2H, m), 2.03 (3H, s), 1.62 - 1.48 (2H, m), 1.18 (3H, d, $J=6.4$ Hz), 0.90 (3H, t, $J=7.5$ Hz).

(R)-1-((*tert*-Butyldimethylsilyl)oxy)butan-2-ol, 3.95

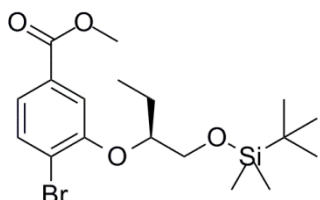
A solution of *tert*-butyldimethylchlorosilane (6.27 g, 41.6 mmol), triethylamine (7.73 mL, 55.5 mmol) and (*R*)-butane-1,2-diol (2.5 mL, 27.7 mmol) in DCM (35 mL) was stirred under nitrogen at RT for 18 h. After this time, the reaction mixture was quenched with ice-cold water (20 mL) and the aqueous layer removed. The aqueous layer was extracted with DCM (20 mL). The combined organics were washed with brine, dried by passing through a hydrophobic frit and the solvent removed *in vacuo*. The crude yellow liquid was loaded onto a 100 g SNAP silica column. The crude material on silica was purified by Biotage SP4 using a gradient of 0 - 20% ethyl acetate in cyclohexane over 24 CV. Fractions containing the desired product were collected and the solvent evaporated *in vacuo* to yield (*R*)-1-((*tert*-butyldimethylsilyl)oxy)butan-2-ol (4.32 g, 21.1 mmol, 76% yield) as a clear liquid. ¹H NMR δ(400 MHz, CDCl₃) ppm: 3.64 (1H, dd, *J*=9.7, 3.3 Hz), 3.60 - 3.53 (1H, m), 3.40 (1H, dd, *J*=9.8, 7.3 Hz), 2.39 (1H, d, *J*=3.7 Hz), 1.50 - 1.41 (2H, m), 0.96 (3H, t, *J*=7.5 Hz), 0.91 (9H, s), 0.08 (6H, s). ¹³C NMR δ(101 MHz, CDCl₃) ppm: 73.2 (O-CH), 66.9 (O-CH₂), 25.9 (CH₂), 25.8 (3 x CH₃), 18.3 (SiC), 9.9 (CH₃), -5.3 (SiCH₃), -5.4 (SiCH₃). IR (neat): 3428, 2930, 1253, 1092. [α_D]^{24.3 °C}_λ(c 0.5, CDCl₃): -7.3°.

(S)-1-((*tert*-Butyldimethylsilyl)oxy)butan-2-ol, 3.96

A solution of *tert*-butyldimethylchlorosilane (6.27 g, 41.6 mmol), triethylamine (7.73 mL, 55.5 mmol) and (*S*)-butane-1,2-diol (2.5 g, 27.7 mmol) in DCM (35 mL) was stirred under nitrogen at RT for 18 h. After this time, the reaction mixture was quenched with ice-cold water (20 mL) and the aqueous layer removed. The aqueous layer was extracted with DCM (20 mL). The combined organics were washed with brine, dried by passing through a hydrophobic frit and the solvent removed *in vacuo*. The crude yellow liquid was loaded onto a 100 g SNAP silica column. The crude material on silica was purified by Biotage SP4 using a gradient of 0 - 15% ethyl acetate in cyclohexane over 24 CV. Fractions containing the desired product were collected and the solvent evaporated *in vacuo* to yield (*S*)-1-((*tert*-butyldimethylsilyl)oxy)butan-2-ol (3.8 g, 18.6 mmol, 67% yield) as a clear liquid. ¹H NMR δ(400 MHz, CDCl₃) ppm: 3.64 (1H, dd, *J*=9.8, 3.4 Hz), 3.60 - 3.52 (1H, m), 3.40 (1H, dd, *J*=9.8, 7.3 Hz), 2.39 (1H, d, *J*=3.7 Hz), 1.50 - 1.41 (2H, m), 0.96 (3H, t, *J*=7.5 Hz), 0.91 (9H, s), 0.08 (6H, s). ¹³C NMR

δ (101 MHz, CDCl₃) ppm: 73.2 (O-CH), 66.9 (O-CH₂), 25.9 (CH₂), 25.8 (3 x CH₃), 18.3 (SiC), 9.9 (CH₃), -5.3 (SiCH₃), -5.4 (SiCH₃). $[\alpha_D]^{24.3 \text{ } ^\circ\text{C}}_{\lambda}(\text{c } 0.5, \text{CDCl}_3)$: +16.3°. IR (neat): 3428, 2930, 1254, 1092

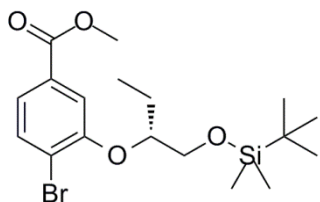
(S)-Methyl 4-bromo-3-((1-((*tert*-butyldimethylsilyl)oxy)butan-2-yl)oxy)benzoate, 3.97



Diisopropyl azodicarboxylate (3.37 mL, 17.3 mmol) was added dropwise over 2 min to a stirred solution of methyl 4-bromo-3-hydroxybenzoate (2.5 g, 10.8 mmol), triphenylphosphine (4.54 g, 17.3 mmol) and (*R*)-1-((*tert*-butyldimethylsilyl)oxy)butan-2-ol (2.65 g, 12.98 mmol) in tetrahydrofuran (75 mL) at 0 °C under N₂. Following stirring at 0 °C for 15 min, the cooling bath was removed and resulting solution was stirred at RT for 16 h. The volatiles were removed under reduced pressure and the mixture was diluted with ethyl acetate (150 mL) then partitioned with aqueous saturated NaHCO₃ (75 mL). The aqueous layer was extracted with ethyl acetate (100 mL). The combined organics were washed with brine (50 mL), dried by passing through a hydrophobic frit and the volatiles were removed under reduced pressure. The crude product was dissolved in DCM/cyclohexane (20 mL) and the resulting precipitate (triphenylphosphine oxide) removed by filtration. The filtrate was collected and the solvent removed *in vacuo*. The resulting yellow gum was dissolved in DCM (10 mL) and loaded onto a 100 g SNAP silica column. The crude material on silica was purified by Biotage SP4 using a gradient of 0 - 10% ethyl acetate in cyclohexane over 14 CV. Fractions containing product were collected and the volatiles were removed under reduce pressure to yield (*S*)-methyl 4-bromo-3-((1-((*tert*-butyldimethylsilyl)oxy)butan-2-yl)oxy)benzoate (3.86 g, 9.25 mmol, 85% yield) as a clear liquid. LCMS (formic acid): *rt* = 1.75 min, MH⁺/- not detected. ¹H NMR δ (400 MHz, CDCl₃) ppm: 7.68 (1H, d, *J*=1.7 Hz), 7.58 (1H, d, *J*=8.3 Hz), 7.47 (1H, dd, *J*=8.2, 1.8 Hz), 4.43 - 4.36 (1H, m), 3.90 (3H, s), 3.82 (1H, dd, *J*=10.9, 6.0 Hz), 3.76 (1H, dd, *J*=10.8, 4.9 Hz), 1.81 - 1.69 (2H, m), 1.01 (3H, t, *J*=7.5 Hz), 0.85 (9H, s), 0.05 (3H, s), 0.01 (3H, s). ¹³C NMR δ (101 MHz, CDCl₃) ppm: 166.4 (C=O), 155.5 (C-O), 133.3 (CH), 130.3 (C-COO), 122.7 (CH), 118.9 (C-Br), 115.9 (CH), 82.1 (OCH), 64.7 (OCH₂), 52.2 (OCH₃), 25.8 (3 x CH₃), 24.3 (CH₂), 18.2 (SiC), 9.5 (CH₃), -5.4 (SiCH₃), -5.5 (SiCH₃). IR (neat): 2929, 1725,

1288, 1230, 1102. HRMS (ESI) exact mass calculated for $C_{18}H_{30}^{79}BrO_4Si$ $[M+H]^+$ m/z 417.1091, found m/z 417.1106. $[\alpha_D]^{24.2^\circ}_\lambda(c\ 0.5, CDCl_3)$: -37.1° .

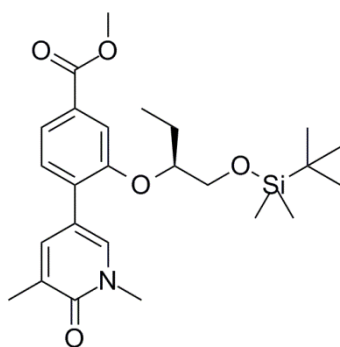
(R)-Methyl 4-bromo-3-((1-((tert-butyldimethylsilyl)oxy)butan-2-yl)oxy)benzoate, 3.98



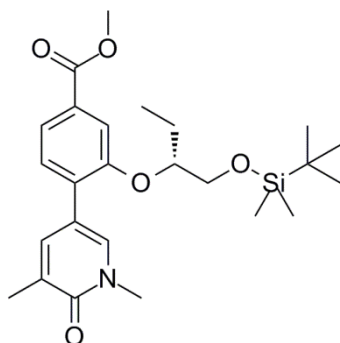
Diisopropyl azodicarboxylate (3.37 mL, 17.3 mmol) was added dropwise over 2 min to a stirred solution of methyl 4-bromo-3-hydroxybenzoate (2.5 g, 10.8 mmol), triphenylphosphine (4.54 g, 17.3 mmol) and (S)-1-((tert-butyldimethylsilyl)oxy)butan-2-ol (2.65 g, 13.0 mmol) in tetrahydrofuran (75 mL) at 0 °C under N_2 . Following stirring at 0 °C for 15 min, the cooling bath was removed and resulting solution was stirred at RT for 16 h. The volatiles were removed under reduced pressure and the mixture was diluted with ethyl acetate (150 mL) then partitioned with aqueous saturated $NaHCO_3$ (75 mL). The aqueous layer was extracted with ethyl acetate (100 mL). The combined organics were washed with brine (50 mL), dried by passing through a hydrophobic frit and the volatiles were removed under reduce pressure. The crude product was dissolved in cyclohexane (20 mL) and the resulting precipitate (triphenylphosphine oxide) removed by filtration. The filtrate was collected and the solvent removed *in vacuo*. The yellow gum was dissolved in DCM (10 mL) and loaded onto a 100 g SNAP silica column. The crude material on silica was purified by Biotage SP4 using a gradient of 0 - 10% ethyl acetate in cyclohexane over 14 CV. Fractions containing product were collected and the volatiles were removed under reduced pressure to yield (R)-methyl 4-bromo-3-((1-((tert-butyldimethylsilyl)oxy)butan-2-yl)oxy)benzoate (2.5 g, 5.99 mmol, 55% yield) as a clear liquid. Impure fractions were collected and the solvent removed *in vacuo* to yield the crude product (1.9 g). The material was dissolved in cyclohexane (2 mL) and loaded onto a 100 g SNAP silica column. The crude material on silica was purified by Biotage Isolera using a gradient of 0 - 10 % ethyl acetate in cyclohexane. Fractions containing pure product were collected and the solvent removed *in vacuo* to yield (R)-methyl 4-bromo-3-((1-((tert-butyldimethylsilyl)oxy) butan-2-yl)oxy)benzoate (100 mg, 0.24 mmol, 2% yield) as a clear liquid. Combined yield 57% LCMS (formic acid): $rt = 1.75$ min, MH^{\pm} not detected. 1H NMR δ (400 MHz, $CDCl_3$) ppm: 7.68 (1H, d, $J=1.7$ Hz), 7.58 (1H, d, $J=8.3$ Hz), 7.47 (1H, dd, $J=8.2, 1.8$ Hz), 4.43 - 4.36 (1H, m), 3.90 (3H, s), 3.82 (1H,

dd, $J=10.8, 6.1$ Hz), 3.76 (1H, dd, $J=10.8, 4.6$ Hz), 1.81 - 1.70 (2H, m), 1.01 (3H, t, $J=7.5$ Hz), 0.85 (9H, s), 0.05 (3H, s), 0.01 (3H, s). ^{13}C NMR δ (101 MHz, CDCl_3) ppm: 166.4 (C=O), 155.5 (C-O), 133.3 (CH), 130.3 (C-COO), 122.7 (CH), 118.9 (C-Br), 115.9 (CH), 82.1 (OCH), 64.7 (OCH₂), 52.2 (OCH₃), 25.8 (3 x CH₃), 24.3 (CH₂), 18.2 (SiC), 9.5 (CH₃), -5.4 (SiCH₃), -5.5 (SiCH₃). IR (neat): 2929, 1725, 1288, 1230, 1102. HRMS (ESI) exact mass calculated for $\text{C}_{18}\text{H}_{30}\text{BrO}_4\text{Si}$ [M+H]⁺ m/z 417.1091, found m/z 417.1087. $[\alpha_D]^{24.2^\circ}_\lambda(c\ 0.5, \text{CDCl}_3)$: +48.6°

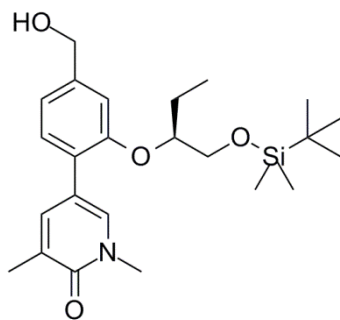
(S)-Methyl 3-((1-((*tert*-butyldimethylsilyl)oxy)butan-2-yl)oxy)-4-(1,5-dimethyl-6-oxo-1,6-dihydropyridin-3-yl)benzoate, 3.99



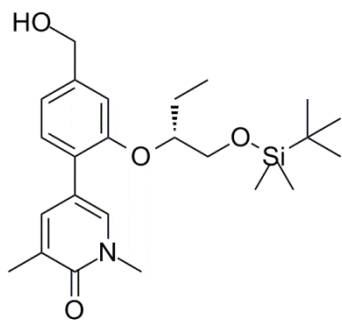
To a solution of (*S*)-methyl 4-bromo-3-((1-((*tert*-butyldimethylsilyl)oxy)butan-2-yl)oxy)benzoate (3 g, 7.19 mmol) and 1,3-dimethyl-5-(4,4,5,5-tetramethyl-1,3,2-dioxaborolan-2-yl)pyridin-2(1H)-one (2.24 g, 8.98 mmol) in 1,4-dioxane (50 mL) and water (2.0 mL) stirred under nitrogen at RT was added palladium tetrakis triphenylphosphine (0.25 g, 0.22 mmol) and 1 M aqueous potassium carbonate (21.6 mL, 21.6 mmol). The reaction mixture was stirred at 95 °C for 1.5 h. After cooling to room temperature, the reaction mixture was diluted with water (100 mL) and extracted with ethyl acetate (3 x 100 mL). The combined organics were extracted with brine (50 mL). The organics were combined, dried by passing through a hydrophobic frit and the solvent was removed under reduced pressure. The resulting brown oil was dissolved in DCM (5 mL) and loaded onto a 200 g Silicycle silica column. The crude material on silica was purified by Biotage Isolera using a gradient of 20 - 80% ethyl acetate in cyclohexane over 20 CV. Fractions containing the desired product were evaporated *in vacuo* and further dried under high vacuum to yield the desired product (*S*)-methyl 3-((1-((*tert*-butyldimethylsilyl)oxy)butan-2-yl)oxy)-4-(1,5-dimethyl-6-oxo-1,6-dihydropyridin-3-yl)benzoate (3.5 g, 6.85 mmol, 95% yield) (90% purity) as a yellow gum. LCMS (formic acid): $t_r = 1.53$ min, MH^+ 460.2. ^1H NMR δ (400 MHz, CDCl_3) ppm: 7.68 (1H, d, $J=1.2$ Hz), 7.64 (1H, dd, $J=8.1, 1.5$ Hz), 7.56 (1H, d, $J=2.4$ Hz), 7.52 (1H, dd, $J=2.3, 1.1$ Hz), 7.29 (1H, d, $J=8.1$ Hz), 4.39 (1H, quin, $J=5.4$ Hz), 3.92 (3H, s), 3.73 (2H, d, $J=4.9$ Hz), 3.60 (3H, s), 2.20 (3H, s), 1.77 - 1.65 (2H, m), 0.95 (3H, t, $J=7.5$ Hz), 0.82 (9H, s), -0.01 (3H, s), -0.01 (3H, s).

(R)-Methyl 3-((1-((*tert*-butyldimethylsilyl)oxy)butan-2-yl)oxy)-4-(1,5-dimethyl-6-oxo-1,6-dihydropyridin-3-yl)benzoate, 3.100

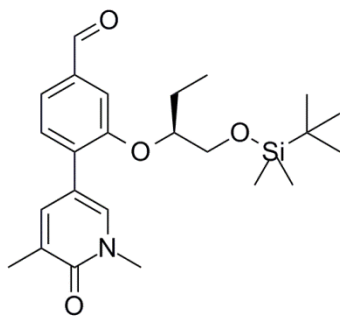
To a solution of (*R*)-methyl 4-bromo-3-((1-((*tert*-butyldimethylsilyl)oxy)butan-2-yl)oxy)benzoate (2.5 g, 5.99 mmol) and 1,3-dimethyl-5-(4,4,5,5-tetramethyl-1,3,2-dioxaborolan-2-yl)pyridin-2(1H)-one (1.87 g, 7.49 mmol) in 1,4-dioxane (40 mL) and water (1.6 mL) stirred under nitrogen at RT was added palladium tetrakis triphenylphosphine (0.21 g, 0.18 mmol) and 1 M aqueous potassium carbonate (18.0 mL, 18.0 mmol). The reaction mixture was stirred at 95 °C for 4 h. After cooling to room temperature, the reaction mixture was diluted with water (100 mL) and extracted with ethyl acetate (3 x 100 mL). The combined organics were extracted with brine (50 mL). The organics were combined, dried by passing through a hydrophobic frit and the solvent was removed under reduced pressure. The resulting brown oil was dissolved in DCM (5 mL) and loaded onto a 200 g Silicycle silica column. The crude material on silica was purified by Biotage Isolera using a gradient of 20 - 80% ethyl acetate in cyclohexane over 20 CV. Fractions containing the desired product were evaporated *in vacuo* and further dried under high vacuum to yield the desired product (*R*)-methyl 3-((1-((*tert*-butyldimethylsilyl)oxy)butan-2-yl)oxy)-4-(1,5-dimethyl-6-oxo-1,6-dihydropyridin-3-yl)benzoate (2.51 g, 5.46 mmol, 91% yield) as a yellow gum. LCMS (formic acid): rt = 1.54 min, MH⁺ 460.4. ¹H NMR δ(400 MHz, CDCl₃) ppm: 7.68 (1H, d, *J*=1.5 Hz), 7.64 (1H, dd, *J*=7.9, 1.6 Hz), 7.55 (1H, d, *J*=2.4 Hz), 7.51 (1H, dd, *J*=2.4, 1.0 Hz), 7.29 (1H, d, *J*=8.1 Hz), 4.39 (1H, quin, *J*=5.4 Hz), 3.92 (3H, s), 3.73 (2H, d, *J*=5.1 Hz), 3.60 (3H, s), 2.20 (3H, s), 1.77 - 1.64 (2H, m), 0.95 (3H, t, *J*=7.5 Hz), 0.82 (9H, s), -0.01 (3H, s), -0.01 (3H, s).

(S)-5-(2-((1-((*tert*-Butyldimethylsilyl)oxy)butan-2-yl)oxy)-4-(hydroxymethyl)phenyl)-1,3-dimethylpyridin-2(1H)-one, 3.101

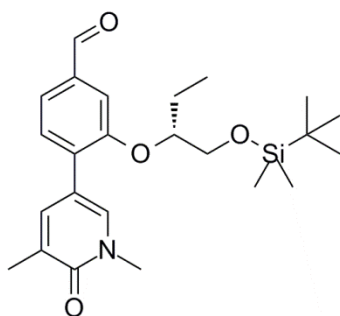
To a solution of (S)-methyl 3-((1-((*tert*-butyldimethylsilyl)oxy)butan-2-yl)oxy)-4-(1,5-dimethyl-6-oxo-1,6-dihydropyridin-3-yl)benzoate (2 g, 4.35 mmol) in DCM (20 mL) stirred under nitrogen and cooled to -78 °C in an dry ice-acetone bath was added a solution of 1 M DIBAL-H in tetrahydrofuran (15 mL, 15 mmol) dropwise during 5 min and the reaction stirred for an additional 10 min. The reaction mixture was warmed to 0 °C and stirred for 20 min. After this time, the reaction was quenched with 10% aqueous citric acid (50 mL) and the mixture stirred at 25 °C overnight. The layers were separated and the aqueous layer was extracted with DCM (2 x 60 mL) and the combined organics were washed with brine (15 mL), dried and concentrated *in vacuo* to provide crude product. The resulting solid was dissolved in DCM (5 mL) and loaded onto a 50 g SNAP silica column. The crude material on silica was purified by Biotage SP4 using a gradient of 50 - 100% ethyl acetate in cyclohexane for 17 CV which eluted the product in two portions. The fractions containing product in each portion were collected separately and the solvent removed under reduced pressure to yield the desired product which was further dried under high vacuum (S)-5-(2-((1-((*tert*-butyldimethylsilyl)oxy)butan-2-yl)oxy)-4-(hydroxymethyl)phenyl)-1,3-dimethylpyridin-2(1H)-one (766 mg, 1.78 mmol, 41% yield) as a clear oil and (S)-5-(2-((1-((*tert*-butyldimethylsilyl)oxy)butan-2-yl)oxy)-4-(hydroxymethyl)phenyl)-1,3-dimethylpyridin-2(1H)-one (270 mg, 0.63 mmol, 14% yield) as a clear oil. LCMS (formic acid): *rt* = 1.30 min, *MH*⁺ 432.3. ¹H NMR δ(400 MHz, CDCl₃) ppm: 7.48 (1H, dd, *J*=2.3, 1.1 Hz), 7.43 (1H, d, *J*=2.2 Hz), 7.19 (1H, d, *J*=7.8 Hz), 7.05 (1H, s), 6.95 (1H, dd, *J*=7.8, 1.5 Hz), 4.69 (2H, s), 4.31 (1H, quin, *J*=5.4 Hz), 3.74 - 3.65 (2H, m), 3.58 (3H, s), 2.18 (3H, s), 1.78 - 1.59 (2H, m), 0.93 (3H, t, *J*=7.5 Hz), 0.83 (9H, s), -0.01 (6H, s). ¹³C NMR δ(101 MHz, CDCl₃) ppm: 162.6 (C=O), 155.7 (C-O), 141.6 (C-CH₂OH), 139.2 (C-CH), 135.3 (N-CH), 129.6 (CH), 128.1 (C-CH₃), 126.0 (C-C), 119.2 (CH), 116.8 (C-C), 112.8 (CH), 80.5 (O-CH), 65.1 (C-CH₂OH), 64.0 (O-CH₂), 37.9 (N-CH₃), 25.8 (SiC(CH₃)₃), 24.2 (CH₂CH₃), 18.2 (SiC(CH₃)), 17.2 (C-CH₃), 9.5 (CH₂CH₃), -5.4 (SiCH₃), -5.5 (SiCH₃). IR (CDCl₃): 3364, 2929, 1652, 1589, 1250, 1097. HRMS (ESI) exact mass calculated for C₂₄H₃₈NO₄Si [*M*+*H*]⁺ *m/z* 432.2565, found *m/z* 432.2569. [*α*_D]^{24.2 °C} (c 0.5, CDCl₃): not detected

(R)-5-(2-((1-((tert-Butyldimethylsilyl)oxy)butan-2-yl)oxy)-4-(hydroxymethyl)phenyl)-1,3-dimethylpyridin-2(1H)-one, 3.102

To a solution of (*R*)-methyl 3-((1-((*tert*-butyldimethylsilyl)oxy)butan-2-yl)oxy)-4-(1,5-dimethyl-6-oxo-1,6-dihydropyridin-3-yl)benzoate (2 g, 4.35 mmol) in DCM (20 mL) stirred under nitrogen and cooled to -78 °C in an dry ice-acetone bath was added a solution of 1 M DIBAL-H in tetrahydrofuran (13 mL, 13 mmol) dropwise during 10 min and the reaction stirred for an additional 20 min. The reaction mixture was warmed to 0 °C and stirred for 1 h. After this time, the reaction was quenched with 10% aqueous citric acid (50 mL) and the mixture stirred at 25 °C overnight. The layers were separated and the aqueous layer was extracted with DCM (2 x 60 mL) and the combined organics were washed with brine (15 mL), dried and concentrated *in vacuo* to provide crude product. The resulting solid was dissolved in DCM (5 mL) and loaded onto a 50 g SNAP silica column. The crude material on silica was purified by Biotage SP4 using a gradient of 25 - 100% ethyl acetate in cyclohexane for 21 CV which eluted the product. The fractions containing product were collected as two batches and the solvent removed under reduced pressure to yield the desired product (*R*)-5-(2-((1-((*tert*-butyldimethylsilyl)oxy)butan-2-yl)oxy)-4-(hydroxymethyl)phenyl)-1,3-dimethylpyridin-2(1H)-one (0.7 g, 1.46 mmol, 34% yield) (90% purity, contains DCM) as a clear oil and (*R*)-5-(2-((1-((*tert*-butyldimethylsilyl)oxy)butan-2-yl)oxy)-4-(hydroxymethyl)phenyl)-1,3-dimethyl pyridin-2(1H)-one (610 mg, 1.41 mmol, 33% yield) as an clear oil. LCMS (formic acid): rt = 1.30 min, MH⁺ 432.4. ¹H NMR δ(400 MHz, CDCl₃) ppm: 7.47 (1H, dd, *J*=2.4, 1.2 Hz), 7.42 (1H, d, *J*=2.4 Hz), 7.18 (1H, d, *J*=7.8 Hz), 7.05 (1H, s), 6.94 (1H, dd, *J*=7.6, 1.5 Hz), 4.69 (2H, s), 4.31 (1H, quin, *J*=5.5 Hz), 3.75 - 3.65 (2H, m), 3.57 (3H, s), 2.18 (3H, s), 1.78 - 1.58 (2H, m), 0.93 (3H, t, *J*=7.5 Hz), 0.83 (9H, s), -0.01 (6H, s). ¹³C NMR δ(101 MHz, CDCl₃) ppm: 162.6 (C=O), 155.6 (C-O), 141.7 (C-CH₂OH), 139.2 (C-CH), 135.3 (N-CH), 129.6 (CH), 128.0 (C-CH₃), 126.0 (C-C), 119.2 (CH), 116.8 (C-C), 112.8 (CH), 80.5 (O-CH), 65.1 (C-CH₂OH), 64.0 (O-CH₂), 37.9 (N-CH₃), 25.8 (SiC(CH₃)₃), 24.1 (CH₂CH₃), 18.2 (SiC(CH₃)), 17.2 (C-CH₃), 9.5 (CH₂CH₃), -5.4 (SiCH₃), -5.5 (SiCH₃). IR (CDCl₃): 3371, 2929, 1652, 1589, 1250, 1098. HRMS (ESI) exact mass calculated for C₂₄H₃₈NO₄Si [M+H]⁺ m/z 432.2565, found m/z 432.2569. [α_D]^{24.3°C}_λ(c 0.5, CDCl₃): not detected

(S)-3-((1-((*tert*-Butyldimethylsilyl)oxy)butan-2-yl)oxy)-4-(1,5-dimethyl-6-oxo-1,6-dihydropyridin-3-yl)benzaldehyde, 3.103

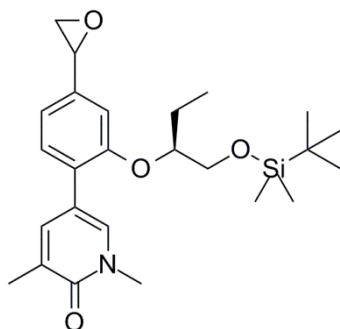
To a solution of (S)-5-(2-((1-((*tert*-butyldimethylsilyl)oxy)butan-2-yl)oxy)-4-(hydroxymethyl)phenyl)-1,3-dimethylpyridin-2(1H)-one (760 mg, 1.76 mmol) in DCM (35 mL) was added 45% iodoxybenzoic acid (stabilised by benzoic acid and isophthalic acid) (1.32 g, 2.11 mmol), portionwise. The reaction mixture was stirred at room temperature for 72 h. LCMS analysis indicated no starting material remained. The reaction mixture was partitioned between DCM (3 x 60 mL) and saturated aqueous sodium bicarbonate solution (75 mL). The organic layers were combined, washed with saturated aqueous sodium bicarbonate solution (60 mL), dried using a hydrophobic frit and evaporated under reduced pressure to give the product (S)-3-((1-((*tert*-butyldimethylsilyl)oxy)butan-2-yl)oxy)-4-(1,5-dimethyl-6-oxo-1,6-dihydropyridin-3-yl)benzaldehyde (804 mg, 1.78 mmol, 100% yield) as a clear gum. LCMS (formic acid): *rt* = 1.46 min, *MH*⁺ 430.3. ¹H NMR δ (400 MHz, CDCl₃) ppm: 9.96 (1H, s), 7.59 (1H, d, *J*=2.4 Hz), 7.54 - 7.51 (2H, m), 7.46 (1H, dd, *J*=7.8, 1.5 Hz), 7.40 (1H, d, *J*=7.8 Hz), 4.43 (1H, quin, *J*=5.4 Hz), 3.79 - 3.70 (2H, m), 3.61 (3H, s), 2.21 (3H, s), 1.79 - 1.64 (2H, m), 0.96 (3H, t, *J*=7.5 Hz), 0.81 (9H, s), -0.02 (6H, s).

(R)-3-((1-((*tert*-Butyldimethylsilyl)oxy)butan-2-yl)oxy)-4-(1,5-dimethyl-6-oxo-1,6-dihydropyridin-3-yl)benzaldehyde, 3.104

To a solution of (R)-5-(2-((1-((*tert*-butyldimethylsilyl)oxy)butan-2-yl)oxy)-4-(hydroxymethyl)phenyl)-1,3-dimethylpyridin-2(1H)-one (700 mg, 1.62 mmol) in DCM (35 mL) was added 45% iodoxybenzoic acid (stabilised by benzoic acid and isophthalic acid) (1.21 g, 1.95 mmol), portionwise. The reaction mixture was stirred at room temperature for 72 h. LCMS analysis indicated no starting material remained. The reaction mixture was partitioned between DCM (3 x 60 mL) and saturated aqueous sodium bicarbonate solution (75 mL). The organic layers were combined, washed with saturated aqueous sodium bicarbonate solution (60 mL), dried using a hydrophobic frit and evaporated under reduced pressure to

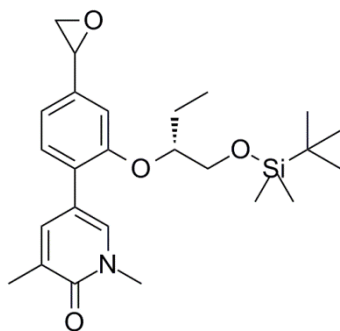
give the product (*R*)-3-((1-((*tert*-butyldimethylsilyl)oxy)butan-2-yl)oxy)-4-(1,5-dimethyl-6-oxo-1,6-dihydropyridin-3-yl)benzaldehyde (642 mg, 1.42 mmol, 88% yield) as a clear gum. LCMS (formic acid): *rt* = 1.46 min, *MH*⁺ 430.3. ¹H NMR δ (400 MHz, CDCl₃) ppm: 9.96 (1H, s), 7.59 (1H, d, *J*=2.4 Hz), 7.54 - 7.51 (2H, m), 7.46 (1H, dd, *J*=7.6, 1.5 Hz), 7.40 (1H, d, *J*=7.6 Hz), 4.43 (1H, quin, *J*=5.4 Hz), 3.79 - 3.70 (2H, m), 3.61 (3H, s), 2.21 (3H, s), 1.79 - 1.63 (2H, m), 0.96 (3H, t, *J*=7.5 Hz), 0.81 (9H, s), -0.02 (6H, s).

5-(2-(((*S*)-1-((*tert*-Butyldimethylsilyl)oxy)butan-2-yl)oxy)-4-(oxiran-2-yl)phenyl)-1,3-dimethylpyridin-2(1H)-one, 3.105



Powdered potassium hydroxide (596 mg, 10.6 mmol) was added in a single portion to a stirred suspension of (*S*)-3-((1-((*tert*-butyldimethylsilyl)oxy)butan-2-yl)oxy)-4-(1,5-dimethyl-6-oxo-1,6-dihydropyridin-3-yl)benzaldehyde (800 mg, 1.77 mmol) and trimethylsulfonium iodide (368 mg, 1.80 mmol) in acetonitrile (7.69 mL) and water (38.4 mL) at RT. The resultant suspension was heated to 65 °C for 30 min and then allowed to cool to RT. The suspension was diluted with ethyl acetate (20 mL) and filtered through a hydrophobic frit. The filtrate was collected and the solvent removed *in vacuo*. The crude gum dissolved in ethyl acetate and diluted with saturated aqueous NaHCO₃ (20 mL). The separated aqueous phase was extracted with ethyl acetate (2 x 20 mL), the combined organic phase was washed with brine (30 mL), passed through a hydrophobic frit and evaporated under reduced pressure to yield 5-(2-(((*S*)-1-((*tert*-butyldimethylsilyl)oxy)butan-2-yl)oxy)-4-(oxiran-2-yl)phenyl)-1,3-dimethylpyridin-2(1H)-one (720 mg, 1.51 mmol, 85% yield) as a pale yellow oil. LCMS (formic acid): *rt* = 1.49 min, *MH*⁺ 444.4. ¹H NMR δ (400 MHz, CDCl₃) ppm: 7.49 - 7.45 (1H, m), 7.45 - 7.41 (1H, m), 7.19 (1H, d, *J*=7.8 Hz), 6.94 - 6.88 (2H, m), 4.29 (1H, quin, *J*=5.4 Hz), 3.85 (1H, dd, *J*=3.9, 2.4 Hz), 3.74 - 3.64 (2H, m), 3.59 (3H, s), 3.15 (1H, ddd, *J*=5.7, 3.9, 2.1 Hz), 2.77 (1H, ddd, *J*=5.5, 2.6, 1.2 Hz), 2.19 (3H, s), 1.77 - 1.60 (2H, m), 0.93 (3H, dd, *J*=14.9, 2.2 Hz), 0.83 (9H, d, *J*=1.0 Hz), -0.01 (6H, s).

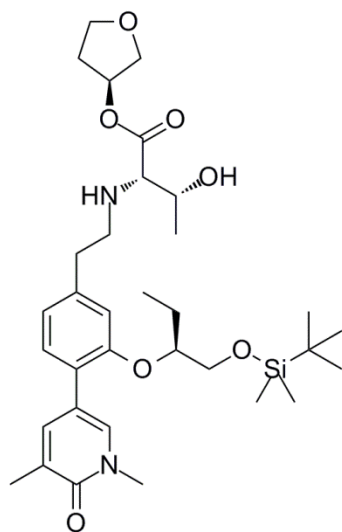
5-(2-(((*R*)-1-((*tert*-Butyldimethylsilyl)oxy)butan-2-yl)oxy)-4-(oxiran-2-yl)phenyl)-1,3-dimethylpyridin-2(1H)-one, 3.106



Powdered potassium hydroxide (454 mg, 8.09 mmol) was added in a single portion to a stirred suspension of (*R*)-3-((1-((*tert*-butyldimethylsilyl)oxy)butan-2-yl)oxy)-4-(1,5-dimethyl-6-oxo-1,6-dihydropyridin-3-yl) benzaldehyde (610 mg, 1.35 mmol) and trimethylsulfonium iodide (281 mg, 1.38 mmol) in acetonitrile (5.86 mL) and Water (29.3 mL) at RT. The

resultant suspension was heated to 65 °C for 30 min and then allowed to cool to RT. The suspension was diluted with ethyl acetate (20 mL) and filtered through a hydrophobic frit. The filtrate was collected and the solvent removed *in vacuo*. The crude gum dissolved in ethyl acetate and diluted with saturated aqueous NaHCO₃ (20 mL). The separated aqueous phase was extracted with ethyl acetate (2 x 20 mL), the combined organic phase was washed with brine (30 mL), passed through a hydrophobic frit and evaporated under reduced pressure to yield 5-(2-(((*R*)-1-((*tert*-butyldimethylsilyl)oxy)butan-2-yl)oxy)-4-(oxiran-2-yl) phenyl)-1,3-dimethylpyridin-2(1H)-one (577 mg, 1.24 mmol, 92% yield) as a yellow gum. LCMS (high pH): *rt* = 1.49 min, MH⁺ 444.4. ¹H NMR δ(400 MHz, CDCl₃) ppm: 7.49 - 7.45 (1H, m), 7.45 - 7.41 (1H, m), 7.19 (1H, d, *J*=7.8 Hz), 6.94 - 6.88 (2H, m), 4.29 (1H, quin, *J*=5.4 Hz), 3.85 (1H, dd, *J*=3.9, 2.7 Hz), 3.74 - 3.64 (2H, m), 3.59 (3H, s), 3.15 (1H, ddd, *J*=5.6, 3.9, 2.2 Hz), 2.77 (1H, ddd, *J*=5.6, 2.5, 1.0 Hz), 2.19 (3H, s), 1.76 - 1.59 (2H, m), 0.93 (3H, td, *J*=7.5, 2.2 Hz), 0.83 (9H, d, *J*=0.7 Hz), -0.01 (6H, s).

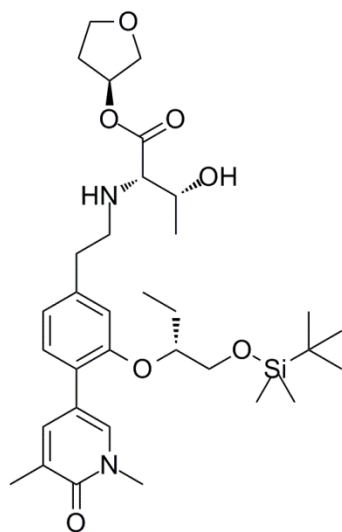
(2S,3R)-(S)-Tetrahydrofuran-3-yl 2-((3-(((S)-1-((tert-butyl)dimethylsilyl)oxy)butan-2-yl)oxy)-4-(1,5-dimethyl-6-oxo-1,6-dihydropyridin-3-yl)phenethyl) amino)-3-hydroxybutanoate, 3.107



To a round bottomed flask was added 5-(2-(((S)-1-((tert-butyl)dimethylsilyl)oxy)butan-2-yl)oxy)-4-(oxiran-2-yl)phenyl)-1,3-dimethylpyridin-2(1H)-one (330 mg, 0.63 mmol) and the flask flushed with nitrogen before dissolution in tetrahydrofuran (5.5 mL). To the solution, cooled in an ice bath, was added boron trifluoride diethyl etherate (0.039 mL, 0.32 mmol). The reaction mixture was stirred at 0 °C for 15 min. After this time, (2S,3R)-(S)-tetrahydrofuran-3-yl 2-amino-3-hydroxybutanoate, hydrochloride (214 mg, 0.95 mmol), triethylamine (0.26 mL, 1.90 mmol) and *p*-toluenesulfonic acid monohydrate (100 mg, 0.53 mmol) was added to aid salt solubility. The mixture was warmed to RT and stirred for 40 min. After this time, sodium triacetoxyborohydride (536 mg, 2.53 mmol) was added and the mixture stirred for 4 days. The reaction mixture was diluted with DCM (50 mL), the mixture washed with saturated aqueous sodium hydrogen carbonate solution (50 mL) and the layers separated. The aqueous was extracted with DCM (2 x 50 mL) and the organics combined, washed with brine (40 mL), dried by passing through a hydrophobic frit and the solvent removed under reduced pressure. The crude gum was dissolved in DCM (3 mL) and loaded onto a 25 g SNAP silica column. The crude material on silica was purified by Biotage SP4 using a gradient of 0 - 10% ethanol in ethyl acetate over 25 CV. Fractions containing the desired product were collected and the solvent removed *in vacuo* to yield a yellow gum. The crude material was dissolved in 1:1 MeOH:DMSO (3 mL) and purified by mass directed autoprep on Xbridge column using 50 – 99% acetonitrile water with an ammonium carbonate modifier. Machine error resulted in only part of the UV peak being collected. The fractions were collected and the solvent was evaporated *in vacuo* to yield the impure product. The crude yellow gum was dissolved in 1:1 MeOH:DMSO (2 mL) and purified by mass directed autoprep on Xbridge column using 50 – 99% acetonitrile water with an ammonium carbonate modifier. The solvent was evaporated *in vacuo* to give the required product (2S,3R)-(S)-tetrahydrofuran-3-yl 2-((3-(((S)-1-((tert-butyl)dimethylsilyl)oxy)butan-2-yl)oxy)-4-(1,5-dimethyl-6-oxo-1,6-

dihydropyridin-3-yl)phenethyl)amino)-3-hydroxy butanoate (58 mg, 0.094 mmol, 15% yield) as a clear gum. Additionally, the waste was collected and the mixture concentrated. The crude solution was dissolved in 1:1 MeOH:DMSO (3 mL) and purified by mass directed autoprep on Xbridge column using 50-99% acetonitrile water with an ammonium carbonate modifier. The solvent was evaporated *in vacuo* to give the required product (2*S*,3*R*)-(S)-tetrahydrofuran-3-yl 2-((3-(((S)-1-((*tert*-butyldimethylsilyloxy)butan-2-yl)oxy)-4-(1,5-dimethyl-6-oxo-1,6-dihydropyridin-3-yl)phenethyl)amino)-3-hydroxybutanoate (80 mg, 0.13 mmol, 21% yield) as a pale yellow gum. LCMS (high pH): *rt* = 1.39 min, *MH*⁺ 617.5. ¹H NMR δ (400 MHz, CDCl₃) ppm: 7.49 (1H, dd, *J*=2.2, 1.0 Hz), 7.44 (1H, d, *J*=2.2 Hz), 7.16 (1H, d, *J*=7.8 Hz), 6.88 - 6.85 (1H, m), 6.82 (1H, dd, *J*=7.7, 1.3 Hz), 5.40 - 5.35 (1H, m), 4.28 (1H, quin, *J*=5.5 Hz), 3.96 - 3.84 (3H, m), 3.80 (1H, d, *J*=10.5 Hz), 3.76 - 3.62 (3H, m), 3.60 (3H, s), 3.06 - 2.96 (2H, m), 2.86 - 2.72 (3H, m), 2.28 - 2.18 (4H, m), 2.06 - 1.98 (1H, m), 1.78 - 1.62 (3H, m), 1.23 (3H, d, *J*=6.1 Hz), 0.95 (3H, t, *J*=7.5 Hz), 0.86 (9H, s), 0.02 (6H, s). ¹³C NMR δ (101 MHz, CDCl₃) ppm: 173.4 (COO), 162.6 (C=O), 155.6 (C-O), 140.0 (C-CH₂), 139.2 (C-CH), 135.2 (N-CH), 129.6 (CH), 128.0 (C-CH₃), 125.0 (C-C), 121.1 (CH), 116.7 (C-C), 114.9 (CH), 80.5 (O-CH), 75.7 (COOCH), 73.0 (O-CH₂ THF), 68.2 (N-CH), 67.8 (CHOH), 66.9 (O-CH₂ THF), 64.1 (O-CH₂), 49.8 (N-CH₂), 37.9 (N-CH₃), 36.7 (C-CH₂), 32.8 (CH₂), 25.8 (SiC(CH₃)₃), 24.2 (CH₂CH₃), 19.4 (CHCH₃), 18.2 (SiC(CH₃)₃), 17.2 (C-CH₃), 9.5 (CH₂CH₃), -5.4 (SiCH₃), -5.5 (SiCH₃). IR (CDCl₃): 3353, 2929, 1731, 1654, 1593, 1250, 1099. HRMS (ESI) exact mass calculated for C₃₃H₅₃N₂O₇Si [M+H]⁺ *m/z* 617.3617, found *m/z* 617.3629. $[\alpha_D]^{24.3^\circ}_\lambda$ (c 0.5, CDCl₃): -17.1 °.

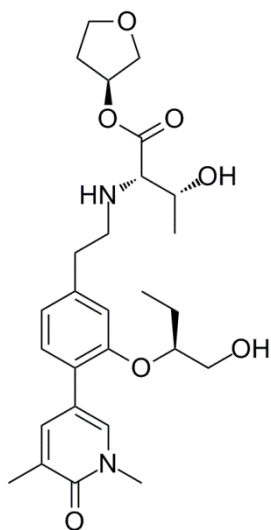
(2S,3R)-(S)-Tetrahydrofuran-3-yl 2-((3-(((R)-1-((tert-butyl)dimethylsilyl)oxy)butan-2-yl)oxy)-4-(1,5-dimethyl-6-oxo-1,6-dihydropyridin-3-yl)phenethyl)amino)-3-hydroxybutanoate, 3.108



To a round bottomed flask was added 5-(2-(((R)-1-((tert-butyl)dimethylsilyl)oxy)butan-2-yl)oxy)-4-(oxiran-2-yl)phenyl)-1,3-dimethylpyridin-2(1H)-one (350 mg, 0.67 mmol) and the flask flushed with nitrogen before dissolution in tetrahydrofuran (5.8 mL). To the solution, cooled in an ice bath, was added boron trifluoride diethyl etherate (0.041 mL, 0.34 mmol). The reaction mixture was stirred at 0 °C for 15 min. After this time, (2S,3R)-(S)-tetrahydrofuran-3-yl 2-amino-3-hydroxybutanoate, hydrochloride (227 mg, 1.01 mmol), triethylamine (0.280 mL, 2.01 mmol) and *p*-toluenesulfonic acid monohydrate (100 mg, 0.53 mmol) was added to aid salt solubility. The mixture was warmed to RT and stirred for 40 min. After this time, sodium triacetoxyborohydride (568 mg, 2.68 mmol) was added and the mixture stirred for 16 h. The reaction mixture was diluted with DCM (50 mL), the mixture washed with saturated aqueous sodium hydrogen carbonate solution (50 mL) and the layers separated. The aqueous was extracted with DCM (2 x 50 mL) and the organics combined, washed with brine (40 mL), dried by passing through a hydrophobic frit and the solvent removed under reduced pressure. The crude gum was dissolved in DCM (3 mL) and loaded onto a 25 g SNAP silica column. The crude material on silica was purified by Biotage SP4 using a gradient of 0 - 10% ethanol in ethyl acetate over 25 CV. Fractions containing the desired product were collected and the solvent removed *in vacuo* to yield a yellow gum. The crude material was dissolved in 1:1 MeOH:DMSO (3 mL) and purified by mass directed autoprep on Xbridge column using 50 – 99% acetonitrile water with an ammonium carbonate modifier. The solvent was evaporated *in vacuo* to give the required product (2S,3R)-(S)-tetrahydrofuran-3-yl 2-((3-(((R)-1-((tert-butyl)dimethylsilyl)oxy)butan-2-yl)oxy)-4-(1,5-dimethyl-6-oxo-1,6-dihydropyridin-3-yl)phenethyl)amino)-3-hydroxybutanoate (130 mg, 0.21 mmol, 31% yield) as a pale yellow gum. LCMS (High pH): rt = 1.40 min, MH⁺ 617.6. ¹H NMR δ(400 MHz, CDCl₃) ppm: 7.47 (1H, dd, *J*=2.3, 1.1 Hz), 7.42 (1H, d, *J*=2.4 Hz), 7.14 (1H, d, *J*=7.8 Hz), 6.84 (1H, s), 6.80 (1H, dd, *J*=7.7, 1.3 Hz), 5.38 - 5.32 (1H, m), 4.26 (1H, quin, *J*=5.5 Hz), 3.95 - 3.82

(3H, m), 3.78 (1H, d, $J=10.8$ Hz), 3.74 - 3.56 (6H, m), 3.04 - 2.92 (2H, m), 2.87 - 2.68 (3H, m), 2.26 - 2.16 (4H, m), 2.04 - 1.95 (1H, m), 1.77 - 1.57 (2H, m), 1.22 (3H, d, $J=6.1$ Hz), 0.93 (3H, t, $J=7.5$ Hz), 0.84 (9H, s), -0.01 (6H, s). ^{13}C NMR δ (101 MHz, CDCl_3) ppm: 173.4 (COO), 162.6 (C=O), 155.6 (C-O), 140.0 (C- CH_2), 139.2 (C-CH), 135.2 (N-CH), 129.6 (CH), 128.0 (C- CH_3), 125.0 (C-C), 121.1 (CH), 116.8 (C-C), 114.9 (CH), 80.5 (O-CH), 75.7 (COOCH), 73.0 (O- CH_2 THF), 68.1 (N-CH), 67.8 (CHOH), 66.9 (O- CH_2 THF), 64.0 (O- CH_2), 49.8 (N- CH_2), 37.9 (N- CH_3), 36.7 (C- CH_2), 32.8 (CH_2), 25.8 ($\text{SiC}(\text{CH}_3)_3$), 24.2 (CH_2CH_3), 19.5 (CHCH_3), 18.2 ($\text{SiC}(\text{CH}_3)_3$), 17.2 (C- CH_3), 9.5 (CH_2CH_3), -5.4 (SiCH_3), -5.5 (SiCH_3). IR (CDCl_3): 3339, 2929, 1731, 1654, 1593, 1250, 1099. HRMS (ESI) exact mass calculated for $\text{C}_{33}\text{H}_{53}\text{N}_2\text{O}_7\text{Si}$ $[\text{M}+\text{H}]^+$ m/z 617.3617, found m/z 617.3643. $[\alpha]_{\text{D}}^{24.4}$ (c 0.5, CDCl_3): -14.2 $^\circ$.

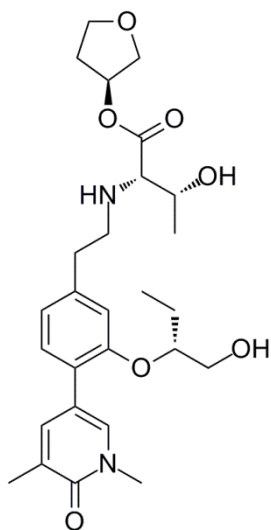
(2S,3R)-(S)-Tetrahydrofuran-3-yl 2-((4-(1,5-dimethyl-6-oxo-1,6-dihydropyridin-3-yl)-3-(((S)-1-hydroxybutan-2-yl)oxy)phenethyl)amino)-3-hydroxybutanoate, 3.109



To a solution of (2S,3R)-(S)-tetrahydrofuran-3-yl 2-((3-(((S)-1-((*tert*-butyldimethylsilyl)oxy)butan-2-yl)oxy)-4-(1,5-dimethyl-6-oxo-1,6-dihydropyridin-3-yl)phenethyl)amino)-3-hydroxybutanoate (40 mg, 0.065 mmol) in tetrahydrofuran (1.25 mL) stirred under nitrogen at 0 $^\circ\text{C}$ was added TBAF (1 M in tetrahydrofuran) (0.091 mL, 0.091 mmol) dropwise. The reaction mixture was stirred at 0 $^\circ\text{C}$ for 3 h. After this time, incomplete conversion to the required product was observed, therefore, an additional portion of TBAF (1 M in tetrahydrofuran) (0.030 mL, 0.030 mmol) was added and stirred for an additional 30 min. Subsequently, the reaction was quenched with dropwise addition of saturated sodium chloride solution (3 mL) and allowed to warm to room temperature. The aqueous layer was then collected and extracted with ethyl acetate (3 x 10 mL). The organic phases were combined, dried by passing through a hydrophobic frit and the solvent removed under reduced pressure to yield the crude product as a yellow oil. The oil was dissolved in DCM (1 mL) and loaded onto a 10 g SNAP silica column. The crude material on silica was purified by Biotage SP4 using a gradient of 0 - 20% ethanol in ethyl acetate over 20

CV. Appropriate fractions were collected and the solvent removed *in vacuo* and further dried under high vacuum to yield (2*S*,3*R*)-(S)-tetrahydrofuran-3-yl 2-((4-(1,5-dimethyl-6-oxo-1,6-dihydropyridin-3-yl)-3-(((*S*)-1-hydroxybutan-2-yl)oxy)phenethyl)amino)-3-hydroxybutanoate (17 mg, 0.034 mmol, 52% yield) as a clear gum. LCMS (high pH): *rt* = 0.85 min, *MH*⁺ 503.4. ¹H NMR δ (400 MHz, CDCl₃) ppm: 7.46 (1H, dd, *J*=2.3, 1.1 Hz), 7.41 (1H, d, *J*=2.2 Hz), 7.16 (1H, d, *J*=7.8 Hz), 6.91 - 6.88 (1H, m), 6.83 (1H, dd, *J*=7.6, 1.5 Hz), 5.37 - 5.31 (1H, m), 4.33 - 4.26 (1H, m), 3.95 - 3.82 (3H, m), 3.77 - 3.60 (4H, m), 3.59 (3H, s), 3.03 - 2.94 (2H, m), 2.86 - 2.73 (3H, m), 2.27 - 2.16 (4H, m), 2.04 - 1.96 (1H, m), 1.73 - 1.65 (2H, m), 1.22 (3H, d, *J*=6.1 Hz), 0.94 (3H, t, *J*=7.5 Hz). IR (CDCl₃): 3364, 2934, 1730, 1652, 1587. HRMS (ESI) exact mass calculated for C₂₇H₃₉N₂O₇ [M+H]⁺ *m/z* 503.2752, found *m/z* 503.2744. $[\alpha_D]^{25.0^\circ C}_\lambda(c\ 0.5, CDCl_3)$: -15.8 °.

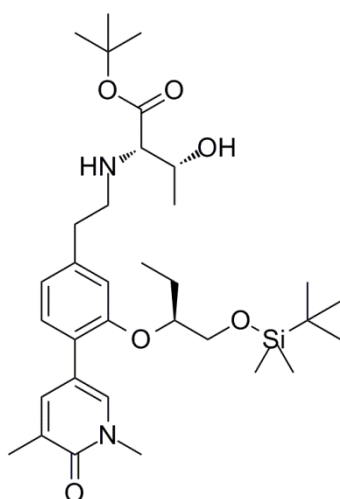
(2*S*,3*R*)-(S)-Tetrahydrofuran-3-yl 2-((4-(1,5-dimethyl-6-oxo-1,6-dihydropyridin-3-yl)-3-(((*R*)-1-hydroxybutan-2-yl)oxy)phenethyl)amino)-3-hydroxybutanoate, 3.110



To a solution of (2*S*,3*R*)-(S)-tetrahydrofuran-3-yl 2-((3-(((*R*)-1-((*tert*-butyldimethylsilyl)oxy)butan-2-yl)oxy)-4-(1,5-dimethyl-6-oxo-1,6-dihydropyridin-3-yl)phenethyl)amino)-3-hydroxybutanoate (60 mg, 0.097 mmol) in tetrahydrofuran (2.0 mL) stirred under nitrogen at 0°C was added TBAF (1 M in tetrahydrofuran) (0.20 mL, 0.20 mmol) dropwise. The reaction mixture was stirred at 0 °C for 1 h. After this time, incomplete conversion to the required product was observed, therefore an additional portion of TBAF (1 M in tetrahydrofuran) (0.050 mL, 0.050 mmol) was added and the mixture stirred for 30 min. Subsequently, the reaction was quenched with dropwise addition of saturated sodium chloride solution (3 mL) and allowed to warm to room temperature. The aqueous layer was then collected and extracted with ethyl acetate (3 x 10 mL). The organic phases were combined, dried over a hydrophobic frit and the solvent removed under reduced pressure to yield the crude product as a yellow oil. The oil was dissolved in DCM (1 mL) and loaded onto a 10 g SNAP silica column. The crude material on silica was purified by Biotage SP4 using a gradient of 0 - 20% ethanol in ethyl acetate over 20 CV. Appropriate

fractions were collected and the solvent removed *in vacuo* and further dried under high vacuum to yield (2*S*,3*R*)-(S)-tetrahydrofuran-3-yl 2-((4-(1,5-dimethyl-6-oxo-1,6-dihydropyridin-3-yl)-3-(((*R*)-1-hydroxybutan-2-yl)oxy)phenethyl)amino)-3-hydroxybutanoate (42 mg, 0.084 mmol, 86% yield) as a clear gum. LCMS (high pH): *rt* = 0.85 min, MH⁺ 503.5. ¹H NMR δ(400 MHz, CDCl₃) ppm: 7.46 (1H, dd, *J*=2.4, 1.0 Hz), 7.42 (1H, d, *J*=2.2 Hz), 7.16 (1H, d, *J*=7.6 Hz), 6.91 - 6.87 (1H, m), 6.84 (1H, dd, *J*=7.8, 1.5 Hz), 5.37 - 5.32 (1H, m), 4.32 - 4.25 (1H, m), 3.93 - 3.82 (3H, m), 3.79 - 3.60 (4H, m), 3.59 (3H, s), 3.03 - 2.95 (2H, m), 2.87 - 2.71 (3H, m), 2.25 - 2.15 (4H, m), 2.02 - 1.95 (1H, m), 1.72 - 1.65 (3H, m), 1.20 (3H, d, *J*=6.1 Hz), 0.94 (3H, t, *J*=7.5 Hz). ¹³C NMR δ(101 MHz, CDCl₃) ppm: 173.4 (COO), 162.6 (C=O), 155.3 (C-O), 140.3 (C-CH₂), 139.1 (C-CH), 135.2 (N-CH), 129.7 (CH), 128.2 (C-CH₃), 125.4 (C-C), 121.9 (CH), 116.6 (C-C), 115.3 (CH), 81.2 (OCH), 75.7 (COOCH), 73.0 (O-CH₂, THF), 68.2 (CHOH), 67.8 (NHCH), 66.9 (O-CH₂, THF), 63.7 (O-CH₂), 49.5 (NHCH₂), 37.9 (N-CH₃), 36.5 (C-CH₂), 32.7 (CH₂), 23.9 (CH₂CH₃), 19.4 (CHCH₃), 17.2 (C-CH₃), 9.6 (CH₂CH₃). IR (CDCl₃): 3352, 2934, 1730, 1652, 1588. HRMS (ESI) exact mass calculated for C₂₇H₃₉N₂O₇ [M+H]⁺ *m/z* 503.2752, found *m/z* 503.2755. [α]_D^{24.9°C}_λ(c 0.5, CDCl₃): -13.8 °.

(2*S*,3*R*)-*tert*-Butyl 2-((3-(((*S*)-1-((*tert*-butyldimethylsilyl)oxy)butan-2-yl)oxy)-4-(1,5-dimethyl-6-oxo-1,6-dihydropyridin-3-yl)phenethyl)amino)-3-hydroxybutanoate, 3.112

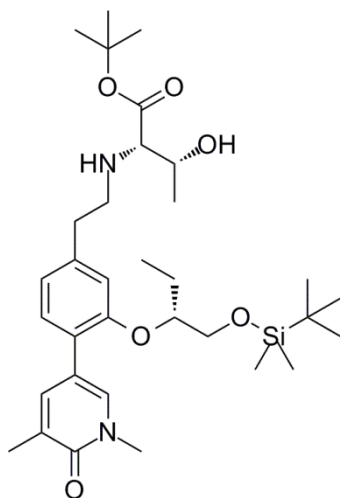


To a round bottomed flask was added 5-(2-(((*S*)-1-((*tert*-butyldimethylsilyl)oxy)butan-2-yl)oxy)-4-(oxiran-2-yl)phenyl)-1,3-dimethylpyridin-2(1*H*)-one (330 mg, 0.63 mmol) and the flask flushed with nitrogen before dissolution in tetrahydrofuran (5.5 mL). To the solution, cooled in an ice bath, was added boron trifluoride diethyl etherate (0.039 mL, 0.32 mmol). The reaction mixture was stirred at 0 °C for 15 min. After this time, (2*S*,3*R*)-*tert*-butyl 2-amino-3-hydroxybutanoate, hydrochloride (201 mg, 0.95 mmol) and triethylamine (0.26 mL, 1.90 mmol) were added. The mixture was warmed to RT and stirred for 40 min. *p*-Toluenesulfonic acid monohydrate (100 mg, 0.53 mmol) was added to aid salt solubility and the mixture stirred for a further 30 min. After this time, sodium

triacetoxyborohydride (536 mg, 2.53 mmol) was added and the mixture stirred for 4 days. The reaction mixture was diluted with DCM (50 mL), the mixture washed with saturated aqueous sodium hydrogen carbonate solution (50 mL) and the layers separated. The aqueous was extracted with DCM (2 x 50 mL) and the organics combined, washed with brine (40 mL), dried by passing through a hydrophobic frit and the solvent removed under reduced pressure. The crude gum was dissolved in DCM (3 mL) and loaded onto a 25 g SNAP silica column. The crude material on silica was purified by Biotage SP4 using a gradient of 60 - 100% ethyl acetate in cyclohexane switching to 0 - 15% ethanol in ethyl acetate over 25 CV. Fractions containing the desired product were collected and the solvent removed *in vacuo* to yield a yellow gum. The crude material was dissolved in 1:1 MeOH:DMSO (2 mL) and purified by mass directed autoprep on Xbridge column using 80-99% acetonitrile water with an ammonium carbonate modifier. The solvent was evaporated *in vacuo* to yield (2*S*,3*R*)-*tert*-butyl 2-((3-(((*S*)-1-((*tert*-butyldimethylsilyl)oxy)butan-2-yl)oxy)-4-(1,5-dimethyl-6-oxo-1,6-dihydropyridin-3-yl)phenethyl)amino)-3-hydroxybutanoate (170 mg, 0.25 mmol, 40% yield) as a pale yellow gum. Impure fractions were collected, the solvent removed *in vacuo* and re-dissolved in 1:1 MeOH:DMSO (1 mL) and purified by mass directed autoprep on Xbridge column using 80 - 99 % acetonitrile water with an ammonium carbonate modifier. The solvent was evaporated *in vacuo* to yield (2*S*,3*R*)-*tert*-butyl 2-((3-(((*S*)-1-((*tert*-butyldimethylsilyl)oxy)butan-2-yl)oxy)-4-(1,5-dimethyl-6-oxo-1,6-dihydropyridin-3-yl)phenethyl)amino)-3-hydroxybutanoate (70 mg, 0.12 mmol, 18% yield) as a clear gum. LCMS (high pH): *rt* = 1.58 min, *MH*⁺ 603.5. ¹H NMR δ (400 MHz, CDCl₃) ppm: 7.47 (1H, dd, *J*=2.4, 1.2 Hz), 7.41 (1H, d, *J*=2.2 Hz), 7.14 (1H, d, *J*=7.8 Hz), 6.86 - 6.83 (1H, m), 6.80 (1H, dd, *J*=7.8, 1.5 Hz), 4.26 (1H, quin, *J*=5.4 Hz), 3.71 (1H, dd, *J*=11.0, 5.4 Hz), 3.66 (1H, dd, *J*=10.8, 4.9 Hz), 3.58 (3H, s), 3.57 - 3.51 (1H, m), 3.02 - 2.93 (1H, m), 2.85 (1H, d, *J*=8.1 Hz), 2.83 - 2.70 (3H, m), 2.18 (3H, s), 1.76 - 1.59 (2H, m), 1.46 (9H, s), 1.21 (3H, d, *J*=6.1 Hz), 0.92 (3H, t, *J*=7.5 Hz), 0.84 (9H, s), -0.01 (6H, s). ¹³C NMR δ (101 MHz, CDCl₃) ppm: 172.9 (COO), 162.6 (C=O), 155.6 (C-O), 140.2 (C-CH₂), 139.3 (C-CH), 135.2 (N-CH), 129.5 (CH), 128.0 (C-CH₃), 124.9 (C-C), 121.2 (CH), 116.8 (C-C), 114.8 (CH), 81.8 (OC(CH₃)₃), 80.5 (O-CH), 69.1 (NHCH), 67.9 (CHOH), 64.0 (O-CH₂), 49.8 (N-CH₂), 37.9 (N-CH₃), 36.7 (C-CH₂), 28.1 (OC(CH₃)₃), 25.8 (SiC(CH₃)₃), 24.2 (CH₂CH₃), 19.3 (CH-CH₃), 18.2 (SiC(CH₃)₃), 17.2 (C-CH₃), 9.5 (CH₂CH₃), -5.4 (SiCH₃), -5.5 (SiCH₃). IR (CDCl₃): 3383, 2930, 1725, 1655, 1595, 1250, 1149, 1099. HRMS (ESI) exact mass

calculated for $C_{33}H_{55}N_2O_6Si$ $[M+H]^+$ m/z 603.3824, found m/z 603.3841. $[\alpha_D]^{24.4}$ °C
 $\lambda(c$ 0.5, $CDCl_3$): -14.2 °.

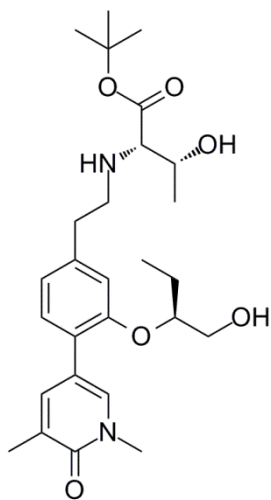
(2S,3R)-tert-Butyl 2-((3-(((R)-1-((tert-butyldimethylsilyl)oxy)butan-2-yl)oxy)-4-(1,5-dimethyl-6-oxo-1,6-dihydropyridin-3-yl)phenethyl)amino)-3-hydroxybutanoate, 3.113



To a round bottomed flask was added 5-(2-(((R)-1-((tert-butyldimethylsilyl)oxy)butan-2-yl)oxy)-4-(oxiran-2-yl)phenyl)-1,3-dimethylpyridin-2(1H)-one (220 mg, 0.42 mmol) and the flask flushed with nitrogen before dissolution in tetrahydrofuran (3.7 mL). To the solution, cooled in an ice bath, was added boron trifluoride diethyl etherate (0.026 mL, 0.21 mmol). The reaction mixture was stirred at 0 °C for 15 min. After this time, (2S,3R)-tert-butyl 2-amino-3-hydroxybutanoate, hydrochloride (134 mg, 0.63 mmol), triethylamine (0.18 mL, 1.27 mmol) and *p*-toluenesulfonic acid monohydrate (60 mg, 0.32 mmol) were added and the mixture stirred at RT for 40 min. After this time, sodium triacetoxyborohydride (357 mg, 1.69 mmol) was added and the mixture stirred for 16 h. The reaction mixture was diluted with DCM (40 mL), the mixture washed with saturated aqueous sodium hydrogen carbonate solution (40 mL) and the layers separated. The aqueous was extracted with DCM (2 x 40 mL) and the organics combined, washed with brine (30 mL), dried by passing through a hydrophobic frit and the solvent removed under reduced pressure. The crude gum was dissolved in DCM (3 mL) and loaded onto a 25 g SNAP silica column. The crude material on silica was purified by Biotage SP4 using a gradient of 60 - 100% ethyl acetate in cyclohexane switching to 0 - 15% ethanol in ethyl acetate over 25 CV. Fractions containing the desired product were collected and the solvent removed *in vacuo* to yield a yellow gum. The crude material was dissolved in 1:1 MeOH:DMSO (2 mL) and purified by mass directed autoprep on Xbridge column using 80-99% acetonitrile water with an ammonium carbonate modifier. The solvent was evaporated *in vacuo* to yield (2S,3R)-tert-butyl 2-((3-(((R)-1-((tert-butyldimethylsilyl)oxy)butan-2-yl)oxy)-4-(1,5-dimethyl-6-oxo-1,6-dihydropyridin-3-yl)phenethyl)amino)-3-hydroxybutanoate (144 mg, 0.24 mmol, 57% yield) as a pale

yellow gum. LCMS (high pH): rt = 1.57 min, MH⁺ 603.5. ¹H NMR δ(400 MHz, CDCl₃) ppm: 7.49 - 7.45 (1H, m), 7.41 (1H, d, *J*=2.2 Hz), 7.14 (1H, d, *J*=7.8 Hz), 6.84 (1H, s), 6.80 (1H, dd, *J*=7.6, 1.2 Hz), 4.26 (1H, quin, *J*=5.4 Hz), 3.74 - 3.64 (2H, m), 3.60 - 3.51 (4H, m), 3.02 - 2.92 (1H, m), 2.86 (1H, d, *J*=7.8 Hz), 2.84 - 2.69 (3H, m), 2.18 (3H, s), 1.76 - 1.59 (2H, m), 1.47 (9H, s), 1.21 (3H, d, *J*=6.1 Hz), 0.93 (3H, t, *J*=7.5 Hz), 0.84 (9H, s), -0.01 (6H, s). ¹³C NMR δ(101 MHz, CDCl₃) ppm: 172.9 (COO), 162.6 (C=O), 155.5 (C-O), 140.2 (C-CH₂), 139.3 (C-CH), 135.2 (N-CH), 129.5 (CH), 128.0 (C-CH₃), 124.9 (C-C), 121.1 (CH), 116.8 (C-C), 114.9 (CH), 81.8 (OC(CH₃)₃), 80.5 (O-CH), 69.0 (NHCH), 67.9 (CHOH), 64.0 (O-CH₂), 49.8 (N-CH₂), 37.9 (N-CH₃), 36.8 (C-CH₂), 28.1 (OC(CH₃)₃), 25.8 (SiC(CH₃)₃), 24.1 (CH₂CH₃), 19.3 (CH-CH₃), 18.2 (SiC(CH₃)₃), 17.2 (C-CH₃), 9.5 (CH₂CH₃), -5.4 (SiCH₃), -5.5 (SiCH₃). IR (CDCl₃): 3382, 2930, 1725, 1655, 1596, 1250, 1149, 1099. HRMS (ESI) exact mass calculated for C₃₃H₅₅O₆N₂Si [M+H]⁺ m/z 603.3824, found m/z 603.3812. [α]_D^{24.3 °C}_λ(c 0.5, CDCl₃): -9.31°

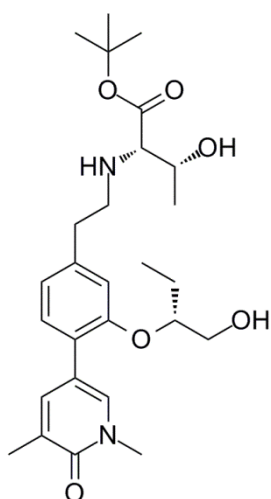
(2*S*,3*R*)-*tert*-butyl 2-((4-(1,5-dimethyl-6-oxo-1,6-dihydropyridin-3-yl)-3-(((*S*)-1-hydroxybutan-2-yl)oxy)phenethyl)amino)-3-hydroxybutanoate, 3.114



To a solution of (2*S*,3*R*)-*tert*-butyl 2-((3-(((*S*)-1-((*tert*-butyldimethylsilyl)oxy)butan-2-yl)oxy)-4-(1,5-dimethyl-6-oxo-1,6-dihydropyridin-3-yl)phenethyl)amino)-3-hydroxybutanoate (70 mg, 0.12 mmol) in tetrahydrofuran (2.1 mL) stirred under nitrogen at 0 °C was added TBAF (1 M in tetrahydrofuran) (0.16 mL, 0.16 mmol) dropwise. The reaction mixture was stirred at 0 °C for 3 h. After this time, incomplete conversion to the required product was observed, therefore an additional portion of TBAF (1 M in tetrahydrofuran) (0.054 mL, 0.054 mmol) was added and stirred for an additional 30 min. Subsequently, the reaction was quenched with dropwise addition of saturated sodium chloride solution (3 mL) and allowed to warm to room temperature. The aqueous layer was then collected and extracted with ethyl acetate (3 x 10 mL). The organic phases were combined, dried by passing through a hydrophobic frit and the solvent removed under reduced pressure to yield the crude product as a yellow oil. The oil was dissolved in DCM (1 mL) and loaded onto a 10 g SNAP silica column. The crude material on silica was purified by Biotage SP4 using a gradient of 0 - 15% ethanol in ethyl acetate over 20 CV. Appropriate fractions were

collected and the solvent removed *in vacuo* and further dried under high vacuum to yield (2*S*,3*R*)-*tert*-butyl 2-((4-(1,5-dimethyl-6-oxo-1,6-dihydropyridin-3-yl)-3-(((*S*)-1-hydroxybutan-2-yl)oxy)phenethyl)amino)-3-hydroxybutanoate (56 mg, 0.12 mmol, 99% yield) as a clear gum. LCMS (high pH): *rt* = 1.02 min, *MH*⁺ 489.5. ¹H NMR δ(400 MHz, CDCl₃) ppm: 7.46 (1H, dd, *J*=2.3, 1.1 Hz), 7.40 (1H, d, *J*=2.2 Hz), 7.16 (1H, d, *J*=7.6 Hz), 6.91 - 6.88 (1H, m), 6.84 (1H, dd, *J*=7.8, 1.5 Hz), 4.32 - 4.26 (1H, m), 3.76 - 3.64 (2H, m), 3.60 - 3.51 (4H, m), 3.04 - 2.95 (1H, m), 2.87 (1H, d, *J*=8.1 Hz), 2.84 - 2.73 (3H, m), 2.19 (3H, s), 1.74 - 1.65 (3H, m), 1.47 (9H, s), 1.21 (3H, d, *J*=6.1 Hz), 0.94 (3H, t, *J*=7.5 Hz). IR (CDCl₃): 3349, 2974, 1725, 1652, 1589, 1154. HRMS (ESI) exact mass calculated for C₂₇H₄₁N₂O₆ [*M*+*H*]⁺ *m/z* 489.2959, found *m/z* 489.2956. [*α*_D]^{24.9°C}_λ(*c* 0.5, CDCl₃): -13.4 °.

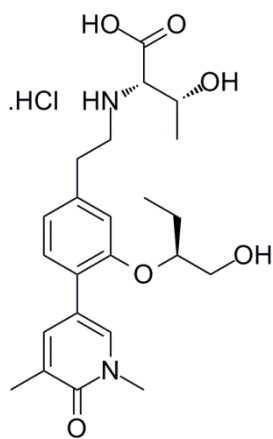
(2*S*,3*R*)-*tert*-Butyl 2-((4-(1,5-dimethyl-6-oxo-1,6-dihydropyridin-3-yl)-3-(((*R*)-1-hydroxybutan-2-yl)oxy)phenethyl)amino)-3-hydroxybutanoate, 3.115



To a solution of (2*S*,3*R*)-*tert*-butyl 2-((3-(((*R*)-1-((*tert*-butyldimethylsilyl)oxy)butan-2-yl)oxy)-4-(1,5-dimethyl-6-oxo-1,6-dihydropyridin-3-yl)phenethyl)amino)-3-hydroxybutanoate (70 mg, 0.10 mmol) in tetrahydrofuran (2.1 mL) stirred under nitrogen at 0 °C was added TBAF (1 M in tetrahydrofuran) (0.21 mL, 0.21 mmol) dropwise. The reaction mixture was stirred at 0 °C for 1 h. After this time, incomplete conversion to the required product was observed, therefore an additional portion of TBAF (1 M in tetrahydrofuran) (0.050 mL, 0.050 mmol) and stirred for 30 min. Subsequently, the reaction was quenched with dropwise addition of saturated sodium chloride solution (3 mL) and allowed to warm to room temperature. The aqueous layer was then collected and extracted with ethyl acetate (3 x 10 mL). The organic phases were combined, dried by passing through a hydrophobic frit and the solvent removed under reduced pressure to yield the crude product as a yellow oil. The oil was dissolved in DCM (1 mL) and loaded onto a 10 g SNAP silica column. the crude material on silica was purified by Biotage SP4 using a gradient of 0 - 15% ethanol in ethyl acetate over 26 CV. Appropriate fractions were collected and the solvent removed *in vacuo* and further dried under high vacuum to yield (2*S*,3*R*)-*tert*-butyl 2-((4-(1,5-dimethyl-6-oxo-1,6-dihydropyridin-3-yl)-3-(((*R*)-1-hydroxybutan-2-

yl)oxy)phenethyl)amino)-3-hydroxybutanoate (51 mg, 0.10 mmol, 100 % yield) as a clear gum. LCMS (high pH): *rt* = 1.03 min, *MH*⁺ 489.4. ¹H NMR δ (400 MHz, CDCl₃) ppm: 7.46 (1H, dd, *J*=2.3, 1.1 Hz), 7.40 (1H, d, *J*=2.2 Hz), 7.15 (1H, d, *J*=7.6 Hz), 6.91 - 6.87 (1H, m), 6.84 (1H, dd, *J*=7.7, 1.3 Hz), 4.32 - 4.25 (1H, m), 3.76 - 3.64 (2H, m), 3.59 (3H, s), 3.58 - 3.50 (1H, m), 3.05 - 2.96 (1H, m), 2.85 (1H, d, *J*=7.8 Hz), 2.83 - 2.71 (3H, m), 2.19 (3H, s), 1.74 - 1.66 (3H, m), 1.47 (9H, s), 1.20 (3H, d, *J*=6.1 Hz), 0.95 (3H, t, *J*=7.6 Hz). ¹³C NMR δ (101 MHz, CDCl₃) ppm: 172.9 (COO), 162.6 (C=O), 155.2 (C-O), 140.4 (C-CH₂), 139.0 (C-CH), 135.2 (N-CH), 129.8 (CH), 128.3 (C-CH₃), 125.4 (C-C), 121.9 (CH), 116.5 (C-C), 115.4 (CH), 82.1 (OC(CH₃)₃), 81.1 (O-CH), 69.0 (NHCH), 67.9 (CHOH), 63.7 (O-CH₂), 49.4 (NHCH₂), 37.9 (N-CH₃), 36.4 (C-CH₂), 28.1 (C(CH₃)₃), 23.8 (CH₂CH₃), 19.4 (CHCH₃), 17.3 (C-CH₃), 9.6 (CH₂CH₃). IR (CDCl₃): 3351, 2974, 1725, 1652, 1589, 1154. HRMS (ESI) exact mass calculated for C₂₇H₄₁N₂O₆ [*M*+*H*]⁺ *m/z* 489.2959, found *m/z* 489.2966. [α _D]^{24.6°C}_λ(*c* 0.5, CDCl₃): -1.6°.

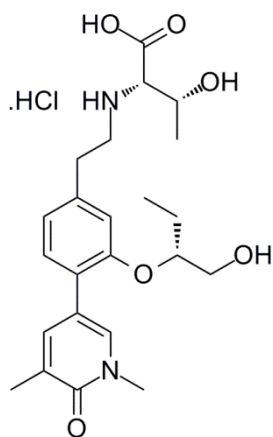
(2*S*,3*R*)-2-((4-(1,5-Dimethyl-6-oxo-1,6-dihydropyridin-3-yl)-3-(((*S*)-1-hydroxybutan-2-yl)oxy)phenethyl)amino)-3-hydroxybutanoic acid, hydrochloride, 3.120



To a solution of (2*S*,3*R*)-*tert*-butyl 2-((4-(1,5-dimethyl-6-oxo-1,6-dihydropyridin-3-yl)-3-(((*S*)-1-hydroxybutan-2-yl)oxy)phenethyl)amino)-3-hydroxybutanoate (25 mg, 0.051 mmol) in tetrahydrofuran (0.5 mL) stirred at RT was added hydrochloric acid (2 M aqueous solution) (300 μ L, 0.60 mmol) dropwise. The reaction mixture was stirred at RT for 24 h. Only a small quantity of product was observed. The reaction was warmed to 50 °C and stirred overnight. The reaction was cooled to RT and the solvent removed under reduced pressure to give a brown gum. The sample was dissolved in 1:1 MeOH:DMSO (1 mL) and purified by mass directed autoprep on Xbridge column using 5 – 30% acetonitrile water with an ammonium carbonate modifier. The solvent was evaporated *in vacuo* and further dried in a vacuum oven for 1 week. To the resulting white solid was added water (0.5 mL) and 2 M aqueous HCl added dropwise. The solvent was evaporated under a stream of nitrogen to yield the desired compound (2*S*,3*R*)-2-((4-(1,5-dimethyl-6-oxo-1,6-dihydropyridin-3-yl)-3-

(((S)-1-hydroxybutan-2-yl)oxy)phenethyl)amino)-3-hydroxybutanoic acid, hydrochloride (23.3 mg, 0.050 mmol, 97% yield) as an off-white solid. LCMS (high pH): rt = 0.57 min, MH⁺ 433.4. ¹H NMR δ(400 MHz, DMSO-*d*₆) ppm: 9.06 (1H, br. s.), 8.96 (1H, br. s.), 7.77 (1H, d, *J*=2.2 Hz), 7.62 - 7.58 (1H, m), 7.25 (1H, d, *J*=7.6 Hz), 6.99 (1H, d, *J*=1.0 Hz), 6.83 (1H, dd, *J*=7.6, 1.2 Hz), 4.32 (1H, quin, *J*=5.3 Hz), 4.14 (1H, quin, *J*=6.2 Hz), 3.91 - 3.83 (1H, m), 3.54 (2H, d, *J*=4.9 Hz), 3.47 (3H, s), 3.33 - 3.13 (2H, m), 3.10 - 2.91 (2H, m), 2.03 (3H, s), 1.75 - 1.52 (2H, m), 1.30 (3H, d, *J*=6.6 Hz), 0.88 (3H, t, *J*=7.5 Hz). HRMS (ESI) exact mass calculated for C₂₃H₃₃N₂O₆ [M+H]⁺ m/z 433.2333, found m/z 433.2344. IR (neat): 3301, 2969, 2427, 1730, 1648.

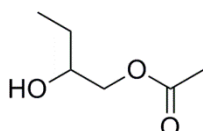
(2S,3R)-2-((4-(1,5-dimethyl-6-oxo-1,6-dihydropyridin-3-yl)-3-(((R)-1-hydroxybutan-2-yl)oxy)phenethyl)amino)-3-hydroxybutanoic acid, hydrochloride, 3.121



To a solution of (2S,3R)-*tert*-butyl 2-((4-(1,5-dimethyl-6-oxo-1,6-dihydropyridin-3-yl)-3-(((R)-1-hydroxybutan-2-yl)oxy)phenethyl)amino)-3-hydroxybutanoate (26 mg, 0.053 mmol) in tetrahydrofuran (0.5 mL) stirred at RT was added hydrochloric acid (2 M aqueous solution) (300 μL, 0.60 mmol) dropwise. The reaction mixture was stirred at RT for 24 h. Only a small quantity of product was observed. The reaction was warmed to 50 °C and stirred overnight. The reaction was cooled to RT and the solvent removed under reduced pressure to give a brown gum. The samples were dissolved in 1:1 MeOH:DMSO (1 mL) and purified by mass directed autoprep on Xbridge column using 5-30% acetonitrile water with an ammonium carbonate modifier. The solvent was evaporated *in vacuo* and further dried in a vacuum oven for 1 week. To the resulting white solid was added water (0.5 mL) and 2 M aqueous HCl added dropwise. The solvent was evaporated under a stream of nitrogen to yield the desired compound (2S,3R)-2-((4-(1,5-dimethyl-6-oxo-1,6-dihydropyridin-3-yl)-3-(((R)-1-hydroxybutan-2-yl)oxy)phenethyl)amino)-3-hydroxybutanoic acid, hydrochloride (12.9 mg, 0.028 mmol, 52% yield) as an off-white solid. LCMS (high pH): rt = 0.56 min, MH⁺ 433.3. ¹H NMR δ(400 MHz, DMSO-*d*₆) ppm: 9.06 (1H, br. s.), 8.93 (1H, br. s.), 7.77 (1H, d, *J*=2.2 Hz), 7.60 (1H, dd, *J*=2.4, 1.0 Hz), 7.25 (1H, d, *J*=7.6 Hz), 6.98 (1H, d, *J*=1.0 Hz), 6.83 (1H, dd, *J*=7.8, 1.2 Hz), 4.32 (1H, quin,

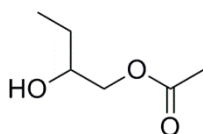
$J=5.3$ Hz), 4.14 (1H, quin, $J=6.2$ Hz), 3.91 - 3.83 (1H, m), 3.54 (2H, d, $J=4.9$ Hz), 3.47 (3H, s), 3.33 - 3.11 (2H, m), 3.10 - 2.91 (2H, m), 2.03 (3H, s), 1.74 - 1.53 (2H, m), 1.30 (3H, d, $J=6.6$ Hz), 0.88 (3H, t, $J=7.5$ Hz). HRMS (ESI) exact mass calculated for $C_{23}H_{33}N_2O_6$ $[M+H]^+$ m/z 433.2333, found m/z 433.2344. IR (neat): 3312, 2969, 1730, 1647.

2-Hydroxybutyl acetate, 3.124²⁸⁸



To a solution of butane-1,2-diol (0.50 mL, 5.55 mmol) in ethyl acetate (9.5 mL) was added porcine pancreatic lipase (0.55 g). The resulting suspension was shaken on an orbit shaker (250 rpm) at 30 °C for 23 h. The insoluble enzyme was removed by filtration and the filtrate analysed by TLC. Permanganate staining indicated a product had formed, although the reaction had not progressed to completion. The filtrate was evaporated *in vacuo* to give a clear liquid which was loaded onto a 25 g SNAP silica column. The crude material on silica was purified by Biotage SP4 using a gradient of 0 - 60% ethyl acetate in cyclohexane over 17 CV. Fractions containing the desired product were collected to yield 2-hydroxybutyl acetate (235 mg, 1.70 mmol, 30 % yield) as a clear liquid. $R_f = 0.30$, 50 % ethyl acetate in cyclohexane. 1H NMR δ (500 MHz, $CDCl_3$) ppm: 4.16 (1H, dd, $J=11.3, 3.0$ Hz), 3.97 (1H, dd, $J=11.5, 7.4$ Hz), 3.81 - 3.74 (1H, m), 2.10 (3H, s), 1.57 - 1.49 (2H, m), 0.99 (3H, t, $J=7.4$ Hz).

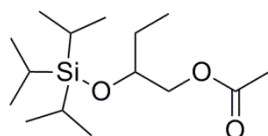
2-Hydroxybutyl acetate, 3.124²⁸⁸



To a solution of butane-1,2-diol (9.94 mL, 111 mmol) in ethyl acetate (190 mL) was added porcine pancreatic lipase (11 g). The resulting suspension was shaken on an orbit shaker (250 rpm) at 30 °C for 47 h. The insoluble enzyme was removed by filtration and the filtrate analysed by TLC. Permanganate staining indicated a product had formed, although the reaction had not progressed to completion. The filtrate was evaporated *in vacuo* to give a clear liquid which was loaded onto two 100 g SNAP silica column. The crude material on silica was purified by Biotage SP4 using a gradient of 0 - 60% ethyl acetate in cyclohexane over 17 CV. Fractions containing the desired product were collected and the solvent removed *in vacuo* to yield 2-hydroxybutyl acetate

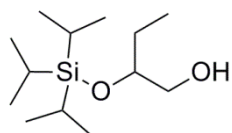
(8.64 g, 65.4 mmol, 59% yield) as a clear liquid. ^1H NMR δ (500 MHz, CDCl_3) ppm: 4.16 (1H, dd, $J=11.3$, 3.0 Hz), 3.97 (1H, dd, $J=11.5$, 7.4 Hz), 3.81 - 3.74 (1H, m), 2.10 (3H, s), 1.57 - 1.49 (2H, m), 0.99 (3H, t, $J=7.4$ Hz). ^{13}C NMR δ (126 MHz, CDCl_3) ppm: 171.2 (C=O), 71.3 (CH-OH), 68.4 (CH_2O), 26.4 (CH_2CH_3), 20.9 (CH_3), 9.7 (CH_2CH_3). IR (neat): 3421, 2968, 1720, 1230.

2-((Triisopropylsilyl)oxy)butyl acetate, 3.129



To a solution of 2-hydroxybutyl acetate (5 g, 37.8 mmol) and triethylamine (10.5 mL, 75 mmol) in DCM (80 mL) stirred under nitrogen at 0 °C was added neat triisopropylsilyl trifluoromethanesulfonate (10.5 mL, 38.7 mmol) dropwise during 5 min. The reaction mixture was stirred at RT for 16 h. The reaction was observed to be complete by TLC staining with permanganate. After this time, the reaction mixture was diluted with DCM (30 mL) and ice-cold water (50 mL) was added to quench reaction. The resultant layers were separated, washing the aqueous layers with DCM (2 x 50 mL). The combined organic layers were washed with saturated aqueous ammonium chloride solution (2 x 50 mL), brine (40 mL), dried by passing through a hydrophobic frit and concentrated *in vacuo*. The crude liquid was loaded onto 2 x 100 g SNAP silica column. The crude material on silica was purified by Biotage SP4 using a gradient of 0 - 10% ethyl acetate in cyclohexane over 20 CV. Fractions containing the desired product were collected and the solvent removed under reduced pressure to yield 2-((triisopropylsilyl)oxy)butyl acetate (6.1 g, 21.1 mmol, 56% yield) as a clear liquid. ^1H NMR δ (400 MHz, CDCl_3) ppm: 4.11 - 3.92 (3H, m), 2.05 (3H, s), 1.65 - 1.50 (2H, m), 1.10 - 1.02 (21H, m), 0.92 (3H, t, $J=7.5$ Hz). ^{13}C NMR δ (101 MHz, CDCl_3) ppm: 171.0 (C=O), 71.2 (O-CH), 67.7 (O- CH_2), 27.5 (CH_2CH_3), 20.9 (COCH_3), 18.07 (3 x CH_3), 18.05 (3 x CH_3), 12.6 (3 x CH), 8.8 (CH_2CH_3). IR (neat): 2944, 2868, 1747, 1230.

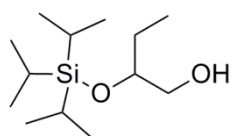
Attempted synthesis of 2-((triisopropylsilyl)oxy)butan-1-ol, 3.130



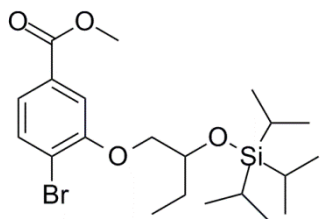
To a solution of 2-((triisopropylsilyl)oxy)butyl acetate (50 mg, 0.17 mmol) in dry methanol (0.86 mL) stirred under nitrogen at room temp was added potassium carbonate (2.4 mg, 0.017 mmol). The reaction mixture was stirred at RT for 30 min. TLC analysis indicated the presence of a product, with starting material remaining. The reaction was stirred for

a further 30 min. After this time, the reaction was still incomplete. An additional portion of potassium carbonate (2.4 mg, 0.017 mmol) was added and the mixture stirred for a further 30 min. After this time, minimal starting material remained. The solvent was removed under reduced pressure, the residue dissolved in DCM (4 mL), filtered and the solvent removed under reduced pressure. The crude residue was dissolved in 1:1 DCM:cyclohexane (2 mL) and loaded onto a 10 g SNAP silica column. The crude material on silica was purified by Biotage SP4 using a gradient of 0 - 25% ethyl acetate in cyclohexane. An individual fraction containing pure material was collected and the solvent removed *in vacuo*. NMR analysis confirmed the major product to be the rearranged isomer 1-((triisopropylsilyl)oxy)butan-2-ol **3.131**. ^1H NMR δ (400 MHz, CDCl_3) ppm: 3.73 (1H, dd, $J=9.5, 3.2$ Hz), 3.63 - 3.55 (1H, m), 3.49 (1H, dd, $J=9.5, 7.6$ Hz), 2.53 (1H, d, $J=3.4$ Hz), 1.53 - 1.40 (2H, m), 1.10 - 1.40 (21H, m), 0.97 (3H, t, $J=7.6$ Hz).

2-((Triisopropylsilyl)oxy)butan-1-ol, 3.130

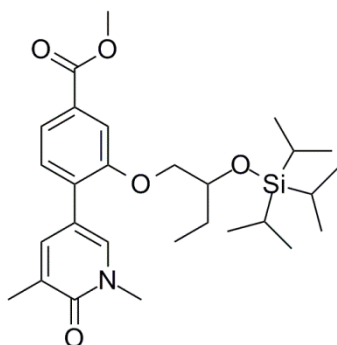


To a solution of 2-((triisopropylsilyl)oxy)butyl acetate (1.4 g, 4.85 mmol) in DCM (23 mL) stirred under nitrogen at -78 °C was added DIBAL-H (1 M in tetrahydrofuran) (10.2 mL, 10.2 mmol) dropwise during 5 min. The reaction mixture was stirred at -78 °C for 1 h. Once the reaction had shown to have gone to completion via TLC, stained with potassium permanganate solution, the reaction mixture was warmed to 0 °C and quenched with 10% aqueous citric acid solution (50 mL). On complete addition of the citric acid solution, the reaction was warmed to RT and stirred overnight. The reaction mixture was extracted with ethyl acetate (3 x 30 mL) and the organic phase was washed with saturated brine (50 mL) and dried using a hydrophobic frit and the solvent evaporated *in vacuo* to give the desired product 2-((triisopropylsilyl)oxy)butan-1-ol (1.2 g, 4.87 mmol, 100% yield) as a clear liquid. ^1H NMR δ (400 MHz, CDCl_3) ppm: 3.85 - 3.77 (1H, m), 3.63 (1H, ddd, $J=11.0, 5.1, 3.7$ Hz), 3.51 (1H, ddd, $J=11.2, 7.1, 4.4$ Hz), 1.92 (1H, dd, $J=7.0, 5.5$ Hz), 1.71 - 1.55 (2H, m), 1.11 - 1.04 (21H, m), 0.88 (3H, t, $J=7.6$ Hz). ^{13}C NMR δ (101 MHz, CDCl_3) ppm: 74.1 (OCH), 65.2 (CH_2OH), 26.7 (CH_2), 18.10 (3 x $\text{CH}(\text{CH}_3)(\text{CH}_3)$), 18.08 (3 x $\text{CH}(\text{CH}_3)(\text{CH}_3)$), 12.5 (3 x SiCH), 9.5 (CH_3). IR (CDCl_3): 3401, 2943, 2867, 1464, 1384, 1247, 1048.

Methyl 4-bromo-3-(2-((triisopropylsilyl)oxy)butoxy)benzoate, 3.132

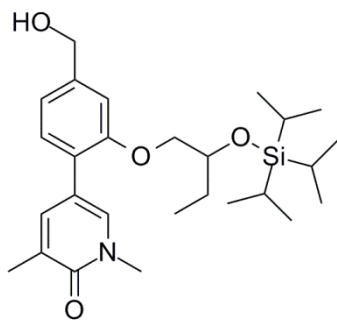
Diisopropyl azodicarboxylate (0.51 mL, 2.60 mmol) was added dropwise over 2 min to a stirred solution of methyl 4-bromo-3-hydroxybenzoate (300 mg, 1.30 mmol), triphenylphosphine (681 mg, 2.60 mmol) and 2-((triisopropylsilyl)oxy)butan-1-ol (384 mg, 1.56 mmol) in tetrahydrofuran (10 mL) at 0 °C under N₂. Following stirring at 0 °C for 15 min, the cooling bath was removed and the solution stirred at RT for 72 h. The volatiles were removed under reduced pressure and the mixture was diluted with ethyl acetate (15 mL) then partitioned with aqueous saturated NaHCO₃ (15 ml). The aqueous layer was extracted with ethyl acetate (15 mL). The combined organics were washed with brine (5 mL), dried by passing through a hydrophobic frit and the volatiles were removed under reduce pressure. The crude product was dissolved in DCM/cyclohexane (2 mL) and the resulting precipitate (triphenylphosphine oxide) was removed by filtration. The filtrate was collected and the solvent removed *in vacuo*. The yellow gum was dissolved in DCM (10 mL) and loaded onto a 50 g SNAP silica column. The crude material on silica was purified by Biotage SP4 using a gradient of 0 - 10% ethyl acetate in cyclohexane over 14 CV. Fractions containing product were collected and the volatiles were removed under reduce pressure to yield methyl 4-bromo-3-(2-((triisopropylsilyl)oxy)butoxy)benzoate (537 mg, 1.17 mmol, 90% yield) as a clear oil. LCMS (formic acid): rt = >2.00 min, MH⁺/- not detected. ¹H NMR δ(400 MHz, CDCl₃) ppm: 7.60 (1H, d, *J*=8.1 Hz), 7.53 (1H, d, *J*=1.7 Hz), 7.50 (1H, dd, *J*=8.1, 1.7 Hz), 4.23 (1H, quin, *J*=5.4 Hz), 4.08 (1H, dd, *J*=9.0, 5.1 Hz), 3.95 (1H, dd, *J*=9.3, 5.6 Hz), 3.92 (3H, s), 1.81 - 1.71 (2H, m), 1.19 - 1.02 (21H, m), 0.98 (3H, t, *J*=7.6 Hz).

Methyl 4-(1,5-dimethyl-6-oxo-1,6-dihydropyridin-3-yl)-3-(2-((triisopropylsilyl)oxy)butoxy)benzoate, 3.133



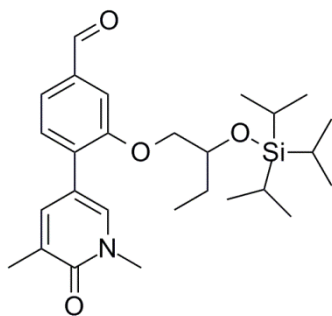
To a solution of methyl 4-bromo-3-(2-((triisopropylsilyl)oxy)butoxy)benzoate (4.5 g, 9.79 mmol) and 1,3-dimethyl-5-(4,4,5,5-tetramethyl-1,3,2-dioxaborolan-2-yl)pyridin-2(1H)-one (3.12 g, 12.5 mmol) in 1,4-dioxane (75 mL) and water (3.0 mL) stirred under nitrogen at RT was added palladium tetrakis triphenylphosphine (0.34 g, 0.29 mmol) and 1 M aqueous potassium carbonate (29.4 mL, 29.4 mmol). The reaction mixture was stirred at 95 °C for 6 h. After cooling to room temperature, the reaction mixture was diluted with water (100 mL) and extracted with ethyl acetate (3 x 100 mL). The combined organics were washed with brine (50 mL), dried by passing through a hydrophobic frit and the solvent was removed under reduced pressure. The resulting yellow oil was dissolved in DCM (5 mL) and loaded onto two 100 g SNAP silica column. The crude material on silica was purified by Biotage SP4 using a gradient of 50 - 100% ethyl acetate in cyclohexane over 14 CV. Fractions containing the desired product were evaporated *in vacuo* and further dried under high vacuum to yield the desired product methyl 4-(1,5-dimethyl-6-oxo-1,6-dihydropyridin-3-yl)-3-(2-((triisopropylsilyl)oxy)butoxy)benzoate (3.5 g, 6.14 mmol, 63% yield) as a yellow gum. LCMS (formic acid): *rt* = 1.73 min, *MH*⁺ 502.3. ¹H NMR δ (400 MHz, CDCl₃) ppm: 7.67 (1H, dd, *J*=7.9, 1.6 Hz), 7.58 (1H, d, *J*=1.2 Hz), 7.54 (1H, d, *J*=2.4 Hz), 7.48 (1H, dd, *J*=2.4, 1.0 Hz), 7.30 (1H, d, *J*=7.8 Hz), 4.12 - 3.97 (3H, m), 3.94 (3H, s), 3.60 (3H, s), 2.20 (3H, s), 1.76 - 1.62 (2H, m), 1.05 - 0.98 (21H, m), 0.93 (3H, t, *J*=7.6 Hz). ¹³C NMR δ (126 MHz, CDCl₃) ppm: 166.7 (COO), 162.6 (C=O), 155.6 (C-O), 138.5 (C-CH), 135.9 (N-CH), 130.9 (C-COO), 130.1 (C-C), 129.2 (CH), 128.5 (C-CH₃), 122.4 (CH), 115.6 (C-C), 112.8 (CH), 71.7 (O-CH), 71.5 (O-CH₂), 52.2 (O-CH₃), 38.0 (N-CH₃), 27.4 (CH₂), 18.1 (6 x CH₃), 17.2 (C-CH₃), 12.5 (3 x SiCH), 8.9 (CH₂CH₃). IR (CDCl₃): 2944, 2867, 1723, 1658, 1288, 1255. HRMS (ESI) exact mass calculated for C₂₈H₄₄NO₅Si [*M*+*H*]⁺ *m/z* 502.2983, found *m/z* 502.2982.

5-(4-(Hydroxymethyl)-2-(2-((triisopropylsilyl)oxy)butoxy)phenyl)-1,3-dimethyl pyridin-2(1H)-one, 3.134



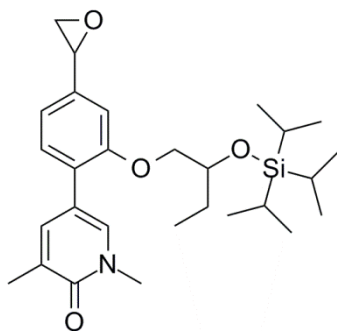
To a solution of methyl 4-(1,5-dimethyl-6-oxo-1,6-dihydropyridin-3-yl)-3-(2-((triisopropylsilyl)oxy)butoxy)benzoate (3.5 g, 6.14 mmol) in DCM (40 mL) stirred under nitrogen and cooled in an dry ice-acetone bath was added a solution of 1 M DIBAL-H in tetrahydrofuran (12.9 mL, 12.9 mmol) dropwise during 5 min and the reaction stirred for an additional 10 min. The reaction mixture was warmed to 0 °C and stirred for 30 min. After this time, a portion of the starting material remained. Therefore, an additional aliquot of 1 M DIBAL-H in tetrahydrofuran (3.0 mL, 3.0 mmol) was added and stirred for a further 15 min. After this time, the reaction was quenched with 10 % aqueous citric acid (45 mL) and the mixture stirred at 25 °C overnight. The layers were separated and the aqueous layer was extracted with DCM (2 x 60 mL) and the combined organics were washed with brine (50 mL), dried by passing through a hydrophobic frit and concentrated *in vacuo* to provide crude product. The resulting yellow gum was dissolved in DCM (5 mL) and loaded onto a 100 g SNAP silica column. The crude material on silica was purified by Biotage SP4 using a gradient of 25 - 100% ethyl acetate in cyclohexane for 20 CV which eluted the product in two peaks. The two peaks containing product were collected separately and the solvent removed under reduced pressure to yield the desired product in each peak. These were combined and further dried under high vacuum to yield 5-(4-(hydroxymethyl)-2-(2-((triisopropylsilyl)oxy)butoxy)phenyl)-1,3-dimethyl pyridin-2(1H)-one (1.51 g, 3.02 mmol, 49% yield) as a clear gum. LCMS (formic acid): rt = 1.54 min, MH⁺ 474.4. ¹H NMR δ(400 MHz, CDCl₃) ppm: 7.44 (1H, dd, *J*=2.3, 1.1 Hz), 7.40 (1H, d, *J*=2.2 Hz), 7.21 (1H, d, *J*=7.8 Hz), 7.01 - 6.94 (2H, m), 4.71 (2H, d, *J*=5.6 Hz), 4.09 - 4.04 (1H, m), 3.98 (1H, dd, *J*=9.3, 4.4 Hz), 3.92 (1H, dd, *J*=9.2, 5.5 Hz), 3.58 (3H, s), 2.19 (3H, s), 1.74 - 1.59 (2H, m), 1.06 - 0.98 (21H, m), 0.92 (3H, t, *J*=7.5 Hz). ¹³C NMR δ(101 MHz, CDCl₃) ppm: 162.6 (C=O), 156.0 (C-O), 141.8 (C-CH₂OH), 139.1 (C-CH), 135.2 (N-CH), 129.5 (CH), 128.2 (C-CH₃), 125.5 (C-C), 119.3 (CH), 116.5 (C-C), 110.7 (CH), 71.6 (OCH), 71.2 (OCH₂), 65.1 (CH₂OH), 37.9 (N-CH₃), 27.4 (CH₂CH₃), 18.1 (6 x CH₃), 17.2 (C-CH₃), 12.5 (3 x SiCH), 8.7 (CH₂CH₃). IR (CDCl₃): 3365, 2941, 2866, 1652, 1248. HRMS (ESI) exact mass calculated for C₂₇H₄₄NO₄Si [M+H]⁺ m/z 474.3034, found m/z 474.3034.

4-(1,5-Dimethyl-6-oxo-1,6-dihydropyridin-3-yl)-3-(2-((triisopropylsilyl)oxy)butoxy)benzaldehyde, 3.135



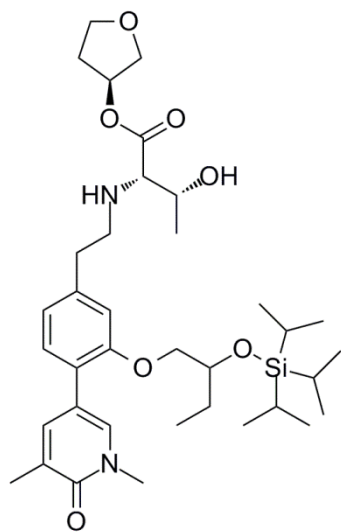
To a solution of 5-(4-(hydroxymethyl)-2-(2-((triisopropylsilyl)oxy)butoxy)phenyl)-1,3-dimethylpyridin-2(1H)-one (1.51 g, 3.09 mmol) in DCM (70 mL) was added 45% iodoxybenzoic acid (stabilised by benzoic acid and isophthalic acid) (2.31 g, 3.71 mmol), portionwise. The reaction mixture was stirred at room temperature for 64 h. The reaction mixture was partitioned between DCM (3 x 100 mL) and saturated aqueous sodium bicarbonate solution (150 mL). The organic layers were combined, washed with saturated aqueous sodium bicarbonate solution (100 mL), dried using a hydrophobic frit and evaporated under reduced pressure to give the desired product 4-(1,5-dimethyl-6-oxo-1,6-dihydropyridin-3-yl)-3-(2-((triisopropylsilyl)oxy)butoxy) benzaldehyde (1.49 g, 3.10 mmol, 100% yield) as a clear gum. LCMS (formic acid): rt = 1.66 min, MH⁺ 472.3. ¹H NMR δ(400 MHz, CDCl₃) ppm: 9.98 (1H, s), 7.58 (1H, d, J=2.4 Hz), 7.53 - 7.46 (2H, m), 7.46 - 7.39 (2H, m), 4.15 - 3.98 (3H, m), 3.61 (3H, s), 2.21 (3H, s), 1.78 - 1.60 (2H, m), 1.05 - 0.98 (21H, m), 0.93 (3H, t, J=7.6 Hz). ¹³C NMR δ(101 MHz, CDCl₃) ppm: 191.4 (CHO), 162.6 (C=O), 156.3 (C-O), 138.3 (C-CH), 136.6 (C-C), 136.2 (N-CH), 132.7 (C-C), 129.6 (CH), 128.6 (C-CH₃), 124.4 (CH), 115.4 (C-C), 110.5 (CH), 71.7 (C-O), 71.6 (C-O), 38.0 (N-CH₃), 27.4 (CH₂CH₃), 18.1 (6 x CH₃), 17.2 (C-CH₃), 12.5 (3 x SiCH), 8.9 (CH₂CH₃). IR (neat): 2942, 2866, 2728, 1694, 1653. HRMS (ESI) exact mass calculated for C₂₇H₄₂NO₄Si [M+H]⁺ m/z 472.2878, found m/z 472.2879.

1,3-Dimethyl-5-(4-(oxiran-2-yl)-2-(2-((triisopropylsilyl)oxy)butoxy)phenyl)pyridin-2(1H)-one, 3.136



Powdered potassium hydroxide (607 mg, 10.8 mmol) was added in a single portion to a stirred suspension of 4-(1,5-dimethyl-6-oxo-1,6-dihydropyridin-3-yl)-3-(2-((triisopropylsilyl)oxy)butoxy)benzaldehyde (850 mg, 1.80 mmol) and trimethylsulfonium iodide (375 mg, 1.84 mmol) in acetonitrile (7.8 mL) and water (39.1 μ L) at RT. The resultant suspension was heated to 65 $^{\circ}$ C for 25 min and then allowed to cool to RT. The suspension was diluted with ethyl acetate (20 mL) and filtered through a hydrophobic frit. The filtrate was collected and the solvent removed *in vacuo*. The crude gum dissolved in ethyl acetate (20 mL) and diluted with saturated aqueous NaHCO_3 (20 mL). The separated aqueous phase was extracted with ethyl acetate (2 x 20 mL), the combined organic phase washed with brine (15 mL), passed through a hydrophobic frit, evaporated under reduced pressure and dried in a vacuum oven to yield 1,3-dimethyl-5-(4-(oxiran-2-yl)-2-(2-((triisopropylsilyl)oxy)butoxy)phenyl)pyridin-2(1H)-one (799 mg, 1.48 mmol, 82% yield) (90% purity) as a pale yellow oil. LCMS (high pH): *rt* = 1.66 min, MH^+ 486.5. ^1H NMR δ (400 MHz, CDCl_3) ppm: 7.43 (1H, s), 7.41 (1H, d, $J=2.2$ Hz), 7.20 (1H, d, $J=7.8$ Hz), 6.94 (1H, dd, $J=7.8, 1.5$ Hz), 6.82 (1H, d, $J=1.5$ Hz), 4.06 (1H, quin, $J=5.2$ Hz), 4.00 - 3.89 (2H, m), 3.87 (1H, dd, $J=3.9, 2.7$ Hz), 3.59 (3H, s), 3.16 (1H, dd, $J=5.5, 4.0$ Hz), 2.81 - 2.77 (1H, m), 2.19 (3H, s), 1.74 - 1.58 (2H, m), 1.02 (21 H, s), 0.92 (3H, t, $J=7.5$ Hz).

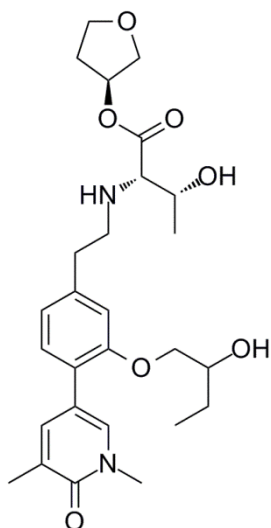
(2S,3R)-(S)-Tetrahydrofuran-3-yl 2-((4-(1,5-dimethyl-6-oxo-1,6-dihydropyridin-3-yl)-3-(2-((triisopropylsilyl)oxy)butoxy)phenethyl)amino)-3-hydroxybutanoate, 3.137



To a round bottomed flask was added 1,3-dimethyl-5-(4-(oxiran-2-yl)-2-(2-((triisopropylsilyl)oxy)butoxy)phenyl)pyridin-2(1H)-one (340 mg, 0.60 mmol) and the flask flushed with nitrogen before dissolution in tetrahydrofuran (5 mL). To the solution, cooled in an ice bath, was added boron trifluoride diethyl etherate (0.037 mL, 0.30 mmol). The reaction mixture was stirred at 0 °C for 15 min. After this time, (2S,3R)-(S)-tetrahydrofuran-3-yl 2-amino-3-hydroxybutanoate, hydrochloride (201 mg, 0.89 mmol), triethylamine (0.250 mL, 1.79 mmol) and *p*-toluenesulfonic acid monohydrate (100 mg, 0.53 mmol) was added to aid salt solubility. The mixture was warmed to RT and stirred for 1 h. After this time, sodium triacetoxyborohydride (504 mg, 2.38 mmol) was added and the mixture stirred overnight. The reaction mixture was diluted with DCM (50 mL), the mixture washed with saturated aqueous sodium hydrogen carbonate solution (50 mL) and the layers separated. The aqueous was extracted with DCM (2 x 50 mL) and the organics combined, washed with brine (40 mL), dried by passing through a hydrophobic frit and the solvent removed under reduced pressure. The crude gum was dissolved in DCM (3 mL) and loaded onto a 25 g SNAP silica column. The crude material on silica was purified by Biotage SP4 using a gradient of 0 - 10% ethanol in ethyl acetate over 25 CV. Fractions containing the desired product were collected and the solvent removed *in vacuo* to yield a yellow gum. The crude material was dissolved in 1:1 MeOH:DMSO (3 mL) and purified by mass directed autoprep on Xbridge column using 80 – 99% acetonitrile water with an ammonium carbonate modifier. The solvent was evaporated *in vacuo* to yield (2S,3R)-(S)-tetrahydrofuran-3-yl 2-((4-(1,5-dimethyl-6-oxo-1,6-dihydropyridin-3-yl)-3-(2-((triisopropylsilyl)oxy)butoxy)phenethyl)amino)-3-hydroxybutanoate (162 mg, 0.25 mmol, 41% yield) as a pale yellow gum. LCMS (high pH): rt = 1.58 min, MH⁺ 659.5. ¹H NMR δ(400 MHz, CDCl₃) ppm: 7.43 (1H, dd, *J*=2.3, 1.1 Hz), 7.41 - 7.37 (1H, m), 7.15 (1H, d, *J*=7.6 Hz), 6.82 (1H, dd, *J*=7.8, 1.5 Hz), 6.75 (1H, s), 5.38 - 5.33 (1H, m), 4.06 (1H, quin, *J*=5.1 Hz), 3.98 - 3.82 (5H, m), 3.81 - 3.74 (1H, m), 3.68 - 3.60 (1H, m), 3.58 (3H, s), 3.05 - 2.96 (2H, m), 2.88 - 2.72 (3H,

m), 2.26 - 2.16 (4H, m), 2.03 - 1.95 (1H, m), 1.74 - 1.59 (3H, m), 1.22 (3H, d, $J=6.4$ Hz), 1.10 - 0.97 (21H, m), 0.92 (3H, t, $J=7.5$ Hz). ^{13}C NMR δ (126 MHz, CDCl_3) ppm: 172.6 (COO), 162.6 (C=O), 155.9 (C-O), 139.8 (C- CH_2), 139.1 (C-CH), 135.1 (N-CH), 129.6 (CH), 128.1 (C- CH_3), 124.5 (C-C), 121.10 (CH Diastereomer a), 121.08 (CH, Diastereomer b), 116.5 (C-C), 112.70 (CH, Diastereomer a), 112.66 (CH, Diastereomer b), 76.0 (COOCH), 73.0 (OCH), 71.7 (OCH $_2$ Diastereomer a), 71.6 (OCH $_2$ Diastereomer b), 71.2 (OCH $_2$ THF), 68.0 (NHCH), 67.6 (CHOH), 66.9 (OCH $_2$ THF), 49.68 (N- CH_2 Diastereomer a), 49.65 (N- CH_2 Diastereomer b), 37.9 (N- CH_3), 36.2 (C- CH_2), 32.8 (CH_2), 27.4 (CH_2CH_3), 19.6 (CHCH_3), 18.1 (3 x $\text{CH}(\text{CH}_3)_2$), 17.2 (C- CH_3), 12.5 (3 x $\text{CH}(\text{CH}_3)_2$), 8.7 (CH_2CH_3 Diastereomer a), 8.7 (CH_2CH_3 Diastereomer b). HRMS (ESI) exact mass calculated for $\text{C}_{36}\text{H}_{59}\text{N}_2\text{O}_7\text{Si}$ $[\text{M}+\text{H}]^+$ m/z 659.4086, found m/z 659.4090. IR (neat): 3356, 2941, 2866, 1732, 1655, 1250.

(2S,3R)-(S)-Tetrahydrofuran-3-yl 2-((4-(1,5-dimethyl-6-oxo-1,6-dihydropyridin-3-yl)-3-(2-hydroxybutoxy)phenethyl)amino)-3-hydroxybutanoate, 3.90



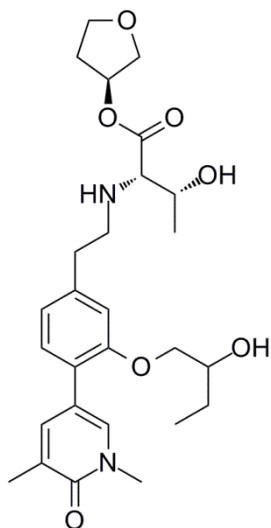
To a solution of (2S,3R)-(S)-tetrahydrofuran-3-yl 2-((4-(1,5-dimethyl-6-oxo-1,6-dihydropyridin-3-yl)-3-(2-((triisopropyl silyl)oxy)butoxy)phenethyl)amino)-3-hydroxy butanoate (162 mg, 0.25 mmol) in tetrahydrofuran (5 mL) stirred under nitrogen at 0 °C was added TBAF (1 M in tetrahydrofuran) (0.37 mL, 0.37 mmol) dropwise. The reaction mixture was stirred at 0 °C for 3 h. Subsequently, the reaction was quenched with dropwise addition of saturated sodium chloride solution (3 mL) and allowed to warm to room temperature. The aqueous layer was then collected and extracted with ethyl acetate (3 x 10 mL). The organic phases

were combined, dried by passing through a hydrophobic frit and the solvent removed under reduced pressure to yield the crude product as a yellow oil. The oil was dissolved in DCM (1 mL) and loaded onto a 10 g SNAP silica column. the crude material on silica was purified by Biotage SP4 using a gradient of 0 - 20% ethanol in ethyl acetate over 20 CV. Appropriate fractions were collected and the solvent removed *in vacuo* and further dried under high vacuum to yield (2S,3R)-(S)-tetrahydrofuran-3-yl 2-((4-(1,5-dimethyl-6-oxo-1,6-dihydropyridin-3-yl)-3-(2-hydroxybutoxy)phenethyl)amino)-3-hydroxybutanoate (95 mg, 0.18 mmol, 73% yield) as a

clear oil. LCMS (high pH): rt = 0.85 min, MH⁺ 503.3. ¹H NMR δ(400 MHz, CDCl₃) ppm: 7.45 (1H, dd, J=2.3, 1.1 Hz), 7.42 - 7.38 (1H, m), 7.16 (1H, d, J=7.6 Hz), 6.85 (1H, dd, J=7.7, 1.3 Hz), 6.79 (1H, d, J=1.2 Hz), 5.37 - 5.32 (1H, m), 4.06 - 3.99 (1H, m), 3.93 - 3.81 (5H, m), 3.77 (1H, d, J=10.5 Hz), 3.67 - 3.57 (4H, m), 3.03 - 2.94 (2H, m), 2.88 - 2.72 (3H, m), 2.26 - 2.17 (4H, m), 2.03 - 1.95 (1H, m), 1.54 - 1.53 (2H, m), 1.21 (3H, d, J=6.1 Hz), 1.01 (3H, t, J=7.5 Hz). ¹³C NMR δ(126 MHz, CDCl₃) ppm: 173.1 (COO), 162.6 (C=O), 155.6 (C-O), 140.3 (C-CH₂), 138.9 (C-CH), 135.1 (N-CH), 129.6 (CH), 128.4 (C-CH₃), 124.6 (C-C), 121.7 (CH), 116.3 (C-C), 113.4 (CH), 75.8 (O-CH), 73.0 (OCH₂), 72.5 (O-CH₂ Diastereomer 1), 72.4 (O-CH₂ Diastereomer 2), 71.5 (CH₂-CHOH), 68.1 (NH-CH-COO), 67.7 (CH₃-CHOH), 66.9 (OCH₂), 49.6 (N-CH₂), 37.9 (N-CH₃), 36.4 (CH₂), 32.8 (C-CH₂), 26.4 (CH₂CH₃), 19.5 (CHCH₃), 17.3 (C-CH₃), 9.9 (CH₂CH₃). IR (neat): 3365, 2929, 1728, 1651. HRMS (ESI) exact mass calculated for C₂₇H₃₉N₂O₇ [M+H]⁺ m/z 503.2752, found m/z 503.2772.

Chiral Separation of **(2S,3R)-(S)-Tetrahydrofuran-3-yl 2-((4-(1,5-dimethyl-6-oxo-1,6-dihydropyridin-3-yl)-3-(2-hydroxybutoxy)phenethyl)amino)-3-hydroxybutanoate, 3.90**

(2S,3R)-(S)-Tetrahydrofuran-3-yl 2-((4-(1,5-dimethyl-6-oxo-1,6-dihydropyridin-3-yl)-3-(2-hydroxybutoxy)phenethyl)amino)-3-hydroxybutanoate (Isomer 1), 3.138

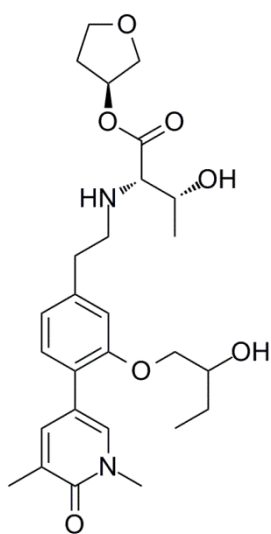


The mixture of diastereoisomers (2S,3R)-(S)-tetrahydrofuran-3-yl 2-((4-(1,5-dimethyl-6-oxo-1,6-dihydropyridin-3-yl)-3-(2-hydroxybutoxy)phenethyl)amino)-3-hydroxybutanoate (130 mg, 0.26 mmol) was separated by chiral HPLC. The HPLC purification was carried out on a Chiralcel OJ-H column (250 x 30 mm, 5 μm packing diameter). The purification was run using 10% ethanol (0.2% v/v isopropylamine) in hexane (0.2% v/v isopropylamine) over 60 min, with a flow rate of 42.5 mL/min. The UV detection was at a wavelength of 280 nm. The first eluting isomer was collected, between 40 and 46 min. Combined

fraction solutions from the first eluting isomer were evaporated to dryness under

reduced pressure to yield (2*S*,3*R*)-(S)-tetrahydrofuran-3-yl 2-((4-(1,5-dimethyl-6-oxo-1,6-dihydropyridin-3-yl)-3-(2-hydroxy butoxy)phenethyl)amino)-3-hydroxybutanoate (Isomer 1) (51 mg, 0.10 mmol) as a clear gum. Chiral HPLC analysis: Chiralcel OJ-H column (250 x 4.6mm) using 10% ethanol (0.2% v/v isopropylamine) in hexane (0.2% v/v isopropylamine) over 60 min, with a flow rate of 1.0 mL/min and a UV detection wavelength of 250 nm: *rt* = 34.27 min, analytical purity >99.5%. LCMS (high pH): *rt* = 0.85 min, *MH*⁺ 503.4. ¹H NMR δ (400 MHz, CDCl₃) ppm: 7.45 (1H, dd, *J*=2.3, 1.1 Hz), 7.39 (1H, d, *J*=2.2 Hz), 7.16 (1H, d, *J*=7.6 Hz), 6.85 (1H, dd, *J*=7.7, 1.3 Hz), 6.79 (1H, d, *J*=1.5 Hz), 5.38 - 5.32 (1H, m), 4.06 - 3.99 (1H, m), 3.94 - 3.81 (5H, m), 3.80 - 3.74 (1H, m), 3.67 - 3.57 (4H, m), 3.03 - 2.95 (2H, m), 2.88 - 2.72 (3H, m), 2.26 - 2.15 (4H, m), 2.03 - 1.95 (1H, m), 1.64 - 1.54 (2H, m), 1.21 (3H, d, *J*=6.1 Hz), 1.01 (3H, t, *J*=7.6 Hz). ¹³C NMR δ (101 MHz, CDCl₃) ppm: 173.4 (COO), 162.6 (C=O), 155.6 (C-O), 140.5 (C-CH₂), 138.8 (C-CH), 135.0 (N-CH), 129.6 (CH), 128.4 (C-CH₃), 124.6 (C-C), 121.7 (CH), 116.3 (C-C), 113.4 (CH), 75.7 (OCH), 73.0 (O-CH₂), 72.5 (O-CH₂), 71.5 (CH-OH), 68.1 (CHNH), 67.8 (CHOH), 66.9 (O-CH₂), 49.6 (NH-CH₂), 37.9 (N-CH₃), 36.6 (C-CH₂), 32.8 (CH₂), 26.4 (CH₂-CH₃), 19.5 (CH-CH₃), 17.2 (C-CH₃), 9.9 (CH₂-CH₃). HRMS (ESI) exact mass calculated for C₂₇H₃₉N₂O₇ [M+H]⁺ *m/z* 503.2752, found *m/z* 503.2748. IR (neat): 3367, 2928, 2874, 1728, 1651. $[\alpha]_D^{24.7^\circ}$ (c 0.5, CDCl₃): -7.5°.

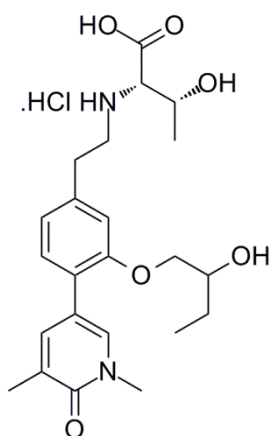
(2*S*,3*R*)-(S)-Tetrahydrofuran-3-yl 2-((4-(1,5-dimethyl-6-oxo-1,6-dihydropyridin-3-yl)-3-(2-hydroxybutoxy)phenethyl)amino)-3-hydroxybutanoate (Isomer 2), 3.139



The mixture of diastereoisomers (2*S*,3*R*)-(S)-tetrahydrofuran-3-yl 2-((4-(1,5-dimethyl-6-oxo-1,6-dihydropyridin-3-yl)-3-(2-hydroxybutoxy)phenethyl)amino)-3-hydroxybutanoate (130 mg, 0.26 mmol) was separated by chiral HPLC. The HPLC purification was carried out on a Chiralcel OJ-H column (250 x 30 mm, 5 μ m packing diameter). The purification was run using 10% ethanol (0.2% v/v isopropylamine) in hexane (0.2% v/v isopropylamine) over 60 min, with a flow rate of 42.5 mL/min. The UV detection was at a wavelength of 280 nm. The second eluting isomer was collected, between 48 and 56 min.

Combined fraction solutions from the second eluting isomer were evaporated to dryness under reduced pressure to yield (2*S*,3*R*)-(S)-tetrahydrofuran-3-yl 2-((4-(1,5-dimethyl-6-oxo-1,6-dihydropyridin-3-yl)-3-(2-hydroxybutoxy)phenethyl)amino)-3-hydroxybutanoate (Isomer 2) (59 mg, 0.12 mmol) as a clear gum. Chiral HPLC analysis: Chiralcel OJ-H column (250 x 4.6mm) using 10% ethanol (0.2% v/v isopropylamine) in hexane (0.2% v/v isopropylamine) over 60 min, with a flow rate of 1.0 mL/min and a UV detection wavelength of 250 nm: *rt* = 38.43 min, analytical purity 96.7%. LCMS (High pH): *rt* = 0.86 min, *MH*⁺ 503.4. ¹H NMR δ (400 MHz, CDCl₃) ppm: 7.45 (1H, dd, *J*=2.2, 1.0 Hz), 7.40 (1H, d, *J*=2.4 Hz), 7.16 (1H, d, *J*=7.6 Hz), 6.85 (1H, dd, *J*=7.7, 1.3 Hz), 6.80 (1H, d, *J*=1.2 Hz), 5.39 - 5.32 (1H, m), 4.06 - 3.99 (1H, m), 3.94 - 3.81 (5H, m), 3.77 (1H, d, *J*=10.8 Hz), 3.68 - 3.57 (4H, m), 3.04 - 2.95 (2H, m), 2.88 - 2.72 (3H, m), 2.27 - 2.15 (4H, m), 2.04 - 1.95 (1H, m), 1.65 - 1.54 (2H, m), 1.21 (3H, d, *J*=6.4 Hz), 1.01 (3H, t, *J*=7.5 Hz). ¹³C NMR δ (101 MHz, CDCl₃) ppm: 173.3 (COO), 162.6 (C=O), 155.6 (C-O), 140.5 (C-CH₂), 138.9 (C-CH), 135.0 (N-CH), 129.6 (CH), 128.4 (C-CH₃), 124.6 (C-C), 121.7 (CH), 116.3 (C-C), 113.4 (CH), 75.7 (C-O), 73.0 (O-CH₂), 72.5 (O-CH₂), 71.5 (CHOH), 68.1 (CHNH), 67.8 (CHOH), 66.9 (OCH₂), 49.6 (NHCH₂), 37.9 (N-CH₃), 36.6 (C-CH₂), 32.8 (CH₂), 26.4 (CH₂CH₃), 19.4 (CHCH₃), 17.2 (C-CH₃), 9.8 (CH₂CH₃). HRMS (ESI) exact mass calculated for C₂₇H₃₉N₂O₇ [*M*+*H*]⁺ *m/z* 503.2752, found *m/z* 503.2737. IR (neat): 3351, 2927, 2874, 1728, 1651. [α _D]^{24.8°C}_λ(c 0.5, CDCl₃): -25.5°.

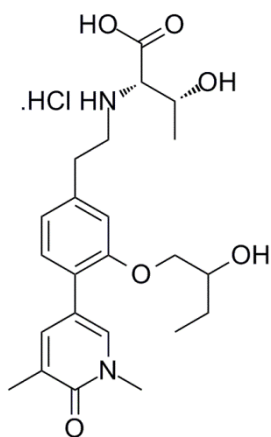
(2*S*,3*R*)-2-((4-(1,5-Dimethyl-6-oxo-1,6-dihydropyridin-3-yl)-3-(2-hydroxybutoxy)phenethyl)amino)-3-hydroxybutanoic acid, hydrochloride (Isomer 1), 3.140



A solution of (2*S*,3*R*)-(S)-tetrahydrofuran-3-yl 2-((4-(1,5-dimethyl-6-oxo-1,6-dihydropyridin-3-yl)-3-(2-hydroxybutoxy)phenethyl)amino)-3-hydroxybutanoate (Isomer 1) (25 mg, 0.050 mmol) in dimethyl sulfoxide (0.25 mL) was added to a solution of pig liver esterase (lyophilized solid) (10 mg), in phosphate buffer solution pH 7.2 (0.5 mL). The mixture was stirred at room temperature for 4 days. Methanol was added, whereupon a thick suspension occurred. The solid was removed by filtration and the resulting solution blown down under a stream of nitrogen. Methanol was added to make the solution up to 1 mL and purified by mass directed autoprep on Xbridge column using 5 – 30%

acetonitrile water with an ammonium carbonate modifier. The solvent was evaporated *in vacuo* and further dried in a vacuum oven for 1 week. To the resulting white solid was added water (0.5 mL) and 2 M aqueous HCl added dropwise. The solvent was evaporated under a stream of nitrogen to yield the desired compound (2*S*,3*R*)-2-((4-(1,5-dimethyl-6-oxo-1,6-dihydropyridin-3-yl)-3-(2-hydroxybutoxy)phenethyl)amino)-3-hydroxybutanoic acid, hydrochloride (Isomer 1) (8.5 mg, 0.018 mmol, 36% yield) as a white solid. LCMS (high pH): *rt* = 0.56 min, *MH*⁺ 433.4. ¹H NMR δ (400 MHz, DMSO-*d*₆) ppm: 9.02 (1H, br. s.), 8.97 (1H, br. s.), 7.81 (1H, d, *J*=2.2 Hz), 7.59 (1H, dd, *J*=2.4, 1.0 Hz), 7.27 (1H, d, *J*=7.6 Hz), 6.95 (1H, d, *J*=1.2 Hz), 6.85 (1H, dd, *J*=7.8, 1.2 Hz), 4.14 (1H, quin, *J*=6.2 Hz), 3.91 (2H, d, *J*=5.1 Hz), 3.88 - 3.83 (1H, m), 3.74 - 3.66 (1H, m), 3.48 (3H, s), 3.33 - 3.13 (2H, m), 3.11 - 2.92 (2H, m), 2.04 (3H, s), 1.63 - 1.50 (1H, m), 1.49 - 1.36 (1H, m), 1.29 (3H, d, *J*=6.4 Hz), 0.91 (3H, t, *J*=7.5 Hz).

(2*S*,3*R*)-2-((4-(1,5-Dimethyl-6-oxo-1,6-dihydropyridin-3-yl)-3-(2-hydroxybutoxy)phenethyl)amino)-3-hydroxybutanoic acid (Isomer 2), 3.141



A solution of (2*S*,3*R*)-(S)-tetrahydrofuran-3-yl 2-((4-(1,5-dimethyl-6-oxo-1,6-dihydropyridin-3-yl)-3-(2-hydroxybutoxy)phenethyl)amino)-3-hydroxybutanoate (25 mg, 0.050 mmol) in dimethyl sulfoxide (0.25 mL) was added to a solution of pig liver esterase (lyophilized solid) (10 mg), in phosphate buffer solution pH 7.2 (0.5 mL). The mixture was stirred at room temperature for 4 days. Methanol was added, whereupon a thick suspension occurred. The solid was removed by filtration and the resulting solution blown down under a stream of nitrogen. Methanol was added to make the solution up to 1 mL, and the sample was purified by mass directed autoprep on Xbridge column using 5 – 30% acetonitrile water with an ammonium carbonate modifier. The solvent was evaporated *in vacuo* and further dried in a vacuum oven for 1 week. To the resulting white solid was added water (0.5 mL) and 2 M aqueous HCl added dropwise. The solvent was evaporated under a stream of nitrogen but the salt was not observed. The desired compound was isolated as the free base (2*S*,3*R*)-2-((4-(1,5-dimethyl-6-oxo-1,6-dihydropyridin-3-yl)-3-(2-hydroxybutoxy)phenethyl)amino)-3-hydroxybutanoic acid (Isomer 2) (11.8 mg, 0.027 mmol, 55% yield) as a white solid. LCMS

GSK Confidential Information – Do not copy

(high pH): rt = 0.56 min, MH+ 433.4. ^1H NMR δ (400 MHz, DMSO- d_6) ppm: 9.14 (1H, br. s.), 7.82 (1H, d, $J=2.2$ Hz), 7.59 (1H, dd, $J=2.4, 1.0$ Hz), 7.26 (1H, d, $J=7.8$ Hz), 6.95 (1H, d, $J=1.2$ Hz), 6.85 (1H, dd, $J=7.7, 1.3$ Hz), 4.83 (1H, br. s.), 4.11 (1H, quin, $J=6.2$ Hz), 3.97 - 3.85 (2H, m), 3.77 (1H, d, $J=5.6$ Hz), 3.74 - 3.64 (1H, m), 3.48 (3H, s), 3.32 - 3.13 (2H, m), 3.10 - 2.91 (2H, m), 2.04 (3H, s), 1.63 - 1.49 (1H, m), 1.49 - 1.35 (1H, m), 1.28 (3H, d, $J=6.6$ Hz), 0.91 (3H, t, $J=7.5$ Hz).

6 References

- (1) Alberts, B.; Johnson, A.; Lewis, J.; Raff, M.; Roberts, K.; Walter, P. *Molecular Biology of the Cell*, 4th Ed.; Garland Science: New York, 2002.
- (2) Mendel, G. *Verhandlungen des naturforschenden Vereines Brünn* **1866**, IV, 3.
- (3) Mendel, G. *J. R. Hortic. Soc.* **1901**, 26, 1.
- (4) Watson, J. D.; Crick, F. H. C. *Nature* **1953**, 171 (4356), 737.
- (5) International Human Genome Sequencing Consortium. *Nature* **2004**, 431 (7011), 931.
- (6) Campbell, N. A.; Reece, J. A. *Biology*, 6th Ed.; Benjamin Cummings: San Francisco, 2002.
- (7) Annunziato, A. *Nat. Educ.* **2008**, 1 (1), 26.
- (8) Wray, J.; Kalkan, T.; Smith, A. G. *Biochem. Soc. Trans.* **2010**, 38 (4), 1027.
- (9) Bigstock: Stem Cells. <http://www.bigstockphoto.com/image-5525840/stock-photo-stem-cells> (accessed Feb 29, 2016).
- (10) Eccleston, A.; DeWitt, N.; Gunter, C.; Marte, B.; Nath, D. *Nature* **2007**, 447 (7143), 395.
- (11) Furusawa, C.; Kaneko, K. *PLoS One* **2013**, 8 (5), e61251.
- (12) Wittkopp, P. J. *PLoS Biol.* **2010**, 8 (3), e1000342.
- (13) Illingworth, R. S.; Bird, A. P. *FEBS Lett.* **2009**, 583 (11), 1713.
- (14) Bird, A. *Gene Dev.* **2002**, 16 (1), 6.
- (15) Fraga, M. F.; Ballestar, E.; Paz, M. F.; Ropero, S.; Setien, F.; Ballestar, M. L.; Heine-Suñer, D.; Cigudosa, J. C.; Urioste, M.; Benitez, J.; Boix-Chornet, M.; Sanchez-Aguilera, A.; Ling, C.; Carlsson, E.; Poulsen, P.; Vaag, A.; Stephan, Z.; Spector, T. D.; Wu, Y.-Z.; Plass, C.; Esteller, M. *P. Natl. Acad. Sci. USA* **2005**, 102 (30), 10604.
- (16) Jarmalaite, S.; Kannio, A.; Anttila, S.; Lazutka, J. R.; Husgafvel-Pursiainen, K. *Int. J. Cancer* **2003**, 106 (6), 913.
- (17) von Zeidler, S. V.; Miracca, E. C.; Nagai, M. A.; Birman, E. G. *Int. J. Mol. Med.* **2004**, 14 (5), 807.
- (18) Lee, K. W. K.; Pausova, Z. *Front. Genet.* **2013**, 4, 1.
- (19) Slotkin, R. K.; Martienssen, R. *Nat. Rev. Genet.* **2007**, 8 (4), 272.
- (20) Tohgi, H.; Utsugisawa, K.; Nagane, Y.; Yoshimura, M.; Genda, Y.; Ukitsu, M. *Mol. Brain Res.* **1999**, 70 (2), 288.
- (21) Lund, G.; Andersson, L.; Lauria, M.; Lindholm, M.; Fraga, M. F.; Villar-Garea, A.; Ballestar, E.; Esteller, M.; Zaina, S. *J. Biol. Chem.* **2004**, 279 (28), 29147.
- (22) Gowers, I. R.; Walters, K.; Kiss-Toth, E.; Read, R. C.; Duff, G. W.; Wilson, A. G. *Cytokine* **2011**, 56 (3), 792.
- (23) Dayeh, T.; Volkov, P.; Salö, S.; Hall, E.; Nilsson, E.; Olsson, A. H.; Kirkpatrick, C. L.; Wollheim, C. B.; Eliasson, L.; Rönn, T.; Bacos, K.; Ling, C.

- PLoS Genet.* **2014**, *10* (3), e1004160.
- (24) Ballestar, E.; Esteller, M.; Richardson, B. C. *J. Immunol.* **2006**, *176* (12), 7143.
- (25) Roach, H. I.; Aigner, T. *Osteoarthr. Cartil.* **2007**, *15* (2), 128.
- (26) Davey, C. A.; Sargent, D. F.; Luger, K.; Maeder, A. W.; Richmond, T. J. *J. Mol. Biol.* **2002**, *319* (5), 1097.
- (27) Phillips, D. M. P. *Proc. Biochem. Soc.* **1961**, *80* (3), 40.
- (28) Allfrey, V. G.; Faulkner, R.; Mirsky, A. E. *Proc. Natl. Acad. Sci. U S A.* **1964**, *51* (5), 786.
- (29) Rossetto, D.; Avvakumov, N.; Côté, J. *Epigenetics* **2012**, *7* (10), 1098.
- (30) Cao, J.; Yan, Q. *Front. Oncol.* **2012**, *2* (26), 1.
- (31) Shiio, Y.; Eisenman, R. N. *Proc. Natl. Acad. Sci. U. S. A.* **2003**, *100* (23), 13225.
- (32) Fukuda, H.; Sano, N.; Muto, S.; Horikoshi, M. *Brief. Funct. Genomic. Proteomic.* **2006**, *5* (3), 190.
- (33) Rothbart, S. B.; Strahl, B. D. *Biochim. Biophys. Acta - Gene Regul. Mech.* **2014**, *1839* (8), 627.
- (34) Turner, B. M. *Nat. Struct. Mol. Biol.* **2005**, *12* (2), 110.
- (35) Shi, Y.; Whetstine, J. R. *Mol. Cell* **2007**, *25* (1), 1.
- (36) Grunstein, M. *Nature* **1997**, *389* (6649), 349.
- (37) Strahl, B. D.; Allis, C. D. *Nature* **2000**, *403* (6765), 41.
- (38) Dhanak, D. *ACS Med. Chem. Lett.* **2012**, *3* (7), 521.
- (39) Mukherjee, K.; Fischer, R.; Vilcinskas, A. *Front. Zool.* **2012**, *9* (1), 25.
- (40) Brown, J. A. *External Presentation, RICT, Nice, France: The Discovery of Small Molecule Inhibitors of Jumonji Enzymes: Probing the Epigenome*; 2013.
- (41) Lau, O. D.; Kundu, T. K.; Soccio, R. E.; Ait-Si-Ali, S.; Khalil, E. M.; Vassilev, A.; Wolffe, A. P.; Nakatani, Y.; Roeder, R. G.; Cole, P. A. *Mol. Cell* **2000**, *5* (3), 589.
- (42) Gajer, J. M.; Furdas, S. D.; Gründer, A.; Gothwal, M.; Heinicke, U.; Keller, K.; Colland, F.; Fulda, S.; Pahl, H. L.; Fichtner, I.; Sippl, W.; Jung, M. *Oncogenesis* **2015**, *4* (2), e137.
- (43) Furdas, S. D.; Kannan, S.; Sippl, W.; Jung, M. *Arch. Pharm. (Weinheim)*. **2012**, *345* (1), 7.
- (44) FDA EPC Text Phrases for Highlights Indications and Usage <http://www.fda.gov/downloads/drugs/guidancecomplianceregulatoryinformation/lawsactsandrules/ucm428333.pdf> (accessed Jun 27, 2015).
- (45) Lauffer, B. E. L.; Mintzer, R.; Fong, R.; Mukund, S.; Tam, C.; Zilberleyb, I.; Flicke, B.; Ritscher, A.; Fedorowicz, G.; Vallero, R.; Ortwine, D. F.; Gunzner, J.; Modrusan, Z.; Neumann, L.; Koth, C. M.; Lupardus, P. J.; Kaminker, J. S.; Heise, C. E.; Steiner, P. *J. Biol. Chem.* **2013**, *288* (37), 26926.

- (46) Rangwala, S.; Zhang, C.; Duvic, M. *Future Med. Chem.* **2012**, *4* (4), 471.
- (47) Marks, P. A. *Oncogene* **2007**, *26* (9), 1351.
- (48) Vandermolen, K. M.; McCulloch, W.; Pearce, C. J.; Oberlies, N. H. *J. Antibiot.* **2011**, *64* (8), 525.
- (49) Ueda, H.; Nakajima, H.; Hori, Y.; Fujita, T.; Nishimura, M.; Goto, T.; Okuhara, M. *J. Antibiot. (Tokyo)*. **1994**, *47* (3), 301.
- (50) Furumai, R.; Matsuyama, A.; Kobashi, N.; Lee, K. H.; Nishiyama, M.; Nakajima, H.; Tanaka, A.; Komatsu, Y.; Nishino, N.; Yoshida, M.; Horinouchi, S. *Cancer Res.* **2002**, *62* (17), 4916.
- (51) Lee, H.-Z.; Kwitkowski, V. E.; Del Valle, P. L.; Ricci, M. S.; Saber, H.; Habtemariam, B. A.; Bullock, J.; Bloomquist, E.; Shen, Y. L.; Chen, X.-H.; Brown, J.; Mehrotra, N.; Dorff, S.; Charlab, R.; Kane, R. C.; Kaminskas, E.; Justice, R.; Farrell, A. T.; Pazdur, R. *Clin. Cancer Res.* **2015**, *21* (12), 2666.
- (52) Poole, R. M. *Drugs* **2014**, *74* (13), 1543.
- (53) Foss, F. M.; Zinzani, P. L.; Vose, J. M.; Gascoyne, R. D.; Rosen, S. T.; Tobinai, K. *Blood* **2011**, *117* (25), 6756.
- (54) Garnock-Jones, K. P. *Drugs* **2015**, *75* (6), 695.
- (55) FDA website. Available: Accelerated Approval Program (2013). <http://www.fda.gov/Drugs/ResourcesForYou/HealthProfessionals/ucm313768.htm> (accessed Jul 9, 2015).
- (56) Falkenberg, K. J.; Johnstone, R. W. *Nat. Rev. Drug Discov.* **2014**, *13* (9), 673.
- (57) Tamkun, J. W.; Deuring, R.; Scott, M. P.; Kissinger, M.; Pattatucci, A. M.; Kaufman, T. C.; Kennison, J. A. *Cell* **1992**, *68* (3), 561.
- (58) Filippakopoulos, P.; Knapp, S. *Nat. Rev. Drug Discov.* **2014**, *13* (5), 337.
- (59) Jones, M. H.; Numata, M.; Shimane, M. *Genomics* **1997**, *45* (3), 529.
- (60) Paillisson, A.; Levasseur, A.; Gouret, P.; Callebaut, I.; Bontoux, M.; Pontarotti, P.; Monget, P. *Genomics* **2007**, *89* (2), 215.
- (61) Wu, S. Y.; Chiang, C. M. *J. Biol. Chem.* **2007**, *282* (18), 13141.
- (62) Rahman, S.; Sowa, M. E.; Ottinger, M.; Smith, J. A.; Shi, Y.; Harper, J. W.; Howley, P. M. *Mol. Cell. Biol.* **2011**, *31* (13), 2641.
- (63) Filippakopoulos, P.; Picaud, S.; Mangos, M.; Keates, T.; Lambert, J. P.; Baryste-Lovejoy, D.; Felletar, I.; Volkmer, R.; Müller, S.; Pawson, T.; Gingras, A. C.; Arrowsmith, C. H.; Knapp, S. *Cell* **2012**, *149* (1), 214.
- (64) Shi, J.; Vakoc, C. R. *Mol. Cell* **2014**, *54* (5), 728.
- (65) Moon, K. J.; Mochizuki, K.; Zhou, M.; Jeong, H. S.; Brady, J. N.; Ozato, K. *Mol. Cell* **2005**, *19* (4), 523.
- (66) LeRoy, G.; Rickards, B.; Flint, S. J. *Mol. Cell* **2008**, *30* (1), 51.
- (67) Vidler, L. R.; Brown, N.; Knapp, S.; Hoelder, S. *J. Med. Chem.* **2012**, *55* (17), 7346.
- (68) Adachi, K.; Endoh, J.-I.; Fujie, N.; Hamada, M.; Hikawa, H.; Ishibuchi, S.;

- Murata, M.; Oshita, K.; Sugahara, K.; Tanaka, M. Thienotriazolodiazepine compound and a medicinal use thereof PCT/JP2006/310709 (WO/2006/129623), 2006.
- (69) Miyoshi, S.; Ooike, S.; Iwata, K.; Hikawa, H.; Sugahara, K. Antitumor Agent PCT/JP2008/073864 (WO/2009/084693), 2009.
- (70) Filippakopoulos, P.; Qi, J.; Picaud, S.; Shen, Y.; Smith, W. B.; Fedorov, O.; Morse, E. M.; Keates, T.; Hickman, T. T.; Felletar, I.; Philpott, M.; Munro, S.; McKeown, M. R.; Wang, Y.; Christie, A. L.; West, N.; Cameron, M. J.; Schwartz, B.; Heightman, T. D.; La Thangue, N.; French, C. A.; Wiest, O.; Kung, A. L.; Knapp, S.; Bradner, J. E. *Nature* **2010**, *468* (7327), 1067.
- (71) Bauer, D. E.; Mitchell, C. M.; Strait, K. M.; Lathan, C. S.; Stelow, E. B.; Lüer, S. C.; Muhammed, S.; Evans, A. G.; Sholl, L. M.; Rosai, J.; Giraldi, E.; Oakley, R. P.; Rodriguez-Galindo, C.; London, W. B.; Sallan, S. E.; Bradner, J. E.; French, C. A. *Clin. Cancer Res.* **2012**, *18* (20), 5773.
- (72) French, C. A. *Annu. Rev. Pathol. Mech. Dis.* **2012**, *7* (1), 247.
- (73) French, C. A.; Ramirez, C. L.; Kolmakova, J.; Hickman, T. T.; Cameron, M. J.; Thyne, M. E.; Kutok, J. L.; Toretsky, J. A.; Tadavarthy, A. K.; Kees, U. R.; Fletcher, J. A.; Aster, J. C. *Oncogene* **2008**, *27* (15), 2237.
- (74) Nicodeme, E.; Jeffrey, K. L.; Schaefer, U.; Beinke, S.; Dewell, S.; Chung, C.-W.; Chandwani, R.; Marazzi, I.; Wilson, P.; Coste, H.; White, J.; Kirilovsky, J.; Rice, C. M.; Lora, J. M.; Prinjha, R. K.; Lee, K.; Tarakhovsky, A. *Nature* **2010**, *468* (7327), 1119.
- (75) Chen, P.; Daugan, A. C.-M.; Gosmini, R. L. M.; Igo, D.; Katrincic, L.; Martres, P.; Nicodemien, E.; Patience, D. Compounds Which Increase Apolipoprotein A-1 Production And Uses Thereof In Medicine PCT/EP2005/010177 (WO 2006/032470 A1), 2006.
- (76) Seal, J. *Internal Presentation, GSK, Stevenage, UK: Bromodomain Introduction*; 2010.
- (77) GlaxoSmithKline. A Study to Investigate the Safety, Pharmacokinetics, Pharmacodynamics, and Clinical Activity of GSK525762 in Subjects With NUT Midline Carcinoma (NMC) and Other Cancers. In: ClinicalTrials.gov [Internet]. Bethesda (MD): National Library of Medicine (US). 2000- [cited 2014 Jul 01]. Available from: <http://clinicaltrials.gov/show/NCT01587703>. NLM Identifier: NCT01587703.
- (78) Zhang, G.; Liu, R.; Zhong, Y.; Plotnikov, A. N.; Zhang, W.; Zeng, L.; Rusinova, E.; Gerona-Nevarro, G.; Moshkina, N.; Joshua, J.; Chuang, P. Y.; Ohlmeyer, M.; He, J. C.; Zhou, M. M. *J. Biol. Chem.* **2012**, *287* (34), 28840.
- (79) Ceribelli, M.; Kelly, P. N.; Shaffer, A. L.; Wright, G. W.; Xiao, W.; Yang, Y.; Mathews Griner, L. A.; Guha, R.; Shinn, P.; Keller, J. M.; Liu, D.; Patel, P. R.; Ferrer, M.; Joshi, S.; Nerle, S.; Sandy, P.; Normant, E.; Thomas, C. J.; Staudt, L. M. *Proc. Natl. Acad. Sci. U. S. A.* **2014**, *111* (31), 11365.
- (80) Wong, C.; Laddha, S. V; Tang, L.; Vosburgh, E.; Levine, A. J.; Normant, E.; Sandy, P.; Harris, C. R.; Chan, C. S.; Xu, E. Y. *Cell Death Dis.* **2014**, *5* (10), e1450.
- (81) Moros, A.; Rodríguez, V.; Saborit-Villarroya, I.; Montraveta, A.; Balsas, P.;

- Sandy, P.; Martínez, A.; Wiestner, A.; Normant, E.; Campo, E.; Pérez-Galán, P.; Colomer, D.; Roué, G. *Leukemia* **2014**, *28* (10), 2049.
- (82) Gehling, V. S.; Hewitt, M. C.; Vaswani, R. G.; Leblanc, Y.; Coité, A.; Nasveschuk, C. G.; Taylor, A. M.; Harmange, J. C.; Audia, J. E.; Pardo, E.; Joshi, S.; Sandy, P.; Mertz, J. A.; Sims, R. J.; Bergeron, L.; Bryant, B. M.; Bellon, S.; Poy, F.; Jayaram, H.; Sankaranarayanan, R.; Yellapantula, S.; Bangalore Srinivasamurthy, N.; Birudukota, S.; Albrecht, B. K. *ACS Med. Chem. Lett.* **2013**, *4* (9), 835.
- (83) Hewitt, M. C.; Leblanc, Y.; Gehling, V. S.; Vaswani, R. G.; Côté, A.; Nasveschuk, C. G.; Taylor, A. M.; Harmange, J.-C.; Audia, J. E.; Pardo, E.; Cummings, R.; Joshi, S.; Sandy, P.; Mertz, J. A.; Sims, R. J.; Bergeron, L.; Bryant, B. M.; Bellon, S.; Poy, F.; Jayaran, H.; Tang, Y.; Albrecht, B. K. *Bioorg. Med. Chem. Lett.* **2015**, *25*, 1842.
- (84) Brand, M.; Measures, A. M.; Wilson, B. G.; Cortopassi, W. A.; Alexander, R.; Höss, M.; Hewings, D. S.; Rooney, T. P. C.; Paton, R. S.; Conway, S. J. *ACS Chem. Biol.* **2015**, *10* (1), 22.
- (85) Hewings, D. S.; Wang, M.; Philpott, M.; Fedorov, O.; Uttarkar, S.; Filippakopoulos, P.; Picaud, S.; Vuppusetty, C.; Marsden, B.; Knapp, S.; Conway, S. J.; Heightman, T. D. *J. Med. Chem.* **2011**, *54* (19), 6761.
- (86) Bamborough, P.; Diallo, H.; Goodacre, J. D.; Gordon, L.; Lewis, A.; Seal, J. T.; Wilson, D. M.; Woodrow, M. D.; Chung, C.-W. *J. Med. Chem.* **2012**, *55* (2), 587.
- (87) Seal, J.; Lamotte, Y.; Donche, F.; Bouillot, A.; Mirguet, O.; Gellibert, F.; Nicodeme, E.; Krysa, G.; Kirilovsky, J.; Beinke, S.; McCleary, S.; Rioja, I.; Bamborough, P.; Chung, C.-W.; Gordon, L.; Lewis, T.; Walker, A. L.; Cutler, L.; Lugo, D.; Wilson, D. M.; Witherington, J.; Lee, K.; Prinjha, R. K. *Bioorg. Med. Chem. Lett.* **2012**, *22* (8), 2968.
- (88) Ran, X.; Zhao, Y.; Liu, L.; Bai, L.; Yang, C.-Y.; Zhou, B.; Meagher, J. L.; Chinnaswamy, K.; Stuckey, J. A.; Wang, S. *J. Med. Chem.* **2015**, *58* (12), 4927.
- (89) Chung, C.-W.; Dean, A. W.; Woolven, J. M.; Bamborough, P. *J. Med. Chem.* **2012**, *55* (2), 576.
- (90) Fish, P.; Filippakopoulos, P.; Bish, G.; Brennan, P.; Bunnage, M. E.; Cook, A.; Fedorov, O.; Gerstenberger, B. S.; Jones, H.; Knapp, S.; Marsden, B.; Nocka, K.; Owen, D. R.; Picaud, S.; Primiano, M.; Ralph, M.; Sciammetta, N.; Trzupsek, J. *J. Med. Chem.* **2012**, *55* (22), 9831.
- (91) Zhao, L.; Cao, D.; Chen, T.; Wang, Y.; Miao, Z.; Xu, Y.; Chen, W.; Wang, X.; Li, Y.; Du, Z.; Xiong, B.; Li, J.; Xu, C.; Zhang, N.; He, J.; Shen, J. *J. Med. Chem.* **2013**, *56* (10), 3833.
- (92) Borah, J. C.; Mujtaba, S.; Karakikes, I.; Zeng, L.; Muller, M.; Patel, J.; Moshkina, N.; Morohashi, K.; Zhang, W.; Gerona-Navarro, G.; Hajjar, R. J.; Zhou, M. M. *Chem. Biol.* **2011**, *18* (4), 531.
- (93) Zhang, G.; Plotnikov, A. N.; Rusinova, E.; Shen, T.; Morohashi, K.; Joshua, J.; Zeng, L.; Mujtaba, S.; Ohlmeyer, M.; Zhou, M. M. *J. Med. Chem.* **2013**, *56* (22), 9251.

- (94) Gosmini, R.; Nguyen, V. L.; Toum, J.; Simon, C.; Brusq, J.-M. G.; Krysa, G.; Mirguet, O.; Riou-Eymard, A. M.; Boursier, E. V.; Trottet, L.; Bamborough, P.; Clark, H.; Chung, C.; Cutler, L.; Demont, E. H.; Kaur, R.; Lewis, A. J.; Schilling, M. B.; Soden, P. E.; Taylor, S.; Walker, A. L.; Walker, M. D.; Prinjha, R. K.; Nicodème, E. *J. Med. Chem.* **2014**, *57* (19), 8111.
- (95) Garnier, J.-M.; Sharp, P. P.; Burns, C. J. *Expert Opin. Ther. Pat.* **2014**, *24* (2), 185.
- (96) Picaud, S.; Wells, C.; Felletar, I.; Brotherton, D.; Martin, S.; Savitsky, P.; Diez-Dacal, B.; Philpott, M.; Bountra, C.; Lingard, H.; Fedorov, O.; Müller, S.; Brennan, P. E.; Knapp, S.; Filippakopoulos, P. *P. Natl. Acad. Sci. USA* **2013**, *110* (49), 19754.
- (97) McLure, K. G.; Gesner, E. M.; Tsujikawa, L.; Kharenko, O. A.; Attwell, S.; Campeau, E.; Wasiaak, S.; Stein, A.; White, A.; Fontano, E.; Suto, R. K.; Wong, N. C. W.; Wagner, G. S.; Hansen, H. C.; Young, P. R. *PLoS One* **2013**, *8* (12), e83190.
- (98) Nicholls, S. J.; Gordon, A.; Johansson, J.; Wolski, K.; Ballantyne, C. M.; Kastelein, J. J. P.; Taylor, A.; Borgman, M.; Nissen, S. E. *J. Am. Coll. Cardiol.* **2011**, *57* (9), 1111.
- (99) Nicholls, S. J.; Gordon, A.; Johansson, J.; Ballantyne, C. M.; Barter, P. J.; Brewer, H. B.; Kastelein, J. J. P.; Wong, N. C.; Borgman, M. R. N.; Nissen, S. E. *Cardiovasc. Drugs Ther.* **2012**, *26* (2), 181.
- (100) Resverlogix Corp. The Effects of RVX000222 on Glucose Metabolism in Individuals With Pre-diabetes. In: ClinicalTrials.gov [Internet]. Bethesda (MD): National Library of Medicine (US). 2000- [cited 2014 Jul 01]. Available from: <http://clinicaltrials.gov/show/NCT01728467>. NLM Identifier: NCT01728467.
- (101) Resverlogix Corp. Clinical Trial for Dose Finding and Safety of RVX000222 in Subjects With Stable Coronary Artery Disease. In: ClinicalTrials.gov [Internet]. Bethesda (MD): National Library of Medicine (US). 2000- [cited 2015 Jun 29]. Available from: <http://clinicaltrials.gov/show/NCT01058018>. NLM Identifier: NCT01058018.
- (102) Oncoethix GmbH. A Phase I, Dose-finding Study of the Bromodomain (Brd) Inhibitor OTX015 in Haematological Malignancies. In: ClinicalTrials.gov [Internet]. Bethesda (MD): National Library of Medicine (US). 2000- [cited 2014 Jul 01]. Available from: <http://clinicaltrials.gov/show/NCT01713582>. NLM Identifier: NCT01713582.
- (103) Albrecht, B. K.; Gehling, V. S.; Hewitt, M. C.; Vaswani, R. G.; Cote, A.; Leblanc, Y.; Nasveschuk, C. G.; Bellon, S.; Bergeron, L.; Campbell, R.; Cantone, N.; Cooper, M. R.; Cummings, R. T.; Jayaram, H.; Joshi, S.; Mertz, J. A.; Neiss, A.; Normant, E.; O'Meara, M.; Pardo, E.; Poy, F.; Sandy, P.; Supko, J.; Sims, R. J.; Harmange, J.-C.; Taylor, A. M.; Audia, J. E. *J. Med. Chem.* **2016**, *59* (4), acs.jmedchem.5b01882.
- (104) Constellation Pharmaceuticals. A Phase 1 Study Evaluating CPI-0610 in Patients With Progressive Lymphoma. In: ClinicalTrials.gov [Internet]. Bethesda (MD): National Library of Medicine (US). 2000- [cited 2014 Jul 01]. Available from: <http://clinicaltrials.gov/show/NCT01949883>. NLM Identifier: NCT01949883.
- (105) Tensha Therapeutics. A Two Part, Multicenter, Open-label Study of TEN-010

- Given Subcutaneously. In: ClinicalTrials.gov [Internet]. Bethesda (MD): National Library of Medicine (US). 2000- [cited 2014 Jul 01]. Available from: <http://clinicaltrials.gov/show/NCT01987362>. NLM Identifier: NCT01987362.
- (106) Bayer. BAY1238097, First in Man. In: ClinicalTrials.gov [Internet]. Bethesda (MD): National Library of Medicine (US). 2000- [cited 2015 Jul 04]. Available from: <http://clinicaltrials.gov/show/NCT02369029>. NLM Identifier: NCT02369029.
- (107) Incyte Corporation. An Open-Label, Dose-Escalation Study of INCB054329 in Patients With Advanced Malignancies. In: ClinicalTrials.gov [Internet]. Bethesda (MD): National Library of Medicine (US). 2000- [cited 2015 Sep 15]. Available from: <http://clinicaltrials.gov/show/NCT02431260>. NLM Identifier: NCT02431260.
- (108) Gilead Sciences. Safety, Tolerability, Pharmacokinetics, and Pharmacodynamics of GS-5829 in Adults With Advanced Solid Tumors and Lymphomas. In: ClinicalTrials.gov [Internet]. Bethesda (MD): National Library of Medicine (US). 2000- [cited 2015 Sep 15]. Available from: <http://clinicaltrials.gov/show/NCT02392611>. NLM Identifier: NCT02392611.
- (109) Houzelstein, D.; Bullock, S. L.; Lynch, D. E.; Grigorieva, E. F.; Wilson, V. A.; Beddington, R. S. P. *Mol. Cell. Biol.* **2002**, 22 (11), 3794.
- (110) Bolden, J. E.; Tasdemir, N.; Clevers, H.; Lowe, S. W.; Bolden, J. E.; Tasdemir, N.; Dow, L. E.; Es, J. H. Van; Wilkinson, J. E.; Zhao, Z. *Cell Rep.* **2014**, 8 (6), 1919.
- (111) Strebhardt, K.; Ullrich, A. *Nat. Rev. Cancer* **2008**, 8 (6), 473.
- (112) Muller, P. Y.; Milton, M. N. *Nat. Rev. Drug Discov.* **2012**, 11 (10), 751.
- (113) Clark, M. A.; Finkel, R.; Ray, J. A.; Whalen, K. *Lippincott's Illustrated Reviews: Pharmacology*, 5th Ed.; Lippincott Williams & Wilkins: Baltimore, 2012.
- (114) De Jong, W. H.; Borm, P. J. A. *Int. J. Nanomedicine* **2008**, 3 (2), 133.
- (115) Allen, T. M.; Cullis, P. R. *Adv. Drug Deliv. Rev.* **2013**, 65 (1), 36.
- (116) Chames, P.; Van Regenmortel, M.; Weiss, E.; Baty, D. *Br. J. Pharmacol.* **2009**, 157 (2), 220.
- (117) Clas, S.-D.; Sanchez, R. I.; Nofsinger, R. *Drug Discov. Today* **2014**, 19 (1), 79.
- (118) Nishida, N.; Yano, H.; Nishida, T.; Kamura, T.; Kojiro, M. *Vasc. Heal. Risk Manag.* **2006**, 2 (3), 213.
- (119) McDonald, D. M.; Baluk, P. *Cancer Res.* **2002**, 62, 5381.
- (120) Cho, K. J.; Moon, H. T.; Park, G.-E.; Jeon, O. C.; Byun, Y.; Lee, Y.-K. *Bioconjug. Chem.* **2008**, 19 (7), 1346.
- (121) Parveen, S.; Misra, R.; Sahoo, S. K. *Nanomedicine NBM* **2012**, 8 (2), 147.
- (122) Hilmer, S. N. *Drug Metab. Dispos.* **2004**, 32 (8), 794.
- (123) Bodley, A.; Liu, L. F.; Israel, M.; Seshadri, R.; Koseki, Y.; Giuliani, F.; Kirschenbaum, S.; Silber, R.; Potmesil, M. *Cancer Res.* **1989**, 49, 5969.

- (124) Gabizon, A.; Catane, R.; Uziely, B.; Kaufman, B.; Safra, T.; Cohen, R.; Martin, F.; Huang, A.; Barenholz, Y. *Cancer Res.* **1994**, *54*, 987.
- (125) Gullotti, E.; Yeo, Y. *Mol. Pharm.* **2009**, *6* (4), 1041.
- (126) Gabizon, A. A. *Cancer Invest.* **2001**, *19* (4), 424.
- (127) Iwanaga, K.; Ono, S.; Narioka, K.; Morimoto, K.; Kakemi, M.; Yamashita, S.; Nango, M.; Oku, N. *Int. J. Pharm.* **1997**, *157* (1), 73.
- (128) Barenholz, Y. *J. Control. Release* **2012**, *160* (2), 117.
- (129) Sawant, R. R.; Torchilin, V. P. *AAPS J.* **2012**, *14* (2), 303.
- (130) Sharma, P.; Banerjee, R.; Narayan, K. P. *J. Pharm. Res.* **2014**, *8* (5), 637.
- (131) Albert, A. *Nature* **1958**, *182* (4633), 421.
- (132) Torchilin, V. P. *Eur. J. Pharm. Sci.* **2000**, *11* (Suppl. 2), S81.
- (133) Stella, V. J.; Himmelstein, K. J. *J. Med. Chem.* **1980**, *23* (12), 1275.
- (134) Rautio, J.; Kumpulainen, H.; Heimbach, T.; Oliyai, R.; Oh, D.; Järvinen, T.; Savolainen, J. *Nat. Rev. Drug Discov.* **2008**, *7* (3), 255.
- (135) Bardsley-Elliot, A.; Noble, S. *Drugs* **1999**, *58* (5), 851.
- (136) Yan, Y.; Kim, H.; Seo, K.; Lee, W. S.; Lee, G.; Woo, J.; Yong, C.; Choi, H. *Mol. Pharm.* **2010**, *7* (6), 2132.
- (137) Jana, S.; Mandlekar, S.; Marathe, P. *Curr. Med. Chem.* **2010**, *17* (32), 3874.
- (138) Gunnarsson, P. O.; Andersson, S.-B.; Johansson, S.-A.; Nilsson, T.; Plym-Forshell, G. *Eur. J. Clin. Pharmacol.* **1984**, *26*, 113.
- (139) Stella, V. J.; Borchardt, R. T.; Hageman, M. J.; Oliyai, R.; Maag, H.; Tilley, J. W. *Prodrugs: Challenges and Rewards*; AAPS Press/Springer: New York, 2007.
- (140) McAuley, A.; Jacob, J.; Kolvenbach, C. G.; Westland, K.; Lee, H. J.; Brych, S. R.; Rehder, D.; Kleemann, G. R.; Brems, D. N.; Matsumura, M. *Protein Sci.* **2008**, *17* (1), 95.
- (141) Janeway, C. A.; Travers, P.; Walport, M.; Shlomchik, M. *Immunobiology: The Immune System in Health and Disease*, New York.; 5th, Ed.; Garland Science, 2001.
- (142) Chari, R. V. J.; Miller, M. L.; Widdison, W. C. *Angew. Chem. Int. Ed.* **2014**, *53* (15), 3796.
- (143) Kohler, G.; Milstein, C. *Nature* **1975**, *256* (5517), 495.
- (144) Nadler, L. M.; Stashenko, P.; Hardy, R.; Kaplan, W. D.; Button, L. N.; Kufe, D. W.; Antman, K. H.; Schlossman, S. F. *Cancer Res.* **1980**, *40*, 3147.
- (145) Klee, G. G. *Arch. Pathol. Lab. Med.* **2000**, *124* (6), 921.
- (146) Morrison, S. L.; Johnson, M. J.; Herzenberg, L. A.; Oi, V. T. *Proc. Natl. Acad. Sci. USA* **1984**, *81* (21), 6851.
- (147) Riechmann, L.; Clark, M.; Waldmann, H.; Winter, G. *Nature* **1988**, *332* (6162), 323.

- (148) McCafferty, J.; Griffiths, A. D.; Winter, G.; Chiswell, D. J. *Nature* **1990**, *348* (6301), 552.
- (149) Jakobovits, A. *Curr. Opin. Biotech.* **1995**, *6* (5), 561.
- (150) Baker, M. P.; Reynolds, H. M.; Lumicisi, B.; Bryson, C. J. *Self. Nonself.* **2010**, *1* (4), 314.
- (151) Schiff, M. H.; Burmester, G. R.; Kent, J. D.; Pangan, A. L.; Kupper, H.; Fitzpatrick, S. B.; Donovan, C. *Ann. Rheum. Dis.* **2006**, *65* (7), 889.
- (152) Ritchie, M.; Tchistiakova, L.; Scott, N. *MAbs* **2013**, *5* (1), 13.
- (153) Mindell, J. A. *Annu. Rev. Physiol.* **2012**, *74*, 69.
- (154) Hamblett, K. J.; Senter, P. D.; Chace, D. F.; Sun, M. M. C.; Lenox, J.; Cerveny, C. G.; Kissler, K. M.; Bernhardt, S. X.; Kopcha, A. K.; Zabinski, R. F.; Meyer, D. L.; Francisco, J. A. *Clin. Cancer Res.* **2004**, *10* (20), 7063.
- (155) Junutula, J. R.; Raab, H.; Clark, S.; Bhakta, S.; Leipold, D. D.; Weir, S.; Chen, Y.; Simpson, M.; Tsai, S. P.; Dennis, M. S.; Lu, Y.; Meng, Y. G.; Ng, C.; Yang, J.; Lee, C. C.; Duenas, E.; Gorrell, J.; Katta, V.; Kim, A.; McDorman, K.; Flagella, K.; Venook, R.; Ross, S.; Spencer, S. D.; Lee Wong, W.; Lowman, H. B.; Vandlen, R.; Sliwkowski, M. X.; Scheller, R. H.; Polakis, P.; Mallet, W. *Nat. Biotechnol.* **2008**, *26* (8), 925.
- (156) McDonagh, C. F.; Turcott, E.; Westendorf, L.; Webster, J. B.; Alley, S. C.; Kim, K.; Andreyka, J.; Stone, I.; Hamblett, K. J.; Francisco, J. A.; Carter, P. *Protein Eng. Des. Sel.* **2006**, *19* (7), 299.
- (157) Axup, J. Y.; Bajjuri, K. M.; Ritland, M.; Hutchins, B. M.; Kim, C. H.; Kazane, S. A.; Halder, R.; Forsyth, J. S.; Santidrian, A. F.; Stafin, K.; Lu, Y.; Tran, H.; Seller, A. J.; Biroc, S. L.; Szydlak, A.; Pinkstaff, J. K.; Tian, F.; Sinha, S. C.; Felding-Habermann, B.; Smider, V. V.; Schultz, P. G. *P. Natl. Acad. Sci. USA* **2012**, *109* (40), 16101.
- (158) Bross, P. F.; Beitz, J.; Chen, G.; Chen, X. H.; Duffy, E.; Kieffer, L.; Roy, S.; Sridhara, R.; Rahman, A.; Williams, G.; Pazdur, R. *Clin. Cancer Res.* **2001**, *7*, 1490.
- (159) US Food and Drug Administration. Fast Track, Breakthrough Therapy, Accelerated Approval and Priority Review <http://www.fda.gov/forconsumers/byaudience/forpatientadvocates/speedingaccessstoimportantnewtherapies/ucm128291.htm> (accessed Jun 23, 2014).
- (160) Paul, S. P.; Taylor, L. S.; Stansbury, E. K.; McVicar, D. W. *Blood* **2000**, *96* (2), 483.
- (161) Jones, R. R.; Bergman, R. G. *J. Am. Chem. Soc.* **1972**, *94* (2), 660.
- (162) Watanabe, C. M. H.; Supekova, L.; Schultz, P. G. *Chem. Biol.* **2002**, *9* (2), 245.
- (163) Hinman, L. M.; Hamann, P. R.; Wallace, R.; Menendez, A. T.; Durr, F. E.; Upešlacis, J. *Cancer Res.* **1993**, *53*, 3336.
- (164) Thorpe, P. E.; Wallace, P. M.; Knowles, P. P.; Relf, M. G.; Brown, A. N. F.; Watson, G. J.; Knyba, R. E.; Wawrzynczak, E. J.; Blake, D. C. *Cancer Res.* **1987**, *47*, 5924.

- (165) US Food and Drug Administration. Mylotarg (gemtuzumab ozogamicin): Market Withdrawal <http://www.fda.gov/safety/medwatch/safetyinformation/safetyalertsforhumanmedicalproducts/ucm216458.htm> (accessed Jun 23, 2014).
- (166) Panowksi, S.; Bhakta, S.; Raab, H.; Polakis, P.; Junutula, J. R. *MAbs* **2014**, *6* (1), 34.
- (167) Drak, J.; Iwasawa, N.; Danishefsky, S.; Crothers, D. M. *P. Natl. Acad. Sci. USA* **1991**, *88* (17), 7464.
- (168) Shen, B.-Q.; Xu, K.; Liu, L.; Raab, H.; Bhakta, S.; Kenrick, M.; Parsons-Reponte, K. L.; Tien, J.; Yu, S.-F.; Mai, E.; Li, D.; Tibbitts, J.; Baudys, J.; Saad, O. M.; Scales, S. J.; McDonald, P. J.; Hass, P. E.; Eigenbrot, C.; Nguyen, T.; Solis, W. A.; Fuji, R. N.; Flagella, K. M.; Patel, D.; Spencer, S. D.; Khawli, L. A.; Ebens, A.; Wong, W. L.; Vandlen, R.; Kaur, S.; Sliwkowski, M. X.; Scheller, R. H.; Polakis, P.; Junutula, J. R. *Nat. Biotechnol.* **2012**, *30* (2), 184.
- (169) Huttunen, K. M.; Raunio, H.; Rautio, J. *Pharmacol. Rev.* **2011**, *63* (3), 750.
- (170) Betsholtz, C. *Nature* **2014**, *509* (7501), 432.
- (171) Lipinski, C. A.; Lombardo, F.; Dominy, B. W.; Feeney, P. J. *Adv. Drug Deliv. Rev.* **1997**, *23*, 3.
- (172) Wager, T. T.; Chandrasekaran, R. Y.; Hou, X.; Troutman, M. D.; Verhoest, P. R.; Villalobos, A.; Will, Y. *ACS Chem. Neurosci.* **2010**, *1* (6), 420.
- (173) Pajouhesh, H.; Lenz, G. R. *NeuroRX* **2005**, *2* (4), 541.
- (174) Yee, R. E.; Cheng, D. W.; Huang, S.-C.; Namavari, M.; Satyamurthy, N.; Barrio, J. R. *Biochem. Pharmacol.* **2001**, *62* (10), 1409.
- (175) Bodor, N.; Farag, H. H.; Brewster, M. E. *Science*. **1981**, *214* (4527), 1370.
- (176) Brewster, M. E.; Anderson, W. R.; Helton, D. O.; Bodor, N.; Pop, E. *Pharm. Res.* **1995**, *12* (5), 796.
- (177) Wu, W. M.; Pop, E.; Shek, E.; Bodor, N. *J. Med. Chem.* **1989**, *32* (8), 1782.
- (178) Estes, K. S.; Brewster, M. E.; Simpkins, J. W.; Bodor, N. *Life Sci.* **1987**, *40* (13), 1327.
- (179) Singh, R. K.; Kumar, S.; Prasad, D. N.; Bhardwaj, T. R. *Med. Chem. Res.* **2013**, *23* (5), 2405.
- (180) Gourand, F.; Mercey, G.; Ibazizène, M.; Tirel, O.; Henry, J.; Levacher, V.; Perrio, C.; Barré, L. *J. Med. Chem.* **2010**, *53* (3), 1281.
- (181) Ishikura, T.; Senou, T.; Ishihara, H.; Kato, T.; Ito, T. *Int. J. Pharm.* **1995**, *116* (1), 51.
- (182) Yoshikawa, T.; Sakaeda (née Kakutani), T.; Sugawara, T.; Hirano, K.; Stella, V. J. *Adv. Drug Deliv. Rev.* **1999**, *36* (2-3), 255.
- (183) Heidelberger, C.; Chaudhuri, N. K.; Danneberg, P.; Mooren, D.; Griesbach, L.; Duschinsky, R.; Schnitzer, R. J.; Plevin, E.; Scheiner, J. *Nature* **1957**, *179* (4561), 663.
- (184) Miwa, M.; Ura, M.; Nishida, M.; Sawada, N.; Ishikawa, T.; Mori, K.; Shimma,

- N.; Umeda, I.; Ishitsuka, H. *Eur. J. Cancer* **1998**, *34* (8), 1274.
- (185) Walko, C. M.; Lindley, C. *Clin. Ther.* **2005**, *27* (1), 23.
- (186) Cortez-Retamozo, V.; Etzrodt, M.; Newton, A.; Rauch, P. J.; Chudnovskiy, A.; Berger, C.; Ryan, R. J. H.; Iwamoto, Y.; Marinelli, B.; Gorbatov, R.; Forghani, R.; Novobrantseva, T. I.; Koteliansky, V.; Figueiredo, J.-L.; Chen, J. W.; Anderson, D. G.; Nahrendorf, M.; Swirski, F. K.; Weissleder, R.; Pittet, M. J. *P. Natl. Acad. Sci. USA* **2012**, *109* (7), 2491.
- (187) Colmegna, I.; Ohata, B. R.; Menard, H. A. *Clin. Pharmacol. Ther.* **2012**, *91* (4), 607.
- (188) Brzezinski, M. R.; Spink, B. J.; Dean, R. A.; Berkman, C. E.; Cashman, J. R.; Bosron, W. F. *Drug Metab. Dispos.* **1997**, *25* (9), 1089.
- (189) Holmes, R. S.; Cox, L. A.; VandeBerg, J. L. *Genetica* **2010**, *138* (7), 695.
- (190) Holmes, R. S.; Wright, M. W.; Laulederkind, S. J. F.; Cox, L. A.; Hosokawa, M.; Imai, T.; Ishibashi, S.; Lehner, R.; Miyazaki, M.; Perkins, E. J.; Potter, P. M.; Redinbo, M. R.; Robert, J.; Satoh, T.; Yamashita, T.; Yan, B.; Yokoi, T.; Zechner, R.; Maltais, L. J. *Mamm. Genome* **2010**, *21* (9), 427.
- (191) Zhang, L.; Hu, Z.; Zhu, C.; Liu, Q.; Zhou, Y.; Zhang, Y. *Acta Biochim. Biophys. Sin.* **2009**, *41* (10), 809.
- (192) Needham, L. A.; Davidson, A. H.; Bawden, L. J.; Belfield, A.; Bone, E. A.; Brotherton, D. H.; Bryant, S.; Charlton, M. H.; Clark, V. L.; Davies, S. J.; Donald, A.; Day, F. A.; Krige, D.; Legris, V.; McDermott, J.; McGovern, Y.; Owen, J.; Patel, S. R.; Pintat, S.; Testar, R. J.; Wells, G. M. A.; Moffat, D.; Drummond, A. H. *J. Pharmacol. Exp. Ther.* **2011**, *339* (1), 132.
- (193) Shi, D.; Yang, J.; Yang, D.; Lecluyse, E. L.; Black, C.; You, L.; Akhlaghi, F.; Yan, B. *J. Pharmacol. Exp. Ther.* **2006**, *319* (3), 1477.
- (194) Bencharit, S.; Morton, C. L.; Xue, Y.; Potter, P. M.; Redinbo, M. R. *Nat. Struct. Biol.* **2003**, *10* (5), 349.
- (195) Redinbo, M. R.; Bencharit, S.; Potter, P. M. *Biochem. Soc. T.* **2003**, *31*, 620.
- (196) Imai, T. *Drug Metab. Pharmacokinet.* **2006**, *21* (3), 173.
- (197) Charlton, M. H.; Brotherton, D. H.; Owen, J.; Clark, V. L.; Testar, R. J.; Davies, S. J.; Moffat, D. F. C. *Med. Chem. Comm.* **2012**, *3* (9), 1070.
- (198) Davidson, A. H.; Patel, S. R.; Mazzei, F. A.; Davies, S. J.; Drummond, A. H.; Moffat, D. F. C.; Baker, K. W. J.; Donald, A. D. G. Enzyme Inhibitors. PCT/GB2006/001605 (WO 2006/117549). PCT/GB2006/001605 (WO 2006/117549), 2006.
- (199) Charlton, M. H.; Moffat, D. F. C.; Davies, S. J.; Drummond, A. H.; Simons, A. L. Imaging Agents. PCT/GB2011/001729 (WO 2012/080705). PCT/GB2011/001729 (WO 2012/080705), 2012.
- (200) Reid, A. H. M.; Protheroe, A.; Attard, G.; Hayward, N.; Vidal, L.; Spicer, J.; Shaw, H. M.; Bone, E. A.; Carter, J.; Hooftman, L.; Harris, A.; De Bono, J. S. *Clin. Cancer Res.* **2009**, *15* (15), 4978.
- (201) Ekroos, M.; Sjogren, T. *Proc. Natl. Acad. Sci.* **2006**, *103* (37), 13682.
- (202) Yan, G.; Zhang, G.; Fang, X.; Zhang, Y.; Li, C.; Ling, F.; Cooper, D. N.; Li, Q.;

- Li, Y.; van Gool, A. J.; Du, H.; Chen, J.; Chen, R.; Zhang, P.; Huang, Z.; Thompson, J. R.; Meng, Y.; Bai, Y.; Wang, J.; Zhuo, M.; Wang, T.; Huang, Y.; Wei, L.; Li, J.; Wang, Z.; Hu, H.; Yang, P.; Le, L.; Stenson, P. D.; Li, B.; Liu, X.; Ball, E. V.; An, N.; Huang, Q.; Zhang, Y.; Fan, W.; Zhang, X.; Li, Y.; Wang, W.; Katze, M. G.; Su, B.; Nielsen, R.; Yang, H.; Wang, J.; Wang, X.; Wang, J. *Nat. Biotechnol.* **2011**, 29 (11), 1019.
- (203) Satoh, T.; Hosokawa, M. *Chem. Biol. Interact.* **2006**, 162 (3), 195.
- (204) Loehry, C. A.; Axon, A. T. R.; Hilton, P. J.; Hider, R. C.; Creamer, B. *Gut* **1970**, 11 (6), 466.
- (205) Fasano, M.; Curry, S.; Terreno, E.; Galliano, M.; Fanali, G.; Narciso, P.; Notari, S.; Ascenzi, P. *IUBMB Life* **2005**, 57 (12), 787.
- (206) Bamborough, P.; Chung, C. *Med. Chem. Commun.* **2015**, 6 (9), 1587.
- (207) de Kloe, G. E.; Bailey, D.; Leurs, R.; de Esch, I. J. P. *Drug Discov. Today* **2009**, 14 (13-14), 630.
- (208) Hopkins, A. L.; Groom, C. R.; Alex, A. *Drug Discov. Today* **2004**, 9 (10), 430.
- (209) Schultes, S.; De Graaf, C.; Haaksma, E. E. J.; De Esch, I. J. P.; Leurs, R.; Krämer, O. *Drug Discov. Today Technol.* **2010**, 7 (3), 157.
- (210) Chung, C.-W. *GSK, Unpublished Results: X-ray Crystallographic Data*; 2015.
- (211) Martinez, C. R.; Iverson, B. L. *Chem. Sci.* **2012**, 3 (7), 2191.
- (212) Craig, P. N. *J. Med. Chem.* **1971**, 14 (8), 680.
- (213) Jaffe, H. H. *Chem. Rev.* **1953**, 53 (2), 191.
- (214) Fujita, T.; Iwasa, J.; Hansch, C. *J. Am. Chem. Soc.* **1964**, 86 (23), 5175.
- (215) Vogel, A. I.; Cresswell, W. T.; Jeffery, G. H.; Leicester, J. *J. Chem. Soc.* **1952**, 514.
- (216) Miyaura, N.; Yanagi, T.; Suzuki, A. *Synth. Commun.* **1981**, 11 (7), 513.
- (217) Feng, Y.; Lo-Grasso, P.; Schroeter, T.; Yin, Y. Urea and Carbamate Compounds and Analogs as Kinase Inhibitors PCT/US2009/005177 (WO 2010/036316), 2010.
- (218) Cayla, N.; Mitchell, D. *GSK, Unpublished Results: 3,4-Dimethoxyphenyl derivative 2.26*; 2012.
- (219) Wang, T.; Ledebuer, M. W.; Duffy, J. P.; Salituro, F. G.; Pierce, A. C.; Zuccola, H. J.; Block, E.; Shlyakter, D.; Hogan, J. K.; Bennani, Y. L. *Bioorg. Med. Chem. Lett.* **2010**, 20 (1), 153.
- (220) Berthelot, M.; Jungfleisch, E. *Ann. Chim. Phys.* **1872**, 26 (4), 396.
- (221) Tute, M. S. *Lipophilicity: A History. In Lipophilicity in Drug Action and Toxicology (eds Pliška, V., Testa, Van de Waterbeemd, B. and H.)*; Wiley-VCH Verlag GmbH: Weinheim, Germany, 1996.
- (222) Koziolok, M.; Grimm, M.; Becker, D.; Iordanov, V.; Zou, H.; Shimizu, J.; Wanke, C.; Garbacz, G.; Weitschies, W. *J. Pharm. Sci.* **2015**, 104 (9), 2855.
- (223) Young, R. J.; Green, D. V. S.; Luscombe, C. N.; Hill, A. P. *Drug Discov. Today* **2011**, 16 (17-18), 822.

- (224) The Biobyte/Daylight cLogP calculator is available from Daylight Chemical Information Systems, Santa Fe, NM. <http://www.daylight.com> (accessed Jun 29, 2013).
- (225) Gillis, E. P.; Burke, M. D. *J. Am. Chem. Soc.* **2007**, *129* (21), 6716.
- (226) Dick, G. R.; Woerly, E. M.; Burke, M. D. *Angew. Chem. Int. Ed.* **2012**, *51* (11), 2667.
- (227) Deng, J. Z.; Paone, D. V.; Ginnetti, A. T.; Kurihara, H.; Dreher, S. D.; Weissman, S. A.; Stauffer, S. R.; Burgey, C. S. *Org. Lett.* **2009**, *11* (2), 345.
- (228) Crowley, B. M.; Potteiger, C. M.; Deng, J. Z.; Prier, C. K.; Paone, D. V.; Burgey, C. S. *Tetrahedron Lett.* **2011**, *52* (39), 5055.
- (229) Jones, K. GSK, *Unpublished Results: pyridazinone*; 2012.
- (230) Igeta, H.; Yamada, M.; Yoshioka, Y.; Kawazoe, Y. *Chem. Pharm. Bull.* **1967**, *15* (9), 1411.
- (231) Greenwood, J. R. *Pyridazinediones and amino acid receptors: theoretical studies, design, synthesis, and evaluation of novel analogues*, PhD Thesis.; University of Sydney, 1999.
- (232) Sulsky, R.; Robl, Jeffrey, A. Pyrazinone Inhibitors of Fatty Acid Binding Protein and Method PCTIUS02/22186 (WO 03/006023 A1), 2003.
- (233) Jones, K. *The Design and Synthesis of Novel Epigenetic Modulators*, PhD Thesis.; 2014.
- (234) Varghese, A.; Jones, K. GSK, *Unpublished Results: Reductive Amination Optimisation*; 2013.
- (235) Varghese, A.; Jones, K. GSK, *Unpublished Results: Slow Valine Ester Hydrolysis*; 2013.
- (236) Mizutani, T.; Ema, T.; Ogoshi, H. *Tetrahedron* **1995**, *51* (2), 473.
- (237) Brown, J. A. GSK, *Unpublished Results: Synthesis of GSK3169442A*; 2012.
- (238) Ishiyama, T.; Murata, M.; Miyaura, N. *J. Org. Chem.* **1995**, *60*, 7508.
- (239) Boys, M. L.; Delisle, R. K.; Hicken, E. J.; Kennedy, A. L.; Mareska, D. A.; Marmsater, F. P.; Munson, M. C.; Newhouse, B.; Rast, B.; Rizzi, J. P.; Rodriguez, M. E.; Topalov, G. T.; Zhao, Q. Substituted N-(1H-Indazol-4-yl)imidazo[1,2-a]pyridine-3-carboxylamide Compounds as Type III Receptor Tyrosine Kinase Inhibitors (WO2012/082689), 2012.
- (240) Brown, J. A. GSK, *Unpublished Results: Pyridinone Boronic Ester Synthesis*; 2013.
- (241) Campbell, M. *PhD Thesis in Preparation, University of Strathclyde and GSK*; 2016.
- (242) Murata, M.; Oyama, T.; Watanabe, S.; Masuda, Y. *J. Org. Chem.* **2000**, *65* (1), 164.
- (243) Lam, K. C.; Marder, T. B.; Lin, Z. *Organometallics* **2010**, *29* (7), 1849.
- (244) Carton, R.; Bit, R. A. GSK, *Unpublished Results: Reductive amination using triethylamine conditions*; 2013.

- (245) Gregory, R. *GSK, Unpublished Results: Cell retention assay*; 2013.
- (246) Gleeson, M. P.; Hersey, A.; Montanari, D.; Overington, J. *Nat. Rev. Drug Discov.* **2011**, *10* (3), 197.
- (247) Peters, J.-U. *J. Med. Chem.* **2013**, *56* (22), 8955.
- (248) Gibson, G. G.; Skett, P. *Introduction to Drug Metabolism*, Third Ed.; Nelson Thornes: Cheltenham, UK, 2001.
- (249) Corey, E. J.; Chaykovsky, M. *J. Am. Chem. Soc.* **1965**, *87* (6), 1353.
- (250) Corey, E. J.; Chaykovsky, M. *J. Am. Chem. Soc.* **1965**, *87* (6), 1345.
- (251) Wittig, G.; Geissler, G. *Justus Liebigs Ann. Chem.* **1953**, *580* (1), 44.
- (252) Gibson (née Thomas), S. E.; Guillo, N.; Middleton, R. J.; Thuilliez, A.; Tozer, M. J. *J. Chem. Soc. Perkin Trans. 1* **1997**, *4*, 447.
- (253) Hirayama, F.; Koshio, H.; Katayama, N.; Kurihara, H.; Taniuchi, Y.; Sato, K.; Hisamichi, N.; Sakai-Moritani, Y.; Kawasaki, T.; Matsumoto, Y.; Yanagisawa, I. *Bioorg. Med. Chem.* **2002**, *10* (5), 1509.
- (254) Penning, T. D.; Russell, M. A.; Chen, B. B.; Chen, H. Y.; Liang, C.-D.; Mahoney, M. W.; Malecha, J. W.; Miyashiro, J. M.; Yu, S. S.; Askonas, L. J.; Gierse, J. K.; Harding, E. I.; Highkin, M. K.; Kachur, J. F.; Kim, S. H.; Villani-Price, D.; Pyla, E. Y.; Ghoreishi-Haack, N. S.; Smith, W. G. *J. Med. Chem.* **2002**, *45* (16), 3482.
- (255) Bit, R. A.; Humphreys, L. D. *GSK, Unpublished Results: Ester Hydrolysis Enzyme Screen*; 2015.
- (256) Jones, K. *GSK, Unpublished results: cyclopentyl and tetrahydrofuranyl esters*; 2013.
- (257) Bit, R. A.; Brown, J. A.; Jones, K. *GSK, Unpublished Results: Unsuccessful Dean-Stark Esterifications With Polar Amino Acids and Polar Alcohols*; 2015.
- (258) Crane, C. M.; Boger, D. L. *J. Med. Chem.* **2009**, *52* (5), 1471.
- (259) Gallenkamp, D.; Gelato, K. A.; Haendler, B.; Weinmann, H. *ChemMedChem* **2014**, *9* (3), 438.
- (260) Hay, D. A.; Fedorov, O.; Martin, S.; Singleton, D. C.; Tallant, C.; Wells, C.; Picaud, S.; Philpott, M.; Monteiro, O. P.; Rogers, C. M.; Conway, S. J.; Rooney, T. P. C.; Tumber, A.; Yapp, C.; Filippakopoulos, P.; Bunnage, M. E.; Müller, S.; Knapp, S.; Schofield, C. J.; Brennan, P. E. *J. Am. Chem. Soc.* **2014**, *136* (26), 9308.
- (261) Hay, D.; Fedorov, O.; Filippakopoulos, P.; Martin, S.; Philpott, M.; Picaud, S.; Hewings, D. S.; Uttakar, S.; Heightman, T. D.; Conway, S. J.; Knapp, S.; Brennan, P. E. *Med. Chem. Commun.* **2013**, *4* (1), 140.
- (262) Hay, D. A.; Fedorov, O.; Martin, S.; Singleton, D. C.; Tallant, C.; Wells, C.; Picaud, S.; Philpott, M.; Monteiro, O. P.; Rogers, C. M.; Conway, S. J.; Rooney, T. P. C.; Tumber, A.; Yapp, C.; Filippakopoulos, P.; Bunnage, M. E.; Müller, S.; Knapp, S.; Schofield, C. J.; Brennan, P. E. *J. Am. Chem. Soc.* **2014**, *136* (26), 9308.
- (263) Hammitzsch, A.; Tallant, C.; Fedorov, O.; O'Mahony, A.; Brennan, P. E.; Hay, D. A.; Martinez, F. O.; Al-Mossawi, M. H.; de Wit, J.; Vecellio, M.; Wells, C.;

- Wordsworth, P.; Müller, S.; Knapp, S.; Bowness, P. *Proc. Natl. Acad. Sci.* **2015**, *112* (34), 10768.
- (264) Theodoulou, N. H.; Bamborough, P.; Bannister, A. J.; Becher, I.; Bit, R. A.; Che, K. H.; Chung, C.-W.; Dittmann, A.; Drewes, G.; Drewry, D. H.; Gordon, L.; Grandi, P.; Leveridge, M.; Lindon, M.; Michon, A.-M.; Molnar, J.; Robson, S. C.; Tomkinson, N. C. O.; Kouzarides, T.; Prinjha, R. K.; Humphreys, P. G. *J. Med. Chem.* **2016**, *59* (4), 1425.
- (265) Atkinson, S. J.; Soden, P. E.; Angell, D. C.; Bantscheff, M.; Chung, C.; Giblin, K. A.; Smithers, N.; Furze, R. C.; Gordon, L.; Drewes, G.; Rioja, I.; Witherington, J.; Parr, N. J.; Prinjha, R. K. *Med. Chem. Commun.* **2014**, *5* (3), 342.
- (266) Hewings, D. S.; Rooney, T. P. C.; Jennings, L. E.; Hay, D. A.; Schofield, C. J.; Brennan, P. E.; Knapp, S.; Conway, S. J. *J. Med. Chem.* **2012**, *55* (22), 9393.
- (267) de Meijere, A. *Angew. Chem. Int. Ed.* **1979**, *18* (11), 809.
- (268) Imai, T. *Drug Metab. Pharmacokinet.* **2006**, *21* (3), 173.
- (269) Wadkins, R. M.; Hyatt, J. L.; Wei, X.; Yoon, K. J. P.; Wierdl, M.; Edwards, C. C.; Morton, C. L.; Obenauer, J. C.; Damodaran, K.; Beroza, P.; Danks, M. K.; Potter, P. M. *J. Med. Chem.* **2005**, *48* (8), 2906.
- (270) Gregory, R.; Ramirez-Molina, C. *GSK, Unpublished Results: IVC +/- Benzil*; 2014.
- (271) Connelly, P. W.; Picardo, C. M.; Potter, P. M.; Teiber, J. F.; Maguire, G. F.; Ng, D. S. *Biochim. Biophys. Acta* **2011**, *1811* (1), 39.
- (272) Gough, P. J.; Gordon, S.; Greaves, D. R. *Immunology* **2001**, *103* (3), 351.
- (273) Humphreys, P. G. *GSK, Unpublished results: Pyridyl Derivatives*; 2014.
- (274) Image generated using TREEspot™ Software Tool and reprinted with permission from KINOMEScan®, a division of DiscoverX Corporation, © DISCOVERX CORPORATION 2010 - See more at: <http://www.discoverx.com/treespot-publication-request-information/#sthash.wfYfWv>.
- (275) Allen, F. H. *Acta Crystallogr. Sect. B Struct. Sci.* **2002**, *58* (3), 380.
- (276) Bruno, I. J.; Cole, J. C.; Edgington, P. R.; Kessler, M.; Macrae, C. F.; McCabe, P.; Pearson, J.; Taylor, R. *Acta Crystallogr. Sect. B Struct. Sci.* **2002**, *58* (3), 389.
- (277) Mitsunobu, O.; Yamada, M.; Mukaiyama, T. *Bull. Chem. Soc. Jpn.* **1967**, *40* (4), 935.
- (278) Humphreys, P. G. *GSK, Unpublished Results: Epoxidation Conditions*; 2014.
- (279) Hoffman, J. M.; Smith, A. M.; Rooney, C. S.; Fisher, T. E.; Wai, J. S.; Thomas, C. M.; Bamberger, D. L.; Barnes, J. L.; Williams, T. M. *J. Med. Chem.* **1993**, *36* (8), 953.
- (280) Humphreys, P. G. *GSK, Unpublished results: Synthesis of diastereomer 174*; 2014.
- (281) Thomas, P. *GSK, Unpublished Results: Computational Modelling of WPF Shelf Groups*; 2014.

- (282) Humphreys, P. G. *GSK, Unpublished results: Design and Synthesis of 2-Dimethoxypropyl Compound 176*; 2014.
- (283) Jackson, S. *GSK, Unpublished Results: Chiral Separation*; 2015.
- (284) Lei, A.; Liu, W.; Liu, C.; Chen, M. *Dalt. Trans.* **2010**, 39 (43), 10352.
- (285) Kazmi, F.; Hensley, T.; Pope, C.; Funk, R. S.; Loewen, G. J.; Buckley, D. B.; Parkinson, A. *Drug Metab. Dispos.* **2013**, 41 (4), 897.
- (286) de Duve, C.; de Barse, T.; Poole, B.; Trouet, A.; Tulkens, P.; Van Hoof, F. *Biochem. Pharmacol.* **1974**, 23 (18), 2495.
- (287) Bit, R. A. *GSK, Unpublished Results: i-propyl and t-butyl ester comparison*; 2015.
- (288) Cesti, P.; Zaks, A.; Klivanov, A. M. *Appl. Biochem. Biotechnol.* **1985**, 11 (5), 401.
- (289) Kumar, I.; Bhide, S. R.; Rode, C. V. *Tetrahedron: Asymmetry* **2007**, 18 (10), 1210.
- (290) Wang, L.; Pratt, J. K.; McDaniel, K. F. Bromodomain Inhibitors PCT/CN2011/002224 (WO 2013/097052 A1), 2013.
- (291) Bennett, M. J.; Betancort, J. M.; Bolor, A.; Kaldor, S. W.; Stafford, J. A.; Veal, J. M. Bromodomain Inhibitors PCT/US2014/061261 (WO 2015/058160 A1), 2015.
- (292) Morrow, C. J.; Rapoport, H. *J. Org. Chem* **1974**, 39 (14), 2116.
- (293) Mayhew, T. M.; Williams, M. A. *Zeitschrift für Zellforsch. und Mikroskopische Anat.* **1974**, 147 (4), 567.

7 Appendix 1

7.1 Macrophage Retention Assay Calculations

7.1.1 Acid 2.95e

Moles of acid from lysate = 0.33 nMoles

Volume of a macrophage²⁹³ = 126 μm^3 = 126 fL

Using 1 million macrophage cells, the total lysate volume = 126 nL

$$\begin{aligned} \text{Lysate Acid Concentration} &= \frac{\text{moles of acid}}{\text{volume}} = \frac{0.33 \times 10^{-9}}{126 \times 10^{-9}} = 2.62 \times 10^{-3} \text{ M} \\ &= 2.62 \text{ mM} \end{aligned}$$

pIC₅₀ of acid **2.59e** = 4.6 \equiv IC₅₀ = 25 μM

$$\frac{2.62 \times 10^{-3}}{25 \times 10^{-6}} = 104.8$$

Therefore, the concentration within the lysate is 100-fold higher than the IC₅₀

7.1.2 Ester 2.58e

Moles of acid from lysate = 0.03 nMoles

Volume of a macrophage²⁹³ = 126 μm^3 = 126 fL

Using 1 million macrophage cells, the total lysate volume = 126 nL

$$\begin{aligned} \text{Lysate Acid Concentration} &= \frac{\text{moles of acid}}{\text{volume}} = \frac{0.03 \times 10^{-9}}{126 \times 10^{-9}} = 0.24 \times 10^{-3} \text{ M} \\ &= 0.24 \text{ mM} \end{aligned}$$

pIC₅₀ of acid **2.58e** = 5.7 \equiv IC₅₀ = 2.0 μM

$$\frac{0.24 \times 10^{-3}}{2.0 \times 10^{-6}} = 120$$

Therefore, the concentration within the lysate is 120-fold higher than the IC₅₀

8 Appendix 2

8.1 BROMOscan™ Bromodomain Phylogenetic Tree

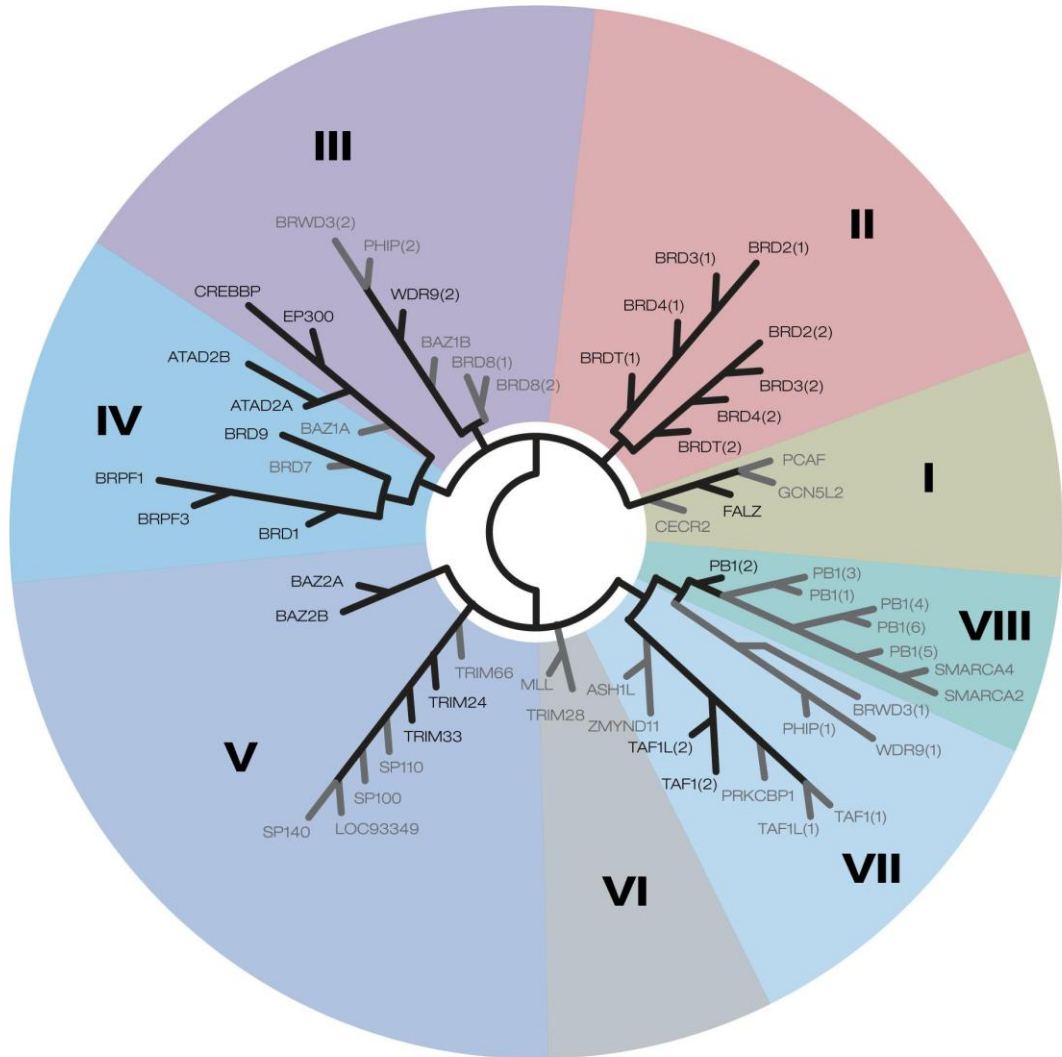


Figure 8.1: Bromodomain phylogenetic tree provided by BROMOscan™, minus activity spots²⁷⁴

9 Appendix 3

9.1 Assay Protocols

Brd4 BD1 FRET Assay

50 nL of test compounds in DMSO were serially diluted 1:3 into a Greiner 384 well low-volume assay plate. To each well was added 5 µL of protein/ligand solution (to an assay buffer of 50 mM HEPES, 150 mM NaCl, 1 mM CHAPS pH7.4, 5% glycerol and 1 mM DTT pH7.4 (using NaOH) was added the fluoroprobe and BRD4-Y390A protein). The assay plate was centrifuged at 1000 rpm for 60 seconds then incubated at RT for 30 min. To each well was added 5 µL of anti-His Eu solution (in assay buffer). The assay plate was centrifuged at 1000 rpm for 60 seconds then incubated at RT for 30 min. The assay plates were read using a Perkin Elmer Envision 2104 reader (emission 1: 665 nm, emission 2: 615 nm).

Human Whole Blood (hWB) MCP-1 Assay

0.5 µL of compounds in 3 mM DMSO were serially diluted (1:3) into a Greiner 96 well flat, clear bottom plate. 130 µL of human whole blood (with added sodium heparin, 10 µL/mL) was added to the compound wells, the plates incubated (37 °C, 5% CO₂) for 30 min, and 10 µL of 2.8 µg/mL LPS diluted in PBS was added. The plates are then incubated at 37 °C, 5% CO₂ overnight. 140 µL of PBS was added to the compound plate and the plates are centrifuged at 1800 rpm for 10 min. 20 µL of the supernatant was transferred to MCP1 coated 96 well MSD plates and incubated for 1.5 h on a plate shaker. 20 µL of 1X sulfo-TAG anti-MCP1 antibody was then added to each well and the plates were incubated for 1 h at RT whilst shaking. The plates were then washed three times with PBS and 0.05% Tween 20 using a plate washer and 150 µL read buffer P/T (2X) was added to the plate. The plates were read using an MSD reader.

CREBBP FRET Assay

100 nL of test compounds in DMSO were serially diluted 1:3 into a Greiner 384 well low-volume assay plate. To each well was added 5 μ L of protein/ligand solution (to an assay buffer of 50 mM HEPES, 150 mM NaCl, 1 mM CHAPS pH7.4, 5% glycerol and 1 mM DTT pH7.4 (using NaOH) was added the fluorophore and CREBBP protein). The assay plate was centrifuged at 1000 rpm for 60 seconds then incubated at RT for 30 min. To each well was added 5 μ L of anti-His Tb solution (in assay buffer). The assay plate was centrifuged at 1000 rpm for 60 seconds then incubated at RT for 30 min. The assay plates were read using a Perkin Elmer Envision 2104 reader (emission 1: 520 nm, emission 2: 495 nm).

CREBBP FP Assay

50 nL of test compounds in DMSO were serially diluted 1:3 into a Greiner 384 well low-volume assay plate. To each well was added 10 μ L of protein/ligand solution (to an assay buffer of 50 mM HEPES, 150 mM NaCl, 1 mM CHAPS pH7.4, 5% glycerol and 1 mM DTT pH7.4 (using NaOH) was added the fluorophore and CREBBP protein). The assay plate was centrifuged at 1000 rpm for 60 seconds then incubated at RT for 1 h. The assay plates were read using a Perkin Elmer Envision 2104 reader (emission 1: p-pol 535 nm, emission 1: s-pol 535 nm)

Brd9 FRET Assay

50 nL of test compounds in DMSO were serially diluted 1:3 into a Greiner 384 well low-volume assay plate. To each well was added 5 μ L of protein/ligand solution (to an assay buffer of 50 mM HEPES, 150 mM NaCl, 1 mM CHAPS pH7.4, 5% glycerol and 1 mM DTT pH7.4 (using NaOH) was added the fluorophore and Brd9 protein). The assay plate was centrifuged at 1000 rpm for 60 seconds then incubated at RT for 30 min. To each well was added 5 μ L of anti-His Eu solution (in assay buffer). The assay plate was centrifuged at 1000 rpm for 60 seconds then incubated at RT for 30 min. The assay plates were read using a Perkin Elmer Envision 2104 reader (emission 1: 665 nm, emission 2: 615 nm).

hCE-1 Specific Activity Assay

30 µL of test compound solution diluted to 100 µM in assay buffer (50 mM sodium phosphate pH 7.5, 100 mM NaCl) was added to the first 8 rows of a Greiner 384 well plate. 30 µL of the enzyme diluted to 100 nM in assay buffer was added to all wells to initiate the reaction. Individual wells (in sequence from Row 1-8) were stopped by the addition of 20 µL 5% formic acid with pipette mixing. Once the time course sequence was complete, the plate was transferred to the autosampler of an Agilent 1100 HPLC system and all wells were analysed on a Phenomenex Gemini 5µ C18 column (50 x 2 mm) using a formic acid modifier.

ChromLogD_{7.4}

The compound, 10 mM in DMSO, was diluted with methanol. The sample was analysed on a LUNA 5µ, C18 (50 x 3.0 mm) column on a Agilent 1100 system using a mobile phase of 50 mM ammonium acetate adjusted to pH7.4, using concentrated ammonia solution and acetonitrile.

Solubility (CLND)

The aqueous solubility of compounds was determined using chemiluminescent nitrogen detection (CLND) as a quantification method. Stock solutions of 10 mM compounds in DMSO were serially diluted in phosphate buffered saline (pH7.4) and analysed by HPLC (Agilent 1100 HPLC system; mobile phase 90% methanol, 10% water; flow rate 0.2 ml/min) using CLND (Antek 8060C chemiluminescent nitrogen detector).

Solubility (FaSSIF)

FaSSIF solution (2.24 mg/mL, pH 6.5) was prepared by the addition of 2.24 mg SIF powder to 0.5 ml assay buffer (3.437 g sodium dihydrogen phosphate, 6.186 g sodium chloride and 0.42 g sodium hydroxide pellets in 500 mL distilled water) and 0.5 ml distilled water. This solution was added to a vial containing compound (1 mg), which was capped, inverted three times, and shaken at 900 rpm for 4 hours. 175 µL

was transferred to a filter plate (0.4 micron pore size), which was centrifuged for 5 min at 2000 rpm to capture the filtrate. The filtrate was analysed by HPLC, and the solubility generated by comparison with HPLC data generated by analysing the compound when fully dissolved in DMSO.

AMP

3.5 µL of lipid solution (1.8% phosphatidylcholine in 1% cholesterol decan solution) was added to a filter plate (Millicell-96-well cell culture plate), the plate shaken for 12 seconds, and then 250 µL of buffer (50 mM phosphate buffer with 0.5% encapsin, pH at 7.4) added to donor side and 100 µL added to the receiver side. The assay plate was shaken for 45 min before adding the test compound (2.5 uL) to the donor side. The assay plates are then incubated at room temperature for 3 h. The donor and receiver solution were then analysed by HPLC.

HSA

10 µl of 10 mM samples were diluted to 100 µl using 50% IPA and 50% water. The samples were analysed by HPLC (column: Chiral Technologies HSA column 50 x 3.0 mm (5 micron), flow rate: 1.8 mL/min, temperature: 30 °C, gradient: 0 to 3.0 minutes 0 to 30% mobile phase B, 3.0 to 5.0 minutes 30% B, 5.0 to 5.1 minutes 30 to 0% B, 5.1 to 6 min 0% B, detection: 254, 210 and 230 nm). The mobile phases were A: ammonium acetate solution in water, 50 mM, adjusted to pH7.4. B: IPA.

HLM IVC

5.85 µL of 0.1 mM test compound and 29.25 µL of liver microsomes (0.5mg/mL final protein concentration) was added to 904.9 µL of 50 mM Potassium Phosphate Buffer in 5.0 mL vial. The mixture was incubated at 37 °C for 5 min to give the bulk mixture. 200 µL stop solution to each tube of a 96 deep well plate. A 40 µL aliquot from the bulk mixture is added to the first well of stop solution for the 0 min time point. 200 µL of cofactor solution (NADPH generating system) was added to 800 µL of the bulk mixture. 50 µL samples were taken at 3, 6, 9, 15, 21 and 30 min and added to the stop solution wells. Samples were analysed by LCMS/MS.

Whole Blood Half Life

995 µL of blood was spiked with 5 µL of a 200 µg/mL test compound solution to produce a 1000 ng/mL incubation solution. An aliquote of spiked blood (25 µL) was removed from the incubation at multiple time points (0, 2, 5, 10, 15, 20, 40, 60, 120, 180 and 240 minutes). Samples were subjected to protein precipitation with organic solvent prior to analysis using LCMS/MS.

Macrophage Retention

M1 macrophages were differentiated from CD14-positive monocytes. The monocytes were diluted to 1 million/mL and then treated with 5 ng/mL GM-CSF, plated at 1 million/well of a 24 well plate and allowed to differentiate for 5 days at 37 °C, 5% CO₂. After 5 days the plate was centrifuged and the medium carefully removed. The cells were treated with 10 µM of the relevant compound for a variety of time points. Additionally, medium containing compound (as above) was added to wells that did not contain any cells (no cell control; NCC) to determine the stability of the compound over time in cell culture medium. The NCC was also set up in lysis buffer (Mammalian Protein Extraction Reagent (MPER)). After the desired amount of time, the supernatant was removed and stored at -20 °C, the cells were washed twice with 500 µL PBS each (which was also stored at -20 °C) and then 100 µL of MPER was added to lyse the cells and the lysate was also then stored at -20 °C. NCC wells were not washed but the supernatant/MPER buffer was removed and stored as above. The samples were then analysed by mass spectrometry. 10 µM supernatants and no cell control samples were diluted 1/10 by adding 10 µL of sample to 90 µL of blank media. To 25 µL of all samples, 25 µL acetonitrile:water was added and all vials were capped and mechanically shaken for 20 min. An aliquot of the supernatant was analysed by LCMS/MS (API4000, SN: J1390111 (Demolishor)).